An Analysis of the Role of *Bacillus oleronius* Proteins in the Pathogenesis of Ocular Rosacea

Maynooth University
National University of Ireland Maynooth

A Thesis Submitted to the National University of Ireland for the Degree of Doctor of Philososphy by

Frederick W. McMahon BSc

Supervisor
Dr Kevin Kavanagh
Department of Biology,
Maynooth University,
Co. Kildare.

Head of Department
Prof. Paul Moynagh
Department of Biology,
Maynooth University,
Co. Kildare.

Co-Supervisor(s):
Dr Finbarr O'Sullivan
National Institute for Cellular Biotechnology,
Dublin City University, Dublin 9.

Dr Emer Reeves
Royal College of Surgeons in Ireland,
Beaumont Hospital, Dublin 9.

October 2015

Declaration of Authorship

This Thesis has not been submitted in whole, or in part to this or any other university for any degree, and is the original work of the author except where ortherwise stated.

Signed:_____ Date:_____

(Frederick W. McMahon BSc)

Abstract

Rosacea is a chronic dermatosis of the central T-zone of the face and eyes. It can be characterised by the presence of inflammatory papules and pustules, persistent non-transient erythema, and flushing episodes. Factors such as alterations in the innate immune response, changes to the vascular network in the skin, the presence of reactive oxygen species within the skin, and neutrophil activation have been suggested as major players in the induction and persistence of the disease. The aetiology of the disease remains unknown but studies suggest a role for bacteria in the induction and persistence of the condition. The aim of the work presented here was to investigate the role of a bacterium, *Bacillus oleronius*, in the pathogenesis of this disfiguring disease.

It was previously established that *B. oleronius* produces two immunogenic proteins that are capable of inducing an immune response in rosacea patients. As part of this project, the serologically reactive proteins were isolated and purified by anion exchange chromatography and ÄKTA FPLC™ for their use in further assays. The expression of the immuno-reactive 62 kDa GroEL protein was analysed in different culture conditions to determine a possible role in the pathogenesis of the disease, and it was observed that the *B. oleronius* increased expression of the 62 kDa GroEL protein in response to stress following alterations in temperature, pH, reactive oxygen species (ROS) presence, and oxygen availability of the local environment.

To investigate the role of *B. oleronius* proteins in the induction of ocular rosacea, a human telomerase-immortalized corneal epithelial (hTCEpi) cell line was used. Exposure of corneal epithelial cells to *B. oleronius* proteins reduced growth in a dose-dependent manner and this corresponded to a decreased rate of cell proliferation and an increase in mean generation time of the epithelial cells. Through FACS analysis, it was shown that corneal epithelial cells stimulated by *B. oleronius* proteins inhibited the hTCEpi cell cycle at the G_1/S transition. It was also observed using label-free mass spectrometry (LF/MS) that exposure of hTCEpi cells to *B. oleronius* proteins leads to alterations in the abundance of proteins that specifically function in poyadenylation (poly (A)) RNA binding.

The effect of *B. oleronius* proteins on immune cells was investigated, and it was observed that exposure of neutrophils to *B. oleronius* protein resulted in neutrophil activation along the inositol 1, 4, 5-triphosphate (IP_3) pathway with calcium (Ca^{2+})

release, cytoskeletal rearrangement and conversion to filamentous (F)-actin, and increased chemotaxis. The effect of *B. oleronius* proteins on the secretion of monocyte-specific and T-cell-specific cytokines was determined by ELISpot/FluoroSpot assays, and it was observed that exposure of peripheral blood mononuclear cells (PBMC) to *B. oleronius* proteins significantly increased the secretion of a range of cytokines ($p < 0.0001$) including IL-1β, IL-10, IL-12p40, IL-23, tumor necrotic factor (TNF)-α, IL-5, IL-13, IL-17A, IL-22, and interferon (IFN)-γ.

The serum from erythematotelangiectatic rosacea patients was analysed for sera reactivity to *B. oleronius* proteins. It was observed that 82% of erythematotelangiectatic rosacea patients were sera reactive to the *B. oleronius* proteins compared to 28% sera reactivity in controls. This population of rosacea patients demonstrated an increased density of *Demodex folliculorum* mites present in the skin but sera reactive rosacea patients also had reduced levels of sebum. Thus, demonstrating altered sebum levels in rosacea patients, and implicating a role for *B. oleronius* in the induction of the skin condition.

The aetiology of rosacea remains unknown but the results presented in this thesis demonstrate that *B. oleronius* proteins may be implicated in the pathogenesis of rosacea, and that the action of these proteins can lead to the induction of an inflammatory response that is a hallmark of the disease.

Publications:

Jarmuda, S., **McMahon, F.,** Zaba, R., O'Reilly, N., Jakubowicz, O., Holland, A., Szkaradkiewicz, A., and Kavanagh, K. 2014. Correlation between serum reactivity to *Demodex*-associated *Bacillus oleronius* proteins, and altered sebum levels and *Demodex* populations in erythematotelangiectatic rosacea patients. *Journal of Medical Microbiology*. 63: 258-262.

McMahon, F. W., Gallagher, C., O'Reilly, N., Clynes, M., O'Sullivan, F., and Kavanagh, K. 2014. Exposure of a corneal epithelial cell line (hTCEpi) to *Demodex*-associated *Bacillus* proteins results in an inflammatory response. *Investigative Ophthalmology and Visual Science*. 55: 7019-7028.

McMahon, F., Banville, N., Bergin, D. A., Smedman, C., Paulie, S., Reeves, E., and Kavanagh, K. 2015. Activation of neutrophils via IP_3 pathway following exposure to *Demodex* associated bacterial proteins. *Inflammation*. (Manuscript In Press).

In Preparation for Submission:

McMahon, F., Gallagher, C., Clynes, M., Carolan, J., O'Sullivan, F., and Kavanagh, K. Alterations to the proteome of corneal epithelial cell line (hTCEpi) induced by exposure to *Bacillus oleronius* proteins at an RNA level, and the implications in ocular rosacea.

Oral Presentations:

Frederick McMahon, Emer P. Reeves, Finbarr O'Sullivan, and Kevin Kavanagh. Title: Characterising the Role of Bacterial Antigens in the Induction and Persistence of the Inflammatory Skin Condition, Rosacea. 12th June, 2012, BioAT Annual Research Day Year 1 at Royal College of Surgeons in Ireland (RCSI).

Fred McMahon and Kevin Kavanagh. Title: The role of bacterial antigens in the induction and persistence of rosacea. 20th July, 2012, NUI Maynooth Biology Department Annual Research Day.

Frederick W. McMahon, Clair Gallagher, Niamh O'Reilly, Martin Clynes, Finbarr O'Sullivan, and Kevin Kavanagh. Title: The role of *Demodex* mites and implications in ocular rosacea – friend or foe? 29th August, 2013, Ulster University at Coleraine. *Winner 1st prize for Best PhD Student Oral Presentation*.

Fred McMahon and Kevin Kavanagh. Title: Characterising the Role of Proteins Extracted from *Bacillus oleronius* in the Induction and Persistence of the Inflammation in Ocular Rosacea. 6th June, 2014. BioAt Annual Research Day Year 3 at Dublin City University (DCU).

Frederick W. McMahon, Clair Gallagher, Niamh O'Reilly, Martin Clynes, Finbarr O'Sullivan, and Kevin Kavanagh. Title: Analysis of the role of *Bacillus oleronius* proteins in the induction of tissue damage and persistent inflammation in Ocular rosacea.11th September, 2014, Charles Darwin House in London, United Kingdom (UK). Society of General Microbiology's Annual General Meeting: Sir Howard Dalton Young Microbiologist of the Year Award (*Semi-finalist*).

Fred McMahon, Clair Gallagher, Niamh O'Reilly, Martin Clynes, Finbarr O'Sullivan, and Kevin Kavanagh. Title: Analysis of the role of *Bacillus oleronius* proteins in the induction of tissue damage and inflammation in Ocular rosacea. 23rd March, 2015, American Academy of Dermatology Annual General Meeting in San Francisco, USA.

Fred McMahon. Title: Characterisation of the role of *Bacillus oleronius* in the disease ocular rosacea. 13th May, 2015, Maynooth University Post-Graduate Research Colloquium Awards (*finalist*).

Poster Presentations:

Fred McMahon, Clair Gallagher, Niamh O'Reilly, Martin Clynes, Finbarr O'Sullivan, and Kevin Kavanagh. Title: Investigation of the Effect of *Bacillus oleronius* Antigens on the Growth of Corneal Epithelium and Ocular Rosacea. 21st, March 2013, Society for General Microbiology Irish Branch Spring Meeting at University College of Dublin (UCD).

Fred McMahon, Clair Gallagher, Niamh O'Reilly, Martin Clynes, Finbarr O'Sullivan, and Kevin Kavanagh. Title: An Investigation of the effect of *Bacillus oleronius* antigens on the Growth of Corneal Epithelial Cells: Implications for Ocular Rosacea. 12th June, 2013, BioAT Annual Research Day Year 2 at NUI Maynooth.

Frederick McMahon and Kevin Kavanagh. Title: An Investigation of the effect of *Bacillus oleronius* antigens on the Growth of Corneal Epithelial Cells: Implications for Ocular Rosacea. 12th September, 2014, NUI Maynooth Biology Department Annual Research Day.

Fred McMahon, Clair Gallagher, Niamh O'Reilly, Martin Clynes, Finbarr O'Sullivan, and Kevin Kavanagh. Title: Analysis of the role of *Bacillus oleronius* proteins in the induction of tissue damage and inflammation in Ocular rosacea. 23rd March, 2015, American Academy of Dermatology Annual General Meeting in San Francisco, USA.

Fred McMahon and Kevin Kavanagh. Title: Generation of the second messenger, inositol 1,4,5-triphosphate (IP_3) by *Demodex*-associated *Bacillus* proteins and it's effect on the activation of neutrophils. 12th June, 2015, NUI Maynooth Biology Department Annual Research Day.

Fred McMahon, Nessa Banville, David A. Bergin, Christian Smedman, Staffan Paulie, Emer Reeves, and Kevin Kavanagh. Title: *Demodex*-associated *Bacillus* proteins generate the second messenger, inositol 1, 4, 5-triphosphate (IP_3) and it's effect on the activation of neutrophils. 17th July, 2015, BioAT Annual Research Day Year 4 at Institute of Technology Tallaght (ITT).

List of Conferences Attended:

Society for General Microbiology Irish Branch Spring Meeting. 21st March, 2013, University College of Dublin (UCD) (Poster Presentation).

New Frontiers in Ophthalmology: Corneal stem cell and Tissue Engineering Symposium. 27th June, 2013, Royal Victoria Eye and Ear Hospital (RVEEH).

Society of General Microbiology Irish Division Autumn Meeting entitled "Gut Microbes – Friend, or Foe?". 29th August, 2013, Ulster University at Coleraine (Oral Presentation). *Won 1st prize for PhD Student Oral Presentation*.

Society of General Microbiology's Annual General Meeting: Sir Howard Dalton Young Microbiologist of the Year Award. 11th September, 2014. Charles Darwin House in London, United Kingdom (UK) (Oral Presentation). *Finalist*.

From Cells to Tissues: Stem Cells, Tissue Repair and Tissue Engineering for Diabetes, Eye Disease and Neurodegenerative Diseases. 16th September, 2014, Dublin City University (DCU).

American Academy of Dermatolgy Annual General Meeting. 23rd March, 2015, Moscone Conference Center in San Francisco, USA (Oral and Poster Presentations).

Acknowledgments

First and foremost, I would like to say my sincerest thanks and gratitude to my supervisor Dr Kevin Kavanagh for all his patience, support and guidance over the course of my PhD thesis. Your enthusiasm to always get through the difficult times is admirable. You are the conductor of the Medical Mycology lab, and now my time has come to depart the station. I would also like to thank my project co-supervisors Dr Finbarr O'Sullivan and Dr Emer Reeves for all your help and support for this thesis. I would also like to say thank you to Dr James Carolan for his assistence with proteomics and use of the Q Exactive™ mass spectrometer.

I would also like to acknowledge the BioAnalysis and Therapeutics (BioAT) programme funded by the Higher Education Authority of Ireland through PRTLI V.

I must also pay many thanks to my fellow Medical Mycologist new and old, Niall, Carla, Louise, Ronan, Ahmed, and Amie, for making the lab an enjoyable place even during the difficult times when science was nothing but a "cruel mistress". And a mention goes to Ger Bear. Many enjoyable tea and coffee breaks were had!

Many thanks to Mr fifty-euro himself, aka Eoin, for all the laughs over the years. We had many tea breaks, and many that were often re-scheduled. Many thanks to Lorraine for all the terrifying inspirational talks. They really helped keep me focused. I want say thanks to everyone in the Biotech and Yeast Genetics labs (Gráinne, Rebecca, Lara, Stephen, Kevin, Elizabeth, Daragh) for always letting me "borrow" reagents, and of course for all the good chats.

I want to pay a special thanks to all the people I have had the opportunity to meet during my PhD, Dr Staffan Paulie and Dr Christian Smedman from my time in Sweden with Mabtech, Dr Clair Gallagher, Dr Erica Hennessy, and Dr Sandra Roche of the NICB in DCU, and to all the admin staff and prep lab staff of the department who were always on hand to help out in any way they possibly could.

I want to say thank you to all my family, Robert, Patrick, and Margaret, William, and Arthur, and to my good friend Dollar$! You were there to listen to all my thesis woes, and we've had many a good laugh.

I want to say a special thanks to my girlfriend Sinéad. If I had known that all I had to do was cycle to Galway and back to meet you then I would have done it sooner. You have been a constant even when times are tough, and your love and support have been invaluable. To our many good times to come!

To my parents, I have not got enough words to say thanks. You have given me the opportunity and support, and have made the sacrifices for me to be in the position that I am now. I can never repay what you have given me. Thank you so much. To my Mam and Dad, I dedicate this thesis.

List of Abbreviations

-ive	Negative
mgf	Mascot Generic File
$[Ca^{2+}]_c$	Cystolic Calcium
+ive	Positive
1-D SDS–PAGE	One-Dimensional Sodium Dodecyl Sulfate Polyacrylamide Gel Electrophoresis
2-D SDS–PAGE	Two-Dimensional Sodium Dodecyl Sulfate Polyacrylamide Gel Electrophoresis
2X YT broth	2X Yeast Tryptone Broth
ABC	ATP Binding Cassette
AID	Advanced Imaging Devices GmbH
ÄKTA FPLC™	ÄKTA Fast Protein Liquid Chromatography™
ALP	Alkaline Phosphatase
ANOVA	Analaysis of Variance
ApoE	Apolipoprotein E
APS	Ammoniun Persulfate
ATP	Adenosine Triphosphate
ATPase	Adenosine 5'-Triphosphatase
AV	Acne Vulgaris Patient
BCIP/NBT	5-Bromo-4-chloro-3-Indolyl-Phosphate/Nitro Blue Tetrazolium
BLAST	Basic Local Alignment Search Tool
BSA	Bovine Serum Albumin
C	Control Subjects
C1 (C1-C2)	Crude *B. oleronius* Protein Preparation 1/2
cADPr	Cyclic Adenosine Diphosphate Ribose
CCL20	Chemokine (C- C Motif) Ligand-20
CDK	Cyclin Dependent Kinase
CHAPS	3-[(3-Cholamidopropyl)Dimethylammonio]-1-Propanesulfonate
CLRs	C-Type Lectin Receptors
Ct	Cycle Threshold
DAB	3, 3'-Diaminobenzidine

DAMPs	Danger-Associated Molecular Patterns
DMEM	Dulbecco's Modified Eagle Medium
DMSO	Dimethyl Sulfoxide
DTT	Dithiothreitol
E1A	Adenovirus Early Region 1A
EC	Endothelial Cell
EDTA	Ethylenediaminetetraacetic Acid
EdU	5-Ethynyl-2'-Deoxyuridine
ELISA	Enzyme-Linked Immunosorbent Assay
ER	Endoplasmic Reticulum
ESI	Electrospray Ionization
F-actin	Filamentous-Actin
F1 (F1-F81)	Eluted *B. oleronius* Protein Fractions 1-81
FACS	Fluorescence-Activated Cell Sorting
FCS	Fetal Calf Serum
FDA	Food and Drug Administration
FDR	False Discovery Rate
FITC	Fluorescein Isothiocyanate
FLICA	Fluorescent-Labeled Inhibitor of Caspases
fMLF	N-Formyl-L-Methionyl-Leucyl-Phenylalanine
fMLP	N-Formyl-L-Methionyl-Leucyl-Phenylalanine
FTICR	Fourier Transform Ion Cyclotron Resonance
g	Force of Gravity
G-actin	Globular-Actin
G_1	Gap-1 Phase of Cell Cycle
G_2	Gap-2 Phase of Cell Cycle
GAPDH	Glyceraldehyde 3-Phosphate Dehydrogenase
GM-CSF	Granulocyte-Macrophage Colony-Stimulating Factor
GO	Gene Ontology
GPCR	G-Protein Coupled Receptor
HEPES	4-(2-Hydroxyethyl)-1-Piperazineethanesulfonic Acid
HLA	Human Leukocyte Antigen
HPLC	High Performance Liquid Chromatography
HPV16-E6/E7	Human Papillomavirus-16-E6/E7

HRP	Horseradish Peroxidase
Hsp	Heat Shock Protein
hTCEpi	Human Telomerase-Immortalized Corneal Epithelial Cell Line
hTERT	Human Telomerase Reverse Transcriptase
IAA	Indole-3-Acetic Acid
ICAM	Intercellular Adhesion Molecule
ICE	Interleukin-1-Beta Converting Enzyme
IEF	Isoelectric Focusing
IL	Interleukin
IL-12p40	Interleukin-12 Subunit 40 kDa
IL-12p70	Interleukin-12 Subunit 70 kDa
IL-12Rβ1	Interleukin-12 Receptor-Beta-1
IL-23R	Interleukin-23 Receptor
INF	Interferon
IP_1	D-*myo*-Inositol 1-Phosphate
IP_3	Inositol 1, 4, 5-Phosphate
IPG	Immobilized pH Gradient
IPL	Intense Pulsed Light
iTRAQ	Isobaric Tags for Relative and Absolute Quantitation
KEGG	Kyoto Encyclopedia of Genes and Genomes
KGM	Keratinocyte Growth Medium
KLK-5	Kallikrein-5
LC/MS	Liquid Chromatography Mass Spectrometry
LESCD	Limbal Epithelial Stem Cell Deficiency
LESCs	Limbal Epithelial Stem Cells
LF/MS	Label-Free Mass Spectrometry
LFQ	Label-Free Quantification
LIT	Linear Ion Trap
LL-37	Cathelicidin
LPS	Lipopolysaccharide
LRR	Leucine-Rich Repeat-Containing Receptors
m/*z*	Mass to Charge Ration
mA	Milliamp (Unit of Electric Current)
MALDI	Matrix Assisted Laser Desorption/Ionization

MGT	Mean Generation Time
MHC	Major Histocompatibility Complex
MIP-3α	Macrophage Inflammatory Protein-3-Alpha
miRNAs	Micro Ribonucleic Acids
MMPs	Matrix Metalloproteinases
MPO	Myeloperoxidase
MS/MS	Tandem Mass Spectrometry
MWCO	Molecular Weight Cut Off
NADPH	Nicotinamide Adenine Dinucleotide Phosphate
NCBI	National Center for Biotechnology Information
NE	Neutrophil Elastase
NF-κB	Nuclear Factor-Kappa-B
NK	Natural Killer T Cell
NLRs	Nucleotide-Binding Oligomerization Domain-Like Receptors
NOD	Nucleotide-Binding Oligomerization Domain
NRS	National Rosacea Society
P1 (P1-P8)	Pure *B. oleronius* Protein Fraction 1 (1-8)
PAMPs	Pathogen-Associated Molecular Patterns
PBMC	Peripheral Blood Mononuclear Cells
PBS	Phosphate Buffered Saline
PHA	Phytohaemagglutinin
PI	Propidium Iodide
PLC	Phospholipase C
Poly (A) RNA	Poyadenylation Ribonucleic Acid
PPAR-γ	Peroxisome Proliferator-Activated Receptor-Gamma
PRR	Pathogen Recognition Receptor
PTPs	Protein Tyrosine Phosphatases
PVDF	Polyvinylidene Fluoride
QIT	Quadropole Ion Trap
R	Eythematotelangiectatic Rosacea Patient
RCSI	Royal College of Surgeons in Ireland
RIG-1	Retinoic Acid-Inducible Gene-1
RLRs	RIG-like Receptors
ROS	Reactive Oxygen Species

RQ	Relative Quantification
S	Synthesis Phase of Cell Cycle
S100A7	S100 Calcium-Binding Protein A7
SA	Streptavidin Red
SBP	Substrate Binding Protein
SD	Seborrheic Dermatitis Patient
SDS	Sodium Dodecyl Sulfate
Seb. Dermatitis	Seborrheic Dermatitis Patient
SERCA	Sacroendoplasmic Reticulum Calcium Transport ATPase
SOCE	Store-Operated Ca^{2+} Entry
SSSB	Standardized Skin Surface Biopsy
SV40	Simian Virus 40
TBS	Tris-Buffered Saline
TEMED	Tetramethylethylenediamine
TFA	Trifluoroacetic Acid
Th	T Helper Cell
TLCK	Tosyl-L-Lysyl-Chloromethane Hydrochloride
TLR	Toll-like Receptor
TMB	3, 3', 5, 5'-Tetramethylbenzidine
TNF-α	Tumor Necrosis Factor-Alpha
TNFAIP3	Tumor Necrosis Factor-Alpha-Induced Protein 3
ToF	Time of Flight
UV	Ultraviolet
UVR	Ultraviolet Radiation
V	Volts (Unit of Electrical Potential (Voltage))
XTT	2, 3-Bis-(2-Methoxy-4-Nito-5-Sulfophenyl)-2H-Tetrazolium-5-Carboxanilide
α	Alpha
β	Beta
γ	Gamma

Table of Contents

Chapter 1: Introduction 1

1.0 Rosacea 2

1.1 Diagnosis of Rosacea 5

1.1.1 Primary Features 5

1.1.2 Secondary Features 5

1.2 Classification of Rosacea Subtypes 6

1.2.1 Subtype I: Erythematotelangiectatic Rosacea 6

1.2.2 Subtype II: Papulopustular Rosacea 9

1.2.3 Subtype III: Phymatous Rosacea 9

1.2.4 Subtype IV: Ocular Rosacea 10

1.2.5 Variants of Rosacea 11

1.3 The Role of *Demodex* Mites in the Skin 13

1.3.1 *Demodex* Mites and Rosacea 15

1.3.2 *Demodex* Mites and Blepharitis 17

1.3.3 *Demodex* Mites and Demodetic Mange 17

1.4 Potential Role of Bacteria in Rosacea 18

1.4.1 *Bacillus oleronius* 18

1.4.2 *Staphylococcus epidermidis* 20

1.4.3 *Helicobacter pylori* 22

1.4.4 *Chlamydophila pneumoniae* 22

1.5 Management and Treatment of Rosacea 15

1.6 Cornea: The Window of the Eye 25

1.6.1 Structure and Function of the Human Cornea 25

1.6.2 Human Telomerase-Immortalized Corneal Epithelial (hTCEpi) Cell Line Model 27

1.7 Neutrophils and the Innate Immune Response 29

1.7.1 Role of Neutrophils in Rosacea 29

1.8 Neutrophil Activation 30

1.9 Neutrophil Chemotaxis and Migration 30

1.10 Neutrophil Killing Mechanisms 31

1.10.1 Oxidative Killing Mechanism 31

1.10.2 Neutrophil Phagocytosis and the Process of Degranulation 32

1.11 Cytokines and the Adaptive Immune Response in Rosacea 35
1.12 Proteomics and Label-Free Mass Spectrometry (LF/MS) 39
1.13 Aims of Study 41

Chapter 2: Materials and Methods 42

2.0 Materials and Methods 43
2.1 Chemicals and Reagents 43
2.2 Sterilisation Procedure 43
2.3 Statistical Methods 43
2.4 Study Populations 43
2.4.1 Erythematotelangiectatic Rosacea Study 43
2.4.2 Ocular Rosacea Patients (Subtype IV Group) and Ocular Rosacea Patients with Erythematotelangiectatic Rosacea (Subtype I & IV Group) Study 44
2.4.3 *Demodex*-Related Blepharitis Study 45
2.5 Bacterial Cell Culture Media 45
2.5.1 Nutrient Agar Medium 45
2.5.2 Nutrient Broth Medium 45
2.5.3 2X Yeast Tryptone (YT) Broth Medium 46
2.6 Phosphate Buffered Saline (PBS) (pH 7.4) 46
2.7 Bacterial Cell Culture Conditions 46
2.8 Glycerol Stocks of *B. oleronius* Cultures 47
2.9 *Bacillus* Lysis Buffer (pH 7.2) 47
2.10 Enzymatic Activity of *B. oleronius* Under Varying Environmental Conditions 48
2.10.1 Analysis of Lipase Activity 48
2.10.2 Analysis of Catalase Activity 48
2.11 General Protein Methodology 49
2.11.1 Bradford Protein Assay 49
2.11.2 Acetone Precipitation of Protein Samples 49
2.11.3 5X Solubilisation Buffer for Protein Sample Loading 50
2.12 Protein Extraction Protocol 50
2.12.1 Protein Extraction from *B. oleronius* Cultures 50
2.12.2 Protein Extraction from hTCEpi Cell Cultures 52

2.13 Trypan Blue Cell Exclusion Assay for Cell Counting 52
2.14 1-D Sodium Dodecyl Sulphate-Polyacrylamide (SDS-PAGE)
Gel Electrophoresis 53
2.14.1 0.5 M Tris – HCl (pH 6.8) 53
2.14.2 1.5 M Tris – HCl (pH 8.9) 53
2.14.3 Sodium Dodecyl Sulphate (SDS) (10%, w/v) 53
2.14.4 Ammonium Persulphate (APS) (10%, w/v) 53
2.14.5 Sodium Dodecyl Sulphate-Polyacrylamide Gel Electrophoresis
(SDS-PAGE) 53
2.14.6 10X Electrode Buffer (pH 8.9) 54
2.14.7 1X Electrode Buffer (pH 8.9) 54
2.14.8 Casting and Electrophoresis of 1-D SDS-PAGE Gels 54
2.15 2-D SDS-PAGE Gel Electrophoresis 55
2.15.1 Isoelectric Focusing (IEF) Buffer 55
2.15.2 Isoelectric Focusing Equilibration Buffer (pH 6.8) 56
2.15.3 Casting of Large-2-D SDS-PAGE Gels 56
2.15.4 Agarose (1%, w/v) Sealing Solution 56
2.15.5 Isoelectric Focusing in the First Dimension 57
2.15.6 IPG Strip Equilibration and 2-D SDS-PAGE in the Second Dimension 58
2.15.7 Comparative Analysis of Differential Protein Expression 59
2.16 Staining of SDS-PAGE Gels 59
2.16.1 Coomassie Brilliant Blue Staining Protocol 59
2.16.2 Colloidal Coomassie Staining Protocol 60
2.17 In-Gel Trypsin Digestion and Liquid Chromatography - Mass
Spectrometry (LC/MS) 60
2.17.1 Preparation of Micro-Centrifuge Tubes and Pipette
Tips for Excision of Protein Bands and Spots for LC/MS 60
2.17.2 De-Staining Buffer 60
2.17.3 Trypsin Digestion Buffer 61
2.17.4 Peptide Extraction Buffer 61
2.17.5 Peptide Resuspension Buffer 61
2.17.6 Trypsin Digestion of Protein Bands and Spots from 1-D and 2-D SDS-
PAGE Gels for LC/MS Analysis 61
2.17.7 Bioinformatic Data Analysis of LC/MS Chromatograms 63

2.18 Label Free Mass Spectrometry (LF/MS) 63
2.18.1 Corneal Epithelial Cell (hTCEpi) Culture and Protein Extraction for LF/MS 63
2.18.2 In-Solution Trypsin Digestion of Protein Samples 64
2.18.3 Pierce® C-18 Spin Column Clean Up and Sample Preparation for LF/MS 65
2.18.4 LF/MS Protein Identification and Quantification 66
2.19 Western Blotting 67
2.19.1 Transfer Buffer (pH 8.3) 67
2.19.2 10X Tris-Buffered Saline (TBS) (pH 7.6) 67
2.19.3 1X TBS Tween®-20 (0.05%, v/v) (pH 7.6) 68
2.19.4 BSA (1%, w/v) Blocking Buffer 68
2.19.5 Western Blotting Protocol 68
2.19.6 Development of Nitocellulose Membrane Blot 69
2.20 Generation of *B. oleronius* Protein Preparations by Anion Exchange Separation using ÄKTA Fast Protein Liquid Chromatography™(ÄKTA FPLC™) and Q-Sepharose™ High Performance Beads 69
2.20.1 ÄKTA FPLC™ Binding Buffer (pH 4.8) 69
2.20.2 ÄKTA FPLC™ Elution Buffer (pH 4.8) 72
2.20.3 Protocol for the Preparation of *B. oleronius* Protein Extracts by Anion Exchange Separation using ÄKTA FPLC™ and Q-Sepharose™ High Performance Beads 72
2.21 Isolation of Peripheral Blood Mononuclear Cells (PBMC) 74
2.22 Isolation of Neutrophils from Fresh Blood 75
2.22.1 1X Saline Solution and 2X Saline Solution 75
2.22.2 Dextran (10%, w/v) 75
2.22.3 Sterile Distilled Water (dH_2O) 75
2.22.4 PBS Glucose (5 mM) 75
2.22.5 Neutrophil Separation from Fresh Blood Protocol 75
2.23 ELISpot Assay to Measure Secreted Cytokine Levels in Isolated Peripheral Blood Mononuclear Cells (PBMC) 76
2.24 FluoroSpot Assay to Measure Secreted Cytokine Levels in Isolated PBMC 78
2.25 Analysis of Endotoxin Activity in *B. oleronius* Protein Preparation by ELISpot 79
2.26 Quantification of D-myo-Inositol 1 Phosphate (IP_1) Levels in Stimulated

Human Neutrophils by *B. oleronius* Proteins 83
2.27 Intracellular Calcium (Ca^{2+}) Flux by Human Neutrophils Exposed to *B. oleronius* Proteins 83
2.28 Analysis of Cytoskeletal Reassembly and Filamentous (F)-Actin Polymerisation Following Exposure of Human Neutrophils to *B. oleronius* Proteins 84
2.28.1 Quantification of G- and F-Actin Distribution Ratios in Stimulated Human Neutrophils 85
2.29 Neutrophil Chemotaxis Induction by *B. oleronius* Proteins 85
2.29.1 Chemotaxis Assay Protocol 85
2.29.2 Fixing and Staining of Cells 85
2.29.3 Counting of Migrated Cells 86
2.30 General Cell Culture Methodolgy 86
2.30.1 Corneal Epithelial (hTCEpi) Cell Culture and Sub-Culture 86
2.30.2 Cryopreservation of hTCEpi Cells in Liquid Nitrogen (N_2) 88
2.30.3 Recovery of hTCEpi Cells from Liquid N_2 88
2.31 The Effect of *B. oleronius* Proteins on the Growth of Corneal Epithelial Cell and Assessment of Cytotoxicity 89
2.31.1 Corneal Cell Cytotoxicity Assay Assessed by XTT Staining 89
2.31.2 Corneal Cell Cytotoxicity Assay Assessed by Crystal Violet (0.25%, w/v) Staining 89
2.32 Corneal Epithelial Cell Proliferation Assay 90
2.33 Cell Cycle Analysis by Fluorescence-Activated Cell Sorting (FACS) 90
2.33.1 Assessment of 5-Ethynyl-2'-Deoxyuridine (EdU) Incorporation on the Growth of Corneal Epithelial Cells by Staining 90
2.33.2 Cell Cycle Analysis by Propidium Iodide Staining and FACS 91
2.34 Caspase-3 and Caspase-7 Immunofluorescence Assay 91
2.35 RNA Extraction of Treated hTCEpi Cells and Gene Expression Analysis 92
2.36 Gelatinase Zymograms to Investigate Matrix Metalloproteinase (MMP) Activity 93
2.37 Enzyme-Linked Immunosorbent Assay (ELISA) to Measure Secreted Cytokine Expression Levels 93
2.37.1 Preparation of Sample to Detect Secreted Cytokine Expression Levels in Patient Serum 93

2.37.2 Preparation of Sample to Detect Secreted Cytokine Expression Levels in hTCEpi Cells Exposed to *B. oleronius* Proteins 94
2.37.3 Preparation of Sample to Detect Secreted Cytokine Expression Levels in Isolated Neutrophil Cells Exposed to *B. oleronius* Proteins 94
2.37.4 ELISA Protocol to Detect Secreted Cytokine and Expression Levels 95
2.38 Standardized Skin Surface Biopsy (SSSB) to Quantify *Demodex* Mite Population 96
2.39 Sebumetric Test to Quantify Abundance of Sebum 96

Chapter 3: An Analysis of the Effect of Culture Conditions on the Proteomic Profile of *Bacillus oleronius* 101

3.0 Introduction 102
3.1 Investigating the Expression of the Immuno-Reactive 62 kDa Protein by *B. oleronius* Under Varying Environmental Conditions 103
3.2 Summary 116
3.3 Proteomic Analysis of *B. oleronius* Grown Under Varying Environmental Conditions 117
3.4 A 2-D SDS-PAGE Investigation of the Expression of the 62 kDa Protein in *B. oleronius* Grown Under Different Environmental Conditions 130
3.5 Analysis of Lipase and Catalase Activity in *B. oleronius* Cultures 136
3.5.1 Lipase Activity in *B. oleronius* Cultures 136
3.5.2 Catalase Activity in *B. oleronius* Cultures 137
3.6 Discussion 141

Chapter 4: An Analysis of the Response of Corneal Epithelial (hTCEpi) Cells to *Bacillus oleronius* Proteins 146

4.0 Introduction 147
4.1 Generation of Crude and Pure *B. oleronius* Protein Preparations 148
4.1.1 Preparation of Crude *B. oleronius* Protein Preparation 148
4.1.2 Preparation of Pure *B. oleronius* Protein Preparation by ÄKTA FPLC™ and Q-Sepharose™ High Performance Beads 148
4.1.3 Summary 152

4.2 Effect of *B. oleronius* Protein on hTCEpi Cell Growth 155
4.3 Effect of *B. oleronius* Protein on hTCEpi Cell Proliferation 155
4.4 Exposure to *B. oleronius* Protein does not Induce Apoptosis in hTCEpi Cells 156
4.5 Effect of *B. oleronius* Protein Exposure on hTCEpi Cell Cycle Progression 156
4.6 Alterations of hTCEpi Gene Expression Induced by *B. oleronius* Protein Exposure 160
4.7 Effect of *B. oleronius* Proteins on Expression of the Defensins, CCL20 and S100A7, in hTCEpi Cells 161
4.8 Cytokine Production in hTCEpi Cells Following Exposure to *B. oleronius* Protein 162
4.9 Effect of *B. oleronius* Protein on Expression of MMP-9 in hTCEpi Cells 169
4.10 Exposure of hTCEpi Cells to *B. oleronius* Proteins Induces Increased MMP-9 Activity and MMP-2 Activity 169
4.11 Summary 170
4.12 Discussion 177

Chapter 5: An Investigation of the Proteomic Response of Corneal Epithelial (hTCEpi) Cells to *Bacillus oleronius* Proteins 182

5.0 Introduction 183
5.1 An Analysis of the Secretome and Proteome of hTCEpi Cells Following Exposure to *B. oleronius* Protein 184
5.1.1 Secretome of hTCEpi Cells Following Exposure to *B. oleronius* Protein Preparations 184
5.1.2 Proteomic Analysis of hTCEpi Cells Following Exposure to *B. oleronius* Protein Preparation 189
5.1.3 Summary 192
5.2 An Investigation of the hTCEpi Cell Proteome Following Exposure to *B. oleronius* Protein 197
5.2.1 An Analysis of the hTCEpi Cell Proteome Following Exposure to *B. oleronius* Protein 197
5.2.2 Summary 199

5.3 An In-Solution Digest Study Investigating the Proteome of hTCEpi Cells Following Exposure to *B. oleronius* Protein by Label Free Mass Spectrometry 204
5.3.1 An Analysis of the hTCEpi Cell Proteome at 24 Hour Following Exposure to Crude *B. oleronius* Protein 204
5.3.2 An Analysis of the hTCEpi Cell Proteome at 72 Hour Following Exposure to Pure *B. oleronius* Protein 217
5.3.3 Summary 222
5.4 Discussion 233

Chapter 6: An Investigation of the Effect of *Bacillus oleronius* Proteins on Isolated Neutrophils and PBMC 237

6.0 Introduction 238
6.1 Assessment of Endotoxin Activity in *B. oleronius* Protein Preparations by TNF-α ELISpot Assays 239
6.2 Exposure of Neutrophils to *B. oleronius* Protein Leads to Increased D-*myo*-Inositol 1-Phosphate (IP_1) Levels 240
6.3 Calcium (Ca^{2+}) Efflux in Neutrophils Exposed to *B. oleronius* Protein 240
6.4 Cytoskeletal Reassembly in Neutrophils Induced by *B. oleronius* Protein 244
6.5 Induction of Neutrophil Chemotaxis in Response to *B. oleronius* Protein 249
6.6 Exposure of Neutrophils to *B. oleronius* Proteins Leads to Elevated IL-1β and IL-6 Secretion 249
6.7 Summary 250
6.8 Investigating the Cytokine Response of Isolated PBMC Following Exposure to *B. oleronius* Protein by FluoroSpot 253
6.9 Investigating the Cytokine of Isolated PBMC Response Following Exposure to *B. oleronius* Protein by ELISpot and FluroSpot 258
6.10 Discussion 266

Chapter 7: An Analysis of the Role of *Bacillus oleronius* Proteins in Erythematotelangiectatic Rosacea, Ocular Rosacea, and *Demodex*-Related Blepharitis.....275

7.0 Introduction.....276

7.1 Investigating the Role of *B. oleronius* in Erythematotelangiectatic Rosacea.....277

7.1.1 Reactivity of Patient Sera to *B. oleronius* Protein.....277

7.1.2 Analysis of Severity of Skin Lesions in Rosacea Patients.....278

7.1.3 Analysis of *Demodex* Mite Population in Study Participants.....278

7.1.4 *B. oleronius* Protein Reactive Rosacea Patients Display Reduced Levels of Sebum in Their Skin.....278

7.1.5 Investigating Cytokine Secretion Levels in Study Participants.....285

7.1.6 Summary.....285

7.2 Analysis of *B. oleronius* Proteins in the Induction of Ocular Rosacea.....289

7.2.1 Assessement of Reactivity to *B. oleronius* Immuno-Reactive 62 kDa and 83 kDa Protein.....289

7.2.2 Investigation of the T Cell Cytokine Response Following Exposure to *B. oleronius* Protein.....290

7.2.3 Summary.....292

7.3 An Assessment of the Role of *B. oleronius* Proteins in *Demodex*-Related Blepharitis.....302

7.3.1 Reactivity of Patient Sera to *B. oleronius* Protein.....302

7.3.2 Summary.....304

7.4 Discussion.....310

Chapter 8: General Discussion.....317

8.0 General Discussion.....318

Chapter 9: Bibliography.....328

Appendix.....386

List of Figures

Chapter 1 1

Figure 1.1 The central T-zone region of the face primarily affected in rosacea 3

Figure 1.2 Subtypes of Rosacea and Characteristics 12

Figure 1.3 Features of ocular rosacea 13

Figure 1.4 An electron micrograph of a *Demodex folliculorum* mite 16

Figure 1.5 Proposed role of *Demodex* mites and the role of *B. oleronius* for the induction of rosacea 21

Figure 1.6 The structure of the human cornea 28

Figure 1.7 Mode of action of neutrophil killing mechanisms 34

Figure 1.8 Toll-like receptor (TLR) signaling pathways 38

Chapter 2 42

Figure 2.1 A representative standard curve of BSA protein for Bradford assay 51

Figure 2.2 A schematic diagram of the orientation of the 'Western blot sandwich' 71

Figure 2.3 A representative standard curve for IP_1 ELISA 87

Figure 2.4 A representative standard curve for TNF-α ELISA 98

Figure 2.5 A representative standard curve for IL-17 ELISA 98

Figure 2.6 A representative standard curve for IL-8 ELISA 99

Figure 2.7 A representative standard curve for IL-6 ELISA 99

Figure 2.8 A representative standard curve for IL-1β ELISA 100

Chapter 3 101

Figure 3.1 A representative growth curve of *B. oleronius* in nutrient broth 105

Figure 3.2 Analysis of the effect of environmental conditions on the expression of *B. oleronius* proteins in nutrient broth (pH 6), by 1-D SDS-PAGE and immunoblot of 62 kDa protein expression 106

Figure 3.3 Analysis of the effect of environmental conditions on the expression of *B. oleronius* proteins in 2X YT broth (pH 6), by 1-D SDS-PAGE and immunoblot of 62 kDa protein expression 107

Figure 3.4 Analysis of the effect of environmental conditions on the expression of *B. oleronius* proteins in nutrient broth (pH 7), by 1-D SDS-PAGE and immunoblot of 62 kDa protein expression 108
Figure 3.5 Analysis of the effect of environmental conditions on the expression of *B. oleronius* proteins in 2X YT broth (pH 7), by 1-D SDS-PAGE and immunoblot of 62 kDa protein expression 109
Figure 3.6 Analysis of the effect of environmental conditions on the expression of *B. oleronius* proteins in nutrient broth (pH 8), by 1-D SDS-PAGE and immunoblot of 62 kDa protein expression 110
Figure 3.7 Analysis of the effect of environmental conditions on the expression of *B. oleronius* proteins in 2X YT broth (pH 8), by 1-D SDS-PAGE and immunoblot of 62 kDa protein expression 111
Figure 3.8 Assessment of the effect of environmental conditions on the expression of the 62 kDa protein in *B. oleronius* cultures in nutrient broth at 30°C 112
Figure 3.9 Assessment of the effect of environmental conditions on the expression of the 62 kDa protein in *B. oleronius* cultures in nutrient broth at 37°C 113
Figure 3.10 Assessment of the effect of environmental conditions on the expression of the 62 kDa protein in *B. oleronius* cultures in 2X YT broth at 30°C..... 114
Figure 3.11 Assessment of the effect of environmental conditions on the expression of the 62 kDa protein in *B. oleronius* cultures in 2X YT broth at 37°C..... 115
Figure 3.12 Master gel of excised 1-D SDS-PAGE *B. oleronius* protein bands for protein identification by LC/MS..... 120
Figure 3.13 Abundance of molecular chaperone GroEL (Band No. 1) in the *B. oleronius* cultures grown under different environmental conditions..... 123
Figure 3.14 Abundance of thioredoxin (Band No. 4) in the *B. oleronius* cultures grown under different environmental conditions..... 124
Figure 3.15 Abundance of peroxidase (Band No. 15) in the *B. oleronius* cultures grown under different environmental conditions..... 125

Figure 3.16 Abundance of superoxide dismutase (Band No. 21) in the *B. oleronius* cultures grown under different environmental conditions 126
Figure 3.17 Abundance of Clp Protease ClpX (Band No. 13) in the *B. oleronius* cultures grown under different environmental conditions 127
Figure 3.18 Abundance of flagellin (Band No. 24) in the *B. oleronius* cultures grown under different environmental conditions 128
Figure 3.19 Abundance of C4-dicarboxylate ABC transporter substrate-binding protein (Band No. 25) in the *B. oleronius* cultures grown under different environmental conditions 129
Figure 3.20 Analysis of the effect of environmental conditions on the expression of *B. oleronius* proteins in nutrient broth (pH 6) at 30°C by 2-D SDS-PAGE and immunoblot of 62 kDa protein expression 131
Figure 3.21 Analysis of the effect of environmental conditions on the expression of *B. oleronius* proteins in nutrient broth (pH 6) at 37°C by 2-D SDS-PAGE and immunoblot of 62 kDa protein expression 132
Figure 3.22 Analysis of the effect of environmental conditions on the expression of *B. oleronius* proteins in 2X YT broth (pH 6) at 30°C by 2-D SDS-PAGE and immunoblot of 62 kDa protein expression 133
Figure 3.23 Analysis of the effect of environmental conditions on the expression of *B. oleronius* proteins in 2X YT broth (pH 6) at 37°C by 2-D SDS-PAGE and immunoblot of 62 kDa protein expression 134
Figure 3.24 The effect of temperature on the expression of the 62 kDa protein in *B. oleronius* cultures resolved by 2-D SDS-PAGE and immunoblotted 135
Figure 3.25 Analysis of lipase activity in the secretome of *B. oleronius* cultures grown under different environmental conditions 138
Figure 3.26 Analysis of lipase activity in the proteome of *B. oleronius* cultures grown under different environmental conditions 139
Figure 3.27 Analysis of catalase activity in *B. oleronius* cultures grown under different environmental conditions 140

Chapter 4 146

Figure 4.1 Crude *B. oleronius* protein preparations demonstrating reactivity to 62 kDa protein 149

Figure 4.2 A representative ÄKTA FPLC™ chromatogram of the fractionation of crude *B. oleronius* protein 150

Figure 4.3 Visualization of *B. oleronius* protein ÄKTA FPLC™ fractions 19 to 36 by Coomassie Staining and Western blotting 153

Figure 4.4 Visualization of ÄKTA FPLC™ generated pure *B. oleronius* protein preparation fractions 1 to 8 by Coomassie Staining and Western blotting 154

Figure 4.5 Effect of *B. oleronius* proteins on hTCEpi cell growth by XTT staining and crystal violet staining 157

Figure 4.6 Exposure of pure *B. oleronius* proteins reduce the rate of cell proliferation of corneal epithelial (hTCEpi) cells 158

Figure 4.7 Non-induction of apoptosis in hTCEpi cells exposed to pure *B. oleronius* proteins 159

Figure 4.8 Effect of EdU exposure on hTCEpi cell growth 163

Figure 4.9 Effect of pure *B. oleronius* protein on hTCEpi cell cycle progression 164

Figure 4.10 Effect of pure *B. oleronius* protein exposure on wound associated gene expression in hTCEpi cells assessed by qRT-PCR 165

Figure 4.11 Expression of CCL20 by hTCEpi cells exposed to pure *B. oleronius* proteins 166

Figure 4.12 Expression of S100A7 by hTCEpi cells exposed to pure *B. oleronius* proteins 167

Figure 4.13 Secretion of IL-6 and IL-8 by hTCEpi cells exposed to *B. oleronius* proteins by ELISA 168

Figure 4.14 Expression of MMP-9 by hTCEpi cells exposed to pure *B. oleronius* proteins 171

Figure 4.15 A representative 1-D gelatinase zymogram (10% w/v) gel image to assess MMP-9 and MMP-2 activity present in hTCEpi cell supernatants following exposure to pure *B. oleronius* proteins 172

Figure 4.16 Fold change of MMP-9 activity in hTCEpi cells exposed to pure *B. oleronius* proteins 173

Figure 4.17 Relative densitometric values of MMP-9 activity from gelatinase (10%, w/v) zymogram gels 174
Figure 4.18 Fold change of MMP-2 activity in hTCEpi cells exposed to pure *B. oleronius* proteins 175
Figure 4.19 Relative densitometric values of MMP-2 activity from gelatinase (10%, w/v) zymogram gels 176

Chapter 5 182

Figure 5.1 Secretome of hTCEpi cells exposed to *B. oleronius* proteins for 24 hour and 72 hour, and resolved by 1-D SDS-PAGE 186
Figure 5.2 Master gel of excised 1-D SDS-PAGE hTCEpi secretome protein bands for protein identification by LC/MS following a 24 hour and a 72 hour exposure to *B. oleronius* proteins 187
Figure 5.3 Proteome of hTCEpi cells exposed to *B. oleronius* proteins for 24 hour and 72 hour, and resolved by 1-D SDS-PAGE 193
Figure 5.4 Master gel of excised 1-D SDS-PAGE hTCEpi proteome protein bands for protein identification by LC/MS following a 24 hour and a 72 hour exposure to *B. oleronius* proteins 194
Figure 5.5 Proteome of hTCEpi cells exposed to *B. oleronius* proteins for 72 hour, and resolved by 2-D SDS-PAGE 200
Figure 5.6 Master gel of excised 2-D SDS-PAGE hTCEpi proteome protein spots for protein identification by LC/MS following a 72 hour exposure to *B. oleronius* proteins 201
Figure 5.7 A Venn diagram illustrating exclusive proteins identified by LF/MS from hTCEpi cells untreated and treated with crude *B. oleronius* protein (6 μg/ml) following a 24 hour exposure 208
Figure 5.8 A volcano plot demonstrating the fold change of hTCEpi proteins identified by LF/MS following a 24 hour exposure to crude *B. oleronius* protein (6 μg/ml) relative to untreated hTCEpi cells 211
Figure 5.9 String network analysis of proteins increased in abundance following a 24 hour exposure of hTCEpi cells to crude *B. oleronius* protein (6 μg/ml) 213
Figure 5.10 String network analysis of proteins decreased in abundance following a

24 hour exposure of hTCEpi cells treated with crude *B. oleronius* protein (6 µg/ml) 216
Figure 5.11 A Venn diagram illustrating exclusive proteins identified by LF/MS from hTCEpi cells untreated and treated with pure *B. oleronius* protein (6 µg/ml) following a 72 hour exposure 223
Figure 5.12 A volcano plot demonstrating the fold change of hTCEpi proteins identified by LF/MS following a 72 hour exposure to crude *B. oleronius* protein (6 µg/ml) relative to untreated hTCEpi cells 226
Figure 5.13 String network analysis of proteins increased in abundance following a 72 hour exposure of hTCEpi cells to pure *B. oleronius* protein (6 µg/ml) 229
Figure 5.14 String network analysis of proteins decreased in abundance following a 72 hour exposure of hTCEpi cells treated with pure *B. oleronius* protein (6 µg/ml) 232

Chapter 6 237

Figure 6.1 Assessment of endotoxin activity and TNF-α secretion in PBMC exposed to LPS by ELISpot 241
Figure 6.2 Assessment of endotoxin activity and TNF-α secretion in PBMC exposed to pure *B. oleronius* protein by ELISpot 242
Figure 6.3 Assessment of endotoxin activity and TNF-α secretion in PBMC exposed to crude *B. oleronius* protein by ELISpot 243
Figure 6.4 Generation of IP_1 by neutrophils exposed to *B. oleronius* proteins 245
Figure 6.5 Release of stored Ca^{2+} by neutrophils exposed to *B. oleronius* proteins 246
Figure 6.6 Cytoskeletal reassembly of neutrophils exposed to *B. oleronius* proteins 247
Figure 6.7 Effect of *B. oleronius* proteins on neutrophil chemotaxis 248
Figure 6.8 Secretion of IL-1β by neutrophils exposed to *B. oleronius* proteins 251
Figure 6.9 Secretion of IL-6 by neutrophils exposed to *B. oleronius* proteins 252
Figure 6.10 Secretion of IL-6 and IL-1β in PBMC exposed to *B. oleronius* proteins by FluoroSpot 254
Figure 6.11 Secretion of IL-6 and TNF-α in PBMC exposed to *B. oleronius* proteins by FluoroSpot 254

Figure 6.12 Secretion of IL-6 and GM-CSF in PBMC exposed to *B. oleronius* proteins by FluoroSpot 255
Figure 6.13 Secretion of IL-6 and IL-10 in PBMC exposed to *B. oleronius* proteins by FluoroSpot 255
Figure 6.14 Secretion of IL-6 and IL-12p40 in PBMC exposed to *B. oleronius* proteins by FluoroSpot 256
Figure 6.15 Secretion of IL-6 and IL-23 in PBMC exposed to *B. oleronius* proteins by FluoroSpot 256
Figure 6.16 Secretion of IL-6 and ApoE in PBMC exposed to *B. oleronius* proteins by FluoroSpot 257
Figure 6.17 Secretion of IL-17A and IL-22 in PBMC exposed to *B. oleronius* proteins by FluoroSpot and ELISpot 260
Figure 6.18 Secretion of IL-17A and IL-31 in PBMC exposed to *B. oleronius* proteins by FluoroSpot and ELISpot 261
Figure 6.19 Secretion of IFN-γ and IL-5 in PBMC exposed to *B. oleronius* proteins by FluoroSpot and ELISpot 262
Figure 6.20 Secretion of IFN-γ and IL-22 in PBMC exposed to *B. oleronius* proteins by FluoroSpot and ELISpot 263
Figure 6.21 Secretion of IFN-γ and IL-31 in PBMC exposed to *B. oleronius* proteins by FluoroSpot and ELISpot 264
Figure 6.22 Secretion of IL-2 and IL-13 in PBMC exposed to *B. oleronius* proteins by ELISpot 265

Chapter 7 275

Figure 7.1 Representative Western blots of sera reactivity of participants in erythematotelangiectatic rosacea study to *B. oleronius* proteins 279
Figure 7.2 Distribution of sera reactivity of participants in erythematotelangiectatic rosacea study to *B. oleronius* protein 280
Figure 7.3 Severity of skin lesions amongst erythematotelangiectatic rosacea patients 282
Figure 7.4 Density of *Demodex* mites in participants of erythematotelangiectatic rosacea study 283

Figure 7.5 Quantity of sebum on the skin of participants in erythematotelangiectatic rosacea study 284
Figure 7.6 Secretion of IL-17 in participants of erythematotelangiectatic rosacea study 286
Figure 7.7 Secretion of TNF-α in participants of erythematotelangiectatic rosacea study 287
Figure 7.8 Secretion of IL-8 in participants of erythematotelangiectatic rosacea study 288
Figure 7.9 Western blots of sera reactivity of study participants to *B. oleronius* protein in ocular rosacea study 294
Figure 7.10 IL-13 secretion by PBMC from controls and patients exposed to *B. oleronius* proteins or anti-CD3 (positive control) in ocular rosacea study 296
Figure 7.11 IL-2 secretion by PBMC from controls and patients exposed to *B. oleronius* proteins in ocular rosacea study 297
Figure 7.12 IL-22 secretion by PBMC from controls and patients exposed to *B. oleronius* proteins in ocular rosacea study 298
Figure 7.13 IL-17A secretion by PBMC from controls and patients exposed to *B. oleronius* proteins in ocular rosacea study 299
Figure 7.14 IL-31 secretion by PBMC from controls and patients exposed to *B. oleronius* proteins in ocular rosacea study 300
Figure 7.15 IFN-γ secretion by PBMC from controls and patients exposed to *B. oleronius* proteins in ocular rosacea study 301
Figure 7.16 Sera reactivity of participants in *Demodex*-related blepharitis study to *B. oleronius* protein 305
Figure 7.17 Representative Western blots of serum reactivity of participants in *Demodex*-related blepharitis study to *B. oleronius* protein 306

List of Tables

Chapter 1 1

Table 1.1 Studies demonstrating the prevalence of rosacea in multiple countries 4

Table 1.2 Primary and secondary features of rosacea 7

Table 1.3 Rosacea subtypes and features 8

Chapter 2 42

Table 2.1 List of phosphatase inhibitors 47

Table 2.2 Reagent volumes for the preparation of 12.5% Bis-acrylamide SDS-PAGE mini-gels 54

Table 2.3 Isoelectric focusing programme used for 2-D SDS-PAGE 57

Table 2.4 A list of the primary antibodies, and the dilutions used for Western blotting 70

Table 2.5 A list of the secondary antibodies, and the dilutions used for Western blotting 70

Table 2.6 List of cytokines analysed by ELISpot 80

Table 2.7 List of cytokines analysed in isolated monocytes by FluoroSpot 81

Table 2.8 List of cytokines analysed in isolated T cells by FluoroSpot 82

Table 2.9 A list of cytokines analysed by ELISA 97

Chapter 3 101

Table 3.1 LC/MS protein band identities from 1-D SDS-PAGE *B. oleronius* cultures grown under varying environmental conditions 121

Table 3.2 Description of sample number and corresponding *B. oleronius* cultures grown under varying environmental conditions 122

Chapter 5 182

Table 5.1 LC/MS protein band identities from 1-D SDS-PAGE of the hTCEpi secretome following a 24 hour and a 72 hour exposure to *B. oleronius* proteins 188

Table 5.2 Fold change of protein band identities from 1-D SDS-PAGE of the hTCEpi secretome following a 24 hour and a 72 hour exposure to *B. oleronius* proteins 188
Table 5.3 LC/MS protein band identities from 1-D SDS-PAGE of the hTCEpi proteome following a 24 hour and a 72 hour exposure to *B. oleronius* proteins 195
Table 5.4 Fold change of protein band identities from 1-D SDS-PAGE of the hTCEpi proteome following a 24 hour and a 72 hour exposure to *B. oleronius* proteins 196
Table 5.5 LC/MS protein spots identities from 2-D SDS-PAGE of the hTCEpi proteome following a 72 hour exposure to *B. oleronius* proteins 202
Table 5.6 Fold change of LC/MS protein spots identities from 2-D SDS-PAGE of the hTCEpi proteome following a 72 hour exposure to *B. oleronius* proteins 203
Table 5.7 LF/MS protein identities exclusive to untreated hTCEpi cells following a 24 hour exposure 209
Table 5.8 LF/MS protein identities exclusive to hTCEpi cells treated with crude *B. oleronius* protein (6 μg/ml) following a 24 hour exposure 210
Table 5.9 LF/MS protein identities from hTCEpi cells exposed to crude *B. oleronius* protein (6 μg/ml) for 24 hour that were increased in abundance relative to untreated hTCEpi cells 212
Table 5.10 LF/MS protein identities from hTCEpi cells exposed to crude *B. oleronius* protein (6 μg/ml) for 24 hour that were decreased in abundance relative to untreated hTCEpi cells 214
Table 5.11 LF/MS protein identities exclusive to untreated hTCEpi cells following a 72 hour exposure 224
Table 5.12 LF/MS protein identities exclusive to hTCEpi cells treated with pure *B. oleronius* protein (6 μg/ml) following a 72 hour exposure 225
Table 5.13 LF/MS protein identities from hTCEpi cells exposed to pure *B. oleronius* protein (6 μg/ml) for 72 hour that were increased in abundance relative to untreated hTCEpi cells 227
Table 5.14 LF/MS protein identities from hTCEpi cells exposed to pure *B. oleronius* protein (6 μg/ml) for 72 hour that were decreased in abundance relative to untreated hTCEpi cells 230

Chapter 7 275

Table 7.1 Erythematotelangiectatic rosacea study population sera reactivity of participants to *B. oleronius* protein 281

Table 7.2 List of study participants in ocular rosacea study and serum reactivity to *B. oleronius* protein 293

Table 7.3 Ocular rosacea study population sera reactivity of participants to *B. oleronius* protein 295

Table 7.4 *Demodex*-related blepharitis study population sera reactivity of participants to *B. oleronius* protein 307

Table 7.5 Sera reactivity of blepharitis patients to *B. oleronius* protein in *Demodex*-related blepharitis study 308

Table 7.6 Sera reactivity of blepharitis patients with ocular Demodicosis infestation to *B. oleronius* protein in *Demodex*-related blepharitis study 308

Table 7.7 Sera reactivity of keratitis patients to *B. oleronius* protein in *Demodex*-related blepharitis study 309

Table 7.8 Sera reactivity of acne patients to *B. oleronius* protein in *Demodex*-related blepharitis study 309

Chapter 1

Introduction

1.0 Rosacea

Rosacea is a chronic inflammatory dermatosis of the central T-zone region of the face, and in some cases it can affect the skin on elbows, chest, shoulders and back. The condition may be characterized by flushing, non-transient erythema, papules, pustules, inflammatory nodules and telangiectasia, and individuals with rosacea can suffer from emotional stress and social stigma from the physical manifestations of the disease (Drummond and Su, 2012; Yamasaki and Gallo, 2009; Blout and Pelletier, 2002). The facial regions primarily affected by rosacea are shown in Figure 1.1.

The course of the disease usually appears in cycles of relapse and remission. Various factors such as vascular and immunological abnormalities, agents responsible for degradation of the structures of connective tissue, changes to the vascular network in the skin, and the presence of reactive oxygen species (ROS) within the skin are believed to play a role in the aetiology of rosacea and it's persistence (Steinhoff *et al*., 2011, 2013; Yamasaki and Gallo, 2009; Gupta and Chaudhry, 2005). A number of trigger factors have been identified by patients to exacerbate the symptoms associated with rosacea, in particular episodes of flushing and facial erythema (Kligman, 2004). These trigger factors include heat, alcohol, spicy foods, hot beverages, menstruation, medications, extreme hot or cold temperatures, and sunlight and ultra violet (UV) exposure (Kligman, 2004). However, these trigger factors are not believed to be involved in the pathogenesis of rosacea, and are considered associated symptoms of the condition.

According to the National Rosacea Society (NRS), rosacea is estimated to affect 16 million Americans, and is highly prevalent in individuals of northern European ancestry, with up to a third having a family history of the facial disease, often referred to as 'Curse of the Celts' (Yamasaki and Gallo, 2009; Del Rosso, 2006). A number of studies have recorded the prevalence of rosacea in Germany (2.2%), Sweden (10%), and Estonia (22%) (Abram *et al*., 2010; Schaefer *et al*., 2008; Berg and Lidén, 1989) (Table 1.1).

The onset of rosacea occurs from the ages of thirty-to-fifty, affecting all racial groups, and the condition affects women more commonly than men depending on the subtype of rosacea (Powell, 2005). Despite the high prevalence of rosacea, the disease remains under-diagnosed by clinicians due to the lack of understanding on the aetiology of rosacea, which has resulted in affected individuals having a range of clinical findings termed as 'rosacea'.

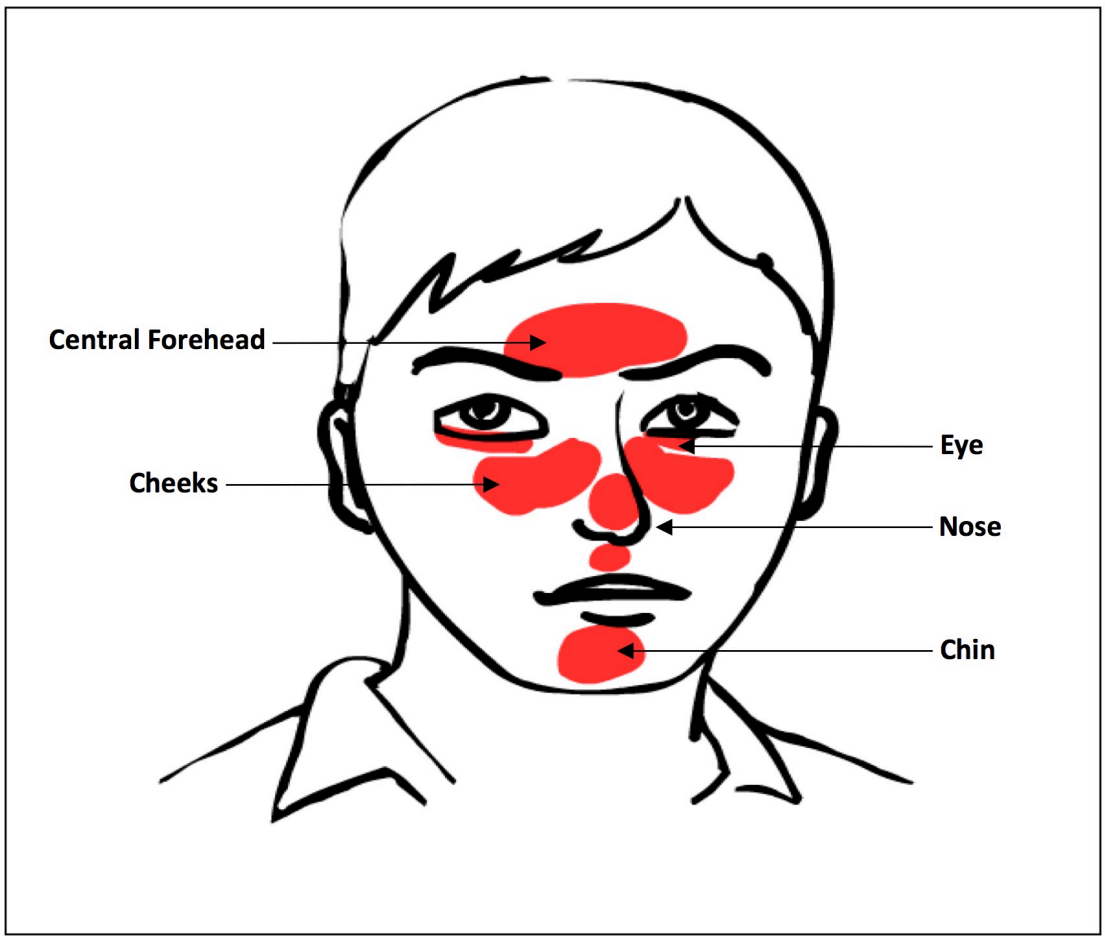

Figure 1.1 The central T-zone region of the face primarily affected in rosacea. [Adapted from the website *http://upload.wikimedia.org/wikipedia/commons/6/6e/Rasacee_couperose_zones.png*]

Table 1.1 Studies demonstrating the prevalence of rosacea in multiple countries. Table was adapted from McAleer *et al*. (2010).

Population	Country	Population Type	Prevalence	Reference
2341	Denmark (Faroe Islands)	Households	0.09%	Lomholt, 1964
809	Sweden	Office Workers	10%	Berg and Lidén, 1989
9290	USA	General Population	1.9%	Engel *et al*, 1988
402	USA	Database of Medical Records	2.1%	Bamford *et al*. 2006
50237	Greece	Database of Dermatology Outpatients	1.22%	Kyriakis *et al*. 2005
48665	Germany	Office Workers	2.2%	Schaefer *et al*. 2008
348	Estonia	General Population	22%	Abram *et al*. 2010

1.1 Diagnosis of Rosacea

Currently, the pathogenesis of rosacea remains unknown, and there is no serological or diagnostic *in vitro* assay available to successfully diagnose the disease. In 2004, a standard grading system for the diagnosis of rosacea was established by the NRS expert committee on the classification and staging of rosacea with the aim of assisting clincians in diagnosing and evaluating rosacea, and to also facilitate a clear line of comunication to a broad range of groups including researchers, dermatologists, patients, and the general public (Wilkin *et al*., 2004). The expert committee concluded that the symptoms associated with rosacea can be categorised into primary and/or secondary features based on the most common patterns or groupings of these for each subtype of rosacea (Table 1.2). The appearance of primary and seconday features can occur together and are taken into account in the assessment of the severity of the condition (Wilkin *et al*., 2004).

1.1.1 Primary Features

Primary features defined by the NRS expert committee include flushing (transient erythema), non-transient erythema (persistent redness on the surface of the facial skin), papules (red dome-shaped elevations of the skin) and pustules (elevations of skin containing fluid consisting of leukocytes), and telangiectasia (dilation of small blood vessels) (Table 1.2) (Wilkin *et al*., 2004). The presence of one or more of these features may be an indication for the diagnosis of rosacea and they have been demonstrated to occur independently or in various combinations with most individuals described as having extremely sensitive skin (Tan and Tope, 2004; Wilkin *et al*., 2002). To assist with diagnosis, the primary features are graded 1 (mild), 2 (moderate), or 3 (severe) (Wilkin *et al*., 2004). It has been suggested that the erythema in rosacea can be subdivided into (a) sole erythema, (b) erythema with telangiectasis, (c) erythema with edema, and (d) erythema with inflammatory papules and nodules, to differentiate between the appearance of perilesional erythema of inflammatory lesions from diffuse facial erythema (Del Rosso, 2012).

1.1.2 Secondary Features

Secondary features include burning or stinging, plaques, appearance of dry skin, edema (soft or solid), ocular manifestations (lid inflammation, sensation of a foreign body, dry eye, blurred vision, and telangiectasia of the conjunctiva and lid margin),

peripheral locations, and phymatous changes (enlargement and thickening of the skin) (Table 1.2) (Wilkin *et al*., 2004). The appearance of ocular manifestations is the most common secondary feature with up to 50% of individuals with rosacea reported to have ocular symptoms (Böhn *et al*., 2014; Elewski *et al*., 2011).

1.2 Classification of Rosacea Subtypes

Rosacea can be classified into different subtypes due to the occurrence of the primary and secondary features of the disease, according to the classification system established by the NRS expert committee. These subtypes, as described by Wilkin *et al*. (2002), are divided into Subtype I: erythematotelangiectatic rosacea, Subtype II: papulopustular rosacea, Subtype III: phymatous rosacea, and Subtype IV: ocular rosacea with the severity of each primary feature graded 1 (mild), 2 (moderate), or 3 (severe) depending upon the presence or absence of a secondary feature (Wilkin *et al*., 2004). Granulomatous rosacea, a variant of rosacea, does not follow other similar morphological patterns and symptoms observed in the subtypes of rosacea. Features of each subtype are summarized in Table 1.3. The classification and grading system defined by the NRS expert committee has been invaluable for physicians in the diagnosis and treatment of rosacea (Wilkin *et al*., 2002, 2004).

1.2.1 Subtype I: Erythematotelangiectatic Rosacea

Patients classified within the erythematotelangiectatic rosacea subtype are often referred to as ‘flushers and blushers’ due to the transient or persistent erythema across the nose and cheeks (Wilkins *et al*., 2002) (Figure. 1.2 (A – C)). A prior history of flushing episodes is highly prevalent amongst individuals diagnosed with this subtype of rosacea but facial flushing may not always be a feature (Powell, 2005; Wilkin *et al*., 2002, 2004). Unlike the facial flushing and blushing that follows embarrassment or other external stimuli and only lasts seconds to a few minutes, facial flushing episodes characteristic of erythematotelangiectatic rosacea patients can last up to 10 minutes (Crawford *et al*., 2004). As the disease progresses for erythematelangiectatic rosacea patients, the grade given for the appearance of the primary feature, telangiectasias, increases to grade 2 (moderate) or grade 3 (severe) (Crawford *et al*., 2004).

Table 1.2 Primary and secondary features of rosacea. Table summarizes the primary and secondary features associated with rosacea. Adapted from Wilkin *et al*. (2004).

Primary Features	Secondary Features
Flushing (Transient Erythema)	Burning or Sting Sensation
	Plaques
Non-Transient Erythema	Appearance of Dry Skin
	Edema
Papules and Pustules	Ocular Manifestations
	Peripheral Location
Telangiectasia	Phymatous Changes

Table 1.3 Rosacea subtypes and features. Table summarizes the characteristics of each subtype of rosacea. Adapted from Wilkin *et al*. (2002).

Rosacea Subtype	Characteristics
Erythematotelangiectatic	Flushing; Persistent Facial Erythema; Telangiectasias; Burning and Stinging Sensations
Papulopustular	Persistent Eyrthema; Transient Facial Papules and Pustules, or Both
Phymatous	Thickened Skin with Irregular Nodularies, can Affect Nose, Forehead, Cheeks, and Ears
Ocular	Sensation of a Foreign Body in the Eye; Burning or Stinging; Dryness; Photosensitivity; Blurred Vision, Telangiectasia and Erythema of Eye Lids
Variant: Granulomatous	Non-Inflammatory Hard Red, Brown or Yellow Cutaneous Papules or Nodules, All of Equal Size

1.2.2 Subtype II: Papulopustular Rosacea

Papulopustular rosacea, also known as classic rosacea, is characterized by persistent erythema and pustules around the mouth, nose and eye regions of the face (Crawford *et al*., 2004; Wilkins *et al*., 2002) (Figure. 1.2 (D – F)). This subtype is often misdiagnosed as acne vulgaris but acne mainly affects younger generations with the presence of comedomes (whiteheads and blackheads) which are not associated with papulopustular rosacea (Powell, 2005; Wilkin *et al*., 2002). Papulopustular rosacea commonly appears in combination with erythematotelangiectatic rosacea and a sensation of burning and stinging is often reported by patients (Wilkin *et al*., 2002). As the features of this subtype increase in grading and worsen, the papules and pustules can form inflammatory lesions or plaques. A prevalence rate of papulopustular roscea of 69% and 2.7% has been recored in Tunisia and Ireland, respectively (Khaled *et al*., 2010; McAleer *et al*., 2010).

1.2.3 Subtype III: Phymatous Rosacea

Phymatous rosacea involves the enlargement and thickening of the skin. It mainly affects the appearance of the nose, giving the nose an enlarged, bulbous and lobulated appearance (Figure. 1.2 (G – I)). This condition is known as rhinophyma and commonly referred to as ‘whiskey nose’. It is a result of hyperplasia of sebaceous glands, connective tissue and blood vessels of the nose, and other primary features such as eythema, telangiectasis, papules and pustules have been described to co-appear with the phymatous subtype (Gupta and Chaundhry, 2005; Wilkin *et al*., 2002). Other areas of the face affected by phymatous rosacea include the chin (gnathophyma), forehead (metophyma), ears (otophyma) and eyelids (blepharophyma) (Crawford *et al*., 2004). The severity of the phymatous rosacea is rated as, (1) least severe with patulous follicles but no contour changes, (2) exhibits contour changes without a nodular component, and (3) changes in contour with a nodular component (Wilkin *et al*., 2004) (Figure. 1.2 (G – I)). A 3.7% prevalence rate of phymatous roscea has been recored in Tunisia (Khaled *et al*., 2010).

1.2.4 Subtype IV: Ocular Rosacea

Ocular rosacea affects the eyes and the eyelids causing symptoms such as blepharitis and keratitis and up to half of those diagnosed with facial rosacea also manifest ocular symptoms (Oltz and Check, 2011; Jenkins *et al*., 1979). The ocular rosacea subtype affects the eyes and has a range of symptoms such as burning or stinging sensation of the eyes, light sensitivity, blurred vision, itching, watery or bloodshot appearance and telangiectases of the conjunctiva and lid margin (Wilkin *et al*., 2002) (Figure. 1.2 (J – L) and Figure 1.3). This condition can appear without other symptoms typical of rosacea but if left untreated patients with ocular rosacea are at risk of vision loss and developing ulcers on the corneal surface (Powell, 2005). Corneal (sterile) ulcers and corneal scarring are associated with severe cases of ocular rosacea and can lead to deterioration in vision and potentially blindness in affected eyes (Kheirkhah *et al*., 2007b). It has been reported that up to 50% of individuals with rosacea experience features associated with ocular manifestations (Böhn *et al*., 2014; Elewski *et al*., 2011).

The appearance of ocular manifestations can be graded depending upon the severitiy of the symptoms as mild (affecting the eye margin or meibomian gland), moderate (affecting the inner lid, fluid secretion, or eye surface), or severe (corneal damage and potential vision loss) (Wilkin *et al*., 2004). Ocular rosacea can be misdiagnosed by clinicians as dermatologists do not routinely investigate ocular symptoms, and opthamologists fail to examine facial skin (Gupta and Chaudhry, 2005). However, this issue is being addressed with an increase in awareness of ocular rosacea and symptoms from a number of research studies involving ocular rosacea and other ocular diseases such as chalazia and ocular Demodicosis that share similar symptoms to ocular rosacea (Liang *et al*., 2014; Li *et al*., 2010; Liu *et* al., 2010; Lacey *et al*., 2009).

1.2.5 Variants of Rosacea

Variants of rosacea are described as not representing morphological patterns or combinations as seen in rosacea subtypes (Wilkin *et al*., 2002, 2004). Granulomatous rosacea is recognized as a variant of rosacea by the NRS expert committee (Wilkin *et al*., 2002, 2004). The condition is characterized by the appearance of papules or nodules on the cheeks that are hard, yellow, brown or red in colour and can lead to severe scarring (Wilkin *et al*., 2002, 2004). The sizes of these vary among patients but have been reported to be of similar size in each individual patient (Wilkin *et al*., 2002). Exposure to ultraviolet radiation (UVR) has been suggested to be a prominent causative factor in the induction of granulomatous rosacea due to the up-regulation of matrix metalloproteinases (MMPs) observed in patients (Jang *et al*., 2011).

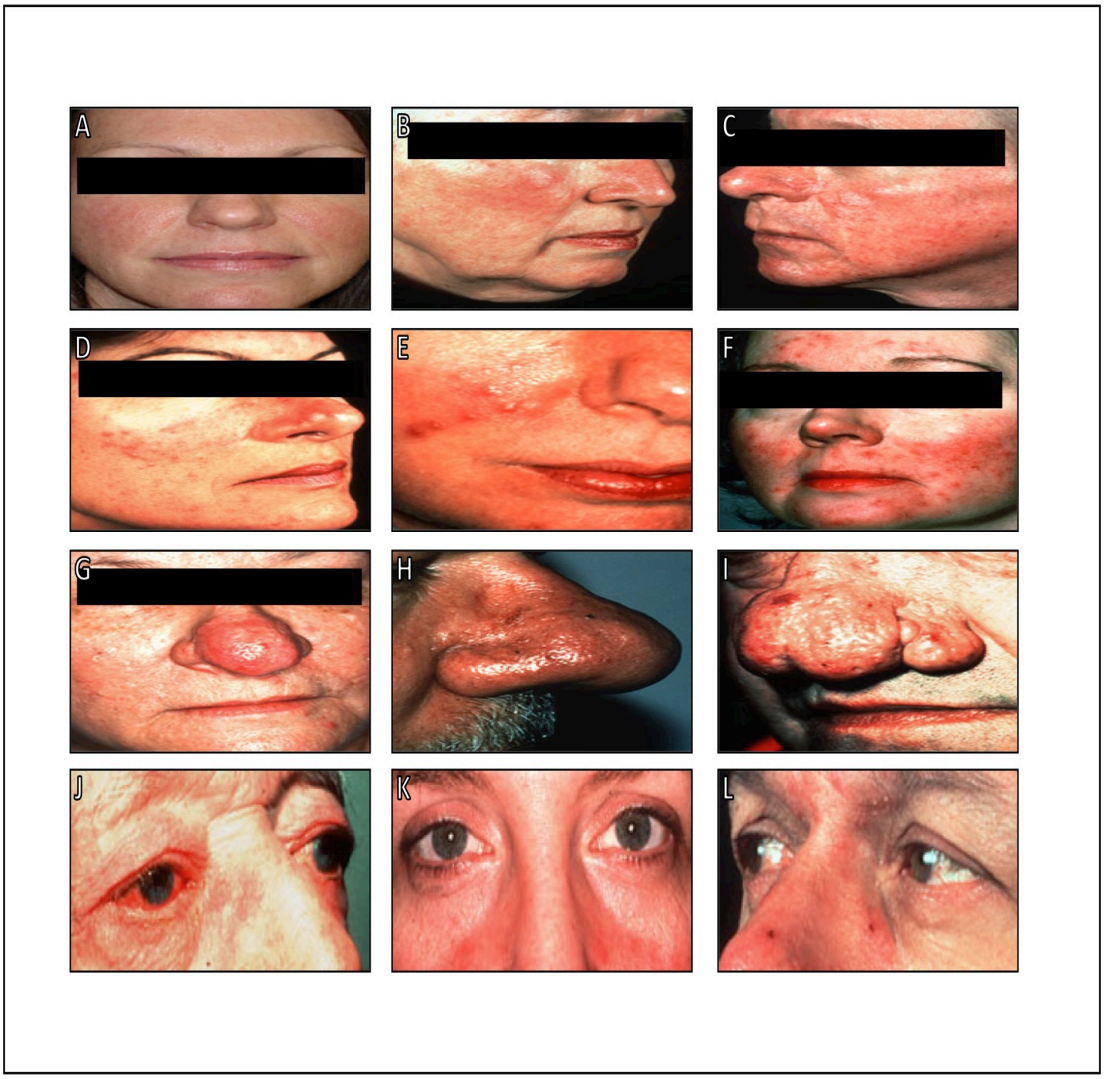

Figure 1.2 Subtypes of Rosacea and Characteristics. (**A** – **C**) Rosacea Subtype I: Erythematotelangiectatic. Telangiectasias and erythema are evident on cheeks and some erythema may also occur on the nose. (**D** – **F**) Rosacea subtype II: Papulopustular. In this example features such as inflammatory papules and pustules can be seen. Erythema is also a common feature of this subtype. (**G** – **I**) Rosacea subtype III: Phymatous. Shown here is advanced rhinophyma. The condition may include fibrosis and thickening of the skin, giving the nose a bulbous appearance, and distended growths of skin known as patulous follicles. Telangiectasia may also be present. (**J** – **L**) Rosacea subtype IV: Ocular. Features of this subtype include erythema and edema in both the upper and lower eyelid, ulcers in the eye, telangiectasia, blepharitis, and blurred vision. Severe cases may result in blindness. [Images adapted from the National Rosacea Society website at *http://www.rosacea.org/patients/faces.php*]

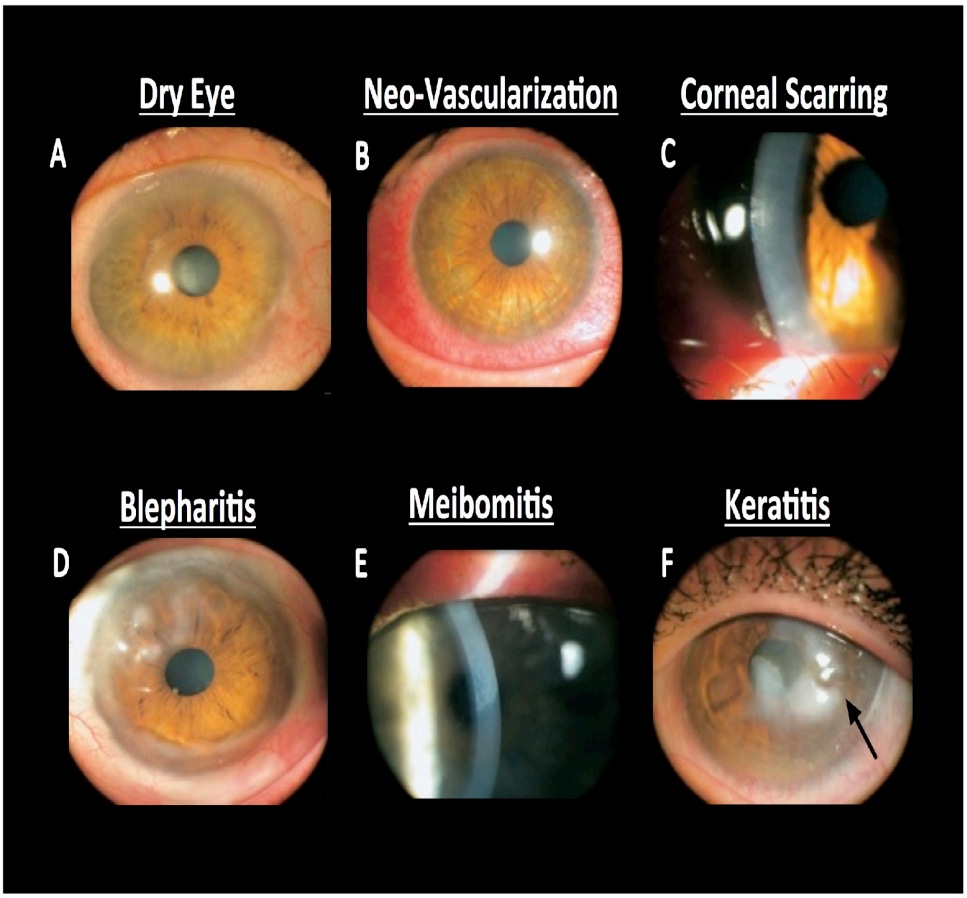

Figure 1.3 Features of ocular rosacea. Features typically associated with ocular rosacea include (**A**) dry eye, (**B**) neo-vascularization, (**C**) corneal scarring, (**D**) blepharitis, (**E**) meibomitis, inflammation of the meibomian gland, and (**F**) keratitis (corneal ulcer indicated by arrow (🡻)). (Adapted from Kheirkhah *et al*., 2007b).

1.3 The Role of *Demodex* Mites in the Skin

Demodex mites are common commensal arachnids that have been found to reside within the pilosebaceous unit of the facial skin and within the meibomian glands of eyelashes in mammals, and are the most common ectoparasites of man (Forton, 2012; Baima and Sticherling, 2002; Basta-Juzbasić *et al*., 2002; Forton and Seys, 1993; Ayres and Anderson, 1932, 1933). Desch and Nutting (1972) identified two distinct species of *Demodex*, both with discrete niches. The larger *Demodex folliculorum* (0.3 – 0.4 mm in length) is located primarily in the hair follicles and eyelashes, and the smaller *Demodex brevis* (0.2 – 0.3 mm in length) resides deep in the pilosebaceous units, and in the meibomian glands (Jing *et al*., 2005; Vance, 1986; Nutting, 1976).

The body of a *Demodex* mite is comprised of the gnathosoma (mouth and oral parts), the podosoma (where four pairs of legs are located), and the opisthosoma (abdominal region) (Forton and Seys, 1993) (Figure 1.4). Unique to the animal kingdom, the *Demodex* lack an anus with wastes being continuosly accumulated and stored in large cells in the abdomen until release following death (Rufli and Mumcuoglu, 1981; Herbert and Nevyas, 1980). Following the death of a *Demodex* mite, the contents are released onto the surface of the skin, and this has been implicated in a number of pathologies including pitryriasis folliculorum, *Demodex*-associated folliculitis, ocular Demodicosis, *Demodex*-related blepharitis, and rosacea (Liang *et al*., 2014; Elston and Elston, 2014; Jarmuda *et al*., 2012; Liu *et al*., 2010; Elston, 2010; Li *et al*., 2010; Lacey *et al*., 2009; Allen *et al*., 2007; Lee and Hsu, 2007; Czepita *et al*., 2007; Crawford *et al*., 2004; Forton, 1998; Vollmer, 1996; Ayres, 1930).

The life cycle of a *Demodex* mite lasts for between 14 – 21 days, and it has been proposed that mites mainly feed on sebum, and that sebum may facilitate the growth of mites on the facial skin and eyelashes (Jarmuda *et al*., 2012; Ní Raghallaigh *et al*., 2012; Rufli and Mumcouglu, 1981; Spickett, 1961; Ayres and Ayres, 1961). However, the role of sebum in the pathogenesis of rosacea has not yet been fully elucidated. Ní Raghallaigh *et al*. (2012) demonstrated that papulopustular rosacea patients have an altered composition of sebaceous gland fatty acids, and suggested that this may result in a disruption or weakening of the integrity of the skin barrier as the population of *Demodex* mites increases. Therefore, the authors conclude that it is the quality of the sebum (sebaceous fatty acids) and not the quantity that is essential

for the increase of the *Demodex* mite population on the surface of the skin and eyelashes.

1.3.1 *Demodex* Mites and Rosacea

The possible role of *D. folliculorum* and *D. brevis* mites in the pathogenesis of rosacea, especially the mechanism of passive transfer of other microorganisms, has been speculated upon for many years (Jarmuda *et al*., 2012). Previous studies have shown that patients affected with rosacea display a higher density of *Demodex* mites, *D. folliculorum* and *D. brevis*, than unaffected controls (Erbağci and Ozgöztaşi, 1998; Bonnar *et al*., 1993; Vance, 1986). Elevated numbers of *Demodex* mites have also been recorded on the eyelashes of patients with ocular rosacea (Li *et al*., 2010). A significantly greater density of the mites per cm^2 was detected in patients with papulopustular rosacea (Bonnar *et al*., 1993). Baima and Sticherling (2002) suggested that the pathogenesis of rosacea increases if the mite density is higher than five per cm^2.

The role of sebum on the facial skin of rosacea patients and the induction of rosacea, has been studied since 1972 (Pye *et al*., 1976). Examination of the composition of the lipids in sebum revealed differences in comparison with controls, which might facilitate the development of larger populations of mites (Ní Raghallaigh *et al*., 2012). The presence of *D. folliculorum* in the sebum secretions from the pilosebaceous unit was found in 90.2% of papulopustular patients and only in 11.9% of healthy controls. Additionally, histological tests of skin samples obtained from these patients revealed that the presence of *Demodex* mites was strongly correlated with substantial perifollicular lymphocytic infiltration (Georgala *et al*., 2001).

It has recently been reported that the prevalence of *Demodex* mites was more common and at higher levels than previously expected in the general population (Thoemmes *et al*., 2014). The prevalence of *Demodex* mites in individuals with rosacea has been proposed to be as high as 60% in a clinical setting and up to 80% following examination of skin biopsies (Yücel and Yilmaz, 2013; Ríos-Yuil and Marcadillo-Perez, 2013). However, the role of the *Demodex* mites in the induction of rosacea is widely debated with them being regarded as an aggravating factor contributing to the condition instead of a causative factor, and that they may act as vessels for transporting pathogenic bacteria around the surface of the face (Wollina, 2014; Holmes, 2013; Lacey, 2009; Powell, 2004).

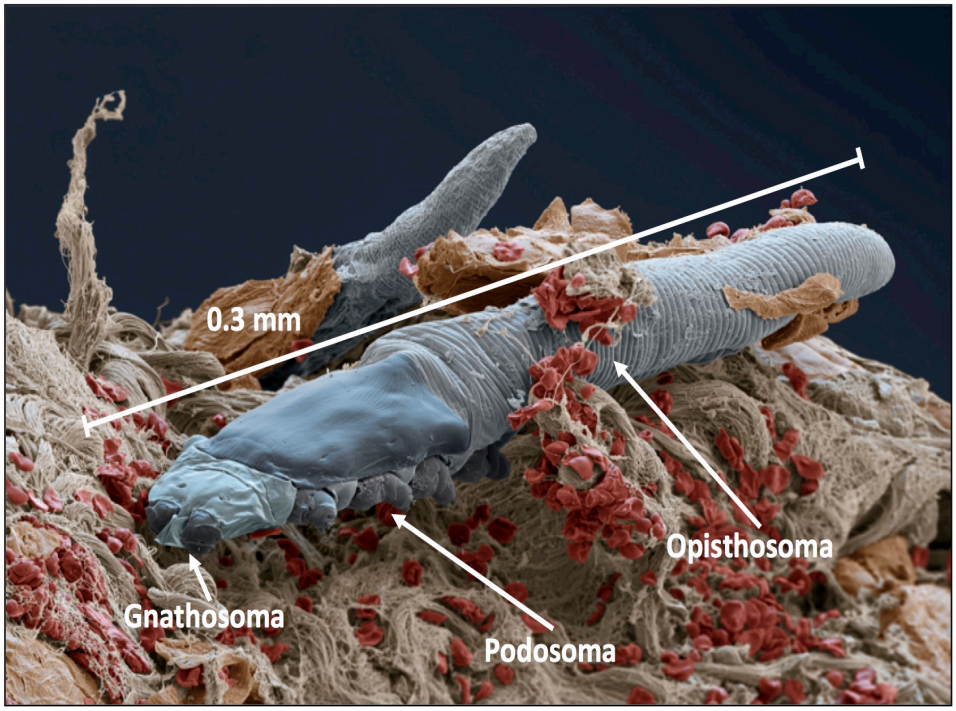

Figure 1.4 An electron micrograph of a *Demodex folliculorum* mite. A scanning electron micrograph image illustrating the body parts of a *D. folliculorum* mite; the gnathosoma containing the mouth and oral parts, the podosoma or thoracic region where four pairs of short legs are found and the abdominal region of the mite, the opisthosoma. [Adapted from the website *http://www.bbc.com/earth/story/20150508-these-mites-live-on-your-face* (Credit: Eye of Science/SPL)]

1.3.2 *Demodex* Mites and Blepharitis

Blepharitis is a chronic inflammatory disease of the eyelid margins that can result in ocular discomfort and irritation, and a loss of vision acuity (Jackson, 2008). A number of studies has implicated increased ocular *Demodex* mite infestation in the induction of a range of ocular pathologies including the ocular surface inflammation of lashes observed in trichiasis and madarosis, meibomian gland dysfunction, and *Demodex*-related blepharitis (Szkaradkiewicz *et al*., 2012; Bernardes and Bonfioli, 2010; Lacey *et al*., 2009; Czepita *et al*., 2007; Gao *et al*., 2007; Kheirkhah *et al*., 2007a, 2007b; Kamoun *et al*., 1999). The symptoms associated with *Demodex*-related blepharitis such as ocular discomfort and irritation, meibomian gland dysfunction, inflammation of the eyelashes, and telangiectasia have also been associated with ocular rosacea (Oltz and Check, 2011; Lacey *et al*., 2009; Crawford *et al*., 2004; Wilkin *et al*., 2002, 2004). Szkaradkiewicz *et al*. (2012) identified *Bacillus oleronius* from epilated eyelashes of severe *Demodex*-related chronic blepharitis patients (18/36) and control subjects (5/30), a bacterium that has previously been implicated in the induction and persistence of rosacea (Jarmuda *et al*., 2012; Li *et al*., 2010; Lacey *et al*., 2009).

1.3.3 *Demodex* Mites and Demodetic Mange

In mammals other than humans, an increase in *Demodex* mite infestation in the pilosebaceous units and hair follicles, and the meibomian glands and eyelashes can result in the development of a debilitating skin disease known as demodetic mange which occurs in a number of free-ranging animals (Nemeth *et al*., 2014). Similar to rosacea, in demodetic mange, *Demodex* species are symbiotic commensal organisms that are host-specific. Each species of mammal is host to specific subset of *Demodex* mite species such as *D. gatoi* and *D. cati* identified in domesticated cats, and *D. canis*, *D. injai*, and *D. cornei* that can be found in domestic dogs (Frank *et al*., 2013; Beale *et al*., 2012; Sastre *et al*., 2012; Chesney, 1988; Kirk, 1949). In animals, the proliferation and increase in *Demodex* mite numbers is associated with alopecia, the development of skin lesions, and a weakend immune system (Nemeth *et al*., 2014; Desch and Nutting, 1974). Reports of demodetic alopecia, similar to animal mange has been described in humans, and responds well to anti-demodetic treatments (García-Vargas *et al*., 2007; Elston *et al*., 2001).

1.4 Potential Role of Bacteria in Rosacea

The aetiology of rosacea is unclear but it is believed that a number of genetic, immunological and environmental factors may be involved. A role for bacteria as contributory factors in the aetiology of the condition has been suggested (Holmes, 2013; Jarmuda *et al*., 2012; Whitfield *et al*., 2010; Lacey *et al*., 2007; Dahl *et al*., 2004). As the *Demodex* move across the skin, it is believed that the mites may act as vectors for the transport of bacteria that may reside on or within the *Demodex* mite, or on the skin surface, and that this mechanism may be involved in the pathogenesis of rosacea (Elston and Elston, 2014; Elston, 2010; Wolf *et al*., 1988).

Bacteria residing within *Demodex* mites may stimulate neutrophil infiltration and activation once released from dead mites residing in the pilosebaceous unit. Similarly, a potential role for bacteria in the induction of rosacea has been suggested since antibiotics (e.g. erythromycin, metronidazole) can be used to treat the condition although these may also exhibit anti-inflammatory properties (Holmes, 2013; Gupta and Chaudhry, 2005).

The microbiota of *Demodex* mites obtained from erythematotelangiectatic rosacea patients, papulopustular rosacea patients, and healthy control subjects was analysed, and it was demonstrated that the microbiota of the *Demodex* mites is subtype-specific with a diverse community of *Demodex*-associated microogranisms identified for each study population (Murillo *et al*., 2014).

1.4.1 *Bacillus oleronius*

B. oleronius is a rod-shaped, non-motile, Gram-negative, endospore-forming bacterium that has previously been isolated from the digestive tract of a termite, *Reticulitermes santonensis*, on Îsle d'Oléron in France where it has been speculated that it may facilitate digestion and the breakdown of lipids (König, 2006; Kuhnigk *et al*., 1995). The bacterium, *B. oleronius*, was first implicated in the pathogenesis of rosacea following it's isolation from a micro-dissected *D. folliculorum* mite extracted from the face of a papulopustular rosacea patient, and it was found to be sensitive to the antibiotics used to treat rosacea (Lacey *et al*., 2007).

Lacey *et al*. (2007) demonstrated that the *B. oleronius* produced immuno-reactive proteins that induced an inflammatory response in 72% (16/22) of papulopustular rosacea patients, but only in 29% (5/17) of control patients ($p = 0.01$). The immuno-reactive proteins produced by *B. oleronius* were found to be 62 kDa and

83 kDa in size. These were further investigated by matrix-assisted laser desorption/ionization-time of flight (MALDI-ToF), and identified as an enzyme involved in carbohydrate metabolism and signal transduction, the phosphoenolpyruvate phosphotransferase sensory system, in the case of the 83 kDa protein, whereas the 62 kDa protein showed similar amino acid sequence to a bacterial heat shock protein, molecular chaperone GroEL, that functions in the correct folding of polypeptides under heat stress conditions (Lacey *et al.*, 2007).

Double-blind seralogical studies have demonstrated a strong correlation between ocular *Demodex* infestation and serum reactivity to these bacterial proteins in patients with ocular rosacea (Li *et al*., 2010). In addition, the presence of eyelid margin inflammation (74.6%; 44/59) ($p = 0.04$) and ocular rosacea (47/59; 80%) ($p = 0.009$) correlated with reactivity to these proteins (Li *et al*., 2010). Similarly, it was demonstrated that 80% (21/26) of erythematotelangiectatic rosacea patients were sera reactive to *B. oleronius* proteins compared to 40% (9/22) of control subjects ($p = 0.004$) (O'Reilly *et al*., 2012c).

The sera reactive 62 kDa and 83 kDa proteins were isolated and purified by ÄKTA fast protein liquid chromatography™ (ÄKTA FPLC™), and are believed to be involved in the pathogenesis of the disease (O'Reilly *et al*., 2012a, 2012b; Lacey *et al*., 2007). An immune response has been shown to be induced in rosacea patients by proteins isolated from *B. oleronius* via the proliferation of peripheral blood mononuclear cells (PBMC) and the activation of neutrophils (O'Reilly *et al*., 2012a; Lacey *et al*., 2007). Neutrophils exposed to *B. oleronius* proteins demonstrated increased migration and elevated release of MMP-9, an enzyme known to degrade collagen, and cathelicidin, an antimicrobial peptide. Exposure of neutrophils to the bacterial proteins resulted in elevated production of IL-8 and TNF-α (O'Reilly *et al*., 2012a). Increased production of IL-8 is a trigger for neutrophil recruitment to the site of infection and TNF-α is indicative of an inflammatory response. Proteins produced by the *B. oleronius* were demonstrated to induce an aberrant wound healing response and an inflammatory response in a human telomerase-immortalized corneal epithelial (hTCEpi) cell line in studies of the corneal epithelial interface in the ocular form of the disease (O'Reilly *et al*. 2012b).

The serological studies from patients with papulopustular, ocular and erythematotelangiectatic rosacea demonstrated elevated reactivity to proteins isolated from *B. oleronius* (O'Reilly *et al*., 2012c; Li *et al*., 2010; Lacey *et al*., 2007). Thus,

suggesting a possible link between the presence of this bacterium and rosacea (Holmes, 2013; Jarmuda *et al*., 2012; Lacey *et al*., 2007, 2009). Interestingly, the *B. oleronius* has also been isolated from *Demodex* mites and eyelashes of patients with chronic blepharitis and increased ocular *Demodex* infestation (Szkaradkiewicz *et al*., 2012). It can be hypothesised that the *Demodex* mites have a role related to rosacea but it is the symbiotic relationship between the *Demodex* mites and *B. oleronius* which may be involved in the pathogenesis of rosacea (Figure 1.5). Together, these studies demonstrate a possible role for *B. oleronius* proteins in the aetiology of rosacea.

1.4.2 *Staphylococcus epidermidis*

Staphylococcus epidermidis is a round-shaped, Gram-positive commensal bacteria that is a natural component of the skin microflora providing protection from invading skin pathogens such as *S. aureus* (Gallo and Nakatsuji, 2011; Cogen *et al*., 2010; Bastos *et al*., 2009). *S. epidermidis* has been shown to display pathogenic properties in opportunistic cicumstances, such as invasion through chronic wounds when the integrity of the natural skin barrier has been disrupted, or from the insertion of medical devices (Uçkay *et al*., 2009; Dowd *et al*., 2008). An alteration in temperature has also been demonstrated as a possible pathogenic mechanism of *S. epidermidis in vivo*, where *S. epidermidis* isolated from rosacea patients were consistently β-hemolytic, and grew better at 37°C than 30°C suggesting a potential link between mesophilic hydrolytic bacteria and rosacea (Dahl *et al*., 2004). The bacterium has also been isolated from the pustules of patients with papulopustular rosacea and from the eyelids of patients with ocular rosacea suggesting a possible role for this bacterium in the induction of these conditions (Whitfeld *et al*., 2011).

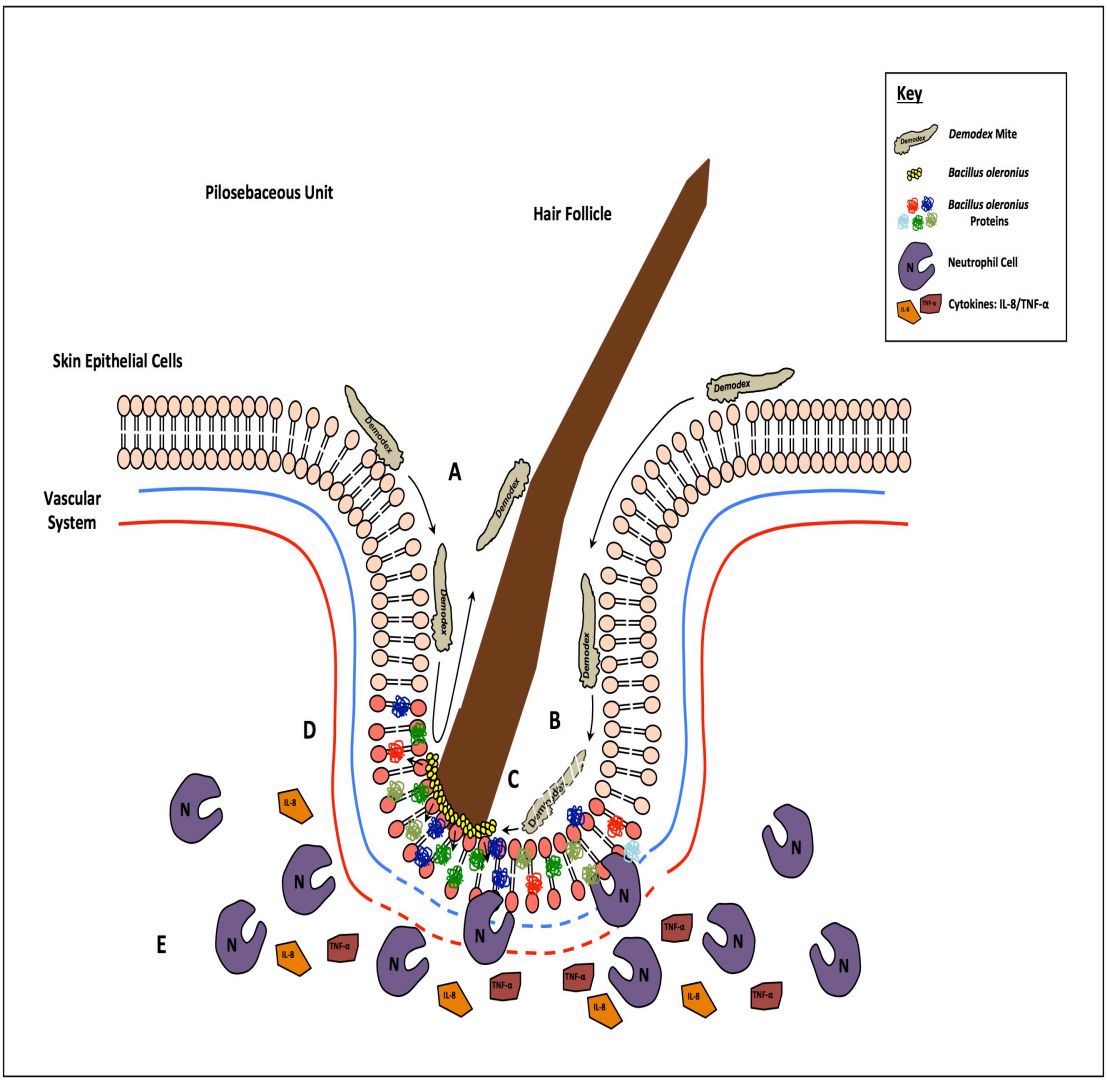

Figure 1.5 Proposed role of *Demodex* mites and the role of *B. oleronius* for the induction of rosacea. (**A**) Increased density of *Demodex* mites that migrate to the pilosebaceous unit. (**B**) The *Demodex* mites die and release bacteria which in turn releases antigenic proteins. (**C**) The bacterial antigenic proteins leave the pilosebaceous unit entering through the epithelial cell surface. (**D**) Induction of an inflammatory response and an immune response. Neutrophils become activated and migrate to the site of infection. Further recruitment of neutrophils occurs through the secretion of IL-8 and TNF-α, and other cytokines and immune cell mediators. (Author's own).

1.4.3 *Helicobacter pylori*

Helicobacter pylori is a helical-shaped, Gram-negative microaerophilic bacteria that resides in the stomach, and is highly prevalent in general populations (Martín-de-Argila *et al*., 1996). A number of studies have implicated *H. pylori* infections in the induction of rosacea (Diaz *et al*., 2003; Rebora *et al*., 1994). However, the role of *H. pylori* in the pathogenesis of rosacea has been widely refuted and considered controversial (Boixeda de Miquel *et al*., 2006; Powell, 2004; Herr and You, 2000; Son *et al*., 1999; Sharma *et al*., 1999). It is more accepted that the improvement of symptoms associated with rosacea is simply because the antibiotic therapy used for the treatment of rosacea and *H. pylori* infections is the same leading to conflicting results, and following a course of antibiotics, an improvement in the skin condition ceased after the eradication of *H. pylori* infection with a relapse of rosacea (Herr and You, 2000). At the moment, evidence to support the role of *H. pylori* in the induction of rosacea does not currently exist.

1.4.4 *Chlamydophila pneumoniae*

Chlamydophila pneumoniae is a Gram-negative bacteria, and an obligate intracellular pathogen that has been linked to a number of common respiratory diseases including pneumoniae and asthma, and central nervous system disorders such as atherosclerosis (Blasi *et al*., 2009). To date, only one study has suggested a role for *C. pneumoniae* in the pathogenesis of rosacea (Fernandez-Obergon and Patton, 2007). The authors detected *C. pneumoniae* antigens present in 40% of malar skin biopsy specimens extracted from rosacea patients, and *C. pneumoniae*-reactive antibodies were present in 80% of rosacea patient serum samples.

1.5 Management and Treatment of Rosacea

Since the aetiology of the disease remains unclear, the management and treatment of rosacea remains a challenge to the clinician and requires a highly individual approach. The classical approach of rosacea therapy has been to target treatment of the inflammatory nodules, pustules, and papules that are features of the skin condition (Wollina, 2014; Powell, 2004). Management with oral antibiotics, mostly from the group of tetracyclines (doxycycline and minocycline), macrolides and metronidazole, or azithromycin, is generally recommended (Wollina, 2014; Bakar *et al*., 2009; Pelle *et al*., 2004; Powell, 2004). Treatment of the papulopustular rosacea or ocular rosacea with oral tetracyclines has been demonstrated to be an effective method of managing and treating these subtypes of rosacea (Kanada *et al*., 2012; Scheinfeld and Berk, 2010; Bakar *et al*., 2009).

The mechanism by which antibiotics successfully treat different subtypes of rosacea is unknown. It has been suggested by Antille *et al*. (2004) that antibiotics work through anti-inflammatory mechanisms, whereas other potent anti-inflammatory drugs (e.g. cyclosporin) are ineffective, and result in the worsening of the condition. Thus, the fact that only selective antibiotics are effective in the treatment of rosacea suggests that a bacterial agent may be involved in the pathogenesis of the disease and supports previous findings which suggests a role for the *D. folliculorum*-related bacterium, *B. oleronius*, in the induction and persistence of inflammation (O'Reilly *et al*., 2012a, 2012b, 2012c; Jarmuda *et al*., 2012; Lacey *et al*., 2007, 2009).

Effective topical therapeutics for the treatment of rosacea include metronidazole and a 15% gel solution of azelaic acid (van Zuuren *et al*., 2011). Topical metronidazole functions as an oxygen scavenger leading to a decrease in reactive oxygen species (ROS), and inhibition of neutrophils and reducing inflammation present at a site of infection (Narayanan *et al*., 2007). In particular, azelaic acid has been shown to be the standard of care for papulopustular rosacea patients (van Zuuren *et al*., 2011; Gollnick and Layton, 2008). Azelaic acid is a US Food and Drug Administration (FDA) approved drug with anti-inflammatory, anti-oxidant, and anti-microbial properties that has been been shown to reduce ROS, and inhibit kallikrein-5 (KLK-5), and thus, increasing serine protease activity (Coda *et al*., 2013; Gollnick and Layton, 2008). It has been demonstrated that individuals diagnosed with rosacea, contain a higher abundance of ROS in their skin, and the action of serine proteases such as cathelicidin (LL-37) and KLK-5 have been suggested to play an important

role in the underlying mechanisms of rosacea (Tisma *et al*., 2009; Yamasaki and Gallo, 2009).

Recently, a topical 1% solution of ivermectin (Soolantra® cream) has been shown in two randomised, double-blind, and controlled studies over a 12 week period, to be an effective treatment for reducing the inflammation and erythema that is a feature of rosacea (Stein *et al*., 2014). Ivermectin is an anti-parasitic drug that targets the farnesoid X receptor ligand of helminths, and it has been reported that treatment of rosacea pateints with ivermectin leads to a decrease in the density of *Demodex* mites on the facial skin, and in turn, the eradication of the *Demodex* mite populations leads to an improvement in the skin barrier and integrity of rosacea patients (Jin *et al*., 2013). Another advantage to vindicate the use of topical ivermectin as a therapy for rosacea is that it is an FDA approved drug and has been found to be completely safe in a range of studies for use in humans, with no side effects (Yardley *et al*., 2014).

Topical calcineurin inhibitors such as 1% solution of pimecrolimus cream or a tacrolimus ointment, that inhibit T-lymphocyte signal transduction and interleukin (IL-2) transcription, have been used to treat rosacea and other skin conditions such as atopic dermatitis with varying degrees of success (Kim *et al*., 2011; Koca *et al*., 2010; Wollina, 2007; Alomar *et al*., 2004). Although treatment of rosacea with topical clacineurin inhibitors has been demostrated to be an effective therapy, adverse effects of topical calcineurin inhibitors has been reported to be an induction of rosacea-like dermatitis and flushing (erythema), that affects the cheeks and forehead (Teraki *et al*., 2012). This has been suggested to be a result of topical immunosuppression leading to an increased density of *Demodex* mites on the facial skin, and perhaps drug interactions with alcoholic beverages (Teraki *et al*., 2012; Ogunleye and James, 2008).

A daily cleanse of the eyelid and eyelashes with a diluted solution of tea tree oil (Cliradex™) has been suggested as an effective therapy for ocular rosacea, and a reduction of the *Demodex* mite population (Lacey *et al*., 2009). Intense pulsed light (IPL) therapies are also employed to treat the diffuse central erythema and telangiectasia that is characteristic of rosacea (Tanghetti *et al*., 2014). A combination of systemic therapy using oral antibiotics and using topical and/or IPL therapies, is the suggested initial therapy of rosacea followed by topical ointments to maintain the skin barrier integrity and manage flare-ups to minimise the impact of the condition on a patients quality of life (Bhatia and Del Rosso, 2012).

1.6 Cornea: The Window of the Eye

1.6.1 Structure and Function of the Human Cornea

Ocular rosacea is characterised by damage to the corneal surface that may lead to visual impairment following damage to tissue and scarring. The cornea is the transparent tissue at the front of the eye that covers the pupil, iris, and the anterior chamber, and is the window of the eye. The cornea, in parallel with the lens, allows for the refraction of light, and the focusing of vision. As well as providing vital sensory information, the cornea protects the eyeball from harmful invading pathogens, acting as a defensive barrier. The cornea consists of five main structural layers of varying thickness, the corneal epithelium (≈ 50 μm thick), the Bowman's layer (≈ 17 μm thick), the corneal stroma (≈ 450 μm thick), the Descemet's membrane (≈ 5 – 20 μm thick), and the corneal endothelium (≈ 5 μm thick) (Ahmad *et al*., 2010; Reinstein *et al*., 2009; Patel *et al*., 2001) (Figure 1.6). Recently, Dua *et al*. (2013) have characterised a novel, pre-Descemet's membrane layer referred to as Dua's layer. However, this has sparked controversy in the field, and has not been fully accepted in the science community when describing the layers of the cornea, instead it is believed that this layer was pre-Descemet stroma, and more correctly a stromal layer (McKee *et al*., 2014). The corneal epithelium is the outermost layer of the cornea, and is constantly exposed to the external environment and responds to external stimuli accordingly (Ahmad *et al*., 2010). Alterations to the structure and functioning of the corneal epithelium results in downstream issues with vision acuity and maintenance of the ocular tissues (Ahmad *et al*., 2010).

The corneal epithelium consists of a non-keratinized stratified squamous epithelial sheet with a capacity for self-renewal and regeneration, covering the entire surface of the avascular cornea to the limbus (Ahmad *et al*., 2010; Robertson *et al*., 2005). The limbus is located at the outer edge of the cornea and forms a barrier between the epithelial sheets of the cornea and conjunctiva (Ahmad *et al*., 2010; Levis and Daniels, 2009). The physical structure of the corneal epithelium consists of five to seven cell layers with a monolayer of columnar cells (basal cells) which can undergo cell division and are situated on a basement membrane (Torricelli *et al*., 2013; Ahmad *et al*., 2010). Resting above this are two to three layers of wing cells, followed by the outermost layer of squamous cells with projections of microvilli which are thought to maintain the integrity of the eye through the glycoprotein, mucin, secreted in tear film

(Ahmad *et al*., 2010; Julio *et al*., 2008; Gipson *et al*., 1995).

A niche of stem cells, known as corneal epithelial stem cells or limbal epithelial stem cells (LESCs), are thought to be located where the limbal epithelium separates the corneal epithelium and conjunctival epithelium, and is composed of a non-keratinized stratified squamous epithelium that is thicker in arrangement compared to the corneal epithelium (Ahmad *et al*., 2010; Notara and Daniels, 2010; Dua and Azuara-Blancon, 2000). LESCs are unipotent or progenitor cells that give rise to differentiated corneal epithelial cells to replenish, renew, and maintain the stability of the corneal epithelial barrier (Moore *et al*., 2002). The limbal palisades of Vogt are thought to be resevoirs for LESCs, providing protection from physical insult, and maintaining the unipotency of the LESCs (Dua *et al*., 2010; Fuchs *et al*., 2004; Dua and Forrester, 1990; Tseng, 1989; Schermer *et al*., 1986; Goldberg and Bron, 1982; Davanger and Evensen, 1971). Shortt *et al*. (2007) suggested two novel, specialised candidate niche structures, limbal crypts and focal stromal projections, that are believed to function in harbouring LESCs in the niche of the limbus.

Injury to the eye by physical trauma, thermal or chemical damage, or systemic infection can result in a depletion of the LESC population, and in turn, result in destruction of the corneal epithelial surface (Vemuganti *et al*., 2009; Hau and Barton, 2009). The loss of LESCs by these means is referred to as limbal epithelial stem cell deficiency (LESCD), and can lead to the absence of an intact corneal epithelial layer, conjunctival epithelial outgrowth, corneal neovascularisation, chronic inflammation, ocular discomfort, and loss of vision (Levis and Daniels, 2009; Tseng, 1996). A successful treatment for LESCD and the restoration of the corneal epithelial structure, and vision has been shown to be corneal grafting or by transplantation of healthy limbal tissue along with a human amniotic membrane substrate due to the anti-inflammatory and anti-angiogenic properties associated with the amnion (Meller *et al*., 2011; Gomes *et al*., 2005; Tsai *et al*., 2000; Kenyon and Tseng, 1989).

The disadvantage to this approach is that its success is dependent upon the availability of suitable donor tissue, as well as the the potential threat of LESCD in the donor eye, the increased likelihood of infection due to immunosuppression, and the supply of the amniotic membrane (Ahmad *et al*., 2010; Levis and Daniels, 2009; Coster *et al*., 1995; Tseng *et al*., 1998; Jenkins *et al*., 1993). Plastic compressed collagen-based bio-substitutes to replace the need for the use of a human amniotic

membrane for the expansion of limbal epithelial cells and restoration of the cornea have been studied with successful results (Levis *et al*., 2010).

1.6.2 Human Telomerase-Immortalized Corneal Epithelial (hTCEpi) Cell Line Model

Previously, cultured cell lines have been developed following transformation with viral oncoproteins such as adenovirus E1A, the SV40 large T-antigen, and HPV16-E6/E7 but this has been used with varying levels of success where the genetic instability, lack of normal cell growth and cell differentiation have been the determining factors for the use of cell lines in research studies (Robertson *et al*., 2005; Mohan *et al*., 2003; Offord *et al*., 1999; Griffith *et al*., 1999; Araki-Sasaki *et al*., 1995; Kahn *et al*., 1993).

Robertson *et al*. (2005) successfully generated an immortalized human corneal epithelial cell line following transfection with a retroviral vector encoding human telomerase reverse transcriptase (hTERT). The hTERT enzyme is a ribonucleoprotein that is typically silent in somatic cells, and allows for cell survival by activating telomerase and maintaining telomere length during cell progression through each mitotic division (Cong *et al*., 2002; Weng *et al*., 1998; Bodnar *et al*., 1998; Vaziri and Benchimol, 1998). This corneal epithelial cell line was named human telomerase-immortalized corneal epithelial (hTCEpi) cell line. The growth and differentiation of hTCEpi cell line was characterised and demonstrated to exhibit similar stratification, differentiation, and desquamation that is observed in normal corneal epithelium (Robertson *et al*., 2005).

The hTCEpi cell line is an excellent model for studying the response of the corneal surface to pathogens or pathogen derived materials (e.g. toxins, antigens). Corneal epithelial (hTCEpi) cells have previously been used to study the interaction of flagellin from pathogenic and non-pathogenic bacteria and in understanding the response of the corneal surface to the combined effect of contact lens and *Pseudomonas aeruginosa* (Maltseva *et al*., 2007; Hozono *et al*., 2006). For this thesis, the hTCEpi cell line model of the corneal epithelial surface was used to characterise the response of corneal epithelial cells to *B. oleronius* proteins, as this may provide an insight into the possible interactions that may be implicated in ocular rosacea.

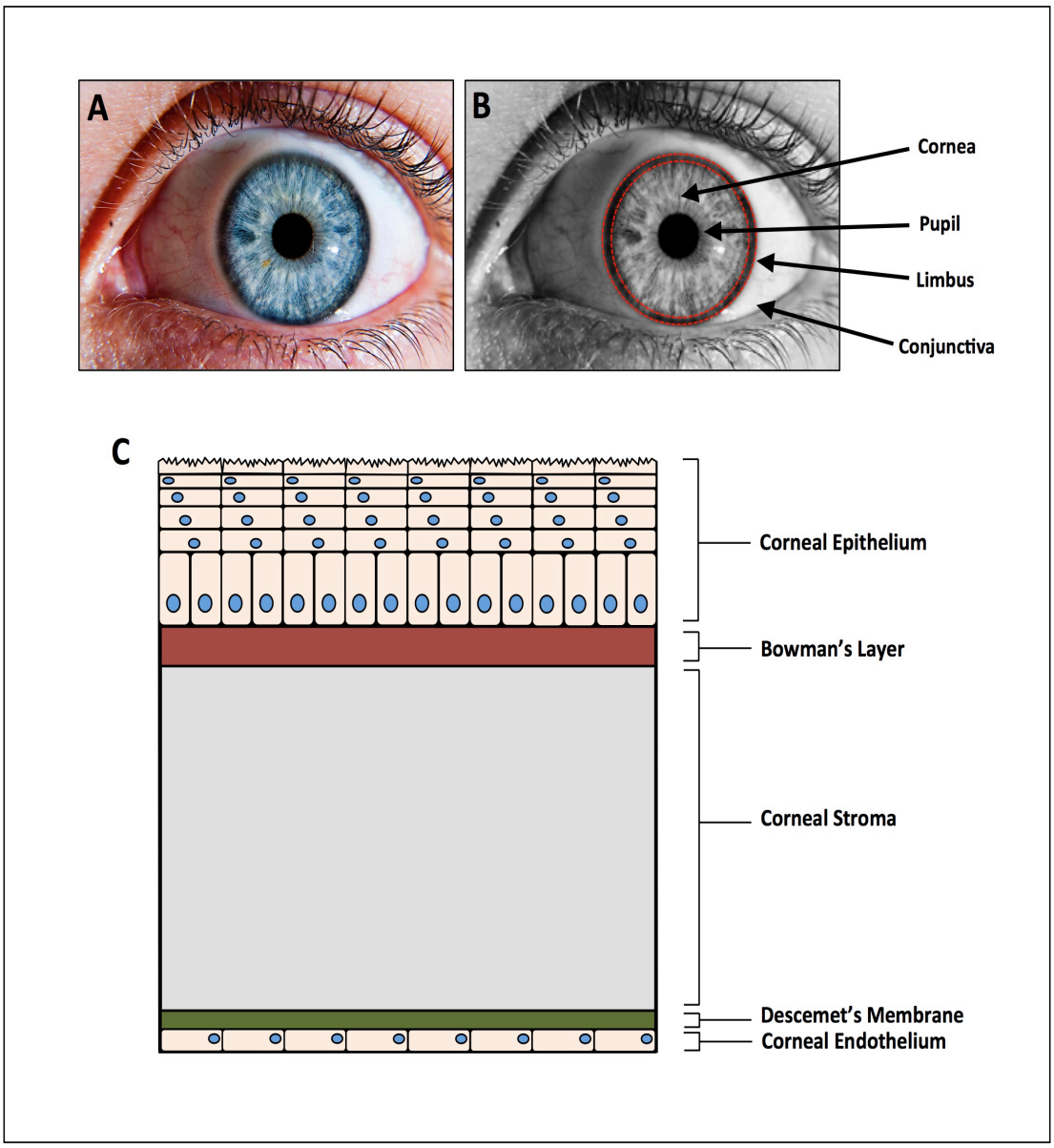

Figure 1.6 The structure of the human cornea. (**A**) A colour photograph of the anterior segment of a human eye. (**B**) A corresponding greyscale image demonstrating the locations of the cornea, pupil, limbus, and conjunctiva. (**C**) A schematic diagram illustrating the structure of the cornea composed of five layers: the corneal epithelium, Bowman's layer, corneal stroma, Descemet's membrane, and the corneal endothelium. (Adapted from Ahmad *et al*., 2010).

1.7 Neutrophils and the Innate Immune Response

The innate immune response is the first line of defence for the body against invading pathogens (Segal, 2005). Neutrophil granulocytes are the most abundant type of white blood cell in mammals and have a critical role in the innate immune response (Segal, 2005). The innate immune response provides non-specific protection against a wide range of microbes through a barrier system such as the skin, the action of chemokines and cytokines, and the activation and recruitment of neutrophils leading to the phagocytosing, killing, and digestion of microbial cells (Bellocchio *et al.*, 2004). It is believed that neutrophils are involved in the pathogenesis of rosacea and may function in the development of inflammation associated with the condition through the production of ROS (hydrogen peroxide), matrix metalloproteinases (MMPs) such as MMP-9, and other proteins produced upon neutrophil degranulation (O'Reilly *et al*., 2012a; Segal, 2005; Lu and Wahl, 2005; Akamatsu *et al.*, 1990; Curnutte *et al*., 1987).

1.7.1 Role of Neutrophils in Rosacea

Neutrophils have been implicated in the pathogenesis of rosacea (Akamatsu *et al*., 1990). Many antibiotics used to treat rosacea such as tetracyclines, azelaic acid, retinoids, and metronidazole, inhibit the production of ROS and the oxidative killing mechanism of NADPH oxidase, suggesting a pivotal role for neutrophils in the disease (Akamatsu *et al*., 1991; Miyachi *et al*., 1986; Yoshioka *et al*., 1986). It is believed that neutrophils can induce increased inflammation in individuals with rosacea through the release of protolytic enzymes during degranulation, leading to increased tissue damage and degradation (Berton *et al*., 2000; Starkey *et al*., 1977). Recently, O'Reilly *et al*. (2012a) have shown that neutrophils express the pro-inflammatory cytokines IL-8 and TNF-α in the presence of *B. oleronius* proteins and that neutrophils release MMP-9 and cathelicidin upon degranulation following exposure to *B. oleronius* stimulatory proteins. The cathelicidin, LL-37 has been shown to be prevalent on the skin of rosacea patients, and possibly dysregulated by the abnormal actions of a serine protease (O'Reilly *et al*., 2012a; Yamasaki and Gallo, 2009; Yamasaki *et al*., 2007).

1.8 Neutrophil Activation

The influx of calcium (Ca^{2+}) ions from the extracellular matrix through the opening of Ca^{2+}-permeable channels subsequently depletes the intracellular Ca^{2+} concentration ($[Ca^{2+}]_c$) and by doing so, mediates the synthesis of inositol 1, 4, 5-triphosphate (IP_3), a Ca^{2+}-mobilizing second messenger, causing the activation of channels located in the endoplasmic reticulum (ER) membranes (Putney, 2007). The resulting intracellular signaling mechanism, known as store-operated Ca^{2+} entry (SOCE), is characterized by the formation of a transient Ca^{2+} spike, which returns to a basal level of $[Ca^{2+}]_c$, dependent on the activity of the plasma membrane and sacro(endo)plasmic reticulum Ca^{2+}-ATPase (SERCA) pumps (Putney, 2007; Taylor, 2004; Berridge, 1995). The SOCE mechanism employed in the activation of neutrophils, is regulated by Orail, and considered the prominent mechanism for Ca^{2+} influx into neutrophils after Ca^{2+} depletion. Another mechanism of neutrophil activation involves the sustaining of the extracellular Ca^{2+} influx in neutrophils stimulated by N-Formyl-L-methionyl-leucyl-phenylalanine (fMLF) through the ryanodine receptor and the action of cyclic ADP-ribose (cADPr) (Patrida-Sanchez *et al*., 2004; Patrida-Sanchez *et al*., 2001).

1.9 Neutrophil Chemotaxis and Migration

Neutrophil chemotaxis involves the migration of neutrophils to areas of tissue damage or sites of bacterial invasion along a chemical gradient. The process of neutrophil migration and circulation to the vascular endothelium begins with the adhesion of the cell to the vascular endothelium following a sequence of steps including tethering, slow rolling, adhesion strengthening, intraluminal crawling and paracellular and transcellular migration (Ley *et al*., 2007). The expression of P-selectin and E-selectin by damaged or inflamed endothelium and interaction with L-selectin on the neutrophil cell surface initiates the adhesion process.

Further interactions between these selectins and glycoproteins such as P-selectin glycoprotein ligand 1 expressed by the endothelium and leukocytes, stimulates the slow rolling action of selectin mediated neutrophil migration through the formation of new bonds before the breaking of older bonds and the release of L-selectin (Yago *et al*., 2007; Riaz *et al*., 2002; Månnson *et al*., 2000). Neutrophils stop rolling and adhere firmly to the target site by the activation of β-integrins, a member of the family of transmembrane glycoproteins containing both β-chains (CD18) and α-chains

(CD11a-d) that interact with intercellular adhesion molecule (ICAM)-1 and ICAM-2 (Li *et al*., 2004; Thorlacius *et al*., 2000; Springer, 1990; Dustin *et al*., 1986).

The chemotactic gradient influences neutrophil transmigration across the endothelium through the release of endothelial-expressed vascular endothelial cadherin facilitated by platelet endothelial cell adhesion molecule 1 and junctional adhesion molecule-A and migration through the endothelial basement membrane and pericyte sheath occurs through the action of $\alpha_6\beta_2$-integrin and proteases (Ley *et al*., 2007; Springer, 1994).

1.10 Neutrophil Killing Mechanisms

1.10.1 Oxidative Killing Mechanism

Once recruited, neutrophils localize to the site of infection, leading to a change in morphology in response to cytokines, and an increase in oxygen uptake leading to a 'respiratory burst' (Manara *et al*., 1991). Baldridge and Gerard (1933) first described the respiratory burst of the neutrophil defence system, by observing a significant increase in the oxygen consumption of canine neutrophils during phagocytosis of bacteria. Later, NADPH was identified as the natural substrate for the oxidative mechanism of killing invading pathogens facilitated by the action of the enzyme complex, NADPH oxidase (Rossi, 1986) (Figure 1.7).

NADPH is a multicomponent enzyme, with the membrane components of the complex consisting of a stable, heterotrimeric flavocytochrome b_{558} composed of two subunits: $gp91^{phox}$ (also known as Nox2) and $p22^{phox}$ and cytosolic components containing four soluble factors: $p67^{phox}$, $p47^{phox}$, $p40^{phox}$, and a small G-protein Rac (Rac1 and Rac2 isoforms) (Bréchard and Tschirhart, 2008). Cell surface receptor activation by soluble inflammatory mediators such as fMLF results in the translocation of the cytosolic components to the plasma or phagosomal membrane, where NADPH oxidase is assembled leading to the generation of ROS and the release of enzyme products by antimicrobial granules (Sheppard *et al*., 2005; Babior *et al*., 2002; Lambeth, 2000).

The activity of the NADPH oxidase complex is triggered by the exposure of the neutrophil to appropriate stimuli, such as an opsonized particle, leading to an increase of oxygen consumption, phagocytosis and vacuolar closure, and the activation of electron transport across the vacuole wall and formation of superoxide (Karnovsky

and Badwey, 1986; Badwey *et al*., 1980; Babior *et al*., 1973). The oxidative killing mechanism of neutrophils is characterized by the production of ROS facilitated through the action of the membrane bound NADPH oxidase, resulting in the single reduction of oxygen to superoxide anion (O_2^-) (Cornutte *et al*., 1987). Immediately O_2^- dismutates from hydrogen peroxide (H_2O_2) and is involved in the generation of other ROS such as, hydroxyl radical (OH^-) or peroxynitrite as a result of an interaction with nitric oxide (NO) (D'Agostino *et al*., 1998). Reeves *et al*. (2002) have shown that formation of O_2^- functions in the dissociation of sequestered proteins through the use of K^+ ions to compensate for the charge within the vacuole environment and by regulation of pH, the vacuolar pH is optimized in the neutral range for serine protease activity. Thus, the killing action of neutrophils is facilitated by activation of proteases by K^+ flux.

1.10.2 Neutrophil Phagocytosis and the Process of Degranulation

The process of neutrophil phagocytosis begins with opsonization of bacterial particles and recognition by various receptors on the neutrophil membrane, followed by the initiation of a complement cascade through interactions with complement receptors such as CR1 (CD35) and CR3 (CD18/11b) and recognition of the complement factors C3b and C4b (Todd, 1996). The Fcγ receptors, FcγRIIA (CD32) and FcγRIIB (CD16b), function in the recognition of IgG antibodies bound to invading bacteria (Witko-Sarsat *et al*., 2000; Indik *et al*., 1995). Together, FcγRIIA and CR3 are the receptors involved in the activation of phagocytosis (Fossati *et al*., 2002).

Ligand binding induces receptors to initiate complex signaling cascades triggering cytoskeletal rearrangement of globular (G)-actin and filamentous (F)-actin, to form pseudopodia and the engulfing of targeted bacteria within a phagocytic vacuole, known as the phagolysosome, by degranulation (Witko-Sarsat *et al*., 2000).

Antimicrobial peptides are stored in different types of granules and are released either to the phagocytic vacuole or to the outside of the cell in response to soluble stimuli within the surrounding environment. The azurophilic granules (primary granules) contain myeloperoxidase (MPO), serine proteases, and antimicrobial proteins, and are considered as the microbicidal component of the neutrophil upon phagocytosis (Klebanoff, 2005). Later in the granule biogenesis process, specific granules (secondary granules) containing lactoferrin and collagenase develop,

followed by the differentiation of gelatinase granules (tertiary granules) (Uriarte *et al*., 2008; Jethwaney *et al*., 2007; Lominadze *et al*., 2005). Secretory vesicles develop within mature neutrophils and contain plasma proteins such as albumin and act as an internal reservoir of membrane and cytokine receptors (Borregaard *et al*., 2007).

Neutrophil elastase (NE), protease 3, and cathepsin G are found in similar amounts within azurophilic granules of neutrophils (Campbell *et al*., 2000). Along with MPO, these proteases are used against targeted bacteria. MPO in the presence of H_2O_2 produces hypochlorous acid, and NE functions in the cleaving of bacterial proteins inside the phagocytic vacuole and activates MMPs such as MMP-9 that degrades the extracellular matrix during inflammation (Lu and Wahl, 2005; Elkington *et al*., 2005; Ferry *et al*., 1997). Human cathelicidin, associated with the secondary granules of neutrophils, is secreted into extracellular space, releasing IL-8 and mediating the recruitment of neutrophils to a target site (Morioka *et al*., 2008).

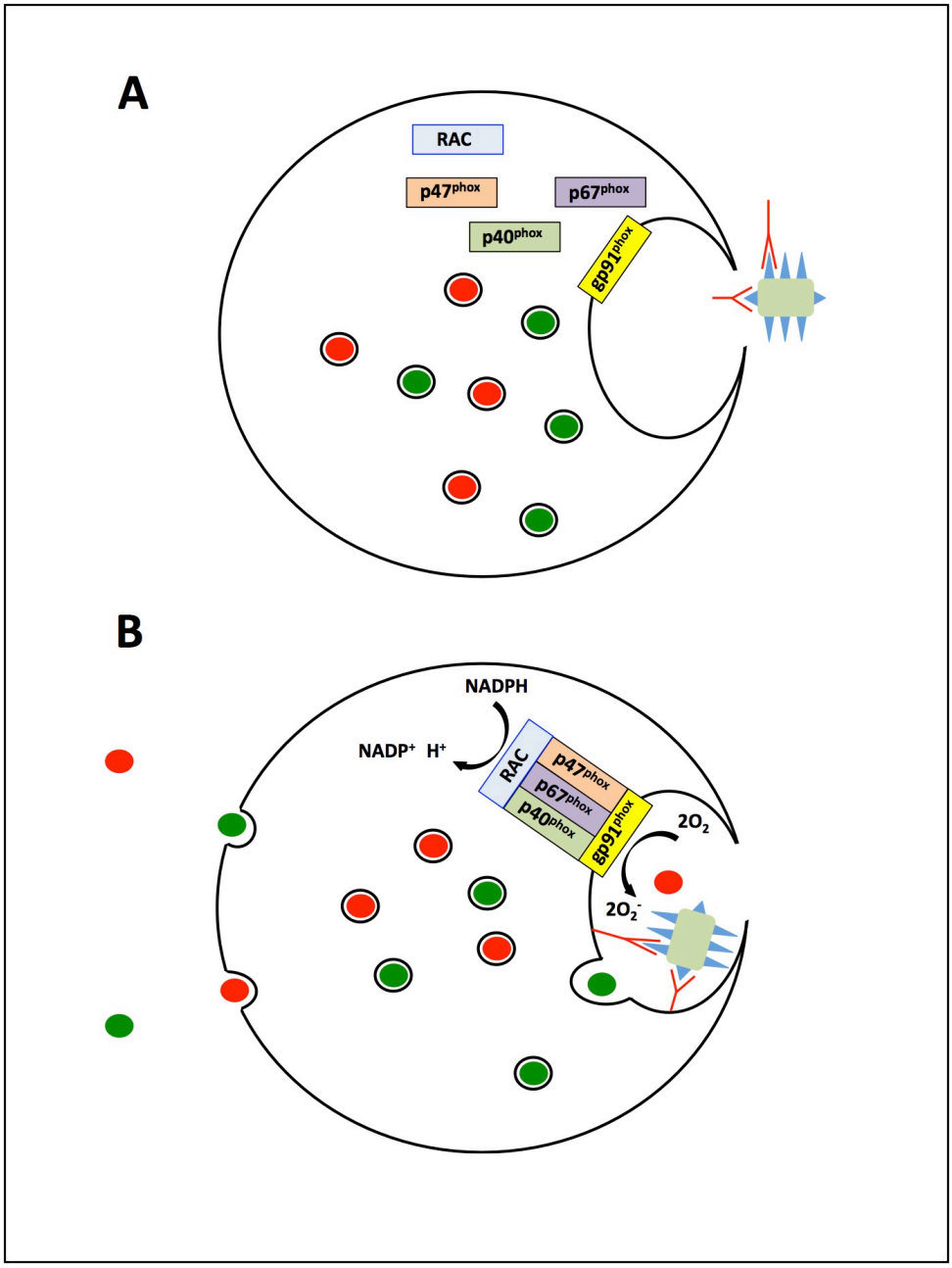

Figure 1.7 Mode of action of neutrophil killing mechanisms. (**A**) Unactivated neutrophil. Microbial pathogen is opsonized for phagocytosis, the NADPH oxidase is non-functional, and antimicrobial peptides are retained in primary (red) and secondary (green) granules intracellularly. (**B**) Activated neutrophil. Phagocytosis of opsonized microbial pathogen, the soluble factors $p40^{phox}$, $p47^{phox}$, $p67^{phox}$, and the G-protein Rac (RAC, Rac1 and Rac2) have translocated from the cytoplasm to bind $gp91^{phox}$ at the cell membrane, and as a result ROS, superoxide anion (O_2^-), is produced from oxygen leading to the conversion of NADPH to $NADP^+$ and H^+. Degranulation has commenced releasing anitmicrobial peptides (red, green) from granules into the phagocytic vacuole and extracellularly. (Adapted from Browne *et al*., 2013).

1.11 Cytokines and the Adaptive Immune Response in Rosacea

Cytokines are small secreted proteins that play an important role in the regulation of the immune response and inflammation, functioning in a pro-inflammatory or an anti-inflammatory capacity, co-ordinating many biological responses (Zhang and An, 2007; Watkins *et al*., 2003; Dinarello, 2000). Following secretion by cells, cytokines can exert their activity in an autocrine fashion (cell signaling self), in a paracrine fashion (cell signaling non-self, neighbouring cell), or in an endocrine fashion (cell signaling non-self, distant neighbouring cell), and can act in a synergistic or antagonistic manner (Zhang and An, 2007; Dinarello, 2000). Cytokines are often pleiotopic, with many cell types secreting the same cytokine or for a single cytokine to act on many cell types (Zhang and An, 2007). However, the dysregulation of cytokines activity can lead to the development of chronic diseases and persistent inflammation (Zhang and An, 2007; Watkins *et al*., 2003; Dinarello, 2000).

Pattern recognition receptors (PRRs) sense a foreign agent, such as a microbial antigen (pathogen-associated molecular patterns (PAMPs)), or following necrosis or cell injury (danger-associated molecular patterns (DAMPs)) that leads to the induction of an adaptive immune response, expansion of T cell populations and the mediation of this response by secretion of cytokines (Iwasaki and Medzhitov, 2015; Chaplin, 2010). The regulation of an adaptive immue response by the innate immune response and secretion of cytokines was first proposed by Janeway (1989). Similarly, dendritic cells are antigen presenting cells that can activate an adaptive immune response (Iwasaki and Medzhitov, 2015).

Commonly secreted pro- and/or anti-inflammatory cytokines include IL-1β, IL-6, and TNF-α, IL-10, and IL-12p40 and these have also been implicated in the process of inducing pathological pain (Watkins *et al*., 2003). Several classes of PRRs have been identified and characterised, and it is widely considered that PRR-mediated sensing initiates the adaptive immune response. These include Toll-like receptors (TLRs), nucleotide-binding oligmerization domain (NOD)-like receptors (NLRs), leucine-rich repeat-containing receptors (LRRs), retinoic acid-inducible gene-1 (RIG-1)-like receptors (RLRs), and C-type lectin receptors (CLRs) (Wu and Chen, 2014; Rathinam *et al*., 2012; Kawai and Akira, 2010) (Figure 1.8).

The synchrony between cytokine secretion, and the adaptive and innate immune systems can be seen when looking at the release of IL-1β. The release of pro-IL-1β is

mediated by the recognition of PAMPs or DAMPs by membrane associated TLR or cytosolic NLR, respectively (Eder, 2009; Watkins *et al*., 1999; Dinarello, 1986, 2011). The binding of TLR ligands, and NLR agonists provides the first signal leading to the release of pro-IL-1β, with a second signal required for the conversion of pro-IL-1β to the active form, IL-1β (Eder, 2009; Watkins *et al*., 1999; Dinarello, 2011, 1986). The second signal involves the cleavage of pro-IL-1β by interleukin-1-converting enzyme (ICE), also known as active caspase-1, triggering the conversion and release of IL-1β, and results in the formation of the caspase-1 inflammasome (Eder, 2009; Ting *et al*., 2008; Agostini *et al*., 2004; Watkins *et al*., 1999; Dinarello, 1986, 2011).

A dysregulation of the immune system, as well as alterations in the vascular network and nervous system, and changes to the integrity of the epidermal skin barrier have been suggested to be implicated in the aetiology of rosacea (Wollina, 2014; Steinhoff *et al*., 2011, 2013; Jarmuda *et al*., 2012; Lacey *et al*., 2009; Yamasaki *et al*., 2007). Currently, the understanding of the adaptive immune response and the mediation of T cells and B cells in rosacea has not been fully elucidated with most research studies focusing on the effects of the vascular system and the role of the innate immune response in the condition (Buhl *et al*., 2015). The involvement of an adaptive immune response and the induction of inflammation have been demonstrated to play a role in many skin pathologies such as acne, psoriasis, and atopic dermatitis (Kelhälä *et al*., 2014; Palau *et al*., 2013; Suárez-Fariñas *et al*., 2013). The role of the adaptive immune response in rosacea has been investigated in a limited number of studies.

Previously, T cells and B cells have been implicated in rosacea following a number of biopsy and histological studies examining cellular infiltrates from rosacea patients (Brown *et al*., 2014; Smith *et al*., 2007; Aloi *et al*., 2000; Rufli and Büchner, 1984). It has been reported that $CD4^+$ T cell populations occur at a higher frequency compared to the number of $CD8^+$ T cells in papulopustular rosacea (Brown *et al*., 2014; Georgala *et al*., 2001). The $CD4^+$ T cell phenotype functions typically as T helper cells (Th) and is associated with immune memory and the mediation of a Th1/Th2 responses, orchestrating the expansion and proliferation of immune cells, and regulating the cellular and humoral immune systems (MacLeod *et al*., 2010; Zhu and Paul, 2008; MacLennan et *al*., 1997).

The skin of rosacea patients is known to contain elevated levels of serine

proteases, cathelicidin (LL-37) and KLK-5, and it has been demostrated that the skin of rosacea patients has incressed expression of TLR-2 (Yamasaki and Gallo, 2011; Yamasaki *et al*., 2007, 2011). Interestingly, the inhibition of KLK-5 has been shown to result in an improvement of the erythema and inflammatory papules associated with rosacea (Two *et al*., 2014). A ligand for TLR-5, flagellin, has also been identified in a study involving human neutrophils stimulated with *B. oleronius* proteins, and this may have a role in the mediation of an adaptive immune response in rosacea (O'Reilly *et al*., 2012a).

Casas *et al*. (2012) quantified *D. folliculorum* mite colonisation in erythematotelangiectatic rosacea and papulopustular rosacea patients using a molecular based PCR technique. The authors also investigated the activation of a skin innate immune response, and demonstrated that genes coding for IL-8, IL-1β, TNF-α, and Cox-1 were increased following examination of facial skin swabs and epidermal scrapings of rosacea patient skin lesions, and observed an increase in the expression for genes coding for the inflammasome. Recently, Buhl *et al*. (2015) characterised an adaptive immune response in erythematotelangiectatic, papulopustular, and phymatous rosacea demonstrating that the activation of Th1/Th17 pathways resulted in an up-regulation of interferon (INF)-γ and IL-17, and increased macrophage infiltration. Thus, further studies are needed to fully understand the role of the adaptive immune response in the induction and persistence of inflammation in the condition.

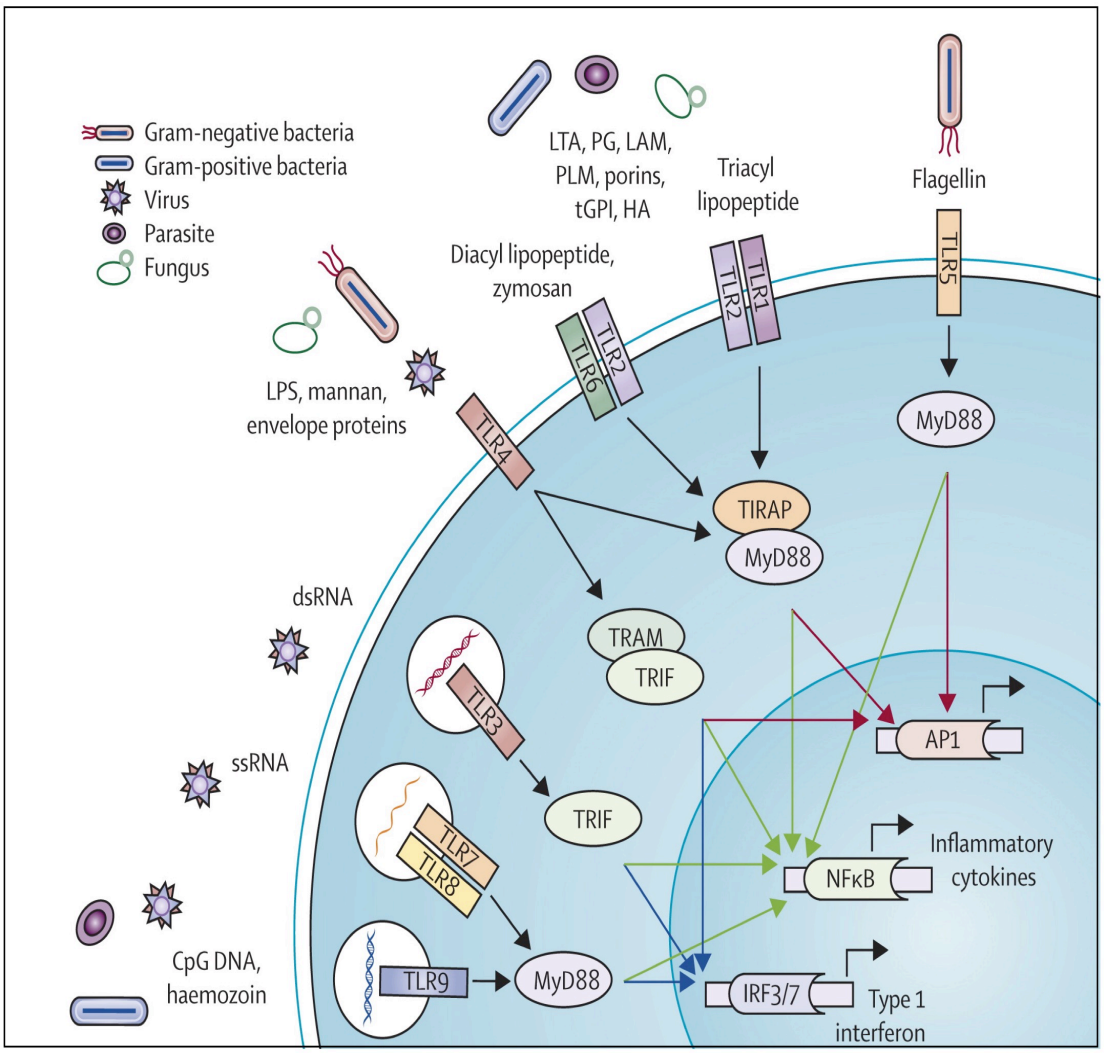

Figure 1.8 Toll-like receptor (TLR) signaling pathways. TLR-2 and TLR-5 have previously been implicated to have a role in the induction of rosacea. (Adapted from Bochud *et al*., 2007).

1.12 Proteomics and Label-Free Mass Spectrometry (LF/MS)

Mass spectrometry (MS)-based proteomics has been shown to be an invaluable technique for studying both the molecular and cellular aspects in systems biology. Many features of proteins to consider such as expression, localization, interaction, domain structure, post-translational modification, and activity add to the complexities involved in a proteomics study but with the increased availability of completed genome sequences and databases, and improved analytical software, the uneviable task of gathering, sorting, and interpreting the large volume of proteomic data has lead to an increase in both the applicability and popularity of an MS-based proteomic technique (Han *et al*., 2008; Aebersold and Mann, 2003). The three main applications of MS in the field of proteomics include listing protein expression, defining protein interactions, and the identification of proteins and sites of protein modifications (Han *et al*., 2008).

MS is a measurement of the mass-to-charge (*m*/*z*) ratio of gas-phase ions. Mass spectrometers are composed of an ion source that converts analyte molecules into gas-phase ions, and a mass analyzer separates the ionized analytes on the basis of *m*/*z* ratio with a detector recording the number of ions at each *m*/*z* value (Michalski *et al*., 2011; Han *et al*., 2008; Aebersold and Mann, 2003). The devlopment of electrospray ionization (ESI) and MALDI, allowed for the ionization of peptides and protein, changing proteomic analyses and advancing MS technology (Fenn *et al*., 1989; Karas and Hillenkamp, 1988). The mass analyzer has been described as the central component of MS technology (Han *et al*., 2008; Aebersold and Mann, 2003). Four types of mass analyzers are available and can be used individually or in combinations as part of a hybrid instrument, thus increasing the capabilites of the mass spectrometer (Han *et al*., 2008). The mass analyzers used include quadrupole mass filter, ion trap (QIT: quadrupole ion trap; LIT or LTQ: linear ion trap), time-of-flight (ToF) mass analyzer, and Fourier-transform ion cyclotron resonance (FTICR) mass analyzer (Han *et al*., 2008; Domon and Aebersold, 2006; Yates, 2004).

The invention of a new type of mass analyzer, the Orbitrap™ revolutionised the field of proteomics (Hu *et al*., 2005; Makarov, 2000). In the Orbitrap™, ions are trapped as they orbit around a central spindle-like electrode that oscillates in harmonic frequency along the axis of *m*/*z* values, which results in an image current in the outer electrodes that is Fourier transformed into a time domain producing a mass spectra (Han *et al*., 2008; Makarov *et al*., 2006; Hardman and Makarov, 2003; Makarov,

2000). In turn, the use of an Orbitrap™ mass analyzer has allowed for the evolution of more powerful commercially available mass spectrometer instruments that have increased resolution, and are capable of analyzing complex protein samples, and this has been demonstrated in numerous studies (Patel *et al*., 2009; Venable *et al*., 2007; Makarov *et al*., 2006; Yates *et al*., 2006; Macek *et al*., 2006).

For the purpose of this thesis, a benchtop Q Exactive™ hybrid Quadrupole-Orbitrap™ mass spectrometer (Thermo Fisher Scientific GmbH, Bremen, Germany) was used to investigate the proteome of hTCEpi cells exposed to *B. oleronius* proteins in a label-free mass spectrometry study. The term 'Exactive' describes the capability of the instrument to analyse small molecules (Michalski *et al*., 2011). The combination of a quadrupole mass filter with a Orbitrap™ mass analyzer allows for an almost instantaneous separation and selection of ions, followed by fragmentation into peptides, and high resoultion analyses in MS and tandem mass spectrometry (MS/MS) ranges (Michalski *et al*., 2011; Geiger *et al*., 2010). The MS spectra data were analysed using MaxQuant with the integrated Andromeda search engine to identify and quantify proteins using methods previously described (Cox *et al*., 2011; Cox and Mann, 2008).

Quantitative-based proteomics has been the basis of many studies taking a global approach to investigate differential protein expression to characterise cellular changes in biological samples, and to identify biomarkers for disease (Griffin *et al*., 2010; Chiang *et al*., 2007; Oh *et al*., 2004, 2007; Shiio *et al*., 2002, 2006). Several challenges remain for the use of a label-free mass spectrometry based experimental approach, such as the quantitation based on the peptide ion peak area measurement, the alignment of chromatograms, the paramaters for peptide quantitation, and normalization (Lai *et al*., 2013). However, it is acknowledged that these challenges can be overcome and that in line with the development of new innovative technology, a label-free approach is a viable option compared to a labelling approach such as isobaric tags for relative and absolute quantitation (iTRAQ) (Michalski *et al*., 2011; Ross *et al*., 2004).

1.13 Aims of Study

The aims of this project were as follows:

1. To investigate the effect of different culture conditions on the *B. oleronius* proteome, and on the expression of the 62 kDa immuno-reactive protein.

2. To isolate and purify *B. oleronius* proteins by ÄKTA FPLC™ for use in further assays involving corneal epithelial (hTCEpi) cells, neutrophils, or peripheral blood mononuclear cells (PBMC).

3. To characterise the effect of *B. oleronius* protein exposure on a corneal epithelial (hTCEpi) cell line and the implications for ocular rosacea.

4. To examine the effect of *B. oleronius* proteins on stimulated neutrophils by the IP_3 pathway of activation.

5. To investigate the cytokine secretion profile of PBMC exposed to *B. oleronius* proteins by ELISpot and/or FlouroSpot assay techniques.

6. To determine the role of *B. oleronius* proteins in erythematotelangiectatic rosacea, ocular rosacea, and *Demodex*-related blepharitis.

Chapter 2

Materials and Methods

2.0 Materials and Methods

2.1 Chemicals and Reagents

All chemicals and reagents were of the highest purity and quality. Unless ortherwise stated chemicals were purchased from Sigma-Aldrich Chemical Co. Ltd. (Dorset, UK). Buffers were prepared using distilled water (dH_2O), and purified using a Millipore-Q apparatus (Millipore, Merck Millipore, Cork, Ireland).

2.2 Sterilisation Procedure

Sterilisation of all equipment, media and buffers was achieved by autoclaving at 121°C with 15 lb per square inch of pressure for 15 minutes. Any chemical or reagent that was unsuitable for autoclaving was filter sterilised using 0.2 μm or 0.45 μm cellulose pore filter discs (Millipore) before use.

2.3 Statistical Methods

The statistical significance was assessed using GraphPad Prism version 5.00 for Mac OS X, GraphPad Software, San Diego California, USA, www.graphpad.com. All experiments were performed on three independent occasions and results presented are given as the mean ± standard error (SE). Statistical tests performed to assess significance were dependent on the distribution of the data, and the data being analysed. Statistical tests used were the Chi-square test, the Student's *t*-test, the Wilcoxon matched-pairs signed rank *t*-test, and one-way ANOVA. A p-value of $p < 0.05$ (*), $p < 0.01$ (**) or $p < 0.001$ (***) were considered statistically significant.

2.4 Study Populations

2.4.1 Erythematotelangiectatic Rosacea Study

Seventy-five erythematotelangiectatic rosacea patients (42 female and 33 male), Fitzpatrick skin phototypes I or II, aged 20-81 years, hospitalized between 01/02/2011 and 16/12/2011 at the Dermatology Clinic, Poznań University of Medical Sciences or treated at the out-patient Dermatology Clinic, were enrolled in the study. Mean age of rosacea patients was 47.07 years (females: 44.95, males: 49.76). Patients did not receive any oral antibiotics, retinoids, glucocorticosteroids, or sulfones for at least 3 months before recruitment to the study.

Fifty-two volunteers (29 female and 24 male), aged 18-89 years constituted the control group. Mean age of the controls was 46.26 years (females: 47.45, males: 44.83). Fourteen volunteers (8 females and 6 males), aged 15-29 years formed the acne vulgaris group with a mean age of 22.93 years (females: 23.75, males: 21.83). The seborrheic dermatitis group consisted of nine volunteers (5 female and 4 male), aged 22-45 years with a mean age of 30.11 (females: 29.4, males: 26.0). The study was approved by the Bioethics Committee of the Poznań University of Medical Sciences (546/10, 17. 06. 2010).

Anamnesis, physical examination and additional tests were performed for all patients. Before enrollment all patients and controls were informed about the nature and the aim of the study and gave their written informed consent. The diagnosis of rosacea was made on the basis of the anamnesis and physical examination. A standard classifications system, published by the National Rosacea Society (NRS), was used in the process of the diagnosis and classification of rosacea subtypes.

2.4.2 Ocular Rosacea Patients (Subtype IV Group) and Ocular Rosacea Patients with Erythematotelangiectatic Rosacea (Subtype I & IV Group) Study

Eighteen consenting volunteers (5 female and 13 male) with an age range between 21-70 years and a mean age of 46.66 years, were recruited for a study to investigate the effect of *B. oleronius* proteins on the cytokine response of isolated PBMC, monocytes and T cells, in collaboration with the Royal Victoria Eye and Ear Hospital (RVEEH) Dublin, Ireland, and Mabtech AB, Nacka Strand, Stockholm, Sweden. Ethical approval for the isolation of human PBMC was approved by the NUIM and RVEEH ethics committee (ref number BSRESC-2012-008). Rosacea patients were clinically diagnosed before enrolment to the study. The volunteers consisted of three groups of 6 volunteers. The control group contained 2 female and 4 male, with an age range between 29-70, and a mean age of 49.7 years. The ocular rosacea group (subtype IV group) consisted of 1 female and 5 male, with an age range between 21-69, and a mean age of 48.8 years. The ocular rosacea with erythematotelangiectatic rosacea group (subtype I and IV group) consisted 2 female and 4 male, with an age range between 27-52 years, and a mean age of 42.2 years.

2.4.3 *Demodex*-Related Blepharitis Study

Seventy consenting volunteers (47 female and 23 male) with an age range between 6-37 years and a mean age of 21.5 years, were recruited for a study to investigate a correlation between blepharitis, *Demodex* infestation, and reactivity of patient sera to *B. oleronius* proteins in collaboration with Dr Lingyi Liang of Zhongshan Opthalmic Center, Sun Yat-sen University Guangzhou, China and Dr Scheffer Tseng of Ocular Surface Center, Miami, Florida, USA. Ethical approval for the study was granted by the Sun Yat-sen University Guangzhou ethics committee (ref number 020-87334825). The volunteers consited of three groups. Group 1 were clinically diagnosed with blepharitis and *Demodex* mite infestation, and contained 37 participants (26 female and 4 male), with an age range between 6-37, and a mean age of 19.9 years. Group 2 were clinically diagnosed with *Demodex* mite infestation and blepharitis-negative, consisted of 17 volunteers (14 female and 3 male), with an age range between 12-35, and a mean age of 25.4 years. Group 3 were clinically diagnosed with *Demodex* mite infestation-negative and blepharitis-negative, and constituted 16 volunteers (7 female and 9 male), with an age range between 6 – 31 years, and a mean age of 21.2 years.

2.5 Bacterial Cell Culture Media

2.5.1 Nutrient Agar Medium

A solution of nutrient agar medium was prepared by dissolving nutrient agar (Oxoid Ltd., Thermo Fisher Scientific, Basingstoke, Hampshire, UK) (28 g/L) by stirring in 1 L of dH_2O. The solution was autoclaved, and allowed to cool until the molten agar was hand hot before pouring under sterile conditions into 9 cm petri dishes (Greiner Bio-One GmbH, Frickenhausen, Germany). The nutrient agar plates were allowed to dry fully and stored at 4°C until needed.

2.5.2 Nutrient Broth Medium

A solution of nutrient broth medium was prepared by dissolving nutrient broth (Oxoid Ltd.) (13 g/L) by stirring in 1 L of dH_2O. The solution was autoclaved and stored at room temperature until needed. For studies involving an investigation of the effect of pH, the pH of the medium was adjusted to pH 6, 7, or 8 accordingly, before autoclaving and storage.

2.5.3 2X Yeast Tryptone (YT) Broth Medium

A solution of 2X yeast tryptone (2X YT) broth medium was prepared by dissolving tryptone (Oxoid Ltd.) (16 g/L), yeast extract (Oxoid Ltd.) (10 g/L) and NaCl (5 g/L) by stirring in 1 L of dH_2O. The solution was autoclaved, and stored at room temperature until needed. For studies involving an investigation of the effect of pH, the pH of the medium was adjusted to pH 6, 7, or 8 accordingly, before autoclaving and storage.

2.6 Phosphate Buffered Saline (PBS) (pH 7.4)

A solution of phosphate buffered saline (PBS) (pH 7.4) was prepared by dissolving PBS tablets (1 tablet per 100 ml dH_2O) in the required volume of dH_2O. The PBS solution was autoclaved and stored at room temperature before use.

2.7 Bacterial Cell Culture Conditions

Cultures of *B. oleronius*, a bacterial strain isolated from the hindgut of a *D. folliculorum* mite of a patient with papulopustular rosacea, were maintained by spreading or streaking colonies onto a nutrient agar plate, with sub-culturing onto freshly prepared nutrient agar plate taking place every 6 to 8 weeks (Lacey *et al*., 2007; Delaney, 2004). From these nutrient agar plates, liquid cultures were aseptically inoculated with one loopful of *B. oleronius* colonies and cultured overnight in an incubator to stationary phase of growth in nutrient broth (pH 7) medium (100 ml) under aerobic (shaking) conditions at 30°C. For experiments involving an evaluation of the proteomic expression profile of the *B. oleronius* under varying environmental conditions, 1 ml of culture was taken from the overnight culture and aseptically added to a fresh culture medium (100 ml).

The environmental conditions examined as part of this research study were as follows: nutrient availability (nutrient broth medium, a nutrient poor environment, or 2X YT broth medium, a nutrient rich environment); pH (medium adjusted to pH 6, pH 7, or pH 8); temperature (30°C, as this is the optimum temperature for *Demodex* mite movement, and 37°C, as this represents body temperature); oxygen availability (cultures were incubated under aerobic or anaerobic conditions with shaking (orbital incubator set to 160 – 180 revolutions per minute (rpm)) or static settings employed, respectively); reactive oxygen species (ROS) (10 mM hydrogen peroxide (H_2O_2) was added to culture medium 4 hour prior to cell harvesting (hour 44 of culture) (indicated

by an arrow in Figures)). All cultures were incubated for 48 hour under the varying environmental conditions described before cell harvesting and protein extractions were performed (Section 2.12.1).

2.8 Glycerol Stocks of *B. oleronius* Cultures

An overnight liquid culture of *B. oleronius* (500 µl) was added to 500 µl of sterile glycerol, and stored at -80°C.

2.9 *Bacillus* Lysis Buffer (pH 7.2)

The *Bacillus* lysis buffer (pH 7.2) was prepared by dissolving piperazine-*N,N*'-bis (2-ethanesulfonic acid) (PIPES) (20 mM), and sodium chloride (NaCl) (5 mM) in dH_2O with stirring, and the pH of the solution was adjusted to pH 7.2 before autoclaving. The non-ionic surfactant, Triton™ X-100 (0.2%, v/v) was added to the solution under aseptic conditions. The lysis buffer was aliquoted into 50 ml universals (Falcon©, Corning Inc., Corning, NY, USA) and stored at 4°C before use. Protease inhibitors (10 µg/ml leupeptin, pepstatin A, aprotinin, and N-a-p-tosyl-L-lysine chloromethyl ketone hydrochloride (TLCK)) and phosphatase inhibitors (phosphatase inhibitor cocktail 2) were added to the *Bacillus* lysis buffer (pH 7.2) on the day of cell harvesting prior to the 4°C cell lysis incubation step. A list of the phosphatase inhibitors used as part of the phosphatase inhibitor cocktail 2 are given in Table 2.1.

Table 2.1 List of phosphatase inhibitors. A list of the phosphatase inhibitors present in the phosphatase inhibitor cocktail 2, added to the *Bacillus* lysis buffer (pH 7.2), and used during protein extractions.

Phosphatase	Inhibitor
Alkaline Phosphatase	Imidazole ($C_3H_4N_2$)
Acid Phosphatase	Sodium Molybdate (Na_2MoO_4), Sodium Tartrate ($C_4H_4Na_2O_6$)
Phosphotyrosyl Phosphatases (PTPs) (general inhibitor)	Sodium Orthovanadate (Vandate, Na_3VO_4)

2.10 Enzymatic Activity of *B. oleronius* Under Varying Environmental Conditions

2.10.1 Analysis of Lipase Activity

The analysis of lipase activity present in *B. oleronius* cultures under varying environmental conditions was assessed using tributyrin agar. The tributyrin agar was prepared by the addition of 20 g tributyrin agar (special peptone (5 g/L), yeast extract (3 g/L), and agar (12 g/L) at pH 7.5) in 1 L of dH_2O. The agar was mixed using a magnetic stir bar, followed by autoclaving. When the tributyrin agar had cooled sufficiently (approximately 80°C), the agar was supplemented with glyceryl tributyrate (10 g/L), the agar was mixed, and inspected to ensure against the emulsification of lipids within the agar before the pouring of 9 cm tributyrin agar plates under aseptic conditions. The agar plates were allowed to dry completely, and 4 gel plugs (wells) were excised from the solidified agar medium of each plate, and labeled accordingly. Bacterial cell superantants (100 µl), and separately, cell lysates in a volume of 100 µl at a concentration of 10 µg/ml were pipetted into the excised wells of the tributyrin agar plates under aseptic conditions, and incubated at 37°C for 12 hours. A blank for the assay was culture medium (100 µl) for cell superantants, and PBS (pH 7.4) (100 µl) for cell lysates. The clear zone of lipolytic activity surrounding the *B. oleronius* culture sample was measured (mm^2) to analyse lipase activity for each environmental condition in otherwise turbid culture medium.

2.10.2 Analysis of Catalase Activity

The analysis of catalase activity present in *B. oleronius* cultures under varying environmental conditions, was achieved by following the method previously described by Larsen and White (1995) with slight modifications. Bacterial cell lysates (10 µg) in volume of 100 µl were added to 17 mM hydrogen peroxide (H_2O_2) (1.8 ml) in a sterile tube. Each sample was thoroughly mixed by pipetting, and left to incubate at room temperature for 15 minutes. The formation of oxygen bubbles in the sample is an indicator of catalase activity. Following the incubation time, the suspension was centrifuged at 10,000 x *g* for 1 minute to stop the reaction. The supernatant was transferred to a 1 ml quartz cuvette (pre-rinsed with ethanol (70%, v/v), and HPLC grade H_2O). The absorbance was measured at 240 nm wavelength, using a UVmini-1240, UV-VIS spectrophotometer (Shimadzu, Mason Technology, Co.

Dublin, Ireland). A blank for the assay consisted of 17 mM H_2O_2, and the fold change of catalase activity of the *B. oleronius* cultures under varying environmental conditions was calculated and expressed as a percentage (%) relative to the positive control, *B. subtilis*.

2.11 General Protein Methodology

2.11.1 Bradford Protein Assay

Bovine serum albumin (BSA) protein standards (2 – 0.125 mg/ml) were prepared in 800 µl of dH_2O, and added to 200 µl Bradford protein assay reagent (Bio-Rad Laboratories, Inc. Hercules, CA, USA) to provide a standard curve using a spectrophotometer (Eppendorf Biophotometer) at 595 nm. The Bradford protein assay reagent was prepared by diluting the Bio-Rad protein assay dye reagent concentrate stock solution (Bio-Rad Laboratories), 1 : 5 with dH_2O to give a working solution which was kept at 4°C. Protein samples (20 µl) were added to 980 µl of Bradford protein assay reagent, placed into a 1 ml cuvette (Sarstedt AG & Co., Nümbrecht, Germany), inverted, and allowed to stand for 5 minutes at room temperature, before the protein concentration was read spectrophotometrically. The unknown protein concentration was determined using the BSA protein standard curve, a representative BSA protein standard curve is given in Figure 2.1.

2.11.2 Acetone Precipitation of Protein Samples

Acetone precipitation was employed to concentrate protein from a dilute sample. The required volume for a specific quantity of protein was calculated following a Bradford protein assay (Section 2.11.1). Into a sterile micro-centrifuge tube, the protein volume calculated and, three times the volume of ice-cold acetone (100%, v/v) added (at a ratio 1 : 3, protein volume : acetone), and placed at -20°C for a minimum of 2 hours or overnight. Acetone was separated from precipitated protein samples by centrifugation at 20,000 x *g* for 30 minutes at 4°C. The acetone was discarded, and the protein pellet was allowed to air dry before preparation for 1-D or 2-D SDS-PAGE (Section 2.14 and Section 2.15, respectively).

2.11.3 5X Solubilisation Buffer for Protein Sample Loading

A 5X solubilisation buffer solution was prepared by dissolving glycerol (8 ml), 0.5 M tris – HCl (pH 6.8) (1 ml), SDS (10%, w/v) (1.6 ml), bromophenol blue (0.5%, w/v) (200 µl), 2-mercaptoethanol (400 µl) in 4 ml of dH_2O. The constituents of the 5X solubilisation buffer were mixed thoroughly by stirring and aliquoted into 500 µl volumes prior to storage at -20°C.

2.12 Protein Extraction Protocol

2.12.1 Protein Extraction from *B. oleronius* Cultures

Cultures of *B. oleronius* were inoculated and set up under varying environmental conditions as described in Section 2.7. Following a 48 hour culture period, cell cultures were aseptically transferred into sterile 50 ml Universals (Falcon©), and harvested by centrifugation at 2,000 x *g* for 20 minutes at room temperature (Beckman GS-6 Centrifuge, Beckman Coulter Inc., Naas, Co. Kildare, Ireland) to pellet the bacterial cells. The supernatant was discarded, and the cells were washed with sterile PBS (pH 7.4) (Section 2.6) twice, and centrifuged at 2,000 x *g* for 15 minutes at room temperature each time. Cells were re-suspended in the *Bacillus* lysis buffer (pH 7.2) supplemented with protease and phosphatase inhibitors (Section 2.9), and incubated at 4°C for a minimum of 1 hour, on a tube rotary wheel (Stuart Rotator SB2, Bibby Scientific Limited, Staffordshire, United Kingdom). The volume of *Bacillus* lysis buffer (pH 7.2) used was dependent on the size of the cell pellet harvested (approximately 1 ml *Bacillus* lysis buffer (pH 7.2) per 100 ml cell culture).

Following the cell lysis, the protein suspension was obtained by centrifuging cell lysates at 6,000 x *g* for 2 minutes at 4°C (Eppendorf Centrifuge 5418, Eppendorf AG, Hamburg, Germany). The supernatant containing extracted proteins was transferred to a sterile 1.7 ml tube, and the protein concentration was quantified using a Bradford protein assay (Section 2.11.1). Protein samples (20 µg) were acetone precipitated (Section 2.11.2) when necessary, or alternatively 5X solubilisation buffer (Section 2.11.3) was added directly to the extracted protein, and boiled for 5 minutes at 90°C on a heating block before sample loading onto 1-D SDS-PAGE gel (Section 2.14.8). All protein sample preparations were stored at -20°C until required.

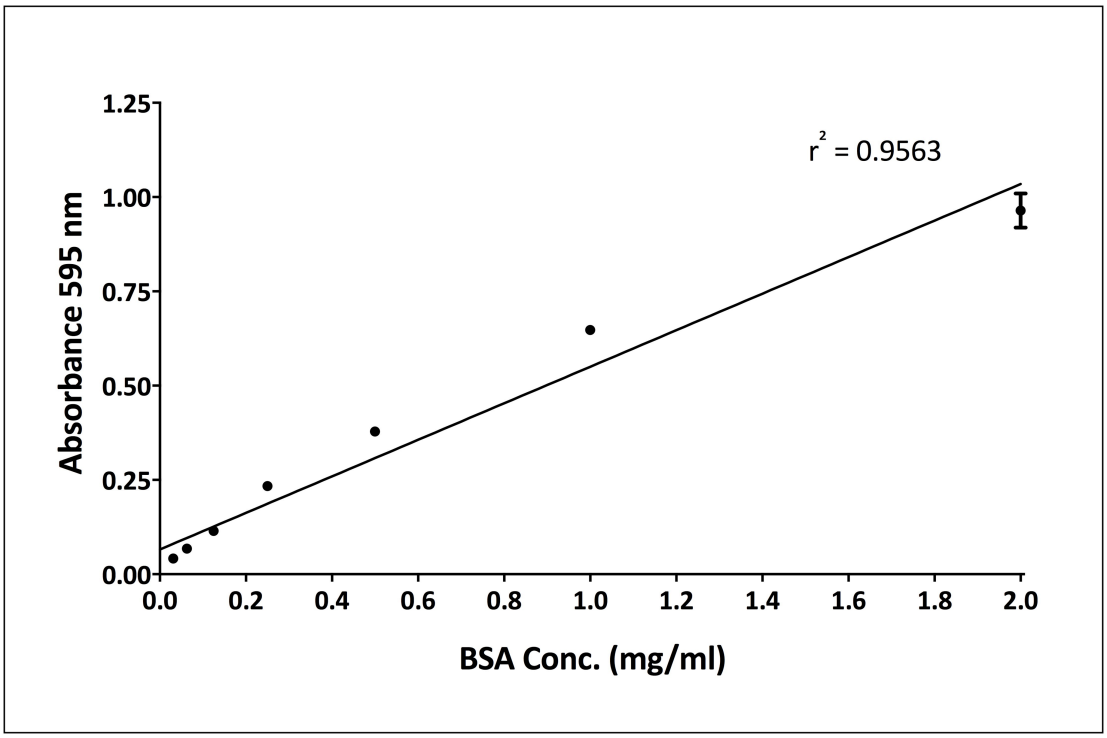

Figure 2.1 A representative standard curve of BSA protein for Bradford assay. A representative standard curve of known concentrations of BSA used to determine the concentration of unknown protein (2 – 0.125 mg/ml).

2.12.2 Protein Extraction from hTCEpi Cell Cultures

Corneal epithelial cells (human telomerase-immortalized corneal epithelial cells (hTCEpi)) were exposed to BSA (2 µg/ml), crude *B. oleronius* proteins (2 µg/ml), or pure *B. oleronius* proteins (2 µg/ml), for 24 hour and 72 hour before cells were harvested by trypsinization (trypsin (0.25%, w/v)-EDTA (0.022%, w/v) in PBS) for 5 minutes. Cells were washed twice in sterile PBS to wash cells and remove media. Protease inhibitors (leupeptin, aprotinin, pepstatin A, TLCK) were added at a concentration of 10 µg/ml to lysis buffer (pH 7.2) (piperazine (20 mM), NaCl (5 mM), Triton™ X-100 (0.2%, v/v), pH 7.2) prior to use, and cells were lysed for 1 hour at 4°C. After lysis, cells were centrifuged at 6000 x *g* for 2 minutes, and soluble proteins (cell supernatant) were collected, and stored at -20°C. Protein concentrations were determined by Bradford assay (Section 2.11.1), acetone precipitated (Section 2.11.2), and proteins were resolved by one-dimensional sodium dodecyl sulphate–polyacrylamide gel electrophoresis (1-D SDS–PAGE), and 2-D SDS–PAGE (Section 2.15). Visualisation was achieved by staining with colloidal Coomassie blue (Section 2.16), and gel pieces of interest were excised and trypsin digested as described by Shevchenko *et al*. (2006) to identify proteins by liquid chromatography-mass spectrometry (LC-MS) (Section 2.17).

2.13 Trypan Blue Cell Exclusion Assay for Cell Counting

Cell counts for assays involving corneal epithelial cells (hTCEpi), and isolated human neutrophil cells were achieved by performing a trypan blue cell exclusion assay (Eichner *et al.,* 1986). A cell suspension (20 µl) was diluted with a trypan blue solution (0.4%, w/v) (60 µl), and PBS (pH 7.4) (20 µl) at a ratio of 1 : 5. An aliquot of this mixture was counted using a haemocytometer (Neubauer improved cell counting chamber, haemocytometer). The number of cells stained, and unstained were recorded. From here, cells that excluded trypan blue were deemed viable, the percentage (%) cell viability was calculated, and the cell count per ml of the cell suspension solution was obtained.

2.14 1-D Sodium Dodecyl Sulphate-Polyacrylamide (SDS-PAGE) Gel Electrophoresis

2.14.1 0.5 M Tris – HCl (pH 6.8)

A solution of 0.5 M Tris-HCl (pH 6.8) was prepared by dissolving 12.1 g trizma base in 150 ml of dH_2O by stirring, and adjusted to pH 6.8 before the final volume was brought to 200 ml with dH_2O. The solution was autoclaved and stored at 4°C until needed.

2.14.2 1.5 M Tris – HCl (pH 8.9)

A solution of 1.5 M Tris-HCl (pH 8.9) was prepared by dissolving 36.3 g trizma base in 150 ml of dH_2O by stirring, and adjusted to pH 8.9 before the final volume was brought to 200 ml with dH_2O. The solution was autoclaved and stored at 4°C until needed.

2.14.3 Sodium Dodecyl Sulphate (SDS) (10%, w/v)

Sodium Dodecyl Sulphate (SDS) (10%, w/v) was prepared by dissolving 10 g SDS in 100 ml of dH_2O by stirring, and stored at room temperature.

2.14.4 Ammonium Persulphate (APS) (10%, w/v)

Ammonium Persulphate (APS) (10%, w/v) was prepared by dissolving 0.1 g APS in 1 ml of dH_2O. The solution was vortexed to ensure a homogenous mixture, and made fresh each time for the casting of 1-D and 2-D sodium dodecyl sulphate-polyacrylamide gel electrophoresis (SDS-PAGE).

2.14.5 Sodium Dodecyl Sulphate-Polyacrylamide Gel Electrophoresis (SDS-PAGE)

Stacking gel (5%) and separating gel (12.5%) mixtures and reagents for one 12.5% bis-acrylamide SDS-PAGE mini-gel are described in Table 2.2. APS (10%, w/v) (Section 2.14.4), and tetramethylethylenediamine (TEMED) were added to the gel mixture last, as these constituents catalyse the polymerization of the 5% stacking and 12.5% separating gels. The volumes were adjusted accordingly depending on the size and number of gels required.

2.14.6 10X Electrode Buffer (pH 8.9)

A 10X electrode buffer (running buffer) (pH 8.9) stock solution was prepared by dissolving tris – base (30 g/L), glycine (144 g/L), and SDS (1%, w/v) (10 g/L) in 1 L of dH_2O by stirring until a homogenous mixture was achieved. The solution was stored at room temperature until needed.

Table 2.2 Reagent volumes for the preparation of 12.5% Bis-acrylamide SDS-PAGE mini-gels. Stacking gel (5%) and separating gel (12.5%) mixtures and reagents for one 12.5% Bis-acrylamide SDS-PAGE mini-gel. The volumes were adjusted accordingly depending on the size and number of gels required.

Reagent	5% Stacking Gel Volumes	12.5% Separating Gel Volume
1.5 M Tris-HCL (pH 8.9) (ml)	-	3
0.5 M Tris-HCL (pH 6.8) (ml)	0.63	-
ProtoGel© (30%, w/v) Bis-Acrylamide (ml)	0.83	5
dH_2O (ml)	3.4	3.8
SDS (10%, w/v) (µl)	50	120
APS (10%, w/v) (µl)	50	75
TEMED (µl)	5	3

2.14.7 1X Electrode Buffer (pH 8.9)

A 1X electrode buffer (running buffer) (pH 8.9) working solution was prepared by adding 100 ml of 10X electrode buffer (pH 8.9) stock to 900 ml of dH_2O. The buffer was mixed thoroughly prior to use and was stored at room temperature.

2.14.8 Casting and Electrophoresis of 1-D SDS-PAGE Gels

Glass plates (Bio-Rad Laboratories) (1.0 mm) were cleaned using ethanol (70%, v/v) prior to placement in a gel casting rig (Mini-Protean II gel casting apparatus, Bio-Rad Laboratories), and were made of acrylamide with 12.5% bis-acrylamide in all experiments. The 12.5% separating gel solution was prepared as described in Table 2.2, and poured between the plates using a 3.5 ml transfer pipette (Sarstedt) and a

layer of SDS (0.1%, v/v) was sprayed on top of the gel to ensure the gel was straight and to remove air bubbles. The gel was allowed to polymerize for approximately 30 minutes at room temperature before the SDS (0.1%, v/v) was removed using Whatman™ filter paper (GE Healthcare, Life Sciences). If excess SDS (10%, v/v) remained on the top layer of the separating gel, it was washed with dH_2O, and Whatman™ filter paper (GE Healthcare, Life Sciences) was used to remove any excess SDS (10%, v/v) and dH_2O. The 5% stacking gel solution was prepared as described in Table 2.2, and poured on the top layer of the polymerized 12.5% separating gel using a 3.5 ml transfer pipette, and a 10-toothed comb was inserted into the gel matrix to cast the wells needed for sample loading onto the gel.

The stacking gel was given time to set (approximately 15 minutes), and placed in either a Mini-Protean® 3 Cell gel rig (Bio-Rad Laboratories) (x 2 gels) or a Mini-Protean® Tetra Cell gel rig (Bio-Rad Laboratories) (x 4 gels). The 12.5% SDS-PAGE gels were immersed with 1X electrode buffer (pH 8.9) (Section 2.14.7) within the gel rig, and the 10-toothed comb was removed carefully. A pre-stained protein marker (6-175 kDa, New England Biolabs, Hertfordshire, UK) (10 µl) was run in the first lane of each gel to identify the molecular weights of the protein bands. Protein samples re-suspended in 5X solubilisation buffer (Section 2.11.3) were boiled for 5 minutes at 90°C on a heating block to denature proteins, and 20 µl of sample (20 µg) was loaded into each well. Proteins were resolved at 60 volts (V), and using a power-pac 300 (Bio-Rad Laboratories) until the protein had sufficiently travelled through the stacking gel matrix, and the voltage was increased to 100 V until the blue tracking dye had moved to approximately 1 cm from the bottom of the separating gel. The stacking gel was carefully removed and discarded, and the separating gel was placed into a clean 15 cm petri-dish for staining (Section 2.16).

2.15 2-D SDS-PAGE Gel Electrophoresis

2.15.1 Isoelectric Focusing (IEF) Buffer

Isoelectric focusing (IEF) buffer was prepared by dissolving urea (8 M), 2 M thiourea, 3-[(3-cholamidopropyl)dimethylammonio]-1-propanesulfonate (CHAPS) (4% w/v), Triton™ X-100 (1% v/v), and tris-HCl (10 mM) in dH_2O. The solution was aliquoted into 1 ml volumes, and stored at -20°C. Carrier ampholytes, immobilised pH gradient (IPG) buffer (pH 4 – 7 L) (0.8%, v/v) (GE Healthcare, Life Sciences),

and a reducing agent, DTT (65 mM) were added to the defrosted aliquots of IEF buffer on the day required, and allowed to stand at room temperature for 15 minutes before the addition of a few grains of bromophenol blue sodium salt to the solution as a tracking dye during electrophoresis.

2.15.2 Isoelectric Focusing Equilibration Buffer (pH 6.8)

Isoelectric focusing equilibration buffer (pH 6.8) was prepared by dissolving glycerol (30%, v/v), SDS (2%, w/v), urea (6 M), tris-HCl (50 mM) in dH_2O. The solution was adjusted to pH 6.8 and aliquoted into 40 ml volumes prior to storage at -20°C. For equilibration of Immobiline™ DryStrip (pH 4 – 7) (GE Healthcare, Life Sciences), the isoelectric focusing equilibration buffer (pH 6.8) was supplemented with a reducing agent, DTT (2%, w/v), or with an alkylating agent, iodoacetamide (IAA) (2.5%, w/v), depending on the strip equilibration step required (Section 2.15.6).

2.15.3 Casting of Large-2-D SDS-PAGE Gels

Glass plates (1.5 mm) (Bio-Rad Laboratories) made up of a front glass plate (200 mm x 200 mm) and a back glass plate (200 mm x 223 mm), separated by a grey glass plate spacer, were cleaned with ethanol (70%, v/v), and carefully arranged into a Protean™ II multi-gel casting chamber rig (Bio-Rad Laboratories). The same constituents and method described in Section 2.14.5 and Table 2.2 were used to produce 12.5% bis-acrylamide gels, however the volumes were adjusted as follows; tris-HCl (1.5 M) (60 ml), bis-acrylamide (30%, w/v) (100 ml), dH_2O (76 ml), SDS (10%, w/v) (2.4 ml), APS (10%, w/v) (1.5 ml), and TEMED (60 µl). Air bubbles were removed before the complete polymerization of the separating gel matrix.

2.15.4 Agarose (1%, w/v) Sealing Solution

An Agarose (1%, w/v) sealing solution was prepared by dissolving agarose (1%, w/v), and bromophenol blue sodium salt (0.5%, w/v) in 1X electrode buffer (pH 8.9) (Section 2.14.7). When the agarose (1%, w/v) sealing solution was first prepared, it was heated till boiling, and left at room temperature to set. Subsequent uses involved heating the solution until it was hand-hot, and quickly placing the agarose (1%, w/v) sealing solution on top of an IPG strip fixed into position on a 2-D SDS-PAGE gel, using a 3.5 ml transfer pipette, to seal the IPG strip in place.

2.15.5 Isoelectric Focusing in the First Dimension

Extracted protein was quantified by a Bradford assay (Section 2.11.1) and acetone precipitated (Section 2.11.2). For a 7 cm IPG strip (Immobiline™ DryStrip (pH 4 – 7), GE Healthcare, Life Sciences), the protein precipitate (150 µg) was resuspended in 125 µl of IEF buffer supplemented with ampholytes, DTT, and bromophenol blue sodium salts (Section 2.15.1). For a 13 cm IPG strip (Immobiline™ DryStrip (pH 4 – 7)), the protein precipitate (400 µg) was resuspended in 250 µl of IEF buffer supplemented with ampholytes, DTT, and bromophenol blue sodium salts (Section 2.15.1). The reconstituted protein sample was transferred into a ceramic strip holder (7 cm or 13 cm, accordingly) (Amersham Pharmacia Biotech, GE Healthcare, Life Sciences) corresponding to the anodic (negative) and cathodic (positive) ends. The IPG strip (pH 4-7, 7 cm and 13 cm) was placed gel-side face down into the protein sample, tilting the strip holder as required to cover the IPG strip, and air bubbles were carefully removed. Prior to IEF, the IPG strips were covered with PlusOne DryStrip cover fluid (GE Healthcare, Life Sciences) (1 ml) using a 3.5 ml transfer pipette. Proteins were isoelectrically focused using an Ettan™ IPGphor II™ focusing system (GE Healthcare, Life Sciences) according to the following 6-step programme (22 hours 15 minutes) (Table 2.3).

Table 2.3 Isoelectric focusing programme used for 2-D SDS-PAGE. Isoelectric focusing in the first dimension 6-step programme (22 hours 15 minutes) applied using an Ettan™ IPGphor II™ focusing system for 2-D SDS-PAGE.

Time	Volts (V)	Mode
8 hours	50 V	Gradient
15 minutes	250 V	Gradient
2 hours	1000 V	Gradient
4 hours	4000 V	Gradient
4 hours	8000 V	Gradient
4 hours	8000 V	Hold

2.15.6 IPG Strip Equilibration and 2-D SDS-PAGE in the Second Dimension

Following isoelectric focusing, IPG strips were kept at -80°C for long term storage, and -20°C for short term storage, or were directly transferred for IPG strip rehydration and equilibration before SDS-PAGE in the second dimension. The IPG strips were first equilibrated for 15 minutes, shaking at room temperature in reducing IEF equilibration buffer (DTT) (2%, w/v) (pH 6.8), followed by a second 15 minute incubation in alkylation IEF equilibration buffer (IAA) (2.5%. w/v) (pH 6.8) (Section 2.15.2).

Equilibrated strips were rinsed briefly in 1X electrode buffer, and placed on top of 12.5% SDS-PAGE gels, overlaid with hand warm agarose (1%, w/v) sealing solution. Mini-2-D SDS-PAGE protein gels (7 cm IPG strips) were resolved at 100 V using either Mini-Protean® 3 Cell gel rig (Bio-Rad Laboratories) or Mini-Protean® Tetra Cell gel rig (Bio-Rad Laboratories), and a power-pac 300 (Bio-Rad Laboratories) until the protein had sufficiently travelled through the separating gel matrix, until the bromophenol blue tracking dye had moved to approximately 1 cm from the bottom of the gel.

The mini-2-D gel was carefully removed and placed into a clean 15 cm petri-dish for protein visualization by colloidal Coomassie staining (Section 2.16). Large-2-D SDS-PAGE protein gels (13 cm IPG strips) were resolved using a Protean Plus™ Dodeca™ Cell (Bio-Rad Laboratories) gel rig system with horizontal electrophoresis. A thin film of DC4 electrical insulating compound (Dow Corning®, Dow Corning Corporation, MI, USA) was smeared onto the bottom side of the large-2-D protein gels (on bottom side of grey glass plate spacer), and the gels were fitted into the protein gel rig system. The chamber was filled with 1X electrode buffer (Section 2.14.7), ensuring that all large-2-D protein gels were covered with buffer.

Large-2-D protein gels were initially electrophoresed for 1 hour at 1 watt (W) per gel, before this was increased to 1.5 W per gel. If the gel rig system was being used overnight, the gel rig cooling system was employed to maintain a temperature between 9 – 10°C to prevent increased protein migration. Protein gels were monitored at regular intervals, and following migration of the bromophenol blue tracking dye to near the bottom of the protein gel, the protein gel was carefully removed, and placed in a dish for colloidal Coomassie staining of proteins (Section 2.16).

2.15.7 Comparative Analysis of Differential Protein Expression

Following de-staining of 1-D and 2-D SDS PAGE gels, images (in triplicate) were recorded as described in Section 2.16, and analysed using Image Quant TL software (GE Healthcare, Life Sciences), and Progenesis SameSpot software (Nonlinear Dynamics, Newcastle Upon Tyne, UK), repsectively, to assess fold-change in protein expression in hTCEpi and *B. oleronius* samples subjected to different treatments and conditions. The level of differential protein expression was determined by analysis of variance (ANOVA) statistical tests, and a p-value < 0.05 was deemed to be statistically significant.

2.16 Staining of SDS-PAGE Gels

Following electrophoresis of 1-D and 2-D SDS-PAGE, gels were placed into a clean 15 cm petri-dish for staining. Proteins resolved by 1-D SDS-PAGE were visualized using the Coomassie Brilliant Blue staining protocol, as described in Section 2.16.1, and proteins separated by 2-D SDS-PAGE were visualized following the colloidal Coomassie staining protocol, given in Section 2.16.2. After the gels had been sufficiently de-stained, gel images were recorded using an ImageScanner™ III (GE Healthcare, Life Sciences) and acquired using LabScan™ 6.0, Epson Scan, Epson Expression™ 10000 XL software (GE Healthcare, Life Sciences).

2.16.1 Coomassie Brilliant Blue Staining Protocol

SDS-PAGE gels were visualized by immersion of gel in Coomassie Brilliant Blue staining solution (Brilliant Blue R (0.2%, w/v), methanol (45%, v/v), acetic acid (10%, v/v), and dH_2O (44.8%, v/v)), overnight on an orbital shaker at room temperature. Following staining, SDS-PAGE gels were de-stained using Coomassie Brilliant Blue de-stain solution (methanol (25%, v/v), acetic acid (10%, v/v), and dH_2O (65%, v/v)), on an orbital shaker at room temperature until blue protein bands were visible against a clear background, and gel images were recorded. The Coomassie Brilliant Blue de-stain solution could be re-used following filtering of the solution through activated charcoal particles. De-stained SDS-PAGE gels were washed (x 3) with dH_2O before being placed in a dish with a spatula of sodium azide and dH_2O, to prevent microbial growth, prior to mass spectrometry analysis.

2.16.2 Colloidal Coomassie Staining Protocol

SDS-PAGE gels were immersed in colloidal Coomassie fixer buffer (ethanol (50%, v/v), phosphoric acid (3%, v/v), and dH_2O (47%, v/v)), for a minimum of 4 hours to overnight on an orbital shaker. Following the protein fixation step, the gels were washed and rehydrated using dH_2O (3 x 20 minute washes). The colloidal Coomassie fixer buffer was completely washed off, and the gels were immersed in the colloidal Coomassie pre-incubation buffer (ammonium sulphate (17%, w/v), methanol (34%, v/v), phosphoric acid (3%, v/v), and dH_2O (46%, v/v)) for 1 hour at room temperature on an orbital shaker, before a spatula tip of SERVA blue G powder (SERVA Electrophoresis GmbH, Heidelberg, Germany) was added. The gels were incubated in the colloidal Coomassie pre-incubation buffer with SERVA blue stain solution overnight or until the proteins were visible. The gels were then washed in dH_2O until the background blue stain was removed and the gels images were recorded. De-stained SDS-PAGE gels were washed (x 3) with dH_2O before being placed in a dish with a spatula of sodium azide and dH_2O, to prevent microbial growth, prior to mass spectrometry analysis.

2.17 In-Gel Trypsin Digestion and Liquid Chromatography - Mass Spectrometry (LC/MS)

2.17.1 Preparation of Micro-Centrifuge Tubes and Pipette Tips for Excision of Protein Bands and Spots for LC/MS

All micro-centrifuge tubes, and pipette tips for liquid chromatography – mass spectrometry (LC/MS) were autoclaved in sealed containers before use. Pipette tips were cut to varied sizes for spot and band excision from 1-D and 2-D SDS-PAGE gels, and placed with all other utensils, scalpels, and blunt needles, that would be in contact with the gel, in a container with acetonitrile (100%, v/v) prior to use, minimising the likelihood of keratin contamination. Micro-centrifuge tubes were washed with acetonitrile (100%, v/v) (1 ml) before the addition of excised spots and bands to the tubes.

2.17.2 De-Staining Buffer

The de-staining buffer was prepared by dissolving ammonium bicarbonate (100 mM) (0.79 g) in 100 ml of high-performance liquid chromatography (HPLC) grade

dH_2O, and subsequently diluting 100 mM ammonium bicarbonate, at a ratio of 1 : 1, with HPLC grade acetonitrile (100%, v/v). The de-staining buffer was made fresh on the day of use, and vortexed every 10 – 15 minutes to ensure a homogenous solution.

2.17.3 Trypsin Digestion Buffer

Lyophilised sequencing grade modified porcine trypsin (Promega, Promega Corporation, Madison, WI, USA) (20 µg) was diluted (100 µl) of trypsin resuspension buffer (composed of 50 mM acetic acid, supplied by the kit from the manufacturer) to yield trypsin buffer (0.2 µg/µl). The trypsin digestion buffer was prepared by adding 10 µl trypsin buffer to 500 µl trypsin reconstitution buffer (ammonium bicarbonate (10 mM) (1 ml), and HPLC grade acetonitrile (100%, v/v) (1 ml)). The trypsin buffer (lyophilised trypsin diluted in trypsin resuspension buffer) was aliquoted in 10 µl volumes, and stored at -20°C for up to 1 month.

2.17.4 Peptide Extraction Buffer

The peptide extraction buffer was prepared by diluting formic acid (5%, v/v) in HPLC grade dH_2O, and acetonitrile (100%, v/v), at a ratio of 1 : 2. The buffer was made fresh on the day of use.

2.17.5 Peptide Resuspension Buffer

The peptide resuspension buffer was composed of formic acid (0.1%, v/v) in HPLC grade dH_2O. The buffer was prepared fresh on the day of use.

2.17.6 Trypsin Digestion of Protein Bands and Spots from 1-D and 2-D SDS-PAGE Gels for LC/MS Analysis

The protocol and guidelines described by Shevchenko *et al*. (2006) were followed for LC/MS analysis. Protein SDS-PAGE gels were washed (3 x 20 minutes) in dH_2O prior to excision of protein bands and spots, and each excised gel plug and gel piece was transferred into an acetonitrile washed micro-centrifuge tube (Section 2.17.1). Excised gel pieces were incubated in de-staining buffer (100 µl) (Section 2.17.2) for 30 minutes at room temperature (or until stain was removed) with vortexing every 10 minutes. Acetonitrile (100%, v/v) (500 µl) was added to dehydrate and shrink each gel piece, turning the gel piece a white colour. Acetonitrile was

removed from each sample, and samples were either stored at -20°C or subjected to further in-gel trypsin digestion.

In-gel trypsin digestion of gel pieces was achieved by adding trypsin digestion buffer (30 µl) (Section 2.17.3) (or enough to cover the gel matrix) to each sample. Samples were incubated at 4°C for 30 minutes to prevent auto-digestion, and allow for penetration of trypsin digestion buffer into the gel piece. If the entire trypsin digestion buffer was absorbed into the gel piece, more was added to cover the gel matrix, and incubated at 4°C for a further 90 minutes to saturate them with trypsin. If required, a further 20 µl 10 mM ammonium bicarbonate in HPLC grade acetonitrile (100%, v/v) was added to the gel pieces to prevent dehydration during the in-gel trypsin digestion process. The samples were placed in a 37°C orbital incubator overnight, set to 160 – 180 rpm, to fully digest peptides.

Digested peptides were centrifuged on a desk top centrifuge (Capsulefuge PMC-060, Tomy Tech USA Inc., Fremont, CA, USA), and the trypsin digestion products, present in the supernatant, were transferred to an acetonitrile washed micro-centrifuge tube. For a double extraction of peptides, peptide extraction buffer (Section 2.17.4) (100 µl) was added to the original gel piece, and incubated for 15 minutes at 37°C with orbital shaking. The supernatant from the second peptide extraction was added to the micro-centrifuge tube containing the trypsin digestion products. The samples were lyophilised using a vacuum centrifuge (Savant DNA120 SpeedVac Concentrator, Thermo Fisher Scientific Inc., Dublin, Ireland) for 2 hours at medium drying rate setting. The lyophilisation step was repeated until complete lyophilisation of the peptides had occurred.

Dried peptide extracts could be stored at -20°C, or immediately prepared for LC/MS analysis, using peptide resuspension buffer (Section 2.17.5) (20 µl). The resuspended samples were vortexed, and sonicated for 5 minutes in a sonication bath (FB15050, Fisher Scientific, Thermo Fisher Scientific Inc.) to aid peptide resuspension, followed by transfer of samples to 0.22 µm cellulose acetate filter spin columns (Spin-X® centrifuge tube filters, Costar®, Corning Incorporated, Corning, NY, USA), and centrifuged at 6,000 x *g* for 15 minutes. The filtrate (10 µl) was added to mass spectrometry vials, taking care to avoid air bubble formation. Analysis of digested peptides was achieved using an Agilent 6340 Ion Trap liquid chromatography mass spectrometer (Agilent Technologies, Santa Clara, CA, USA) using acetonitrile elution.

2.17.7 Bioinformatic Data Analysis of LC/MS Chromatograms

The relative mass-to-charge (*m*/*z*) ratio was detected from ionized particles, as fragmented protein samples were eluted through the column of the Agilent 6340 Ion Trap LC/MS (Agilent Technologies). The chromatogram data files generated were saved as mascot generic files (.mgf), and further analysed using the mascot MS/MS ion search engine database (www.matrixscience.com), to determine protein identities. The following settings were employed for data analysis; Database: NCDInR; Taxonomy: *Homo sapiens* (human) for proteomic studies involving hTCEpi cells, or Bacteria (*Eubacteria*) for proteomic studies involving *B. oleronius*; Enzyme: Trypsin; Allow up to: 2 missed cleavages; Fixed modifications: Carboxymethyl; Variable modifications: Oxidation (M); Quantitation: None; Peptide tol. ± : 2 Da; MS/MS tol. ± : 1 Dalton (Da); Peptide charge: 1+, 2+ and 3+; Data format: Mascot generic; Instrument: ESI-TRAP; Report top: AUTO hits. Following mascot MS/MS ion search, a mascot score above 67 was deemed to be a significant match for the protein identity ($p < 0.05$). The mass error tolerance was 1 Da allowing for a maximum of no more than two missed cleavages. Protein sequences identified were verified through BLAST (Basic Local Alignment Search Tool) searches of the protein sequences (Protein BLAST) on the National Center for Biotechnology Information (NCBI) (www.ncbi.nlm.nih.gov) and Uniprot (www.uniprot.org) website.

2.18 Label Free Mass Spectrometry (LF/MS)

2.18.1 Corneal Epithelial Cell (hTCEpi) Culture and Protein Extraction for LF/MS

Corneal epithelial cells (hTCEpi) were cultured at a density 5 x 10^5 cells/well in 6-well tissue culture plates (Corning), and were maintained in Keratinocyte Growth Medium (KGM™)-2 supplemented with KGM™-2 SingleQuot™ kit supplements and growth factors (Lonza Ltd., Basel, Switzerland) in a 5% carbon dioxide (CO_2) humidified atmosphere incubator at 37°C. Cells were exposed to *B. oleronius* crude (6 µg/ml), and pure (6 µg/ml) protein preparations for 24 hour and 72 hour, respectively (preparation of *B. oleronius* protein preparations is described in Section 2.20). Cultured hTCEpi cells were harvested by trypsinization using 1 ml trypsin buffer (trypsin (0.25%, w/v)-EDTA (0.022%, w/v) in PBS) for 5 minutes, or until the cells had detached, before using an equal volume trypsin neutralisation medium

(Dulbecco's modified eagle medium (DMEM) (95%, v/v) (Gibco®, Invitrogen, Thermo Fisher Scientific Inc., Life Technolgies) supplemented with FCS (5%, v/v)) to inhibit the action of trypsin, followed by centrifugation of the cell suspension at 200 x *g* for 5 minutes.

The cell pellet was resuspended in 3 ml sterile PBS, and the centrifugation step was repeated, before *ex situ* cell lysis in 500 µl cell lysis buffer (urea (8 M), thiourea (2 M), and tris-HCl (0.1 M) (pH 8.0) dissolved in HPLC grade dH_2O, supplemented with protease inhibitors (10 µg/ml) (aprotinin, leupeptin, pepstatin A, and TLCK), and phosphatase inhibitors (phosphatase inhibitor cocktail 2 (Table 2.1)) for 2 hours at room temperature using a rotary wheel (Stuart Rotator SB2, Bibby Scientific Limited, Staffordshire, UK). The extracted protein lysates were stored at -20°C prior to in-solution trypsin digestion, and sample preparation for LF/MS.

2.18.2 In-Solution Trypsin Digestion of Protein Samples

Label free mass spectrometry (LF/MS) shotgun proteomics was applied to protein extracted from human corneal epithelial cells (hTCEpi) exposed to crude *B. oleronius* proteins (6 µg/ml) for 24 hour (untreated hTCEpi cells – Vs – crude *B. oleronius* protein (6 µg/ml) treated hTCEpi cells), and from human corneal epithelial cells (hTCEpi) exposed to pure *B. oleronius* proteins (6 µg/ml) for 72 hour (untreated hTCEpi cells – Vs – pure *B. oleronius* protein (6 µg/ml) treated hTCEpi cells). Samples were quantified by Bradford protein assay (Section 2.11.1), protein (60 µg) was acetone precipitated (Section 2.9), and the protein pellet was resuspended in 15 µl sample resuspension buffer (urea (8 M), thiourea (2 M), tris-HCl (0.1 M) (pH 8.0) dissolved in HPLC grade dH_2O), followed by the addition of 125 µl ammonium bicarbonate (50 mM). The protein sample was reduced by adding 1 µl DTT (0.5 M) (prepared by dissolving DTT (0.03856 g) in 500 µl ammonium bicarbonate (50 mM)), and incubated at 56°C for 20 minutes.

Samples were cooled to room temperature, and alkylated by the addition of 2.7 µl IAA (0.55 M) (prepared by dissolving IAA (0.1017 g) in 1 ml ammonium bicarbonate (50 mM)), and incubated at room temperature for 15 minutes in the dark, away from light. Following reduction and alkylation, 1 µl ProteaseMAX™ Surfactant Trypsin Enhancer stock (Promega) (1%, w/v stock dissolved in ammonium bicarbonate (50 mM)), and 1 µl trypsin (Promega) (0.5 µg/µl) (sequencing grade trypsin (20 µg) dissolved in trypsin resuspension buffer (40 µl)) was added to each

protein sample, and incubated at 37°C overnight. Trifluoroacetic acid (TFA) (1 µl) was added to each tryptic digest sample, and incubated at room temperature for 5 minutes. The samples were centrifuged at 13,000 x *g* for 10 minutes, and the supernatant was aliquoted into sterile micro-centrifuge tubes of equal volume (77.5 µl yields ≈ 30 µg protein). The micro-centrifuge tubes were kept at -20°C for storage prior to C18 column clean up and sample preparation for LF/MS.

2.18.3 Pierce® C-18 Spin Column Clean Up and Sample Preparation for LF/MS

Pierce® C-18 spin columns (Thermo Scientific, Life Technologies, Rockford, IL, USA) containing C-18 reverse-phase resin were used for the recovery, and purification of tryptic digested peptides for identification by mass spectrometry. The Pierce® C-18 spin columns were first activated by adding 200 µl activation solution (acetonitrile (50%, v/v) in HPLC grade dH_2O) to each column to rinse the walls of the column, and wet the resin, followed by centrifugation at 1500 x *g* for 1 minute. The flow-through was discarded and the column activation step was repeated. The flow-through was discarded, 200 µl equilibration solution (TFA (0.5%, v/v), acetonitrile (5%, v/v) in HPLC grade dH_2O) was added to the C-18 column, and the columns were centrifuged at 1500 x *g* for 1 minute. The flow-through was discarded, and the equilibration step was repeated. Tryptic digested peptide samples were mixed with sample buffer 1 (TFA (2%, v/v), acetonitrile (20%, v/v) in HPLC grade dH_2O), at ratio of 3 : 1 (tryptic digested peptide sample : sample buffer 1), and were loaded to the top of the C-18 resin bed, and the column was transferred to a new sterile micro-centrifuge tube (receiver tube). The tryptic digested peptide samples loaded on to the top of the resin bed of the column were centrifuged at 1500 x *g* for 1 minute.

The flow-through was collected, re-applied to the C-18 resin bed, and the columns were centrifuged at 1500 x *g* for 1 minute twice more, to ensure complete sample binding to the C-18 resin. The columns were transferred to new sterile micro-centrifuge tubes (receiver tubes), and 200 µl wash buffer (TFA (0.5%, v/v), acetonitrile (5%, v/v) in HPLC grade dH_2O) was added, and the columns were centrifuged at 1500 x *g* for 1 minute. The flow-through was discarded, and the wash step was repeated to remove contaminants. The columns were transferred to new sterile micro-centrifuge tubes (receiver tubes), and 25 µl elution buffer (acetonitrile (70%, v/v) in HPLC grade dH_2O) was added, and the columns were centrifuged at 1500 x *g* for 1 minute. The elution step was repeated, and the eluent (≈ 75 µl)

transferred to a new sterile micro-centrifuge tube, and the samples were lyophilised using a vacuum centrifuge (Savant DNA120 SpeedVac Concentrator, Thermo Fisher Scientific Inc., Dublin, Ireland) for 2 hours at a medium drying rate setting. The lyophilisation step was repeated until complete lyophilisation of the peptides had occurred.

Dried peptide extracts could be stored at -20°C, or immediately prepared for LF/MS analysis, by resuspension in 32 µl of Q Exactive™ loading buffer (TFA (0.05%, v/v) in acetonitrile (2%, v/v)). The resuspended samples were vortexed, and sonicated for 5 minutes in a sonication bath (FB15050, Fisher Scientific, Thermo Fisher Scientific Inc.) to aid peptide resuspension. The digested peptide samples were centrifuged at 13,400 x *g* for 5 minutes to pellet insoluble material, and the supernatant (10 µl) was transferred to mass spectrometry vials, taking care to avoid air bubble formation. The purified peptides (1 µg) were analysed on a Q Exactive™ high resolution mass spectrometer (Thermo Fisher Scientific) connected to a Dionex UltiMate® 3000 RSLnano liquid chromatography system (Thermo Fisher Scientific). Peptides were separated by an increasing acetonitrile gradient on a BioBasic™ C18 Picofrit™ column (100 mm length, 75 mm inner diameter) (Thermo Fisher Scientific), using a 120 minutes reverse phase gradient at a flow rate of 250 nl/min. All data were acquired from the mass spectrometer operating in an automatic dependent switching mode. A high resolution MS scan (300 – 2000 Da) was performed using the Orbitrap to select the 15 most intense ions prior to MS/MS.

2.18.4 LF/MS Protein Identification and Quantification

Protein identification from the MS/MS data extrapolated from the Q Exactive™ was performed using the Andromeda search engine (Cox *et al*., 2011) in MaxQuant (version 1.2.2.5; http://maxquant.org/). The following search parameters were used: first search peptide tolerance of 20 ppm, second search peptide tolerance 4.5 ppm with cysteine carbamidomethylation as a fixed modification and N-acetylation of protein and oxidation of methionine as variable modifications and a maximum of 2 missed cleavage sites allowed. False discovery rate (FDR) was set to 1% for both peptides and proteins, and the FDR was estimated following searches against a target-decoy database. Peptides with minimum length of seven amino acid length were considered for identification and proteins were only considered indentified when more than one unique peptide for each protein was observed.

Results processing, statistical analyses and graphics generation were conducted using Perseus v. 1.5.0.31. Label free quantification (LFQ) intensities were log_2-transformed and ANOVA of significance, and t-tests between untreated hTCEpi cells – Vs – crude *B. oleronius* protein (6 µg/ml) treated hTCEpi cells after a 24 hour exposure, and from hTCEpi cells – Vs – crude *B. oleronius* protein (6 µg/ml) treated hTCEpi cells following a 72 hour exposure. A p-value of less than 0.05 and significance was determined using FDR correction (Benjamini-Hochberg). Proteins that had non-existent values (indicative of absence or very low abundance in a sample) were included in the study only when they were completely absent from one group and present in at least three of the four replicates in the second group (hereafter referred to as qualitatively differentially abundant proteins). The Blast2GO suite of software tools was utilised to assign gene ontology terms (GO terms) relating to biological processes, molecular function and cellular component. Enzyme commission (EC) numbers and Kyoto Encyclopaedia of Genes and Genomes (KEGG) pathway mapping was performed as part of the Blast2GO annotation pipeline, as well as string network (string-db.org) to assess known and predicted protein-protein interactions (Conesa and Götz, 2008).

2.19 Western Blotting

2.19.1 Transfer Buffer (pH 8.3)

Transfer buffer (pH 8.3) was prepared by dissolving tris-base (25 mM) (3.03 g/L), and glycine (192 mM) (14.4 g/L) in a solution composed of methanol (20%, v/v), and dH_2O (80%, v/v). The buffer should not require pH adjustment once all constituents are fully solubilised. The solution was stored at 4°C, and mixed thoroughly before Western blotting.

2.19.2 10X Tris-Buffered Saline (TBS) (pH 7.6)

A 10X tris-buffered saline (TBS) (pH 7.6) stock solution was prepared by dissolving tris-HCL (0.5 M) (78.7 g), and tris-HCL (1.5M) (86.65 g) in 1 L of dH_2O. Prior to the solution being brought up to the final volume, the buffer was adjusted to pH 7.6. The buffer was autoclaved, and stored at room temperature until needed. After each use the buffer would be re-autoclaved, and the pH monitored to prevent against contamination, and maintain the shelf-life of the solution.

2.19.3 1X TBS Tween®-20 (0.05%, v/v) (pH 7.6)

A 1X TBS Tween®-20 (0.05%, v/v) (pH 7.6) working solution was prepared by adding 100 ml 10X TBS (pH 7.6) stock to 900 ml dH_2O, and supplemented with detergent, Tween®-20 (0.05%, v/v) (500 µl) using a 3.5 ml transfer pipette. The solution was mixed thoroughly prior to use as wash buffer, and used immediately within 2 days.

2.19.4 BSA (1%, w/v) Blocking Buffer

A bovine serum albumin (BSA) (1%, w/v) blocking buffer solution was prepared by dissolving BSA (1 g) in 100 ml of 1X TBS Tween®-20 (0.05%, v/v). The solution was filter-sterilized using 0.45 µm cellulose pore filter discs, and stored at 4°C.

2.19.5 Western Blotting Protocol

Extracted protein (20 µg for 1D SDS-PAGE; 125 µg for 2D SDS-PAGE) from *B. oleronius*, corneal epithelial (hTCEpi) cells, or neutrophil cells were separated under reducing conditions by 1-D SDS-PAGE (Section 2.14) or by 2-D SDS-PAGE (Section 2.15). Following electrophoresis, resolved proteins were transferred onto a nitrocellulose membrane (Fisher Scientific) and placed into the correct 'Western blot sandwhich' orientation (sponge, Whatman™ filter paper, SDS-PAGE gel, nitrocellulose membrane, Whatman™ filter paper, sponge) (Figure 2.2). The 'Western blot sandwhich' was arranged into position using a wet transfer rig apparatus (Bio-Rad Laboratories) and submerged in transfer buffer (pH 8.3) (Section 2.19.1) along with an ice-block before transferring at 70 V, 400 mA for 70 minutes using a power-pac 300 (Bio-Rad Laboratories).

Following protein transfer, the nitrocellulose membrane blot was placed into a clean 15 cm petri-dish, and the quality of protein transfer onto the blot was assessed using Ponceau-S-Red solution (10 ml). The Ponceau-S-Red solution was removed by washing (x 3) the nitrocellulose membrane blot with 1X TBS Tween®-20 (0.05%, v/v) (pH 7.6) (Section 2.19.3). The nitrocellulose membrane blot was placed into a new 15 cm petri-dish, and the membrane was blocked for 1 hour at room temperature on an orbital shaker, using BSA (1%, w/v) blocking buffer (Section 2.19.4) (30 ml). After the incubation period, the blocking buffer was removed, and the primary antibody, diluted in BSA (1%, w/v) blocking buffer (20 ml), was added to the

membrane blot, and incubated at 4°C overnight on a rocker. A list of primary antibodies, and the dilutions used can be seen in Table 2.4.

The primary antibody was removed, and the membrane blot was washed (x 3) for 20 minutes in 1X TBS Tween®-20 (0.05%, v/v) (pH 7.6) on an orbital shaker, followed by the addition of horseradish-peroxidase (HRP)-linked IgG secondary antibody, diluted in BSA (1%, w/v) blocking buffer (20 ml), and incubated at room temperature for 2 hours on an orbital shaker. A list of secondary antibodies, and the dilutions used can be seen in Table 2.5. The secondary antibody was removed after the incubation period, and the membrane blot was washed (x 3) for 20 minutes in 1X TBS Tween®-20 (0.05%, v/v) (pH 7.6) on an orbital shaker before development of the nitrocellulose membrane blot.

2.19.6 Development of Nitocellulose Membrane Blot

Immuno-reactive protein bands were visualized by incubating the membranes for 10 minutes in 0.01 g diaminobenzidine tetrahydrochloride (DAB) in 15 ml of tris–HCl (100 mM) (pH 7.6) containing 15 µl of hydrogen peroxide (Sigma) before washing in dH_2O, followed by air-drying in a laminar safety cabinet. Western blot images were recorded using an ImageScanner™ III (GE Healthcare, Life Sciences) and acquired using LabScan™ 6.0, Epson Scan, Epson Expression™ 10000 XL software (GE Healthcare, Life Sciences). Immuno-bands were quantified by densitometry using Image J software, and the fold change relative to an unstimulated or untreated control sample was calculated to assess expression levels of target protein.

2.20 Generation of *B. oleronius* Protein Preparations by Anion Exchange Separation using ÄKTA Fast Protein Liquid Chromatography™ (ÄKTA FPLC™) and Q-Sepharose™ High Performance Beads

2.20.1 ÄKTA FPLC™ Binding Buffer (pH 4.8)

The protein ÄKTA fast protein liquid chromatography™ (ÄKTA FPLC™) binding buffer (pH 4.8) was prepared by dissolving piperazine (20 mM) (6.047 g/L), and NaCl (10 mM) (0.584 g/L) in dH_2O. The pH of the buffer was adjusted to pH 4.8

Table 2.4 A list of the primary antibodies, and the dilutions used for Western blotting.

Primary Antibody	Source (raised in)	Company	Western Blot Dilution
Anti-MMP-9	Rabbit	Sigma	1/500
Anti-CCL20	Rabbit	Abnova	1/500
Anti-S100A7	Rabbit	Sigma	1/600
Anti-62 kDa *B. oleronius* Protein	Rabbit	Generated In-House from Collaboration with DCU	1/5000
Anti-Actin	Mouse	Millipore	1/5000
Patient Serum	Human	Institution Collaborations	1/100

Table 2.5 A list of the secondary antibodies, and the dilutions used for Western blotting.

Secondary Antibody	Source (raised in)	Company	Western Blot Dilution
Anti-Rabbit IgG HRP-Linked	Goat	Sigma	1/1000
Anti-Mouse IgG HRP-Linked	Goat	Sigma	1/1000
Anti-Human IgG HRP-Linked	Sheep	GE Healthcare	1/1000

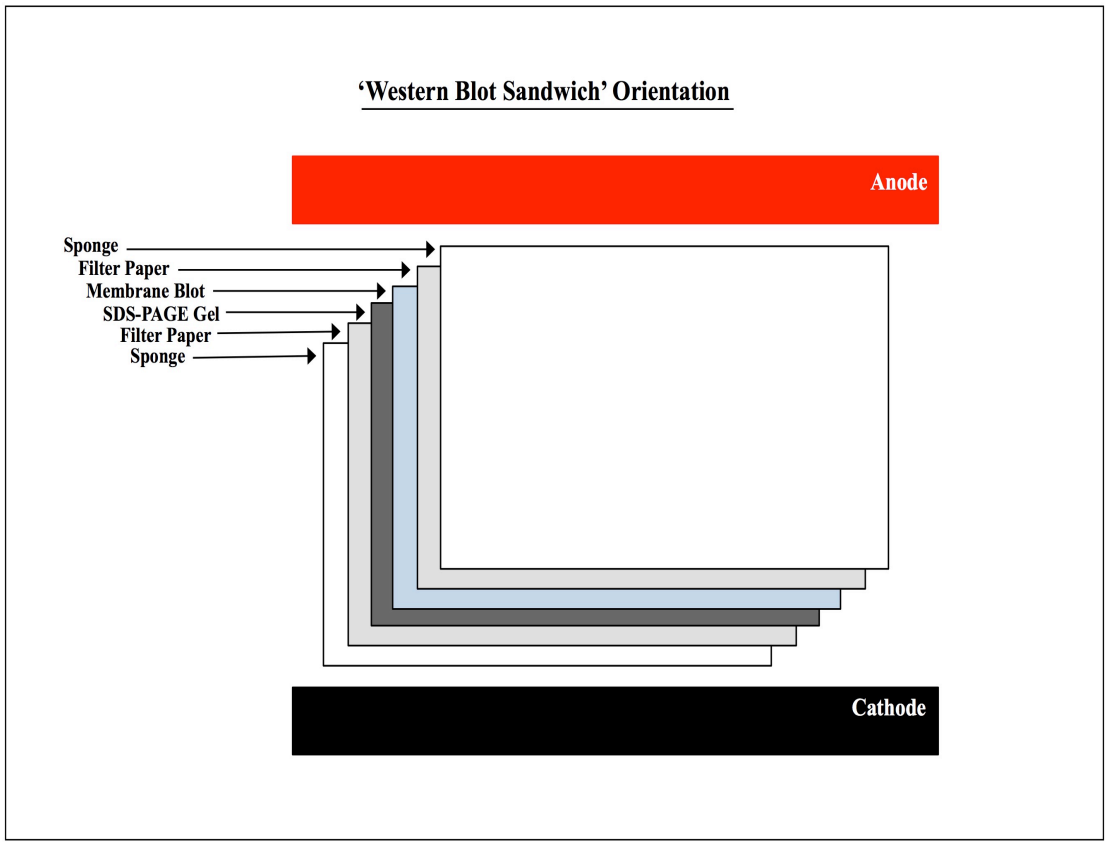

Figure 2.2 A schematic diagram of the orientation of the 'Western blot sandwich'. A representative schematic diagram illustrating the orientation of the 'Western blot sandwich': sponge - filter paper - SDS-PAGE gel - membrane blot - filter paper - sponge from cathode (black) to anode (red) direction. (Author's own).

before being brought to the final volume. The ÄKTA FPLC™ binding buffer (pH 4.8) was autoclaved, and stored at 4°C. Before the process of fractionating the crude *B. oleronius* protein lysate, the buffer was filter sterilised through a 0.2 µm cellulose pore filter disc twice before application to the ÄKTA FPLC™ column (Amersham Biosciences, Little Chalfont, Buckinghamshire, England, UK), and ÄKTA Purifier 100 system instrument (Amersham Biosciences). The ÄKTA FPLC™ binding buffer (pH 4.8) was termed 'buffer A' as it passed through the column when the ÄKTA Purifier 100 system instrument was switched on.

2.20.2 ÄKTA FPLC™ Elution Buffer (pH 4.8)

The protein ÄKTA FPLC™ elution buffer (pH 4.8) was prepared by dissolving piperazine (20 mM) (6.047 g/L), and NaCl (1 M) (58.44 g/L) in dH_2O. The pH of the buffer was adjusted to pH 4.8 before being brought to the final volume. The ÄKTA FPLC™ elution buffer (pH 4.8) was autoclaved, and stored at 4°C. Before the process of fractionating the crude *B. oleronius* protein lysate, the buffer was filter sterilised through a 0.2 µm cellulose pore filter disc twice before application to the ÄKTA FPLC™ column (Amersham Biosciences), and ÄKTA Purifier 100 system instrument (Amersham Biosciences). The ÄKTA FPLC™ elution buffer (pH 4.8) was termed 'buffer B' as it passed through the column when the ÄKTA Purifier 100 system instrument was switched on.

2.20.3 Protocol for the Preparation of *B. oleronius* Protein Extracts by Anion Exchange Separation using ÄKTA FPLC™ and Q-Sepharose™ High Performance Beads

Cultures of *B. oleronius* were incubated at 30°C in nutrient broth (Oxoid Ltd) under aerobic conditions to stationary phase of growth before protein extractions were performed as described by Lacey *et al*. (2007), and in Section 2.12.1. The abundance of protein was quantified through a Bradford assay (Section 2.11.1), the protein was pelleted by acetone precipitation (Section 2.11.1) to a stock concentration of 200 µg/ml, resuspended in sterile PBS (pH 7.4), and filter sterilised through a 0.2 µm cellulose pore filter disc. The protein preparation generated was termed crude *B. oleronius* protein and was diluted to a working concentration required for each assay (termed as 'crude' protein in the figures, tables, and text of thesis).

The generation of the pure *B. oleronius* protein preparation began by collecting

the starting material, consisting of crude *B. oleronius* protein lysates obtained from the *B. oleronius* cultures, and resuspension in ÄKTA FPLC™ binding buffer (pH 4.8) (15 ml) (Section 2.20.1). The resuspended protein buffer was filter sterilised through a 0.45 µm cellulose pore filter disc, and the filtrate is resuspended in a solution of ÄKTA FPLC™ binding buffer (pH 4.8) containg Q-sepharose™ high performance beads (GE Healthcare, Life Sciences) (20 ml), and inverted on a rotary wheel for 1 hour at 4°C. Following the binding incubation period, the material containing the *B. oleronius* protein in ÄKTA FPLC™ binding buffer (pH 4.8) with Q-sepharose™ high performance beads was loaded onto an ÄKTA FPLC™ column (2 x 5 cm) (Amersham Biosciences), and placed into position on ÄKTA Purifier 100 system instrument (Amersham Biosciences).

The loaded column was equilibrated by passing ÄKTA FPLC™ binding buffer (pH 4.8) (buffer A) through the column at a 0.5 ml/min flow rate with 100% gradient buffer A selected using the Unicorn 5.0 chromatography computer software (Amersham Biosciences). The loaded column was equilibrated for a minimum of 1 hour, and during equilibration, the material settled to the bottom of the column, and was tightly packed together within the column before fractionation of the *B. oleronius* protein. Following equilibration of the column, the ÄKTA FPLC™ elution buffer (pH 4.8) (buffer B) was passed through the column at a 0.5 ml/min flow rate, and set a 50% buffer A to buffer B 30 ml linear gradient for 30 minutes to separate protein bound to the Q-sepharose™ high performance beads by anion exchange separation, as 1 ml fractions were collected. After 30 minutes, 1 ml fractions were collected for a further 15 minutes at a 50% buffer A to buffer B gradient. Subsequently, the saline gradient was adjusted to 100% buffer B for 10 minutes to completely elute bound *B. oleronius* protein from the beads before the gradient was altered to 100% buffer A. A representative ÄKTA FPLC™ chromatogram can be seen in Figure 4.2.

The collected protein fractions were prepared for 1-D SDS-PAGE electrophoresis by denaturing and boiling in 5X solubilisation buffer (Section 2.11.3). The resolved protein fractions were visualized by staining with Coomassie blue (Section 2.16), and immunoblotted (Section 2.19) against our in-house generated anti-rabbit anti-62 kDa antibody to ensure the purification of the crude *B. oleronius* protein to isolate 'pure' proteins of interest. Following de-staining of gels and assessment of reactivity to the anti-62 kDa antibody, the fractions of interest were pooled, and filter concentrated using 3000 molecular weight cut off (MWCO)

Vivaspin®-20 filter columns (Vivaproducts, Vivaproducts Inc., GE Healthcare, Littleton, MA, USA) by centrigation at 3,500 x *g* for 45 minutes. The concentrated protein was quantified by a Bradford assay (Section 2.11.1), and the protein was pelleted by acetone precipitation (Section 2.11.2) to a stock concentration of 200 µg/ml, and resuspended in sterile PBS (pH 7.4), and filter sterilised through a 0.2 µm cellulose pore filter disc. The protein preparation generated was termed pure *B. oleronius* protein and was diluted to a working concentration required for each assay (termed as 'pure' protein in the figures, tables, and text of thesis). The pure *B. oleronius* protein preparations were resolved by 1-D SDS-PAGE, the pure fractions were visualized by Coomassie staining, immunoblotted against the anti-rabbit anti-62 kDa antibody to ensure isolation of the 'pure' proteins of interest. The generation of the *B. oleronius* protein preparations has previously been described by O'Reilly *et al*. (2012a).

2.21 Isolation of Peripheral Blood Mononuclear Cells (PBMC)

Fresh blood of healthy volunteers was collected in heparin-EDTA treated tubes following informed consent and approval of the National University of Ireland Maynooth (NUIM) ethics board committee (ref number BSRESC-2012-008) to isolate peripheral blood mononuclear cells (PBMC). A population of PBMC was isolated by mixing one volume of blood with one volume of PBS (a ratio of 1 : 1), and the diluted blood was carefully layered on top of Ficoll-Pacque™ PLUS (GE Healthcare, Life Sciences Uppsala, Sweden) using a 3.5 ml transfer pipette. The diluted blood was separated by centrifugation at 400 x *g* for 30 minutes at room temperature, and slow braking to obtain the PBMC band from the density gradient.

The plasma layer was discarded, the PBMC fraction was collected, and added to at least 3 volumes (6 ml) of PBS before centrifuging at 750 x *g* for 10 minutes at room temperature. The PBMC pellet was washed twice in 10 ml cell culture medium (Roswell Park Memorial Institute (RPMI)-1640 GlutaMAX™ (Gibco®, Invitrogen, Life Technologies products, Bio-Sciences, Dún Laoghaire, Dublin, Ireland) supplemented with fetal calf serum (FCS) (10%, v/v) (Gibco®)), and centrifuged at 250 x *g* for 10 minutes at room temperature. The isolated PBMC population was counted using a haemocytometer (Neubauer improved cell counting chamber, haemocytometer), and cell viability was assessed using the trypan blue cell exclusion assay (Section 2.13).

2.22 Isolation of Neutrophils from Fresh Blood

2.22.1 1X Saline Solution and 2X Saline Solution

A 1X saline solution was prepared by dissolving sodium chloride (NaCl) (9 g) in 1 L of dH_2O. A 2X saline solution was prepared by dissolving NaCl (18 g) in 1 L of dH_2O. The solutions were autoclaved, and stored at 4°C until needed.

2.22.2 Dextran (10%, w/v)

A dextran (10%, w/v) solution was prepared by dissolving dextran sulfate sodium salt form *Leuconostoc spp.* (5 g) in Dulbecco's PBS (DPBS) (pH 7.4) (Gibco®) (50 ml). Contents were mixed through vortexing, and filter sterilised using 0.45 μm cellulose pore filter discs. The solution was prepared fresh.

2.22.3 Sterile Distilled Water (dH_2O)

Sterile dH_2O was prepared by autoclaving dH_2O (1 L), and kept at 4°C before use.

2.22.4 PBS Glucose (5 mM)

A 5 mM PBS glucose solution was freshly prepared on the day of neutrophil isolation from donor blood samples, and composed of glucose (0.045 g) dissolved into 1X DPBS (pH 7.4) (50 ml). The solution was gently mixed, and filter sterilised using 0.45 μm cellulose pore filter discs before use.

2.22.5 Neutrophil Separation from Fresh Blood Protocol

Ethical approval for the isolation of human neutrophils was supplied by NUIM ethics committee (ref number BSRESC-2012-008). Human neutrophils were isolated from healthy consenting volunteers by dextran (10%, w/v) sedimentation gradient, and lymphoprep™ centrifugation (Axis-Shield PoC AS, Oslo, Norway) as described (Reeves *et al.,* 2002). Briefly, fresh blood (15 ml) from consenting healthy volunteers was collected in heparin-EDTA beaded vials under vacuum by a qualified phlebotomist, and added to a sterile 50 ml universal (Corning), followed by the addition of 1X saline solution (20 ml) (Section 2.22.1), and dextran (10 %, w/v) (3.5 ml) (Section 2.22.2). The solution was inverted 3 – 4 times carefully to ensure an homogenous mixture of the constituents. The universal cap was loosened, and the

solution was left to sediment for 20 minutes a room temperature to separate the cellular components present in the donated blood. Following the dextran (10%, w/v) sucrose sedimentation, the supernatant was carefully removed using a 3.5 ml transfer pipette, and transferred into a fresh sterile 50 ml universals, and the transferred contents were carefully underlayed with 6 ml of lymphoprep™ before being centrifuged at 1400 x *g* for 10 minutes at room temperature. The dark red, bottom layer containing the heparin beads of the first 50 ml universal were discarded.

After separation of the blood sample by centrifugation, the supernatant was removed and discarded, and the cell pellet (red in colour), containing white blood cells (lymphocytes but the majority of which are neutrophils) and red blood cells (erythrocytes), was lysed by resuspension of the cell pellet in sterile dH_2O (20 ml) (Section 2.22.3) by quickly and carefully inverting the 50 ml universal 4 to 5 times, followed by the addition of 2X saline solution (20 ml) (Section 2.22.1) to minimise the lysis of neutrophils. The lysed cell suspension was centrifuged at 800 x *g* for 5 minutes at room temperature. If the cell pellet was red in colour, due to a high proportion of red blood cells present in the cell suspension, the cell lysis step of the cell pellet, and the centrifugation step were repeated until the cell pellet was a creamy white colour to signify the isolation of neutrophils from the donated blood samples. The cell pellet was resuspended in 1 ml PBS glucose (5 mM) (Section 2.22.4), cell viabiltiy was assessed using the trypan blue cell exclusion assay (Eichner *et al.,* 1986) (Section 2.13), and neutrophil cell counts were used accordingly for assays.

2.23 ELISpot Assay to Measure Secreted Cytokine Levels in Isolated Peripheral Blood Mononuclear Cells (PBMC)

An ELISpot assay was performed to investigate the cytokine secretion from isolated peripheral blood mononuclear cells (PBMC), monocytes and T cells. A list of the cytokines investigated to examine the monocyte and T cell immune responses to the crude and pure *B. oleronius* proteins, and the dilutions for the capture and the detection antibodies, and the cell density per well for each cytokine target can be seen in Table 2.6. The assay was performed following guidelines of the suppliers (Mabtech AB, Nacka Strand, Stocknolm, Sweden). Briefly, a polyvinylidene fluoride (PVDF) membrane 96-well micro-plate (MAIPSWU, Millipore, Bedford, MA, USA) was prepared by activating the membrane with 50 µl/well ethanol (70%, v/v) for 1 minute, followed by a wash step (x 5) with sterile dH_2O (200 µl/well). The capture

antibody (100 µl/well) for the target cytokine was prepared by dilution in PBS (pH 7.4) to the assay concentration, added to the ELISpot micro-plate, and incubated overnight at 4°C. The coating antibody was removed by washing (x 5) with sterile PBS (pH 7.4) (200 µl/well).

The PVDF membrane was blocked using culture medium (RPMI-1640 GlutaMAX™ (Gibco®) supplemented fetal calf serum (FCS) (10%, v/v) (Gibco®)) (200 µl/well) for a minimum of 30 minutes at room temperature. The medium was removed, and isolated PBMC, monocytes and T cells (Section 2.21), were added to each well at the stated cell density (Table 2.6), with the following treatments (unstimulated, crude *B. oleronius* protein (5 µg/ml), pure *B. oleronius* protein (5 µg/ml), and either LPS (100 ng/ml) for investigating the monocyte cytokine response, or to examine the T cell cytokine response, phytohemagglutinin (PHA) (5 µg/ml) or anti-CD3 (1/1000 dilution from the supplier's kit), were employed as positive controls) to a final volume of 200 µl/well, and incubated at 37°C with a 5% CO_2 humidified atmosphere for 24 hour for isolated monocytes, and 48 hour for examining T cells. The 96-well ELISpot micro-plate was covered with foil to prevent evaporation for the duration of the incubation period.

After the incubation time-period, the culture medium and unbound cells were removed, and the micro-plate was washed (x 5) with sterile PBS (pH 7.4) (200 µl/well). The biotinylated detection antibody (100 µl/well) for the target cytokine was prepared by dilution in PBS (pH 7.4) containing FCS (0.5%, v/v) (the diluent was filter-sterilised before use) to the assay concentration, added to the ELISpot micro-plate, and incubated at room temperature for 2 hours. The detection antibody was removed by washing (x 5) with sterile PBS (pH 7.4) (200 µl/well), followed by the addition of streptavidin conjugated with alkaline phosphatase (ALP) (Streptavidin-ALP) (100 µl/well), diluted 1/1000 in PBS with FCS (0.5%, v/v), for 1 hour at room temperature.

The Streptavidin-ALP was removed by washing (x 5) with sterile PBS (pH 7.4) (200 µl/well), followed by the addition of substrate solution (100 µl/well), composed of 5-bromo-4-chloro-3-indoyl phosphate/nitro blue tetrazolium (BCIP/NBT)-plus. The substrate was left on the plate to develop until the formation of spots on the membrane was visible. The ELISpot micro-plate was washed in water to stop colour development, and left to air-dry. The analysis and counting of spots was performed using an Advanced Imaging Devices (AID) iSpot ELISpot plate reader

system, and ELISpot 3.5 computer software, or ELISpot ELISpot 6.0 spectrum computer software (AID GmbH, Straßberg, Germany).

2.24 FluoroSpot Assay to Measure Secreted Cytokine Levels in Isolated PBMC

A FluoroSpot assay was performed to investigate the cytokine secretion from isolated peripheral blood mononuclear cells (PBMC), monocytes and T cells. A list of the cytokines investigated to examine the monocyte and T cell immune responses to the crude and pure *B. oleronius* proteins, and the dilutions for the capture and the detection antibodies, and the cell density per well for each cytokine target can be seen in Table 2.7 and Table 2.8, respectively. The assay was performed by following guidelines of the suppliers (Mabtech). Briefly, a low-flourescent PVDF membrane 96-well IPFL micro-plate (Millipore) was prepared by activating the membrane with 15 µl/well ethanol (35%, v/v) for 1 minute, followed by a wash step (x 5) with sterile dH_2O (200 µl/well).

The addition of the dual capture antibodies, incubation of cells and treatments, and dual detection antibodies for the target cytokines was achieved by following the protocol described for the ELISpot assay (Section 2.23). Following incubation of the cytokine target detection antibodies conjugated with BAM (green flouresence), fluorescein isothiocyanate (FITC) (green flouresence), or biotinylated streptavidin red (SA) (red flouresence), the micro-plate was washed (x 5) with PBS (pH 7.4) (200 µl/well), and the FluoroSpot micro-plate was developed by the addition of anti-BAM-green, anti-FITC-green, or SA-550-red corresponding to the conjugated detection antibody (100 µl/well) for 1 hour at room temperature, and protected from light. The development solutions were prepared by dilution in filter-sterilised PBS (pH 7.4) containing BSA (0.1%, w/v), and are described in Table 2.7 and Table 2.8.

The FluoroSpot micro-plate was washed (x 5) with PBS (pH 7.4) (200 µl/well) to remove excess development solution, and Fluoresence enhancer II was added, 50 µl/well, for 15 minutes at room temperature. The contents of the micro-plate were discarded, and the residual Fluorescence enhancer II was removed by blotting the micro-plate firmly against clean paper towels. The underdrain of the Fluorospot micro-plate (the soft plastic cover under the plate) was removed, and the micro-plate was left to dry in a dark place before the recording and analysis of fluorescently-labeled secreted spots using an AID iSpot FluoroSpot micro-plate reader system, and ELISpot 6.0 spectrum computer software (AID GmbH).

2.25 Analysis of Endotoxin Activity in *B. oleronius* Protein Preparation by ELISpot

Fresh blood from healthy volunteers was collected in heparin-EDTA treated tubes following informed consent and approval of the NUI Maynooth ethics committee (BSRESC-2012-008) to isolate peripheral blood mononuclear cells (PBMC) according to the method described by Smedman *et al.* (2009, 2012), and described in Section 2.21. To confirm the absence of endotoxin contamination in both the crude and pure *B. oleronius* protein preparations, tumor necrosis factor **(**TNF)-α ELISpot cytokine assays were performed using isolated PBMC, at a density of 5 x 10^5 cells/well, and treated with crude or pure *B. oleronius* protein (2, 0.2, 0.002, and 0.0002 µg/ml), lipopolysaccharide (LPS) (10, 1, 0.1, and 0.001 ng/ml), and with or without the addition of polymyxin B (10 µg/ml) to specific sample wells to inhibit LPS activity if present.

The assay was performed according to manufacturer's guidelines (Mabtech), and decribed in Section 2.23, with analysis of PBMC TNF-α secreted spots recorded using an AID iSpot ELISpot micro-plate reader system, and ELISpot 3.5 computer software, and ELISpot 6.0 spectrum computer software (AID GmbH). A titre of LPS concentrations (10, 1, 0.1, and 0.001 ng/ml) with and without polymyxin B (10 µg/ml) was also performed using an IL-6 FluoroSpot assay to examine the functionality of polymyxin B, and followed the FluoroSpot assay protocol described in Section 2.24. The recording and analysis of fluorescently-labeled secreted spots using an AID iSpot FluoroSpot micro-plate reader system, and ELISpot 6.0 spectrum computer software (AID GmbH).

Table 2.6 List of cytokines analysed by ELISpot. A list of the cytokines investigated by ELISpot to examine the monocyte and T cell immune responses to the crude and pure *B. oleronius* proteins, and the dilutions for the capture and the detection antibodies, and the cell density per well for each cytokine target.

Cytokine Target	Company	Product Code	ELISpot Micro-Plate	Capture Antibody (conc.)	Capture Antibody Dilution (conc.)	Biotinylated Detection Antibody (conc.)	Biotinylated Detection Antibody Dilution (conc.)	Enzyme/Substrate	Cells per Well
IL-2	Mabtech AB	3445-2AW-Plus	MAIPSWU (Millipore)	MT2A91/2C95 (0.5 mg/ml)	1/50 (10 µg/ml)	MT8G10-Biotin (0.5 mg/ml)	1/2000 (0.25 µg/ml)	Streptavidin ALP/ BCIP/NBT-plus	2.5×10^5
IL-5	Mabtech AB	3490-2AW-Plus	MAIPSWU (Millipore)	TRK5 (1 mg/ml)	3/200 (15 µg/ml)	5A10-Biotin (1 mg/ml)	1/1000 (1 µg/ml)	Streptavidin ALP/ BCIP/NBT-plus	2.5×10^5
IL-6	Mabtech AB	3460-2A	MAIPSWU (Millipore)	13A5 (1 mg/ml)	3/200 (15 µg/ml)	39C3-Biotin (1 mg/ml)	1/1000 (1 µg/ml)	Streptavidin ALP/ BCIP/NBT-plus	5×10^3
IL-12p40	Mabtech AB	3450-2A	MAIPSWU (Millipore)	MT86/221 (0.5 mg/ml)	1/50 (10 µg/ml)	MT618-Biotin (0.5 mg/ml)	1/500 (1 µg/ml)	Streptavidin ALP/ BCIP/NBT-plus	5×10^4
IL-13	Mabtech AB	3470-2AW-Plus	MAIPSWU (Millipore)	IL13-I (0.5 mg/ml)	1/50 (10 µg/ml)	IL13-3-Biotin (0.5 mg/ml)	1/500 (1 µg/ml)	Streptavidin ALP/ BCIP/NBT-plus	2.5×10^5
IL-17A	Mabtech AB	3520-2AW-Plus	MAIPSWU (Millipore)	MT44.6 (0.5 mg/ml)	1/50 (10 µg/ml)	MT504-Biotin (0.5 mg/ml)	1/1000 (0.5 µg/ml)	Streptavidin ALP/ BCIP/NBT-plus	2.5×10^5
IL-22	Mabtech AB	3475-2AW-Plus	MAIPSWU (Millipore)	MT12A3 (0.5 mg/ml)	1/50 (10 µg/ml)	MT7B27-Biotin (0.5 mg/ml)	1/1000 (0.5 µg/ml)	Streptavidin ALP/ BCIP/NBT-plus	2.5×10^5
IL-31	Mabtech AB	3530-2AW-Plus	MAIPSWU (Millipore)	MT31/88 (0.5 mg/ml)	1/50 (10 µg/ml)	MT158-Biotin (0.5 mg/ml)	1/5000 (0.1 µg/ml)	Streptavidin ALP/ BCIP/NBT-plus	2.5×10^5
IFN-γ	Mabtech AB	3420-2AW-Plus	MAIPSWU (Millipore)	1-D1K (1 mg/ml)	3/200 (15 µg/ml)	7-B6-1-Biotin (1 mg/ml)	1/1000 (1 µg/ml)	Streptavidin ALP/ BCIP/NBT-plus	2.5×10^5
TNF-α	Mabtech AB	3510-2A	MAIPSWU (Millipore)	TNF3/4 (0.5 mg/ml)	3/100 (15 µg/ml)	TNF5-Biotin (0.5 mg/ml)	1/1000 (0.5 µg/ml)	Streptavidin ALP/ BCIP/NBT-plus	5×10^3

Table 2.7 List of cytokines analysed in isolated monocytes by FluoroSpot. A list of the cytokines investigated by FluoroSpot to examine the monocyte immune responses to the crude and pure *B. oleronius* proteins, and the dilutions for the capture and the detection antibodies, and the cell density per well for each cytokine target.

Cytokine Targets	Company	Product Code	FluoroSpot Micro-Plate	Cells per Well	Capture Antibody (conc.)		Capture Antibody Dilution (conc.)		Detection Antibody (conc.)		Detection Antibody Dilution (conc.)		Fluorophore Conjugate (dilution)	
					FL1 (Green Channel)	FL2 (Red Channel)	FL1 (Green Channel)	FL2 (Red Channel)	FL1 (Green Channel)	FL2 (Red Channel)	FL1 (Green Channel)	FL2 (Red Channel)	FL1 (Green Channel)	FL2 (Red Channel)
IL-6 / IL-1β	Mabtech AB	N/A	IPFL (Millipore)	5×10^3	13A5 (1 mg/ml)	IL1β-I (1 mg/ml)	3/200 (15 µg/ml)	3/200 (15 µg/ml)	39C3-BAM	IL1β-II-Biotin (1 mg/ml)	1/200	1/500 (2 µg/ml)	Anti-BAM-490 (1/200)	SA-550 (1/200)
IL-6 / IL-10	Mabtech AB	N/A	IPFL (Millipore)	5×10^4	13A5 (1 mg/ml)	9D7 (1 mg/ml)	3/200 (15 µg/ml)	3/200 (15 µg/ml)	39C3-BAM	12G8-Biotin (1 mg/ml)	1/200	1/500 (2 µg/ml)	Anti-BAM-490 (1/200)	SA-550 (1/200)
IL-6 / IL-12p40	Mabtech AB	FS-1314-2	IPFL (Millipore)	5×10^4	13A5 (1 mg/ml)	MT86/221 (0.5 mg/ml)	3/200 (15 µg/ml)	3/100 (15 µg/ml)	39C3-BAM	MT618-Biotin (0.5 mg/ml)	1/200	1/250 (2 µg/ml)	Anti-BAM-490 (1/200)	SA-550 (1/200)
IL-6 / IL-23	Mabtech AB	FS-1314-2	IPFL (Millipore)	5×10^4	13A5 (1 mg/ml)	MT86/221 (0.5 mg/ml)	3/200 (15 µg/ml)	3/100 (15 µg/ml)	39C3-BAM	MT618-Biotin (0.5 mg/ml)	1/200	1/250 (2 µg/ml)	Anti-BAM-490 (1/200)	SA-550 (1/200)
IL-6 / TNF-α	Mabtech AB	FS-1309-2	IPFL (Millipore)	5×10^3	13A5 (1 mg/ml)	TNF3/4 (0.5 mg/ml)	3/200 (15 µg/ml)	3/100 (15 µg/ml)	39C3-BAM	TNF5-Biotin (0.5 mg/ml)	1/200	1/500 (1 µg/ml)	Anti-BAM-490 (1/200)	SA-550 (1/200)
IL-6 / GM-CSF	Mabtech AB	FS-1315-2	IPFL (Millipore)	5×10^3	13A5 (1 mg/ml)	21C11 (1 mg/ml)	3/200 (15 µg/ml)	3/200 (15 µg/ml)	39C3-BAM	23B6-Biotin (1 mg/ml)	1/200	1/500 (2 µg/ml)	Anti-BAM-490 (1/200)	SA-550 (1/200)

Table 2.8 List of cytokines analysed in isolated T cells by FluoroSpot. A list of the cytokines investigated by FluoroSpot to examine the T cell immune responses to the crude and pure *B. oleronius* proteins, and the dilutions for the capture and the detection antibodies, and the cell density per well for each cytokine target.

Cytokine Targets	Company	Product Code	FluoroSpot Micro-Plate	Cells per Well	Capture Antibody (conc.)		Capture Antibody Dilution (conc.)		Detection Antibody (conc.)		Detection Antibody Dilution (conc.)		Fluorophore Conjugate (dilution)	
					FL1 (Green Channel)	FL2 (Red Channel)	FL1 (Green Channel)	FL2 (Red Channel)	FL1 (Green Channel)	FL2 (Red Channel)	FL1 (Green Channel)	FL2 (Red Channel)	FL1 (Green Channel)	FL2 (Red Channel)
IL-17A / IL-22	Mabtech AB	FS-1314-2	IPFL (Millipore)	2.5×10^5	MT44.6 (0.5 mg/ml)	MT12A3 (0.5 mg/ml)	3/100 (15 µg/ml)	3/100 (15 µg/ml)	MT504-BAM	MT7B27-Biotin (0.5 mg/ml)	1/200	1/1000 (0.5 µg/ml)	Anti-BAM-490 (1/200)	SA-550 (1/200)
IL-17A / IL-31	Mabtech AB	N/A	IPFL (Millipore)	2.5×10^5	MT44.6 (0.5 mg/ml)	MT31/88 (0.5 mg/ml)	3/100 (15 µg/ml)	1/50 (10 µg/ml)	MT504-BAM	MT158-Biotin (0.5 mg/ml)	1/200	1/500 (1 µg/ml)	Anti-BAM-490 (1/200)	SA-550 (1/200)
IFN-γ / IL-5	Mabtech AB	FS-0108-2	IPFL (Millipore)	2.5×10^5	1-D1K (1 mg/ml)	TRK5 (1 mg/ml)	3/200 (15 µg/ml)	3/200 (15 µg/ml)	7-B6-1-FS-FITC	5A10-Biotin (1 mg/ml)	1/200	1/500 (2 µg/ml)	Anti-FITC-490 (1/200)	SA-550 (1/200)
IFN-γ / IL-17A	Mabtech AB	FS-0103-2	IPFL (Millipore)	2.5×10^5	1-D1K (1 mg/ml)	MT44.6 (0.5 mg/ml)	3/200 (15 µg/ml)	3/100 (15 µg/ml)	7-B6-1-FS-FITC	MT504-Biotin (0.5 mg/ml)	1/200	1/250 (2 µg/ml)	Anti-FITC-490 (1/200)	SA-550 (1/200)
IFN-γ / IL-22	Mabtech AB	FS-0118-2	IPFL (Millipore)	2.5×10^5	1-D1K (1 mg/ml)	MT12A3 (0.5 mg/ml)	3/200 (15 µg/ml)	3/100 (15 µg/ml)	7-B6-1-FS-FITC	MT7B27-Biotin (0.5 mg/ml)	1/200	1/1000 (0.5 µg/ml)	Anti-FITC-490 (1/200)	SA-550 (1/200)
IFN-γ / IL-31	Mabtech AB	N/A	IPFL (Millipore)	2.5×10^5	1-D1K (1 mg/ml)	MT31/88 (0.5 mg/ml)	3/200 (15 µg/ml)	1/50 (10 µg/ml)	7-B6-1-FS-FITC	MT158-Biotin (0.5 mg/ml)	1/200	1/500 (1 µg/ml)	Anti-FITC-490 (1/200)	SA-550 (1/200)

2.26 Quantification of D-myo-Inositol 1 Phosphate (IP_1) Levels in Stimulated Human Neutrophils by *B. oleronius* Proteins

The abundance of D-*myo*-inositol 1 phosphate (IP_1) in neutrophils was assessed using an IP-One (IP_1) ELISA assay kit (Cisbio Bioassays, Codolet, France), and following the manufacturer's guidelines. Freshly isolated human neutrophils (Section 2.22) (5 x 10^6/ml) were resuspended in stimulation buffer (pH 7.4) (1X: 4-(2-hydroxyethyl)-1-piperethanesulfonic acid (HEPES) (10 mM), calcium chloride ($CaCl_2$) (1 mM), magnesium chloride ($MgCl_2$) (0.5 mM), potassium chloride (KCl) (4.2 mM), sodium chloride (NaCl) (146 mM), glucose (5.5 mM), and lithium chloride (LiCl (50 mM)(provided in the assay kit), and stimulants (fMLP: 1 μ M, IL-8: 10 ng/ml, BSA: 2 μg/ml, crude *B. oleronius* protein: 2 μg/ml and 6 μg/ml, and pure *B. oleronius* protein: 2 μg/ml and 6 μg/ml) at 37°C for 1 hour. Cells were lysed in a 2% lysis reagent (potassium fluoride (KF) (0.03%, w/v), sodium azide (NaN_3) (0.001%, w/v), and Triton™ X-100 (0.25%, w/v) in dH_2O) (provided the assay kit) for 30 minutes at 37°C. From this, cell supernatants were transferred to a coated 96-well microplate supplied with the kit, and IP_1-HRP conjugate and anti-IP_1 monoclonal antibody (MAB) were added for 3 hours at room temperature. The IP_1 ELISA plate was developed using a 3, 3', 5, 5'-tetramethylbenzidine (TMB) substrate, and read at absorbance 450 nm on a BioTek Synergy™ HT (BioTek Instruments Inc., Vermont, USA) microplate reader to generate a standard curve, and from the standard cure, quantify levels of IP_1 in stimulated human neutrophils. A representative standard cure is given in Figure 2.3.

2.27 Intracellular Calcium (Ca^{2+}) Flux by Human Neutrophils Exposed to *B. oleronius* Proteins

Intracellular calcium (Ca^{2+}) levels were measured using the Fluo-4 NW calcium assay kit (Molecular Probes™, Invitrogen, Life Technologies) and the protocol was followed according to the manufacturer's guidelines. Briefly, cells were seeded at a density of 2 x 10^5 cells/well, and resuspended in 5 mM PBS glucose (40 μl) (Section 2.22.5) onto a 96-well microplate (Nunc™ U96 PP 0.5 ml, poly-D-lysine-coated), and incubated at 37°C for 30 minutes. Ater the incubation period, the Flou-4 NW dye mix (40 μl/well) supplied with assay kit was added. Plates were wrapped in foil to protect from light, and incubated for a further 30 minutes at 37°C. The stimulants (fMLP: 1 μM, IL-8: 10 ng/ml, crude *B. oleronius* proteins: 2 μg/ml, and pure *B. oleronius*

proteins: 2 μg/ml) (10 μl) were warmed to 37°C prior to stimulation of human neutrophils. The Ca^{2+} fluorescence was determined immediately at 494 nm wavelength , and read at 10-second intervals for a total of 90 seconds with stimulation of human neutrophils occurring after 40 seconds (indicated by arrow (🡻) in the Figure for the thesis) on a BioTek Synergy™ HT (BioTek Instruments, Inc., P.O. Box 998, Highland Park, Vermont, USA) microplate reader.

2.28 Analysis of Cytoskeletal Reassembly and Filamentous (F)-Actin Polymerisation Following Exposure of Human Neutrophils to *B. oleronius* Proteins

The cytoskeletal resassembly of filamentous (F)-actin and globular (G)-actin abundance was analysed following the method described by Jayachandran *et al*. (2007). Neutrophils were isolated and resuspended at a density of 1 x 10^7 cells per treatment and stimulated with IL-8 (10 ng/ml), crude *B. oleronius* protein preparation (2 μg/ml), or pure *B. oleronius* protein preparation (2 μg/ml) in a water bath at 37°C for 10 minutes, prior to pelleting of cells (300 x *g* for 5 minutes at 4°C) and washed with 5 mM PBS glucose (1 ml) (Section 2.22.5). Cells were lysed in F-actin stabilisation buffer (50 mM piperazine-N, N′-bis (2-ethanesulfonic acid) (PIPES) at pH 6.9, 50 mM potassium chloride (KCl), 5 mM magnesium chloride ($MgCl_2$), 5 mM ethylene glycol tetraacetic acid (EGTA), 5% (v/v) glycerol, 0.1% (v/v) Turgitol© NP-40, 0.1% (v/v) Triton™ X-100, 0.1% (v/v) Tween®-20, 0.1% (v/v) 2-mercaptoethanol in the presence of 1 mM ATP, phosphatase inhibitors (sodium orthovanadate (Na_3VO_4), and sodium fluoride (NaF)) (0.5 ml) and protease inhibitors (TLCK, pepstatin A, phenylmethylsulfonyl fluoride (PMSF), leupeptin) at 37°C for 10 minutes. Lysates were fractionated at 100,000 x *g* for 2 hours at 37°C using polycarbonate thickwall (16 x 76 mm) centrifuge tubes (Beckman Coulter), a 70.1 Ti rotor (Beckman Coulter), and an Optima™ L-100 XP Ultracentrifuge (Beckman Coulter). Following centrifugation, the supernatant (G-actin) was transferred to a fresh tube, and the pellet (F-actin) was resuspended to the same volume as that of the supernatant with ice-cold dH_2O containing 10 μM cytochalasin D to inhibit the polymerization of actin. The sample was incubated on ice for 1 hour to allow dissociation, and resuspension of F-actin.

2.28.1 Quantification of G- and F-Actin Distribution Ratios in Stimulated Human Neutrophils

Equal volumes of extracted subcellular neutrophil fractions were loaded onto a 1-D SDS-PAGE, and separated under reducing conditions (Section 2.14). Following electrophoresis, resolved proteins were transferred onto a nitrocellulose membrane (Fisher Scientific), using a wet blotter transfer rig in transfer buffer for Western blotting (Section 2.19), the abundance of G- and F-actin was detected using an anti-actin primary antibody (Table 2.4), and corresponding mouse anti-human IgG secondary antibody (Table 2.5) before blot development. Western blot images were recorded using an ImageScanner™ III (GE Healthcare, Life Sciences) and acquired using LabScan™ 6.0, Epson Scan, Epson Expression™ 10000 XL software (GE Healthcare, Life Sciences). Immuno-bands were quantified by densitometry using Image J software (National Institutes of Health (NIH), Bethesda, MD, USA), and the distribution ratios between the abundance of G- and F-actin for each treatment was calculated.

2.29 Neutrophil Chemotaxis Induction by *B. oleronius* Proteins

2.29.1 Chemotaxis Assay Protocol

Chemotaxis assays were performed in triplicate, and using a multi-well chemotaxis chamber (Neuro Probe Inc., Gaithersburg, MD, USA), and a 5 μm pore filter (Neuro Probe Inc.) set up to the manufacturer's guidelines with the stimulants (N-formyl-methionyl-leucyl-phenaylalanine (fMLP): 1 μM, IL-8: 10 ng/ml, crude *B. oleronius* protein: 2 μg/ml, pure *B. oleronius* protein: 2 μg/ml) (in a final volume of 80 μl in PBS glucose (5 mM) (Section 2.22.5)) were added to the bottom of the chamber with a positive meniscus to create a chemotactic gradient. Human neutrophils (2×10^5 cells/well) (Section 2.22) were resuspended in 5 mM PBS glucose, added to each well (200 μl) of the multi-well chemotaxis chamber, and placed in a 37°C for 30 minutes.

2.29.2 Fixing and Staining of Cells

After the incubation period, the 5 μm pore filter was removed from the chamber for fixing and staining of migrated neutrophils. The cell side of the filter was placed in methanol for 2 minutes at room temperature, and allowed to air dry for

5 minutes, followed by covering the cell side of the filter with Stain A (Speedy-Diff Solution "A", Clin-Tech Limited, Guildford, UK) for 5 minutes and then in Stain B (Speedy-Diff Solution "B", Clin-Tech) for a further 5 minutes. The cell side of the filter was washed with PBS (pH 7.4), and the filter was allowed to air-dry before counting of migrated neutrophils.

2.29.3 Counting of Migrated Cells

Cells that had completely migrated through the filter were counted in 5 random high-power fields of vision (magnification 40x) per well per treatment by light microscopy. A chemotactic index was used to express the chemotactic activity and was measured by calculating the number of cells migrated to the chemokine divided by the number of cells that migrated spontaneously to the chemotaxis buffer, and the fold change of neutrophil chemotaxis was calculated relative to the unstimulated control.

2.30 General Cell Culture Methodolgy

2.30.1 Corneal Epithelial (hTCEpi) Cell Culture and Sub-Culture

Human telomerase-immortalized corneal epithelial cells (hTCEpi) (sourced from Tissue Engineering Lab, NICB, DCU) were maintained in Keratinocyte Growth Medium (KGM™)-2 supplemented with KGM™-2 SingleQuot™ kit supplements and growth factors (bovine pitutary extract (BPE), human epidermal growth factor (hEGF), recombinant human insulin, hydrocortisone, and GA-1000 (a combination of gentamicin and amphotericin B)) (Lonza, Basel, Switzerland) (corneal epithelial (hTCEpi) culture medium), in a 5% CO_2 incubator at 37°C, and passaged (harvested) every 3 to 5 days depending on cell culture confluency.

Cultured hTCEpi cells were harvested for sub-culturing, and assays, by trypsinization using 1 ml trypsin buffer (trypsin (0.25%, w/v)-EDTA (53 mM) (0.022%, w/v) in PBS) for 5 minutes, or until the cells had detached, before using equal volumes of trypsin neutralisation medium (Dulbecco's modified eagle medium (DMEM) (Gibco®) (95%, v/v) supplemented with FCS (5%, v/v)) to inhibit the action of trypsin, followed by centrifugation of the cell suspension at 200 x *g* for 5 minutes. The cell pellet was resuspended in 3 ml sterile PBS, and the centrifugation

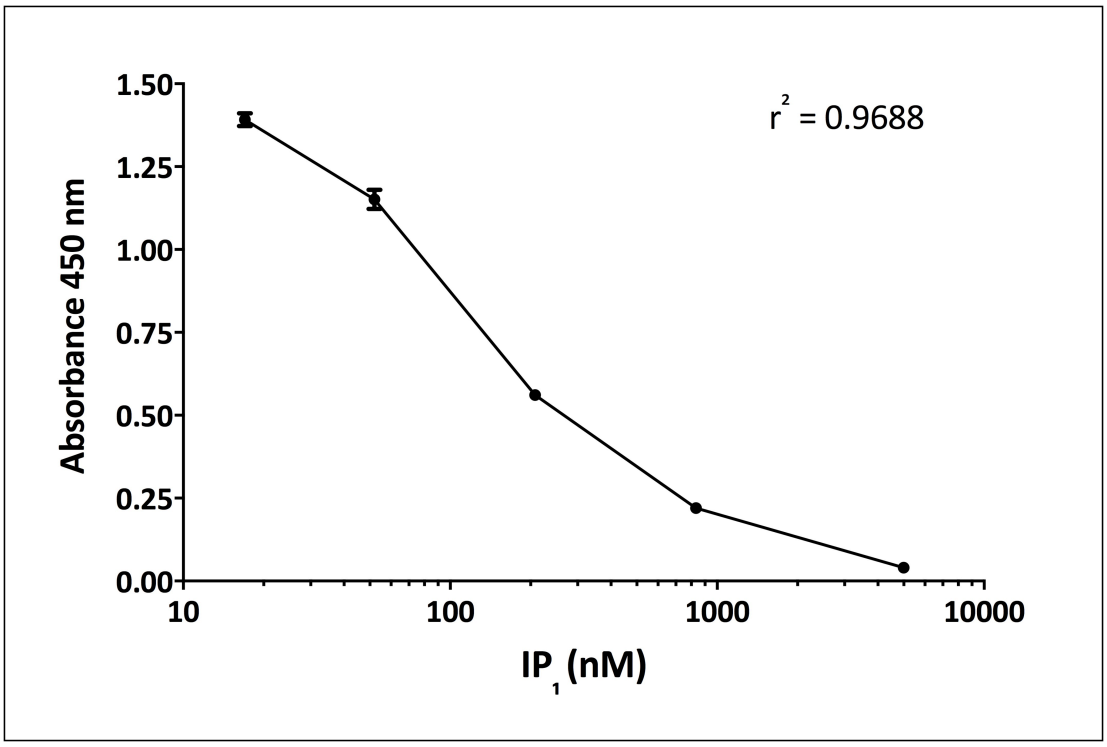

Figure 2.3 A representative standard curve for IP_1 ELISA. A representative standard curve used to measure the production of secreted IP_1 following stimulation of neutrophils by *B. oleronius* proteins.

step was repeated, before resuspension in 1 ml corneal epithelial (hTCEpi) culture medium. Cell counts were achieved using the trypan blue cell exclusion method (Section 2.13) used accordingly for sub-culturing, cryopreservation, and hTCEpi assays. Cells were left to adhere overnight before exposure to the *B. oleronius* proteins, unless stated.

2.30.2 Cryopreservation of hTCEpi Cells in Liquid Nitrogen (N_2)

Corneal epithelial (hTCEpi) cells were cultured to the exponential phase of growth (approximately 60% confluency), and harvested by trypsinization (trypsin (0.25%, w/v)-EDTA (0.022%, w/v) in PBS). Cells counts were performed using the trypan blue cell exclusion method (Section 2.13) before resuspension of hTCEpi cells (2×10^6 cells/ml) in cryopreservation buffer (Dulbecco's modified eagle medium (DMEM) (Gibco®) (80%, v/v), supplemented with FCS (10%, v/v), and DMSO (10%, v/v) aliquoted to 1 ml volumes using cryovials, and transferred to a Mr Frosty™ freezing container (Nalgene®, Thermo Scientific) (contained ice-cold methanol (100 ml) and was stored at -80°C the night before use) and stored at -80°C overnight before the cyrovials were placed in a liquid N_2 (-195.79°C) tank for long term storage. The cryopreservation buffer was kept at 4°C before use.

2.30.3 Recovery of hTCEpi Cells from Liquid N_2

Corneal epithelial (hTCEpi) cells were recovered from liquid N_2 (-195.79°C) storage by rapid thawing of cells using pre-warmed cell recovery medium (DMEM (95%, v/v) supplemented with FCS (5%, v/v)) (10 ml of recovery medium for a 1 ml aliquot of cells per cryovial). The cell recovery process was performed quickly to promote cell viability, and was achieved by swiftly pipetting cells into suspension with the recovery medium followed centrifugation at 200 x *g* for 3 minutes. Recovered cells were washed (x 2) in corneal cell culture medium, and centrifuged again before transfer to a T-75 cm^2 or T-175 cm^2 tissue culture flask (Corning). The flasks were placed in a 5% CO_2 humidified atmosphere incubator at 37°C for 1 hour followed by a medium change to remove unattached cells (non viable).

2.31 The Effect of *B. oleronius* Proteins on the Growth of Corneal Epithelial Cell and Assessment of Cytotoxicity

Human corneal epithelial cells (hTCEpi) were seeded onto a 96-well tissue culture plate (Corning) at a density of 1 x 10^3 cells/well, and exposed to BSA, crude *B. oleronius* proteins, and pure *B. oleronius* proteins at concentrations of 1, 2, 4, 6 and 8 µg/ml for a duration of 6 days. Following the assay incubation time period, the growth of hTCEpi cells and cytotoxicity of the *B. oleronius* treatments was assessed by crystal violet (0.25%, w/v) staining, and by 2, 3, -bis-(-2-4-nitro-5-sulfophenyl)-2H-tetrazolium-5-carboxanilide inner salt (XTT) staining. Images were captured on a Nikon TiE microscope (magnification 10x) for the assay (scale bar: 200 µm).

2.31.1 Corneal Cell Cytotoxicity Assay Assessed by XTT Staining

Following the 6 day culture period of the assay, the medium was removed, and each sample well was washed (x 3) with sterile PBS (200 µl). XTT stain (*In vitro* Toxicology Assay Kit, XTT based, Sigma) was reconstituted in 5 ml corneal epithelial (hTCEpi) cell culture medium, pre-warmed and fully solublised before the addition of 20 µl/well XTT stain, and incubated for 2 hours in a 5% CO_2 incubator at 37°C. Following incubation, the plate was read at absorbance 450 nm on a BioTek Synergy™ HT (BioTek Instruments Inc., Vermont, USA) microplate reader. The percentage growth of viable hTCEpi cells for each treatment was calculated relative to the untreated control hTCEpi cells. All cytotoxic assays were performed in triplicate, and to be within 10% standard deviation from the mean.

2.31.2 Corneal Cell Cytotoxicity Assay Assessed by Crystal Violet (0.25%, w/v) Staining

Following the 6 day culture period of the assay, the medium was removed, and each sample well was washed (x 3) with sterile PBS (200 µl). An aqueous solution containing crystal violet (0.25%, w/v) was prepared, and 100 µl crystal violet (0.25%, w/v) stain was added to each sample well for 10 minutes at room temperature. Following the staining period, each well was washed (x 4) with sterile dH_2O (200 µl), and allowed to air-dry for 10 minutes at room temperature. The stain colour was solubilized by the addition of 100 µl/well glacial acetic acid (33%, v/v), and the plate was read at absorbance 570 nm on a BioTek Synergy™ HT (BioTek Instruments Inc., Vermont, USA) microplate reader. The percentage growth of

hTCEpi cells for each treatment was calculated relative to the untreated control hTCEpi cells. All cytotoxic assays were performed in triplicate, and to be within 10% standard deviation from the mean.

2.32 Corneal Epithelial Cell Proliferation Assay

Human corneal epithelial cells (hTCEpi) were seeded onto a 6-well tissue culture plate (Corning) at a density of 5 x 10^5 cells/well and exposed to pure *B. oleronius* proteins at concentrations of 2 and 6 µg/ml. Cell counts were performed on Day 0, 1, 2, 3, and 6 using a haemocytometer and cell viability was measured using the trypan blue cell exclusion method (Section 2.13). Corneal epithelial cells were co-cultured with the *B. oleronius* proteins for the duration of the assay. Images were captured on a Nikon TiE microscope (magnification 10x) for the assay (scale bar: 200 µm). The mean generation time (MGT) was calculated between day 2 (N_0), and day 3 (N_t) according to the following formula to assess the rate of proliferation, and cell doubling time of corneal epithelial cells exposed to the *B. oleronius* proteins.

$$MGT = \frac{(\log_{10} N_t - \log_{10} N_0)}{\log_{10} 2}$$

2.33 Cell Cycle Analysis by Fluorescence-Activated Cell Sorting (FACS)

2.33.1 Assessment of 5-Ethynyl-2'-Deoxyuridine (EdU) Incorporation on the Growth of Corneal Epithelial Cells by Staining

The cytotoxicity of incorporating 5-Ethynyl-2'-Deoxyuridine (EdU) into hTCEpi cell cultures was assessed to determine suitability of hTCEpi cells for use with the Click-it™ EdU flow cytometry assay kit (Invitrogen, Life Technologies). Titrations of EdU at 1, 1.25, 1.5, 1.75, 2, 2.5, 5, and 10 µM were exposed to corneal epithelial (hTCEpi) cells for 6 days, as described in Section 2.32, followed by staining with crystal violet (0.25%, v/v) to assess hTCEpi cell growth relative to the untreated control hTCEpi cells (Section 2.33.2).

2.33.2 Cell Cycle Analysis by Propidium Iodide Staining and FACS

Fluorescence-activated cell sorting (FACS) through propidium iodide (PI) staining was performed with the assistance of Dr Clair Gallagher (DCU) to analyse the phases of the corneal epithelial cell cycle following exposure to *B. oleronius* proteins. Human corneal epithelial cells (hTCEpi) were seeded into 6-well plates (Corning) at a density of 1 x 10^4 cells/well. Cells attached during a 2 hour incubation, and were treated using KGM-Gold media (Lonza) alone, or KGM-Gold media supplemented with pure *B. oleronius* proteins (6 µg/ml). Following 48 hour exposure, hTCEpi cells were harvested using trypsin (0.25%, w/v)-EDTA (0.022%, w/v) in PBS, PBS washed, and fixed with ice cold 90% methanol (Sigma). Samples were stained using propidium iodide (Biotium Inc., Hayward, CA, USA) according to the manufacturer's instructions, and analyzed using a Guava easyCyte HT flow cytometer (Millipore, EMD Millipore, Billerica, MA, USA). The percentages of cells in Gap-1 (G_1), Synthesis (S), and Gap-2 (G_2) phases of the cell cycle were calculated using the ModFit LT 3.2 DNA cell-cycle analysis software (Verity Software House, Topsham, ME, USA).

2.34 Caspase-3 and Caspase-7 Immunofluorescence Assay

Corneal epithelial cells were cultured for 3 days in culture dishes (CELLVIEW™, cell culture dish with glass bottom, TC, 35 mm, 1 compartment, Greiner Bio-one GMbH) (2 x 10^5 cells/well) under the following conditions; untreated, dimethyl sulfoxide (DMSO) (1%, v/v), and pure *B. oleronius* protein (6 µg/ml) before washing with 1X apoptosis wash buffer (supplied with assay kit), and staining for caspase-3/7 activity, and assessed following the guidelines in the Image-iT™ LIVE Red Caspase-3 and -7 Detection Kit (Invitrogen). The fluorescent labelled inhibitor of caspases (FLICA) reagent was prepared by the addition of DMSO (50 µl) to the vial of lyophilized FLICA reagent (FAM-DEVD-FMK caspase-3 and -7 reagent) to give a 150X FLICA reagent stock solution.

The 150X FLICA reagent stock solution was diluted 5-fold in PBS to give a 30X FLICA reagent stock solution. Following preparation of assay reagents, the cultured corneal epithelial (hTCEpi) cells were washed with warm culture medium before the addition of 1X FLICA reagent (30-fold dilution from 30X FLICA reagent stock solution). A sufficient volume of stain was added to cover the cell monolayer (500 µl), and cells were incubated for 1 hour under culture conditions, and protected

from light. After the incubation period, the cells were washed with warm culture medium, followed by the addition of a 1000-fold diluted preparation of 1 mM Hoescht 3334 stain. A sufficient volume of stain was added to cover the cell monolayer (500 µl), and cells were incubated for 10 minutes in a 5% CO_2 incubator at 37°C, and protected from light. Cells were washed with warm 1X apoptosis wash buffer (supplied with assay kit) before the capturing of images.

Cells were stained with fluorescent labelled inhibitor of caspases (FLICA) reagent (excitation/emission at 550/595 nm) (green fluorescence) that becomes covalently and irreversibly coupled to active caspase-3 and -7, and Hoescht 33342 stain was used as a nuclear stain (excitation/emission at 350/461 nm) (blue fluorescence) to visualize hTCEpi cells positive and negative for caspase-3/7. Images were captured on a Nikon TiE microscope (magnification 40x) controlled using MetaMorph software. Images were analysed using MetaMorph software (Molecular Devices, Berkshire, UK). Cells positively expressing active caspase-3 and -7 stained a yellow fluorescence on captured images demonstrating the induction of apoptosis. Results represent experiments performed in triplicate and determined for five fields of view per treatment for each repeat of the assay.

2.35 RNA Extraction of Treated hTCEpi Cells and Gene Expression Analysis

The analysis of gene expression in treated hTCEpi cells was achieved with the assistance of Dr Clair Gallagher (DCU). Corneal cells (hTCEpi) (6×10^4/well) were seeded in 6-well culture dishes and exposed to pure *B. oleronius* proteins (0, 2, or 6 µg/ml) for 5 days, with feeding and treatment on alternate days. Following PBS washes (x 3), Tri-reagent (1 ml/ well) was applied and RNA extracted according to manufacturer's instructions (Sigma). RNA concentration was determined using a NanoDrop spectrophotometer (ND-1000, Labtech International, UK) and complimentary DNA (cDNA) synthesized using a high-capacity RNA to cDNA kit (Applied Biosystems, Carlsbad, CA, USA). Amplification of chemokine ligand-20 (CCL20), interleukin (IL)-1β, IL-6, IL-8, S100A7, and tumor necrotic factor (TNF) targets was performed using TaqMan Gene Expression Assays (Hs01011368_m1, Hs01555410_m1, Hs00985639_m1, Hs00174103_m1, Hs00161488_m1, Hs00174128_m1, respectively) in conjunction with an ABI 7500 Fast Real-time PCR thermal cycler (Applied Biosystems). Resultant cycle threshold (Ct) values from real-time PCR expression analyses, were normalized against human glyceraldehyde 3-

phosphate dehydrogenase (GAPDH) endogenous control expression (Hs99999905_m1) and changes in expression calculated using the relative quantification (RQ) = 2−ΔΔCt equation. All experiments were performed on three independent occasions and results presented are given as the mean ± standard error (SE).

2.36 Gelatinase Zymograms to Investigate Matrix Metalloproteinase (MMP) Activity

Cell supernatants collected from cell proliferation assays at days 3 and 6 following exposure of hTCEpi cells to pure *B. oleronius* proteins at 2 and 6 µg/ml, were filter concentrated using 3000 molecular weight cut off (MWCO) Vivaspin®-20 filter columns (Vivaproducts, Vivaproducts Inc., GE Healthcare, Littleton, MA, USA) by centrifugation at 3,500 x *g* for 45 minutes. Concentrated protein samples were prepared for loading (protein sample (5 µl), 2X native sample buffer without SDS (5 µl) (Novex®, Invitrogen, Life Technologies), and loading dye (3 µl)) onto a Novex® 10% zymogram (gelatin) gels (Invitrogen, Life Technologies), composed of tris-glycine (10%, w/v) with gelatin (0.1%, w/v) as the substrate incorporated into the solidifed gel. Following electrophoresis at 125 V, 40 milliamps (mA) for 90 minutes, the zymogram gels were incubated in 1X zymogram renaturing buffer (Invitrogen, Life Technologies) for 30 minutes at room temperature, left at 37°C overnight in 1X zymogram developing buffer (Invitrogen, Life Technologies) and stained with colloidal Coomassie blue for 2 hours prior to de-staining of gels in distilled water and recording of gel images (Section 2.16).

2.37 Enzyme-Linked Immunosorbent Assay (ELISA) to Measure Secreted Cytokine Expression Levels

2.37.1 Preparation of Sample to Detect Secreted Cytokine Expression Levels in Patient Serum

In collaboration with Dr Stanisław Jarmuda and colleagues of Poznań University of Medical Sciences in Poland, samples of peripheral blood (20 ml) from the cubital vein were collected from all study participants between 8 am and 1 pm into EDTA-heparin tubes (Monovette, Sarstedt). The blood was centrifuged at 500 x *g* for 10 minutes. The serum specimen was separated into three parts, and stored at -20°C

until assayed. The secretion levels of the expressed cytokines, TNF-α and IL-8, were measured using commercial ELISA kits (mini-development ELISA kit; PeproTech, Rocky Hill, NJ, U.S.A.) according to the manufacturer's guidelines (Table 2.9). Representative standard curves to detect unknown expression levels of TNF-α and IL-17, and IL-8 can be seen in Figure 2.4, and Figure 2.5, and Figure 2.6, respectively.

2.37.2 Preparation of Sample to Detect Secreted Cytokine Expression Levels in hTCEpi Cells Exposed to *B. oleronius* Proteins

Corneal epithelial (hTCEpi) cells were seeded onto 6-well tissue culture plates (Corning) at a density of 5 x 10^5 cells/well, and exposed to crude *B. oleronius* protein (2 μg/ml), or pure *B. oleronius* protein (2 μg/ml) for 24 hour or 72 hour. At each time-point, the sample supernatants were collected, and centrifuged at 200 x *g* for 2 minutes before transfer to a fresh sterile 1.7 ml micro-centrifuge tube, and storage at -20°C until assayed. The secretion levels of the expressed cytokines, IL-8 and IL-6, were measured using commercial ELISA kits (mini-development ELISA kit; PeproTech, Rocky Hill, NJ, U.S.A.) according to the manufacturer's guidelines (Table 2.9). Representative standard curves to detect unknown expression levels of IL-8 and IL-6 can be seen in Figure 2.6 and Figure 2.7, respectively.

2.37.3 Preparation of Sample to Detect Secreted Cytokine Expression Levels in Isolated Neutrophil Cells Exposed to *B. oleronius* Proteins

Isolated human neutrophils (1 x 10^6/well in Roswell Park Memorial Institute (RPMI)-1640 GlutaMAX™ media (Gibco®) supplemented with 5% (v/v) FCS) from fresh donated blood (Section 2.10), were added to each well of a 24-well flat-bottomed tissue culture plate (BD Falcon™, BD Biosciences, Oxford, UK), and incubated for 16 and 24 hour. Cells were treated with 2 μg/ml and 6 μg/ml of both the crude and pure *B. oleronius* protein preparations, and IL-8 (10 ng/ml). Cell culture supernatants were harvested at each of the indicated time-points, and centrifuged at 200 x *g* for 2 minutes before transfer to a fresh sterile 1.7 ml micro-centrifuge tube, and storage at -20°C until assayed. Neutrophil cell viability was assessed using the trypan blue cell excluison method (Section 2.10) for the duration of the assay. The secretion levels of the expressed cytokines, IL-6 and IL-1β, were measured using commercial ELISA kits (Mabtech) according to the instructions given in the

manufacturer's guidelines (Table 2.9). Representative standard curves to detect unknown expression levels of IL-6 and IL-1β can be seen in Figure 2.7 and Figure 2.8, respectively.

2.37.4 ELISA Protocol to Detect Secreted Cytokine and Expression Levels

A list of the cytokines investigated, and the concentrations of the capture antibody, detection antibody, streptavidin conjugated enzyme/substrate, and the absorbance optical density measured for each cytokine enzyme-linked immunosorbent assay (ELISA) is detailed in Table 2.9. All ELISAs were achieved by following the guidelines stated by the manufacturer, and performed in triplicate. Briefly, each 96-well ELISA micro-plate (Nunc™, Thermo Scientific) was coated overnight with the cytokine target capture antibody (100 µl/well), diluted to working concentration in PBS, the micro-plate was sealed with an adhesive protective cover, and incubated overnight at room temperature.

Each ELISA micro-plate was washed (x 2) with PBS (200 µl/well), followed by a 1 hour incubation at room temperature in blocking buffer (1% w/v bovine serum albumin (BSA) in PBS, and filter-sterilised before use with a 0.45 µm cellulose filter disc). After blocking, the micro-plate was washed (x 5) with PBS containing Tween®-20 (0.05%, v/v) (200 µl/well), the standard curve dilutions were prepared, and sample/standard (100 µl/well) was added, and incubated for 2 hours at room temperature. The micro-plate was washed (x 5) with PBS containing Tween®-20 (0.05%, v/v) (200 µl/well), followed by the addition of the detection antibody, diluted to the working concentration in blocking buffer, for 1 hour at room temperature.

The micro-plate was washed (x 5) with PBS containing Tween®-20 (0.05%, v/v) (200 µl/well), before the addition of streptavidin-HRP (100 µl/well), diluted according to the manufacturer's guidelines, and incubation for 1 hour at room temperature. The micro-plate was washed (x 5) with PBS containing Tween®-20 (0.05%, v/v) (200 µl/well), followed by the addition of 3, 3', 5, 5'-tetramethylbenzidine (TMB) (100 µl/well) substrate solution at room temperature, and protected from light. The micro-plate was developed for 15-20 minutes, and the reaction stopped by the addition of stop solution (1 N sulfuric acid (H_2SO_4): prepared by dissolving concentrated H_2SO_4 (27.5 ml) in dH_2O (972.5 ml)) (50 µl/well). Each ELISA plate was read at a specific absorbance wavelength according to the manufacturer's instructions using a BioTek Synergy™ HT (BioTek

Instruments Inc., Vermont, USA) microplate reader. The standard curves generated were used to detect the cytokine expression levels for each sample assayed.

2.38 Standardized Skin Surface Biopsy (SSSB) to Quantify *Demodex* Mite Population

The recording of the standard skin surface biopsy (SSSB) to quantify *Demodex* mite population present in patients involved in the study (Section 2.4.1) collaborating with the University of Medical Sciences, Poznań in Poland was achieved with the assistance of Dr Stanisław Jarmuda and colleagues. One drop of cyanoacrylate adhesive was placed on a glass slide with a pre-marked square surface area of 1 cm^2. The slide was applied to the skin on a patient's face. After 30 seconds the slide was removed gently and one drop of immersion oil was added. A coverslip was placed on the sample and the specimen was examined under an optical microscope (magnified 40x and 100x). The number of mites per 1 cm^2 was determined by microscopic examination.

2.39 Sebumetric Test to Quantify Abundance of Sebum

The sebumetric test of patients involved in the study (Section 2.4.1) collaborating with the University of Medical Sciences, Poznań in Poland was achieved with the assistance of Dr Stanisław Jarmuda and colleagues. The level of sebum secretion by skin was measured using a Sebumeter® SM 815 Courage-Khazaka (Courage-Khazaka electronic GmbH, Köln, Germany) as recommended by the manufacturer. A piece of 0.1 mm tape on a measuring probe, equipped with a spring to assure constant and even pressure, was placed on the skin of the patient's chin for 30 seconds. The probe was then inserted into the sebumeter, where the amount of sebum on the surface of the skin was assessed and expressed as $\mu g/cm^2$.

Table 2.9 A list of cytokines analysed by ELISA. A detailed list of the capture anitbodies, detection antibodies, enzyme/substrate complex, and the optical density measured for each cytokine investigated by ELISA.

Cytokine Target	Company	Product Code	Capture Antibody (conc.)	Capture Antibody Dilution (conc.)	Biotinylated Detection Antibody (conc.)	Biotinylated Detection Antibody Dilution (conc.)	Enzyme/Substrate	Optical Density (Absorbance)
IL-8	PeproTech	900-TM18	Recombinant hIL-8 (100 µg/ml)	1/200 (0.5 µg/ml)	Recombinant hIL-8-Biotin (100 µg/ml)	1/200 (0.5 µg/ml)	Streptavidin-HRP/ TMB	450 nm
IL-6	PeproTech	900-TM16	Recombinant hIL-6 (100 µg/ml)	1/100 (1 µg/ml)	Recombinant hIL-6-Biotin (100 µg/ml)	1/200 (0.5 µg/ml)	Streptavidin-HRP/ TMB	450 nm
	Mabtech AB	3460-1H-6	13A5 (1 mg/ml)	1/2000 (0.5 µg/ml)	29C3-Biotin (1 mg/ml)	1/1000 (1 µg/ml)	Streptavidin-HRP/ TMB	450 nm
IL-1β	Mabtech AB	3415-1H-6	IL1β-I (1 mg/ml)	1/500 (2 µg/ml)	IL1β-II-Biotin (1 mg/ml)	1/1000 (1 µg/ml)	Streptavidin-HRP/ TMB	405 nm
TNF-α	PeproTech	900-M25	Recombinant hTNF-α (100 µg/ml)	1/100 (1 µg/ml)	Recombinant hTNF-α-Biotin (100 µg/ml)	1/200 (0.5 µg/ml)	Streptavidin-HRP/ TMB	450 nm
IL-17	Mabtech AB	3520-1H-6	MT44.6 (0.5 mg/ml)	1/50 (10 µg/ml)	MT504-Biotin (0.5 mg/ml)	1/1000 (0.5 µg/ml)	Streptavidin-HRP/ TMB	450 nm

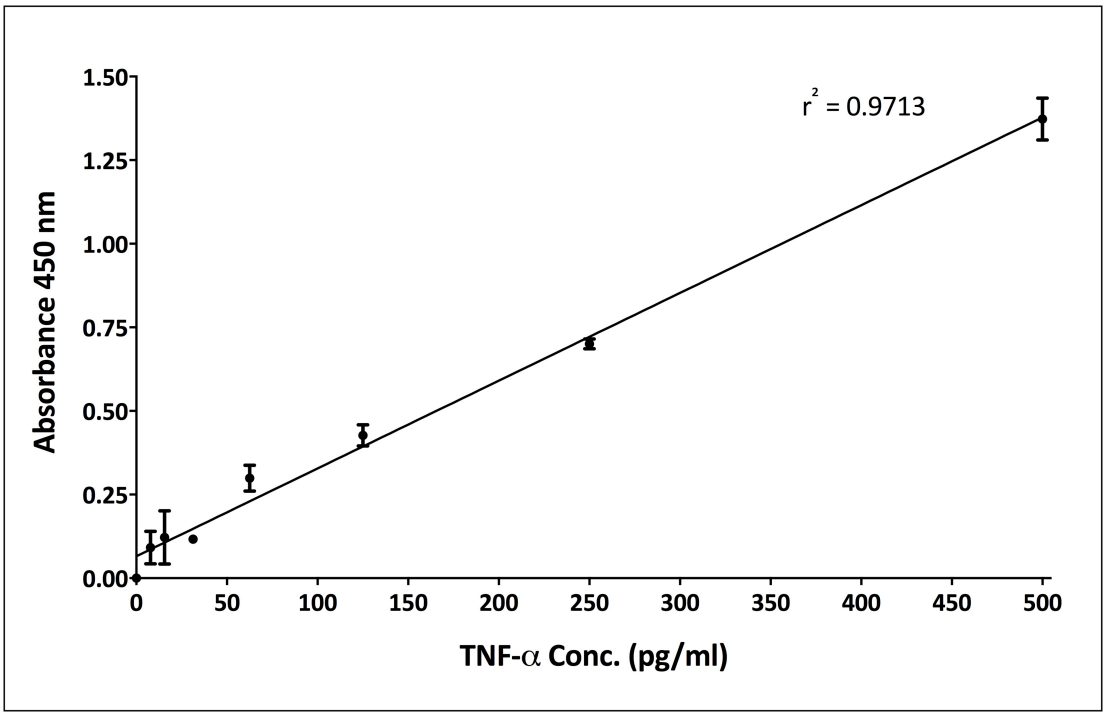

Figure 2.4 A representative standard curve for TNF-α ELISA. A representative standard curve used to measure the production of secreted TNF-α.

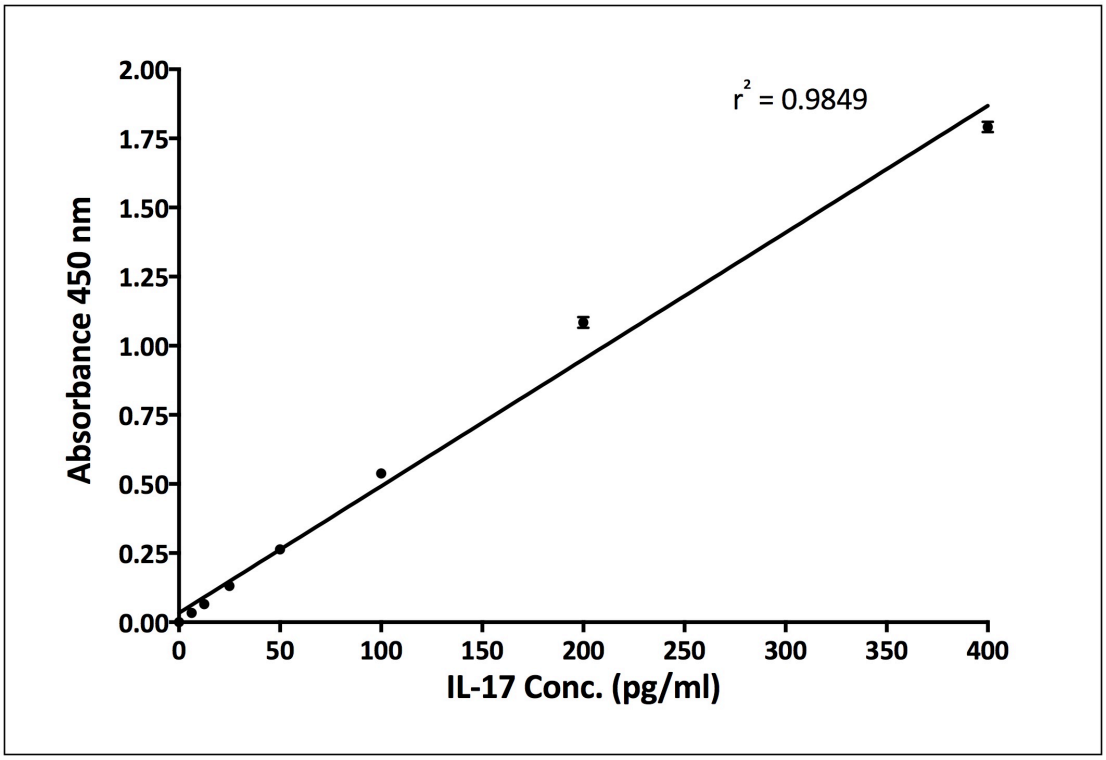

Figure 2.5 A representative standard curve for IL-17 ELISA. A representative standard curve used to measure the production of secreted IL-17.

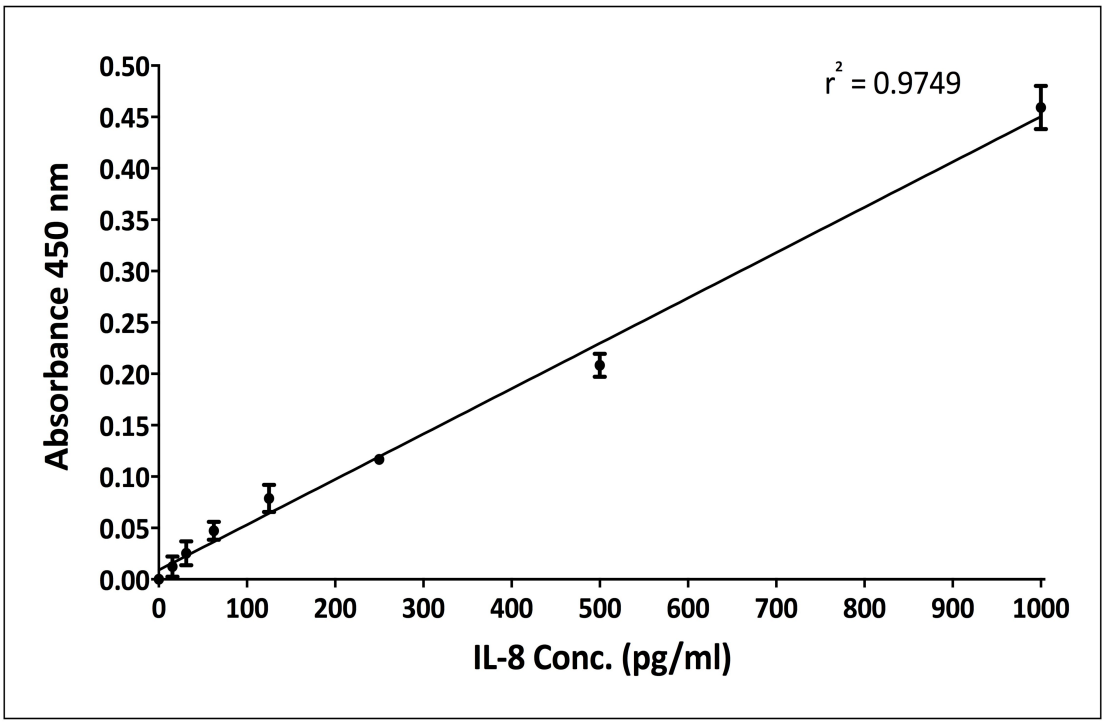

Figure 2.6 A representative standard curve for IL-8 ELISA. A representative standard curve used to measure the production of secreted IL-8.

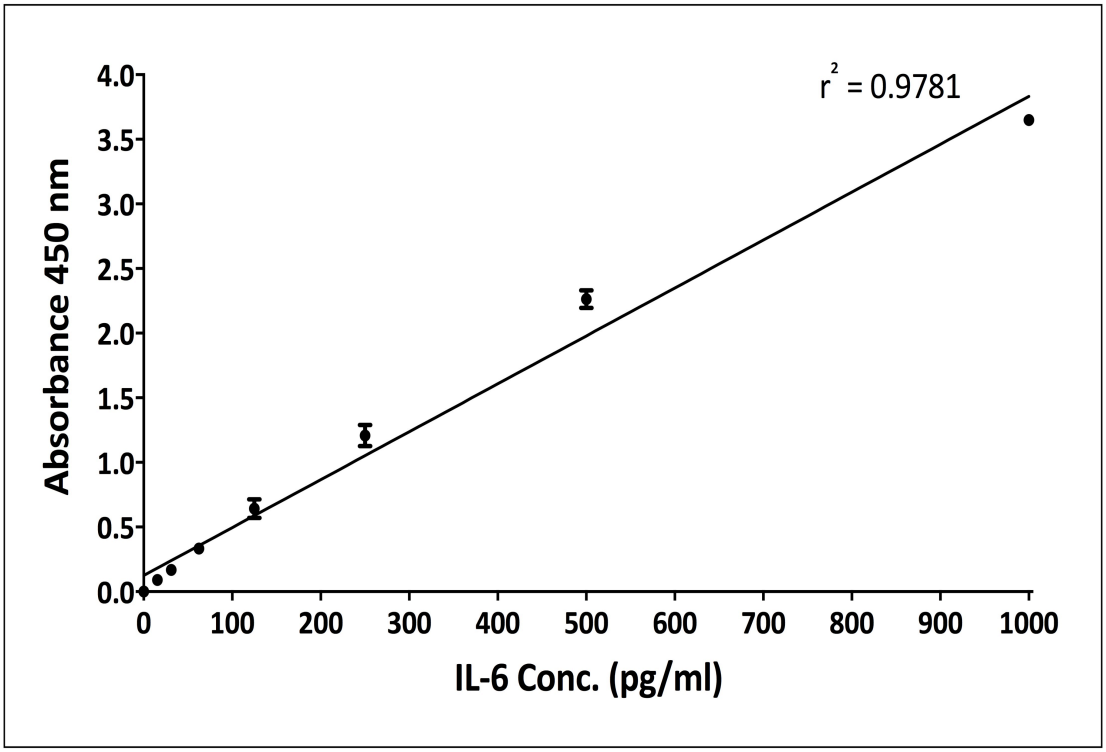

Figure 2.7 A representative standard curve for IL-6 ELISA. A representative standard curve used to measure the production of secreted IL-6.

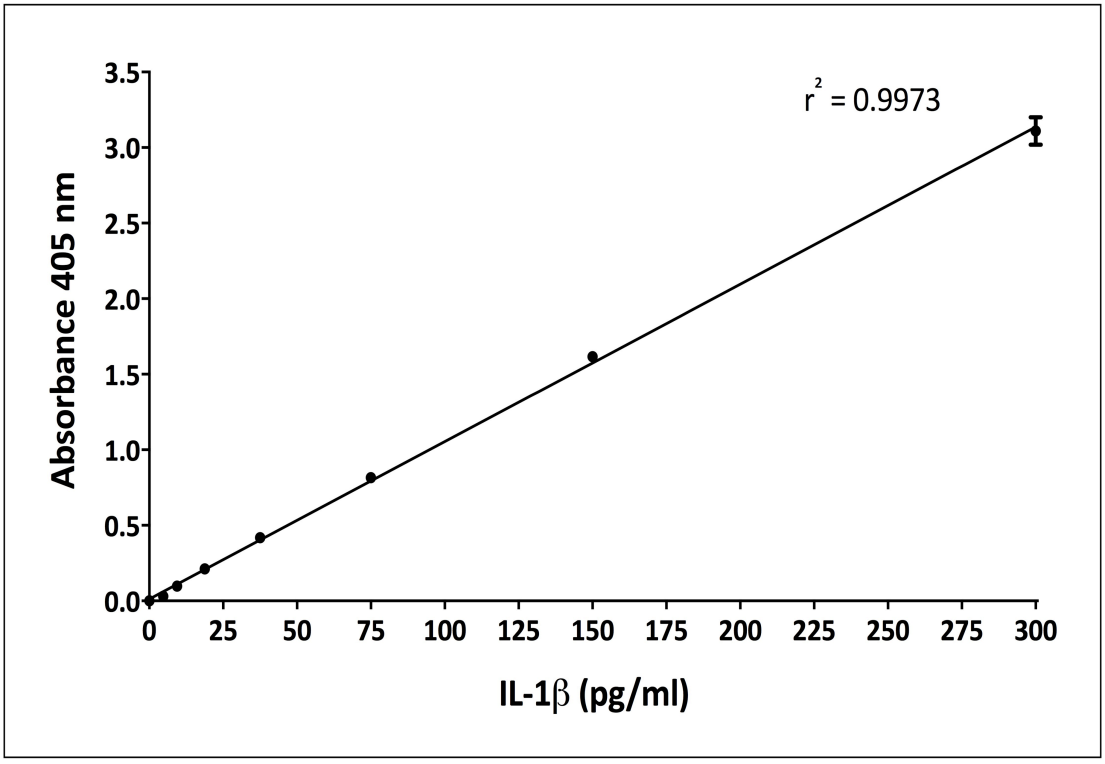

Figure 2.8 A representative standard curve for IL-1β ELISA. A representative standard curve used to measure the production of secreted IL-1β.

Chapter 3

An Analysis of the Effect of Culture Conditions on the Proteomic Profile of *Bacillus oleronius*

3.0 Introduction

Previous studies have shown that the facial skin of patients affected with rosacea display a higher density of *Demodex* mites than unaffected controls (Erbağci and Ozgöztaşi, 1998; Bonnar *et al*., 1993; Vance, 1986). Lacey *et al*. (2007) isolated *B. oleronius* from the hindgut of a *D. folliculorum* mite of a papulopustular rosacea patient, and demonstrated that the bacterium produced immunogenic proteins with the capacity to induce an inflammatory response and peripheral blood mononuclear cell (PBMC) proliferation in 72% of papulopustular rosacea patients but only in 29% of controls ($p = 0.0105$). The antigenic proteins produced by the *B. oleronius* were further analysed by matrix-assisted laser desorption/ionization-time of flight (MALDI-ToF) mass spectrometry. The 62 kDa protein was identified as GroEL, a chaperone protein with an amino acid sequence homologous to a bacterial heat shock protein. The 83 kDa protein was identified as an enzyme involved in carbohydrate metabolism and signal transduction of the phosphoenolpyruvate phosphotransferase sensory system. From the results, it was suggested that *B. oleronius* was implicated in rosacea, and it was hypothesised that the bacterium may be involved in the pathogenesis of the disease resulting in an immune-based inflammatory cascade (Lacey *et al.*, 2007).

The pathogenic role of *Demodex* mite infestation is unclear as the mites can be found in asymptomatic individuals (Liu *et al*., 2010; Kemal *et al*., 2005). It has been suggested that the *Demodex* mites are a naturally occurring commensal organism of the skin flora of mammalian hosts, and that the role of the mites in the aetiology of rosacea is as a vessel for pathogenic microbes. The endosymbiotic relationship between the *Demodex* mites and *B. oleronius* is believed to be an element involved in the pathogenesis of rosacea. Recently, Li *et al*. (2010) have shown a strong correlation between serum reactivity to the *B. oleronius* proteins and eyelid inflammation ($p = 0.04$) and ocular rosacea ($p = 0.01$). Western blotting has also demonstrated correlations between serum reactivity to the immunogenic *B. oleronius* proteins and erythematotelangiectatic rosacea (O'Reilly *et al*., 2012c). The immunogenic *B. oleronius* proteins were isolated and purified by anion exchange chromatography using Q-Sepharose™ beads and ÄKTA FPLC™, and induced an immune response by the activation of neutrophils and an aberrant wound healing response in a corneal epithelial (hTCEpi) cell line (O'Reilly *et al*., 2012a, 2012b). The

aim of the work presented in this Chapter was to investigate the effect of different culture conditions on the production of the *B. oleronius* immunogenic proteins.

3.1 Investigating the Expression of the Immuno-Reactive 62 kDa Protein by *B. oleronius* Under Varying Environmental Conditions

It has previously been demonstrated that patients with erythematotelangiectatic rosacea, papulopustular roscaea, and ocular rosacea are sera reactive to the *B. oleronius* 62 kDa protein (O'Reilly *et al*., 2012c; Li *et al*., 2010; Lacey *et al*., 2007). The environmental conditions employed to investigate the production of the immuno-reactive 62 kDa protein, were as follows: nutrient availability (nutrient broth medium (a nutrient poor environment), or 2X YT broth medium (a nutrient rich environment)); pH (medium adjusted to pH 6, pH 7, or pH 8); temperature (30°C, as this is the optimum temperature for *Demodex* mite movement, and 37°C, as this represents body temperature); oxygen availability (cultures were incubated under aerobic or anaerobic static conditions); reactive oxygen species (ROS) (10 mM hydrogen peroxide (H_2O_2) was added to culture medium 4 hour prior to cell harvesting (at hour 44 of culture growth) (indicated by an arrow in Figure 3.1)). All cultures were incubated for 48 hour before cell harvesting and protein extractions were performed as decribed in Section 2.12.1. A representative growth curve of *B. oleronius* cultured in nutrient broth media (pH 8), under aerobic conditions cultured at 30°C for 48 hour, with (blue line) or without (red line) the addition of 10 mM hydrogen peroxide (H_2O_2) at hour 44 of culture growth (indicated by arrow (🡻)) is given in Figure 3.1.

Following cell harvesting and protein extraction, protein preparations from each *B. oleronius* culture were resolved by 1-D SDS-PAGE (Figure 3.2 – 3.7). The production of the immuno-reactive 62 kDa protein was assessed by Western blotting (Figure 3.8 – 3.11). In nutrient broth media and at 30°C, an increase in the of the 62 kDa protein was observed at pH 6 for each environmental condition analysed compared to pH 7 and pH 8 (Figure 3.8). At pH 7 there is no change in the production of the 62 kDa protein but a reduced level of expression is observed compared to 62 kDa protein production at pH 6, and a significant reduction was seen following the addition of 10 mM H_2O_2 under aerobic conditions ($p < 0.05$). A culture pH of 8 most closely resembles the alkaline environment of the *Demodex* mite midgut (Erban and Hubert, 2010; König *et al*., 2002). Cultures at pH 8 demonstrated a significant

reduction in the production of the 62 kDa protein under aerobic conditions ($p < 0.001$) compared to the pH 6 *B. oleronius* cultures (Figure 3.8).

In nutrient broth at 37°C, the production of the 62 kDa protein was decreased compared to that in the 30°C *B. oleronius* cultures. At 37°C, *B. oleronius* cultures at pH 8 demonstrated increased production of the 62 kDa protein in contrast to the levels recorded for the pH 8 *B. oleronius* cultures at 30°C (Figure 3.9). A significant decrease in the production of the 62 kDa protein was observed in aerobic cultures at pH 6 following the addition of 10 mM H_2O_2 compared to the pH 8 *B. oleronius* cultures ($p < 0.05$) (Figure 3.9). A significant reduction in the expression of the 62 kDa protein was observed in *B. oleronius* cultures at pH 7 compared to *B. oleronius* aerobic cultures at pH 6 without the addition of 10 mM H_2O_2 ($p < 0.05$). Similarly, relative to *B. oleronius* anaerobic cultures at pH 8 with the addition of 10 mM H_2O_2, a significant decrease in the production of the 62 kDa protein was observed in *B. oleronius* cultures at pH 7 ($p < 0.05$) (Figure 3.9).

The production of the 62 kDa protein was similar for the pH conditions analysed in 2X YT broth media at 30°C. Under aerobic conditions, there was a significant reduction in the production of the 62 kDa protein observed in the *B. oleronius* cultures at pH 7 compared to pH 8 ($p < 0.05$) (Figure 3.10). Anaerobic conditions resulted in a significant decreased expression of the 62 kDa protein at pH 7 ($p < 0.001$), and at pH 8 ($p < 0.05$) compared to *B. oleronius* cultures at pH 6. Following the addition of 10 mM H_2O_2, a similar significant decrease in production of the 62 kDa protein was evident at pH 7 ($p < 0.001$), and at pH 8 ($p < 0.05$) compared to the *B. oleronius* cultures at pH 6 (Figure 3.10).

The expression of the 62 kDa protein was similar for the pH conditions analysed in 2X YT broth at 37°C, and when compared to the expression of the 62 kDa protein from cultures in 2X YT broth at 30°C (Figure 3.11). However, a significant reduction in expression of the 62 kDa protein was observed at pH 7 relative to anaerobic conditions at pH 6 and 8 without the addition of 10 mM H_2O_2 ($p < 0.001$).

The environment surrounding *B. oleronius* can alter the expression of the immuno-reactive 62 kDa protein, and the varied expression levels are induced in response to stresses for the *B. oleronius*. In an environment similar to the natural habitat of the bacterium within the gut of the *Demodex* mite (an alkali, low nutrient environment with poor oxygen availability), there was low expression of the 62 kDa protein compared to the higher expression levels observed for the different

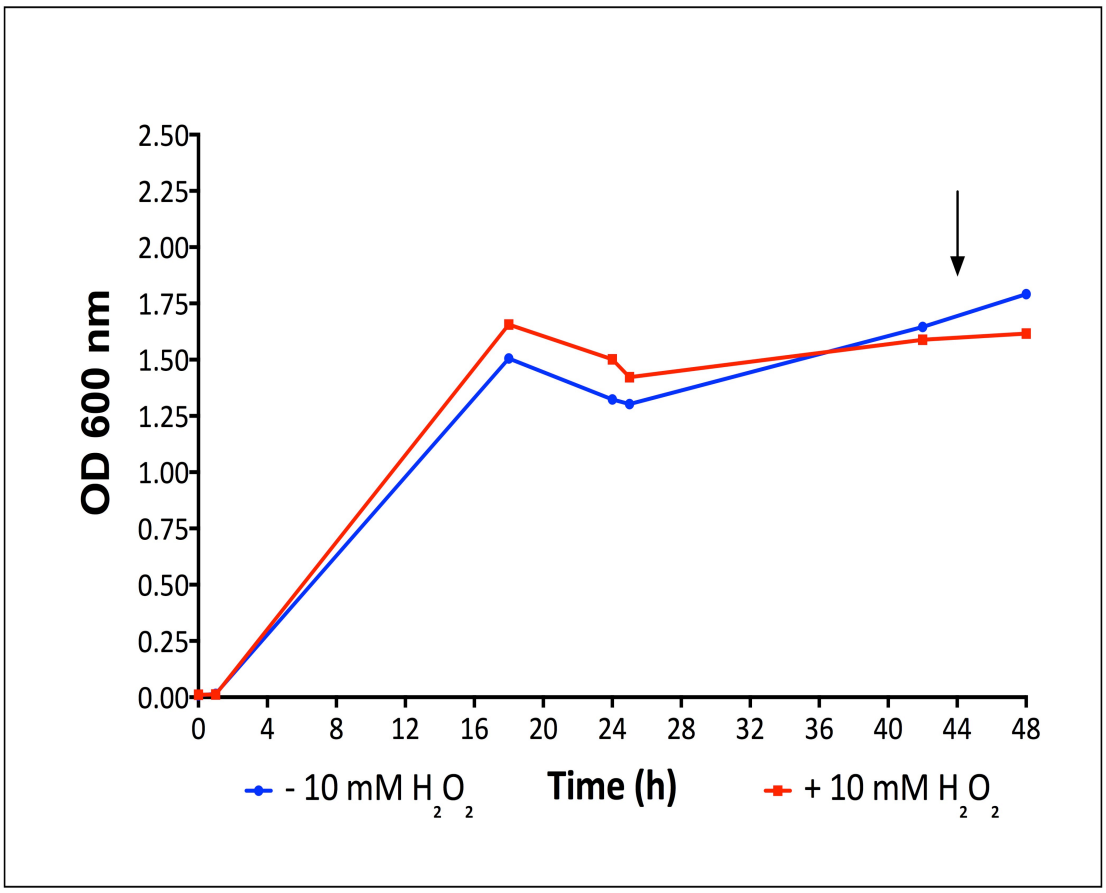

Figure 3.1 A representative growth curve of *B. oleronius* in nutrient broth. Growth curve of *B. oleronius* in nutrient broth media (pH 8), under aerobic conditions cultured at 30°C for 48 hour, with (blue line) or without (red line) the addition of 10 mM hydrogen peroxide (H_2O_2) at hour 44 of culture growth (Indicated by arrow (🡻)). (n = 3, for each culture condition).

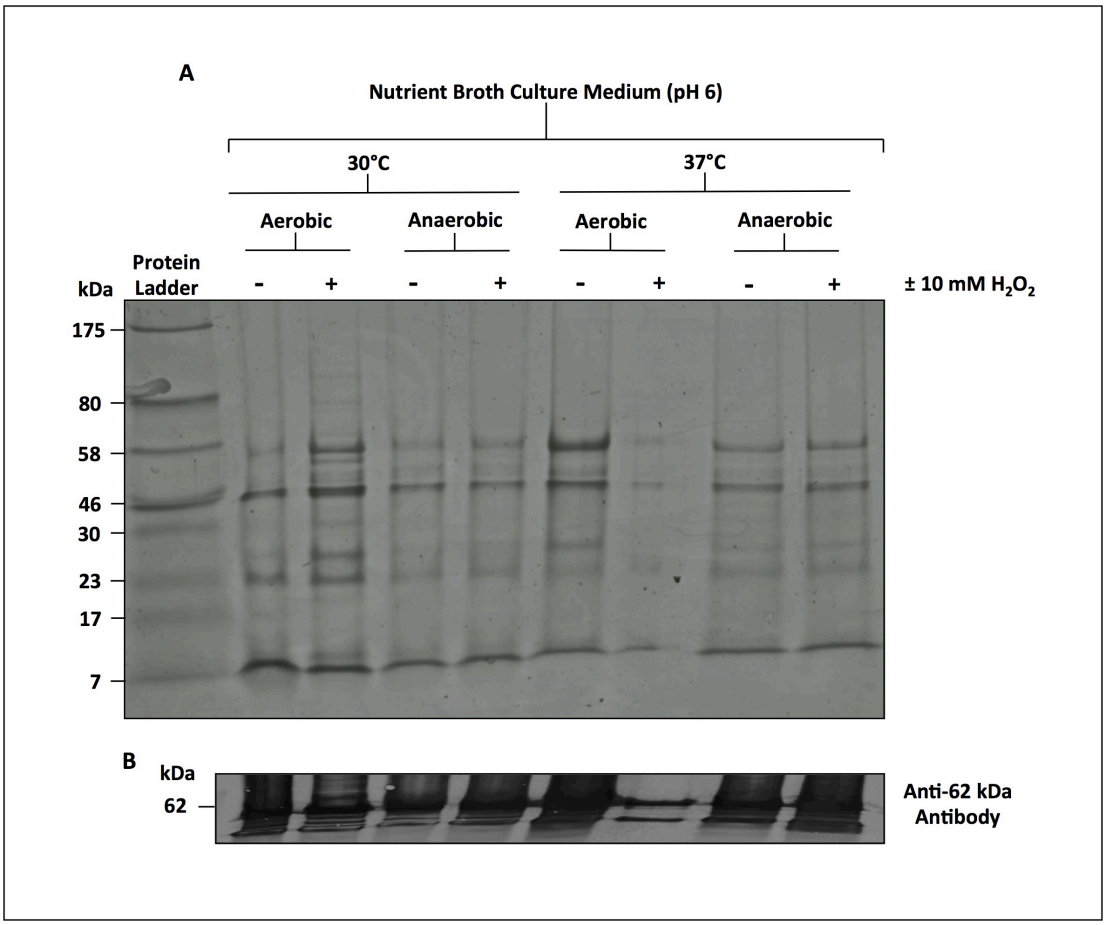

Figure 3.2 Analysis of th effect of environmental conditions on the expression of *B. oleronius* proteins in nutrient broth (pH 6), by 1-D SDS-PAGE and immunoblot of 62 kDa protein expression. Resolved protein preparations of the *B. oleronius* 48 hour cultures in nutrient broth medium (pH 6) under different environmental conditions including temperature (30°C or 37°C), oxygen availability (aerobic or anaerobic), and ROS (± 10 mM H_2O_2). The addition of 10 mM H_2O_2 occurred 4 hour prior to protein extraction. (**A**) Proteins were visualized by Coomassie staining, and (**B**) the abundance of the 62 kDa *B. oleronius* protein was assessed by Western blotting. (n = 3, for each culture condition).

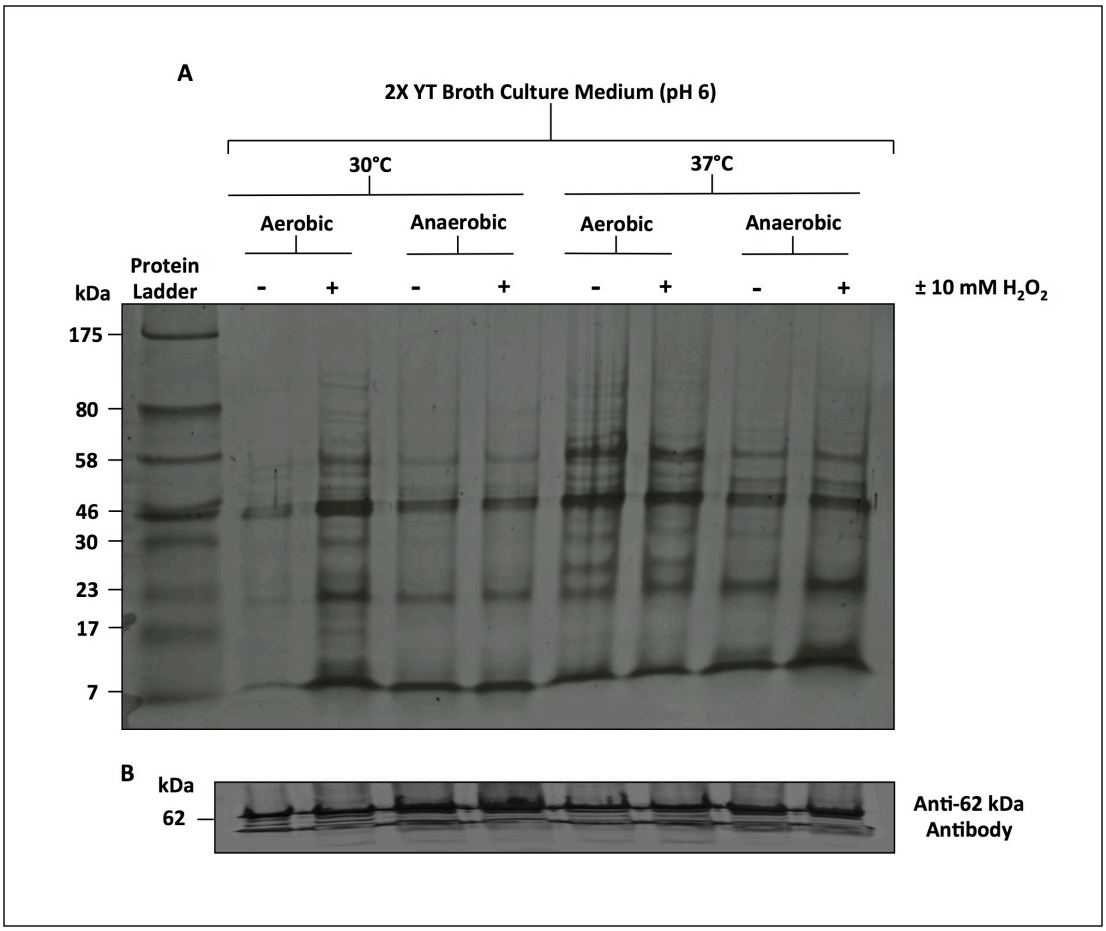

Figure 3.3 Analysis of the effect of environmental conditions on the expression of *B. oleronius* proteins in 2X YT broth (pH 6), by 1-D SDS-PAGE and immunoblot of 62 kDa protein expression. Resolved protein preparations of the *B. oleronius* 48 hour cultures in 2X YT broth medium (pH 6) under different environmental conditions including temperature (30°C or 37°C), oxygen availability (aerobic or anaerobic), and ROS (± 10 mM H_2O_2). The addition of 10 mM H_2O_2 occurred 4 hour prior to protein extraction. (**A**) Proteins were visualized by Coomassie staining, and (**B**) the abundance of the 62 kDa *B. oleronius* protein was assessed by Western blotting. (n = 3, for each culture condition).

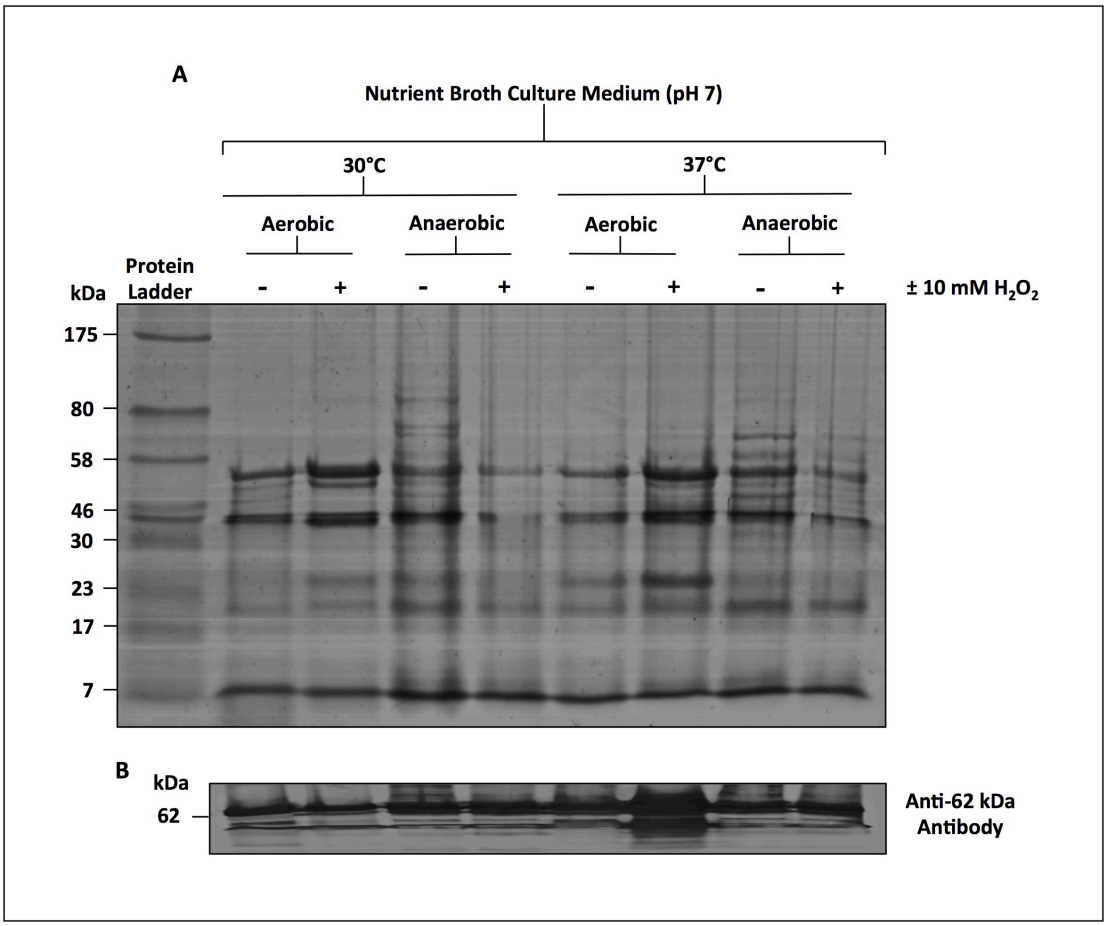

Figure 3.4 Analysis of the effect of environmental conditions on the expression of *B. oleronius* proteins in nutrient broth (pH 7), by 1-D SDS-PAGE and immunoblot of 62 kDa protein expression. Resolved protein preparations of the *B. oleronius* 48 hour cultures in nutrient broth medium (pH 7) under different environmental conditions including temperature (30°C or 37°C), oxygen availability (aerobic or anaerobic), and ROS (± 10 mM H_2O_2). The addition of 10 mM H_2O_2 occurred 4 hour prior to protein extraction. (**A**) Proteins were visualized by Coomassie staining, and (**B**) the abundance of the 62 kDa *B. oleronius* protein was assessed by Western blotting. (n = 3, for each culture condition).

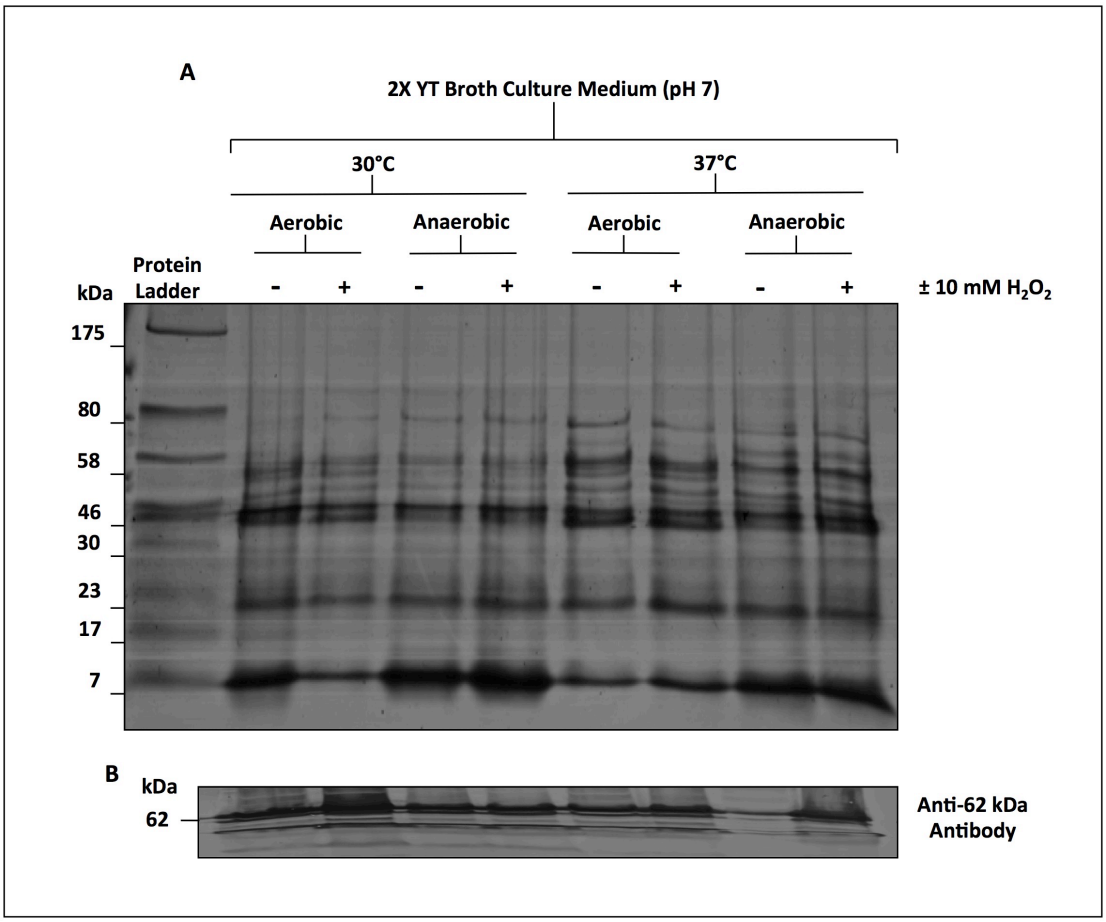

Figure 3.5 Analysis of the effect of environmental conditions on the expression of *B. oleronius* proteins in 2X YT broth (pH 7), by 1-D SDS-PAGE and immunoblot of 62 kDa protein expression. Resolved protein preparations of the *B. oleronius* 48 hour cultures in 2X YT broth medium (pH 7) under different environmental conditions including temperature (30°C or 37°C), oxygen availability (aerobic or anaerobic), and ROS (± 10 mM H_2O_2). The addition of 10 mM H_2O_2 occurred 4 hour prior to protein extraction. (**A**) Proteins were visualized by Coomassie staining, and (**B**) the abundance of the 62 kDa *B. oleronius* protein was assessed by Western blotting. (n = 3, for each culture condition).

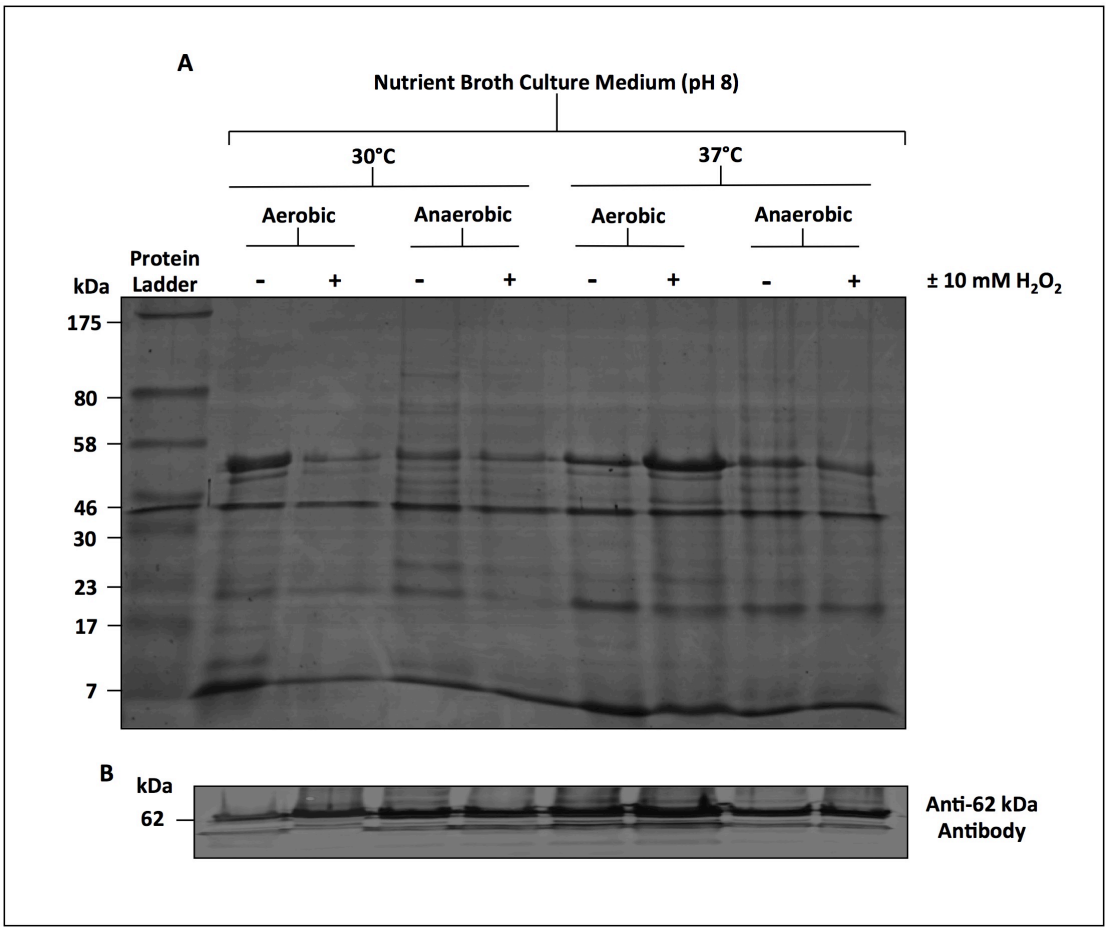

Figure 3.6 Analysis of the effect of environmental conditions on the expression of *B. oleronius* proteins in nutrient broth (pH 8), by 1-D SDS-PAGE and immunoblot of 62 kDa protein expression. Resolved protein preparations of the *B. oleronius* 48 hour cultures in nutrient broth medium (pH 8) under different environmental conditions including temperature (30°C or 37°C), oxygen availability (aerobic or anaerobic), and ROS (± 10 mM H_2O_2). The addition of 10 mM H_2O_2 occurred 4 hour prior to protein extraction. (**A**) Proteins were visualized by Coomassie staining, and (**B**) the abundance of the 62 kDa *B. oleronius* protein was assessed by Western blotting. (n = 3, for each culture condition).

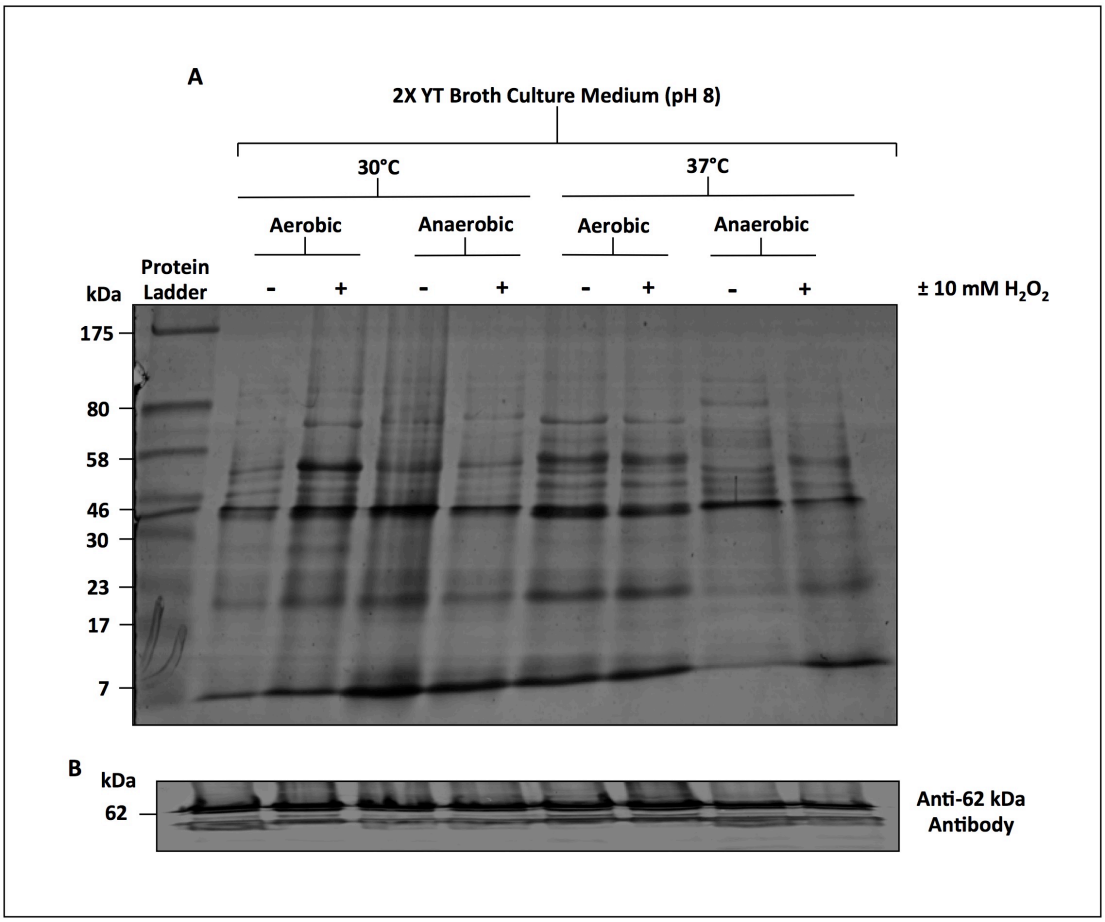

Figure 3.7 Analysis of the effect of environmental conditions on the expression of *B. oleronius* proteins in 2X YT broth (pH 8), by 1-D SDS-PAGE and immunoblot of 62 kDa protein expression. Resolved protein preparations of the *B. oleronius* 48 hour cultures in 2X YT broth medium (pH 8) under different environmental conditions including temperature (30°C or 37°C), oxygen availability (aerobic or anaerobic), and ROS (± 10 mM H_2O_2). The addition of 10 mM H_2O_2 occurred 4 hour prior to protein extraction. (**A**) Proteins were visualized by Coomassie staining, and (**B**) the abundance of the 62 kDa *B. oleronius* protein was assessed by Western blotting. (n = 3, for each culture condition).

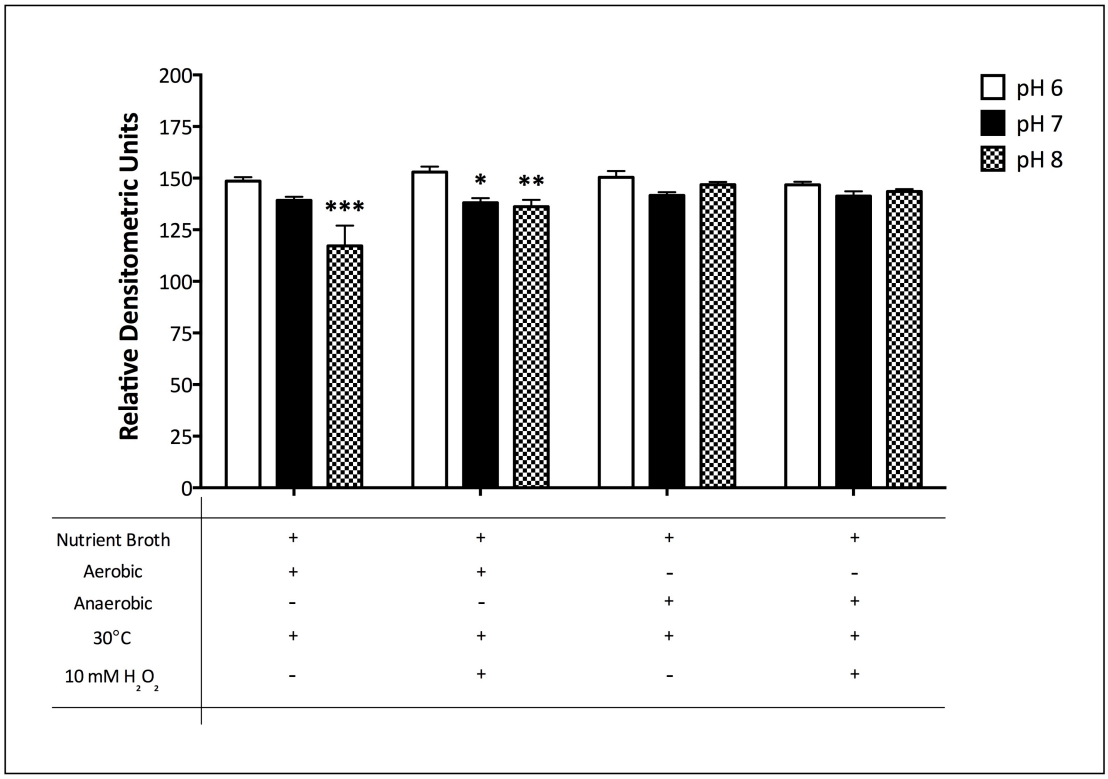

Figure 3.8 Assessment of the effect of environmental conditions on the expression of the 62 kDa protein in *B. oleronius* cultures in nutrient broth at 30°C. The effect of varying environmental conditions on the abundance of the 62 kDa protein from *B. oleronius* cultures resolved by 1-D SDS-PAGE. The expression of the 62 kDa protein was assessed using Image J software. (Significance: * = $p < 0.05$, ** = $p < 0.01$, *** = $p < 0.001$). (n = 3, for each culture condition).

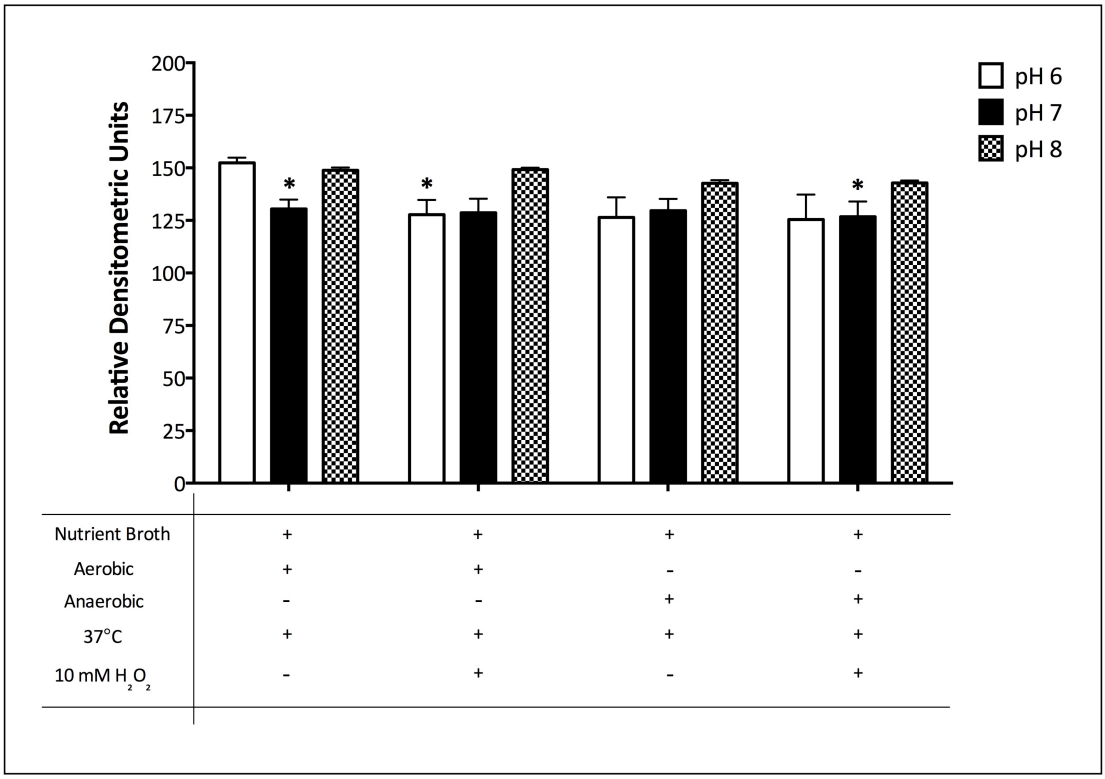

Figure 3.9 Assessment of the effect of environmental conditions on the expression of the 62 kDa protein in *B. oleronius* cultures in nutrient broth at 37°C. The effect of varying environmental conditions on the abundance of the 62 kDa protein from *B. oleronius* cultures resolved by 1-D SDS-PAGE. The expression of the 62 kDa protein was assessed using Image J software. (Significance: * = $p < 0.05$). (n = 3, for each culture condition).

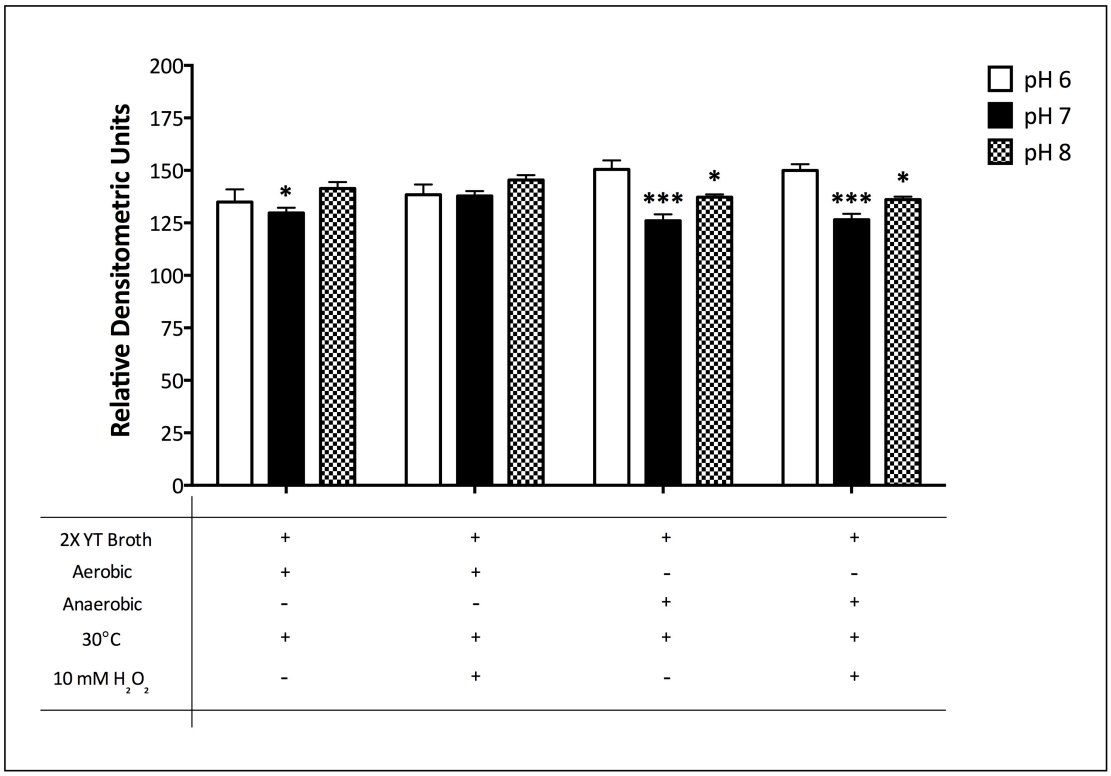

Figure 3.10 Assessment of the effect of environmental conditions on the expression of the 62 kDa protein in *B. oleronius* cultures in 2X YT broth at 30°C. The effect of varying environmental conditions on the abundance of the 62 kDa protein from *B. oleronius* cultures resolved by 1-D SDS-PAGE. The expression of the 62 kDa protein was assessed using Image J software. (Significance: * = $p < 0.05$, *** = $p < 0.001$). (n = 3, for each culture condition).

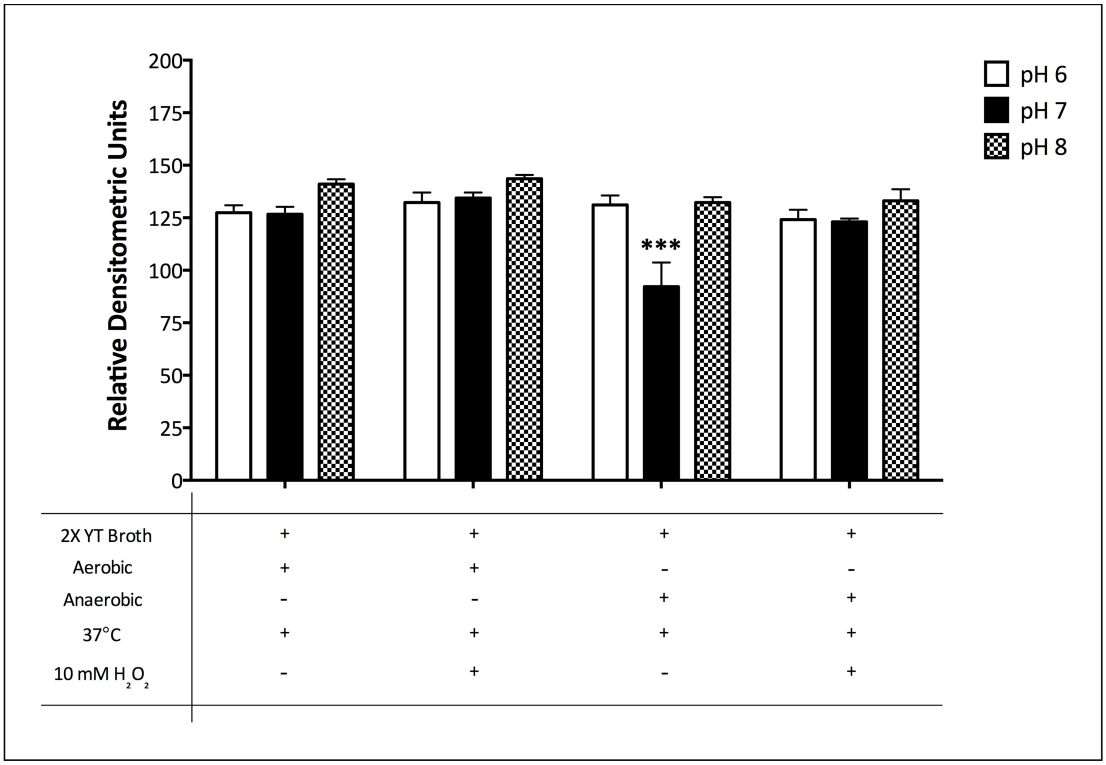

Figure 3.11 Assessment of the effect of environmental conditions on the expression of the 62 kDa protein in *B. oleronius* cultures in 2X YT broth at 37°C. The effect of varying environmental conditions on the abundance of the 62 kDa protein from *B. oleronius* cultures resolved by 1-D SDS-PAGE. The expression of the 62 kDa protein was assessed using Image J software. (Significance: * = $p < 0.05$, *** = $p < 0.001$). (n = 3, for each culture condition).

pH conditions, suggesting that increased abundance of the 62 kDa protein may be induced by *B. oleronius* under stress (Figure 3.8). In similar environmental conditions at 37°C, the production of the 62 kDa protein increases in the *B. oleronius* cultures at pH 8, as the bacterium possibly adapts to the higher temperature (Figure 3.9). A nutrient rich environment (2X YT broth media) for the *Bacillus* increases the production of the 62 kDa protein in 30°C *B. oleronius* cultures at pH 8 (Figure 3.10), and decreases the expression of the 62 kDa protein at 37°C (Figure 3.11) compared to similar temperatures with nutrient poor environments. This indicates a possible correlation between a plentiful source of nutrients and that the production of the immuno-reactive 62 kDa protein is dependent upon the host in which the bacterium resides, either the *Demodex* mite or human.

3.2 Summary

The production and expression of the immuno-reactive 62 kDa protein by *B. oleronius* was assessed in different environmental conditions. It was observed that the expression of the 62 kDa protein was increased in response to the stress of a change in pH, temperature, and oxygen availability, and that the expression of the 62 kDa protein may be host-specific.

3.3 Proteomic Analysis of *B. oleronius* Grown Under Varying Environmental Conditions

Following electrophoresis of the *B. oleronius* grown under different environmental conditions, the proteome was investigated by LC/MS to identify differential abundance of proteins. A master gel of excised protein bands resolved by 1-D SDS-PAGE can be seen in Figure 3.12. A list of protein band identities is given in Table 3.1. The identified proteins are shown to function in a wide range of biological processes including metabolism, serine protease activity, transmembrane protein processes, signaling, cell motility, heat shock response and oxidative stress response. A description of each sample and corresponding *B. oleronius* culture grown under different environmental conditions investigated at pH 6, 7, and 8, for this proteomic study is given in Table 3.2.

The results of the *B. oleronius* proteome analysis demonstrate that the abundance of proteins corresponds to the growth of the *B. oleronius*. In general, it was seen that the *B. oleronius* grew best at pH 8, in an environment similar to the hindgut of the *Demodex* mite (Erban and Hubert, 2010; König *et al*., 2002). The fold change in *B. oleronius* protein abundance and the effect of different environmental conditions on protein abundance can be seen in Figure 3.13 – 3.19, and in the Appendix (Table A3.1). The fold change values given are relative to the optimal environmental condition of the *B. oleronius* residing in the hindgut of the *Demodex* mite (Sample number 1 at pH 8).

The molecular chaperone GroEL was identified in *B. oleronius* cultures by LC/MS (Band No: 1) (Figure 3.13). The chaperone protein, GroEL, has been shown to have homolgy to a bacterial heat shock protein, and functions in proper folding of polypeptides under stress conditions (Hemmingsen *et al*., 1988; Hendrix, 1979). Cultures of *B. oleronius* demonstrated increased abundance of GroEL in nutrient poor conditions at pH 6, and in nutrient rich conditions at pH 8. A significant change in abundance was observed between pH 8 and pH 6 culture conditions. In nutrient broth media with high oxygen availability (aerobic culture) at 30°C, a significant increase in protein abundance was seen at pH 8 compared to pH 6 ($p = 0.0282$). Whereas, the addition of H_2O_2 to nutrient broth *B. oleronius* cultures at 30°C lead to higher abundance of the GroEL in *B. oleronius* cultures at pH 6 compared to the *B. oleronius* cultures at pH 8 in aerobic and anaerobic ($p = 0.0001$) conditions. At 37°C, the abundance of GroEL increased significantly at pH 8 compared to the *B. oleronius*

anaerobic cultures at pH 6 inoculated with ($p = 0.0065$), or without ($p = 0.0039$) 10 mM H_2O_2. In 2X YT broth media, the abundance of GroEL increased at pH 8 compared to pH 6 cultures in aerobic ($p = 0.0001$), and anaerobic ($p = 0.0379$) conditions.

Proteins associated with oxidative stress such as thioredoxin (Band No: 4) (Figure 3.14), peroxidase (Band No: 15) (Figure 3.15), and superoxide dismutase (Band No: 21) (Figure 3.16) were identified in the *B. oleronius* cultures. Thioredoxin are a group of dithiol-disulfide oxidoreductases of the thioredoxin system, and function in an antioxidant capacity in numerous cellular functions, protecting the cell from ROS and environmental stress, and regulating programmed cell death and the inflammatory system, and promoting protein folding (Collett and Messens, 2010; Nakamura *et al*., 2005; Landino *et al*., 2004; Kern *et al*., 2003). At 37°C, the abundance of thioredoxin increased in *B. oleronius* grown in nutrient broth at pH 6 following the addition of 10 mM H_2O_2 compared to pH 8 cultures ($p = 0.0106$), and compared to 2X YT broth (pH 8) cultures at 30°C ($p < 0.0001$). At pH 7, the abundance of thioredoxin significantly increased compared to pH 8 aerobic cultures in 2X YT broth media at 30°C ($p = 0.0346$) and at 37°C ($p = 0.0113$) (Figure 3.14).

Peroxidase is an enzyme that catalyzes the oxidation of a substrate by reducing peroxide to water, and is often located in the peroxisomes of cells (Wang *et al*., 2015; Ross *et al*., 2000). Interestingly, without the addition of 10 mM H_2O_2, the abundance of peroxidase was observed to be significantly increased in the *B. oleronius* cultures at pH 8 compared to pH 6 cultures in 2X YT media in anaerobic conditions at 30°C ($p = 0.017$). Similarly, an increase in peroxidase was observed in nutrient broth (pH 8), anaerobic cultures at 30°C ($p = 0.0026$), and at 37°C ($p = 0.0098$) compared to *B. oleronius* cultures at pH 6. An increased abundance of peroxidase was observed in the aerobic *B. oleronius* cultures in nutrient broth media at pH 6 compared to the *B. oleronius* cultures at pH 7 ($p = 0.0298$) (Figure 3.15).

Superoxide dismutase is an enzyme that catalyzes the breakdown of superoxide into hydrogen peroxide and water, and is involved in cell signaling pathways, and the regulation and detoxification of ROS (Landis and Tower, 2005). At pH 8 the abundance of superoxide dismutase from the *B. oleronius* cultures is significantly increased compared to the pH 6 media conditions in nutrient broth, anaerobic cultures without the addition of 10 mM H_2O_2 at 30°C ($p = 0.0283$), and at 37°C ($p = 0.009$), and in 2X YT broth cultures at 30°C under anaerobic conditions without the addition

of 10 mM H_2O_2 ($p = 0.0097$) (Figure 3.16).

The serine proteases, subtilisin-like peptidase S8 (Band No: 11 and 12) and Clp protease ClpX (Band No: 13) (Figure 3.17), catalyze the hydrolysis of peptide bonds (Di Cera, 2009; Page and Di Cera, 2008; Siezen and Leunissen, 1997). The abundance of the Clp protease ClpX is significantly increased in the *B. oleronius* nutrient broth (pH 6) cultures in aerobic conditions at 30°C compared to pH 8 ($p = 0.0255$) culture conditions, and at 37°C compared to pH 7 ($p = 0.0322$) and pH 8 ($p = 0.0205$) culture conditions.

Flagellin (Band No: 24) (Figure 3.18) is a structural protein that forms flagellin filaments that function in motility and adhesion for bacterial cell growth and survival, and has been shown to activate the immune response mediated by the Toll-like receptor (TLR)-5 cell signaling pathway (Ramos *et al*., 2004; MacNab, 2003; Mizel *et al*., 2003; Smith *et al*., 2003). It was observed in anaerobic, nutrient broth media at 37°C cultures, that with or without the addition of 10 mM H_2O_2, the abundance of flagellin was significantly increased in *B. oleronius* cultures at pH 8 compared to pH 6 ($p = 0.0058$, and $p = 0.0161$, respectively). In 2X YT broth, anaerobic conditions at 30°C, the abundance of flagellin increased at pH 8 compared to the *B. oleronius* cultures at pH 7 ($p = 0.0264$).

Proteins involved in transmembrane processes were identified by LC/MS, such as ATP F_0F_1 synthase subunit beta (Band No: 14 and 23), sugar ATP binding cassette (ABC) transporter substrate-binding protein (SBP) (Band No: 20), and C4-dicarboxylate ABC transporter SBP (Band No: 25) (Figure 3.19). The membrane-bound ATP synthase (F_0F_1-ATPase) of bacteria catalyze the synthesis of ATP from ADP and inorganic phosphate (Deckers-Hebestreit and Altendorf, 1996). The abundance of the transmembrane proteins were influenced by the external environment of the *B. oleronius*, with significantly increased abundance of the sugar ABC transporter SBP observed in *B. oleronius* cultures at pH 8. The significantly increased abundance levels were also seen in nutrient broth cultures without the addition of 10 mM H_2O_2, at 30°C in aerobic ($p = 0.0282$) conditions, and in 2X YT broth at 30°C in aerobic ($p = 0.0001$), and anaerobic ($p = 0.0379$) conditions. A significant increase in abundance of the sugar ABC transporter SBP was observed in *B. oleronius* cultures following the addition of 10 mM H_2O_2 in 30°C anaerobic, nutrient broth (pH 6) cultures compared to the *B. oleronius* cultures at pH 8 ($p = 0.0001$).

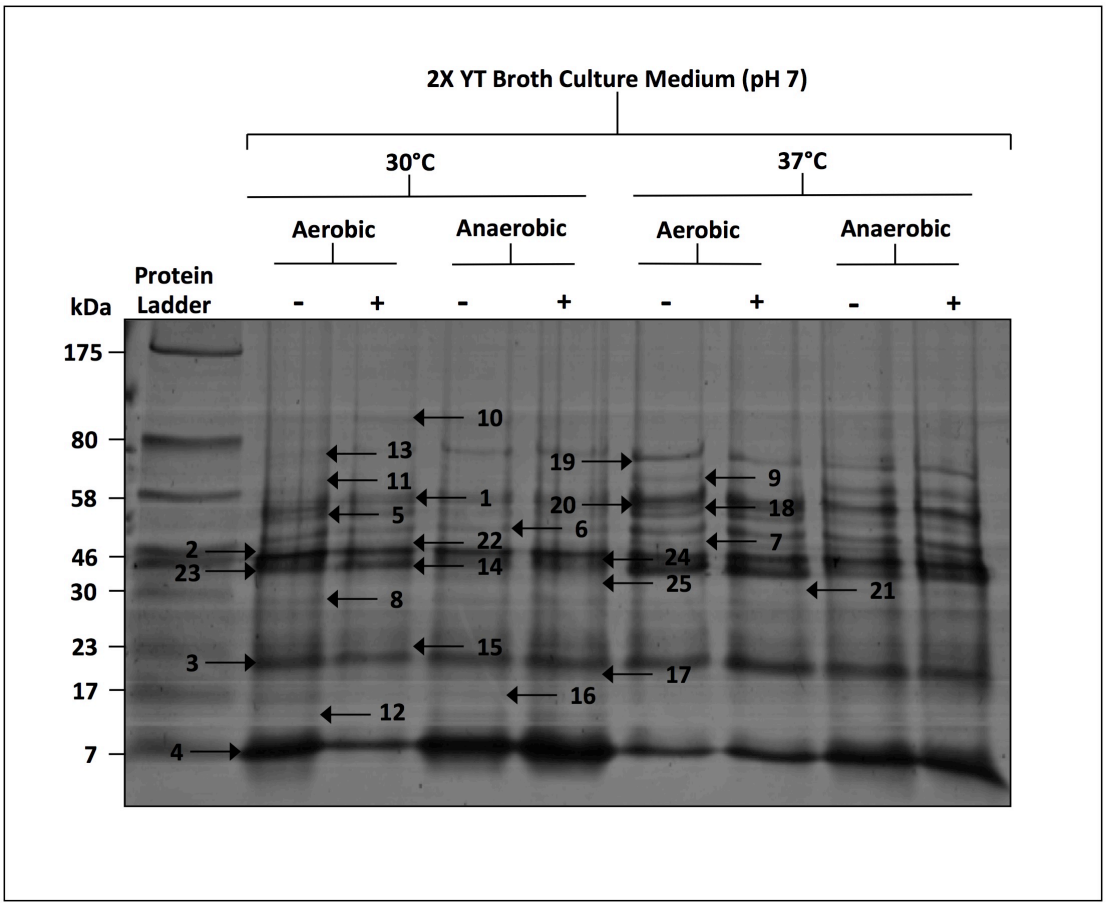

Figure 3.12 Master gel of excised 1-D SDS-PAGE *B. oleronius* protein bands for protein identification by LC/MS. Master gel of excised protein bands resolved by 1-D SDS-PAGE, and identified through LC/MS from the proteome of *B. oleronius* cells under varying environmental conditions, and cultured for 48 hour before cell harvesting. **(**Arrow (🡻) indicates bands excised for identification by LC/MS).

Table 3.1 LC/MS protein band identities from 1-D SDS-PAGE *B. oleronius* cultures grown under varying environmental conditions. (*: indicates protein identities discussed further).

Band No:	Protein Identity	Organism	M_r (nominal mass)	pI	Mascot Score	Sequence Coverage	Accession No:	UniProt Protien Function
1*	Molecular Chaperone GroEL	*Bacillus*	57400	4.77	1063	39%	WP_034766062	Polypetide Folding Under Stress Conditions
2	30S Ribosomal Protein S1	*Bacillus vietnamensis*	41911	4.72	274	19%	WP_034760590	Plays a Role in Sporulation
3	Cyclase	*Bacillus vietnamensis*	22939	4.72	142	29%	WP_034758131	Plays a Role in Sporulation
4*	Thioredoxin	*Bacillus methanolicus*	20566	4.78	216	19%	WP_003348753	Oxidoreductase Activity of Disulfide Proteins
5	1-Pyrroline-5-Carboxylate Dehydrogenase	*Bacillus vietnamensis*	59992	4.93	242	8%	WP_034756375	Oxidoreductase
6	Enolase	*Bacillus vietnamensis*	46684	4.62	1005	43%	WP_034764211	Catalyses Enzymatic Reactions in Glycolysis
7	Enolase	*Thiomicrospira crunogena XCL-2*	45832	4.82	75	3%	Q31G68	Catalyses Enzymatic Reactions in Glycolysis
8	Peptidase M29	*Bacillus vietnamensis*	45500	4.75	312	23%	WP_034761231	Aminopeptidase Activity
9	Inorganic Pyrophosphatase	*Bacillus vietnamensis*	33722	4.65	516	34%	WP_034764465	Catalyses Enzymatic Reactions in Lipid Metabolism
10	Putative Secreted Protein	*Listeria ivanovii FSL F6-596*	12671	9.12	80	17%	WP_003719615	Riboflavin Biosynthesis
11	Peptidase S8	*Bacillus vietnamensis*	155817	4.52	228	5%	WP_034758084	Serine Protease
12	Peptidase S8	*Bacillus vietnamensis*	155817	4.52	341	6%	WP_034758084	Serine Protease
13*	Clp Protease ClpX	*Bacillus vietnamensis*	90508	5.86	1442	35%	WP_034766028	Stress Response Protease
14	ATP F0F1 Synthase Subunit Beta	*Bacillus vietnamensis*	50627	4.74	359	18%	WP_034765166	ATP Binding
15*	Peroxidase	*Bacillus vietnamensis*	18334	4.75	93	19%	WP_034756208	Response to Oxidative Stress
16	Thioredoxin	*Bacillus methanolicus*	20566	4.78	124	15%	WP_003348753	Oxidoreductase Activity of Disulfide Proteins
17	Fructose-Bisphosphate Aldolase	*Bacillus marisflavi*	30562	4.88	310	30%	WP_048004831	Catalyses Enzymatic Reactions in Glycolysis
18	Elongation Factor Tu	*Bacillus*	43682	4.92	825	51%	WP_003235058	Protein Synthesis
19	Aconitate Hydratase	*Bacillus vietnamensis*	99283	4.98	419	13%	WP_034759297	Catalyses Enzymatic Reactions in Tricarboxylic Acid Cycle
20	Sugar ABC Transporter Substrate-Binding Protein	*Bacillus aquimaris*	49691	4.85	352	25%	WP_044339160	Transmembrane Protein Processes
21*	Superoxide Dismutase	*Bacillus vietnamensis*	22352	5.15	265	34%	WP_034757581	Response to Oxidative Stress
22	Protein prkA	*Bacillus vietnamensis*	73146	5.9	680	28%	WP_034760298	Protein Kinase Activity
23	ATP F0F1 Synthase Subunit Beta	*Bacillus vietnamensis*	50627	4.74	490	27%	WP_034765166	ATP Binding
24*	Flagellin	*Bacillus sp. 2_A_57_CT2*	44170	4.95	475	28%	WP_009331966	Ciliary or Flagellar Motility
25*	C4-Dicarboxylate ABC Transporter Substrate-Binding Protein	*Bacillus vietnamensis*	34518	4.57	479	37%	WP_034763524	Transmembrane Protein Processes

Table 3.2 Description of sample number and corresponding *B. oleronius* cultures grown under varying environmental conditions. Each *B. oleronius* culture sample was investigated at pH 6, 7, and 8. (2X YT broth: 2X yeast tryptone broth, H_2O_2: hydrogen peroxide).

Sample Number	Environmental Culture Condition				
	Medium	Aerobic	Anaerobic	10 mM H_2O_2	Temperature (°C)
1	Nutrient Broth	+	-	-	30
2	Nutrient Broth	+	-	+	30
3	Nutrient Broth	-	+	-	30
4	Nutrient Broth	-	+	+	30
5	Nutrient Broth	+	-	-	37
6	Nutrient Broth	+	-	+	37
7	Nutrient Broth	-	+	-	37
8	Nutrient Broth	-	+	+	37
9	2X YT Broth	+	-	-	30
10	2X YT Broth	+	-	+	30
11	2X YT Broth	-	+	-	30
12	2X YT Broth	-	+	+	30
13	2X YT Broth	+	-	-	37
14	2X YT Broth	+	-	+	37
15	2X YT Broth	-	+	-	37
16	2X YT Broth	-	+	+	37

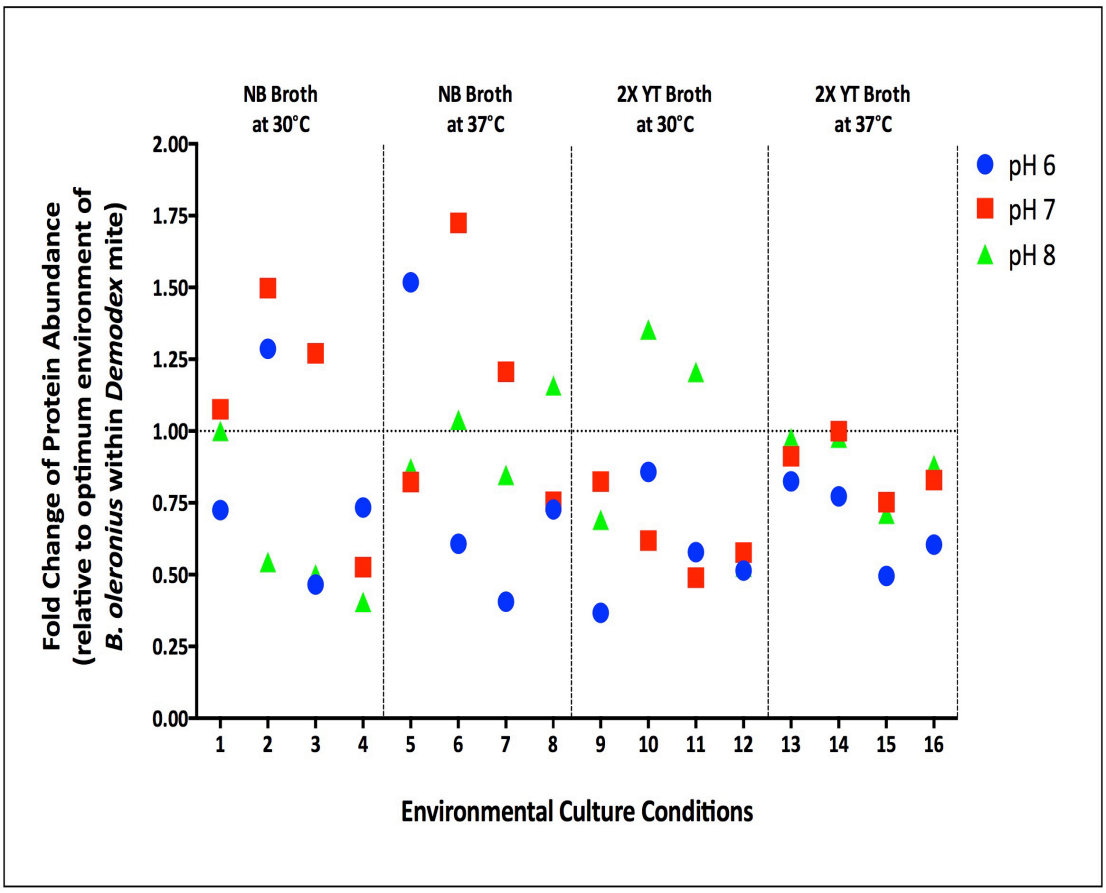

Figure 3.13 Abundance of molecular chaperone GroEL (Band No. 1) in the *B. oleronius* cultures grown under different environmental conditions. Fold change of protein abundance is given for the environmental conditions assessed at pH 6, 7, and 8 relative to the optimum environmental condition of the *B. oleronius* residing in the hindgut of the *Demodex* mite (Sample number 1 at pH 8) (nutrient broth medium (pH 8), aerobic, - 10 mM H_2O_2, 30°C). The environmental culture conditions 1 to 16 represent the culture condition examined at pH 6, 7, and 8, and are described in Table 3.2. (n = 3, for each culture condition).

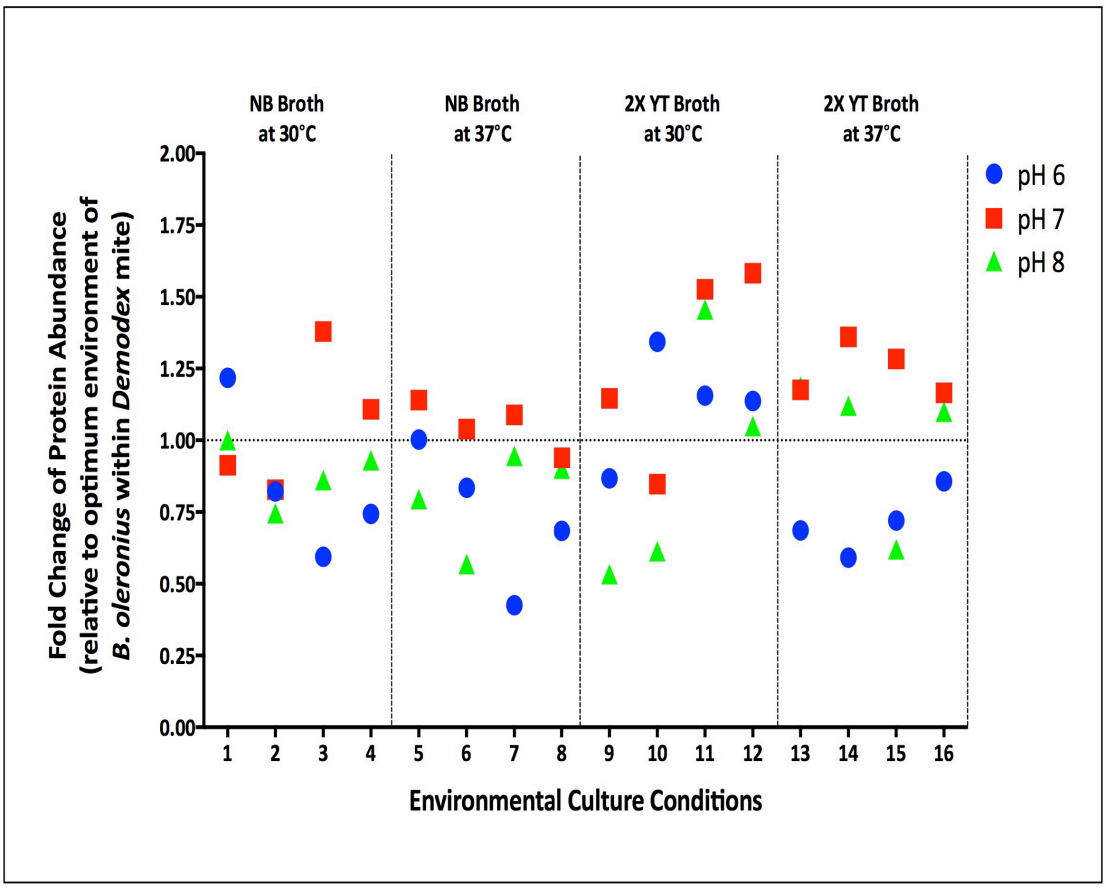

Figure 3.14 Abundance of thioredoxin (Band No. 4) in the *B. oleronius* cultures grown under different environmental conditions. Fold change of protein abundance is given for the environmental conditions assessed at pH 6, 7, and 8 relative to the optimum environmental condition of the *B. oleronius* residing in the hindgut of the *Demodex* mite (Sample number 1 at pH 8) (nutrient broth medium (pH 8), aerobic, - 10 mM H_2O_2, 30°C). The environmental culture conditions 1 to 16 represent the culture condition examined at pH 6, 7, and 8, and are described in Table 3.2. (n = 3, for each culture condition).

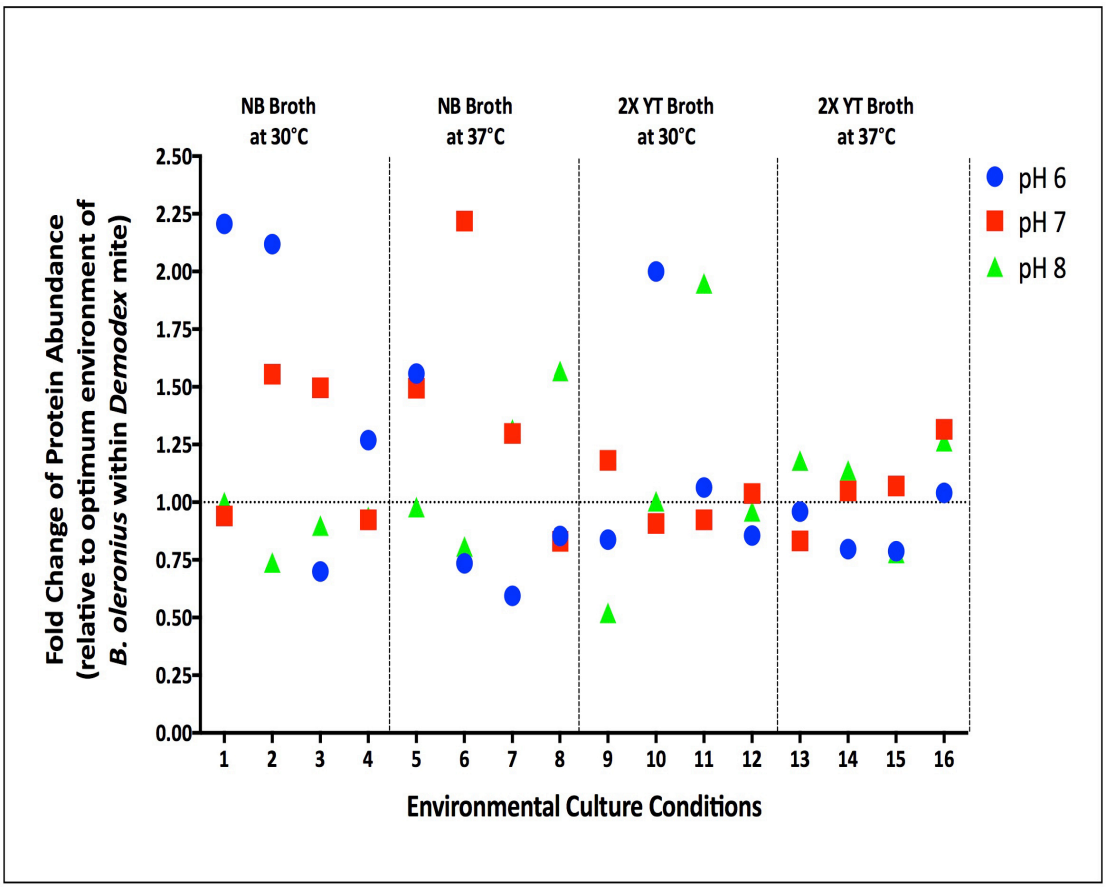

Figure 3.15 Abundance of peroxidase (Band No. 15) in the *B. oleronius* cultures grown under different environmental conditions. Fold change of protein abundance is given for the environmental conditions assessed at pH 6, 7, and 8 relative to the optimum environmental condition of the *B. oleronius* residing in the hindgut of the *Demodex* mite (Sample number 1 at pH 8) (nutrient broth medium (pH 8), aerobic, - 10 mM H_2O_2, 30°C). The environmental culture conditions 1 to 16 represent the culture condition examined at pH 6, 7, and 8, and are described in Table 3.2. (n = 3, for each culture condition).

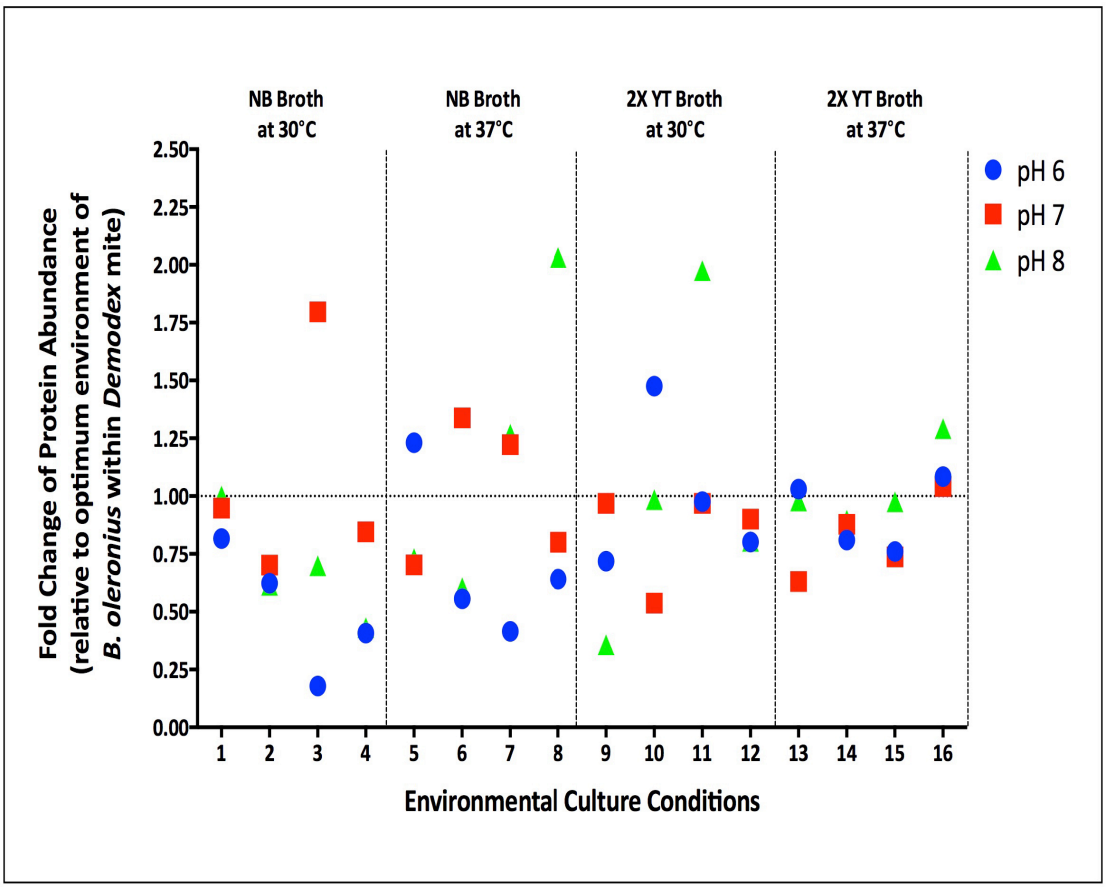

Figure 3.16 Abundance of superoxide dismutase (Band No. 21) in the *B. oleronius* cultures grown under different environmental conditions. Fold change of protein abundance is given for the environmental conditions assessed at pH 6, 7, and 8 relative to the optimum environmental condition of the *B. oleronius* residing in the hindgut of the *Demodex* mite (Sample number 1 at pH 8) (nutrient broth medium (pH 8), aerobic, - 10 mM H_2O_2, 30°C). The environmental culture conditions 1 to 16 represent the culture condition examined at pH 6, 7, and 8, and are described in Table 3.2. (n = 3, for each culture condition).

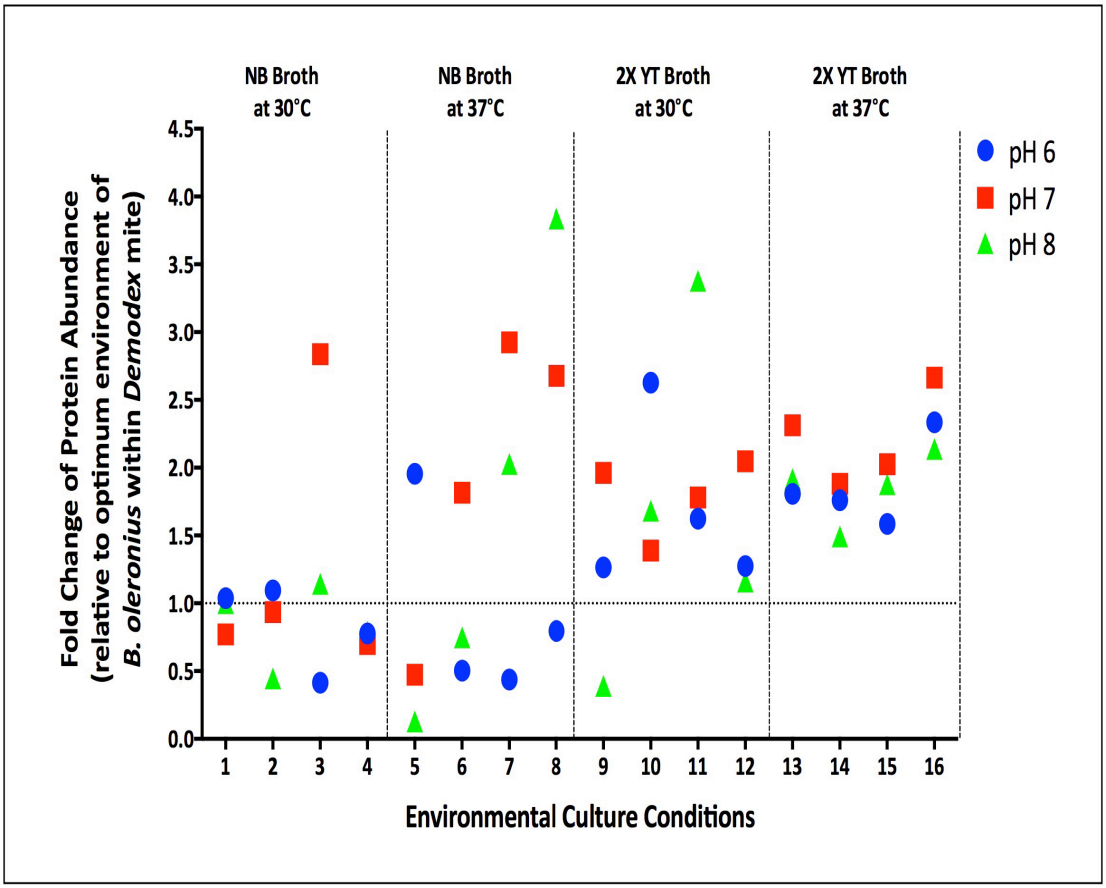

Figure 3.17 Abundance of Clp Protease ClpX (Band No. 13) in the *B. oleronius* cultures grown under different environmental conditions. Fold change of protein abundance is given for the environmental conditions assessed at pH 6, 7, and 8 relative to the optimum environmental condition of the *B. oleronius* residing in the hindgut of the *Demodex* mite (Sample number 1 at pH 8) (nutrient broth medium (pH 8), aerobic, - 10 mM H_2O_2, 30°C). The environmental culture conditions 1 to 16 represent the culture condition examined at pH 6, 7, and 8, and are described in Table 3.2. (n = 3, for each culture condition).

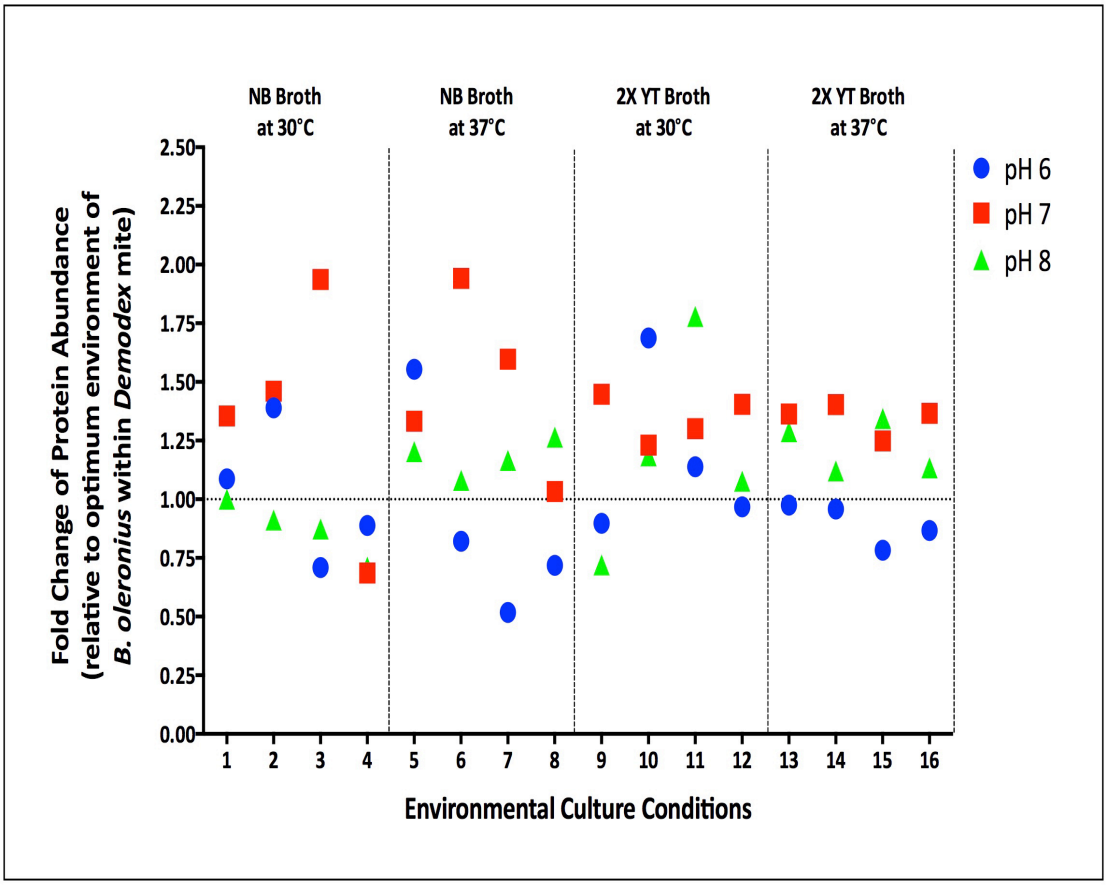

Figure 3.18 Abundance of flagellin (Band No. 24) in the *B. oleronius* cultures grown under different environmental conditions. Fold change of protein abundance is given for the environmental conditions assessed at pH 6, 7, and 8 relative to the optimum environmental condition of the *B. oleronius* residing in the hindgut of the *Demodex* mite (Sample number 1 at pH 8) (nutrient broth medium (pH 8), aerobic, - 10 mM H_2O_2, 30°C). The environmental culture conditions 1 to 16 represent the culture condition examined at pH 6, 7, and 8, and are described in Table 3.2. (n = 3, for each culture condition).

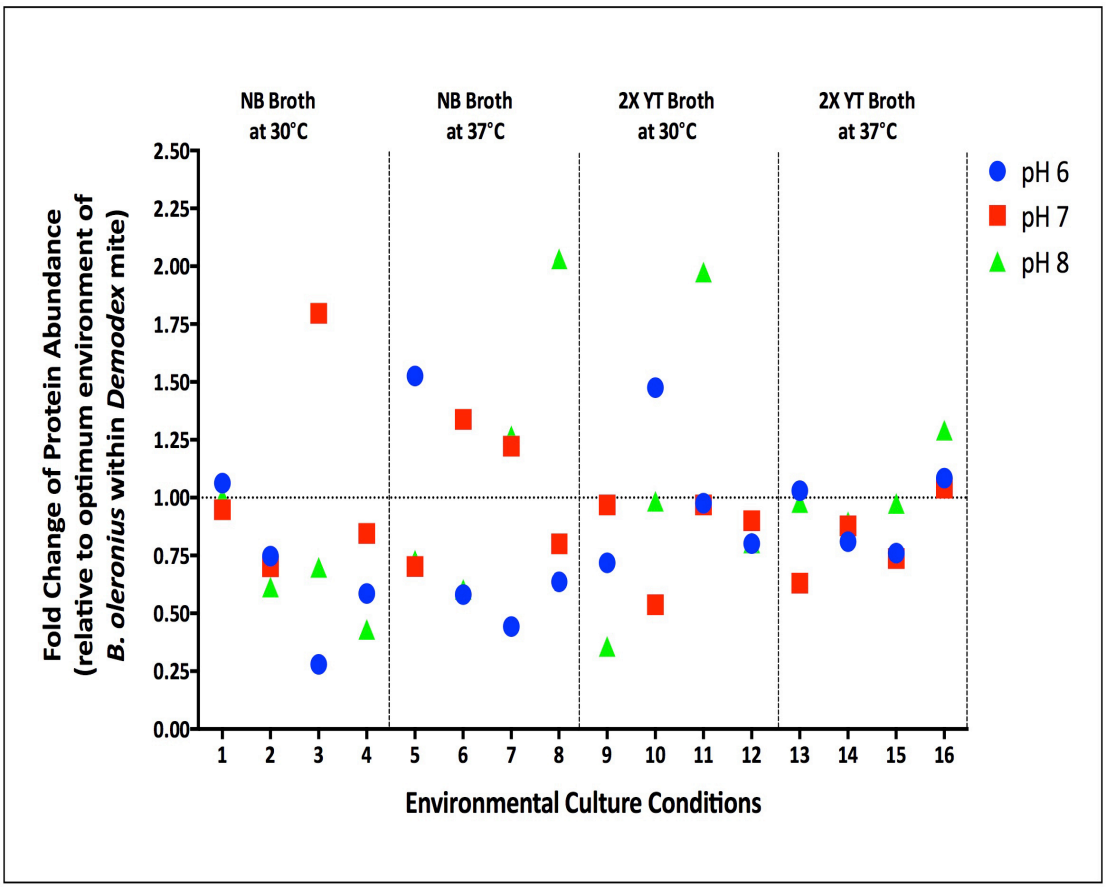

Figure 3.19 Abundance of C4-dicarboxylate ABC transporter substrate-binding protein (Band No. 25) in the *B. oleronius* cultures grown under different environmental conditions. Fold change of protein abundance is given for the environmental conditions assessed at pH 6, 7, and 8 relative to the optimum environmental condition of the *B. oleronius* residing in the hindgut of the *Demodex* mite (Sample number 1 at pH 8) (nutrient broth medium (pH 8), aerobic, - 10 mM H_2O_2, 30°C). The environmental culture conditions 1 to 16 represent the culture condition examined at pH 6, 7, and 8, and are described in Table 3.2. (n = 3, for each culture condition).

3.4 A 2-D SDS-PAGE Investigation of the Expression of the 62 kDa Protein in *B. oleronius* Grown Under Different Environmental Conditions

From the 1-D SDS-PAGE study investigating the expression of the immuno-reactive 62 kDa protein, specific environmental conditions were further examined by 2-D SDS-PAGE. The environmental conditions examined were: nutrient availability; pH; and temperature. All cultures were incubated for 48 hour under aerobic conditions with shaking, and under the varying environmental conditions described before cell harvesting and protein extractions were performed (Section 2.12.1).

Following electrophoresis of *B. oleronius*, proteins were (A) visualised on 2-D SDS-PAGE gels by colloidal Coomassie staining, and (B) the abundance of the 62 kDa protein was assessed by Western blotting (Figure 3.20 – 3.23). The expression of the 62 kDa protein was assessed using Image J densitometric software, and changes between the environmental conditions can be seen in Figure 3.24.

An increase in temperature resulted in a significant increase in expression of the immuno-reactive 62 kDa protein in *B. oleronius* cultures at 30°C to 37°C (pH 6: $p = 0.0461$; pH 8: $p = 0.0206$). The culture grown at pH 8 and 30°C, resembles the micro-environment of the hindgut of the *Demodex* mite where the *B. oleronius* naturally resides as an endosymbiont (Erban and Hubert, 2010; König *et al*., 2002). Interestingly, an increase in temperature correlates with a significant rise in the production of the 62 kDa protein in response to a heat stress ($p = 0.0206$). At 37°C, the pH 6 closer to that of the skin results in higher expression levels of the 62 kDa protein compared to the alkaline pH 8 of the gut of *Demodex* mite ($p < 0.0001$), suggesting that the *B. oleronius* produces increased levels of the 62 kDa protein in response to stress from the surrounding environment (Figure 3.24).

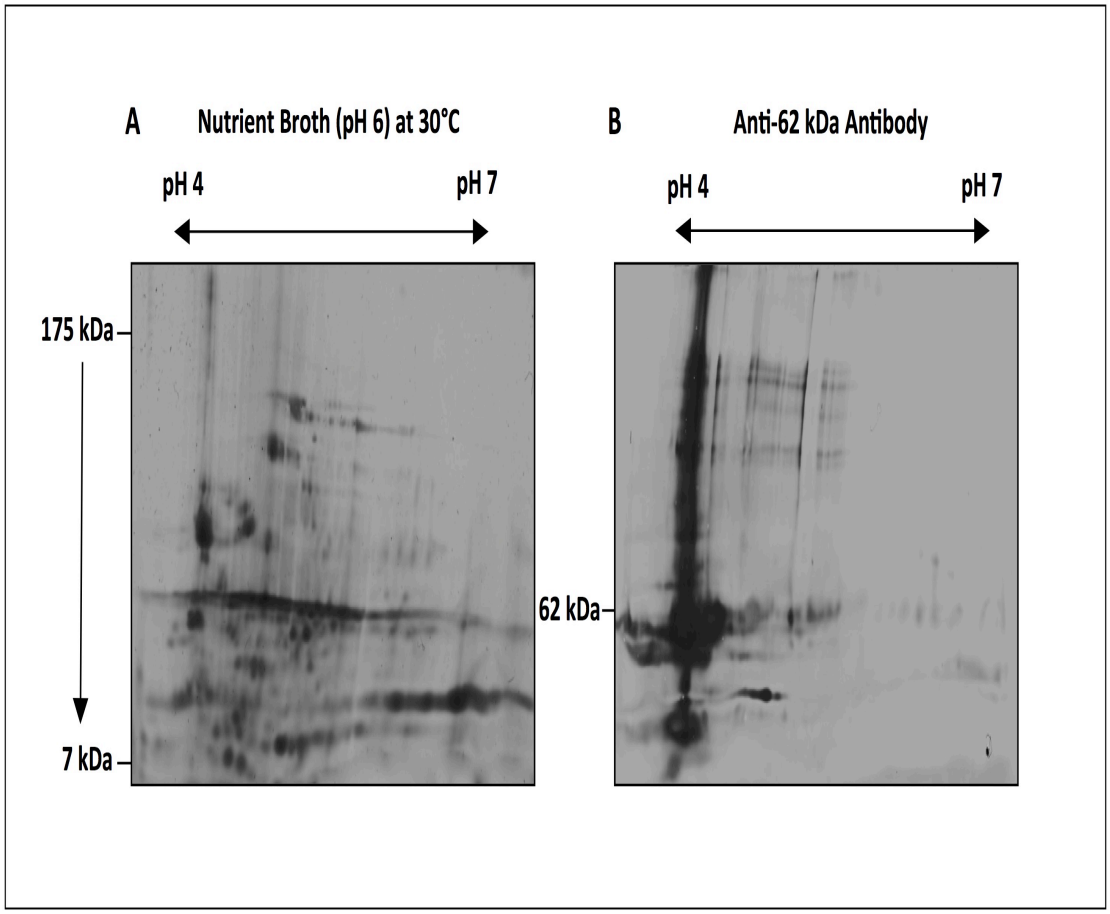

Figure 3.20 Analysis of the effect of environmental conditions on the expression of *B. oleronius* proteins in nutrient broth (pH 6) at 30°C by 2-D SDS-PAGE and immunoblot of 62 kDa protein expression. (**A**) Protein harvested from nutrient broth medium (pH 6) cultures of *B. oleronius* at 30°C for 48 hour, and resolved by 2-D SDS-PAGE before visualization by colloidal Coomassie staining, and (**B**) the abundance of the 62 kDa protein was assessed by Western blotting. (n = 3, for each culture condition).

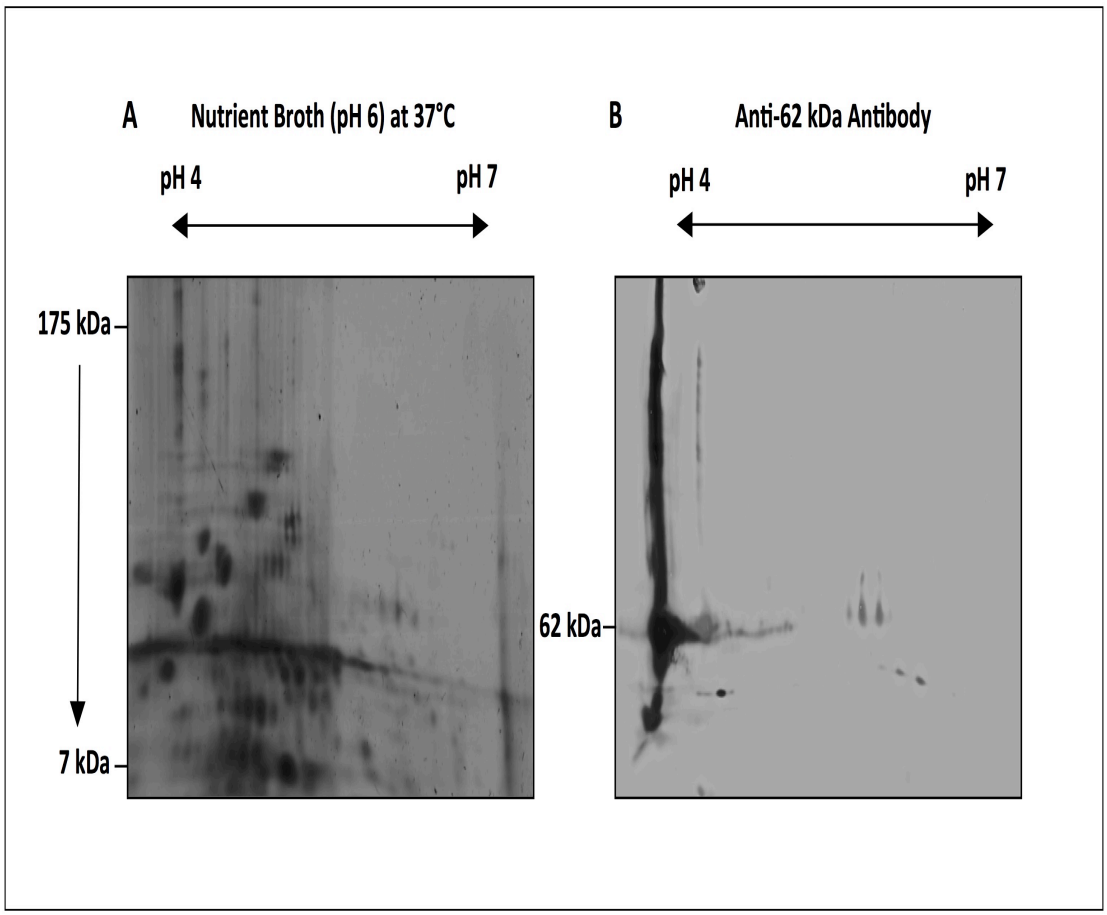

Figure 3.21 Analysis of the effect of environmental conditions on the expression of *B. oleronius* proteins in nutrient broth (pH 6) at 37°C by 2-D SDS-PAGE and immunoblot of 62 kDa protein expression. (**A**) Protein harvested from nutrient broth medium (pH 6) cultures of *B. oleronius* at 37°C for 48 hour, and resolved by 2-D SDS-PAGE before visualization by colloidal Coomassie staining, and (**B**) the abundance of the 62 kDa protein was assessed by Western blotting. (n = 3, for each culture condition).

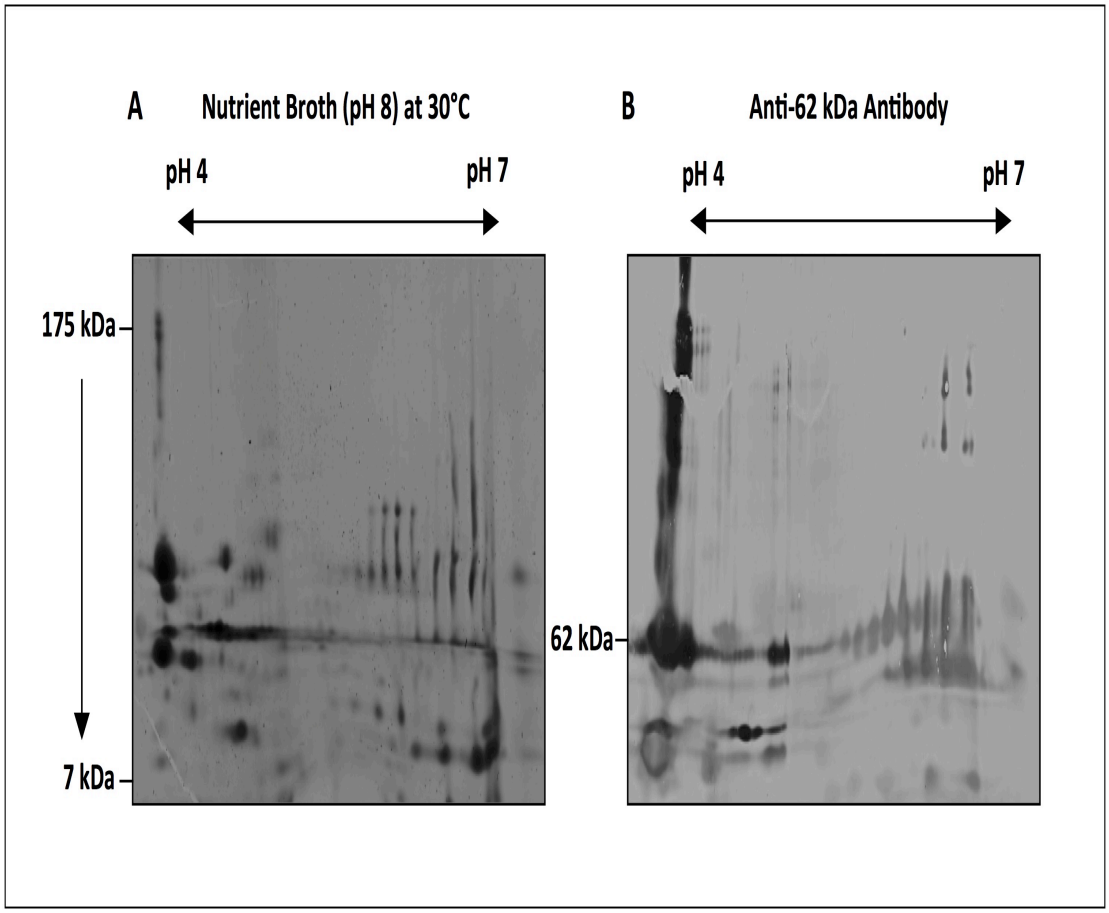

Figure 3.22 Analysis of the effect of environmental conditions on the expression of *B. oleronius* proteins in 2X YT broth (pH 6) at 30°C by 2-D SDS-PAGE and immunoblot of 62 kDa protein expression. (**A**) Protein harvested from nutrient broth medium (pH 8) cultures of *B. oleronius* at 30°C for 48 hour, and resolved by 2-D SDS-PAGE before visualization by colloidal Coomassie staining, and (**B**) the abundance of the 62 kDa protein was assessed by Western blotting. (n = 3, for each culture condition).

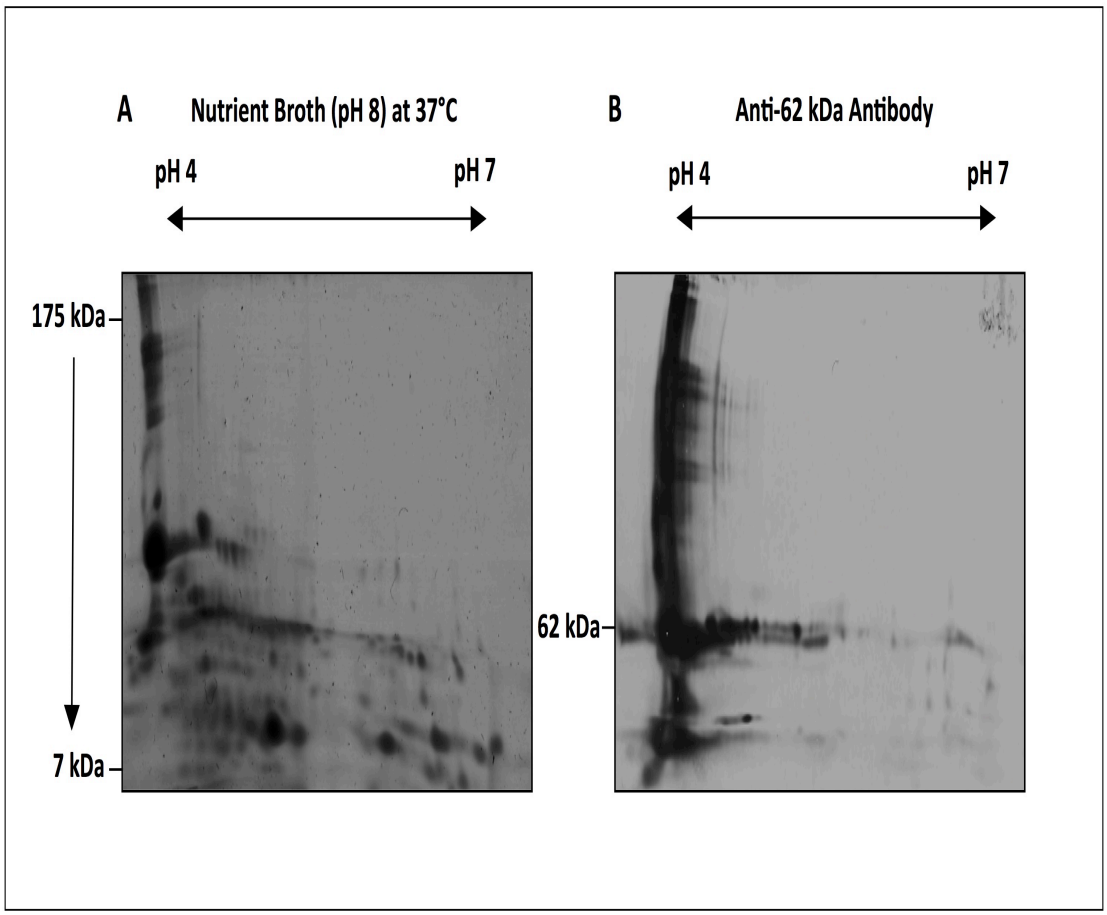

Figure 3.23 Analysis of the effect of environmental conditions on the expression of *B. oleronius* proteins in 2X YT broth (pH 6) at 37°C by 2-D SDS-PAGE and immunoblot of 62 kDa protein expression. (**A**) Protein harvested from nutrient broth medium (pH 8) cultures of *B. oleronius* at 37°C for 48 hour, and resolved by 2-D SDS-PAGE before visualization by colloidal Coomassie staining, and (**B**) the abundance of the 62 kDa protein was assessed by Western blotting. (n = 3, for each culture condition).

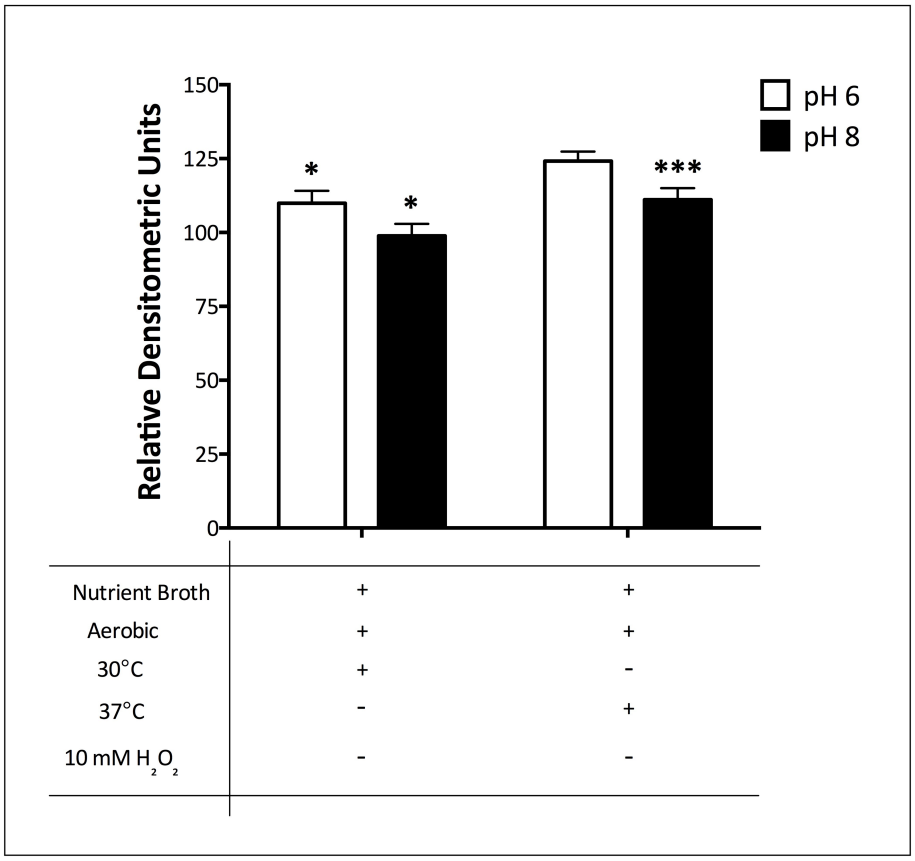

Figure 3.24 The effect of temperature on the expression of the 62 kDa protein in *B. oleronius* cultures resolved by 2-D SDS-PAGE and immunoblotted. The effect of varying environmental conditions on the abundance of the 62 kDa protein from *B. oleronius* cultures resolved by 2-D SDS-PAGE. The expression of the 62 kDa protein was assessed using Image J software. (Significance: * = $p < 0.05$, *** = $p < 0.001$). (n = 3, for each culture condition).

3.5 Analysis of Lipase and Catalase Activity in *B. oleronius* Cultures

The lipase and catalase activity of *B. oleronius* cells grown under different environmental conditions was analysed. Bacterial lipases have been implicated in the manifestation of meibomian gland dysfunction in blepharitis, and may have a role in the aetiology of ocular rosacea and other eye diseases (Liang *et al*., 2014; Li *et al*., 2010; McCulley and Shine, 2003; Dougherty and McCulley, 1986). Catalase functions to protect a cell against oxidative stress induced by ROS, and it has been demonstrated that individuals diagnosed with rosacea, contain a higher abundance of ROS in their skin (Tisma *et al*., 2009; Yamasaki and Gallo, 2009). The environmental conditions examined were described in Section 2.10. The environmental conditions were selected on the basis of differential expression of the immuno-reactive 62 kDa protein observed from Western blot analyses from the 1-D SDS-PAGE (Section 3.3), and 2-D SDS-PAGE (Section 3.4) investigations of the *B. oleronius* cultures. For both enzymatic investigations, the positive control was *B. subtilis* cultured in nutrient broth (pH 7) at 30°C, as the bacterium has been previously characterised as lipase-positive (Dröge *et al*., 2006; Eggert *et al*., 2000, 2003), and catalase-positive (Naclerio *et al*., 1995; Loewen and Switala, 1987).

3.5.1 Lipase Activity in *B. oleronius* Cultures

The analysis of lipase activity present in *B. oleronius* cultures grown under different environmental conditions was assessed using tributyrin agar (Section 2.10.1). Lipase activity was detected in the secretome of the *B. oleronius* cultures investigated with the level of lipase activity varying with each environmental condition analysed (Figure 3.25). At pH 8, bacteria grown in nutrient broth demonstrated that a change in temperature, from 30°C to 37°C, significantly increased the activity of lipase in the bacterium ($p = 0.002$). In 2X YT broth, there were significantly increased levels of lipase detected for both pH 6 and pH 8 *B. oleronius* cultures at 30°C ($p = 0.0027$, and $p = 0.0151$, respectively) and at 37°C ($p = 0.0089$, and $p = 0.0479$, respectively) relative to the nutrient broth (pH 8) cultures at 30°C. Similary in 2X YT broth, significantly increased levels of lipase were observed for both pH 6 and pH 8 *B. oleronius* cultures at 30°C ($p = 0.0054$, and $p = 0.0086$, respectively) and at 37°C ($p = 0.0048$, and $p = 0.032$, respectively) and relative to nutrient broth (pH 6) cultures at 37°C. However, 2X YT broth (pH 8) cultures at 30°C showed a significantly reduced lipase activity at 37°C compared to

the *B. subtilis* control (p = 0.0316) (Figure 3.25).

The analysis of the cell lysate of the *B. oleronius* cultures demonstrated a capacity to produce lipase (Figure 3.26). However, the levels of lipase were reduced compared to the levels of lipase detected in the secretome of *B. oleronius* cultures. Similarly, the activity of lipase present in the cell lysates of nutrient broth (pH 8) cultures increased with temperature, and was observed to be significantly increased at 37°C (p = 0.0153) (Figure 3.26). Interestingly, the cell lysates of cultures at pH 6 and 37°C, an environment that describes the conditions on the skin of the human body, demonstrated an increase in lipase activity relative to the *B. subtilis* positive control but was not deemed to be statistically significant (Figure 3.26).

3.5.2 Catalase Activity in *B. oleronius* Cultures

The analysis of catalase activity in *B. oleronius* cultures, was achieved by following the method described by Larsen and White (1995). Catalase activity was observed to be similar in *B. oleronius* cultures for each of the different environmental conditions investigated. A higher level of catalase activity was observed in cultures taken from a low nutrient environment. In nutrient broth at pH 6, the temperature did not alter catalase activity. In contrast, cultures grown at pH 8 showed a change in the level of catalase activity with an increased level of catalase activity observed at 30°C (68.75%), compared to *B. oleronius* cultures grown at 37°C (41.75%). *B. oleronius* grown in an environment rich with nutrients (2X YT broth) cultured at 30°C showed similar levels of catalase activity to *B. oleronius* cultures grown in nutrient poor environments. An increase of catalase activity was observed in 2X YT broth (pH 8) cultures (72.75%) compared to 2X YT broth (pH 6) cultures (56%). At 37°C and a nutrient rich environment, there was a decrease of catalase activity at pH 8 (61.75%) and at pH 6 (38.5%) compared to the 30°C cultures (Figure 3.27).

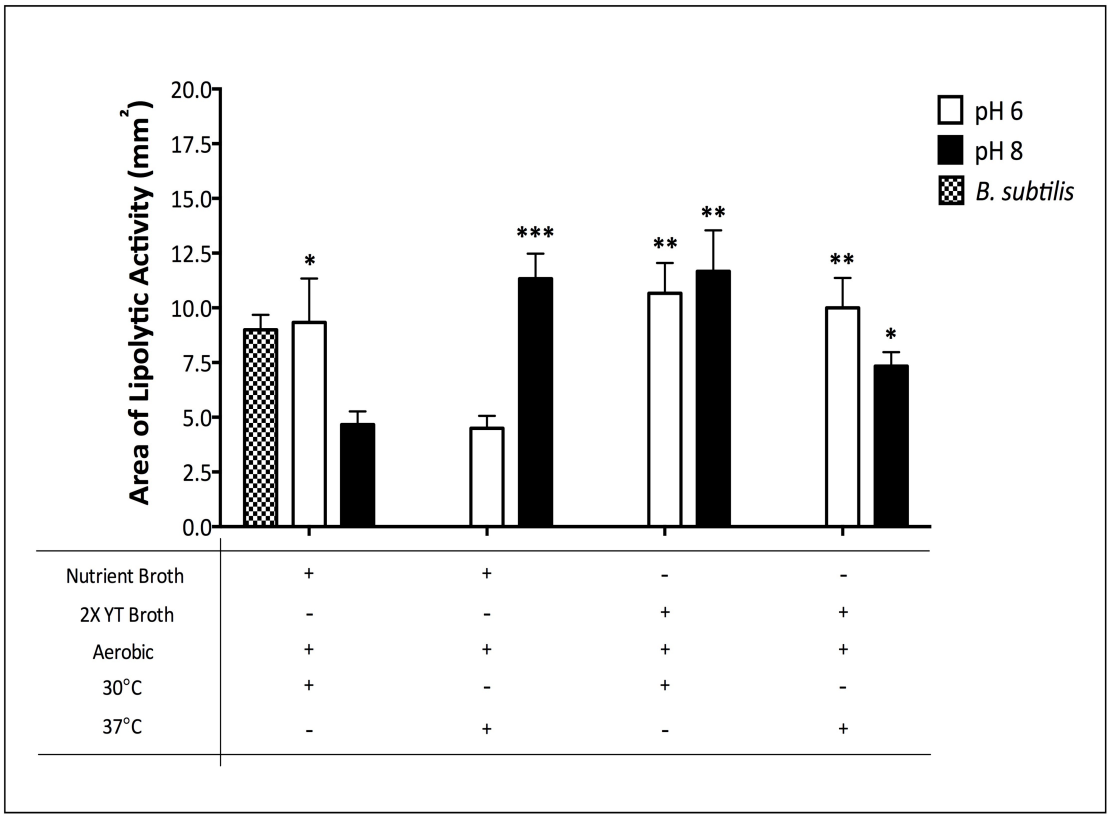

Figure 3.25 Analysis of lipase activity in the secretome of *B. oleronius* cultures grown under different environmental conditions. Lipase activity present in the secretome of *B. oleronius* cultures grown under different environmental conditions. *B. subtilis*, was used as a positive control for the assay. (Significance: * = $p < 0.05$, ** = $p < 0.01$, *** = $p < 0.001$). (n = 3, for each culture condition).

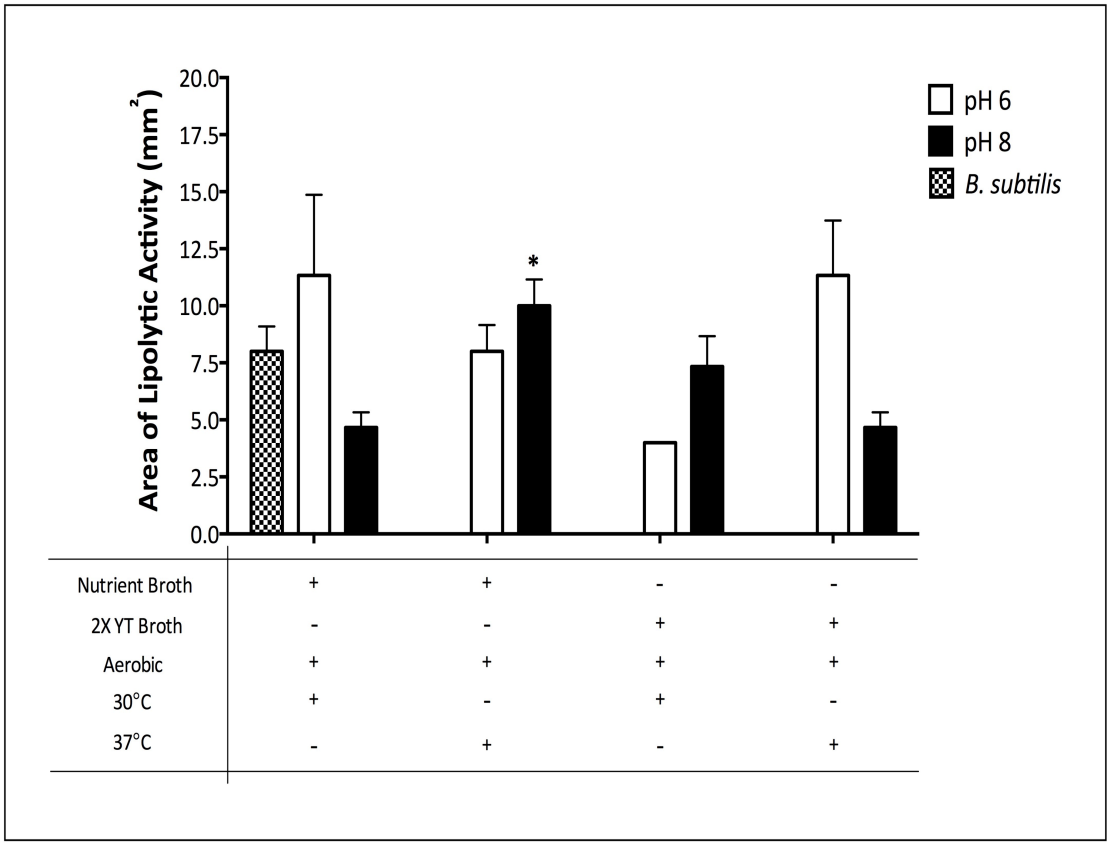

Figure 3.26 Analysis of lipase activity in the proteome of *B. oleronius* cultures grown under different environmental conditions. Lipase activity present in the proteome of *B. oleronius* cultures grown under different environmental conditions. *B. subtilis*, was used as a positive control for the assay. (Significance: * = $p < 0.05$). (n = 3, for each culture condition).

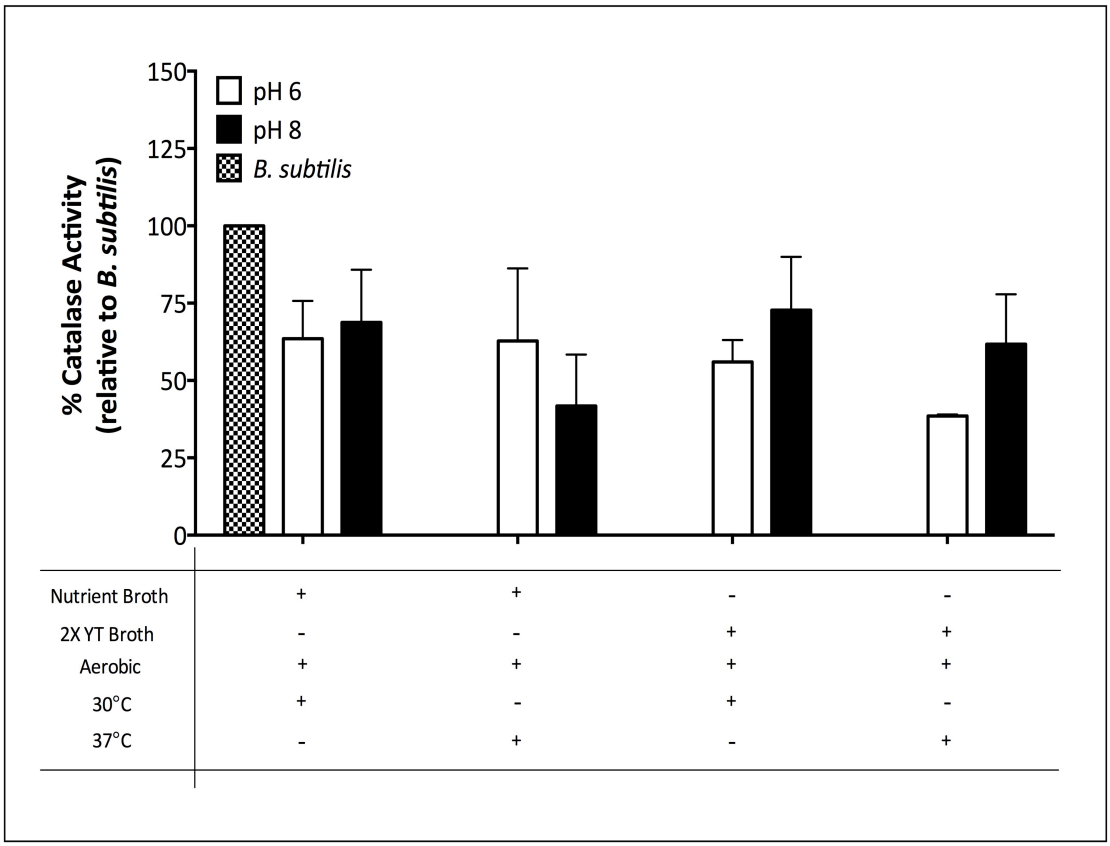

Figure 3.27 Analysis of catalase activity in *B. oleronius* cultures grown under different environmental conditions. The percentage (%) of catalase activity of *B. oleronius* cultures grown under different environmental conditions relative to that produced by *B. subtilis*. *B. subtilis* was grown under nutrient broth (pH 7), aerobic conditions at 30°C, and *B. oleronius* catalase activity was compared to this. (n = 3, for each culture condition).

3.6 Discussion

The research initially undertaken by Delaney (2004), lead to the isolation of *B. oleronius* from a *D. folliculorum* mite extracted from the facial skin of a papulopustular rosacea patient. It was demonstrated that the *B. oleronius* produced immunogenic proteins that show high levels of serum reactivity in erythematotelangiectatic rosacea patients, papulopustular rosacea patients, and ocular rosacea patients (O'Reilly *et al*., 2012c; Li *et al*., 2010; Lacey *et al*., 2007). The results of serological studies lead to further investigations examining the biological effects of the immunogenic *B. oleronius* proteins to determine the role of the bacterium in the induction and persistence of rosacea.

The abundance of the 62 kDa GroEL chaperone protein was analysed in *B. oleronius* cultures grown in different environmental conditions by 1-D and 2-D electrophoresis and immunoblotting (Section 3.1 and 3.4, respectively). It has been established that a high population of *Demodex* mites can be found residing in the pilo-sebaceous units of the skin in rosacea patients compared to controls (Zhao *et al*., 2010; El Shazly *et al*., 2001; Erbağci & Ozgöztaşi, 1998; Abd-El-Al *et al*., 1997; Bonnar *et al*., 1993; Forton and Seys, 1993; Vance, 1986). The pathogenicity of the parasitic acaridid facial mites have been intensely studied by dermatologists and scientists since their discovery by Henle and Berger (1841), to understand their role on the skin of humans (Aylesworth and Vance, 1982). Akilov and Mumcuoglu (2003) showed that individuals with the human leukocyte antigen (HLA) Cw2 and Cw4 haplotypes were more suseptible to Demodicosis, increased *Demodex* mite infestation in the surface of the skin, and have a decreased natural killer T cell population, respectively.

The effect of temperature on the viability of *D. folliculorum* and *D. brevis* mites was assessed, and it was suggested that variations of temperature may lead to alterations in the microbiota of the *Demodex*, and thus, non-pathogenic microbes, such as *B. oleronius*, may switch from a non-pathogenic to a pathogenic state due to a change in the local environment of the microbe (Zhao *et al*., 2009). Casas *et al*. (2012) quantified *D. folliculorum* mite colonisation in erythematotelangiectatic rosacea and papulopustular rosacea patients using a molecular based PCR technique. The authors also investigated the activation of a skin innate immune response, and found the gene expression of IL-8, IL-1β, TNF-α, and Cox-1 to be increased following facial skin swabs and epidermal scrapings of rosacea patients skin lesions,

and observed an increase in the expression for genes coding for the inflammasome.

Features of the skin microenvironment including aerobicity, temperature, pH, and lipid composition could influence *Demodex* mite population growth, and thus, the onset of symptoms associated with rosacea by a microbial agent (Holmes, 2013; Ní Raghallaigh *et al*., 2012; Grice and Segre, 2011; Leyden *et al*., 1975; Somerville, 1969). A study by Murillo *et al*. (2014) identified the microbiota of *Demodex* mites isolated from controls and rosacea patients. The authors identified *Bacillus* species in *Demodex* mites of rosacea patients (Murillo *et al*., 2014). The results presented in Section 3.1 and 3.4, demonstrate that the production of the immuno-reactive 62 kDa GroEL chaperone protein is dependent upon the host in which the bacterium resides, either the *Demodex* mite or human. The cultures grown at pH 8 and 30°C, resembles the micro-environment of the gut of the *Demodex* mite where the *B. oleronius* may reside as an endosymbiont (Erban and Hubert, 2010; König *et al*., 2002). Interestingly, an increase of temperature correlates with a significant rise in the production of the 62 kDa protein ($p = 0.0206$). At pH 6 and 37°C, the pH closer to that of the skin results in higher expression of the 62 kDa protein compared to the pH 8 of the gut of *Demodex* mite ($p < 0.0001$) (Figure 3.21), suggesting that *B. oleronius* produces increased levels of the immuno-reactive 62 kDa protein in response to stress from the surrounding environment.

The most prevalent bacteria found to inhabit the skin of healthy individuals is *Staphylococcus epidermidis*. The effect of temperature on protein expression, has previously been investigated in *S. epidermidis*, demonstrating that temperature regulates bacterial protein production, as *S. epidermidis* isolated from rosacea patients' skin was shown to be consistently β-hemolytic compared to non-hemolytic in controls (Cheung *et al*., 2012; Dahl *et al*., 2004). The research study also revealed that the β-hemolytic *S. epidermidis* isolates secreted more protein and different proteins at 37°C compared to cells grown at 30°C (Dahl *et al*., 2004). It is believed that *S. epidermidis* may be implicated in the pathogenesis of rosacea as pure growths of *S. epidermidis* were isolated from a pustule on the cheeks (9/15), and eyelids (4/15), of papulopustular rosacea patients, with no pure growth of *S. epidermidis* isolated from the cheeks and eyelids of control subjects (Whitfeld *et al*., 2011). The surface skin temperature of individuals with rosacea is elevated compared to healthy individuals, with the transient episodes of periodic flushing and increasing blood flow that is believed to be one of the explainations for this occurrence. It is possible that

alterations in temperature and the microenvironment of the *B. oleronius* can result in the *B. oleronius* upregulating the secretion of proteins that mediate an immune and persistent inflammatory response in rosacea.

The composition and quantity of sebum present on the skin of rosacea patients has been a subject of interest for understanding the underlying mechanisms of the disease since 1976 (Pye *et al*., 1976). The fatty acid profile of the skin surface lipid layer was assessed in papulopustular rosacea patients, and demonstrated that the sebum of papulopustular roascea patients contained increased levels of myristic acid, and reduced levels of arachidic acid, behenic acid, tricosanoic acid, lignoeric acid, cis-11-eicosanoic acid compared to the sebum analysed from controls (Ní Raghallaigh *et al*., 2012). The authors suggest that fatty acid composition present on the skin may be related to the skin barrier integrity (Ní Raghallaigh *et al*., 2012). It is believed that the *Demodex* mites residing in the pilo-sebaceous units of the skin and meibomian glands of the eyes, may increase in populations, as they feed on the host's sebum and epithelial cells (Liang *et al*., 2014; Forton, 2012; Liu *et* al., 2010; Lacey *et al*., 2009). The bacterium, *B. oleronius*, has been identified residing in the hindgut of the *Demodex* mite, and it is thought that the *B. oleronius* may function in a commensal capacity during feeding, for the digestion of sebum, in a similar manner to *Bacillus* species have previously reported to reside in the hindguts of the termite, *Reticulitermes santonesis* (König, 2006; Kuhnigk *et al*., 1995). Here, it was observed that the *B. oleronius* produced lipases in different environmental conditions that may potentially alter the sebum composition on the skin of rosacea patient's and allow for *Demodex* mite populations to increase (Figure 3.25 and Figure 3.26).

The activity of catalase in *B. oleronius* cultures grown under various environmental culture conditions was investigated (Section 3.5.2). The *B. oleronius* cultures produced similar levels of catalase activity in the different environmental conditions analysed. Catalase functions in the conversion of hydrogen peroxide to water and oxygen, and thus, protecting a cell from oxidative stresses induced by ROS. ROS are known to activate an innate immune response in the human body, and it can be suggested that the protective effect of catalase, can enable the *B. oleornius* to survive and persist during the course of an infection. As mentioned earlier, it has been demonstrated that individuals diagnosed with rosacea, contain a higher abundance of ROS in their skin (Tisma *et al*., 2009; Yamasaki and Gallo, 2009). The ROS primarily found in the skin of rosacea patients were LL-37, a form of cathelicidin derived from

neutrophils present on infected or injured skin, and kallikrein-5 (KLK-5), a serine protease of the kallikrein family of proteases, that cleaves and activates cathelicidin (Meyer-Hoffert *et al*., 2011; Yamasaki *et al*., 2007; Yamasaki *et al*., 2006). KLK-5 is believed to mediate centrofacial vascular changes of the centrofacial region, consequently leading to the production of the persistent non-transient facial erythema and inflammation, characteristic in rosacea (Two and Del Rosso, 2014; Del Rosso *et al*., 2013a, 2013b, 2013c ; McAleer *et al*., 2009; Koczulla *et al*., 2003)

The results presented in this Chapter support previous findings describing an involvement of *B. oleronius* in rosacea. The expression of the 62 kDa GroEL chaperone protein by *B. oleronius*, was investigated in varying environmental conditions, and demonstrated that the *B. oleronius* increased the expression of the 62 kDa protein in response to stress. The expression of the 62 kDa protein is reduced in an environment resembling the conditions of the hindgut of the *Demodex* mite (Erban and Hubert, 2010; König *et al*., 2002).

A LC/MS study investigating the proteome of the *B. oleronius* grown under varying environmental conditions demonstrated that the *Bacillus* produces a wide range of proteins that function in metabolism, transmembrane protein processes, signaling, serine proteases, motility, and in response to heat shock and oxidative stresses, and that the expression of these proteins is altered in response to the conditions of the surrounding environment. The pathogenic potential of the *B. oleronius* can be induced by a change in the environment, from the hindgut of the *Demodex* mite to the human skin and body, leading to the increased abundance of GroEL, thioredoxin, peroxidase, superoxide dismutase, Clp protease ClpX, ABC transporters, and flagellin that have been shown to activate the immune response.

The activity of catalase and lipase in the *B. oleronius* were analysed. It was observed that catalase activity increased in an environment similar to the conditions of the body, suggesting that the *B. oleronius* has the capacity to protect itself against the oxidative killing mechanisms of neutrophils and the innate immune system, and persist. The fatty acid composition of rosacea patients has been shown to be different compared to controls, and it can be hypothesised that an altered sebum content may promote the proliferation of *Demodex* populations, and therefore, allow for an environment for the *B. oleronius* to flourish in number. Following the end of the life cycle of the *Demodex* mite, and the release of *B. oleronius* and other microbes from their acaridid host to the skin surface of the mammalian host, it may be postulated that

the environmental changes induces a proteomic change in the phenotype of the *B. oleronius*, leading to the pathogenesis of rosacea.

Chapter 4

An Analysis of the Response of Corneal Epithelial (hTCEpi) Cells to *Bacillus oleronius* Proteins

4.0 Introduction

Ocular rosacea affects the eyes and the eyelids causing symptoms such as blepharitis and keratitis and up to half of those diagnosed with facial rosacea also manifest ocular symptoms (Oltz and Check, 2011; Jenkins *et al*., 1979). Corneal (sterile) ulcers and corneal scarring are associated with severe cases of ocular rosacea and can lead to a deterioration in vision and potentially blindness in affected eyes (Kheirkhah *et al*., 2007b). While the classification of rosacea is now well established there is no agreement on the aetiology of the condition. A number of factors have been implicated in the induction and persistence of rosacea including alterations in the dermal immune response, increased dermal vascularisation, and the presence of ROS in the skin (Yamasaki and Gallo, 2009). In a study by Li *et al*. (2010) it was demonstrated that individuals with ocular rosacea and high *Demodex* mite infestation were serum immunoreactive to *B. oleronius* proteins ($p = 0.009$).

Corneal epithelial cells (hTCEpi) are an excellent model for studying the response of the corneal surface to pathogens or pathogen derived materials (e.g. toxins, antigens) and may give an insight into the response of the cornea to bacterial interactions in ocular rosacea. Corneal epithelial cells have previously been used to study the interaction of flagellin from pathogenic and non-pathogenic bacteria and in understanding the response of the corneal surface to the combined effect of contact lens and *Pseudomonas aeruginosa* (Maltseva *et al*., 2007; Hozono *et al*., 2006). It has previously been demonstrated that exposure of hTCEpi cells to the *B. oleronius* proteins leads to an aberrant wound healing response (O'Reilly *et al*., 2012b). Thus implicating a role for *B. oleronius* in ocular rosacea and the possible generation of ocular sterile ulcers on the corneal surface.

The aim of the work presented in this Chapter was (1) to isolate *B. oleronius* proteins for use in futher *in vitro* biological assays involving corneal epithelial (hTCEpi) cells, and human neutrophils and PBMC, and (2) to characterise the response of corneal epithelial cells exposed to the *B. oleronius* proteins and to determine if exposure to the *B. oleronius* proteins might give an indication as to how these bacterial proteins induce the erythema that is a feature of ocular rosacea (Oltz and Check, 2011; Jenkins *et al*., 1979). The elucidation of the role of these proteins in inducing the symptoms of ocular rosacea could open the possibility of developing new therapeutic strategies for the control of this disfiguring condition.

4.1 Generation of Crude and Pure *B. oleronius* Protein Preparations

4.1.1 Preparation of Crude *B. oleronius* Protein Preparation

Cultures of *B. oleronius* were incubated at 30°C in nutrient broth, under aerobic conditions to the stationary phase before protein extractions were performed (Section 2.12.1). The crude *B. oleronius* protein preparation generated was resolved by 1-D SDS-PAGE, followed by Western blotting to assess reactivtiy to the 62 kDa protein of interest (Figure 4.1). The crude *B. oleronius* protein preparation was used for assays investigating the effect of *B. oleronius* proteins on human corneal epithelial cells (hTCEpi cell line), and isolated PBMC (Section 2.21) and neutrophils (Section 2.22).

4.1.2 Preparation of Pure *B. oleronius* Protein Preparation by ÄKTA FPLC™ and Q-Sepharose™ High Performance Beads

The immuno-reactive proteins were isolated to form the 'pure' *B. oleronius* protein preparation, and were identified by O'Reilly *et al*. (2012a) using LC/MS to contain proteins implicated in response to oxidative stress, e.g. Kat E1, vegetative catalase 1, superoxide dismutase, and alkyl hydroperoxide reductase, flagellin, and bacterial heat shock protein, GroEL. The pure *B. oleronius* protein preparation was generated through anion exhange chromatography of isolated fractions of interest present in the crude *B. oleronius* protein lysate along a saline gradient using Q-Sepharose™ high performance beads and ÄKTA FPLC™.

The starting material consisting of crude *B. oleronius* protein lysates obtained from the *B. oleronius* cultures (Section 2.20), was resuspended in ÄKTA FPLC™ binding buffer (pH 4.8), sterile-filtered using 0.45 µm cellulose pore filter discs, and incubated for 1 hour with ÄKTA FPLC™ binding buffer (pH 4.8) and Q-Sepharose™ high performance beads at 4°C prior to loading onto the ÄKTA FPLC™ column. The starting material was fractionated from the Q-Sepharose™ beads based on charge by increasing the saline gradient using the ÄKTA FPLC™ elution buffer (pH 4.8) to dissociate the charged protein from within the column of the ÄKTA Purifier 100 system instrument. A representative chromatogram from the preparation of the pure *B. oleronius* protein from the crude extract using ÄKTA FPLC™ and Q-Sepharose™ high performance beads can be seen in Figure 4.2. The UV 280 nm

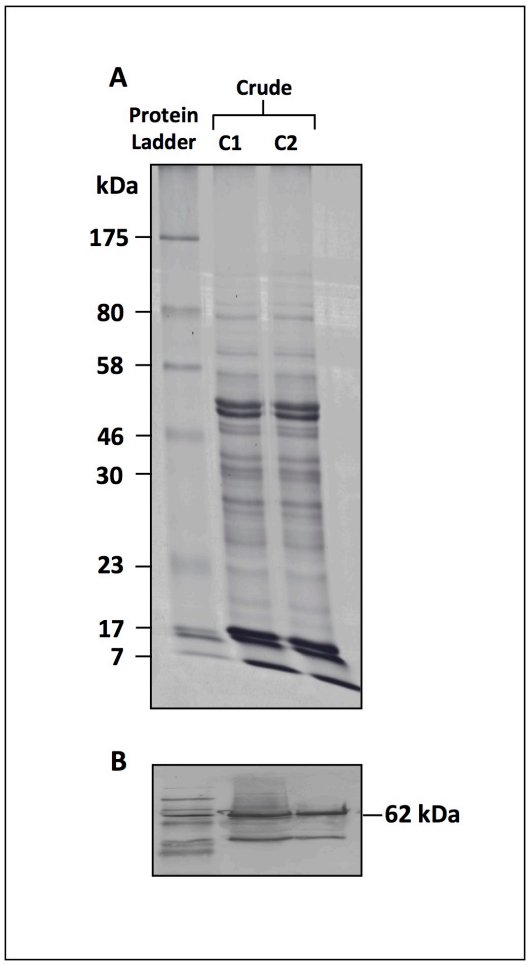

Figure 4.1 Crude *B. oleronius* protein preparations demonstrating reactivity to 62 kDa protein. (A) Crude *B. oleronius* protein preparations (labeled C1 and C2) (20 µg) were resolved by 1-D SDS-PAGE (Section 2.14), and visualized by Coomassie staining (Section 2.16.1). (**B**) Immunoblots of crude *B. oleronius* protein preparations, C1 and C2, demonstrating reactivity of the crude preparation to *B. oleronius* anti-62 kDa protein (Section 2.19).

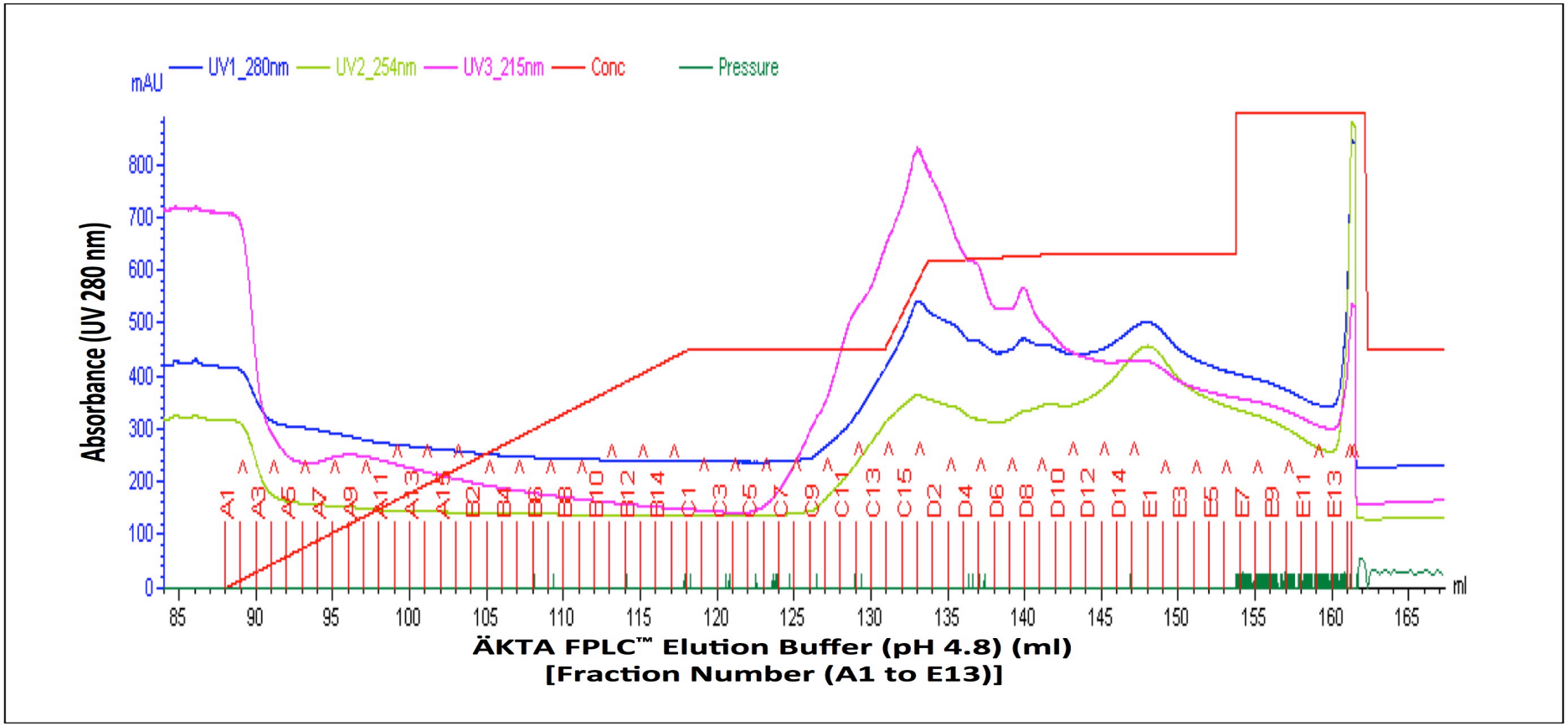

Figure 4.2 A representative ÄKTA FPLC™ chromatogram of the fractionation of crude *B. oleronius* protein. A representative chromatogram from the preparation of the pure *B. oleronius* protein from the crude extract using ÄKTA FPLC™ and Q-Sepharose™ High Performance Beads. The absorbance UV 280 nm (blue line) measures protein concentration, and the concentration (conc) (red line) illustrates the salt gradient and elution of protein from the Q-Sepharose™ beads in the ÄKTA FPLC™ column with the collection of fractions (A1 to E13).

(blue line) measures protein concentration, and the concentration (conc) (red line) illustrates the salt gradient and elution of protein from the Q-Sepharose™ beads in the ÄKTA FPLC™ column with the collection of fractions, labelled A1 to E13.

The collected fractions were labelled, and prepared for 1-D SDS-PAGE, with Coomassie brilliant blue staining and immunoblotting against the anti-62 kDa protein employed to identify isolated fractions of interest containing a high abundance of the 62 kDa protein of interest. The process can be seen in Figure 4.3, and in the Appendix (Figure A4.1 – A4.5). Fractions 1 to fraction 81, labelled F1 to F81, are resolved by 1-D SDS-PAGE with protein visualised by Coomassie brilliant blue staining, and each fraction was assessed for reactivity to the 62 kDa protein by Western blotting. During the ÄKTA FPLC™ separation of the starting material, the crude *B. oleronius* lysate, reactivity of the 62 kDa protein appeared at fraction 23 (F23) (Figure 4.3 A and B), and continued to be eluted from the ÄKTA FPLC™ column until fraction 69 (F69) (Figure A4.4 C and D in the Appendix).

Fractions 23 to 69 were processed further for purification, and filter concentrated by centrifugation using 3000 MWCO Vivaspin®-20 filter columns (Section 2.20.3) to give 8 fractions of pure *B. oleronius* protein preparations, labelled P1 to P8 (Figure 4.4). The pure *B. oleronius* protein preparations were resolved by electrophoresis, and stained with Coomassie brilliant blue stain to visualize the protein content of each pure fraction. The purity of each fraction was determined by Western blotting against the 62 kDa protein, and the abundance of the 62 kDa protein of interest in each pure *B. oleronius* protein preparation was quantified. The pure *B. oleronius* protein preparation was used for assays investigating the effect of positively immuno-reactive *B. oleronius* proteins found in rosacea patients, on human corneal epithelial cells (hTCEpi cell line), and isolated PBMC (Section 2.21) and neutrophils (Section 2.22). A representative Western blot demonstrating the presence of the 62 kDa protein in pure *B. oleronius* protein preparations following fractionation of crude *B. oleronius* protein can be seen in the appendix (Figure A4.6).

4.1.3 Summary

Cultures of *B. oleronius* were harvested and protein was extracted to form the crude *B. oleronius* protein (200 μg/ml) stock preparation. The crude *B. oleronius* protein was loaded onto an ÄKTA FPLC™ column, and fractionated using a saline gradient and Q-sepharose™ high performance beads. Fractions of interest containing the 62 kDa protein were visualized by Coomassie staining and Western blotting, pooled by filter-centrifugation, and acetone precipitated to generate the pure *B. oleronius* protein (200 μg/ml) stock preparation. The crude and pure *B. oleronius* protein preparations were used for *in vitro* biological assays involving corneal epithelial (hTCEpi) cells, and immune cells, neutrophils and PBMC.

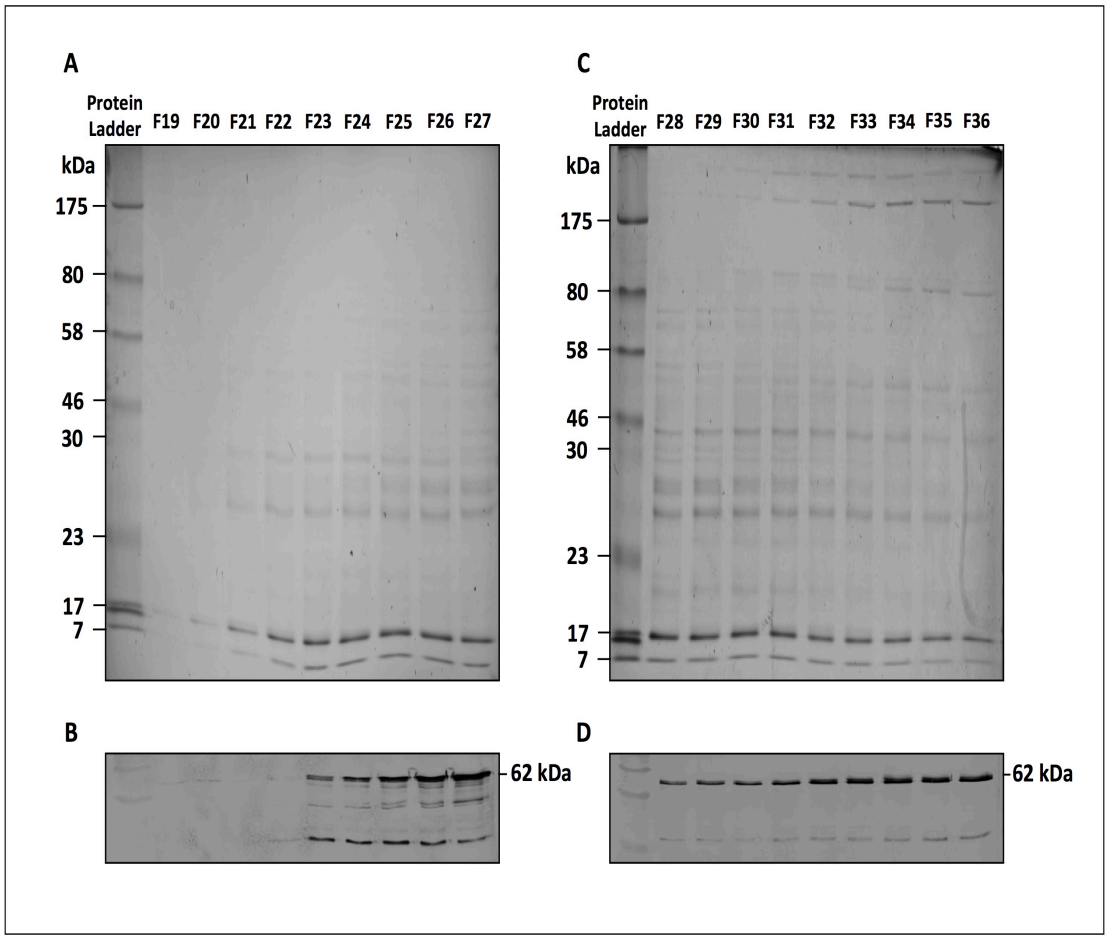

Figure 4.3 Visualization of *B. oleronius* protein ÄKTA FPLC™ fractions 19 to 36 by Coomassie Staining and Western blotting. Preparation of pure *B. oleronius* protein by assessing fractions for the abundance of the protein of interest, the 62 kDa *B. oleronius* protein. (**A**) Fractions 19 to 27 (F19 – F27) of crude *B. oleronius* protein eluted from the Q-sepharose™ high performance beads of the ÄKTA FPLC™ column were resolved by 1-D SDS-PAGE with visualization by Coomassie staining, and (**B**) assessment of reactivity to anti-62 kDa *B. oleronius* protein by Western blotting. (**C**) Fractions 28 to 36 (F28 – F36) of crude *B. oleronius* protein eluted from the Q-sepharose™ high performance beads of the ÄKTA FPLC™ column were resolved by 1-D SDS-PAGE with visualization by Coomassie staining, and (**D**) assessment of reactivity to anti-62 kDa protein by Western blotting.

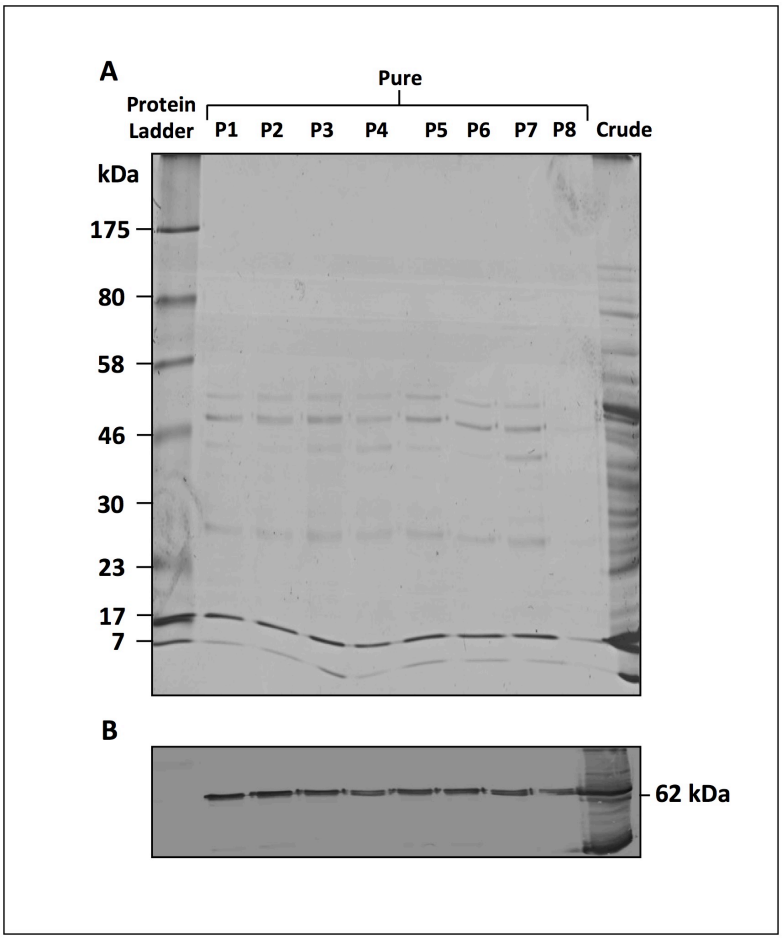

Figure 4.4 Visualization of ÄKTA FPLC™ generated pure *B. oleronius* protein preparation fractions 1 to 8 by Coomassie Staining and Western blotting. (**A**) Fractions of pure *B. oleronius* protein preparations labeled P1 to P8 (P1 – P8) obtained from separation of crude *B. oleronius* protein from the Q-sepharose™ high performance beads of the ÄKTA FPLC™ column were resolved by 1-D SDS-PAGE with visualization by Coomassie staining, and (**B**) assessment of reactivity to anti-62 kDa *B. oleronius* protein by Western blotting. Crude *B. oleronius* protein (20 µg) was resolved, and immunoblotted alongside the pure *B. oleronius* protein preparations to assess the abundance and purification of the anti-62 kDa protein.

4.2 Effect of *B. oleronius* Protein on hTCEpi Cell Growth

The effect of the crude and pure *B. oleronius* protein preparations (2, 4, 6, and 8 μg/ml) on the growth of corneal epithelial (hTCEpi) cells (1 x 10^3 cells/well), and the cytotoxic effect following a 6 day exposure was assessed by XTT staining and crystal violet staining (Section 2.31) (Figure 4.5).

Exposure of corneal epithelial (hTCEpi) cells to BSA protein (protein control) did not have a negative effect on hTCEpi cell growth. Staining of pure *B. oleronius* protein treated hTCEpi cells with XTT, showed a significant dose-dependent reduction in corneal epithelial cell growth relative to the untreated control cells from 68% cell growth following exposure to 2 μg/ml protein ($p < 0.01$) to 55% cell growth following exposure to 8 μg/ml protein ($p < 0.001$). Treatment of hTCEpi cells to the crude *B. oleronius* protein reduced cell growth, and a siginificant decrease in cell growth was recorded using 6 μg/ml protein (62%) ($p < 0.001$), and 8 μg/ml protein (63%) ($p < 0.001$) relative to untreated hTCEpi cells (Figure 4.5A).

Following crystal violet staining, exposure of hTCEpi cells to the pure *B. oleornius* protein produced a significant decrease in cell growth relative to the untreated control cells at 2 μg/ml protein (70%) ($p < 0.01$), 4 μg/ml protein (69%) ($p < 0.05$), 6 μg/ml protein (73%) ($p < 0.05$), and 8 μg/ml protein (68%) ($p < 0.01$). Similarly, the growth of hTCEpi cells was reduced in the presence of crude *B. oleronius* protein in a dose-dependent manner, with a significant decrease in growth following exposure of hTCEpi cells to 4 μg/ml protein (73%) ($p < 0.05$), 6 μg/ml protein (70%) ($p < 0.01$), and 8 μg/ml protein (69%) ($p < 0.01$) (Figure 4.5B).

4.3 Effect of *B. oleronius* Protein on hTCEpi Cell Proliferation

Exposure of corneal epithelial cells to 2 or 6 μg/ml *B. oleronius* protein reduced the growth rate of cells over a 6 day period (Section 2.32) (Figure 4.6). Cell proliferation was reduced by 34% and 42% in those cultures that were exposed to 2 and 6 μg/ml pure *B. oleronius* protein, respectively, compared to the total cell number in the untreated control after a 72 hour incubation period. The mean generation time (MGT) for cells during the log phase of growth between day 2 and day 3 of exposure to *B. oleronius* proteins (2 and 6 μg/ml) was calculated to be 91 hour and 123 hour, respectively, while it was 76 hour in the control. A significant decrease in corneal epithelial cell growth was observed at day 3 following exposure to pure *B. oleronius* protein (6 μg/ml) ($p = 0.0185$) and reduced growth of corneal

epithelial cells following 6 days exposure to 2 or 6 µg/ml pure *B. oleronius* protein was significant ($p = 0.0111$ and $p = 0.0133$, respectively). During the course of a 6 day exposure to the pure *B. oleronius* protein at 2 and 6 µg/ml, a statistical difference in total cell number between the two doses at each time-point was not observed but a dose-dependent increase in the MGT at day 3 between the pure *B. oleronius* protein at 2 and 6 µg/ml was found to be statistically significant ($p = 0.0427$).

4.4 Exposure to *B. oleronius* Protein does not Induce Apoptosis in hTCEpi Cells

To investigate if the reduced hTCEpi cell growth and decreased rate of cell proliferation was due to an apoptotic effect induced by exposure to *B. oleronius* proteins, the activity of caspase-3 and caspase-7 was assessed (Section 2.34). The cleavage of caspases, a family of cysteine-aspartic acid specific proteases, represents a distinctive feature of early apoptosis. The exposure of corneal epithelial cells to 6 µg/ml pure *B. oleronius* protein did not induce increased production of caspase-3 and -7. Following a 72 hour exposure, the pure *B. oleronius* protein preparation showed that 3.09% of corneal cells were positive for the apoptotic markers caspase-3 and -7, compared to 3.16% of control cells. In contrast 61.34% of corneal cells exposed to DMSO (1%, v/v) (positive control) were positive for these markers ($p < 0.0001$) (Figure 4.7). The non-induction of caspases following exposure to pure *B. oleronius* protein preparation suggests that the effect on growth of corneal epithelial cells is anti-proliferative rather than via the induction of apoptosis.

4.5 Effect of *B. oleronius* Protein Exposure on hTCEpi Cell Cycle Progression

The effect of *B. oleronius* proteins on the cell cycle was first intended to be investigated using the Click-it™ EdU flow cytometry assay kit (Invitrogen, Life Technologies). However, co-culturing hTCEpi cells with various concentrations of EdU (1, 1.25, 1.5, 1.75, 2, 2.5, 5, and 10 µM) demonstrated an adverse effect on the growth of the corneal cells for the duration of the assay (Figure 4.8).

Alternatively, propidium iodide staining was used to determine the effect of pure *B. oleronius* protein (6 µg/ml) exposure on hTCEpi progression through the cell cycle. By comparing the DNA content of untreated hTCEpi cells (Figure 4.9A), and *B. oleronius* proteins-treated hTCEpi cells (Figure 4.9B) it was observed that exposure to *B. oleronius* proteins induced significant G_1 phase arrest ($p = 0.0015$) by

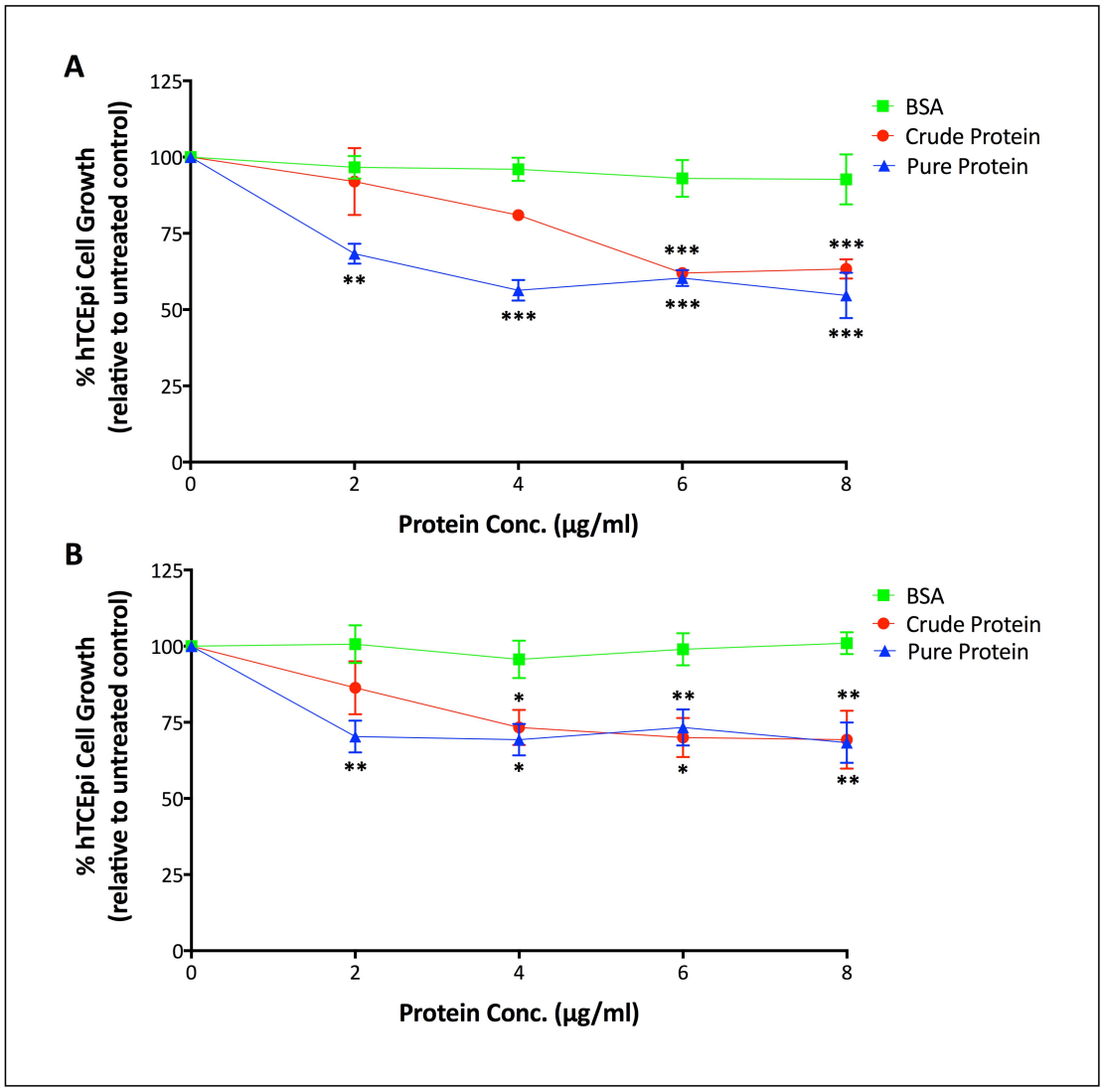

Figure 4.5 Effect of *B. oleronius* proteins on hTCEpi cell growth by XTT staining and crystal violet staining. Assessment of hTCEpi cell growth following a 6 day exposure to BSA (2, 4, 6, and 8 µg/ml), and crude and pure *B. oleronius* protein (2, 4, 6, and 8 µg/ml) by (**A**) XTT staining, and (**B**) crystal violet (0.25%, w/v) staining. (Significance: * = $p < 0.05$, ** = $p < 0.01$, *** = $p < 0.001$).

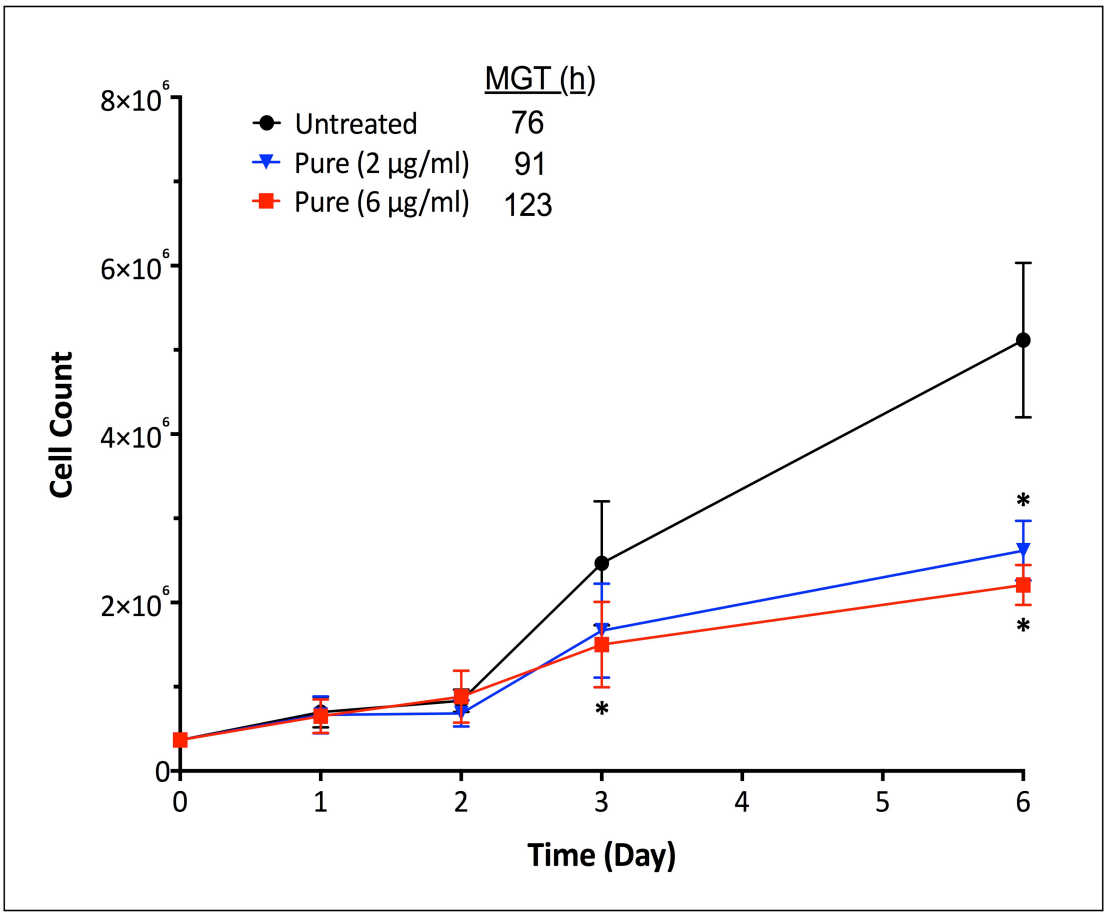

Figure 4.6 Exposure of pure *B. oleronius* proteins reduce the rate of cell proliferation of corneal epithelial (hTCEpi) cells. The MGT for hTCEpi cells during the log phase of growth between day 2 and day 3 of exposure to *B. oleronius* proteins at 2 and 6 µg/ml was calculated to be 91 hour and 123 hour, respectively, compared to untreated cells (76 hour). (Significance: * = $p < 0.05$). (MGT: mean generation time).

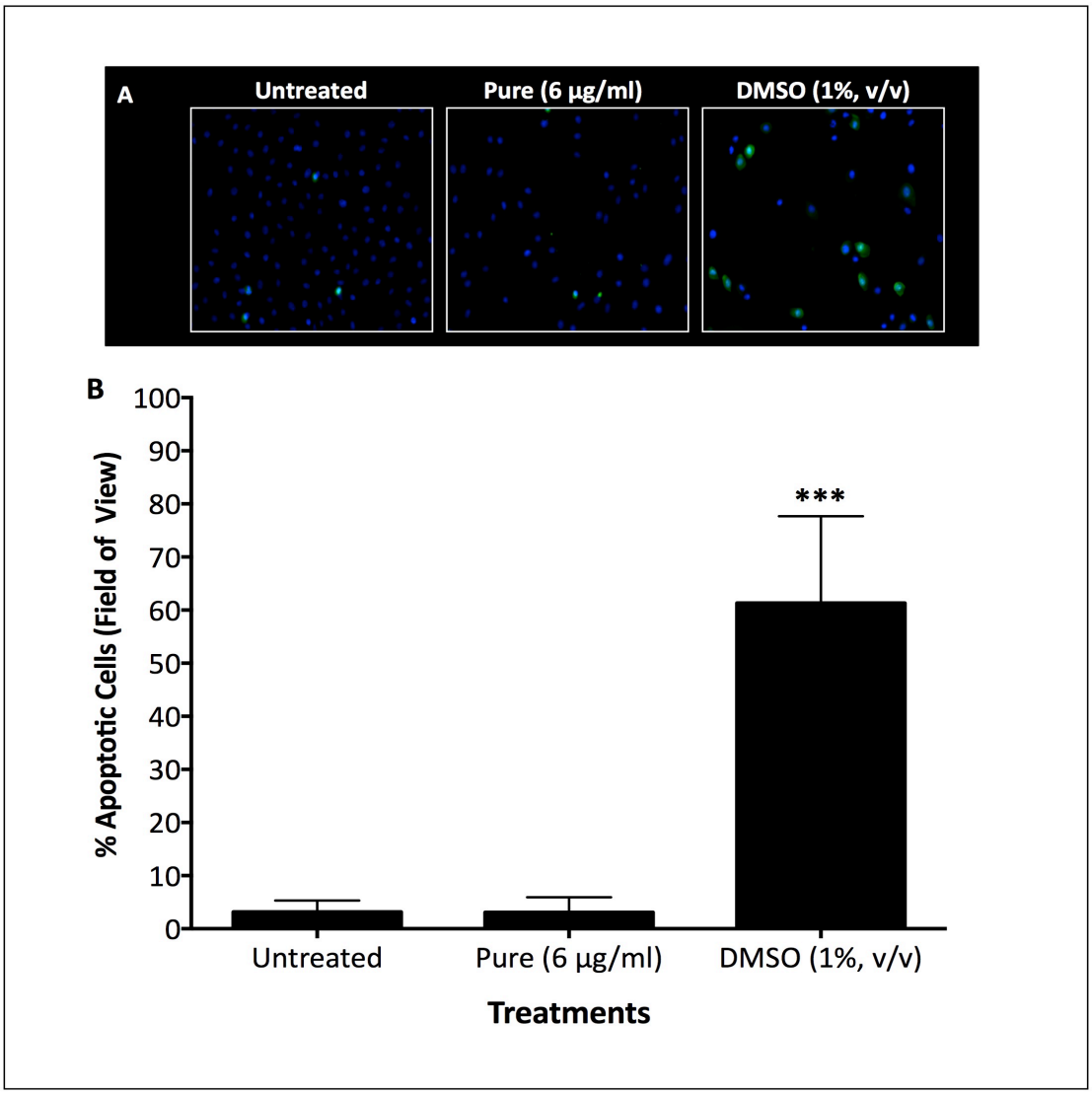

Figure 4.7 Non-induction of apoptosis in hTCEpi cells exposed to pure *B. oleronius* proteins. (**A**) Corneal epithelial cells (hTCEpi) were exposed to pure *B. oleronius* proteins (pure 6 µg/ml), and DMSO (1%, v/v) (positive control), untreated (PBS) for 3 days, and caspase-3 and -7 activity was assessed by capturing immunofluorescence images followed through MetaMorph software analysis. (**B**) The induction of caspase-3 and -7 activity after 3 days exposure to the pure *B. oleronius* protein preparation was not observed with 3.09% of corneal cells positive for caspase-3 and -7 after 72 hour stimulation compared to 3.16% of untreated cells, and 61.34% of corneal cells exposed to DMSO (1%, v/v) ($p < 0.0001$), suggesting an anti-proliferative effect of the pure *B. oleronius* protein treatment rather than an apoptotic effect. FLICA was used to stain for caspase activity (Ex/Em: 550/595 nm), and Hoescht 33342 (Ex/Em: 350/461 nm) was used as a nuclear stain for the assay. (Magnification: 40x) (Significance: *** = P <0.0001).

increasing the percentage of hTCEpi cells in the G_1 phase from 58.66% to 72.91% (Figure 4.9C). Accordingly, the percentage of cells in the S phase also decreased (from 39.13% to 25.61%) concurrent with *B. oleronius* protein-treatment ($p = 0.002$) (Figure 4.10C), suggesting that exposure to *B. oleronius* proteins may reduce hTCEpi cell proliferation by inhibiting progression from the G_1 growth phase to the S (synthesis) phase of the cell cycle.

4.6 Alterations of hTCEpi Gene Expression Induced by *B. oleronius* Protein Exposure

To assess the effect of pure *B. oleronius* protein exposure on hTCEpi gene expression, the expression of a number of genes which are known to participate in pro-inflammatory, immune-modulation, and defence-associated activities during wound healing was assessed (Figure 4.10). Immediately following barrier disruption in a healthy wound, pro-inflammatory cytokines including IL-6, IL-8, IL-1β, and TNF-α are released. These cytokines function in the acute phase to stimulate inflammation and attract immune cells to the site of injury. However, if pro-inflammatory cytokines continue to be secreted at elevated concentrations after the acute phase, complications may result. It was observed in hTCEpi cells exposed to both low (2 μg/ml) and high (6 μg/ml) concentrations of pure *B. oleronius* protein, resulted in a significant over-expression of pro-inflammatory cytokines IL-1β (3.6-fold; $p = 0.0027$, and 3.0-fold; $p = 0.0083$, respectively) and TNF-α (4.9-fold; $p = 0.0019$, and 5.1-fold; $p = 0.0014$, respectively) relative to untreated cells (Figure 4.10).

Interleukins are regulators of the corneal response to injury and IL-1β acts as a pro-inflammatory mediator, stimulating stromal fibroblasts to secrete chemokines and amplify inflammatory responses while TNF-α also plays important roles in corneal inflammation and wound healing (Wilson and Esposito, 2009; Sakimoto *et al*., 2008). The highest relative increase of cytokines expression were observed to be IL-6 (11.6-fold; $p = 0.0337$) and IL-8 (7.8-fold; $p = 0.0378$) following exposure of cells to 6 μg/ml pure *B. oleronius* protein. Secreted IL-6 is known to be elevated in chronic wounds and over-production of IL-6 protein may lead to the development of autoimmune inflammatory diseases (Ishihara and Hirano, 2002; Grellner *et al*., 2000). Elevated IL-8 has been observed in wounds which display retarded healing and IL-8 may directly contribute to this effect by inhibition of keratinocyte replication (Iocono

et al., 2000). In the cornea, IL-8 over-expression has also been associated with ulcer formation via chemoattraction of macrophages and subsequent destruction of tissue (Oka *et al*., 2006). While not itself a cytokine, over-expression of CCL20 (2.8-fold; p = 0.0355) was also observed in cells exposed to pure *B. oleronius* protein (6 µg/ml). CCL20 affects corneal wound healing indirectly by the attraction of specialised IL-22-secreting γδ T cells which induce an inflammatory response (Li *et al*., 2011).

The antimicrobial peptide psoriasin-coding gene S100A7 displayed over expression at both 2 µg/ml and 6 µg/ml pure *B. oleronius* protein exposure (4.3-fold; p = 0.0124, and 5.1-fold; p = 0.0022, respectively). The S100A7 protein was first discovered due to its over-secretion in the inflammatory skin disease psoriasis, and is known to be present at the ocular surface in both tear films and corneal epithelium, however associations with corneal disease are as yet not defined (Garreis *et al*., 2011).

4.7 Effect of *B. oleronius* Proteins on Expression of the Defensins, CCL20 and S100A7, in hTCEpi Cells

Corneal epithelial (hTCEpi) cells were exposed to pure *B. oleronius* proteins (2 µg/ml and 6 µg/ml) for 24, 48, and 72 hour, as described in Section 2.32, and Western blots were performed to assess the effect on the expression of the defensins, CCL20 and S100A7 (Figure 4.11, and Figure 4.12, respectively). The results revealed increased expression of CCL20 in corneal cells exposed to pure *B. oleronius* proteins at 2 µg/ml and 6 µg/ml, with a 2.1-fold (p = 0.0323) and 2.9-fold increase, respectively, relative to the control at 24 hour. An increase of CCL20 expression was observed at 48 hour, with a 2.6-fold (p = 0.0057) and 3.9-fold (p = 0.0178) increase of CCL20 expression following exposure to the 2 µg/ml and 6 µg/ml pure *B. oleronius* protein preparations, respectively. At 72 hour, CCL20 expression in corneal cells treated with 2 µg/ml and 6 µg/ml pure *B. oleronius* proteins showed a 2.5-fold (p = 0.0024) and 4.1-fold (p = 0.0129) increase, respectively, compared to the control (Figure 4.11).

Similarly, an increase in the expression of S100A7 was observed in corneal epithelial cells exposed to pure *B. oleronius* proteins (2 and 6 µg/ml). At 24 hour, a 2.4-fold and 5.7-fold (p = 0.005) increase in expression of S100A7 compared to the control was recorded. At 48 hour, the 6 µg/ml dose of pure *B. oleronius* protein extract induced a 5.1-fold increase in the expression of S100A7 (p = 0.0012). An

increase of S100A7 expression was evident at 72 hour following exposure to the 2 µg/ml and 6 µg/ml pure *B. oleronius* proteins preparations with a 2.3-fold ($p = 0.0163$) and 3.8-fold ($p = 0.0103$) increase was observed for each dose, respectively. A significant dose-dependent response between the 2 µg/ml and 6 µg/ml pure *B. oleronius* protein preparations for the increased expression of S100A7 was recorded following 24 hour ($p = 0.0005$), 48 hour ($p < 0.0001$), and 72 hour ($p = 0.0002$) exposure of corneal epithelial (hTCEpi) cells to the pure *B. oleronius* proteins (Figure 4.12).

4.8 Cytokine Production in hTCEpi Cells Following Exposure to *B. oleronius* Protein

Analysis of the production of cytokines by hTCEpi cells exposed to crude and pure *B. oleronius* protein preparations (2 µg/ml) for 24 hour and 72 hour revealed increased production of IL-6 and IL-8 (Section 2.37) (Figure 4.13A, and Figure 4.13B, respectively). There was a statistically significant increase in the secretion of IL-6 in cells exposed to pure *B. oleronius* protein preparation at 24 hour and 72 hour (277 pg/ml; $p < 0.0001$, and 249 pg/ml; $p = 0.0014$, respectively). A significant increase in IL-6 secretion was also observed in cells exposed to crude *B. oleronius* protein preparation at 24 hour (84 pg/ml; $p = 0.0255$). The increased production of IL-6 following exposure of the corneal epithelial cells to the pure *B. oleronius* protein (2 µg/ml) compared to the crude *B. oleronius* protein (2 µg/ml) was statistically significant at 24 hour ($p = 0.0034$) but not at 72 hour (Figure 4.13A).

At 24 hour, IL-8 secretion reached the highest level in cells exposed to crude *B. oleronius* protein (2 µg/ml) preparation (226 pg/ml; $p = 0.0003$), and this was also significant compared to pure *B. oleronius* protein (2 µg/ml) treated hTCEpi cells ($p = 0.0485$). Pure *B. oleronius* protein (2 µg/ml) preparation also stimulated IL-8 secretion at 24 hour and 72 hour. At 72 hour, exposure of hTCEpi cells to to the pure *B. oleronius* protein (2 µg/ml) preparation resulted in significant level of IL-8 secretion compared to untreated hTCEpi cells (157 pg/ml; $p = 0.0003$) (Figure 4.13B).

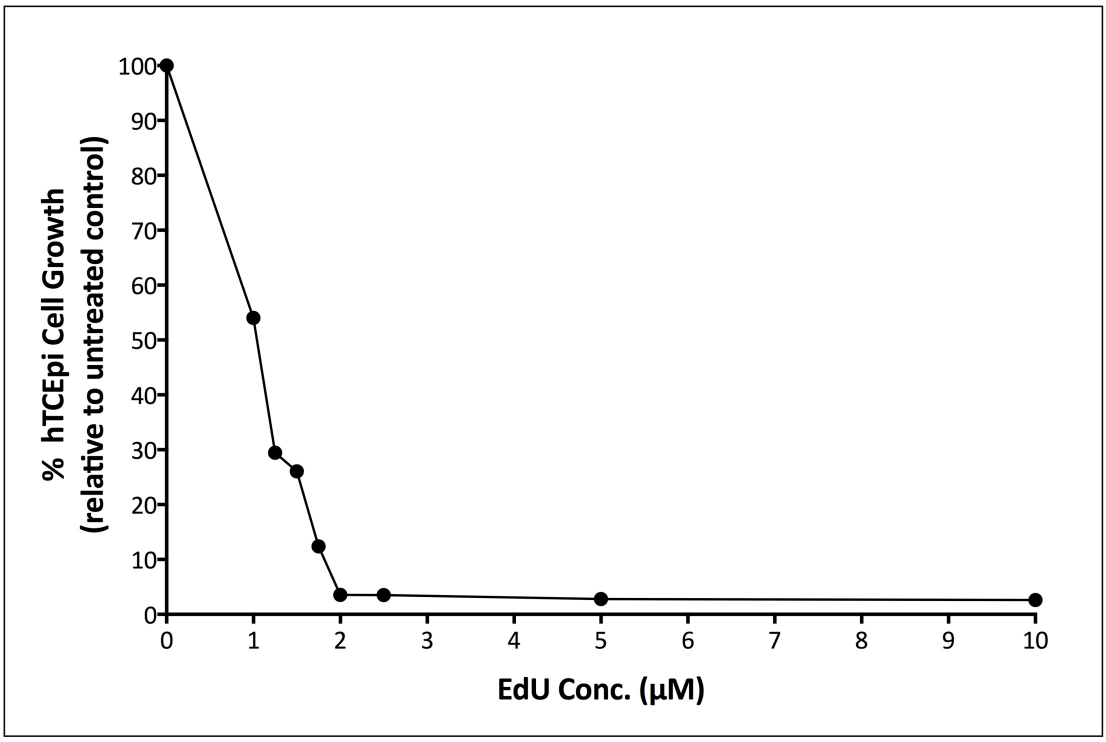

Figure 4.8 Effect of EdU exposure on hTCEpi cell growth. Reduced hTCEpi cell growth in the presence of the compound, EdU at 1, 1.25, 1.5, 1.75, 2, 2.5, 5, and 10 µM. The percentage hTCEpi growth of cells was calculated relative to the untreated control hTCEpi cells.

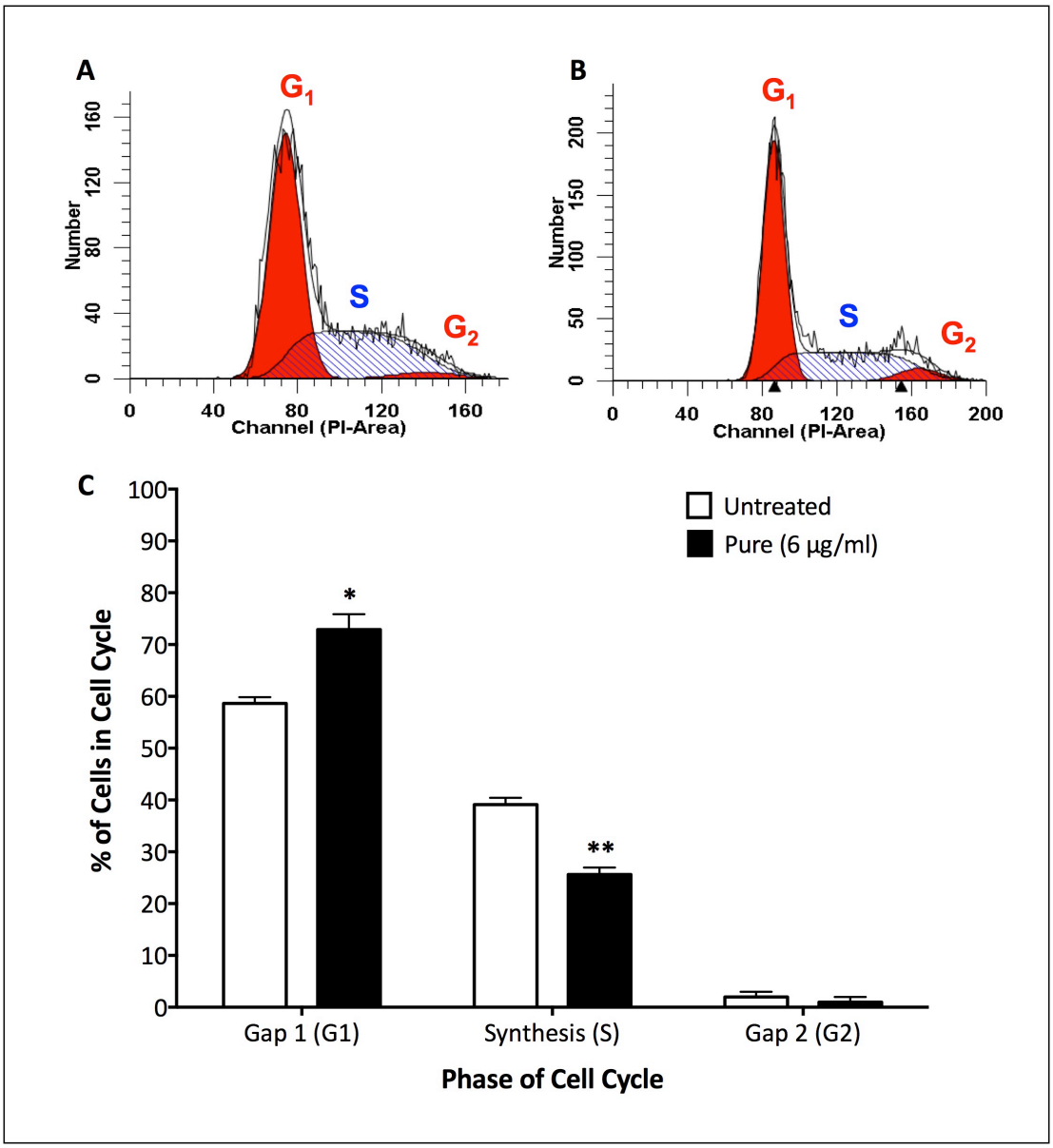

Figure 4.9 Effect of pure *B. oleronius* protein on hTCEpi cell cycle progression. Cell cycle characteristics of both (**A**) untreated, and (**B**) pure *B. oleronius* protein treated (pure 6 µg/ml) hTCEpi cells were assessed by DNA content analysis through propidium iodide staining following a 48 hour exposure period. (**C**) Pure *B. oleronius* protein treated cells demonstrate an increased proportion of cells in G_1 phase and a decreased proportion of cells in the S phase relative to untreated controls, indicating that exposure to pure *B. oleronius* protein (pure 6 µg/ml) inhibits transition from the G_1 growth phase into the S phase ($p = 0.0015$, and $p = 0.002$, respectively. (Significance: * = $p < 0.05$, ** = $p < 0.001$). (G_1: Gap-1 phase, S: Synthesis phase, G_2: Gap-2 phase).

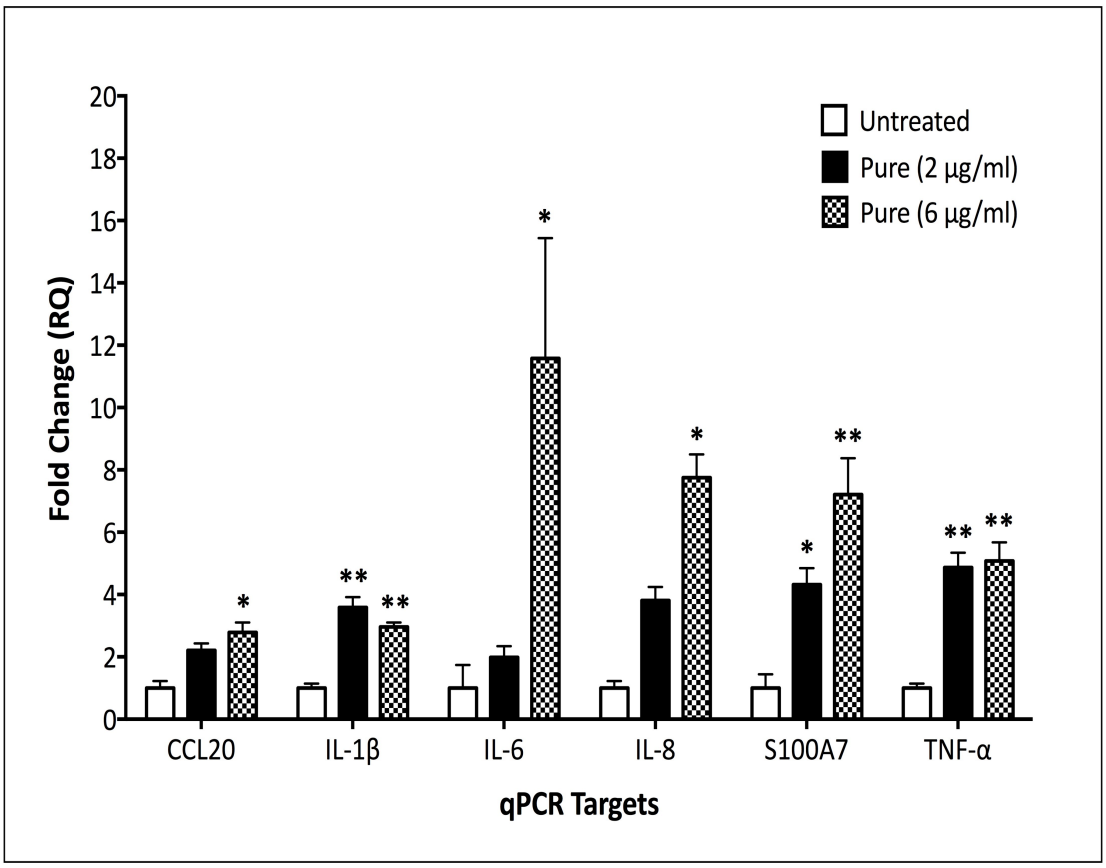

Figure 4.10 Effect of pure *B. oleronius* protein exposure on wound associated gene expression in hTCEpi cells assessed by qRT-PCR. Pure *B. oleronius* protein (pure 6 µg/ml) exposure induced significant overexpression of cytokines IL-1β (3.0-fold; p = 0.0083), IL-6 (11.6-fold; p = 0.0337), IL-8 (7.8-fold; p = 0.0378), TNF-α (5.1-fold; p = 0.0014), immune modulating CCL20 (2.8-fold; p = 0.0355), and defence-associated S100A7 (5.1-fold; p = 0.0022) relative to untreated control hTCEpi cells. Lower *B. oleronius* protein concentration (pure 2 µg/ml) also induced overexpression of targets IL-1β (3.6-fold; p = 0.0027), S100A7 (4.3-fold; p = 0.0124) and TNF-α (4.9-fold; p = 0.0019). (Significance: * = $p < 0.05$, ** = $p < 0.001$). (RQ: relative quantification to the GAPDH enodgenous house-keeping gene).

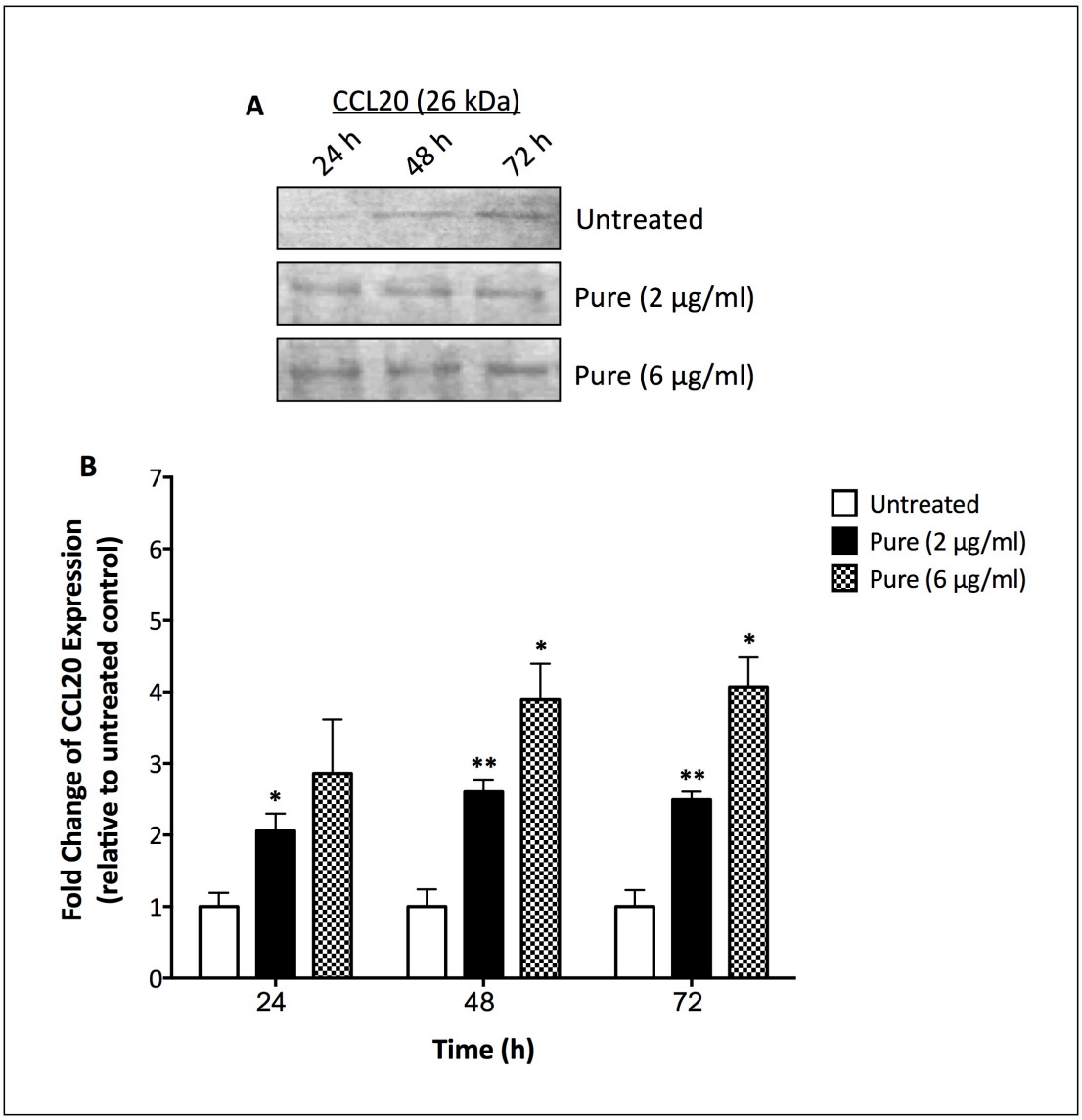

Figure 4.11 Expression of CCL20 by hTCEpi cells exposed to pure *B. oleronius* proteins. (**A**) The expression of CCL20 by corneal epithelial cells following treatment to pure *B. oleronius* proteins (pure 2 and 6 µg/ml) was assessed by Western blot at 24, 48, and 72 hour post-stimulation. (**B**) Exposure to the lower concentration of protein (pure 2 µg/ml) increased the expression of CCL20 at 24 hour (2.1-fold; $p = 0.0323$), at 48 hour (2.6-fold; $p = 0.0057$), and at 72 hour (2.5-fold; $p = 0.0024$), and at the higher dose of pure *B. oleronius* protein (pure 6 µg/ml), where a significant increase of CCL20 expression was recorded at 48 hour (3.9-fold; $p = 0.0178$), and 72 hour (4.1-fold; $p = 0.0129$). (Significance: * = $p < 0.05$, ** = $p < 0.01$).

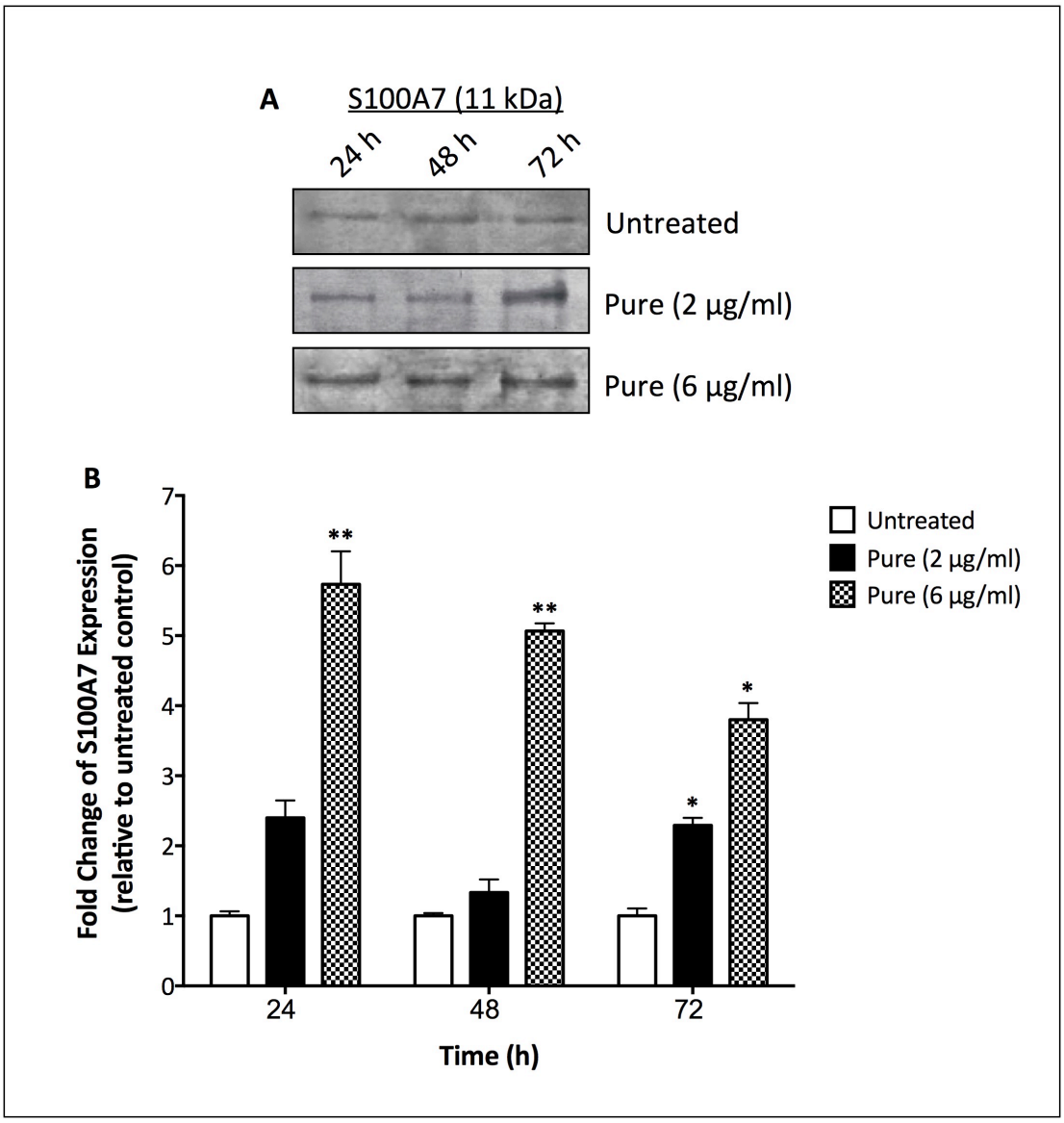

Figure 4.12 Expression of S100A7 by hTCEpi cells exposed to pure *B. oleronius* proteins. (**A**) The expression of S100A7 following exposure of corneal epithelial cells to the pure *B. oleronius* protein preparations (2 and 6 µg/ml) was investigated at 24, 48, and 72 hour by Western blot. (**B**) The expression of S100A7 was shown to be significantly increased following exposure of corneal epithelial cells to the higher concentration of pure *B. oleronius* protein (pure 6 µg/ml) at 24 hour (5.7-fold; $p = 0.005$), 48 hour (5.1-fold; $p = 0.0012$), and at 72 hour (3.8-fold; $p = 0.0103$), and at the lower concentration (pure 2 µg/ml) after 72 hour stimulation (2.3-fold; $p = 0.0163$). (Significance: * = $p < 0.05$, ** = $p < 0.001$).

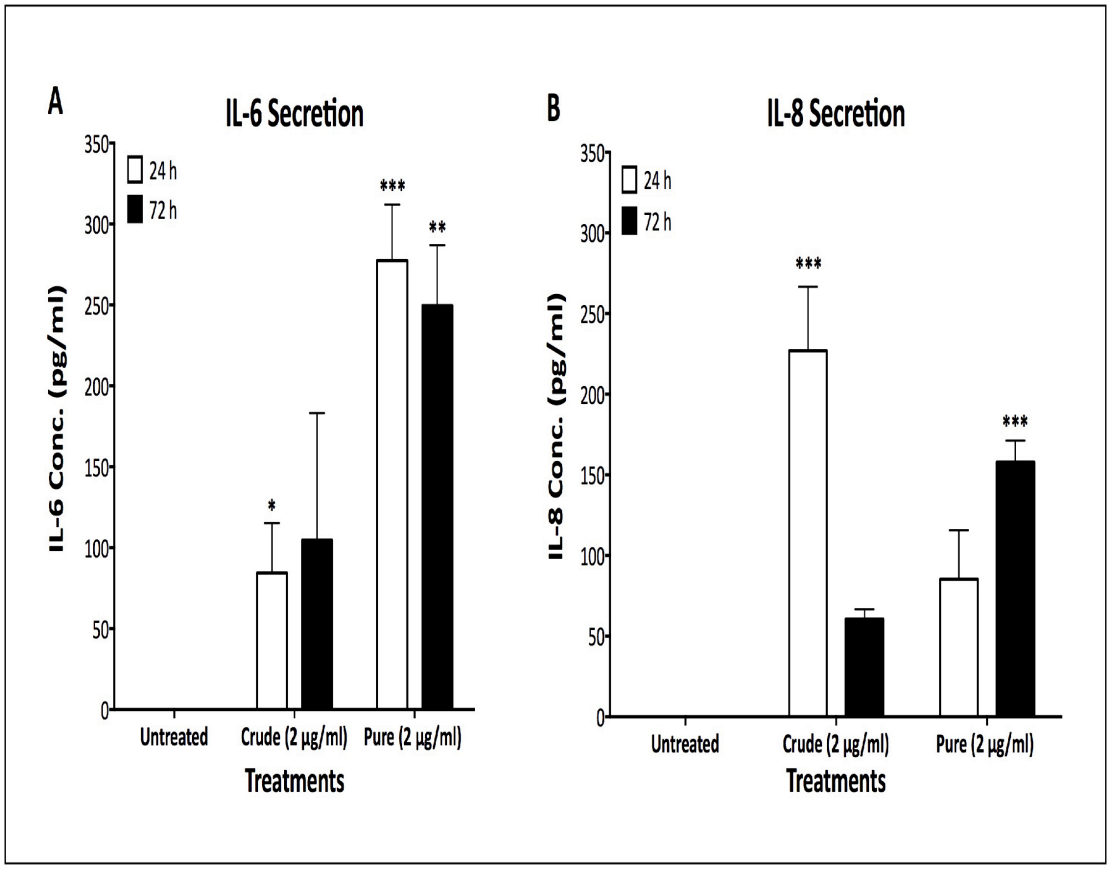

Figure 4.13 Secretion of IL-6 and IL-8 by hTCEpi cells exposed to *B. oleronius* proteins by ELISA. (**A**) IL-6 and (**B**) IL-8 secreted by corneal epithelial cells in response to crude (crude 2 µg/ml) and pure *B. oleronius* (pure 2 µg/ml) protein preparations were assessed 24 hour and 72 hour post-stimulation, by ELISA (Section 2.39). There was a statistically significant increase in the secretion of IL-6 in cells exposed to pure *B. oleronius* protein preparation at 24 hour and 72 hour ($p < 0.0001$, and $p = 0.0014$, respectively). A significant increase in IL-6 secretion was also observed in cells exposed to crude *B. oleronius* protein preparation at 24 hour ($p = 0.0255$). IL-8 secretion reached the highest level in cells exposed to crude *B. oleronius* protein preparation at 24 hour (230 pg/m; $p = 0.0003$). Pure *B. oleronius* protein preparation also stimulated IL-8 secretion at 24 hour and 72 hour. (Significance: * = $p < 0.05$, ** = $p < 0.01$, *** = $p < 0.001$).

4.9 Effect of *B. oleronius* Protein on Expression of MMP-9 in hTCEpi Cells

Corneal epithelial cells were exposed to pure *B. oleronius* proteins (2 µg/ml and 6 µg/ml) for 24, 48 and 72 hour. Cell culture supernatants were collected, filter-concentrated by centrifugation using 3000 MWCO Vivaspin®-20 filter columns, and resolved by 1-D SDS-PAGE (Section 2.14). Proteins were transferred and probed to assess the effect of *B. oleronius* proteins on the expression of MMP-9 (Section 2.19). The results revealed increased expression of MMP-9 in corneal cells exposed to pure *B. oleronius* proteins at 2 µg/ml and 6 µg/ml, with a 2.2-fold ($p < 0.0001$) and 3.5-fold ($p = 0.0096$) increase, respectively, relative to the control at 24 hour. A 1.5-fold ($p = 0.0355$) and 3.2-fold ($p = 0.003$) increase in MMP-9 expression was observed at 48 hour, following exposure to the 2 and 6 µg/ml pure *B. oleronius* protein preparations, respectively. At 72 hour, MMP-9 expression in corneal cells treated with 2 and 6 µg/ml pure *B. oleronius* proteins showed a 1.3-fold and 2.2-fold increase, respectively, compared to the control. A significant dose-dependent response between the 2 µg/ml and 6 µg/ml pure *B. oleronius* protein concentrations for the expression of MMP-9 was not observed at 24 hour, or 72 hour post-stimulation but a significant difference in dose-response was recorded at 48 hour ($p = 0.0105$) (Figure 4.14).

4.10 Exposure of hTCEpi Cells to *B. oleronius* Proteins Induces Increased MMP-9 Activity and MMP-2 Activity

Corneal epithelial (hTCEpi) cells were exposed to 2 or 6 µg/ml *B. oleronius* protein preparations for up to 6 days, and MMP-9 activity was measured by gelatinase zymograms (10%, w/v) (Section 2.36). A representative 1-D Coomassie stained gel image of filter-concentrated hTCEpi supernatant samples exposed to pure *B. oleronius* protein resolved using gelatinase zymogram (10%, w/v) gels to detect MMP-9 activity (92 kDa) and MMP-2 activity (72 kDa) can be seen in Figure 4.15. A representative de-stained gelatinase zymogram (10%, w/v) can be seen in the Appendix (Figure A4.7).

The results revealed a significant dose-dependent increase in MMP-9 (gelatinase B) activity over the course of the experiment (Figure 4.16A). A 1.8-fold ($p = 0.0134$) and 2.3-fold ($p = 0.0215$) increase in MMP-9 activity was observed following stimulation of corneal epithelial cells with 2 and 6 µg/ml pure *B. oleronius* protein after 3 days exposure, respectively (Figure 4.16B). At day 6, a 1.5-fold

increase in MMP-9 activity was recorded after exposure of corneal epithelial cells to the pure *B. oleronius* protein (2 µg/ml), and a statistically significant increase in MMP-9 activity was observed in cells exposed to the higher dose of pure *B. oleronius* protein preparation (6 µg/ml) ($p = 0.0186$) and 2.2-fold increase was observed at day 6 compared to untreated corneal epithelial cells (Figure 4.16B). The relative densitometric values of MMP-9 activity in treated hTCEpi samples calculated using Image J software are given in Figure 4.17. MMP-9 plays a role in tissue degradation but is also a trigger for neo-vascularisation *in vivo*. The growth of new blood vessels is a feature of corneal damage in ocular rosacea (Oltz and Check, 2011; Kheirkhah *et al*., 2007b).

Following development and de-staining of the gelatin zymogram (10%, w/v) gels, active MMP-2 (gelatinase A) was detected in the treated hTCEpi samples (Figure 4.18A). At day 6, a 1.3-fold increase in MMP-2 activity was observed following exposure to 2 µg/ml pure *B. oloernius* protein, and a statistically significant 1.9-fold increase in MMP-2 activity was observed in cells exposed to pure *B. oleronius* protein extract (6 µg/ml) ($p = 0.0129$) compared to the untreated control (Figure 4.18B). The relative densitometric values of MMP-2 activity in treated hTCEpi samples calculated using Image J software are given in Figure 4.19.

4.11 Summary

Exposure of corneal epithelial (hTCEpi) cells to the pure or crude *B. oleronius* protein preparations demonstrated a dose-dependent decrease in the growth of the hCTEpi cells, and a decreased rate of cell proliferation, with an increased mean generation time (MGT) recorded compared to untreated hTCEpi cells at 72 hour. Through immunofluorescence staining, it was demonstrated that the apoptotic markers, caspase-3 and caspase-7 were not induced by exposure to the pure *B. oleronius* proteins. However, it was determined by FACS analysis and propidium iodide staining that pure *B. oleronius* proteins acted upon the hTCEpi cells in an anti-proliferative capacity by inhibiting progression from the G_1 growth phase to the S phase of the cell cycle. Corneal epithelial (hTCEpi) cells exposed to *B. oleronius* proteins demonstrated an increase in gene expression of IL-6, IL-8, CCL20, S100A7, IL-1β, IL-6, IL-8, and TNF-α was observed in cells exposed to the *Bacillus* proteins. In addition, MMP-9 production (3.2-fold; $p = 0.003$) and activity (2.2-fold; $p = 0.0186$) were elevated.

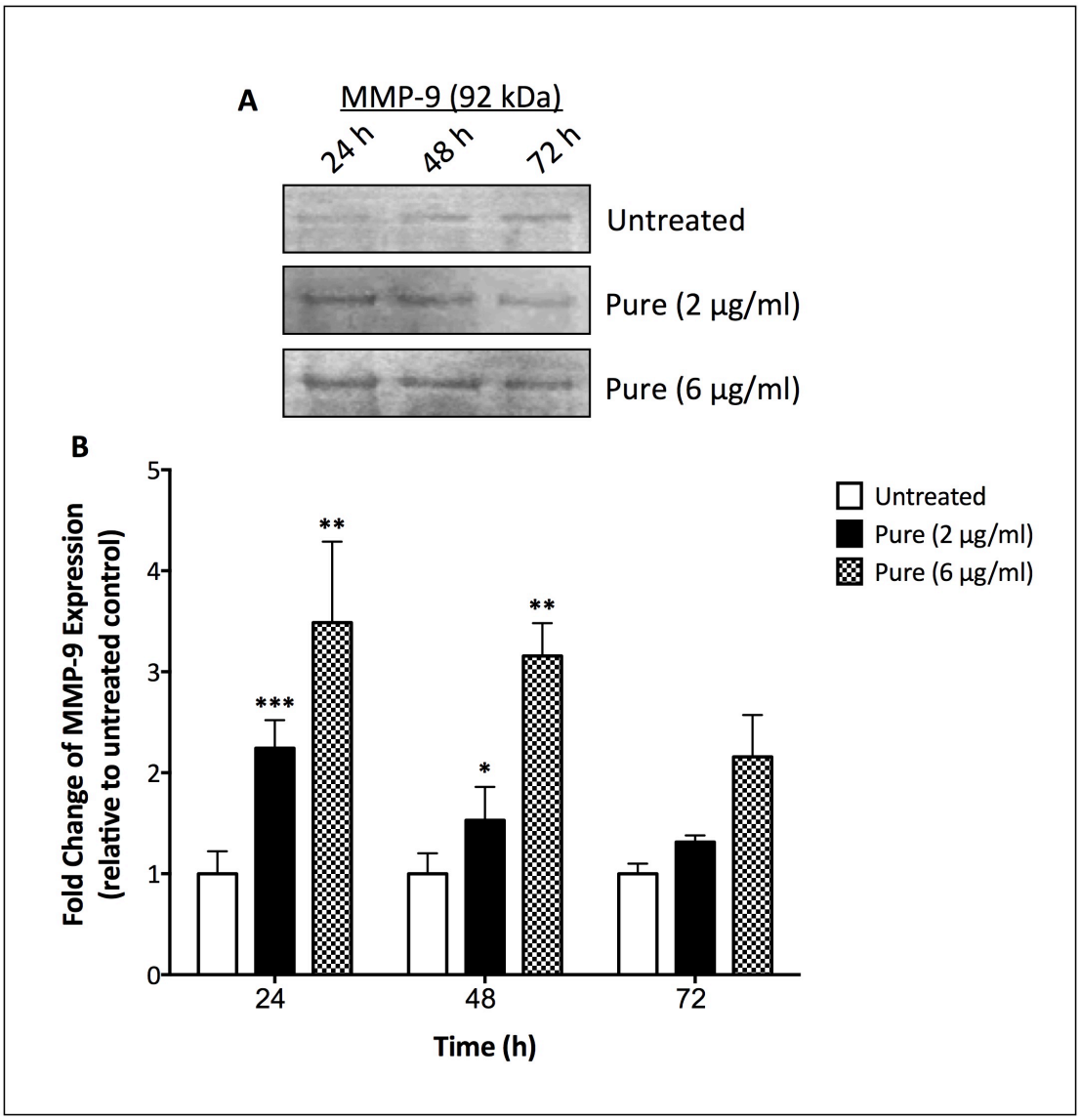

Figure 4.14 Expression of MMP-9 by hTCEpi cells exposed to pure *B. oleronius* proteins. (**A**) The expression of MMP-9, in supernatants of corneal epithelial cells exposed to pure *B. oleronius* protein preparations (pure 2 and 6 µg/ml) were assessed through Western blotting at 24, 48, and 72 hour post-stimulation. (**B**) The secretion of MMP-9 increased following exposure to the protein concentration at the lower dose (pure 2 µg/ml) at 24 hour (2.2-fold; $p < 0.0001$), and at 48 hour (1.5-fold; $p = 0.0355$), and a dose-dependent response was observed following exposure to the higher concentration of pure *B. oleronius* protein (pure 6 µg/ml) at 24 hour (3.5-fold; $p = 0.0096$), and 48 hour (3.2-fold; $p = 0.003$). (Significance: * = $p < 0.05$, ** = $p < 0.01$, *** = $p < 0.001$).

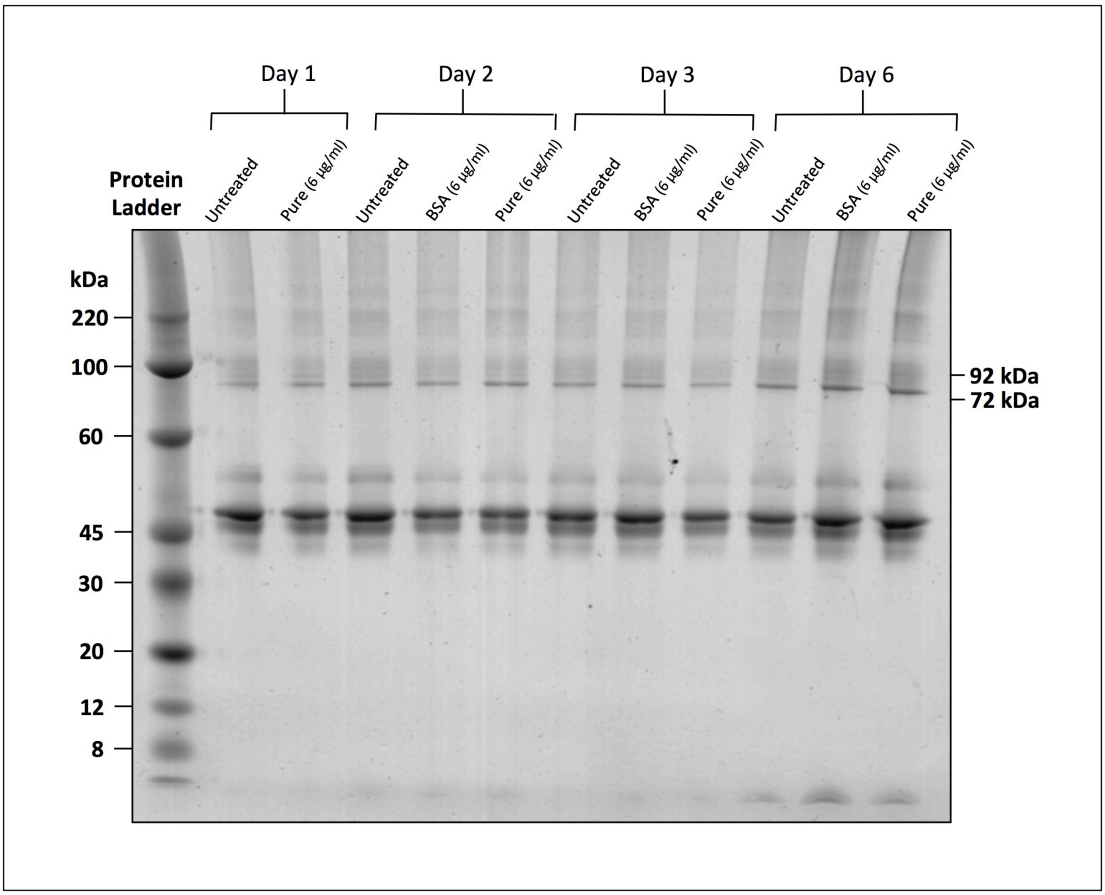

Figure 4.15 A representative 1-D gelatinase zymogram (10% w/v) gel image to assess MMP-9 and MMP-2 activity present in hTCEpi cell supernatants following exposure to pure *B. oleronius* proteins. A representative 1-D gelatinase zymogram (10% w/v) gel image of filter-concentrated hTCEpi supernatant samples exposed to pure *B. oleronius* protein. Corneal epithelial (hTCEpi) cell samples were resolved using gelatinase zymogram (10%, w/v) gels to detect MMP-9 activity (92 kDa) and MMP-2 activity (72 kDa) (Section 2.38). The gel was stained and de-stained using Coomassie brilliant blue staining protocol (Section 2.16.1).

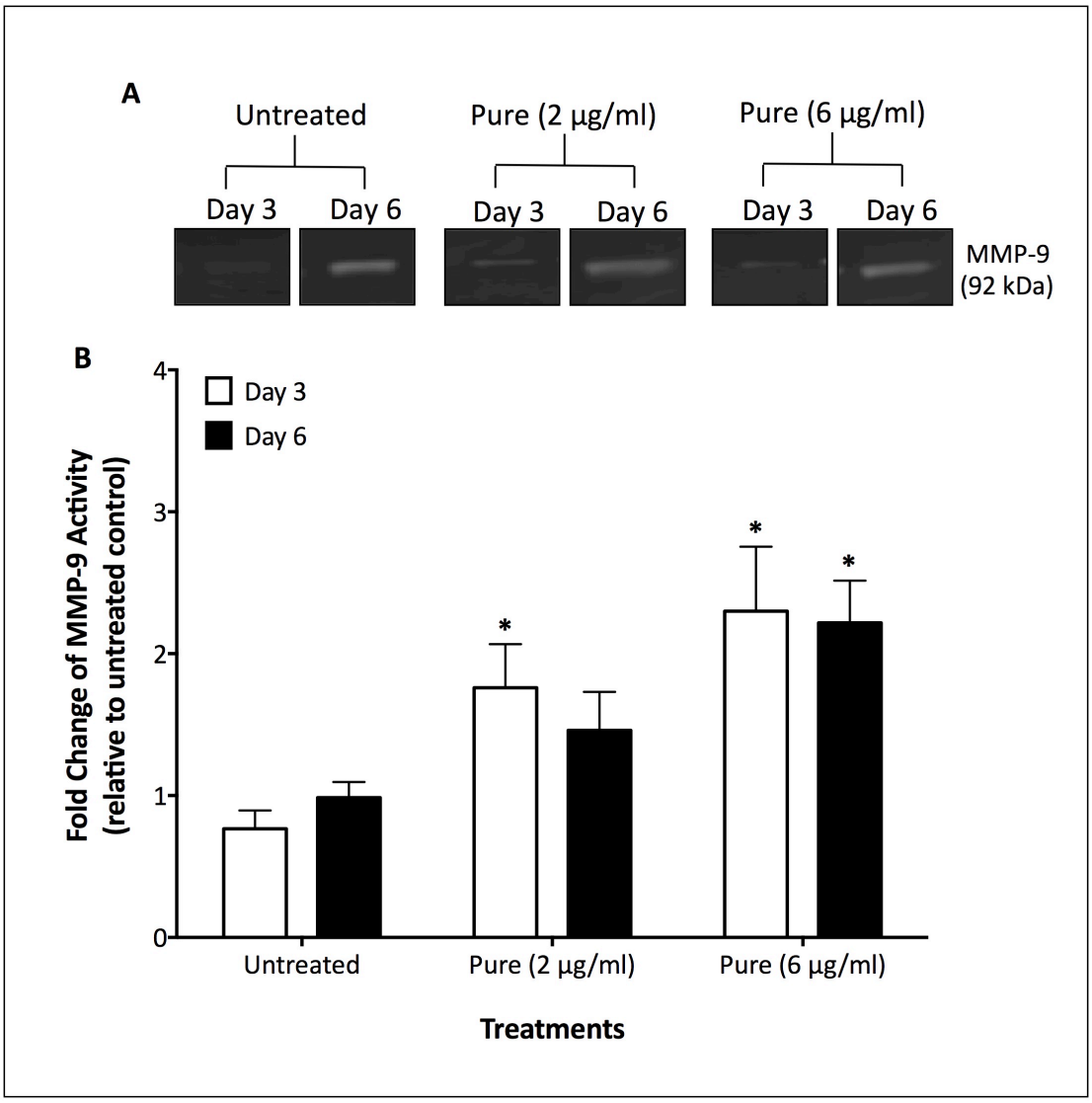

Figure 4.16 Fold change of MMP-9 activity in hTCEpi cells exposed to pure *B. oleronius* proteins. (**A**) Increased enzymatic activity of MMP-9 in corneal epithelial cells exposed to pure *B. oleronius* proteins (pure 2 and 6 µg/ml), 3 days and 6 days post-stimulation was observed compared to the untreated control (Section 2.38). (**B**) The activity of MMP-9 increases following exposure of hTCEpi cells to the pure *B. oleronius* protein (pure 2 and 6 µg/ml) preparations, and a significant increase in MMP-9 activity was recorded at day 6 after exposure to 6 µg/ml pure *B. oleronius* protein ($p = 0.046$). (Significance: * = $p < 0.05$).

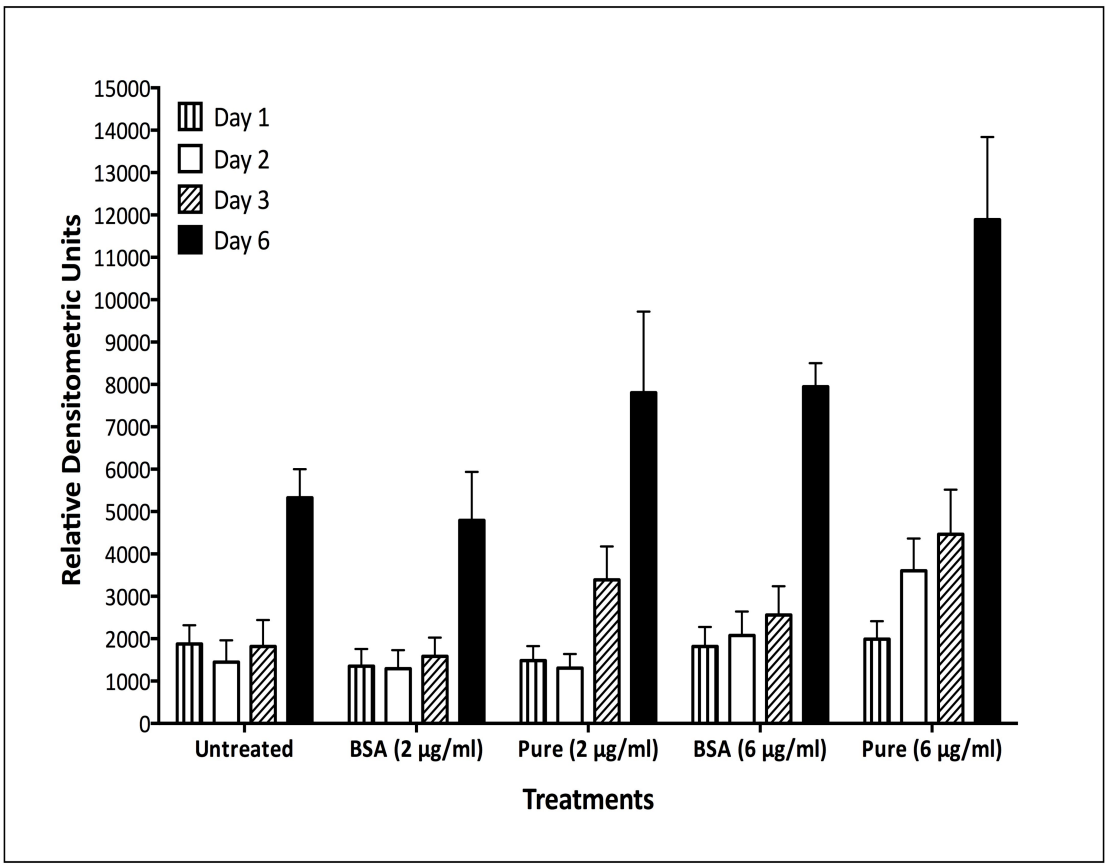

Figure 4.17 Relative densitometric values of MMP-9 activity from gelatinase (10%, w/v) zymogram gels. The relative densitometric values of MMP-9 activity in treated hTCEpi samples were calculated using Image J software (Section 2.36).

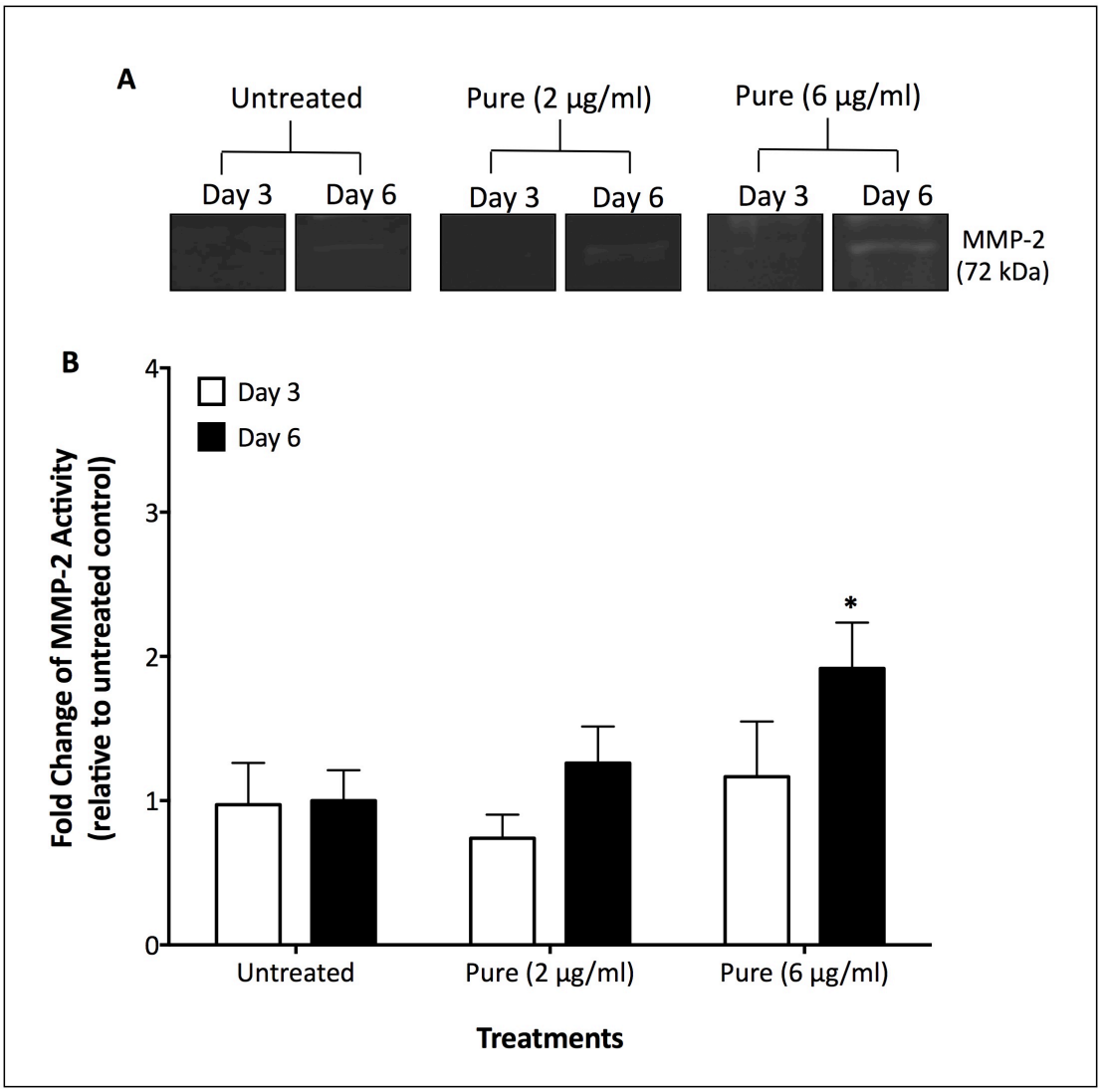

Figure 4.18 Fold change of MMP-2 activity in hTCEpi cells exposed to pure *B. oleronius* proteins. (**A**) Increased enzymatic activity of MMP-2 in corneal epithelial cells exposed to pure *B. oleronius* proteins (pure 2 and 6 µg/ml), 3 days and 6 days post-stimulation was observed compared to the untreated control (Section 2.38). (**B**) The activity of MMP-2 increases following exposure of hTCEpi cells to the *B. oleronius* protein preparations, and a significant increase of MMP-2 activity was recorded at day 6 after exposure to pure *B. oleronius* 6 µg/ml protein ($p = 0.0197$). (Significance: * = $p < 0.05$).

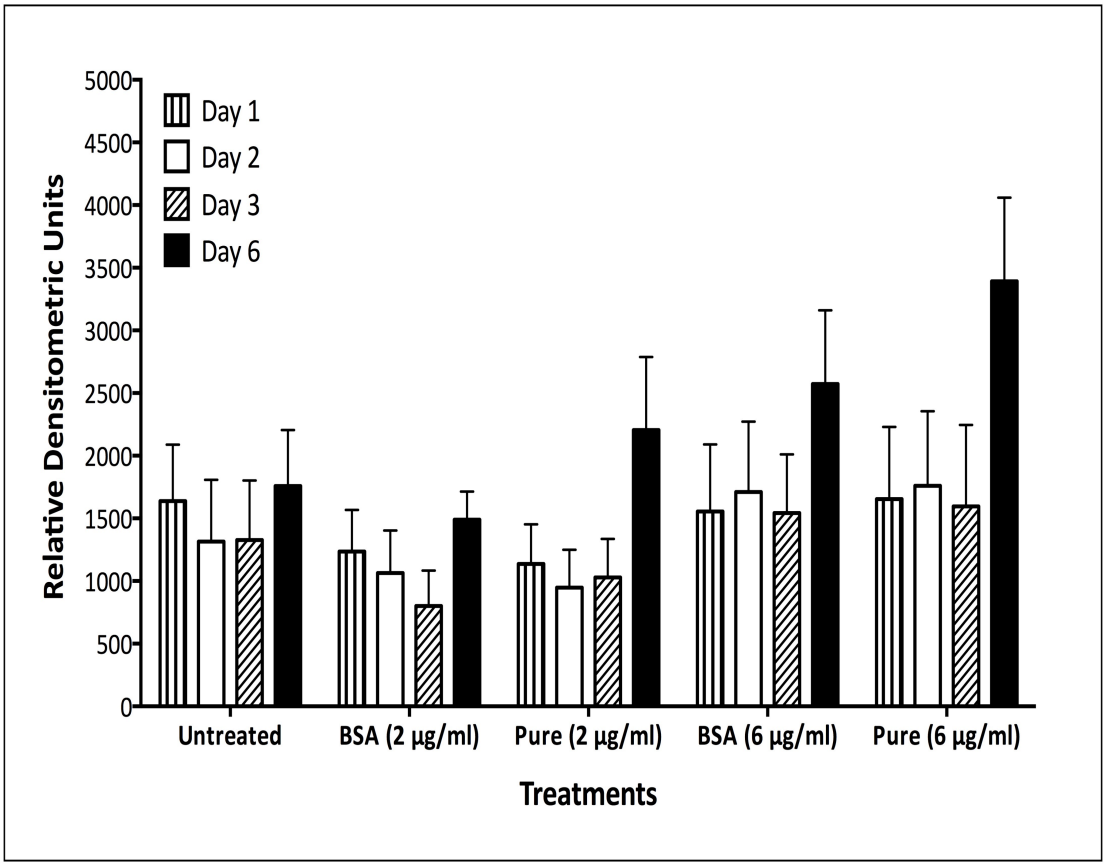

Figure 4.19 Relative densitometric values of MMP-2 activity from gelatinase (10%, w/v) zymogram gels. The relative densitometric values of MMP-2 activity in treated hTCEpi samples were calculated using Image J software (Section 2.36).

4.12 Discussion

The purification technique involving the separation of proteins of interest from the crude protein extracted from the *B. oleronius* by anion exchange, using Q-Sepharose™ high performance beads and ÄKTA FPLC™, has been previously employed by Lacey *et al*. (2007), and O'Reilly *et al*. (2012a, 2012b). The starting material, consisting of the crude *B. oleronius* protein extracted from *B. oleronius* cultures, was fractionated based on protein charge in the ÄKTA column as the saline gradient was increased. The eluted fractions were assessed for abundance of the immunogenic *B. oleronius* proteins of interest by 1-D SDS-PAGE, using Coomassie staining and Western blotting (Figure A4.1 – A4.5) (Section 4.1). Immunoblots were probed with a polyclonal antibody (anti-62 kDa), specific for the 62 kDa *B. oleronius* protein, that was generated in rabbit by Lacey *et al*. (2007). The pure *B. oleronius* protein preparation was used for *in vitro* biological assays to investigate the role of *B. oleronius* proteins in the pathogenesis of rosacea.

The pure *B. oleronius* protein extract contains a mixture of proteins that have been found to be serologically positive in 80% of erythematotelangiectatic rosacea patients and 40% of controls, following Western blotting (O'Reilly *et al*., 2012c). Similar levels of sera reactivity to the *B. oleronius* proteins have been recorded in studies involving papulopustular and ocular rosacea (Li *et al*., 2010; Lacey *et al*., 2007). The immuno-reactive proteins have been identified by O'Reilly *et al*. (2012a) using LC/MS to contain proteins implicated in response to oxidative stress, i.e. Kat E1, vegetative catalase 1, superoxide dismutase, and alkyl hydroperoxide reductase (small subunit), in the formation of bacterial cell wall, hypothetical protein Noc_2222, bacterial cell mobility, flagellin, and bacterial heat shock protein (Hsp) and chaperone, GroEL.

The skin of rosacea patients has been demonstrated to produce increased levels of ROS, and proteins involved in bacterial responses to oxidative stress have been identified in the pure *B. oleronius* protein preparation (O'Reilly *et al*., 2012a; Tisma *et al*., 2009; Yamasaki and Gallo, 2009). The hypothetical protein Noc_2222, described as a component of the pure *B. oleronius* protein preparation, functions in the synthesis of peptidoglycan for the formation of bacterial cell walls. Peptidoglycan is recognised as a pathogen-associated molecular pattern (PAMP) resulting in the establishment of an innate immunne response (Dziarski, 2004).

Flagellin is a globular protein that forms the flagellum, and functions in

bacterial cell motility. It was identified by LC/MS as a component of the pure *B. oleronius* protein preparation (O'Reilly *et al*., 2012a). It is a known ligand for Toll-like receptor (TLR)-5 activation, leading to increased production of the pro-inflammatory cytokines, IL-8 and TNF-α, in activated neutrophils (O'Reilly *et al*., 2012c; Vance *et al*., 2009). A specific function of IL-8 involves the recruitment and activation of neutrophils, leading to a flux of calcium (Ca^{2+}) ions, and increased production of ROS, and the release of antimicrobial enzymes from stored granules (Bergin *et al*., 2010; Lapinet *et al*., 2000). The cytokine TNF-α functions in many pro-inflammatory capacities in the human body, and has been reported to enhance phagocytosis and cytotoxicity in neutrophils (Sohn *et al*., 2007; Schwabe and Brenner, 2006; van Dervort *et al*., 1994).

The gene coding for the GroE protein of *E. coli*, first isolated from lambda and T4 bacteriophages, was described as a host gene essential for morphogenesis (Coppo *et al*., 1973; Georgopoulos *et al*., 1973; Stenberg, 1973). From here, GroE and its related proteins, GroES and GroEL, were characterised as being a member of the heat shock protein 60 kDa (Hsp60) protein family, later termed 'chaperonins' (Hemmingsen *et al*., 1988; Hendrix, 1979). The genes coding for *groES* and *groEL* were isolated, cloned, and characterised in the *B. subtilis* Marburg 168 strain, demonstrating that *Bacillu*s species contain chaperonins (Tozawa *et al*., 1992). Chaperonins function in protein folding and assembly of newly synthesised polypeptides, preventing misfolding and promoting refolding, while being assisted by the cofactor, GroES (Khor *et al*., 2004; Hemmingsen *et al*., 1988).

The 62 kDa protein has been identified in the pure *B. oleronius* protein preparation by mass spectrometry as GroEL, a member of the chaperonin family of heat shock proteins located in the cytoplasm of bacterial cells (O'Reilly *et al*., 2012a; Lacey *et al*., 2007). The protein identified by these authors was shown to have homology to the GroEL chaperonin protein sequenced from *B. subtilis* (accession number 1906220B). Chaperonins are involved in a range of biochemical processes including folding, refolding, assembly, and translocation of proteins, that can be induced due to physiological stresses experienced by a bacterial cell (Goloubinoff *et al*., 1989; Kusukawa *et al*., 1989; Ostermann *et al*., 1989; Rothman, 1989; van Dyk *et al*., 1989; Bockhareva *et al*., 1988; Hendrix, 1979).

The proteins of the pure *B. oleronius* protein preparation demonstrate a capacity to induce an immune response in rosacea patients as decribed by previous studies

(O'Reilly *et al*., 2012a, 2012b, 2012c; Li *et al*., 2010; Lacey *et al*., 2007). The crude *B. oleronius* protein and pure *B. oleronius* protein preparations generated here were used for further analysis to characterise the effect of *B. oleronius* on corneal epithelial (hTCEpi) cells, neutrophils, and PBMC, to elucidate the possible underlying pathogenic mechanisms implicating *B. oleronius* in rosacea.

In a previous study, the response of the hTCEpi cells to *B. oleronius* proteins in terms of alterations in cell migration and invasiveness was characterised (O'Reilly *et al*., 2012b). The results indicated increased cell migration and invasiveness following exposure of the cells to the *B. oleronius* proteins. Cells exposed to *B. oleronius* proteins showed a dose dependent increase in the expression of genes coding for *matrix metalloprotease-3* (*MMP-3*) (61-fold) and *matrix metalloprotease-9* (*MMP-9*) (300-fold). This dose dependent increase in gene expression was also reflected in elevated levels of MMP-9 protein and increased matrix metalloprotease activity in the culture supernatant. These results suggest a possible link between exposure to *B. oleronius* proteins and the development of corneal damage in ocular rosacea patients.

The results presented here demonstrate that exposure of a corneal epithelial cell line to *B. oleronius* proteins results in a reduction in cell proliferation and the induction of an inflammatory response as indicated by the increased expression of genes coding for IL-6, IL-1β, IL-8, S100A7 and TNF-α, elevated MMP-9 production and activity (Figure 4.5 – 4.16). A dose response was observed when corneal epithelial cells were exposed to different concentrations of *B. oleronius* protein, and this effect is particularly evident in changes in cell proliferation (MGT at day 3: $p = 0.0427$) (Figure 4.5 and Figure 4.6), S100A7 expression after 24 hour ($p = 0.0005$), 48 hour ($p < 0.0001$), and 72 hour ($p = 0.0002$) exposure) (Figure 4.12), and MMP-9 expression after 48 hour exposure ($p = 0.0105$) (Figure 4.14). Corneal damage is one of the features of ocular rosacea and leads to the degradation of the corneal surface and the formation of sterile ulcers and corneal scaring (Oltz and Check, 2011; Kheirkhah *et al*., 2007b). It was previously demonstrated that exposure of corneal epithelial (hTCEpi) cells to *B. oleronius* proteins to induce an aberrant wound healing response in cultured hTCEpi cells and could possibly lead to damage to the corneal surface, thus implicating a role for *B. oleronius* in ocular rosacea (O'Reilly *et al*., 2012b).

Exposure of corneal epithelial cells to the *B. oleronius* protein preparation

reduced the rate of proliferation and the anti-proliferative effect was demonstrated to be due to G_1 phase arrest (Figure 4.9). Exposure of hTCEpi cells to the *B. oleronius* proteins did not induce apoptosis, consequently the reduction in cell proliferation was not due to increased levels of cell death. The elevated expression of the cytokines IL-1β, IL-6, IL-8 and TNF-α has been shown in a number of inflammatory corneal pathologies (Karthikeyan *et al*., 2011; Prada *et al*., 2003). The elevation of these cytokines results in angiogenesis, inflammation and sterile ulcer formation due to the up-regulation of MMP-9 (Gordon *et al*., 2009; Oka *et al*., 2006; Prada *et al*., 2003). However, a recent study demonstrated no increase in these cytokines in the tear fluid of rosacea patients and an up-regulation of these cytokines in ocular rosacea patients was not observed (Topcu-Yilmaz *et al*., 2013). The lack of expression may be due to the ocular rosacea patients possessing only mild symptoms and thus alterations in expression were too low to be detected. CCL-20/MIP-3α is similar functionally to the β-defensins in its role as an anti-bacterial agent and the recruitment of cells into the cornea following wounding (Li *et al*., 2011; Heimer *et al*., 2010; Shirane *et al*., 2004). It has been shown to be up regulated by the cytokines IL-1β and TNF-α in cornea (Huang *et al*., 2007).

The exposure of hTCEpi cells to *B. oleronius* proteins induced the increased expression and activity of MMP-9 (Figure 4.14, and Figure 4.16, respectively). MMP-9 is expressed during cell migration and matrix remodeling in cornea wound repair by the corneal epithelium (Daniels *et al*., 2003). It also controls timing of the inflammation response around cornea repair (Mohan *et al*., 2002). However, its expression is finely balanced and elevated levels of MMP-9 have been demonstrated to have a negative role in epithelial cell replication and barrier function in the cornea (Pflugfelder *et al*., 2005). In this context, elevation of MMP-9 has been linked to a number of corneal pathologies including sterile ulcer formation and ocular rosacea (Dursun *et al*., 2001; Fini *et al*., 1998; Alfonso *et al*., 1995). The results presented here show the effect of *B. oleronius* proteins on transformed corneal cells over a short time frame and demonstrate that the increased expression and activity of MMP-9 corresponds with an increased mean generation time and decreased corneal cell proliferation at day 3, a G_1/S transition block in the cell cycle at day 2, increased expression of S100A7 and CCL-20/MIP-3α, and increased production of IL-6 and IL-8.

Elevated densities of *Demodex* mites on the eyelashes are a feature of ocular

rosacea but their role in the aetiology of the condition is unclear (Oltz and Check, 2011; Yamasaki and Gallo, 2009; Kheirkhah *et al*., 2007a, 2007b; Diaz-Perez, 1994; Vance, 1986). Previously a positive correlation between serum reactivity to *B. oleronius* proteins and ocular rosacea was demonstrated, thus suggesting a role for this bacterium in the condition (Li *et al*., 2010). One possible scenario linking the elevated density of *Demodex* mites and the induction of corneal damage involves the release of the contents of bacterial cells and proteins from dead *Demodex* mites on the eyelashes. These may fall onto the corneal surface and induce an aberrant wound healing response (O'Reilly *et al*., 2012b). In addition the results presented here indicate the induction of an inflammatory response which would contribute to the degradation of corneal tissue and the induction of sterile ulcers or scarring *in vivo*. Understanding the interaction of *Demodex*-associated *B. oleronius* proteins with the corneal surface may aid in the design of specific therapies to reduce the severity of symptoms arising from this interaction.

Chapter 5

An Investigation of the Proteomic Response of Corneal Epithelial (hTCEpi) Cells to *Bacillus oleronius* Proteins

5.0 Introduction

It has been demonstated that patients with ocular rosacea and increased incidence of *Demodex* infestation are highly sera reactive to *B. oleronius* proteins (Li *et al*., 2010). A previous study by O'Reilly *et al*. (2012b) demonstrated alterations in the growth rate and motility of corneal epithelial (hTCEpi) cells exposed to *B. oleronius* proteins. It also was demonstrated that treatment of hTCEpi cells with *B. oleronius* proteins resulted in a dose-dependent decrease in β1-integrin and an increase of vinculin. The observed aberrant wound healing response in hTCEpi cells exposed to the *B. oleronius* proteins corresponded with an increase in the gene expression of *MMP-3* and *MMP-9*. The changes induced in hTCEpi cells as a result of exposure to the *B. oleronius* protein suggests a possible link between *B. oleronius* and the development of corneal damage in ocular rosacea patients. Here, alterations in the hTCEpi proteome following exposure to *B. oleronius* protein were analysed to identify proteins that may be involved in the development of this disease.

The aim of the work presented in this Chapter was (1) to investigate changes in the secretome and proteome of hTCEpi cells treated with *B. oleronius* proteins following a 24 hour and a 72 hour exposure, by 1-D SDS-PAGE; (2) to analyse alterations in the proteome of hTCEpi cells treated with *B. oleronius* proteins following a 72 hour exposure by 2-D SDS-PAGE; and (3) to investigate the proteomic profile of hTCEpi cells exposed to the crude or pure *B. oleronius* protein preparations using label-free mass spectrometry (LF/MS). The identification of changes in the abundance of hTCEpi cell proteins may potentially help to elucidate the pathogenic effect of *B. oleronius* proteins on the corneal epithelial surface and in the induction of the symptoms associated with ocular rosacea.

5.1 An Analysis of the Secretome and Proteome of hTCEpi Cells Following Exposure to *B. oleronius* Protein

A description of the protocols followed for 1-D SDS-PAGE and the subsequent identification of proteins isolated from the secretome and proteome of hTCEpi cells by LC/MS can be seen in Section 2.14, and Section 2.17, respectively.

5.1.1 Secretome of hTCEpi Cells Following Exposure to *B. oleronius* Protein Preparations

The secretome of corneal epithelial (hTCEpi) cells treated with BSA (6 µg/ml) (protein-control), pure *B. oleronius* protein (2 and 6 µg/ml), and crude *B. oleronius* protein (2 and 6 µg/ml) for 24 hour and 72 hour was investigated by LC/MS to identify secreted proteins from the hTCEpi cells. Prior to LC/MS analysis, treated hTCEpi sample supernatants were collected for each time-point, and resolved by 1-D SDS-PAGE (Figure 5.2). Following electrophoresis, staining, and de-staining of gels, protein bands were excised and prepared for LC/MS analysis to identify proteins, and assess differential protein abundance in the secretome of hTCEpi cells. A master gel of protein bands excised for mass spectrometry is given in Figure 5.2. Identified proteins were subjected to relative densitometric analysis using Image Quant software, to quantify abundance, and the differential protein abundance. A list of identified proteins from the secretome of hTCEpi cells exposed to *B. oleronius* proteins can be seen in Table 5.1.

Transferrin (Band No: 1) was identified following LC/MS analysis of the secretome of hTCEpi cells. Transferrin is an iron-binding protein the functions in the regulation and transport of free iron *in vivo* (Gomme *et al*., 2005). After 24 hour, the abundance of transferrin was increased following treatment of hTCEpi cells with the pure *B. oleronius* protein preparations at 2 µg/ml (1.6-fold) and 6 µg/ml (2.1-fold). Exposure of hTCEpi cells to the 2 µg/ml or 6 µg/ml crude *B. oleronius* protein demonstrated increased abundance of transferrin at 24 hour (1.9-fold, and 1.6-fold, respectively), and at 72 hour (1.4-fold, and 2.6-fold, respectively) compared to untreated hTCEpi cells (Table 5.2). However, the changes in the abundance of transferrin were deemed not to be statistically significant.

Phosphatidylethanolamine-binding protein 1 preprotein (Band No: 2), is a serine protease inhibitor that has been demonstrated to inhibit the kinase activity of RAF1, modulating the Raf-MEK-ERK signaling pathway (Rath *et al*., 2008). The Raf-MEK-

ERK signaling pathway is conserved in metazoans and is involved in the transmission of extracellular signals into the nucleus, regulating cell proliferation and differention, and protects a cell from apoptosis (Wellbrock *et al*., 2004; Murakami and Morrison, 2001). The abundance of phosphatidylethanolamine-binding protein 1 preprotein was elevated in hTCEpi cells treated with the pure or crude *B. oleronius* protein preparations relative to the untreated hTCEpi cells. At 72 hour, the increased abundance of the serine protease inhibitor following exposure of hTCEpi cells to the 2 µg/ml pure *B. oleronius* protein preparation was observed to be statistically significant compared to treatment with the 2 µg/ml crude *B. oleronius* protein preparation ($p = 0.0451$) (Table 5.2).

Fibronectin 1 (Band No: 3) is an ubiquitous component of the extracellular matrix that functions as a regulator of cellular processes such as cell adhesion and mobility, and tissue repair, and acts a scaffold protein to maintain cell and tissue organization, and the arrangement of the extracellular matrix (To and Midwood, 2011; Potts and Campbell, 1996). The abundance of fibronectin 1 was observed to be altered following treatment of hTCEpi cells with the *B. oleronius* protein preparations. A 72 hour exposure of hTCEpi cells to the 6 µg/ml pure *B. oleronius* protein preparation was calculated to be statistically significant (1.9-fold; $p = 0.0395$) (Table 5.2).

Peroxisome assembly protein 12 (Band No: 4), functions in the correct folding and importation of proteins into the peroxisomes of cells, with a role in cell metabolism and the detoxification of ROS (Okumoto *et al*., 1998; Lazarow and Fujiki, 1985). The abundance of peroxisome assembly protein 12 was observed to be increased at 24 hour in hTCEpi cells treated with the 2 µg/ml or 6 µg/ml pure *B. oleronius* protein preparations compared to untreated hTCEpi cells (2.5-fold, and 2.6-fold, respectively), and the increase of abundance was calculated to be statistically significant ($p = 0.0419$, and $p = 0.0284$, respectively). Exposure of hTCEpi cells to the 6 µg/ml pure *B. oleronius* protein preparation resulted in an increase of abundance at 24 hour (2.6-fold), and a decrease of abundance at 72 hour (0.6-fold) ($p = 0.0314$) (Table 5.2).

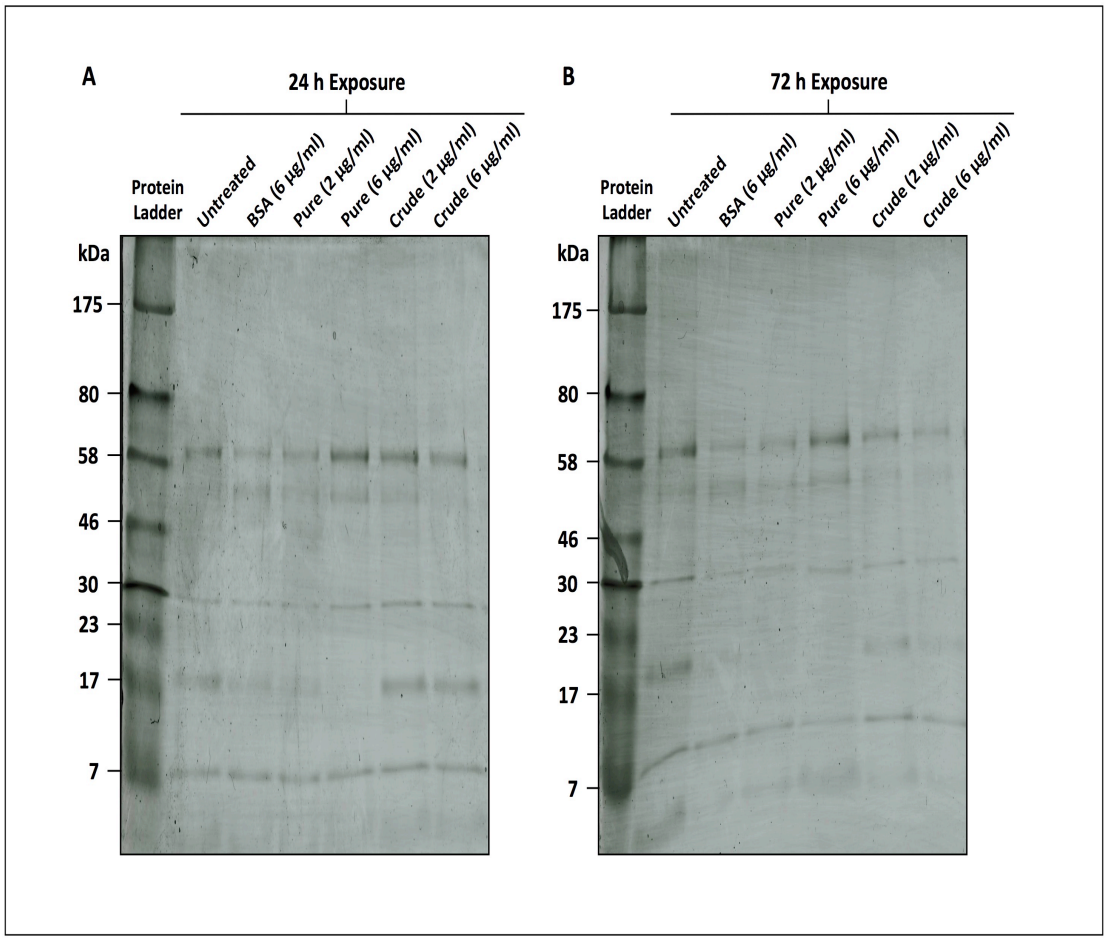

Figure 5.1 Secretome of hTCEpi cells exposed to *B. oleronius* proteins for 24 hour and 72 hour, and resolved by 1-D SDS-PAGE. Resolved 1-D SDS-PAGE images of the secretome of corneal epithelial (hTCEpi) cells treated with BSA (6 µg/ml), crude *B. oleronius* (2 µg/ml and 6 µg/ml), and pure *B. oleronius* protein (2 µg/ml and 6 µg/ml) for (**A**) a 24 hour, and (**B**) a 72 hour exposure prior to LC/MS protein identification and Image Quant densitometric software analysis. (n = 4, for each treatment).

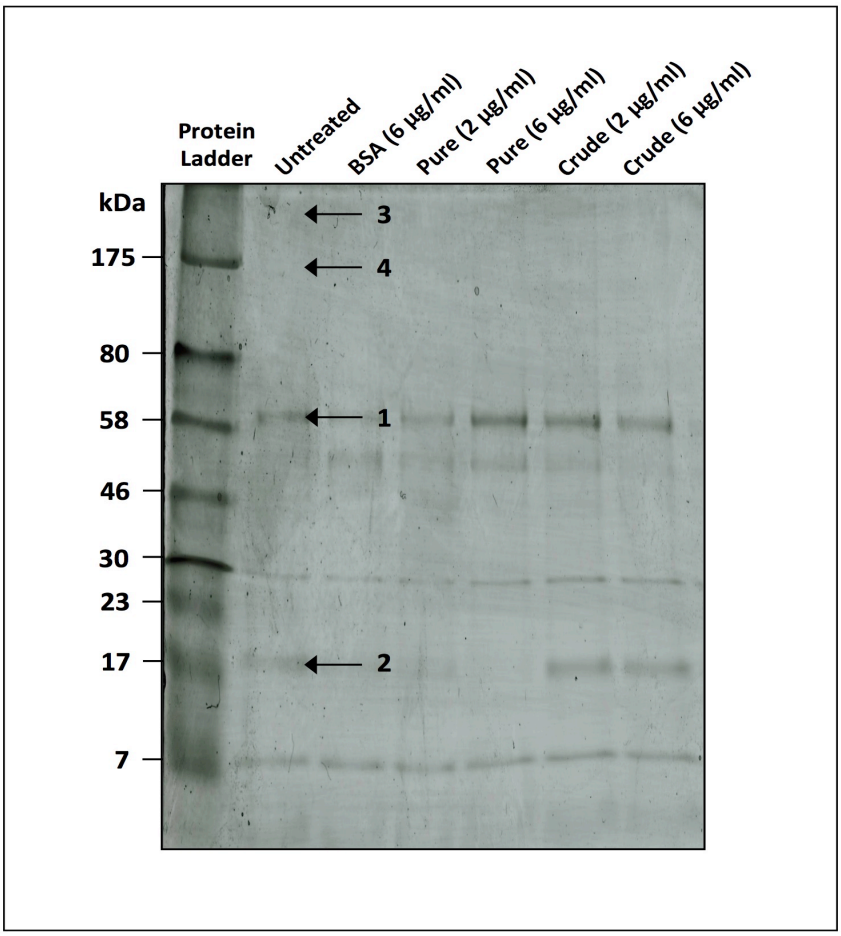

Figure 5.2 Master gel of excised 1-D SDS-PAGE hTCEpi secretome protein bands for protein identification by LC/MS following a 24 hour and a 72 hour exposure to *B. oleronius* proteins. Master gel of excised protein bands resolved by 1-D SDS-PAGE, and identified through LC/MS from the supernatants of hTCEpi cells treated and exposed to *B. oleronius* proteins for 24 hour and 72 hour. **(**Arrow (🡻) indicates bands excised for identification by LC/MS).

Table 5.1 LC/MS protein band identities from 1-D SDS-PAGE of the hTCEpi secretome following a 24 hour and a 72 hour exposure to *B. oleronius* proteins.

Band No.	Protein Identity	Organism	M_r (nominal mass)	pI	Mascot Score	Sequence Coverage	Accession No.	UniProt Protien Function
1	Transferrin	*Homo sapiens*	79350	6.97	950	23%	AAH59367	Iron Uptake
2	Phosphatidylethanolamine-Binding Protein 1 Preproprotein	*Homo sapiens*	21160	7.01	62	10%	NP_002558	Serine Protease Inhibitor
3	Fibronectin 1	*Homo sapiens*	243125	5.60	1247	19%	AAI17177	Cell adhesion and Mobility, Tissue Repair, and Maintenance of Cell Shape
4	Peroxisome Assembly Protein 12	*Homo sapiens*	41061	9.21	55	7%	NP_000277	Protein Import into Peroxisomes

Table 5.2 Fold change of protein band identities from 1-D SDS-PAGE of the hTCEpi secretome following a 24 hour and a 72 hour exposure to *B. oleronius* proteins. Fold change of protein abundance are relative to the untreated hTCEpi cells at 24 hour or 72 hour, respectively. (n = 4, for each treatment).

Band No.	Protein Identity	Untreated		BSA (6 µg/ml)		Pure (2 µg/ml)		Pure (6 µg/ml)		Crude (2 µg/ml)		Crude (6 µg/ml)	
		24 h	72 h	24 h	72 h	24 h	72 h	24 h	72 h	24 h	72 h	24 h	72 h
1	Transferrin	1.0	1.0	0.8	1.2	1.6	1.0	2.1	1.6	1.9	1.4	1.6	2.6
2	Phosphatidylethanolamine-Binding Protein 1 Preproprotein	1.0	1.0	0.7	0.9	1.6	0.7	1.5	1.5	1.4	1.3	1.3	2.3
3	Fibronectin 1	1.0	1.0	1.3	1.0	1.1	1.2	1.2	1.9	1.0	1.4	0.8	2.7
4	Peroxisome Assembly Protein 12	1.0	1.0	1.3	0.7	2.5	0.9	2.6	0.6	2.4	1.4	2.1	1.3

5.1.2 Proteomic Analysis of hTCEpi Cells Following Exposure to *B. oleronius* Protein Preparation

The proteome of corneal epithelial (hTCEpi) cells treated with BSA (6 µg/ml) (protein-control), pure *B. oleronius* protein (2 and 6 µg/ml), and crude *B. oleronius* protein (2 and 6 µg/ml) for 24 hour and 72 hour was investigated by LC/MS. Prior to LC/MS analysis, treated hTCEpi cells were harvested for each time-point, protein was extracted, and resolved by 1-D SDS-PAGE (Figure 5.3). Following electrophoresis, staining, and de-staining of gels, protein bands were excised and prepared for LC/MS analysis to identify proteins, and assess differential protein abundance of the proteome of hTCEpi cells. A master gel of protein bands excised for mass spectrometry is given in Figure 5.4. A list of identified proteins from the proteome of hTCEpi cells exposed to *B. oleronius* proteins can be seen in Table 5.3.

A number of molecular chaperone heat shock proteins including 90 kDa heat shock protein (Band No: 4), heat shock cognate 71 kDa protein isoform 1 (Band No: 10), and 60 kDa heat shock protein, mitochondrial (Band No: 16) were identified by LC/MS analysis (Figure 5.4). Heat shock proteins (Hsps) are members of the chaperonins family of proteins and are known to be molecular chaperones that assist with the correct folding of polypeptides induced by heat stress conditions, and can be classifed according to molecular mass in kilodaltons (Urbak and Vorum, 2010; Arrigo and Simon, 2010; Hartl and Hayer-Hartl, 2002; Groenen *et al*., 1994; Linquist and Craig, 1988).

Exposure of corneal epithelial (hTCEpi) cells to *B. oleronius* protein resulted in an increase in abundance of Hsp90 (Band No: 4) at 24 hour and 72 hour. At 24 hour, treatment of hTCEpi cells with 2 µg/ml or 6 µg/ml pure *B. oleronius* protein preparations resulted in elevated abundance of Hsp90 relative to that in untreated hTCEpi cells (2.5-fold, and 2.2-fold, respectively). Similarly, following a 72 hour exposure to the 2 µg/ml or 6 µg/ml pure *B. oleronius* protein preparations, the abundance of Hsp90 was observed to be increased compared to the untreated hTCEpi cells (1.7-fold, and 1.6-fold, respectively). The increased abundance of Hsp90 was statistically significant following exposure to the 2 µg/ml pure *B. oleronius* protein preparation after 24 hour ($p = 0.0633$), and following exposure to the 6 µg/ml pure *B. oleronius* protein preparation after 72 hour ($p = 0.0362$) (Table 5.4). The abundance of heat shock cognate 71 kDa protein isoform 1 (Band No: 10) was decreased in abundance at 24 hour following treatment with the pure *B. oleronius*

protein preparations at 2 µg/ml (1.0-fold) and 6 µg/ml (0.6-fold; p = 0.0295), or crude *B. oleronius* protein at 2 µg/ml (0.4-fold) and 6 µg/ml (0.5-fold), relative to the untreated hTCEpi cells. At 72 hour, the abundance of heat shock cognate 71 kDa protein isoform 1 was increased following treatment with the pure *B. oleronius* protein preparations at 2 µg/ml (1.3-fold) and 6 µg/ml (2.1-fold; p = 0.0296), or crude *B. oleronius* protein at 2 µg/ml (2.3-fold; p = 0.0296) and 6 µg/ml (1.5-fold), relative to the untreated hTCEpi cells (Table 5.4). The increase of Hsp abundance between 24 hour and 72 hour exposure was deemed to be significant following treatment of hTCEpi cells with 6 µg/ml pure *B. oleronius* protein preparation (p = 0.0272), 2 µg/ml crude *B. oleronius* protein preparation (p = 0.012), and 6 µg/ml crude *B. oleronius* protein preparation (p = 0.0045) (Table 5.4).

Treatment of hTCEpi cells with the *B. oleronius* protein preparations resulted in an increase in the abundance of Hsp60 (Band No: 16) relative to untreated hTCEpi cells. Exposure to the 2 µg/ml or 6 µg/ml pure *B. oleronius* protein preparations lead to increased protein abundance at 24 hour (1.8-fold, and 1.9-fold, respectively), and at 72 hour (1.2-fold, and 1.2-fold, respectively). The increase of Hsp60 abundance following 24 hour exposure to the 6 µg/ml pure *B. oleronius* protein preparation was deemed to be significant compared to a 24 hour exposure to the 6 µg/ml crude *B. oleronius* protein preparation (p = 0.0156) (Table 5.4).

Peroxiredoxin-1 (Band No: 12) is an anti-oxidant enzyme containing a single conserved cysteine residue, that catalyses the thiol-dependent reduction of peroxides and ROS (Jarvis *et al*., 2012; Hofmann *et al*., 2002; Fujii and Ikeda, 2002; Rhee *et al*., 2001). The role of peroxiredoxin-1 *in vivo* has been linked with cell signaling and the stimulation of pro-inflammatory cytokine secretion, and has been implicated in a number of eye disorders including oxidative stress-induced cataracts and the development of pterygium, an overgrowth of the conjunctiva on to the corneal surface (Klebe *et al*., 2014; Jarvis *et al*., 2012; Riddell *et al*., 2010; Neumann *et al*., 2009; Pak *et al*., 2006). At 24 hour, the increased abundance of peroxiredoxin following a 24 hour exposure to the 6 µg/ml pure *B. oleronius* protein preparation was significant relative to the 2 µg/ml pure *B. oleronius* protein preparation (p = 0.0086). At 72 hour, the abundance of peroxiredoxin-1 was observed to be reduced following treatment with the 2 µg/ml or 6 µg/ml pure *B. oleronius* protein preparations (Table 5.4). The reduced abundance of peroxiredoxin following a 72 hour exposure to the 6 µg/ml pure *B. oleronius* protein preparation was significant relative to untreated hTCEpi cells

($p = 0.0465$).

A number of proteins that function in a range of cellular processes were identified by LC/MS analysis. These proteins include elongation factor 2 (Band No: 3), annexin A2 isoform 2 (Band No: 6), histone H2B (Band No: 7), 14-3-3 sigma (Band No: 11), protein S100-A11 (Band No: 13), and ubiquitin activating enzyme E1 (Band No: 14). Annexin A2 and 14-3-3 sigma have been demonstrated to modulate the cell cycle and regulate cell growth in a number of studies, in particular studies that focus on the mechanisms of cell divivsion in cancer cell lines and tumor growth (Wang *et al*., 2015; Chaudhary *et al*., 2014; Zhang *et al*., 2013; Wang *et al*., 2012; Lee and Lozano, 2006; Gilmore *et al*., 2004; Tanaka *et al*., 2004; Yang *et al*., 2003; Hermeking *et al*., 1997).

Exposure of hTCEpi cells to the 2 μg/ml or 6 μg/ml pure *B. oleronius* protein preparations resulted in an increase in the abundance of annexin A2 at 24 hour (2.1-fold, and 1.6-fold, respectively) and a decrease in abundance at 72 hour (0.8-fold, and 0.8-fold, respectively), compared to untreated hTCEpi cells. The increase of annexin A2 abundance at 24 hour following exposure to the 2 μg/ml pure *B. oleronius* protein preparation was significant relative to the untreated hTCEpi cells ($p = 0.0372$) (Table 5.4).

The abundance of 14-3-3 sigma was decreased in hTCEpi cells following treatment with the *B. oleronius* protein preparations. Exposure to the 2 μg/ml or 6 μg/ml pure *B. oleronius* protein preparations lead to a reduction in the abundance of 14-3-3 sigma protein at 24 hour (0.7-fold, and 0.8-fold, respectively), and at 72 hour (0.5-fold; $p = 0.0039$, and 0.4-fold; $p = 0.0047$, respectively) relative to untreated hTCEpi cells. Similarly, exposure to the 2 μg/ml or 6 μg/ml crude *B. oleronius* protein preparations resulted in a decrease in the abundance of 14-3-3 sigma protein at 72 hour (0.2-fold; $p = 0.0004$, and 0.3-fold; $p = 0.0009$, respectively) compared to untreated hTCEpi cells (Table 5.4).

The protein S100-A11 is a member of calcium binding proteins that function in a range of biological processes including the differentiation and cornification of keratinocytes (Tu *et al*., 2001). Protein S100-A11 has been implicated in dry eye syndrome and pterygium (Riau *et al*., 2009; Zhou *et al*., 2009). The abundance of protein S100-A11 was elevated at 24 hour following exposure to the 2 μg/ml or 6 μg/ml pure *B. oleronius* protein preparations (3.4-fold, and 2.4-fold, respectively), and to the 2 μg/ml or 6 μg/ml crude *B. oleronius* protein preparations (2.9-fold, and

3.0-fold, respectively) compared to the untreated hTCEpi cells. However, the abundance of protein S100-A11 was significantly reduced at 72 hour following exposure to the 2 μg/ml or 6 μg/ml pure *B. oleronius* protein preparations (0.3-fold; $p = 0.0004$, and 0.3-fold; $p < 0.0001$, respectively), and to the 2 μg/ml or 6 μg/ml crude *B. oleronius* protein preparations (0.2-fold; $p < 0.0001$, and 0.4-fold; $p = 0.0067$, respectively) compared to the untreated hTCEpi cells (Table 5.4).

5.1.3 Summary

Exposure to pure or crude *B. oleronius* protein preparation demonstrates alterations in the abundance of proteins from the secretome and proteome of hTCEpi cells at 24 hour and 72 hour. The identified proteins are associated with many biological processes, and support previous findings that have shown the hTCEpi cells to become more motile and invasive following treatment with the *B. oleronius* protein preparations. Also, structural proteins such as myosin-9 and profilin-1 were observed to be altered in abundance following exposure of hTCEpi cells to the *B. oleronius* protein preparations.

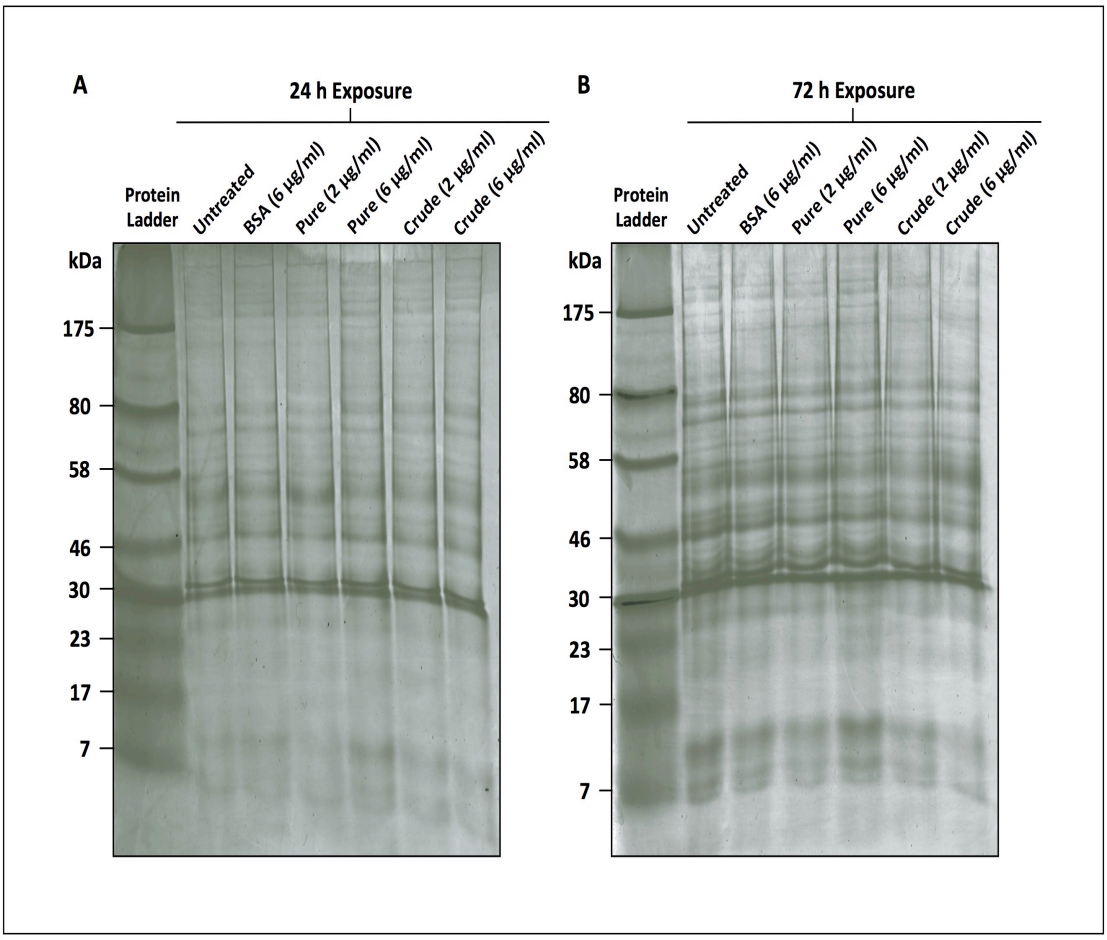

Figure 5.3 Proteome of hTCEpi cells exposed to *B. oleronius* proteins for 24 hour and 72 hour, and resolved by 1-D SDS-PAGE. Resolved 1-D SDS-PAGE images of the proteome of corneal epithelial (hTCEpi) cells treated with BSA (6 µg/ml), pure *B. oleronius* (2 µg/ml and 6 µg/ml), and crude *B. oleronius* protein (2 µg/ml and 6 µg/ml) for (**A**) a 24 hour, and (**B**) a 72 hour exposure prior to LC/MS protein identification and Image Quant densitometric software analysis. (n = 4, for each treatment).

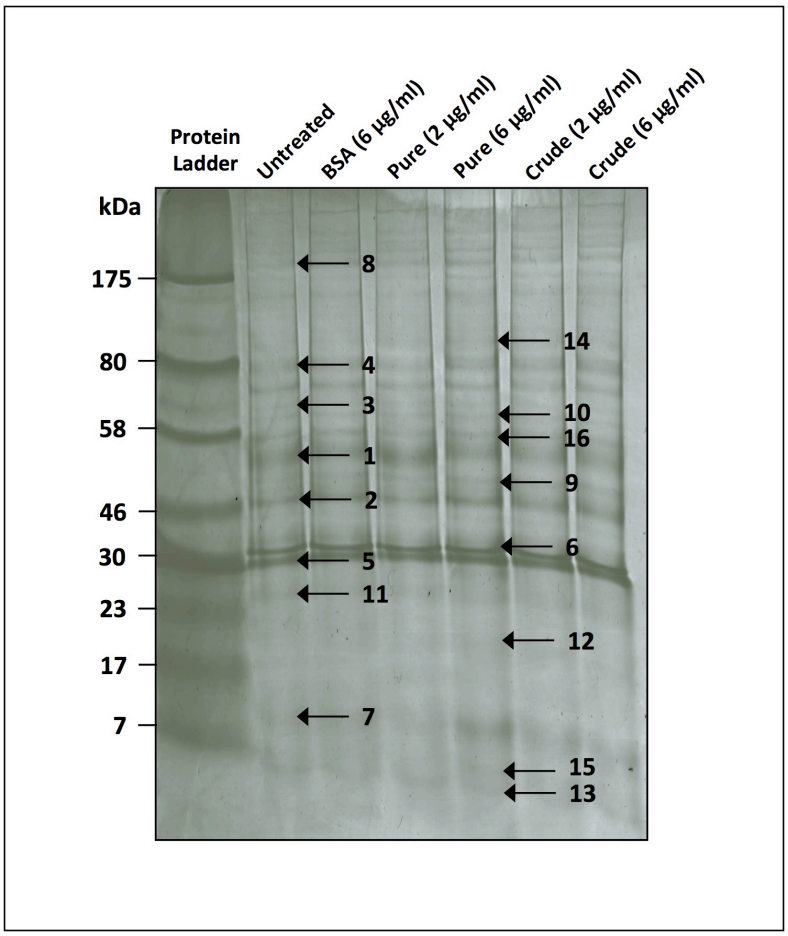

Figure 5.4 Master gel of excised 1-D SDS-PAGE hTCEpi proteome protein bands for protein identification by LC/MS following a 24 hour and a 72 hour exposure to *B. oleronius* proteins. Master gel of excised protein bands resolved by 1-D SDS-PAGE, and identified through LC/MS from the whole cell lysates of hTCEpi cells treated and exposed to *B. oleronius* proteins for 24 hour and 72 hour. **(**Arrow (🡻) indicates bands excised for identification by LC/MS).

Table 5.3 LC/MS protein band identities from 1-D SDS-PAGE of the hTCEpi proteome following a 24 hour and a 72 hour exposure to *B. oleronius* proteins.

Band No.	Protein Identity	Organism	M_r (nominal mass)	pI	Mascot Score	Sequence Coverage	Accession No.	UniProt Protien Function
1	Transketolase	*Homo sapiens*	68447	7.90	242	18%	CAA47919	Catalyses Enzymatic Reactions of the Pentose Phosphate Pathway
2	Beta-Tubulin	*Homo sapiens*	50249	4.75	510	29%	AAB59507	Constituent of Microtubules
3	Elongation Factor 2	*Homo sapiens*	96263	6.41	242	10%	NP_001952	Protein Synthesis
4	90 kDa Heat Shock Protein	*Homo sapiens*	83590	4.97	519	17%	AAA36025	Molecular Chaperone that Assist Polypetide Folding Under Stress Conditions
5	Beta Actin Variant	*Homo sapiens*	42086	5.37	613	43%	BAD96752	Cytoskeletal Structure
6	Annexin A2 Isoform 2	*Homo sapiens*	38812	7.57	214	12%	NP_004030	Regulation of Cell Growth
7	Histone H2B	*Homo sapiens*	13928	10.31	368	53%	CAB02542	DNA Binding and Replication
8	Myosin-9	*Homo sapiens*	227668	5.50	150	2%	NP_002464	Regulation of Cytokinesis and Maintenance of Cell Shape
9	Pyruvate Kinase	*Homo sapiens*	58421	7.58	300	21%	CAA39849	Catalyses Enzymatic Reactions in Glycolysis
10	Heat Shock Cognate 71 kDa Protein Isoform 1	*Homo sapiens*	71086	5.37	344	11%	NP_006588	Molecular Chaperone that Assist Polypetide Folding Under Stress Conditions
11	Chain A, Binary Complex of 14-3-3 Sigma and P53 Pt387-Peptide	*Homo sapiens*	28226	4.68	435	39%	3LW1_A	Regulation of Cell Cycle and Cell Growth
12	Peroxiredoxin-1	*Homo sapiens*	22328	8.27	191	20%	NP_002565	Response to Oxidative Stress
13	Protein S100-A11	*Homo sapiens*	11849	6.56	171	32%	NP_005611	Keratinocyte Differentiation and Cornification
14	Ubiquitin Activating Enzyme E1	*Homo sapiens*	118817	5.57	155	6%	CAA40296	Catalyses Enzymatic Reactions in Ubiquitination of Proteins
15	Profilin-1	*Homo sapiens*	15219	8.44	73	22%	NP_005013	Regulation Cytoskeletal Structure by Actin Binding
16	60 kDa Heat Shock Protein, Mitochondrial	*Homo sapiens*	61190	5.70	126	8%	NP_002147	Molecular Chaperone that Assist Polypetide Folding Under Stress Conditions

Table 5.4 Fold change of protein band identities from 1-D SDS-PAGE of the hTCEpi proteome following a 24 hour and a 72 hour exposure to *B. oleronius* proteins. Fold change of protein abundance are relative to the untreated hTCEpi cells at 24 hour or 72 hour, respectively. (n = 4, for each treatment).

Band No.	Protein Identity	Untreated		BSA (6 µg/ml)		Pure (2 µg/ml)		Pure (6 µg/ml)		Crude (2 µg/ml)		Crude (6 µg/ml)	
		24 h	72 h	24 h	72 h	24 h	72 h	24 h	72 h	24 h	72 h	24 h	72 h
1	Transketolase	1.0	1.0	1.1	1.2	1.7	1.3	0.7	0.9	0.6	1.0	0.3	1.1
2	Beta-Tubulin	1.0	1.0	0.7	0.8	0.6	0.8	0.7	1.4	0.5	1.0	0.4	0.9
3	Elongation Factor 2	1.0	1.0	0.7	0.6	0.4	0.7	0.6	0.5	0.6	0.4	0.8	0.4
4	90 kDa Heat Shock Protein	1.0	1.0	1.2	1.0	2.5	1.7	2.2	1.6	2.4	1.8	2.1	1.5
5	Beta Actin Variant	1.0	1.0	0.9	1.4	1.1	0.9	1.2	1.7	0.8	1.2	1.0	1.2
6	Annexin A2 Isoform 2	1.0	1.0	1.0	1.2	2.1	0.8	1.6	0.8	0.7	0.8	1.3	1.2
7	Histone H2B	1.0	1.0	1.1	0.8	0.9	0.5	0.6	1.2	1.1	0.4	0.5	0.5
8	Myosin-9	1.0	1.0	1.0	1.0	1.0	1.8	0.9	1.0	1.0	1.8	0.6	1.5
9	Pyruvate Kinase	1.0	1.0	1.1	0.8	1.2	0.6	1.4	0.8	1.1	0.9	0.8	0.8
10	Heat Shock Cognate 71 kDa Protein Isoform 1	1.0	1.0	0.8	1.0	1.0	1.3	0.6	2.1	0.4	2.3	0.5	1.5
11	Chain A, Binary Complex of 14-3-3 Sigma and P53 Pt387-Peptide	1.0	1.0	1.2	0.7	0.7	0.5	0.8	0.4	0.7	0.2	1.0	0.3
12	Peroxiredoxin-1	1.0	1.0	0.7	1.0	0.9	0.8	1.1	0.5	1.0	0.6	1.1	0.8
13	Protein S100-A11	1.0	1.0	1.3	0.5	3.4	0.3	2.4	0.3	2.9	0.2	3.0	0.4
14	Ubiquitin Activating Enzyme E1	1.0	1.0	0.8	0.9	0.9	1.2	0.9	1.5	0.6	1.2	0.8	1.3
15	Profilin-1	1.0	1.0	1.0	0.4	1.6	0.3	1.0	0.3	2.3	0.3	1.4	0.5
16	60 kDa Heat Shock Protein, Mitochondrial	1.0	1.0	0.9	0.9	1.8	1.2	1.9	1.2	1.3	1.2	1.0	1.2

5.2 An Investigation of the hTCEpi Cell Proteome Following Exposure to *B. oleronius* Protein

A description of the protocols followed for 2-D SDS-PAGE and the subsequent identification of proteins isolated from hTCEpi cells by LC/MS can be seen in Section 2.15, and Section 2.17, respectively.

5.2.1 An Analysis of the hTCEpi Cell Proteome Following Exposure to *B. oleronius* Protein

Corneal epithelial (hTCEpi) cells were exposed to crude *B. oleronius* protein (2 μg/ml), and pure *B. oleronius* protein (2 μg/ml) for 24 hour and 72 hour, harvested, and proteins were resolved in the first and second dimension prior to LC/MS analysis (Figure 5.5). A master gel of protein spots excised for mass spectrometry is given in Figure 5.6. A list of identified proteins from the proteome of hTCEpi cells exposed to *B. oleronius* proteins at 72 hour can be seen in Table 5.5. A discernible change in the abundance of identified proteins was not observed in hTCEpi cells following a 24 hour exposure to *B. oleronius* proteins but differences in the abundance of hTCEpi proteins was observed at 72 hour and the fold change in abundance relative to untreated hTCEpi cells was calculated (Table 5.6).

A number of similar proteins from the 1-D SDS-PAGE proteomic study were subsequently identified in the hTCEpi 2-D SDS-PAGE proteomic study. These include annexin V (Spot No: 2), 14-3-3 protein sigma (Spot No: 3), thioredoxin isoform 1 (Spot No: 9), protein S100-A11 (Spot No: 11), annexin A3 (Spot No: 12), heat shock protein gp96 precursor (Spot No: 14), elongation factor 2 (Spot No: 17), and heat shock protein beta-1 (Spot No: 20). These proteins function in many biological processes such as cell cycle and cell growth, keratinocyte differentiation, in response to oxidative stress, protein synthesis, and protein folding under heat stress conditions. At 72 hour, exposure of hTCEpi cells to *B. oleronius* protein preparations resulted in an alteration in the abundance of these proteins (Table 5.6).

Protein S100-A11 (Spot No: 11) is a calcium binding protein that is involved in the remodeling of the membrane and facilitating the joining of lipid segments on the membrane surface, and the differentiation of keratinocytes (Eckert *et al*., 2004; Tu *et al*., 2001). Protein S100-A11 has been implicated in dry eye syndrome and pterygium (Riau *et al*., 2009; Zhou *et al*., 2009). The abundance of protein S100-A11 was observed to be significantly decreased in hTCEpi cells treated with crude

B. oleronius protein (2 μg/ml) relative to untreated hTCEpi cells (0.5-fold; p = 0.0374). However, exposure of hTCEpi cells to the pure *B. oleronius* protein (2 μg/ml) preparation resulted in a significant increase of protein S100-A11 compared to untreated hTCEpi cells (1.7-fold; p = 0.0486).

Calreticulin precursor (Spot No: 16) and calmodulin (salmon) (Spot No: 24) regulate the movement of Ca^{2+} ions and play a role in cell signaling (Bandyopadhyay *et al*., 2002; Means, 1994; Walker *et al*., 1983). Exposure of hTCEpi to the crude or pure *B. oleronius* protein (2 μg/ml) preparations was observed to result in the increase of the calcium regulating proteins calreticulin precursor and calmodulin (salmon).

Structural proteins such as stathmin isoform a (Spot No: 6), laminin-binding protein (Spot No: 13), and tropomyosin-3-*ROS1* fusion protein (Spot No: 15) were identified by LC/MS. Laminin-binding proteins have been demonstrated to function in cell adhesion, and maintaining the structural integrity of the cornea (Keresztes and Lajtos, 1997; McCarthy *et al*., 1985; Carlsson *et al*., 1981). Treatment of hTCEpi cells with crude *B. oleronius* protein (2 μg/ml) resulted in a significant increase in the abundance of laminin-binding protein relative to untreated hTCEpi cells (1.3-fold; p = 0.0205). Increased hTCEpi cell migration and cell invasiveness was previously observed following exposure of hTCEpi cells to *B. oleronius* proteins (O'Reilly *et al*., 2012b).

Proteins involved in the enzymatic reactions in metabolism were identified by LC/MS, including platelet-activating factor acetylhydrolase (Spot No: 7), triosephosphate isomerase (Spot No: 8), malate dehydrogenase (Spot No: 18), and alpha-enolase (Spot No: 19), and peptidyl-prolyl cis-trans isomerase A (Spot No: 21). Platelet-activating factor acetylhydrolase has been shown to be implicated as a lipid messenger, and to have a role in atherosclerosis in an anti-inflammatory capacity (Chen, 2004; Arai *et al*., 2002). An increase in the abundance of platelet-activating factor acetylhydrolase was observed at 72 hour, and may indicate that the exposed hTCEpi are responding to the *B. oleronius* proteins.

Alterations to the proteome of hTCEpi cells may lead to changes in the phenotype of hTCEpi cells induced by the presence of *B. oleronius* proteins leading to the corneal epithelial sheet becoming unstable, with increased cell movement, and altered cell – cell adhesion that may result in the formation of ocular ulcers that are associated with ocular rosacea *in vivo*.

5.2.2 Summary

A 2-D SDS-PAGE analysis of the hTCEpi proteome following a 72 hour exposure to crude or pure *B. oleronius* protein (2 μg/ml) demonstrated changes in the abundance of a range of proteins. Similar proteins were identified in the 1-D SDS-PAGE study (Section 5.1), and these include annexin V, 14-3-3 protein sigma, thioredoxin isoform 1, protein S100-A11, annexin A3, heat shock protein gp96 precursor, elongation factor 2, and heat shock protein beta-1. These proteins function in many physiological processes such as cell cycle and cell growth, keratinocyte differentiation, in response to oxidative stress, protein synthesis, and protein folding under heat stress conditions. Alterations in the abundance of the hTCEpi proteome may play an important role in inducing changes to the corneal epithelial monolayer *in vitro*.

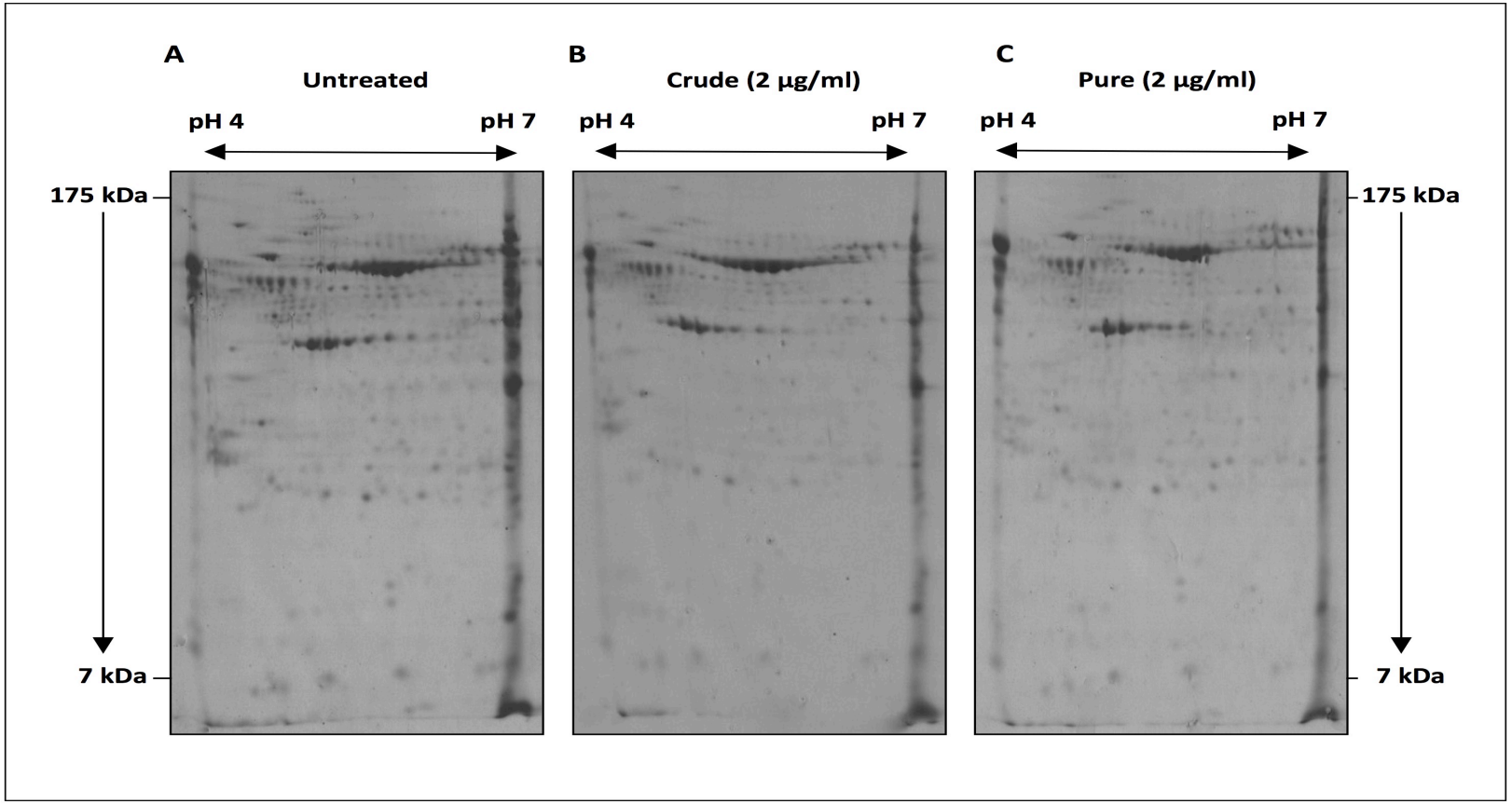

Figure 5.5 Proteome of hTCEpi cells exposed to *B. oleronius* proteins for 72 hour, and resolved by 2-D SDS-PAGE. Resolved 2-D SDS-PAGE images of corneal epithelial (hTCEpi) cells (**A**) untreated, and treated with (**B**) crude *B. oleronius* (2 µg/ml), and (**C**) pure *B. oleronius* protein (2 µg/ml) for a 72 hour exposure prior to LC/MS protein identification and progenesis SameSpot densitometric software analysis. (n = 4, for each treatment).

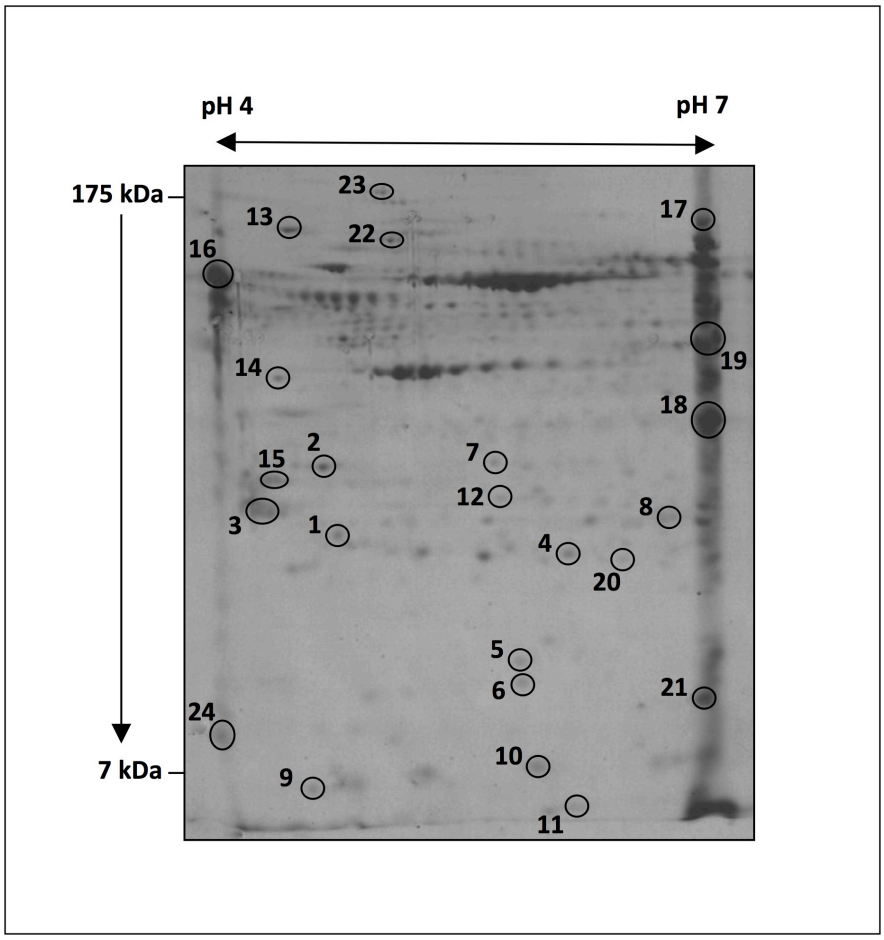

Figure 5.6 Master gel of excised 2-D SDS-PAGE hTCEpi proteome protein spots for protein identification by LC/MS following a 72 hour exposure to *B. oleronius* proteins. Master gel of excised protein spots resolved by 2-D SDS-PAGE, and identified through LC/MS from the whole cell lysates of hTCEpi cells treated and exposed to *B. oleronius* proteins for 24 hour and 72 hour. (Circles (O) indicate spots excised for identification by LC/MS).

Table 5.5 LC/MS protein spots identities from 2-D SDS-PAGE of the hTCEpi proteome following a 72 hour exposure to *B. oleronius* proteins.

Spot No.	Protein Identity	Organism	M_r (nominal mass)	pI	Mascot Score	Sequence Coverage	Accession No.	UniProt Protien Function
1	Rho GDP-Dissociation Inhibitor 1 Isoform a	*Homo sapiens*	23251	5.02	548	38%	NP_004300	Regualation of Rho Proteins and Transcription
2	Chain A, the Effect of Metal Binding on the Structure of Annexin V and Implications for Membrane Binding	*Homo sapiens*	35840	4.94	144	53%	1ANW_A	Regulation of Cell Growth
3	14-3-3 Protein Sigma	*Homo sapiens*	27873	4.68	167	62%	NP_006133	Regulation of Cell Cycle and Cell Growth
4	Glutathione S-Transferase-P1c	*Homo sapiens*	23587	5.43	176	58%	AAC13869	Oxidoreductase
5	Dismutase, Cu/Zn Superoxide	*Homo sapiens*	16024	8.44	74	18%	0808265A	Response to Oxidative Stress
6	Stathmin Isoform a	*Homo sapiens*	17292	5.76	81	60%	NP_005554	Regulation of Microtubule Structure
7	Platelet-Activating Factor Acetylhydrolase IB Subunit Beta Isoform a	*Homo sapiens*	25727	5.57	63	20%	NP_002563	Catalyses Enzymatic Reactions in Lipid Metabolism and Degradation
8	Triosephosphate Isomerase	*Homo sapiens*	26807	6.51	209	56%	1HTI_A	Catalyses Enzymatic Reactions in Glycolysis
9	Thioredoxin Isoform 1	*Homo sapiens*	12020	4.82	96	51%	NP_003320	Oxidoreductase Activity of Disulfide Proteins
10	Galectin-1	*Homo sapiens*	15054	5.34	194	80%	NP_002296	Regulation of Apoptosis, Cell Proliferation, and Cell Diiferentiation
11	Protein S100-A11	*Homo sapiens*	11849	6.56	305	59%	NP_005611	Keratinocyte Differentiation and Cornification
12	Annexin A3	*Homo sapiens*	36527	5.63	113	29%	NP_005130	Regulation of Cell Growth
13	Laminin-Binding Protein	*Homo sapiens*	31890	4.84	139	35%	CAA43469	Cell Adhesion and Migration
14	Heat Shock Protein gp96 Precursor	*Homo sapiens*	90312	4.73	391	42%	AAK74072	Molecular Chaperone that Assist Polypetide Folding Under Stress Conditions
15	Tropomyosin-3-*ROS1* Fusion Protein	*Homo sapiens*	83238	4.9	101	18%	BAM95192	Regulation Cytoskeletal Structure by Actin Binding
16	Calreticulin Precursor	*Homo sapiens*	48286	4.29	70	29%	NP_004334	Regulation of Ca^{2+} Ions and Cell Signaling
17	Elongation Factor 2	*Homo sapiens*	96263	6.41	351	46%	NP_001952	Protein Synthesis
18	Malate Dehydrogenase, Mitochondrial Precursor	*Homo sapiens*	35945	8.92	145	27%	NP_005909	Catalyses Oxidoreductase Reactions in Tricarboxylic Acid Cycle
19	Alpha-Enolase Isoform 1	*Homo sapiens*	47487	7.01	542	77%	NP_001419	Catalyses Enzymatic Reactions in Glycolysis
20	Heat Shock Protein Beta-1	*Homo sapiens*	22826	5.98	97	64%	NP_001531	Molecular Chaperone that Assist Polypetide Folding Under Stress Conditions
21	Peptidyl-Prolyl Cis-Trans Isomerase A	*Homo sapiens*	18233	7.68	223	66%	NP_066953	Catalyses Enzymatic Reactions in Ribosomes Biogenesis
22	Phosphoglycerate Mutase 1	*Homo sapiens*	28902	6.67	120	43%	NP_002620	Catalyses Enzymatic Reactions in Glycolysis
23	Transitional Endoplasmic Reticulum ATPase	*Homo sapiens*	89962	5.14	450	33%	NP_009057	ATP Binding
24	Calmodulin (Salmon)	*Homo sapiens*	16696	4.09	155	61%	MCON	Regulation of Ca^{2+} Ions and Cell Signaling

Table 5.6 Fold change of LC/MS protein spots identities from 2-D SDS-PAGE of the hTCEpi proteome following a 72 hour exposure to *B. oleronius* proteins. Fold change calculated is relative to untreated hTCEpi cells. (n = 4, for each treatment). (Significance: * = $p < 0.05$).

Spot No:	Protein Identity	Untreated	Crude *B. oleronius* Protein (2 µg/ml)	Pure *B. oleronius* Protein (2 µg/ml)
1	Rho GDP-Dissociation Inhibitor 1 Isoform a	1.0	1.3	1.5
2	Chain A, the Effect of Metal Binding on the Structure of Annexin V and Implications for Membrane Binding	1.0	1.4	1.2
3	14-3-3 Protein Sigma	1.0	1.1	0.9
4	Glutathione S-Transferase-P1c	1.0	1.2	1.2
5	Dismutase, Cu/Zn Superoxide	1.0	1.3	1.3
6	Stathmin Isoform a	1.0	1.3	0.9
7	Platelet-Activating Factor Acetylhydrolase IB Subunit Beta Isoform a	1.0	1.9	1.5
8	Triosephosphate Isomerase	1.0	0.9	1.1
9	Thioredoxin Isoform 1	1.0	2.5	0.8
10	Galectin-1	1.0	1.1	1.3
11	Protein S100-A11	1.0	0.5*	1.7*
12	Annexin A3	1.0	1.9	1.7
13	Laminin-Binding Protein	1.0	1.3*	0.8
14	Heat Shock Protein gp96 Precursor	1.0	1.0	0.8
15	Tropomyosin-3-*ROS1* Fusion Protein	1.0	1.3	1.0
16	Calreticulin Precursor	1.0	1.4	1.2
17	Elongation Factor 2	1.0	1.0	1.0
18	Malate Dehydrogenase, Mitochondrial Precursor	1.0	1.1	0.8
19	Alpha-Enolase Isoform 1	1.0	0.9	0.8
20	Heat Shock Protein Beta-1	1.0	2.4	2.4
21	Peptidyl-Prolyl Cis-Trans Isomerase A	1.0	1.0	0.8
22	Phosphoglycerate Mutase 1	1.0	1.1	0.8
23	Transitional Endoplasmic Reticulum ATPase	1.0	1.0	1.0
24	Calmodulin - Salmon	1.0	2.3	3.1

5.3 An In-Solution Digest Study Investigating the Proteome of hTCEpi Cells Following Exposure to *B. oleronius* Protein by Label Free Mass Spectrometry

An in-solution digest study of the hTCEpi cell proteome following a 24 hour exposure to crude *B. oleronius* protein (6 μg/ml), and a 72 hour exposure to pure *B. oleronius* protein (6 μg/ml) was analysed using label free mass spectrometry (LF/MS) (Section 2.18).

5.3.1 An Analysis of the hTCEpi Cell Proteome at 24 Hour Following Exposure to Crude *B. oleronius* Protein

Following a 24 hour exposure of hTCEpi cells to the crude *B. oleronius* protein (6 μg/ml) preparation, proteins were identified using MaxQuant and Blast2Go computer software (Section 2.18). LF/MS analysis demonstrated 13 proteins (red) to be exclusive to untreated hTCEpi cells, and 3 proteins (blue) to be exclusive to crude *B. oleronius* protein (6 μg/ml) treated hTCEpi cells following a 24 hour exposure (Figure 5.7). A total of 1616 proteins (purple) were observed to be similar to both untreated and treated hTCEpi cells (Figure 5.7). For a protein to be considered exclusive or unique, it must be detected in a minimum of 3 out of 4 replicates of one treatment, and undetected in 4 out of 4 replicates of the other comparative treatment. The proteins identified to be exclusive to untreated hTCEpi cells and those treated with crude *B. oleronius* protein (6 μg/ml) following a 24 hour exposure can be seen in Table 5.7, and Table 5.8, respectively.

At 24 hour, ubiquitin-associated protein 2 (Gene: UBAP2) and glioma tumor suppressor candidate gene 2 protein (Gene: GLTSCR2) were identified to be exclusive to untreated hTCEpi cells, and to function specifically in polyadenylation (poly (A)) RNA binding (Table 5.7). These poly (A) RNA binding proteins play an important role in a range of physiological processes including signal transduction, target degradation of proteins and protein synthesis, cell survival, cell cycle and migration, cell proliferation, apoptosis, regulation of transcription, and response to DNA damage (Zhao *et al*., 2015; Zhou *et al*., 2014; Vlachostergios *et al*., 2012; Yamaguchi *et al*., 2012; Wei and Lin, 2012; Kim *et al*., 2008; Sakamoto *et al*., 2003). Other proteins exclusive to untreated hTCEpi cells share similar biological functions (Table 5.7). These include translocon-associated protein subunit gamma (Gene: SSR3), peptidyl-prolyl cis-trans isomerase FKBP11 (Gene: FKBP11), ubiquitin-conjugating enzyme E2 Z (Gene: UBE2Z), and tyrosine-protein kinase BAZ1B

(Gene: BAZIB) that function in translation and signal transduction, chaperone-mediated protein folding, and the regulation of apoptosis and transcription, respectively (Broering *et al*., 2015; Yamaguchi *et al*., 2011; Markson *et al*., 2009; Lu *et al*., 2008). It can be hypothesized that proteins identified as exclusive to untreated hTCEpi cells are required for the maintenance of a healthy corneal surface, and that they were not detected following a 24 hour exposure to the crude *B. oleronius* protein (6 µg/ml) preparation may suggest a possible mechanism of disease for the development of ocular rosacea.

A small number of proteins were identified as exclusive to hTCEpi cells following a 24 hour exposure to the crude *B. oleronius* protein (6 µg/ml) preparation (Table 5.8). These include leukocyte elastase inhibitor (Gene: SERPINB1), Rho-associated protein kinase 1 (Gene: ROCK1), and rab11 family-interacting protein 5 (Gene: RAB11FIP5). Leukocyte elastase inhibitor is a member of the serpin superfamily and is a serine protease inhibitor (Huntington, 2011). Leukocyte elastase inhibitor has been demonstrated to have a role in cell survival by the inhibition of caspase-dependent cell death, and to also induce caspase-independent apoptosis through the activity of DNase II (Pardon-Barthe *et al*., 2008; Torriglia *et al*., 2008). The intracellular location of the protein, either the cytoplasm or the nucleus, is related to the pro-survival or pro-apoptotic function of the protein (Pardon-Barthe *et al*., 2007, 2008; Torriglia *et al*., 2008). Recently, Justet *et al*. (2015) demonstrated that the expression of leukocyte elastase inhibitor increased during wound healing in bovine corneal endothelial cells, and suggested that the production of ROS may result in the increase of the serine protease inhibitor.

Rho-associated protein kinase 1 has been demonstrated to be implicated in the proliferation and differentiation of airway epithelial cells, and in the regulation of cadherin and cell adhesion (Horani *et al*., 2013; Smith *et al*., 2012). Therapeutic inhibition of Rho-associated protein kinase 1 has been reported to promote adheren junction stability, and tissue organization (Wójack-Stothard *et al*., 2001). Rab11 family-interacting protein 5 is a membrane protein GTPase that is essential for the transport of proteins between cellular compartments (Oehlke *et al*., 2011; Prekeris *et al*., 2000).

Following a 24 hour exposure, the increased abundance of the exclusive proteins, leukocyte elastase inhibitor, Rho-associated protein kinase 1, and rab11 family-interacting protein 5, identified from hTCEpi cells treated with crude

B. oleronius protein (6 μg/ml) preparation suggests that a stress response is induced by hTCEpi cells resulting in the a re-structuring of the corneal epithelial monolayer. Similarly, the crude *B. oleronius* protein preparation has previously been shown to increase cell migration in hTCEpi cells, and lead to the development of an aberrant wound healing response (O'Reilly *et al*., 2012b).

Following a 24 hour exposure of hTCEpi cells to crude *B. oleronius* protein (6 μg/ml), a number of proteins were observed to be differentially expressed when depicted on a volcano plot with –Log (p – value) (y-axis) plotted against the Log to the base 2 of fold change ([Log_2 (fold change)]) (Figure 5.8). A value greater than –Log (1.3) was considered to be statistically significant ($p < 0.05$). Identified proteins that were increased or decreased in abundance following exposure to crude *B. oleronius* protein (6 μg/ml) relative to untreated hTCEpi cells can be seen in Table 5.9, and Table 5.10, respectively.

Proteins observed to be increased in abundance function in a range of physiological processes. These include poly (A) RNA binding, protein transport, actin-binding, signal transduction, epidermal development and morphogenesis, and cell cycle and apoptosis, and response to oxidative stress (Table 5.9). An increase of thioredoxin (Gene: PDIA3) abundance was observed in hTCEpi cells treated with the crude *B. oleronius* protein preparation compared to untreated hTCEpi cells.

String network analysis showed a collection of increased abundant proteins to share a homologous function, poly (A) RNA binding (Figure 5.9). Proteins associated with poly (A) RNA binding include U5 small nuclear ribonucleoprotein (Gene: SNRNP40), fragile X mental retardation syndrome-related protein 1 (Gene: FXR1), putative RNA-binding protein 3 (Gene: RBM3), transitional endoplasmic reticulum ATPase (Gene: VCP), and eukaryotic translation initiation factor 4H (Gene: EIF4H) (Table 5.9). As mentioned earlier, these proteins have a wide range of biological functions such as targeted protein degradation and synthesis, and cell cycle and proliferation (Zhao *et al*., 2015; Zhou *et al*., 2014; Vlachostergios *et al*., 2012; Yamaguchi *et al*., 2012; Wei and Lin, 2012; Kim *et al*., 2008; Ciechanover, 2005; Sakamoto *et al*., 2003). Eukaryotic translation initiation factor 4H has been demonstrated to function in the regulation of cell differentiation and increased abundance has been associated with increased rates of cell proliferation (Blázquez-Domingo *et al*., 2005; Fingar *et al*., 2004).

A number of proteins were found to be significantly decreased in abundance relative to that in untreated hTCEpi cells (Table 5.10). Of these proteins, a majority were observed by a string network to function specifically in poly (A) RNA binding (Figure 5.10). Theses protein identities include transportin-1 (Gene: TNPO1), 60S ribosomal protein L27 (Gene: RPL27), x-ray repair cross-complementing protein 6 (Gene: XRCC6), 40S ribosomal protein S11 (Gene: RPS11), interleukin enhancer-binding factor 2 (Gene: ILF2), constitutive coactivator of PPAR-gamma-like protein 1 (Gene: FAM120A), protein DEK (Gene: DEK), trifunctional enzyme subunit beta (Gene: HADHB), RNA-binding protein 39 (Gene: RBM39), ATP-dependent RNA helicase DDX54 (Gene: DDX54), deoxynucleotidyltransferase terminal-interacting protein 2 (Gene: DNTTIP2), proline-, glutamic acid-, leucine-rich protein 1 (Gene: PELP1), glioma tumor suppressor candidate region gene 2 protein (Gene: GLTSCR2), and ribonucleases P/MRP protein subunit POP1 (Gene: POP1) (Table 5.10).

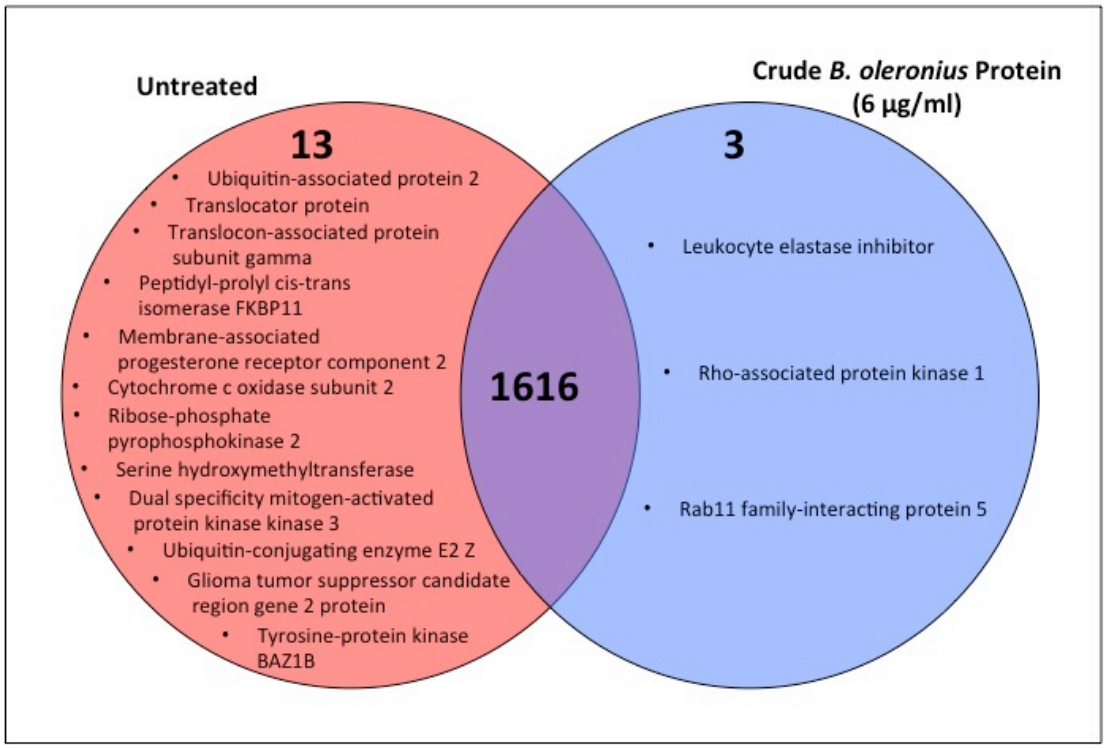

Figure 5.7 A Venn diagram illustrating exclusive proteins identified by LF/MS from hTCEpi cells untreated and treated with crude *B. oleronius* protein (6 µg/ml) following a 24 hour exposure. LF/MS analysis demonstrated 13 proteins (red) to be exclusive to untreated hTCEpi cells, and 3 proteins (blue) to be exclusive to crude *B. oleronius* protein (6 µg/ml) treated hTCEpi cells following a 24 hour exposure. A total of 1616 proteins (purple) were observed to be similar in both untreated and treated hTCEpi cells. For a protein to be considered exclusive or unique, it must be detected in a minimum of 3 out of 4 replicates of one treatment, and undetected in 4 out of 4 replicates of the other comparative treatment. Proteins were identified using MaxQuant and Blast2Go computer software (Section 2.18). LF/MS: label free mass spectrometry. (n = 4, for each treatment).

Table 5.7 LF/MS protein identities exclusive to untreated hTCEpi cells following a 24 hour exposure. For a protein to be considered exclusive or unique, it must be detected in a minimum of 3 out of 4 replicates of one treatment, and undetected in 4 out of 4 replicates of the other comparative treatment. Proteins were identified using MaxQuant and Blast2Go computer software (Section 2.18). LF/MS: label free mass spectrometry. (n = 4, for each treatment).

Gene	Untreated LFQ Intensity				Crude *B. oleronius* Protein (6 µg/ml) LFQ Intensity				MS/MS Count	Peptides	Sequence Coverage (%)	Mol. Weight (kDa)	Protein Identity	UniProt Protein Function
	1	2	3	4	1	2	3	4						
UBAP2	3.20E+07	2.00E+07	0	2.47E+07	0	0	0	0	7	3	6.6	87.90	Ubiquitin-Associated Protein 2	Poly (A) RNA Binding Protein
TSPO	1.31E+07	8.87E+06	0	2.78E+07	0	0	0	0	8	1	21.5	11.90	Translocator Protein	Lipid Transport
SSR3	4.80E+07	1.72E+07	0	3.45E+07	0	0	0	0	5	2	10.3	20.16	Translocon-Associated Protein Subunit Gamma	Translation
PPP2R5E	1.78E+07	1.29E+07	1.66E+07	0	0	0	0	0	2	2	6.6	46.18	Serine/Threonine-Protein Phosphatase 2A 56 kDa Regulatory Subunit Epsilon Isoform	Signal Transduction
FKBP11	4.33E+07	7.33E+06	0	2.76E+07	0	0	0	0	5	2	20.5	15.77	Peptidyl-Prolyl Cis-Trans Isomerase FKBP11	Chaperone-Mediated Protein Folding
PGRMC2	1.78E+07	1.06E+07	0	2.61E+07	0	0	0	0	3	2	9.9	23.82	Membrane-Associated Progesterone Receptor Component 2	Lipid Binding
MT-CO2	5.75E+07	1.54E+08	5.91E+07	0	0	0	0	0	11	4	19.4	25.57	Cytochrome C Oxidase Subunit 2	Electron Transport
PRPS2	0	6.14E+07	4.25E+07	4.39E+07	0	0	0	0	5	5	20.4	34.77	Ribose-Phosphate Pyrophosphokinase 2	Nucleotide Biosynthesis
SHMT1	1.57E+07	2.43E+07	0	1.43E+07	0	0	0	0	4	4	21.8	44.55	Serine Hydroxymethyltransferase, Cytosolic	Transferase
MAP2K3	9.51E+06	0	5.86E+06	1.43E+07	0	0	0	0	2	2	9.2	39.32	Dual Specificity Mitogen-Activated Protein Kinase Kinase 3	Serine/Threonine Protien Kinase
UBE2Z	0	1.40E+07	1.95E+07	2.39E+07	0	0	0	0	8	3	22	28.08	Ubiquitin-Conjugating Enzyme E2 Z	Regulation of Apoptosis
GLTSCR2	5.52E+07	5.81E+07	3.27E+07	3.60E+07	0	0	0	0	4	3	14.9	54.39	Glioma Tumor Suppressor Candidate Region Gene 2 Protein	Poly (A) RNA Binding Protein
BAZ1B	1.15E+07	0	8.85E+06	8.80E+06	0	0	0	0	4	2	1.3	170.45	Tyrosine-Protein Kinase BAZ1B	Regulation of Transcription

Table 5.8 LF/MS protein identities exclusive to hTCEpi cells treated with crude *B. oleronius* protein (6 µg/ml) following a 24 hour exposure. For a protein to be considered exclusive or unique, it must be detected in a minimum of 3 out of 4 replicates of one treatment, and undetected in 4 out of 4 replicates of the other comparative treatment. Proteins were identified using MaxQuant and Blast2Go computer software (Section 2.18). LF/MS: label free mass spectrometry. (n = 4, for each treatment).

Gene	Untreated LFQ Intensity				Crude *B. oleronius* Protein (6 µg/ml) LFQ Intensity				MS/MS Count	Peptides	Sequence Coverage (%)	Mol. Weight (kDa)	Protein Identity	UniProt Protein Function
	1	2	3	4	1	2	3	4						
SERPINB1	0	0	0	0	1.01E+07	1.18E+07	0	1.05E+07	5	4	14	42.74	Leukocyte Elastase Inhibitor	Serine Protease Inhibitor
ROCK1	0	0	0	0	6.37E+07	5.98E+07	5.34E+07	0	4	4	4.9	158.17	Rho-Associated Protein Kinase 1	Serine/Threonine Protien Kinase
RAB11FIP5	0	0	0	0	2.46E+07	1.24E+07	1.11E+07	0	4	2	5.5	70.41	Rab11 Family-Interacting Protein 5	Protein Transport

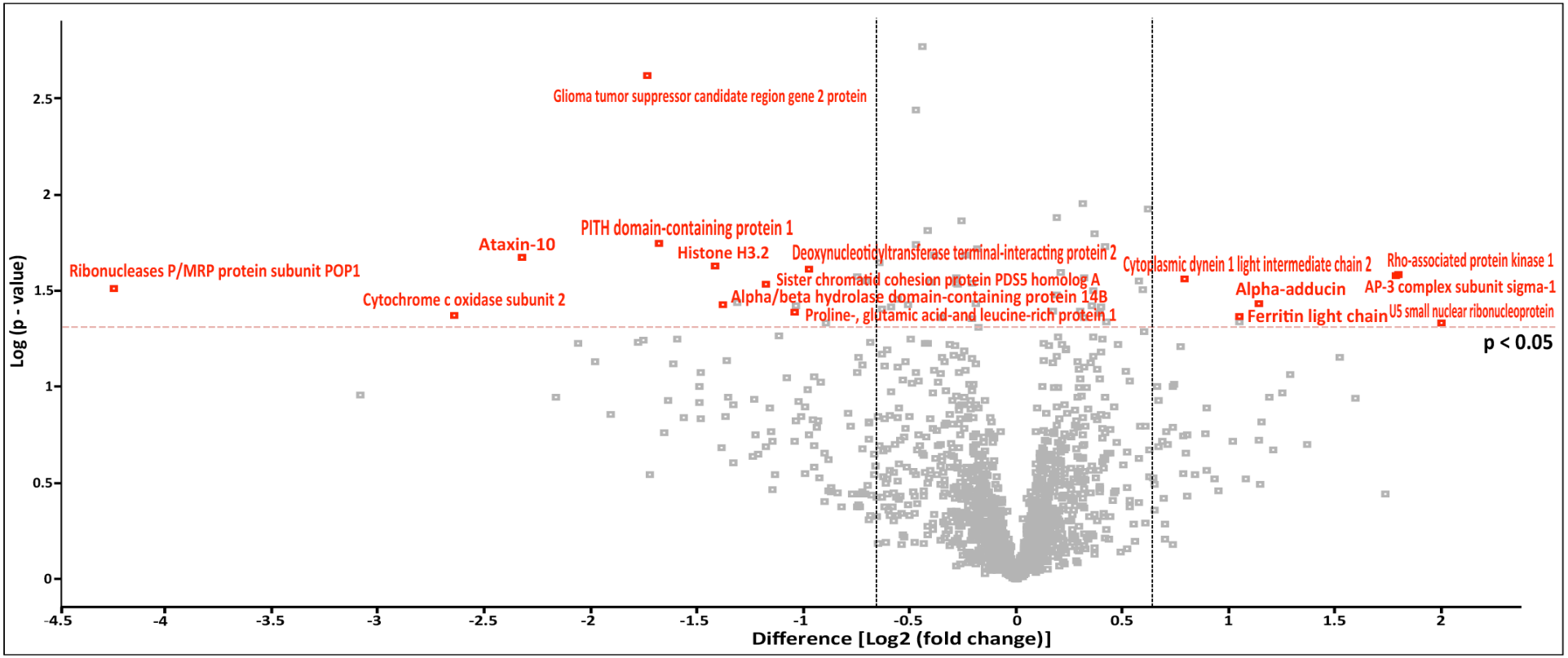

Figure 5.8 A volcano plot demonstrating the fold change of hTCEpi proteins identified by LF/MS following a 24 hour exposure to crude *B. oleronius* protein (6 µg/ml) relative to untreated hTCEpi cells. LF/MS analysis (Section 2.18) demonstrating the distribution of hTCEpi proteins increased and decreased in abundance following a 24 exposure to crude *B. oleronius* protein (6 µg/ml) relative to untreated hTCEpi cells. Identities (red) above -Log of 1.3 are considered statistically significant (red dashed line). LF/MS: label free mass spectrometry. (n = 4, for each treatment).

Table 5.9 LF/MS protein identities from hTCEpi cells exposed to crude *B. oleronius* protein (6 µg/ml) for 24 hour that were increased in abundance relative to untreated hTCEpi cells. LF/MS: label free mass spectrometry. (n = 4, for each treatment).

Gene	Untreated LFQ Intensity	Crude Protein (6 µg/ml) LFQ Intensity	MS/MS Count	Peptides	Sequence Coverage (%)	Mol. Weight (kDa)	Protein Identity	-Log (p-Value)	Difference [Log_2 (fold change)]	UniProt Protein Function
SNRNP40	24.05	26.05	10	3	21	39.31	U5 Small Nuclear Ribonucleoprotein 40 kDa Protein	1.33	2.00	Poly (A) RNA Binding Protein
AP3S1	24.34	26.14	10	2	14	21.73	AP-3 Complex Subunit Sigma-1	1.58	1.80	Protein Transport
ROCK1	23.49	25.28	4	4	4.9	158.17	Rho-Associated Protein Kinase 1	1.58	1.79	Serine/Threonine Protien Kinase
ADD1	22.74	23.86	7	2	3.8	69.98	Alpha-Adducin	1.39	1.12	Actin-Binding
FTL	26.20	27.25	12	4	34.9	20.02	Ferritin Light Chain	1.34	1.05	Iron Storage
DTYMK	25.59	26.21	22	7	30.7	23.82	Thymidylate Kinase	1.92	0.62	Nucleotide Biosynthesis
DYNC1LI2	25.62	26.22	15	5	17.1	45.00	Cytoplasmic Dynein 1 Light Intermediate Chain 2	1.51	0.60	Transport
METAP1	26.24	26.82	32	8	41.4	37.81	Methionine Aminopeptidase	1.55	0.58	Protease
CTBP1	24.45	24.87	15	4	10.7	46.40	C-Terminal-Binding Protein 1	1.34	0.43	Regulation of Transcription
PDIA3	28.79	29.21	16	12	58.5	13.52	Thioredoxin	1.73	0.42	Oxidative Stress
NUDT5	27.09	27.50	42	7	42.9	24.33	ADP-Sugar Pyrophosphatase	1.42	0.40	Hydrolase
FXR1	26.98	27.37	49	12	23.2	69.72	Fragile X Mental Retardation Syndrome-Related Protein 1	1.38	0.39	Poly (A) RNA Binding Protein
NDRG3	25.20	25.57	16	4	24.4	29.72	Protein NDRG3	1.80	0.37	Signal Transduction
PPP1R18	27.07	27.44	58	12	33.9	67.94	Phostensin	1.50	0.37	Actin-Binding
PLOD1	25.92	26.27	21	6	13.5	83.55	Procollagen-Lysine, 2-Oxoglutarate 5-Dioxygenase 1	1.42	0.36	Epidermis Development
LMNA	27.75	28.07	47	75	88.3	65.13	Prelamin-A/C	1.57	0.32	Apoptosis
MAT2B	26.26	26.58	20	6	42.1	28.95	Methionine Adenosyltransferase 2 Subunit Beta	1.36	0.32	Metabolism
RBM3	28.58	28.90	50	7	62.4	17.17	Putative RNA-Binding Protein 3	1.95	0.32	Poly (A) RNA Binding Protein
TRIOBP	25.09	25.39	20	7	17	68.04	TRIO and F-Actin-Binding Protein	1.39	0.30	Cell Cycle
PLOD3	26.97	27.18	52	16	31.8	84.78	Procollagen-Lysine, 2-Oxoglutarate 5-Dioxygenase 3	1.60	0.21	Epidermis Morphogenesis
VCP	32.01	32.20	547	69	73.3	89.32	Transitional Endoplasmic Reticulum ATPase	1.88	0.19	Poly (A) RNA Binding Protein
EIF4H	29.17	29.36	95	11	65.8	25.20	Eukaryotic Translation Initiation Factor 4H	1.48	0.19	Poly (A) RNA Binding Protein
TPM3	32.71	32.88	423	36	79.4	29.03	Tropomyosin Alpha-3 Chain	1.40	0.17	Actin-Binding

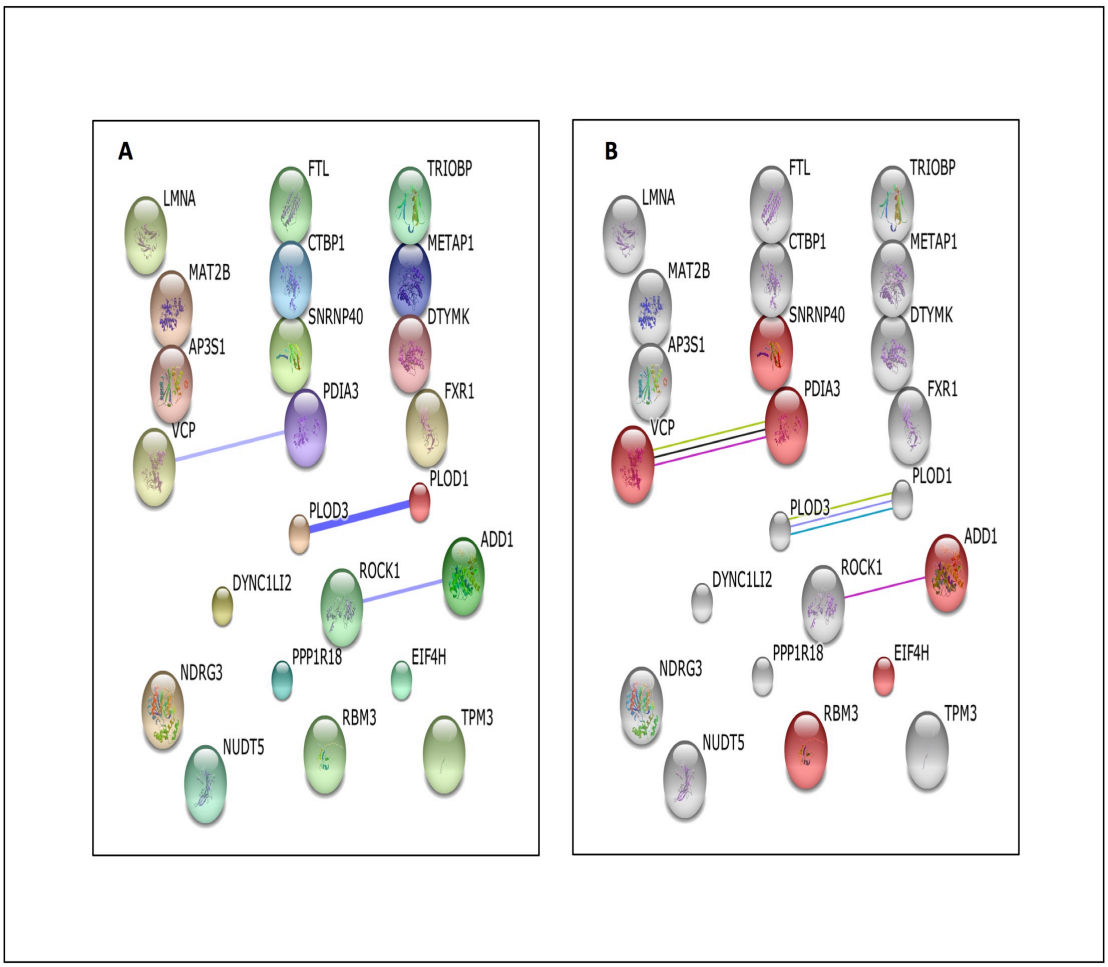

Figure 5.9 String network analysis of proteins increased in abundance following a 24 hour exposure of hTCEpi cells to crude *B. oleronius* protein (6 µg/ml). (**A**) String network of proteins increased in abundance following a 24 hour exposure of hTCEpi cells with crude *B. oleronius* protein (6 µg/ml). (**B**) Proteins (red) that function as Poly (A) RNA binding proteins. (n = 4, for each treatment).

Table 5.10 LF/MS protein identities from hTCEpi cells exposed to crude *B. oleronius* protein (6 µg/ml) for 24 hour that were decreased in abundance relative to untreated hTCEpi cells. LF/MS: label free mass spectrometry. (n = 4, for each treatment).

Gene	Untreated LFQ Intensity	Crude Protein (6 µg/ml) LFQ Intensity	MS/MS Count	Peptides	Sequence Coverage (%)	Mol. Weight (kDa)	Protein Identity	-Log (p-Value)	Difference [Log_2 (fold change)]	UniProt Protein Function
TNPO1	27.61	27.43	44	13	29	101.31	Transportin-1	1.31	-0.18	Poly (A) RNA Binding Protein
RPL27	29.10	28.92	74	10	63.2	15.80	60S Ribosomal Protein L27	1.72	-0.18	Poly (A) RNA Binding Protein
PRKAR2A	26.98	26.79	52	14	51.6	43.07	cAMP-Dependent Protein Kinase Type II-Alpha Regulatory Subunit	1.43	-0.19	Nucleotide-Binding
XRCC6	29.88	29.68	189	32	52.7	69.84	X-Ray Repair Cross-Complementing Protein 6	1.36	-0.20	Poly (A) RNA Binding Protein
RPS11	30.37	30.16	171	25	79.7	18.43	40S Ribosomal Protein S11	1.54	-0.21	Poly (A) RNA Binding Protein
PSMA3	27.07	26.83	35	9	39.5	27.65	Proteasome Subunit Alpha Type-3	1.69	-0.24	Threonine Protease
ILF2	28.05	27.79	61	12	48.7	43.06	Interleukin Enhancer-Binding Factor 2	1.86	-0.26	Poly (A) RNA Binding Protein
RPL38	28.24	27.97	38	5	57.1	8.22	60S Ribosomal Protein L38	1.53	-0.27	RNA Binding
VDAC1	29.67	29.39	132	22	78.4	30.77	Voltage-Dependent Anion-Selective Channel Protein 1	1.54	-0.28	Transport
FAM120A	25.77	25.49	17	6	11.4	121.89	Constitutive Coactivator of PPAR-Gamma-like Protein 1	1.57	-0.28	Poly (A) RNA Binding Protein
GLOD4	26.92	26.58	25	7	33.2	33.23	Glyoxalase Domain-Containing Protein 4	1.36	-0.35	Mitochondrial Protein
DECR1	25.16	24.78	10	5	20.6	34.99	2,4-Dienoyl-CoA Reductase, Mitochondrial	1.68	-0.38	Oxidoreductase
DEK	27.02	26.61	26	7	22.9	42.67	Protein DEK	1.55	-0.40	Poly (A) RNA Binding Protein
ATP5F1	23.78	23.37	7	2	16.4	22.28	ATP Synthase Subunit B, Mitochondrial	1.81	-0.41	Ion Transport
NCAPG	25.46	25.02	15	6	7.9	114.33	Condensin Complex Subunit 3	2.77	-0.44	Cell Cycle
HADHB	28.02	27.55	58	13	39.4	48.88	Trifunctional Enzyme Subunit Beta, Mitochondrial	1.74	-0.47	Poly (A) RNA Binding Protein
RBM39	27.73	27.26	59	12	34.1	57.09	RNA-Binding Protein 39	2.44	-0.47	Poly (A) RNA Binding Protein
DDX54	23.47	22.96	3	3	4.3	98.59	ATP-Dependent RNA Helicase DDX54	1.42	-0.51	Poly (A) RNA Binding Protein
HMOX2	27.18	26.63	40	9	50.3	36.03	Heme Oxygenase 2	1.45	-0.56	Oxidoreductase
HUWE1	26.06	25.48	16	7	3.7	374.19	E3 Ubiquitin-Protein Ligase HUWE1	1.42	-0.59	Ligase
RAB1B	27.71	27.08	41	9	52.1	18.48	Ras-Related Protein Rab-1B	1.41	-0.63	Nucleotide-Binding

Table 5.10 (Continued) LF/MS protein identities from hTCEpi cells exposed to crude *B. oleronius* protein (6 µg/ml) for 24 hour that were decreased in abundance relative to untreated hTCEpi cells. LF/MS: label free mass spectrometry. (n = 4, for each treatment).

Gene	Untreated LFQ Intensity	Crude Protein (6 µg/ml) LFQ Intensity	MS/MS Count	Peptides	Sequence Coverage (%)	Mol. Weight (kDa)	Protein Identity	-Log (p-Value)	Difference [Log_2 (fold change)]	UniProt Protein Function
PLP2	26.08	25.43	15	2	18.4	16.69	Proteolipid Protein 2	1.64	-0.64	Ion Transport
CKAP5	25.60	24.90	25	8	5.9	218.52	Cytoskeleton-Associated Protein 5	1.55	-0.70	Cell Cycle
SLC25A6	28.04	27.30	36	20	61.4	32.87	ADP/ATP Translocase 3	1.57	-0.75	Transport
NELFB	24.17	23.27	5	3	6.6	65.70	Negative Elongation Factor B	1.33	-0.89	Regulation of Transcription
DNTTIP2	24.63	23.66	11	3	6.6	84.47	Deoxynucleotidyltransferase Terminal-Interacting Protein 2	1.61	-0.97	Poly (A) RNA Binding Protein
PELP1	24.44	23.40	11	3	5.9	110.09	Proline-, Glutamic Acid- and Leucine-Rich Protein 1	1.42	-1.04	Poly (A) RNA Binding Protein
PDS5A	24.26	23.09	5	3	4	150.83	Sister Chromatid Cohesion Protein PDS5 Homolog A	1.53	-1.18	Cell Cycle
ABHD14B	25.56	24.25	15	4	31.9	22.35	Alpha/Beta Hydrolase Domain-Containing Protein 14B	1.44	-1.31	Hydrolase
HIST2H3A	28.32	26.91	13	22	75	15.39	Histone H3.2	1.63	-1.41	DNA-Binding
PITHD1	24.62	22.94	8	3	23.3	24.12	PITH Domain-Containing Protein 1	1.74	-1.68	Cell Differentiation
GLTSCR2	25.39	23.66	4	3	14.9	54.39	Glioma Tumor Suppressor Candidate Region Gene 2 Protein	2.62	-1.73	Poly (A) RNA Binding Protein
ATXN10	26.17	23.84	11	6	27.3	46.29	Ataxin-10	1.67	-2.32	Protein Homotrimerization
MT-CO2	25.36	22.72	11	4	19.4	25.57	Cytochrome C Oxidase Subunit 2	1.37	-2.64	Electron Transport
POP1	28.46	24.22	10	3	3.8	114.71	Ribonucleases P/MRP Protein Subunit POP1	1.51	-4.24	Poly (A) RNA Binding Protein

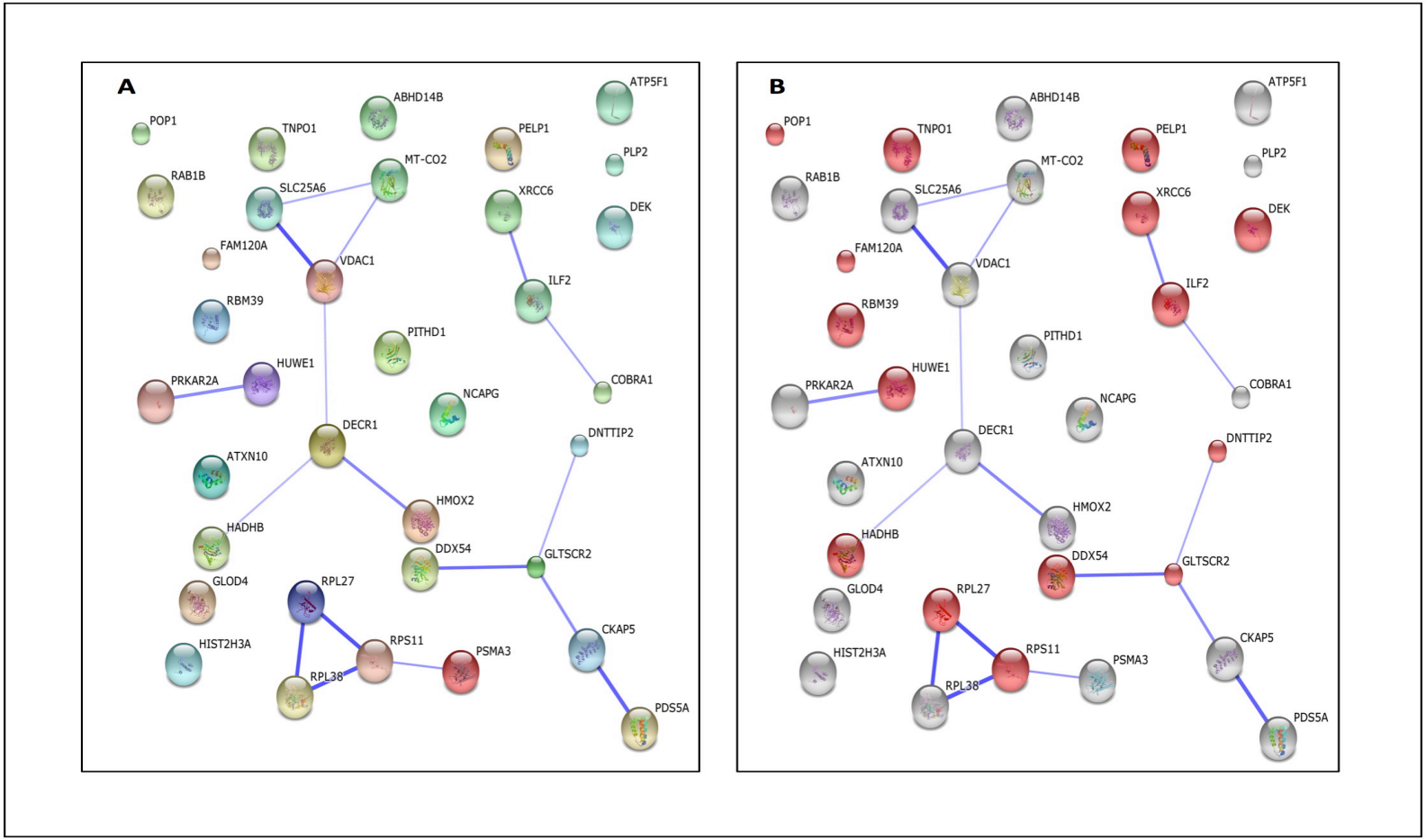

Figure 5.10 String network analysis of proteins decreased in abundance following a 24 hour exposure of hTCEpi cells treated with crude *B. oleronius* protein (6 µg/ml). (**A**) String network of proteins decreased in abundance following a 24 hour exposure of hTCEpi cells with crude *B. oleronius* protein (6 µg/ml). (**B**) Proteins (red) that function as Poly (A) RNA binding proteins. (n = 4, for each treatment).

5.3.2 An Analysis of the hTCEpi Cell Proteome at 72 Hour Following Exposure to Pure *B. oleronius* Protein

Following a 72 hour exposure of hTCEpi cells to the pure *B. oleronius* protein (6 µg/ml) preparation, proteins were identified using MaxQuant and Blast2Go computer software (Section 2.18). LF/MS analysis demonstrated 7 proteins (red) to be exclusive to untreated hTCEpi cells, and 7 proteins (green) to be exclusive to crude *B. oleronius* protein (6 µg/ml) treated hTCEpi cells following a 72 hour exposure (Figure 5.11). A total of 1854 proteins (brown) were observed to be similar to both untreated and treated hTCEpi cells (Figure 5.11). For a protein to be considered exclusive or unique, it must be detected in a minimum of 3 out of 4 replicates of one treatment, and undetected in 4 out of 4 replicates of the other comparative treatment. The proteins identified to be exclusive to untreated hTCEpi cells and treated with pure *B. oleronius* protein (6 µg/ml) following a 72 hour exposure can be seen in Table 5.11, and Table 5.12, respectively.

Proteins exclusive to untreated hTCEpi cells following a 72 hour incubation include tumor suppressor p53-binding protein 1 (Gene: TP53BP1), ADP-ribosylation factor-like protein 1 (Gene: ARL1), E3 ubiquitin-protein ligase BRE1B (Gene: RNF40), cullin-7 (Gene: CUL7), geranylgeranyl transferase type-2 subunit alpha (Gene: RABGGTA), nuclear pore complex protein Nup88 (Gene: NUP88), and NIF3-like protein 1 (Gene: NIF3L1) (Table 5.11). Tumor suppressor p53-binding protein has been demonstrated to be expressed in response to DNA damage and has also been reported to be expressed in central and peripheral human corneal endothelial cells and is believed to regulate cell growth and proliferation at the corneal endothelium (Paull and Whikehart, 2005; Ward *et al*., 2003; Rappold *et al*., 2001). Cullin-7 has previously been implicated in regulating cell growth by interacting with the p53 tumor suppressor protein and induces the development of the epithelial to mesenchymal transition (Fu *et al*., 2010; Sarikas *et al*., 2008; Andrews *et al*., 2006).

Proteins identified as exclusive to hTCEpi cells exposed to the pure *B. oleronius* protein (6 µg/ml) preparation can be seen in Table 5.12. Interestingly, of these proteins, RNA binding protein FOX-1 homolog (Gene: RBM9) and argininosuccinate synthase (Gene: ASS1) have been associated with poly (A) RNA binding (Tseng *et al*., 2013; Norris *et al*., 2002). Nesprin-2 (Gene: SYNE2) and smoothelin (Gene: SMTN) have been shown to play a role in actin-binding and cell

proliferation and differentiation during a wound healing response (Rashmi *et al*., 2012; van der Loop *et al*., 1996). Tumor necrosis factor α-induced protein 3 (TNFAIP3)-interacting protein 1 (Gene: TNIP1) is an inhibitor of NF-κB and TNF-α induced apoptosis, and has been associated in individuals with psoriasis (Kawasaki *et al*., 2010; Verstrepen *et al*., 2009; Oshima *et al*., 2009; Nair *et al*., 2009).

Similar to hTCEpi cells exposed to crude *B. oleronius* protein (6 μg/ml) preparation for 24 hour, it was observed that hTCEpi cells treated with pure *B. oleronius* protein (6 μg/ml) preparation for 72 hour, the serine protease inhibitor, leukocyte elastase inhibitor (Gene: SERPINB1) was exclusive to hTCEpi cells exposed to *B. oleronius* proteins. As described above, leukocyte elastase inhibitor can function in either a pro-survival or pro-apoptotic capacity, and the expression of the serine protease inhibitor increases during the wound healing response (Justet *et al*., 2015; Pardon-Barthe *et al*., 2007, 2008; Torriglia *et al*., 2008).

Following a 72 exposure of hTCEpi cells to pure *B. oleronius* protein (6 μg/ml), a number of proteins were observed to be differentially expressed when depicted on a volcano plot with –Log (p – value) (y-axis) plotted against the Log to the base 2 of fold change ([Log_2 (fold change)]) (Figure 5.12).

Proteins that were observed to be increased in abundance were shown to be involved in a wide range of physiological processes including cell signaling, cell adhesion, apoptosis, iron binding, response to oxidative stress, actin-binding and cytoskeletal organization, and poly (A) RNA binding (Table 5.13). String network analysis of increased abundant proteins did not show a collection of proteins with a homologous function (Figure 5.13).

An increased abundance of superoxide dismutase (Gene: SOD2) was detected in hTCEpi cells treated with the pure *B. oleronius* protein (6 μg/ml) preparation relative to untreated hTCEpi cells. Superoxide dismutase functions in cell signaling, and protects a cell by the regulation and detoxification of ROS *in vivo* (Landis and Tower, 2005).

A number of proteins that function in cell adhesion such as laminin subunit beta 3 (Gene: LAMB3), laminin subunit gamma-2 (Gene: LAMC2), and laminn subunit beta-1 (Gene: LAMB1) (Keresztes and Lajtos, 1997; McCarthy *et al*., 1985; Carlsson *et al*., 1981). It has previously been reported that human corneal epithelial cells are capable of rapid adhesion (Kurpakus *et al*., 1999). Thus, an increased abundance of laminin proteins may be related to the increased hTCEpi cell migration and cell

invasiveness previousy observed following exposure of hTCEpi cells to *B. oleronius* proteins (O'Reilly *et al*., 2012b).

Nuclear factor NF-κB p100 subunit (Gene: NFKB2) was observed to be significantly increased in abundance in hTCEpi cells exposed to the pure *B. oleronus* protein (6 μg/ml) relative to untreated hTCEpi cells. Nuclear factor NF-κB p100 subunit has been shown to be involved in the regulation of transcription, and in the induction of an inflammatory and an immune response (Lawrence, 2009; Dobrzanski *et al*., 1994). Thus, demonstrating a capacity within the pure *B. oleronius* protein (6 μg/ml) preparation to induce an inflammatory and an immune response in hTCEpi cells.

The serine protease inhibitor, plasminogen activator inhibitor 2 (Gene: SERPINB2), was significantly increased in abundance in pure *B. oleronius* protein (6 μg/ml) treated hTCEpi cells compared to untreated hTCEpi cells. The conversion of plasminogen to plasmin has previously been shown to have a role in the plasminogen cascade in corneal and conjunctival cells and has been associated in physiological and pathological ocular processes, and plasminogen activator inhibitor has been demonstrated to be expressed in the corneal epithelium (Williams *et al*., 1999; Whitelock *et al*., 1997; Fini *et al*., 1996).

Following a 72 hour exposure of hTCEpi cells with the pure *B. oleronius* protein (6 μg/ml) preparation, a collection of identified proteins were found to function in poly (A) RNA binding. These include argininosuccinate synthase (Gene: ASS1), RNA binding protein Fox-1 homolog (Gene: RBM2), mitochondrial ribonuclease P protein 1 (Gene: TRMT10C), superkiller viralicidic activity 2-like 2 (Gene: SKIV2L2), and G-rich sequence factor 1 (Gene: GRSF1) (Table 5.13).

Argininosuccinate synthase and RNA binding protein Fox-1 homolog were observed to be exclusive to hTCEpi cells exposed to the pure *B. oleronius* protein (6 μg/ml) preparation, and have been shown to regulate downstream processes of poly (A) RNA binding mediating protein synthesis and as a negative regulator of estrogen receptor signaling (Tseng *et al*., 2013; Norris *et al*., 2002). Mitochondrial ribonuclease P protein 1 is involved in the maturation of precursors that contain mRNAs, rRNAs, and tRNAs by cleavage of the 5' ends of the tRNAs, and is required for mitochondrial translational processes for the synthesis of protein (Li *et al*., 2015; Reinhard *et al*., 2015). Superkiller viralicidic activity 2-like 2 plays a role in pre-mRNA splicing and is required for the processing of rRNA (Schilders *et al*., 2007).

The G-rich sequence factor 1 protein has been reported to regulate RNA processing in mitochondrial RNA granules, (Antonicka *et al*., 2013; Jourdain *et al*., 2013). The increased abundance of these poly (A) RNA binding processes suggests that exposure of hTCEpi cells to the pure *B. oleronius* protein (6 μg/ml) affects the normal cellular RNA processes and the synthesis of protein by the corneal epithelial (hTCEpi) cells.

A number of proteins were significantly decreased in abundance relative to untreated hTCEpi cells (Table 5.14). The proteins cyclin-dependent kinase 6 (Gene: CDK6), epidermal growth factor receptor substrate 15 (Gene: EPS15), and Ras suppressor protein 1 (Gene: RSU1) were observed to be significantly decreased in abundance following a 72 hour exposure of hTCEpi cells to pure *B. oleronius* protein (6 μg/ml) (Table 5.14). Cyclin-dependent kinase 6 and epidermal growth factor receptor substrate 15 have previously been demonstrated to play an important role in the cell proliferation and cell growth, regulating the cell cycle, and promoting cell adherence at corneal epithelial cell junctions (Arpitha *et al*., 2013; Teckchandani *et al*., 2012; Roxrud *et al*., 2008). The Ras suppressor protein 1 is a member of the Ras GTPase superfamily of proteins and is believed to have a role in the Ras signal transduction pathway that is involved in cell proliferation, differentiation, senescence, and apoptosis (Castellano and Downward, 2011; Wittinghofer and Pai, 1991; Bourne *et al*., 1990; Satoh *et al*., 1987; Field *et al*., 1987). The decrease in abundance of these proteins in hTCEpi cells exposed to the pure *B. oleronius* protein (6 μg/ml) preparation may be part of the underlying cellular mechanisms that results in decreased hTCEpi growth and proliferation, and may lead to an irregular corneal epithelial sheet formation *in vivo* where there is a greater likelihood of prolonged exposure to *B. oleronius* proteins.

Similar to the 24 hour exposure of hTCEpi cells to the crude *B. oleronius* protein (6 μg/ml) preparation, a collection of proteins were observed by a string network to function specifically in poly (A) RNA binding (Figure 5.14). These protein identities include serine/arginine repetitive matrix protein 1 (Gene: SRRM1), protein SON (Gene: SON), serine/arginine-rich splicing factor 9 (Gene: SRSF9), eukaryotic translational initiation factor 5B (Gene: EIF5B), nucleolin (Gene: NCL), desmoplakin (Gene: DSK), plectin (Gene: PLEC), and x-ray repair cross-complementing protein 5 (Gene: XRCC5) (Table 5.14).

The serine/arginine repetitive matrix protein 1 has been shown to facilitate pre-mRNA processing functioning as a splicing coactivator by promoting transcript 3'-

end cleavage, and in turn influencing downstream steps involved in gene expression and the export of mRNA from the nucleus (Szymczyna *et al*., 2003; McCracken *et al*., 2002; Blencowe *et al*., 2000, 1998; Eldridge *et al*., 1999). The protein SON is a spliceosome-associated mRNA cofactor that has been shown to coordinate and control mitotic cell cycle progression by RNA splicing (Ahn *et al*., 2011; Huen *et al*., 2010). A decrease in the abundance of the protein SON may contribute to the reduction in hTCEpi cell proliferation following exposure to pure *B. oleronius* protein that was observed in Section 4.3. The serine/arginine-rich splicing factor 9 protein has been shown to be involved in constitutive splicing and modulating the selection of alternative splice sites for pre-mRNA processing (Kondo *et al*., 2004; Wang *et al*., 2005; Wang *et al*., 2004).

Eukaryotic translational initiation factor 5B plays a key role in catalyzing the initiation of the eukaryotic translational complex of RNA processing, and has been demonstrated to regulate larval growth and germline development in *C. elegans* (Fernández *et al*., 2013; Hiraishi *et al*., 2013; Yu *et al*., 2006; Singh *et al*., 2005). Nucleolin is multifunctional and has been shown to be involved in rRNA synthesis and influence gene silencing, senescence, and regulation of the cell cycle (Olson *et al*., 2000; Parada and Roader, 1999; Pederson, 1998).

Desmoplakin is involved in the organization of the desmosomal cadherin-plakoglobin complexes and has been demonstrated to be essential in epithelial sheet formation (Pigors *et al*., 2015; Vasioukhin *et al*., 2001). Plectin has been shown to promote stable cell adhesion of epithelial cells underlying the extracellular matrix, by the formation of hemidesmosome, a multi-protein complex (Gundesli *et al*., 2010; Koster *et al*., 2003). A decrease in the abundance of desmoplakin and plectin may result in the loss of cell adherence and an increase of cell migration and motility that was previously observed in hTCEpi cells exposed to the pure *B. oleronius* protein preparation (O'Reilly *et al*., 2012b).

The x-ray repair cross-complementing protein 5 is a single-stranded DNA-dependent ATP-dependent helicase that has a role in chromosomal translocation, binding to double-stranded DNA in a cell cycle dependent manner, and functions in response to DNA damage (Roberts *et al*., 2010; Willis *et al*., 2002; Chung *et al*., 1996; Tuteja *et al*., 1994). The decrease in the abundance of the collection of proteins that function in poly (A) RNA binding suggests that exposure of hTCEpi cells to the pure *B. oleronius* protein (6 μg/ml) preparation trigger a disruption of the corneal

epithelial surface and may result in the characteristic symptoms that are associated with ocular rosacea.

5.3.3 Summary

LF/MS analysis of hTCEpi cells exposed to crude *B. oleronius* protein (6 µg/ml) and pure *B. oleronius* protein (6 µg/ml) for 24 hour and 72 hour, respectively, resulted in specific changes to the proteome of the hTCEpi cells. Intrestingly, exposure of hTCEpi cells to either *B. oleronius* protein preparation showed leukocyte elastase inhibitor to be exclusive to *B. oleronius* protein treated hTCEpi cells. A large number of proteins identified following exposure to the crude or pure *B. oleronius* protein preparation were observed by string network analysis to function in poly (A) RNA binding. These identified proteins may collectively play a role in the disruption of the corneal epithelial surface and formation of ocular sterile ulcers that are associated with ocular rosacea.

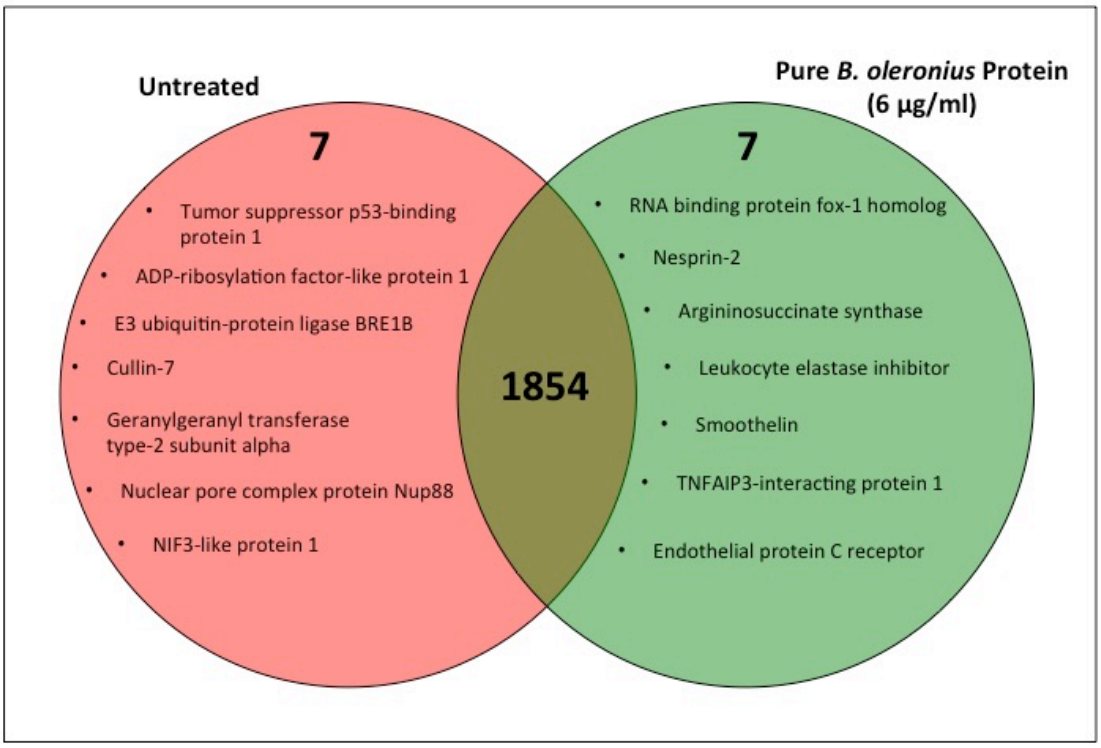

Figure 5.11 A Venn diagram illustrating exclusive proteins identified by LF/MS from hTCEpi cells untreated and treated with pure *B. oleronius* protein (6 µg/ml) following a 72 hour exposure. LF/MS analysis demonstrated 7 proteins (red) to be exclusive to untreated hTCEpi cells, and 7 proteins (green) to be exclusive to crude *B. oleronius* protein (6 µg/ml) treated hTCEpi cells following a 72 hour exposure. A total of 1854 proteins (brown) were observed to be similar to both untreated and treated hTCEpi cells. For a protein to be considered exclusive or unique, it must be detected in a minimum of 3 out of 4 replicates of one treatment, and undetected in 4 out of 4 replicates of the other comparative treatment. Proteins were identified using MaxQuant and Blast2Go computer software (Section 2.18). LF/MS: label free mass spectrometry. (n = 4, for each treatment).

Table 5.11 LF/MS protein identities exclusive to untreated hTCEpi cells following a 72 hour exposure. For a protein to be considered exclusive or unique, it must be detected in a minimum of 3 out of 4 replicates of one treatment, and undetected in 4 out of 4 replicates of the other comparative treatment. Proteins were identified using MaxQuant and Blast2Go computer software (Section 2.18). LF/MS: label free mass spectrometry. (n = 4, for each treatment).

Gene	Untreated LFQ Intensity				Pure *B. oleronius* Protein (6 µg/ml) LFQ Intensity				MS/MS Count	Peptides	Sequence Coverage (%)	Mol. Weight (kDa)	Protein Identity	UniProt Protein Function
	1	2	3	4	1	2	3	4						
TP53BP1	1.92E+07	1.58E+07	0	1.64E+07	0	0	0	0	5	4	4.3	209.02	Tumor Suppressor p53-Binding Protein 1	Response to DNA Damage
ARL1	1.20E+07	2.15E+07	0	2.28E+07	0	0	0	0	5	2	40.4	5.85	ADP-Ribosylation Factor-like Protein 1	Nucleotide-Binding
RNF40	1.36E+07	0	1.79E+07	1.84E+07	0	0	0	0	5	3	7.1	79.01	E3 Ubiquitin-Protein Ligase BRE1B	Chromatin Regulator
CUL7	2.01E+07	1.80E+07	0	1.81E+07	0	0	0	0	6	2	1.2	191.16	Cullin-7	Epithelial to Mesenchymal Transition
RABGGTA	1.08E+07	1.32E+07	1.47E+07	1.61E+07	0	0	0	0	4	3	7.1	65.07	Geranylgeranyl Transferase Type-2 Subunit Alpha	Zinc Ion Binding
NUP88	1.29E+07	1.32E+07	2.61E+07	1.95E+07	0	0	0	0	5	3	6.3	83.54	Nuclear Pore Complex Protein Nup88	mRNA Transport
NIF3L1	4.91E+07	3.38E+07	0	3.07E+07	0	0	0	0	3	2	8.3	38.98	NIF3-like Protein 1	Transcription Factor Binding

Table 5.12 LF/MS protein identities exclusive to hTCEpi cells treated with pure *B. oleronius* protein (6 µg/ml) following a 72 hour exposure. For a protein to be considered exclusive or unique, it must be detected in a minimum of 3 out of 4 replicates of one treatment, and undetected in 4 out of 4 replicates of the other comparative treatment. Proteins were identified using MaxQuant and Blast2Go computer software (Section 2.18). LF/MS: label free mass spectrometry. (n = 4, for each treatment).

Gene	Untreated LFQ Intensity				Pure *B. oleronius* Protein (6 µg/ml) LFQ Intensity				MS/MS Count	Peptides	Sequence Coverage (%)	Mol. Weight (kDa)	Protein Identity	UniProt Protein Function
	1	2	3	4	1	2	3	4						
RBM9	0	0	0	0	2.49E+07	1.84E+07	0	2.17E+07	5	2	22.6	23.76	RNA Binding Protein Fox-1 Homolog	Poly (A) RNA Binding Protein
SYNE2	0	0	0	0	0	5.64E+07	6.62E+07	6.35E+07	4	4	0.7	787.71	Nesprin-2	Actin-Binding
ASS1	0	0	0	0	5.02E+07	4.94E+07	0	4.17E+07	7	2	12.9	46.53	Argininosuccinate Synthase	Poly (A) RNA Binding Protein
SERPINB1	0	0	0	0	1.14E+07	1.13E+07	0	1.16E+07	3	3	9	42.74	Leukocyte Elastase Inhibitor	Serine Protease Inhibitor
SMTN	0	0	0	0	2.94E+07	3.48E+07	0	3.79E+07	9	8	13.9	98.92	Smoothelin	Actin-Binding
TNIP1	0	0	0	0	0	9.32E+06	1.81E+07	1.06E+07	3	3	6.5	66.01	TNFAIP3-Interacting Protein 1	Inflammatory Response
PROCR	0	0	0	0	3.24E+07	3.32E+07	0	2.54E+07	8	2	10.9	26.67	Endothelial Protein C Receptor	Blood Coagulation

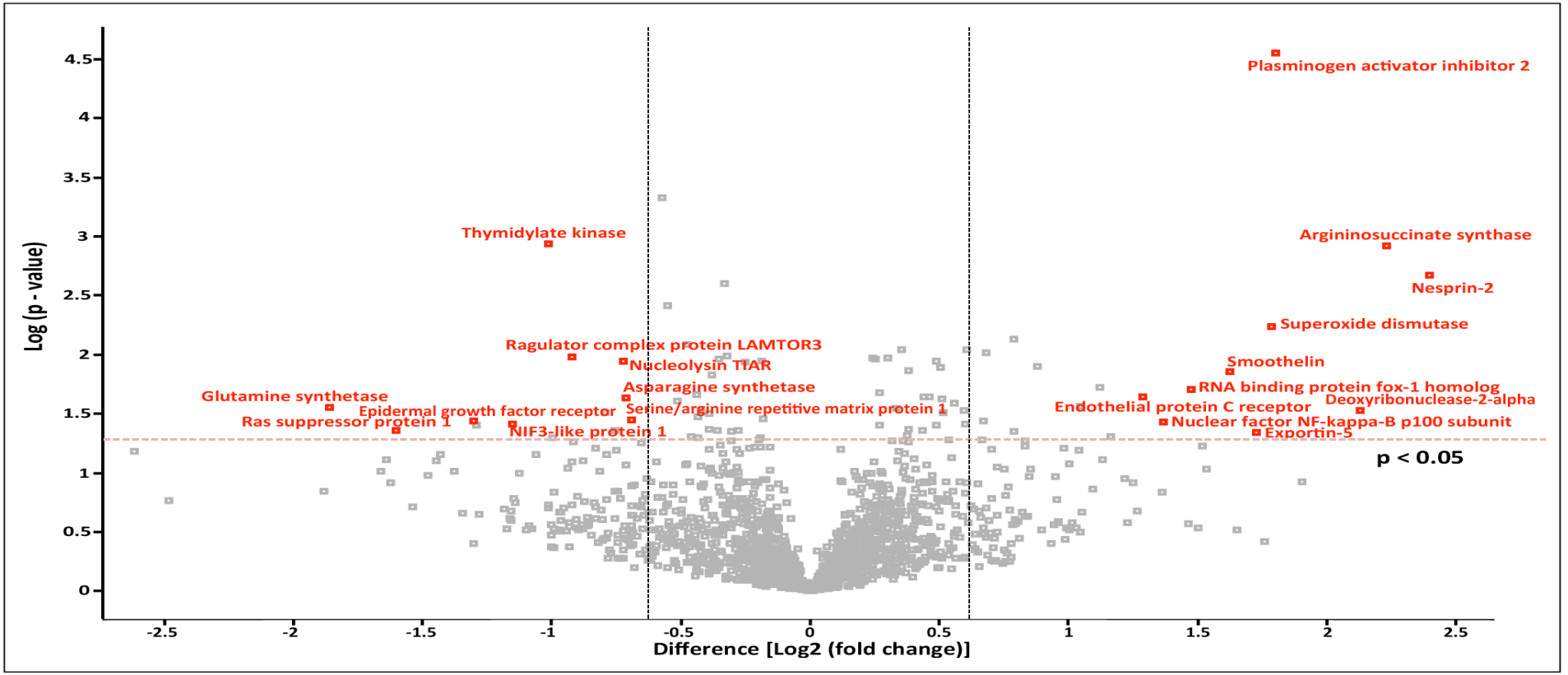

Figure 5.12 A volcano plot demonstrating the fold change of hTCEpi proteins identified by LF/MS following a 72 hour exposure to crude *B. oleronius* protein (6 µg/ml) relative to untreated hTCEpi cells. LF/MS analysis (Section 2.18) demonstrating the distribution of hTCEpi proteins increased and decreased abundance following a 72 exposure to crude *B. oleronius* protein (6 µg/ml) relative to untreated hTCEpi cells. Identities (red) above -Log of 1.3 are considered statistically significant (red dashed line). LF/MS: label free mass spectrometry. (n = 4, for each treatment).

Table 5.13 LF/MS protein identities from hTCEpi cells exposed to pure *B. oleronius* protein (6 µg/ml) for 72 hour that were increased in abundance relative to untreated hTCEpi cells. LF/MS: label free mass spectrometry. (n = 4, for each treatment).

Gene	Untreated LFQ Intensity	Pure Protein (6 µg/ml) LFQ Intensity	MS/MS Count	Peptides	Sequence Coverage (%)	Mol. Weight (kDa)	Protein Identity	-Log (p-Value)	Difference [Log_2 (fold change)]	UniProt Protein Function
SYNE2	23.05	25.45	4	4	0.7	787.71	Nesprin-2	2.67	2.40	Actin-Binding
ASS1	22.98	25.21	7	2	12.9	46.53	Argininosuccinate Synthase	2.92	2.23	Poly (A) RNA Binding Protein
DNASE2	23.19	25.33	11	4	14.1	33.62	Deoxyribonuclease-2-Alpha	1.50	2.14	Apoptosis
SERPINB2	28.18	29.98	99	22	56.1	46.60	Plasminogen Activator Inhibitor 2	4.56	1.80	Serine Protease Inhibitor
SOD2	27.61	29.40	56	11	81.8	19.73	Superoxide Dismutase	2.23	1.78	Oxidative Stress
XPO5	23.70	25.42	11	7	8.4	136.31	Exportin-5	1.34	1.73	RNA-Binding
SMTN	23.18	24.81	9	8	13.9	98.92	Smoothelin	1.85	1.63	Actin-Binding
RBM9	22.85	24.32	5	2	22.6	23.76	RNA Binding Protein Fox-1 Homolog	1.70	1.48	Poly (A) RNA Binding Protein
NFKB2	24.57	25.94	15	4	7.8	96.68	Nuclear Factor NF-kappa-B p100 Subunit	1.40	1.37	Regulation of Transcription
PROCR	23.32	24.60	8	2	10.9	26.67	Endothelial Protein C Receptor	1.61	1.29	Blood Coagulation
CYB5R1	22.31	23.47	5	3	10.8	34.09	NADH-Cytochrome b5 Reductase 1	1.31	1.16	Lipid Biosynthesis
MRPS16	23.51	24.63	10	4	43.1	15.35	28S Ribosomal Protein S16, Mitochondrial	1.73	1.12	Ribosomal Protein
RAB34	22.44	23.48	3	2	43.1	5.84	Ras-Related Protein Rab-34	1.57	1.05	Protein Transport
SQSTM1	25.78	26.66	38	8	23.6	47.69	Sequestosome-1	1.90	0.88	Zinc Ion Binding
NDUFA5	26.12	26.91	19	6	55.2	13.46	NADH Dehydrogenase [Ubiquinone] 1 Alpha Subcomplex Subunit 5	1.35	0.79	Electron Transport
ALDH1A3	30.89	31.67	328	44	79.1	56.11	Aldehyde Dehydrogenase Family 1 Member A3	2.13	0.79	Oxidoreductase
LAMB3	29.35	30.03	247	56	64.8	129.57	Laminin Subunit Beta-3	2.02	0.68	Cell Adhesion
LAMC2	29.38	30.05	205	52	53.1	130.97	Laminin Subunit Gamma-2	1.44	0.67	Cell Adhesion

Table 5.13 (Continued) LF/MS protein identities from hTCEpi cells exposed to pure *B. oleronius* protein (6 µg/ml) for 72 hour that were increased in abundance relative to untreated hTCEpi cells. LF/MS: label free mass spectrometry. (n = 4, for each treatment).

Gene	Untreated LFQ Intensity	Pure Protein (6 µg/ml) LFQ Intensity	MS/MS Count	Peptides	Sequence Coverage (%)	Mol. Weight (kDa)	Protein Identity	-Log (p-Value)	Difference [Log_2 (fold change)]	UniProt Protein Function
DYNC1LI1	24.18	24.79	10	5	14.1	56.58	Cytoplasmic Dynein 1 Light Intermediate Chain 1	2.04	0.61	Cell Cycle
GMFB	26.10	26.70	22	5	51.4	16.71	Glia Maturation Factor Beta	1.41	0.60	Growth Factor
PLOD2	26.64	27.24	47	16	35.1	81.17	Procollagen-Lysine,2-Oxoglutarate 5-Dioxygenase 2	1.53	0.59	Iron Ion Binding
NAMPT	28.63	29.19	76	23	53.6	55.52	Nicotinamide Phosphoribosyltransferase	1.59	0.56	Cell-Cell Signaling
TRMT10C	23.70	24.21	9	4	14.1	47.35	Mitochondrial Ribonuclease P Protein 1	1.51	0.51	Poly (A) RNA Binding Protein
SKIV2L2	25.28	25.78	21	10	14.5	117.80	Superkiller Viralicidic Activity 2-like 2	1.63	0.51	Poly (A) RNA Binding Protein
MAP7D1	26.55	27.06	59	18	30.9	92.82	MAP7 Domain-Containing Protein 1	1.89	0.51	Cytoskeletal Organization
TPM4	30.81	31.30	165	34	82.7	28.52	Tropomyosin Alpha-4 Chain	1.94	0.49	Actin-Binding
PGM3	25.39	25.88	12	3	13.4	51.08	Phosphoacetylglucosamine Mutase	1.40	0.49	Metabolism
STAM2	23.55	24.01	6	2	6.9	58.16	Signal Transducing Adapter Molecule 2	1.64	0.46	Protein Transport
PRPF4	25.04	25.49	21	9	23	58.32	U4/U6 Small Nuclear Ribonucleoprotein Prp4	1.64	0.44	mRNA Processing
LAMB1	24.36	24.79	23	7	5.8	198.04	Laminin Subunit Beta-1	1.36	0.43	Cell Adhesion
P4HA2	27.11	27.49	49	11	30.2	60.63	Prolyl 4-Hydroxylase Subunit Alpha-2	1.37	0.38	Iron Ion Binding
LUZP1	26.99	27.37	54	21	26.5	120.27	Leucine Zipper Protein 1	1.86	0.38	Protein Biosynthesis
ALDH2	24.42	24.79	14	6	16.6	56.38	Aldehyde Dehydrogenase, Mitochondrial	1.31	0.37	Oxidoreductase
FHL2	25.11	25.46	13	4	24.4	32.19	Four and a Half LIM Domains Protein 2	2.04	0.35	Regulation of Transcription
ATP5E	23.41	23.74	6	2	37.3	5.78	ATP Synthase Subunit Epsilon, Mitochondrial	1.55	0.33	Ion Transport
LIMA1	29.92	30.22	245	40	58	85.22	LIM Domain and Actin-Binding Protein 1	1.97	0.30	Actin-Binding
GRSF1	26.65	26.92	29	7	37.6	41.63	G-Rich Sequence Factor 1	1.68	0.27	Poly (A) RNA Binding Protein
PSMD9	26.35	26.62	47	10	42.8	24.55	26S Proteasome Non-ATPase Regulatory Subunit 9	1.40	0.27	Chaperone Protein
TLN1	30.66	30.92	380	96	51.6	269.76	Talin-1	1.96	0.25	Vinculin Binding
DNAJC7	25.39	25.63	15	9	22.9	56.44	DnaJ Homolog Subfamily C Member 7	1.97	0.24	Heat Shock Protein

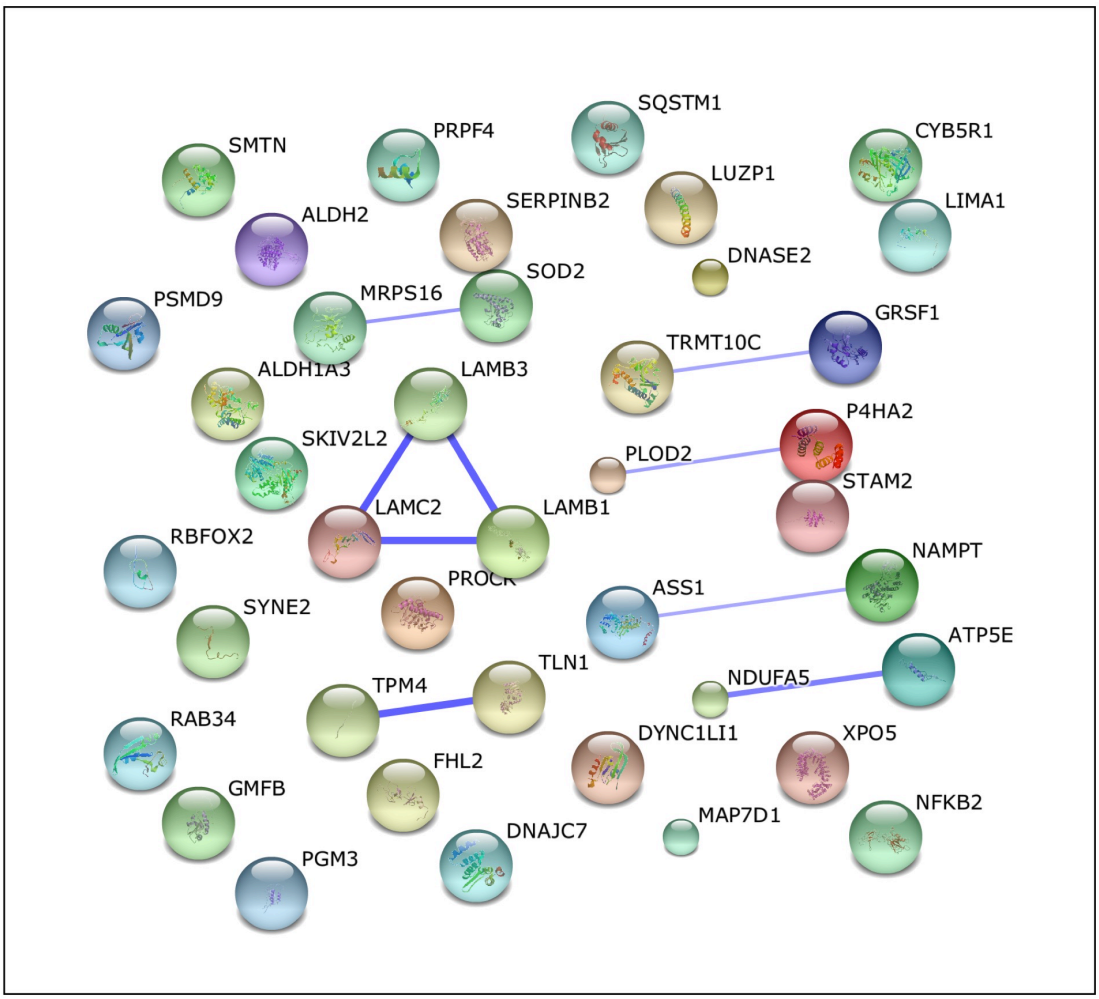

Figure 5.13 String network analysis of proteins increased in abundance following a 72 hour exposure of hTCEpi cells to pure *B. oleronius* protein (6 µg/ml). String network of proteins decreased in abundance following a 72 hour exposure of hTCEpi cells with crude *B. oleronius* protein (6 µg/ml). (n = 4, for each treatment).

Table 5.14 LF/MS protein identities from hTCEpi cells exposed to pure *B. oleronius* protein (6 µg/ml) for 72 hour that were decreased in abundance relative to untreated hTCEpi cells. LF/MS: label free mass spectrometry. (n = 4, for each treatment).

Gene	Untreated LFQ Intensity	Pure Protein (6 µg/ml) LFQ Intensity	MS/MS Count	Peptides	Sequence Coverage (%)	Mol. Weight (kDa)	Protein Identity	-Log (p-Value)	Difference [Log_2 (fold change)]	UniProt Protein Function
XRCC5	31.09	30.91	284	47	81.1	82.70	X-Ray Repair Cross-Complementing Protein 5	1.46	-0.18	Poly (A) RNA Binding Protein
FBL	29.26	29.07	89	14	57.6	33.78	rRNA 2-O-Methyltransferase Fibrillarin	1.95	-0.19	Calmodulin-Binding
PLEC	33.98	33.72	2394	420	78.3	516.19	Plectin	1.94	-0.25	Poly (A) RNA Binding Protein
SRM	27.25	26.98	40	12	54	33.82	Spermidine Synthase	1.36	-0.28	Transferase
ADK	27.58	27.28	49	10	44.3	36.58	Adenosine Kinase	1.35	-0.30	Nucleotide-Binding
DSP	31.52	31.20	656	161	64.7	331.77	Desmoplakin	1.99	-0.32	Poly (A) RNA Binding Protein
PPP3CA	26.77	26.44	30	11	33.7	52.67	Serine/Threonine-Protein Phosphatase 2B Catalytic Subunit Alpha Isoform	2.60	-0.33	Calmodulin-Binding
NCL	32.65	32.30	360	48	48.7	76.61	Nucleolin	1.96	-0.35	Poly (A) RNA Binding Protein
WARS	28.30	27.94	61	14	33.3	53.17	Tryptophan--tRNA Ligase, Cytoplasmic	1.36	-0.36	Nucleotide-Binding
EIF5B	28.12	27.74	50	17	23	138.83	Eukaryotic Translation Initiation Factor 5B	1.83	-0.38	Poly (A) RNA Binding Protein
FKBP5	28.95	28.55	111	26	59.7	51.21	Peptidyl-Prolyl Cis-Trans Isomerase FKBP5	1.50	-0.39	Chaperone Protein
DARS	27.96	27.57	62	23	56.9	57.14	Aspartate--tRNA Ligase, Cytoplasmic	1.37	-0.39	Nucleotide-Binding
ANXA8	30.75	30.33	152	32	85	36.88	Annexin A8	1.53	-0.42	Blood Coagulation
JUP	28.40	27.97	69	26	45.1	81.74	Junction Plakoglobin	1.30	-0.43	Cell Adhesion
CKMT1B	27.87	27.43	33	7	47.5	29.19	Creatine Kinase U-Type, Mitochondrial	1.47	-0.44	Nucleotide-Binding
SRSF9	26.57	26.13	29	10	56.6	25.54	Serine/Arginine-Rich Splicing Factor 9	1.66	-0.44	Poly (A) RNA Binding Protein
COPB1	29.29	28.83	108	27	42.3	107.14	Coatomer Subunit Beta	1.31	-0.46	Protein Transport
PHGDH	29.18	28.70	83	24	49.7	56.65	D-3-Phosphoglycerate Dehydrogenase	2.09	-0.47	Serine Biosynthesis
SON	26.50	25.98	27	9	10.3	232.30	Protein SON	1.61	-0.51	Poly (A) RNA Binding Protein
PPP1R7	26.81	26.26	22	10	42.9	36.84	Protein Phosphatase 1 Regulatory Subunit 7	2.42	-0.55	Regulation of Enzyme Activity
PSAT1	27.72	27.15	52	20	60.5	40.42	Phosphoserine Aminotransferase	3.32	-0.57	Serine Biosynthesis

Table 5.14 (Continued) LF/MS protein identities from hTCEpi cells exposed to pure *B. oleronius* protein (6 µg/ml) for 72 hour that were decreased in abundance relative to untreated hTCEpi cells. LF/MS: label free mass spectrometry. (n = 4, for each treatment).

Gene	Untreated LFQ Intensity	Pure Protein (6 µg/ml) LFQ Intensity	MS/MS Count	Peptides	Sequence Coverage (%)	Mol. Weight (kDa)	Protein Identity	-Log (p-Value)	Difference [Log_2 (fold change)]	UniProt Protein Function
SRRM1	24.11	23.43	6	4	7.1	102.12	Serine/Arginine Repetitive Matrix Protein 1	1.45	-0.69	Poly (A) RNA Binding Protein
ASNS	24.99	24.27	12	9	18.6	54.82	Asparagine Synthetase [Glutamine-Hydrolyzing]	1.64	-0.71	Asparagine Biosynthesis
TIAL1	25.17	24.45	12	5	18.1	41.59	Nucleolysin TIAR	1.95	-0.72	Nucleotide-Binding
RAB3GAP2	25.20	24.45	10	8	10.3	155.98	Rab3 GTPase-Activating Protein Non-Catalytic Subunit	1.36	-0.76	Regulation of GTPase Activity
RABGGTA	23.69	22.90	4	3	7.1	65.07	Geranylgeranyl Transferase Type-2 Subunit Alpha	1.51	-0.79	Rab GTPase Binding
LAMTOR3	26.09	25.17	15	1	19.7	12.94	Ragulator Complex Protein LAMTOR3	1.98	-0.92	Regulation of GTPase Activity
DTYMK	26.78	25.76	21	6	30.2	23.82	Thymidylate Kinase	2.94	-1.01	Transferase
NIF3L1	24.94	23.79	3	2	8.3	38.98	NIF3-like Protein 1	1.41	-1.15	Transcription Factor Binding
CDK6	25.97	24.68	13	6	24.5	36.94	Cyclin-Dependent Kinase 6	1.41	-1.29	Cell Cycle
EPS15	25.42	24.12	7	5	12.4	98.66	Epidermal Growth Factor Receptor Substrate 15	1.44	-1.30	Protein Transport
RSU1	26.00	24.40	9	6	39.7	31.54	Ras Suppressor Protein 1	1.36	-1.60	Signal Transduction
GLUL	27.27	25.41	41	17	58.7	42.06	Glutamine Synthetase	1.56	-1.86	Nucleotide-Binding

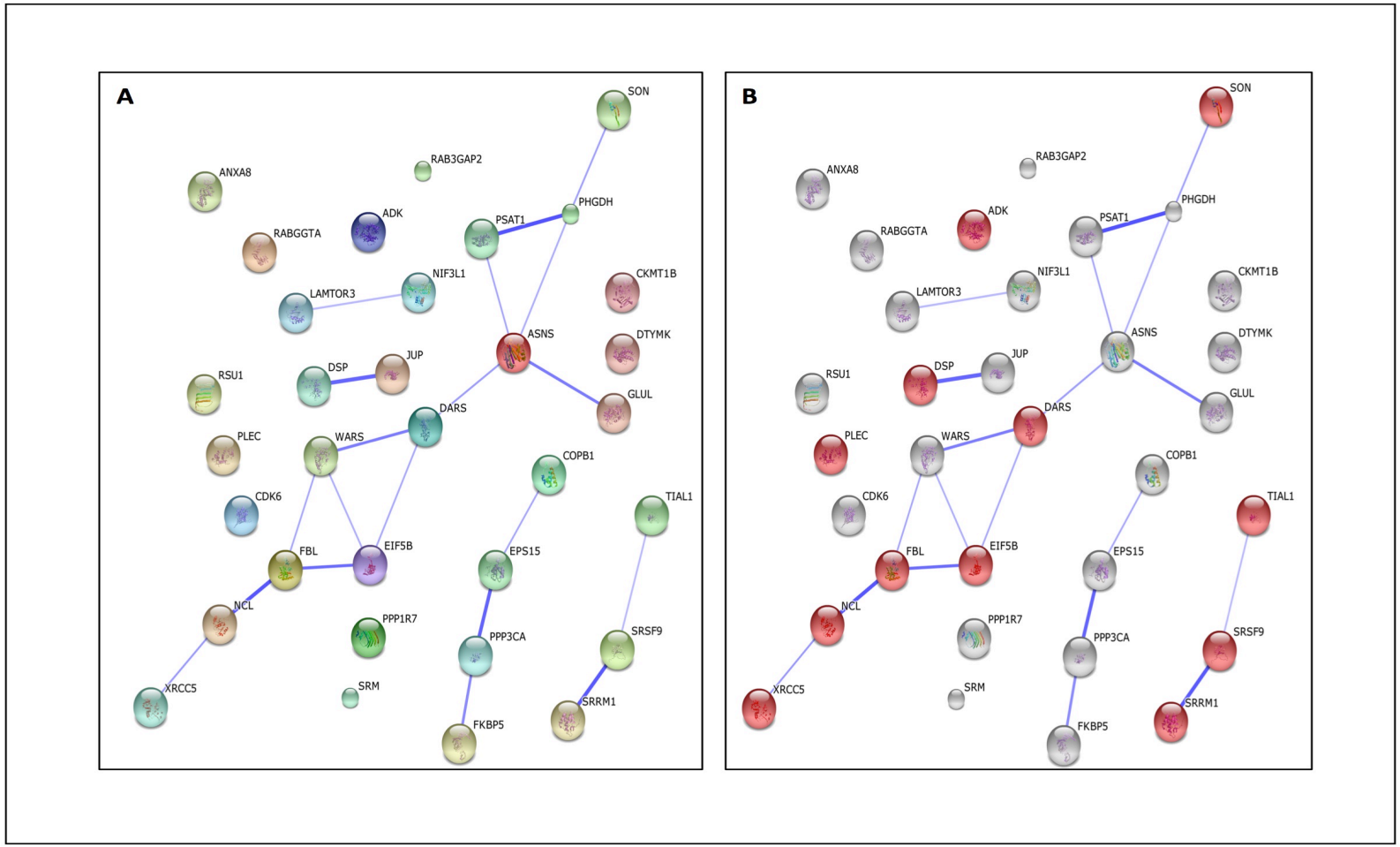

Figure 5.14 String network analysis of proteins decreased in abundance following a 72 hour exposure of hTCEpi cells treated with pure *B. oleronius* protein (6 µg/ml). (**A**) String network of proteins decreased in abundance following a 72 hour exposure of hTCEpi cells with pure *B. oleronius* protein (6 µg/ml). (**B**) Proteins (red) that function as Poly (A) RNA binding proteins. (n = 4, for each treatment).

5.4 Discussion

The bacterium, *B. oleronius*, was previously isolated from the hindgut of a *Demodex* mite of a patient with papulopustular rosacea, and two proteins were identified to be sera reactive in rosacea patients with erythematotelangiectatic, papulopustular, and ocular rosacea (O'Reilly *et al*., 2012c; Li *et al*., 2010; Lacey *et al*., 2007). Theses immungenic proteins were isolated and purified by ÄKTA FPLC, and shown to induce the activation of human neutrophils (O'Reilly *et al*., 2012a). Furthermore, the effect of *B. oleronius* proteins on a corneal epthelial cell line (hTCEpi) was used to investigate the potential role of *B. oleronius* in the development of ocular rosacea (O'Reilly *et al*., 2012b). The results indicated alterations in the phenotype of hTCEpi cells exposed to the *B. oleronius* proteins leading to increased cell migration and cell invasiveness, and an increase of matrix metalloproteinases, *MMP-3* and *MMP-9*. Thus, suggesting an aberrant wound healing response induced in hTCEpi cells exposed to *B. oleronius* proteins. Here, the proteomic response of hTCEpi cells to the *B. oleronius* protein preparations was investigated to identify proteins that may implicate *B. oleronius* in ocular rosacea.

A 24 hour or 72 hour exposure of hTCEpi cells to the pure or crude *B. oleronius* proteins lead to alterations in the profile of the secretome and proteome of hTCEpi cells by 1-D SDS-PAGE (Figure 5.1, and Figure 5.3, respectively). The identified proteins are associated with many biological processes, and support previous findings that have shown the hTCEpi cells to become more motile and invasive following treatment with the *B. oleronius* protein preparations (O'Reilly *et al*., 2012b). It was demonstrated that the *B. oleronius* proteins may have a capacity to alter the corneal epithelial surface causing the symptoms associated with ocular rosacea.

The secretome of hTCEpi cells was investigated following a 24 hour and 72 hour exposure to *B. oleronius* proteins, and the abundance of the identified proteins was calculated (Table 5.1 and Table 5.2). Transferrin was identified following LC/MS analysis of the secretome of hTCEpi cells. Transferrin is an iron-binding protein that functions in the regulation and transport of free iron *in vivo* (Gomme *et al*., 2005). Transferrin has been associated with the growth and differentiation of cells, and has been related to many biological processes including embryo-morphogenesis, mitogenesis, chemotaxis, cell proliferation, neurotrophic activity, and angiogenesis (Paez *et al*., 2002; Ohtsuka *et al*., 2001; Carlevaro *et al*., 1997; Bruinink *et al*., 1996; Sirbasku *et al*., 1991; Shim-Oka *et al*., 1986). The

binding and release of iron by transferrin has been demonstrated to be regulated by a pH – anion mechanism (He *et al*., 2000). Carbonate and chloride ions have been shown to be important for the stability and functionality of the iron-binding site, respectively (He *et al*., 2000). Transferrin has been shown to be involved in promoting the growth of pathogenic bacteria *in vivo* by the sequestering of free iron (Teehan *et al*., 2004; Parkkinen *et al*., 2002). The increase in the abundance of transferrin in hTCEpi cells may facilitate the growth and pathogenic potential of *B. oleronius* proteins leading to the induction of an inflammatory response and to alterations to the phenotype of hTCEpi cells and extracellular matrix causing disruption of the corneal epithelial surface (Table 5.2).

Peroxisome assembly protein 12 functions in the correct folding and import of proteins into the peroxisomes of cells, that a role in cell metabolism and the detoxification of ROS (Okumoto *et al*., 1998; Lazarow and Fujiki, 1985). These proteins function in an antioxidant capacity in numerous cellular functions, protecting the cell from ROS and environmental stress, and regulating programmed cell death and the inflammatory system, and promoting protein folding (Collett and Messens, 2010; Nakamura *et al*., 2005; Landino *et al*., 2004; Kern *et al*., 2003). The increase in abundance of peroxisome assembly protein 12 in hTCEpi cells exposed to the *B. oleronius* protein preparations suggests that the hTCEpi cells are responding to the oxidative stress induced by the presence of the *B. oleronius* proteins (Table 5.2).

Exposure to pure or crude *B. oleronius* protein preparation demonstrates alterations in the abundance of proteins from the proteome of hTCEpi cells at 24 hour and 72 hour using 1-D SDS-PAGE (Table 5.3, and Table 5.4, respectively). Alterations in the proteome of hTCEpi cells exposed to the *B. oleronius* proteins was also assessed at 72 hour using 2-D SDS-PAGE (Table 5.5, and Table 5.6). Proteins that function in the regulation of the cell cycle, cell growth, and keratinocyte differentiation (annexin A2, 14-3-3 sigma, and protein S100-A11) were altered in abundance following treatment of hTCEpi cells to the *B. oleronius* protein preparations (Section 5.1.2 and Section 5.2.1). Also, structural proteins such as myosin-9 and profilin-1 were observed to be altered in abundance following exposure of hTCEpi cells to the *B. oleronius* protein preparations, suggesting that the *B. oleronius* poroteins are inducing a phenotypic change to the hTCEpi cells. Previously, O'Reilly *et al*. (2012b) demonstrated that exposure of hTCEpi cells to *B. oleronius* proteins resulted in a change in hTCEpi cell structure, increasing hTCEpi

cell invasiveness and migration.

It was observed that exposure of hTCEpi cells to either the crude or pure *B. oleronius* protein preparation resulted in either increased or decreased protein abundance at either 24 hour or 72 hour. This was most notable in the case of the abundance of protein S100-A11 (Table 5.4 and Table 5.5). The crude *B. oleronius* protein preparation contains proteins extracted from *B. oleronius* cell lysates and represent all proteins present in the *B. oleronius*. Whereas, the pure *B. oleronius* protein preparation contains a collection of proteins that have been previously shown to be serolgically reactive in rosacea patients, and was purified using ÄKTA FPLC™ (Section 4.1) (O'Reilly *et al*., 2012c; Li *et al*., 2010; Lacey *et al*., 2007). It can be suggested that the observed difference may be due in part to the composition of protein in each *B. oleronius* protein preparation, and that the different protein preparations can cause altered biological responses *in vitro*.

Heat shock proteins (Hsps) are members of the chaperonins family of proteins and are known to be molecular chaperones that assist with the correct folding of polypeptides induced by heat stress conditions, and can be classifed according to molecular mass in kilodaltons (Urbak and Vorum, 2010; Arrigo and Simon, 2010; Hartl and Hayer-Hartl, 2002; Groenen *et al*., 1994; Linquist and Craig, 1988). Hsps are involved in cell growth and the cell cycle, with cyclin dependent kinase (CDK) Hsp70 phosphorylation reported to regulate the abundance of G_1 cyclin and cell cycle progression (Truman *et al*., 2012).

The expression of Hsps has been shown to be of vital importance to maintaining the differentiated structures of the eye such as the retinal pigment epithelium (Urbak and Vorum, 2010; Arrigo and Simon, 2010; Strunnikova *et al*., 2001). In response to heat-induced stress, tissue insult or injury, oxidative stress or disease, the abundance of Hsps is up-regulated to facilitate the folding of damaged proteins to reorganise the tissues of the eye (Li *et al*., 2003; Omar and Papolla, 1993; Georgopolous and Welch, 1993; Dasgupta *et al*., 1992; Linquist and Craig, 1988). The expression of Hsps has been implicated in range of eye diseases including uveal melanoma, glaucoma, and cataracts (Urbak and Vorum, 2010; Missotten *et al*., 2003; Tezel *et al*., 2000). In the current work, it was observed that Hsp60, Hsp70, and Hsp90 were elevated in abundance following exposure to the *B. oleronius* protein preparations relative to untreated hTCEpi cells. These Hsps are vital for the organisation of tissue structures in the eye, and have been implicated in a number of eye disorders, and that an

increase of these Hsps may result in the disorganization of the corneal epithelial surface that is associated with ocular rosacea (Section 5.1.2 and Section 5.2.1).

A LF/MS study was used to globally analyse the proteome of hTCEpi cells exposed to crude *B. oleronius* proteins (6 μg/ml) for 24 hour, and exposed to pure *B. oleronius* proteins (6 μg/ml) for 72 hour (Section 5.3.1, and Section 5.3.2, respectively). A small number of proteins were observed to be exclusive (unique) to hTCEpi cells exposed to the crude or pure *B. oleronius* (6 μg/ml) protein preparations (Figure 5.7, and Figure 5.11, respectively). Leukocyte elastase inhibitor protein was found to be exclusive to hTCEpi cells treated with the crude or pure *B. oleronius* protein (6 μg/ml) preparation.

Exposure to the crude or pure *B. oleronius* protein (6 μg/ml) preparations resulted in alterations in the abundance of proteins identified from hTCEpi cells (Figure 5.8, and Figure 5.12, respectively). It was observed using string network analysis and UniProt that a group of proteins related to poly (A) RNA binding were increased or decreased in abundance following exposure of hTCEpi cells with crude or pure *B. oleronius* protein (6 μg/ml) preparation (Tables 5.11 – 5.14). Poly (A) RNA binding proteins play an important role in a range of physiological processes including signal transduction, target degradation of proteins and protein synthesis, cell survival, cell cycle and migration, cell proliferation, apoptosis, regulation of transcription, and response to DNA damage (Zhao *et al*., 2015; Zhou *et al*., 2014; Vlachostergios *et al*., 2012; Yamaguchi *et al*., 2012; Wei and Lin, 2012; Kim *et al*., 2008; Ciechanover, 2005; Sakamoto *et al*., 2003). The change in the abundance of the proteins that function in poly (A) RNA binding suggests that exposure of hTCEpi cells to the *B. oleronius* protein results in alterations in hTCEpi cells at a RNA processing level that may lead a disruption of the corneal epithelial surface. These identified proteins may collectively play a role in the disruption of the corneal epithelial surface and formation of ocular sterile ulcers that are associated with ocular rosacea, and may lead to the development of an effective therapy for the treatment of this condition.

Chapter 6

An Investigation of the Effect of *Bacillus oleronius* Proteins on Isolated Neutrophils and PBMC

6.0 Introduction

Rosacea patients demonstrate an elevated density of *Demodex* mites in their skin compared to controls (Erbağci and Özgöztaşi, 1998; Bonner *et al*., 1993; Vance, 1986), and the role of these ectoparasites in the induction of the condition has been the subject of some debate. *Demodex* mites reside within the pilosebaceous unit and inflammation in cases of papulopustular rosacea is often centred on this structure raising the possibility that the trigger for erythema is located there. The nature of the sebum produced on the faces of rosacea patients is different to that in controls and this may facilitate the growth in the *Demodex* population (Ní Raghallaigh *et al*., 2012). It has been suggested that the elevated density of *Demodex* mites may irritate the lining of the pilosebaceous unit and initiate an inflammatory response (Jarmuda *et al*., 2012). A number of studies have suggested that bacteria may play a role in the induction of rosacea (O'Reilly *et al*., 2012a, 2012b, 2012c; Li *et al*., 2010; Whitfeld *et al*., 2011; Lacey *et al*., 2007; Dahl *et al*., 2004).

Neutrophils play a central role in the innate immune response against pathogens and a role in the aetiology of rosacea has been suggested (Akamatsu *et al*., 1990). The infiltration of neutrophils has been shown to be a key feature of the erythema observed in rosacea affected areas of skin, and one suggestion was that antibiotics used in the management of rosacea reduced this process (Akamatsu *et al*., 1991; Miyachi *et al*., 1986; Yoshioka *et al*., 1986). Thus, suggesting exposure of neutrophils to proteins from *B. oleronius* resulted in activation as measured by the release of enzymes via the process of degranulation and the production of inflammatory cytokines (O'Reilly *et al*., 2012c). It was previously reported that peripheral mononuclear cells (PBMC) stimulated with the *B. oleronius* proteins lead to PBMC proliferation, demonstrating a capacity to induce an inflammatory response in rosacea patients (Lacey *et al*., 2007).

The aim of this Chapter was (1) to characterise the response of neutrophils to *B. oleronius* proteins, and (2) to characterise the cytokine secretion profile of isolated PBMC following exposure to *B. oleronius* protein. This may explain how the release of these proteins from *Demodex* mites in the pilosebaceous unit could lead to the activation of the immune response and persistent inflammation which are associated with rosacea.

6.1 Assessment of Endotoxin Activity in *B. oleronius* Protein Preparations by TNF-α ELISpot Assays

The crude and pure *B. oleronius* protein preparations were extracted and purified as described in Section 2.20. To ensure the effects on isolated neutrophils and PBMC following exposure to crude and pure *B. oleronius* protein preparations were not caused by the presence of an endotoxin, the protein preparations were tested against PBMC in a TNF-α ELISpot assay (Section 2.25) to detect minimal amounts of LPS and assess for endotoxin activity.

Isolated PBMC (Section 2.21) were seeded into a 96-well microplate at a density of 5 x 10^5 cells/well, and treated with crude or pure *B. oleronius* protein (2, 0.2, 0.002, and 0.0002 µg/ml), lipopolysaccharide (LPS) (10, 1, 0.1, and 0.001 ng/ml), and with or without the addition of polymyxin B (10 µg/ml) to specific sample wells to inhibit LPS activity if present. Titrations of LPS were performed by ELISpot (Section 2.23) and FluoroSpot (Section 2.24) to confirm the inhibitory effect of the addition of polymyxin B, and a reduction in spot formation (Figure 6.1, and Figure A6.1, respectively). Representative images of LPS stimulated PBMC with or without the addition of polymyxin B can be seen in the Appendix (Figure A6.2 – A6.3).

Addition of LPS led to an increase in the number of TNF-α-secreting cells which at 0.01 and 0.001 ng/ml LPS were effectively inhibited by the action of polymyxin B (10 µg/ml), and the reduction of TNF-α-secreting cells was calculated to be significant ($p = 0.0032$ and $p = 0.0063$, respectively) (Figure 6.1). In contrast, polymyxin B had little or no effect on the TNF-α-inducing capacity of PBMC exposed to both the pure (Figure 6.3) and crude (Figure 6.4) *B. oleronius* protein preparations at 2, 0.2, 0.002, and 0.0002 µg/ml, demonstrating that the induction of TNF-α secretion by PBMC was not due to the presence of the endotoxin, LPS. Representative images of TNF-α ELISpot assay following exposure of PBMC to the crude or pure *B. oleronius* proteins, with or without the addition of polymyxin B, can be seen in the Appendix (Figure A6.4 and Figure A6.5).

6.2 Exposure of Neutrophils to *B. oleronius* Protein Leads to Increased D-*myo*-Inositol 1-Phosphate (IP_1) Levels

The quantification of IP_1 in neutrophils was performed as described (Section 2.26), as this can be used as a measure of inositol 1, 4, 5-triphosphate (IP_3), a second messenger involved in neutrophil signaling (Bokoch, 1995). An increase in IP_1 production was observed following exposure of neutrophils to the pure *B. oleronius* protein preparation at 2 µg/ml (4.7-fold; $p = 0.016$) and 6 µg/ml (4.4-fold; $p = 0.02$), relative to that in unstimulated cells (Figure 6.4). Exposure of neutrophils to the crude *B. oleronius* protein extract lead to an increase of IP_1 in 2 µg/ml (13.9-fold; $p = 0.011$) and 6 µg/ml (10.9-fold; $p = 0.032$) treatments, and these values were similar to IP_1 levels detected for neutrophils stimulated with fMLP (1 µM) (13.8-fold; $p = 0.0146$) and IL-8 (10 ng/ml) (8.5-fold; $p = 0.0046$) (Figure 6.4).

6.3 Calcium (Ca^{2+}) Efflux in Neutrophils Exposed to *B. oleronius* Protein

Previously it was shown that exposure of neutrophils to *B. oleronius* protein preparations lead to neutrophil activation and degranulation (O'Reilly *et al*., 2012c). The activation of neutrophils is characterized by the rapid movement of intracellular Ca^{2+} ions stored in the calciosomes induced by IP_3 receptor binding (Thelen and Wirthmueller, 1994; Billah, 1993; Lew, 1990; Rossi, 1986). Stimulation of neutrophils with *B. oleronius* protein preparations resulted in a rise in released Ca^{2+} (Figure 6.5). The increase in Ca^{2+} levels was significant following exposure of neutrophils to the crude *B. oleronius* protein preparation (2 µg/ml) (1.4-fold; $p = 0.030$) at 10 seconds. At 40 seconds post-injection, Ca^{2+} flux was increased in neutrophils exposed to crude *B. oleronius* protein (1.5-fold; $p = 0.021$), pure *B. oleronius* protein (1.3-fold; $p = 0.003$), and IL-8 (1.3-fold; $p = 0.003$). Stimulation of neutrophils with fMLP (1 µM) resulted in an increase in Ca^{2+} levels compared to the unstimulated control at 10 seconds (1.1-fold), 20 seconds (1.2-fold), 30 seconds (1.2-fold), and 40 seconds (1.2-fold) post-injection but was not statistically significant.

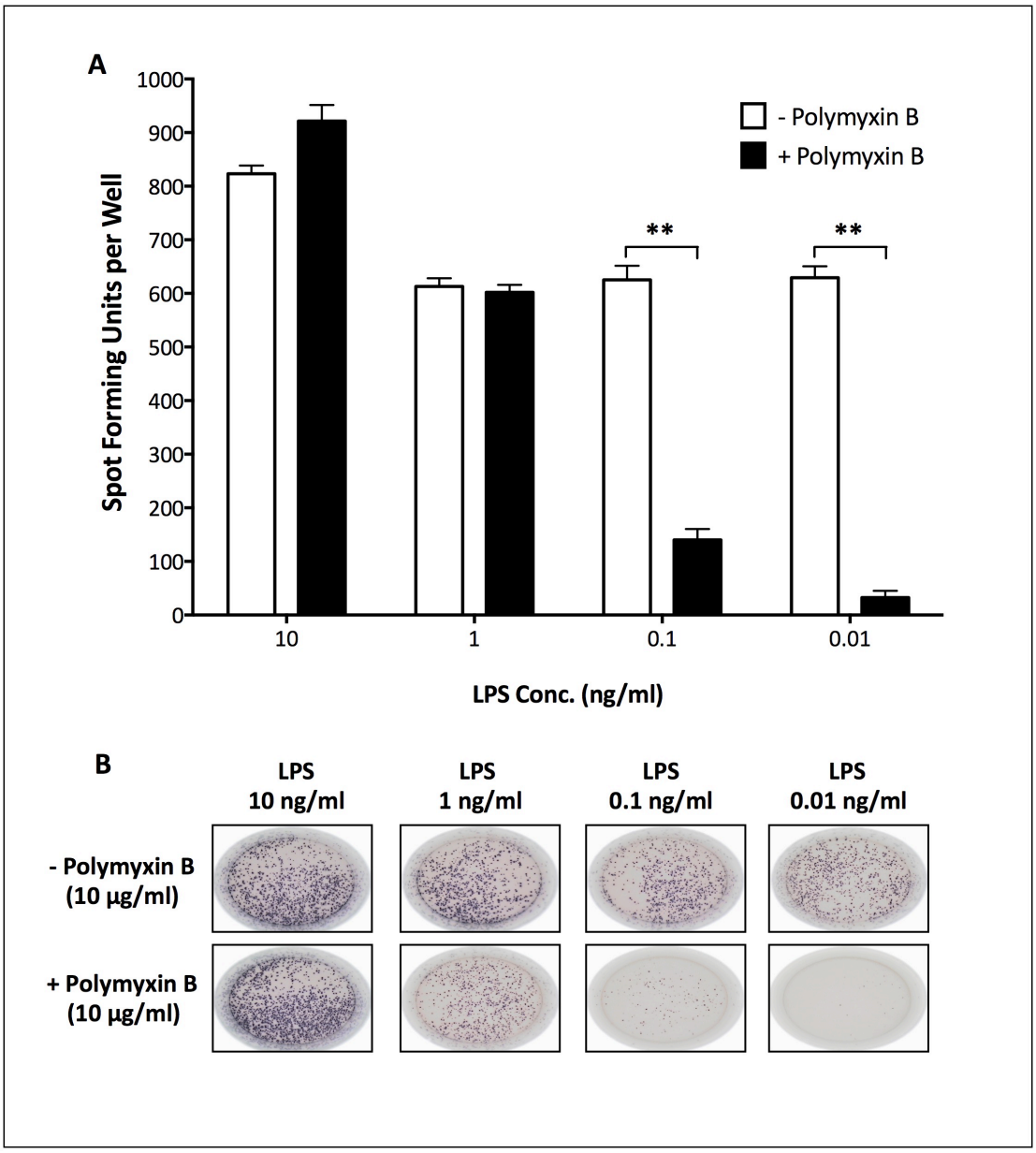

Figure 6.1 Assessment of endotoxin activity and TNF-α secretion in PBMC exposed to LPS by ELISpot. (**A**) Investigating the endotoxin properties of pure and crude *B. oleronius* protein preparations through TNF-α ELISpot, by performing titrations of LPS (10 – 0.01 ng/ml) to examine spot formation induced by endotoxin activity, and inhibition of endotoxin activity by polymyxin B (10 µg/ml) at 0.1 ng/ml LPS. The inhibition of spot formation at 0.1 ng/ml and 0.001 ng/ml LPS following the addition of polymyxin B was significant. (**B**) Representative ELISpot images of spot formation and inhibition were recorded. (n = 3, experiment performed in triplicate). (Significance: ** = $p < 0.01$).

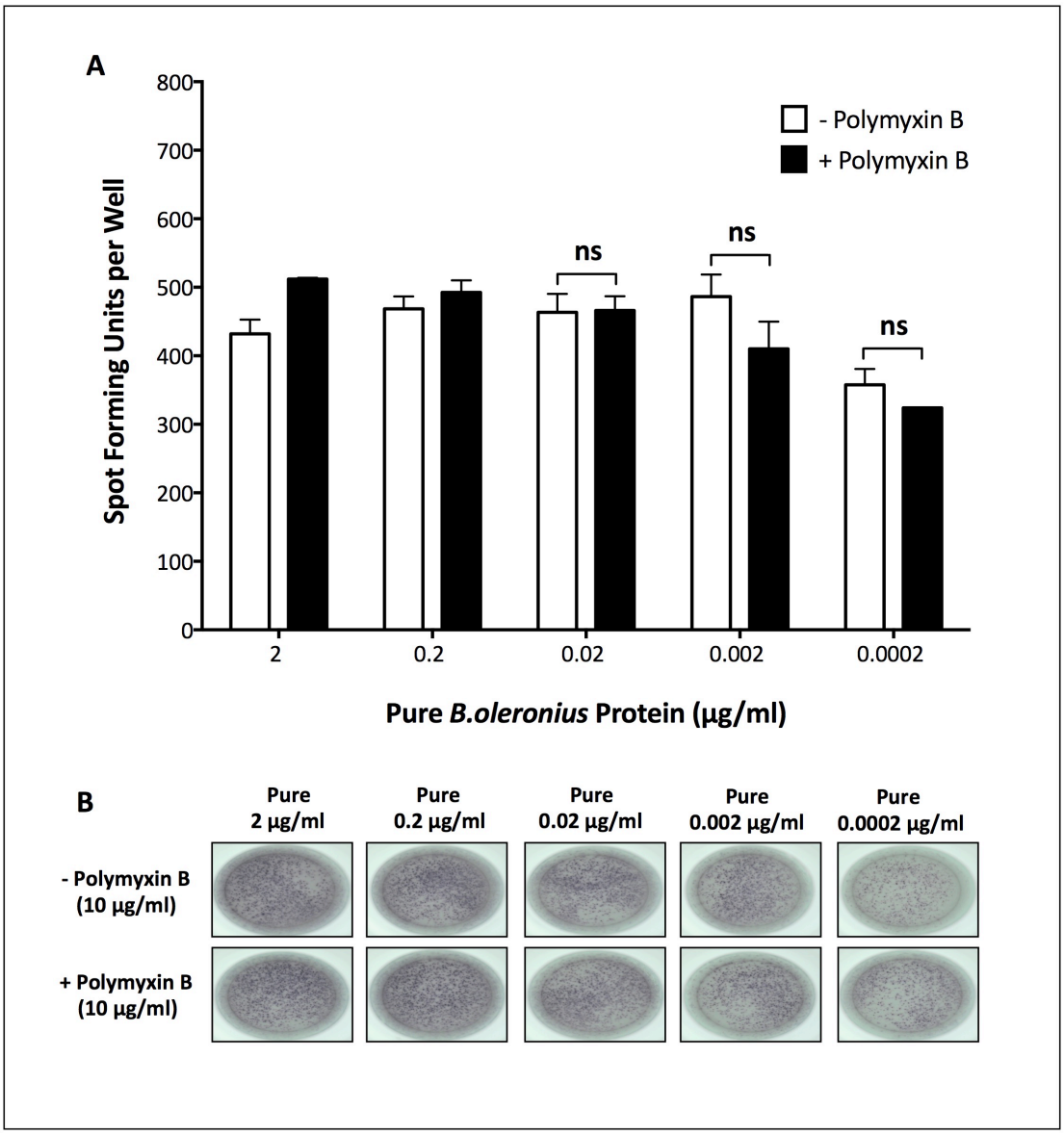

Figure 6.2 Assessment of endotoxin activity and TNF-α secretion in PBMC exposed to pure *B. oleronius* protein by ELISpot. (**A**) Investigating the endotoxin properties of pure *B. oleronius* protein preparations through TNF-α ELISpot. (**B**) Representative ELISpot images of spot formation and inhibition were recorded. (n = 3, experiment performed in triplicate). (ns: not significant).

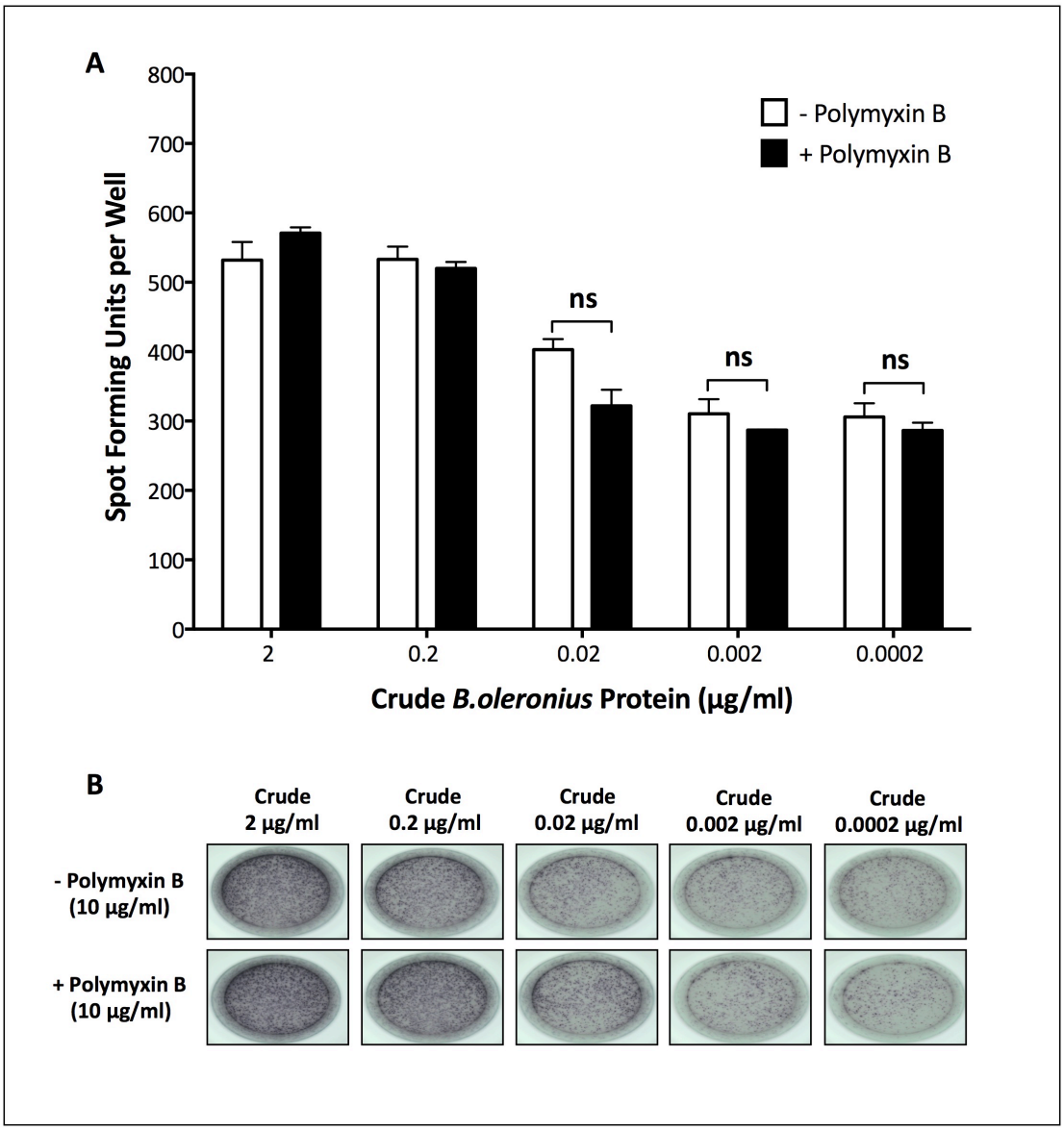

Figure 6.3 Assessment of endotoxin activity and TNF-α secretion in PBMC exposed to crude *B. oleronius* protein by ELISpot. (**A**) Investigating the endotoxin properties of crude *B. oleronius* protein preparations through TNF-α ELISpot. (**B**) Representative ELISpot images of spot formation and inhibition were recorded. (n = 3, experiment performed in triplicate). (ns: not significant).

6.4 Cytoskeletal Reassembly in Neutrophils Induced by *B. oleronius* Protein

The ability of activated neutrophils to perform the morphological and functional changes required to phagocytose and kill an opsonized pathogen is dependent upon the conversion of G-actin to F-actin (Pollard and Cooper, 2009). In this experiment, neutrophils were exposed to crude and pure *B. oleronius* protein preparations (2 and 6 μg/ml) for 10 minutes, and the relative abundance of G-actin and F-actin was measured by Western blot (Figure 6.6A). The distribution ratio was calculated (Figure 6.6B), and the relative densitometric units of G-actin and F-actin were quantified (Figure 6.6C). In unstimulated neutrophils the abundance of G-actin exceeded that of F-actin by 2.6-fold. Stimulation of cells with IL-8 (10 ng/ml) lead to an increase in F-actin (1.7-fold; $p = 0.025$), and a relative decline in G-actin (0.7-fold; $p = 0.028$) compared to unstimulated neutrophils, demonstrating the cytoskeletal conversion of G-actin to F-actin.

Neutrophils exposed to pure *B. oleronius* protein preparation (2 and 6 μg/ml) showed significantly elevated levels of F-actin (2.0-fold; $p = 0.011$, and 1.5-fold; $p = 0.024$, respectively) and reduced abundance of G-actin (0.6-fold; $p = 0.048$, and 0.8-fold; $p = 0.025$, respectively). The increase in F-actin following exposure of neutrophils to pure *B. oleronius* protein at 6 μg/ml was significant compared to pure *B. oleronius* protein at 2 μg/ml ($p = 0.019$), and crude *B. oleronius* protein at 6 μg/ml ($p = 0.008$) (Figure 6.6C).

The relative levels of F-actin were increased in neutrophils exposed to crude *B. oleronius* protein (1.4-fold), as a result of exposure to *B. oleronius* protein at 2 μg/ml ($p = 0.04$). Exposure of neutrophils to crude *B. oleronius* protein at 6 μg/ml induced a 1.7-fold increase in F-actin but this did not reach significance ($p = 0.0557$). The abundance of G-actin declined significantly following exposure of neutrophils to crude *B. oleronius* protein preparation at 2 μg/ml and 6 μg/ml (0.7-fold; $p = 0.0165$, and 0.7-fold; $p = 0.0147$, respectively) relative to unstimulated cells (Figure 6.6C).

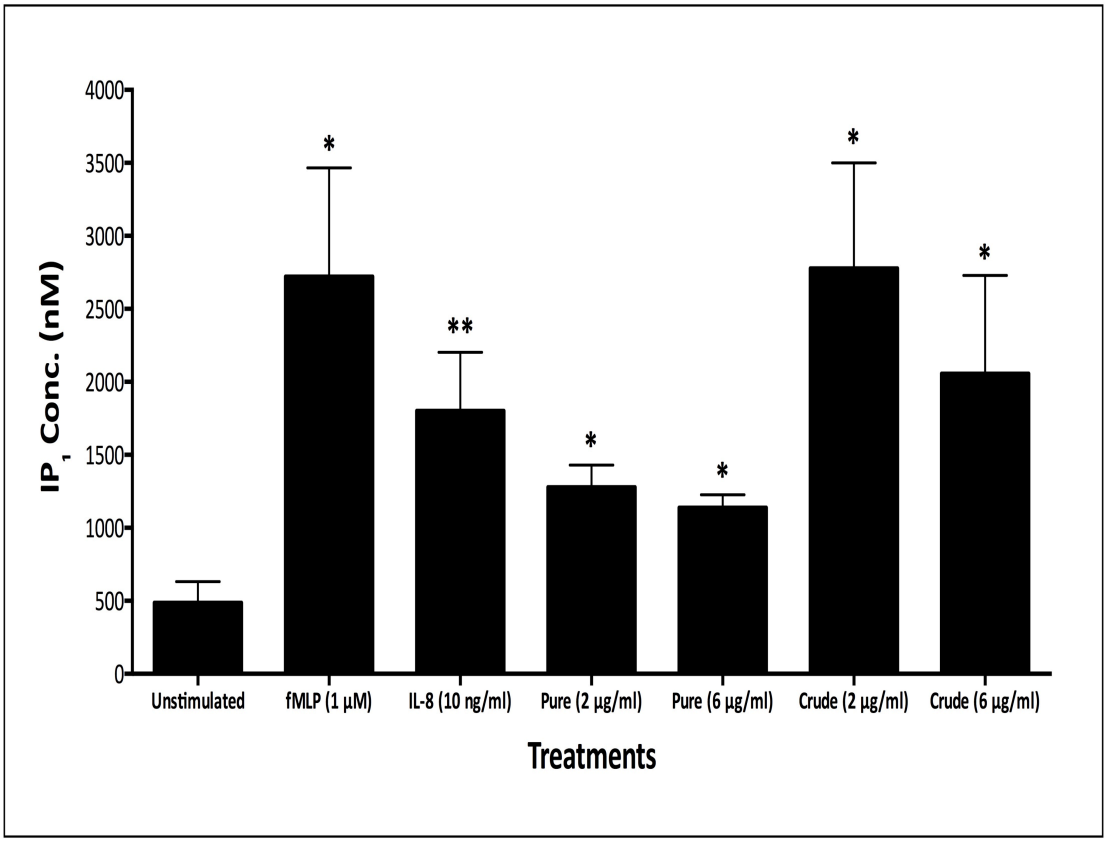

Figure 6.4 Generation of IP_1 by neutrophils exposed to *B. oleronius* proteins. Neutrophils were exposed to PBS (unstimulated), fMLP (1 µM), IL-8 (10 ng/ml), pure *B. oleronius* protein (2 µg/ml and 6 µg/ml), and crude *B. oleronius* protein (2 µg/ml and 6 µg/ml) for 10 minutes, and the effect on IP_1 formation in cytosols was quantified (Section 2.26). (Significance: * = $p < 0.05$, ** = $p < 0.01$). (n = 3, experiment performed in triplicate).

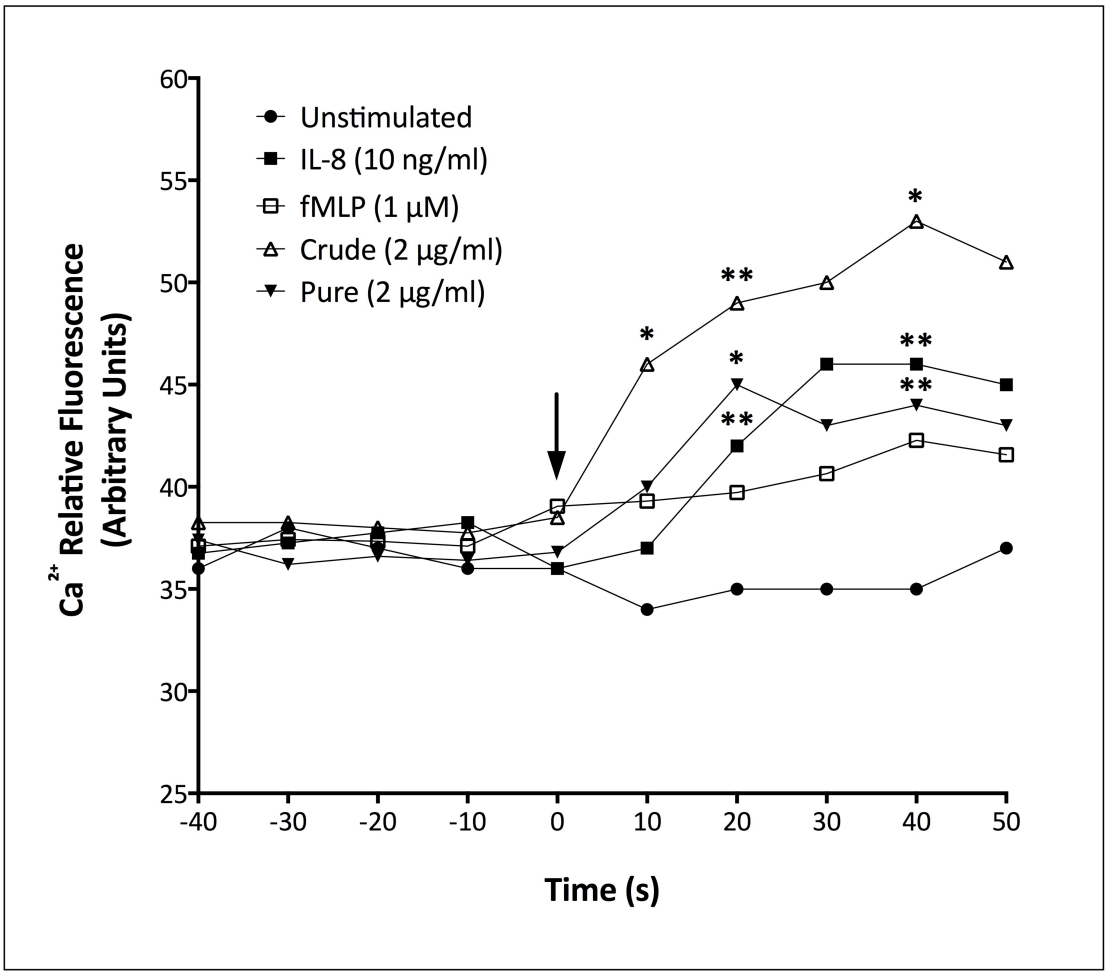

Figure 6.5 Release of stored Ca^{2+} by neutrophils exposed to *B. oleronius* proteins. The effect of *B. oleronius* protein preparation on stored Ca^{2+} flux and release in neutrophils was examined. Isolated neutrophils were exposed to PBS (unstimulated), IL-8 (10 ng/ml) (positive control), fMLP (1 µM) (positive control), crude *B. oleronius* protein (2 µg/ml), or pure *B. oleronius* protein (2 µg/ml), and the effect of cytosolic Ca^{2+} flux was measured (Section 2.27). Stimulation of neutrophils by the different treatments occurred at 0 seconds (s) (injection of stimulants indicated by arrow (🡻)). (Significance: * = $p < 0.05$, ** = $p < 0.01$). (Figure is a representative of one repeat of the assay performed in triplicate (n = 3), and the statistics are representative of the assay performed in triplicate relative to the unstimulated control).

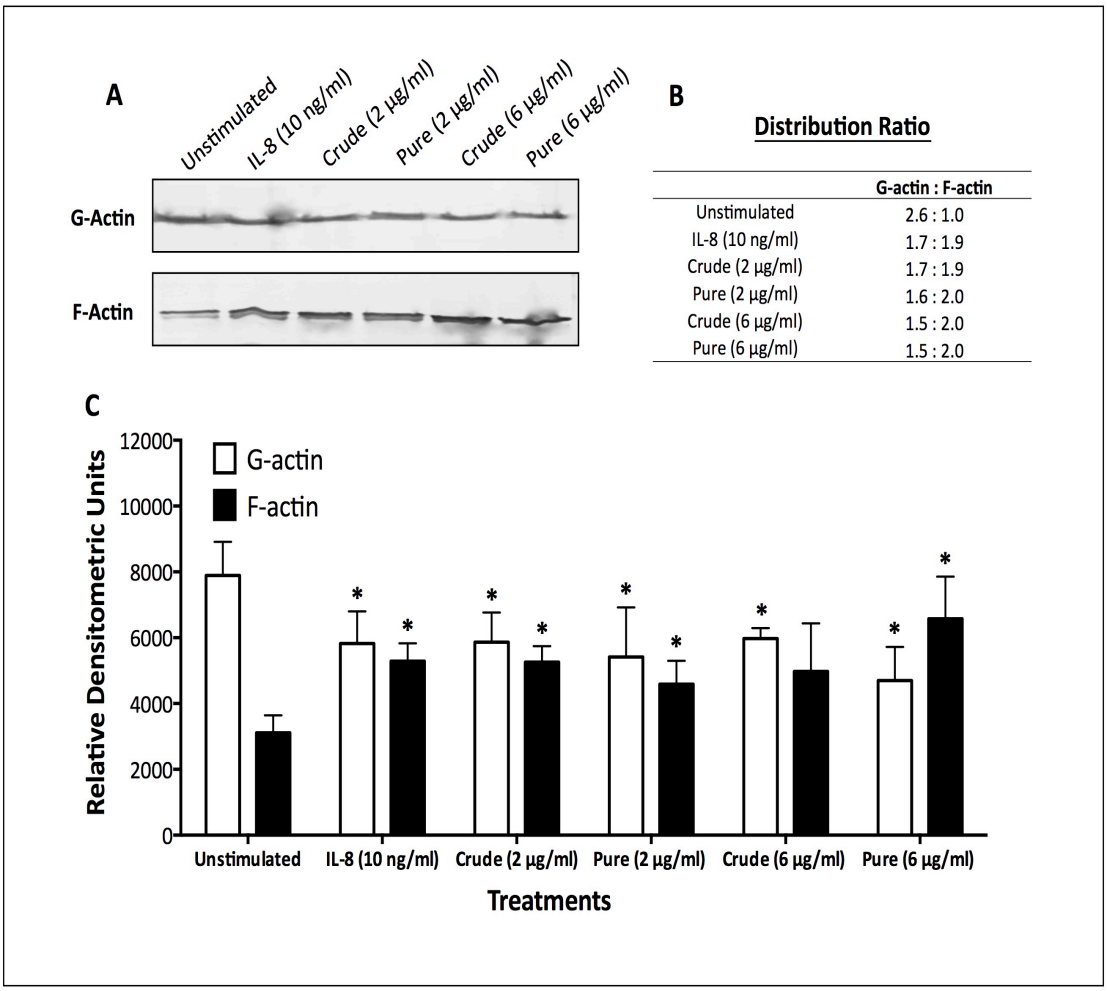

Figure 6.6 Cytoskeletal reassembly of neutrophils exposed to *B. oleronius* proteins. Alterations in the conversion of G-actin to F-actin in neutrophils exposed to crude and pure *B. oleronius* protein preparations (2 µg/ml and 6 µg/ml) was investigated by assessing the abundances of G-actin and F-actin for each treatment by (**A**) Western blot, (**B**) the distribution ratio of the G-actin : F-actin were calculated, and (**C**) the abundance of G-actin and F-actin for each treatment was quantified using Image J densitometric software (Section 2.28). (Significance: * = $p < 0.05$). (n = 3, experiment performed in triplicate).

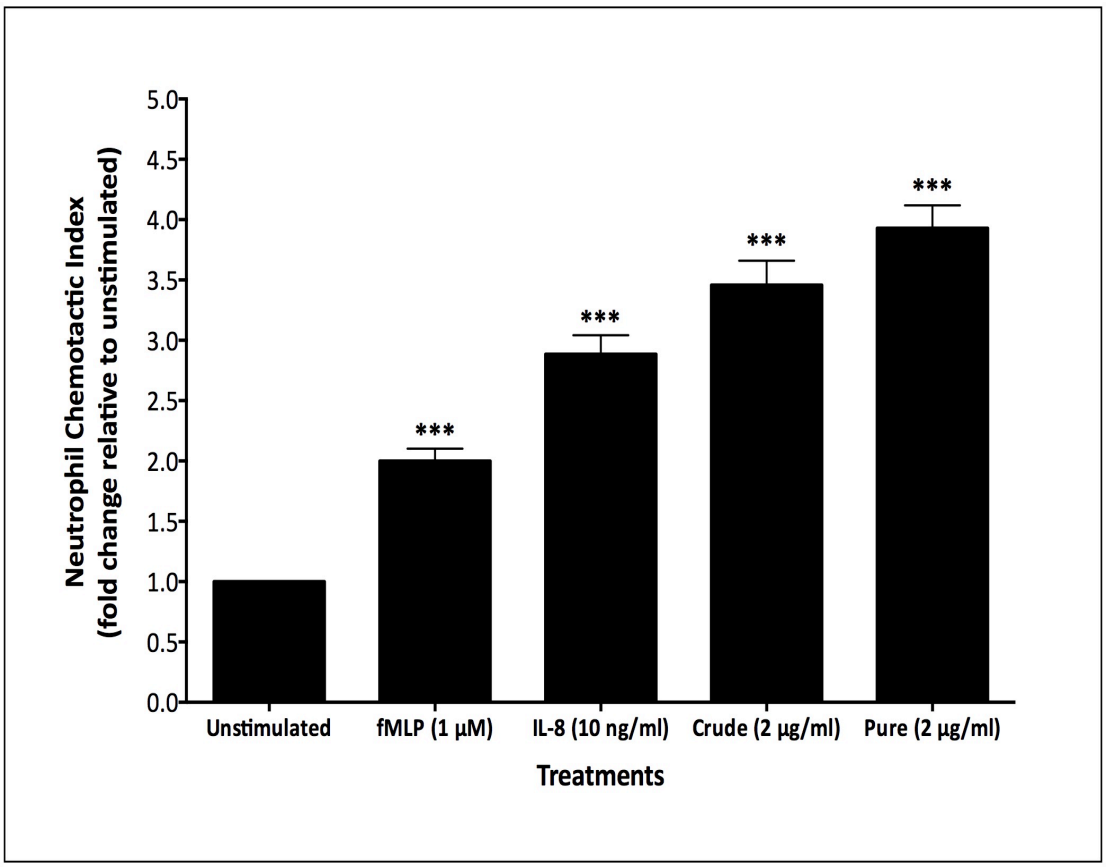

Figure 6.7 Effect of *B. oleronius* proteins on neutrophil chemotaxis. The effect of *B. oleronius* protein preparations on neutrophil chemotaxis was investigated by exposing isolated neutrophils to fMLP (1 µM), IL-8 (10 ng/ml), pure *B. oleronius* protein (2 µg/ml), and crude *B. oleronius* protein (2 µg/ml) for 30 minutes, and the effect on neutrophil migration along a chemotactic gradient was quantified using a Boyden chamber (Section 2.29). (Significance: *** = $p < 0.001$). (n = 3, experiment performed in triplicate).

6.5 Induction of Neutrophil Chemotaxis in Response to *B. oleronius* Protein

Exposure of neutrophils to *B. oleronius* protein preparation has previously been shown to lead to activation and an increase in mobility of neutrophils (O'Reilly *et al*., 2012c). The effect of *B. oleronius* crude (2 μg/ml) and pure (2 μg/ml) protein preparations on neutrophil chemotaxis was investigated. The results demonstrated that exposure to IL-8 (10 ng/ml) (positive control) lead to a 2.9-fold ($p < 0.0001$) increase in neutrophil chemotaxis. Exposure to the crude *B. oleronius* protein preparation or to the pure *B. oleronius* protein preparation induced a 3.5-fold ($p < 0.0001$) or 3.9-fold ($p < 0.0001$) increase in migration of neutrophils toward a chemotactic gradient, respectively (Figure 6.7).

6.6 Exposure of Neutrophils to *B. oleronius* Proteins Leads to Elevated IL-1β and IL-6 Secretion

Cytokine secretion by neutrophils exposed to *B. oleronius* protein preparation can be used as an indicator of activation (O'Reilly *et al*., 2012c). The effect of *B. oleronius* protein preparations on the ability of neutrophils to secrete IL-1β and IL-6 was investigated. IL-1β is a pro-inflammatory cytokine, and also functions in cell proliferation and the induction of apoptosis (Brink *et al*., 2000). IL-6 is a pro-inflammatory cytokine associated with the response to bacterial infection and high levels of expression have been recorded in psoriatic skin (Grossman *et al.*, 1989).

Neutrophils exposed to pure *B. oleronius* protein (2 and 6 μg/ml) demonstrated significant increased secretion of in IL-1β following 16 hour and 24 hour incubation relative to unstimulated neutrophils ($p < 0.0001$) (Figure 6.8). There was a significant increase in IL-1β by neutrophils exposed to pure *B. oleronius* protein at 2 μg/ml (201 pg/ml; $p = 0.0005$), and at 6 μg/ml (150 pg/ml; $p = 0.0003$) after 16 hour, and after 24 hour exposure at 2 μg/ml (89 pg/ml; $p = 0.0009$) and at 6 μg/ml (83 pg/ml; $p < 0.0001$) pure *B. oleronius* protein. In contrast, cells exposed to the crude *B. oleronius* protein preparation (2 and 6 μg/ml) showed no altered IL-1β secretion (Figure 6.8).

Neutrophils exposed to 2 or 6 μg/ml pure or crude *B. oleronius* protein preparations demonstrated increased secretion of IL-6 ($p < 0.001$) with the highest amount occurring at 24 hour (Figure 6.9). IL-6 production increased 2.5-fold and 2.2-fold following exposure of neutrophils to 2 and 6 μg/ml pure *B. oleronius* proteins ($p < 0.0001$, and $p = 0.0048$, respectively) after 16 hour.

Treatment of neutrophils with the crude *B. oleronius* protein preparation at 2 μg/ml and 6 μg/ml produced similar levels of IL-6 (198 pg/ml, and 202 pg/ml, respectively) compared to IL-6 production following stimulation by IL-8 (positive control). After 24 hour, IL-6 production increased 1.8-fold and 1.9-fold following exposure of neutrophils to pure *B. oleronius* protein ($p = 0.0001$, and $p = 0.0018$, respectively). Exposure of neutrophils to crude *B. oleronius* protein at 2 μg/ml and 6 μg/ml showed similar levels of IL-6 (407 pg/ml, and 348 pg/ml, respectively) compared to 423 pg/ml IL-6 production following stimulation by IL-8.

6.7 Summary

The activity of an endotoxin contaminant in the crude *B. oleronius* protein and pure *B. oleronius* protein preparation was assessed by TNF-α ELISpot. The results showed that spot formation was not inhibited by the addition of polymyxin B, suggesting that the effects of the crude and pure *B. oleronius* protein preparations are not due to the presence of endotoxin. Neutrophils exposed to the crude or pure *B. oleronius* proteins leads to the generation of IP_1, a breakdown product of the second messenger IP_3, and an indicator of neutrophil activation along the IP_3 pathway. The release of stored Ca^{2+} was observed following stimulation of neutrophils to *B. oleronius* proteins. Cytoskeletal reassembly and distribution, the conversion of G-actin to F-actin, was increased in *B. oleronius* protein treated neutrophils, with a positive neutrophil chemotaxis and migration response induced by the crude or pure *B. oleronius* proteins. The secretion levels of IL-1β and IL-6 were shown to be elevated in neutrophils exposed to the *B. oleronius* protein preparations that may result in the development of an inflammatory response.

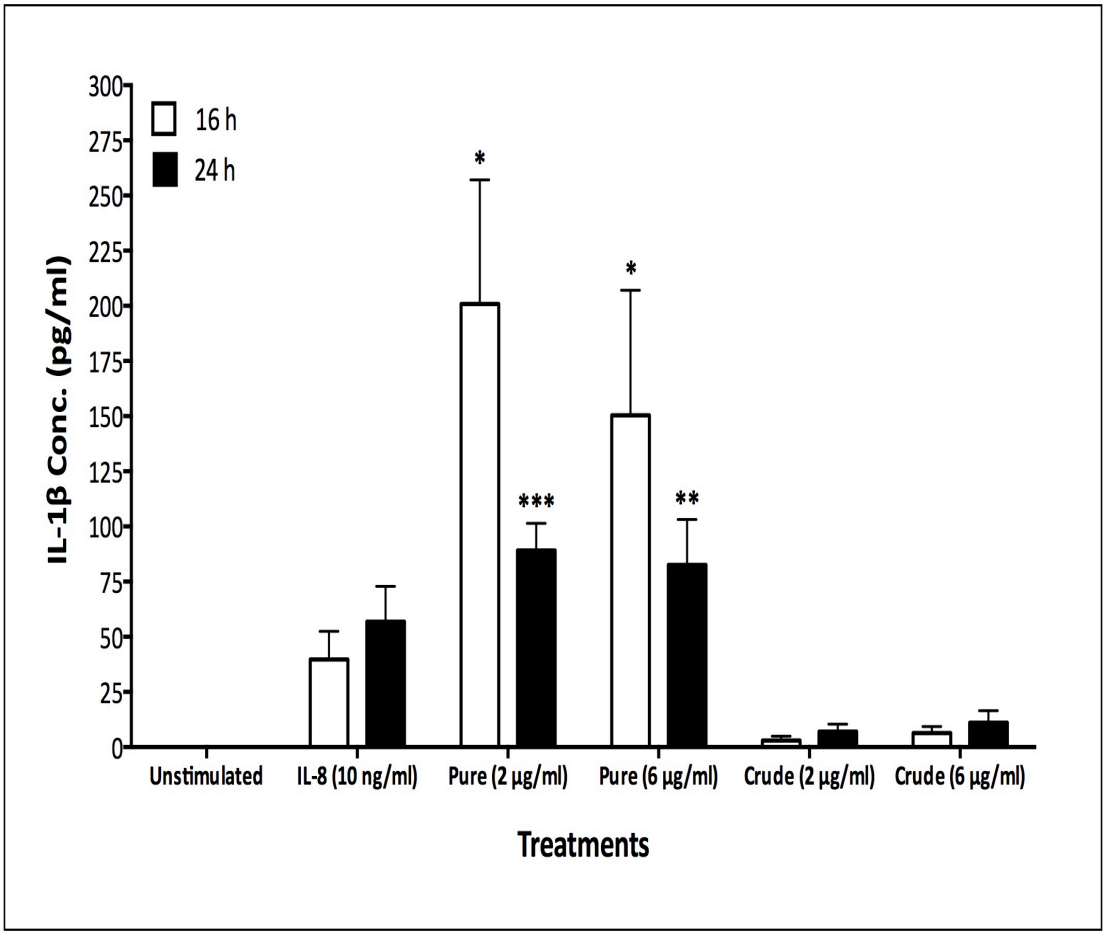

Figure 6.8 Secretion of IL-1β by neutrophils exposed to *B. oleronius* proteins. Neutrophils were exposed to IL-8 (10 ng/ml), pure *B. oleronius* protein (2 and 6 µg/ml), or crude *B. oleronius* protein (2 and 6 µg/ml), for 16 hour and 24 hour. The secretion of the pro-inflammatory cytokine, IL-1β, was measured by ELISA (Section 2.37). (Significance: * = $p < 0.05$, ** = $p < 0.01$, *** = $p < 0.001$). (n = 3, experiment performed in triplicate).

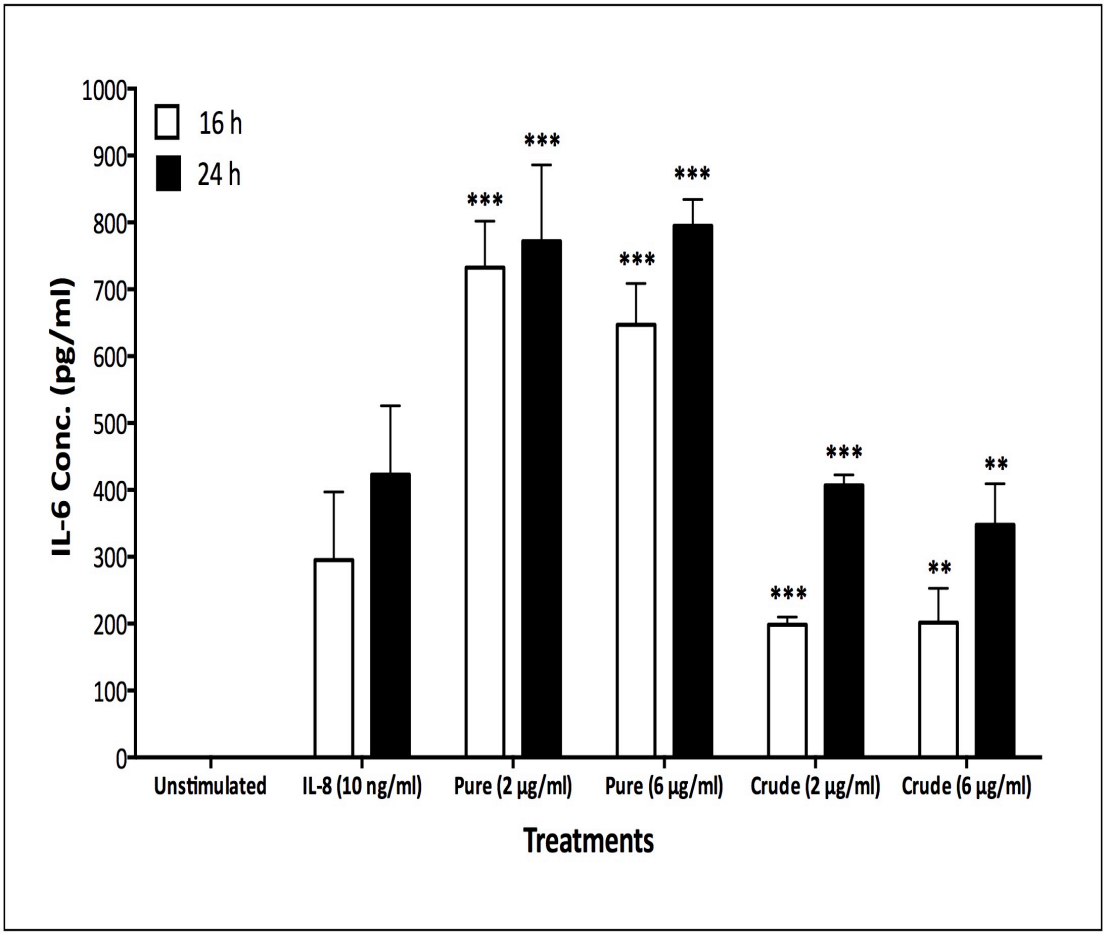

Figure 6.9 Secretion of IL-6 by neutrophils exposed to *B. oleronius* proteins. Neutrophils were exposed to IL-8 (10 ng/ml), pure *B. oleronius* protein (2 and 6 µg/ml), or crude *B. oleronius* protein (2 and 6 µg/ml), for 16 hour and 24 hour. The secretion of the pro-inflammatory cytokine, IL-6, was measured by ELISA (Section 2.37). (Significance: ** = $p < 0.01$, *** = $p < 0.001$). (n = 3, experiment performed in triplicate).

6.8 Investigating the Cytokine Response of Isolated PBMC Following Exposure to *B. oleronius* Protein by FluoroSpot

Cytokines are the key regulators of the immune response against an infectious agent, and depending upon the specific cytokines secreted, these can result in a pro- or anti-inflammatory response. The monocyte cell population, acquired from the isolation of PBMC (Section 2.21) from healthy volunteers, were exposed to the crude and pure *B. oleronius* protein (5 µg/ml) preparations, and the cytokine signaling response was characterised by FluoroSpot (Section 2.24). Dual-labeling fluorescence of the target cytokines was employed to measure co-secreting cells. The secretion of IL-6 (green fluorescence) was analysed for each assay. The target cytokines were IL-6 and IL-1β (IL-6/IL-1β), IL-6 and TNF-α (IL-6/TNF-α), IL-6 and granulocyte macrophage colony-stimulating factor (GM-CSF) (IL-6/GM-CSF), IL-6 and IL-10 (IL-6/IL-10), IL-6 and IL-12p40 (IL-6/IL-12p40), IL-6 and IL-23 (IL-6/IL-23), and IL-6 and apolipoprotein E (ApoE) (IL-6/ApoE). Exposure of monocytes from the isolated PBMC population to the crude or pure *B. oleronius* protein (5 µg/ml) preparation lead to a significant increase in IL-6 secretion relative to the unstimulated PBMC ($p < 0.0001$, and $p < 0.0001$, respectively) (Figure 6.10 – 6.16).

The levels of secreted IL-1β (Figure 6.10), TNF-α (Figure 6.11), GM-CSF (Figure 6.12), IL-10 (Figure 6.13), IL-12p40 (Figure 6.14), and IL-23 (Figure 6.15) were significantly elevated following stimulation of PBMC with the crude or pure *B. oleronius* protein preparations compared to unstimulated PBMC ($p < 0.0001$, and $p < 0.0001$, respectively). Similarly, the number of co-secreting cells of IL-6/IL-1β (Figure 6.10), IL-6/TNF-α (Figure 6.11), and IL-6/GM-CSF (Figure 6.12), IL-6/IL-10 (Figure 6.13), IL-6/IL-12p40 (Figure 6.14), and IL-6/IL-23 (Figure 6.15) was observed to be significantly increased in crude and pure *B. oleronius* protein treated PBMC with a higher number of IL-6/IL-1β, IL-6/IL-10, IL-6/IL-12p40, and IL-6/IL-23 co-secreting cells detected following stimulation with the pure *B. oleronius* protein ($p < 0.0001$, and $p < 0.0001$, respectively) (Figure 6.10 and Figure 6.13 – 6.15).

The secretion of apolipoprotein E (ApoE) was induced at lower levels relative to unstimulated PBMC, following stimulation with the crude or pure *B. oleronius* protein. The number of double-secreting cells of IL-6/ApoE following exposure to the *B. oleronius* proteins was shown to be similar to unstimulated PBMC and deemed not to be statistically significant (Figure 6.16).

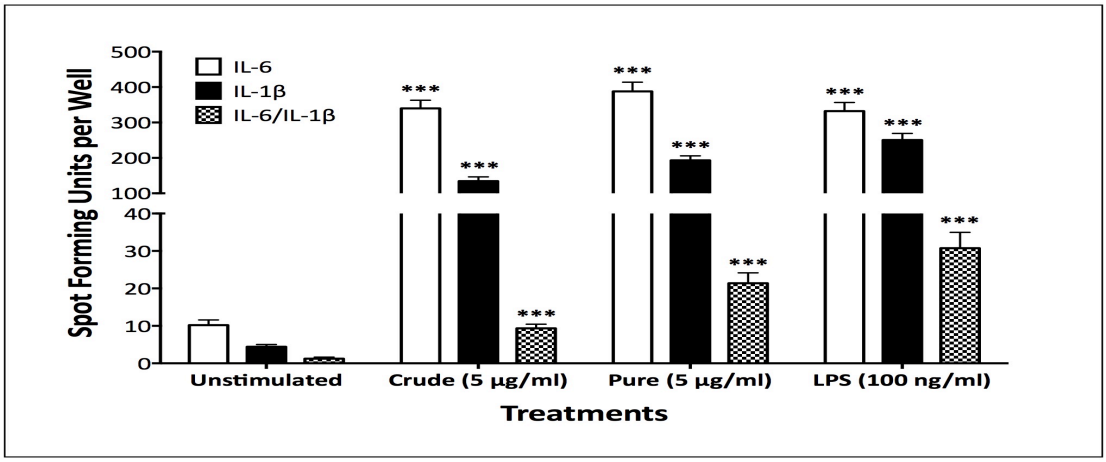

Figure 6.10 Secretion of IL-6 and IL-1β in PBMC exposed to *B. oleronius* proteins by FluoroSpot. Secretion of the cytokines, IL-6 (green fluorescence) and IL-1β (red fluorescence), by isolated PBMC from healthy volunteers (n = 6), following a 48 hour incubation with stimulation by untreated (culture media), crude *B. oleronius* protein (5 µg/ml), pure *B. oleronius* protein (5 µg/ml), or anti-CD3 (1 ng/ml) (positive control), determined by FluoroSpot. PBMC co-expressing IL-6 and IL-1β (IL-6/IL-1β) (yellow fluorescence) were detected. (Significance: *** = $p < 0.001$).

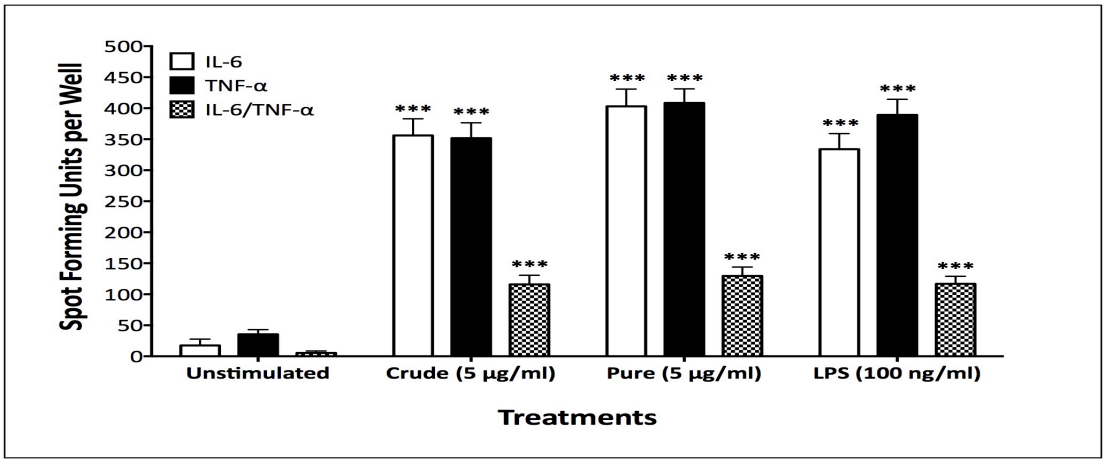

Figure 6.11 Secretion of IL-6 and TNF-α in PBMC exposed to *B. oleronius* proteins by FluoroSpot. Secretion of the cytokines, IL-6 (green fluorescence) and TNF-α (red fluorescence), by isolated PBMC from healthy volunteers (n = 6), following a 48 hour incubation with stimulation by untreated (culture media), crude *B. oleronius* protein (5 µg/ml), pure *B. oleronius* protein (5 µg/ml), or anti-CD3 (1 ng/ml) (positive control), determined by FluoroSpot. PBMC co-expressing IL-6 and TNF-α (IL-6/TNF-α) (yellow fluorescence) were detected. (Significance: *** = $p < 0.001$).

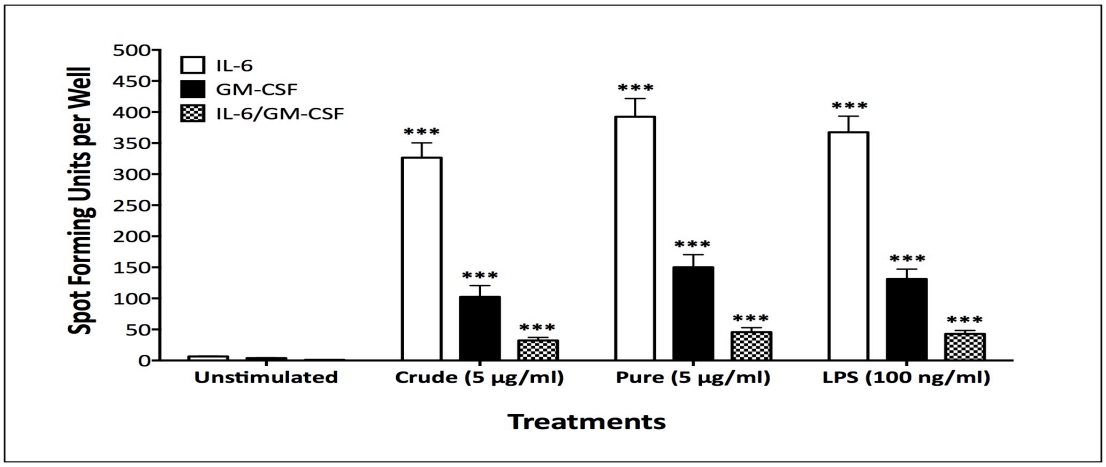

Figure 6.12 Secretion of IL-6 and GM-CSF in PBMC exposed to *B. oleronius* proteins by FluoroSpot. Secretion of the cytokines, IL-6 (green fluorescence) and GM-CSF (red fluorescence), by isolated PBMC from healthy volunteers (n = 6), following a 48 hour incubation with stimulation by untreated (culture media), crude *B. oleronius* protein (5 µg/ml), pure *B. oleronius* protein (5 µg/ml), or anti-CD3 (1 ng/ml) (positive control), determined by FluoroSpot. PBMC co-expressing IL-6 and GM-CSF (IL-6/GM-CSF) (yellow fluorescence) were detected. (Significance: *** = $p < 0.001$).

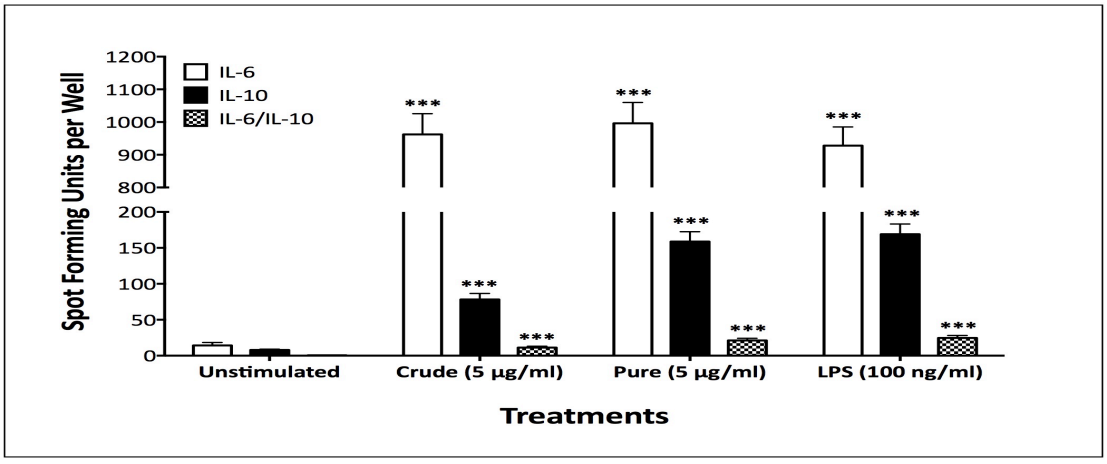

Figure 6.13 Secretion of IL-6 and IL-10 in PBMC exposed to *B. oleronius* proteins by FluoroSpot. Secretion of the cytokines, IL-6 (green fluorescence) and IL-10 (red fluorescence), by isolated PBMC from healthy volunteers (n = 6), following a 48 hour incubation with stimulation by untreated (culture media), crude *B. oleronius* protein (5 µg/ml), pure *B. oleronius* protein (5 µg/ml), or anti-CD3 (1 ng/ml) (positive control), determined by FluoroSpot. PBMC co-expressing IL-6 and IL-10 (IL-6/IL-10) (yellow fluorescence) were detected. (Significance: *** = $p < 0.001$).

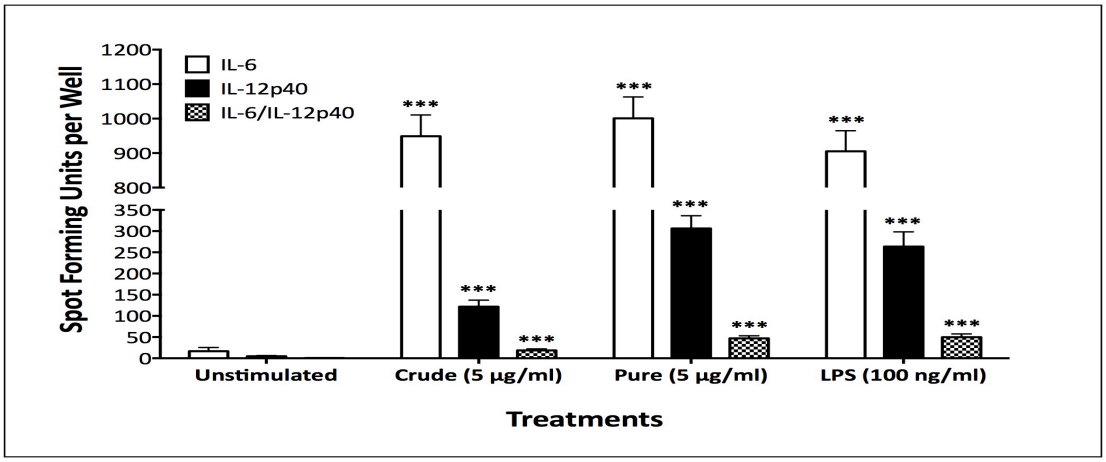

Figure 6.14 Secretion of IL-6 and IL-12p40 in PBMC exposed to *B. oleronius* proteins by FluoroSpot. Secretion of the cytokines, IL-6 (green fluorescence) and IL-12p40 (red fluorescence), by isolated PBMC from healthy volunteers (n = 6), following a 48 hour incubation with stimulation by untreated (culture media), crude *B. oleronius* protein (5 µg/ml), pure *B. oleronius* protein (5 µg/ml), or anti-CD3 (1 ng/ml) (positive control), determined by FluoroSpot. PBMC co-expressing IL-6 and IL-12p40 (IL-6/IL-12p40) (yellow fluorescence) were detected. (Significance: *** = $p < 0.001$).

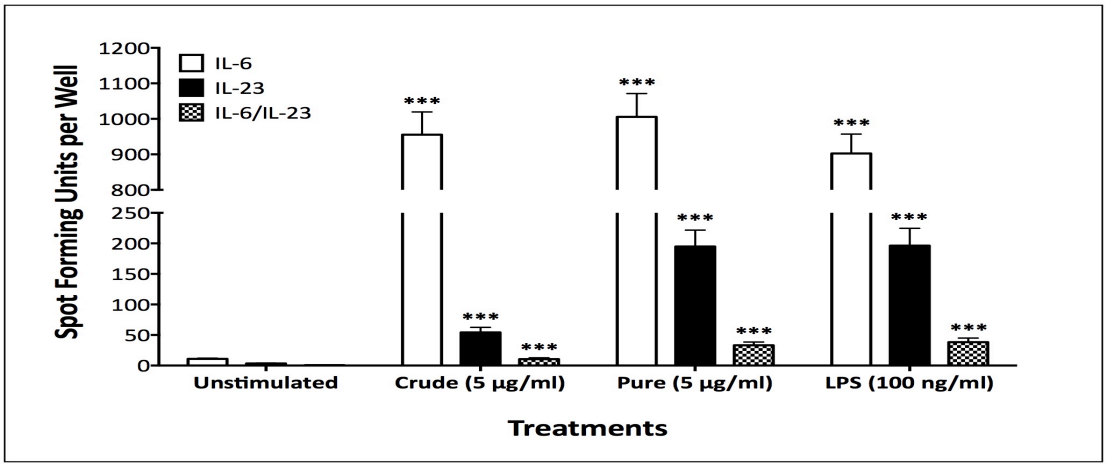

Figure 6.15 Secretion of IL-6 and IL-23 in PBMC exposed to *B. oleronius* proteins by FluoroSpot. Secretion of the cytokines, IL-6 (green fluorescence) and IL-23 (red fluorescence), by isolated PBMC from healthy volunteers (n = 6), following a 48 hour incubation with stimulation by untreated (culture media), crude *B. oleronius* protein (5 µg/ml), pure *B. oleronius* protein (5 µg/ml), or anti-CD3 (1 ng/ml) (positive control), determined by FluoroSpot. PBMC co-expressing IL-6 and IL-23 (IL-6/IL-23) (yellow fluorescence) were detected. (Significance: *** = $p < 0.001$).

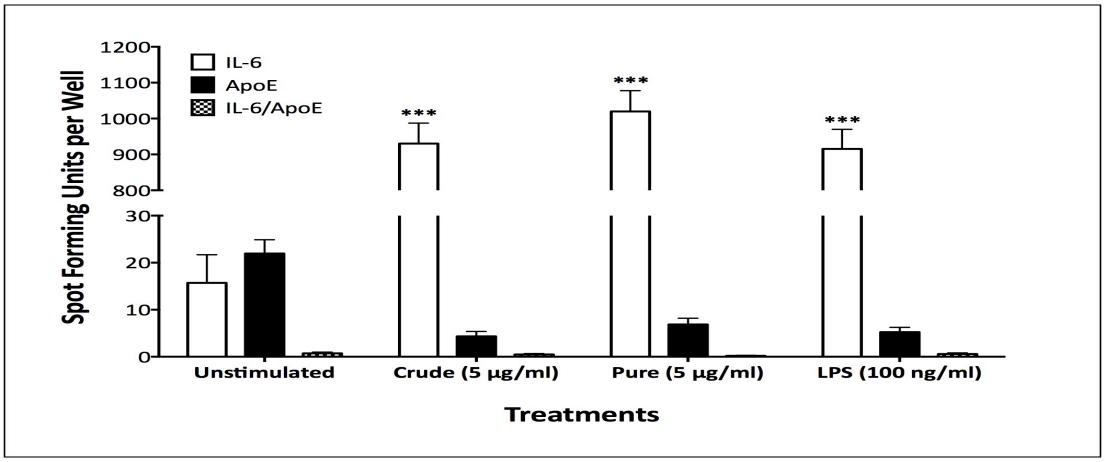

Figure 6.16 Secretion of IL-6 and ApoE in PBMC exposed to *B. oleronius* proteins by FluoroSpot. Secretion of the cytokines, IL-6 (green fluorescence) and ApoE (red fluorescence), by isolated PBMC from healthy volunteers (n = 6), following a 48 hour incubation with stimulation by untreated (culture media), crude *B. oleronius* protein (5 µg/ml), pure *B. oleronius* protein (5 µg/ml), or anti-CD3 (1 ng/ml) (positive control), determined by FluoroSpot. PBMC co-expressing IL-6 and ApoE (IL-6/ApoE) (yellow fluorescence) were detected. (Significance: *** = $p < 0.001$).

6.9 Investigating the Cytokine Response of Isolated PBMC Following Exposure to *B. oleronius* Protein by ELISpot and FluroSpot

Cytokines that are specifically secreted by T cells are responsible for mediating an adaptive immune response against a pathogenic agent. Isolated PBMC were exposed to the crude and pure *B. oleronius* protein (5 µg/ml) to characterise the cytokine signaling response using ELISpot (Section 2.23) and FluoroSpot (Section 2.24) assay techniques. The T-cell specific cytokines analysed by ELISpot were IL-2, IL-5, IL-13, IL-17A, IL-22, IL-31, and IFN-γ. The FluoroSpot assay allowed for dual-labeling fluorescence of the target cytokines to measure cytokine secretion and to quantify the number of co-secreting cells. The target cytokines for analysis using FluoroSpot were IL-17A and IL-22 (IL-17A/IL-22), IL-17A and IL-31 (IL-17A/IL-31), IFN-γ and IL-5 (IFN-γ/IL-5), IFN-γ and IL-22 (IFN-γ/IL-22), and IFN-γ and IL-31 (IFN-γ/IL-31). The secretion of IL-17A or IFN-γ were analysed using the green fluorescence channel for each assay (Figure 6.17A – 6.21A).

It was demonstrated by FluoroSpot, that secetion of IL-17A, and the number of co-secreting IL-17A/IL-22 cells were increased significantly following exposure of PBMC to the pure *B. oleronius* protein preparation relative to unstimulated PBMC ($p < 0.05$, and $p < 0.05$, respectively) (Figure 6.17A, and Figure 6.18A, respectively). Through ELISpot, the levels of secreted IL-17A were shown to be significantly higher in PBMC treated with the crude *B. oleronius* protein ($p < 0.05$) or pure *B. oleronius* protein ($p < 0.01$) compared to unstimulated PBMC (Figure 6.17B, and Figure 6.18B, respectively).

The secretion of IL-22 was significantly increased in PBMC exposed to the crude *B. oleronius* protein (5 µg/ml) or pure *B. oleronius* protein (5 µg/ml) preparations using FluroSpot ($p < 0.01$, and $p < 0.001$, respectively), and ELISpot ($p < 0.001$, and $p < 0.001$, respectively) compared to unstimulated PBMC (Figure 6.17). The secretion of IL-31 was detected by FluoroSpot and ELISpot but a difference between unstimulated PBMC and PBMC treated with crude or pure *B. oleronius* protein was not observed (Figure 6.18, and Figure 6.21, respectively).

An increase of IFN-γ secretion was observed in PBMC stimulated with the crude *B. oleronius* protein ($p < 0.001$) or pure *B. oleronius* protein ($p < 0.001$) preparations relative to unstimulated PBMC using (A) FluoroSpot or (B) ELISpot assay techniques (Figure 6.19 – 6.22). Similarly, it was demonstrated that stimulation of PBMC with the crude or pure *B. oleronius* protein preparations significantly

elevated the levels of secreted IL-5 using FluoroSpot ($p < 0.01$, and $p < 0.01$, respectively) and ELISpot ($p < 0.001$, and $p < 0.001$, respectively) analysis (Figure 6.19). Exposure of PBMC to the pure *B. oleronius* protein preparation lead to statistically higher levels of IFN-γ/IL-5 co-secreting cells ($p < 0.05$) (Figure 6.19A).

The secretion of IL-22 was shown to be significantly increased in PBMC exposed to the crude or pure *B. oleronius* protein prepartions relative to unstimulated PBMC following analysis by FluoroSpot ($p < 0.001$, and $p < 0.01$, respectively) and ELISpot ($p < 0.001$, and $p < 0.001$, respectively) (Figure 6.20). A change in the number of IFN-γ/IL-22 co-secreting cells was not observed.

Stimulation of PBMC with the *B. oleronius* protein preparations did not significantly alter the secretion levels of IL-2 relative to unstimulated PBMC by ELISpot (Figure 6.22A). However, ELISpot analysis demonstrated a significant rise in the secretion of IL-13 by PBMC treated with the crude *B. oleronius* protein ($p < 0.001$) or pure *B. oleronius* protein ($p < 0.001$) preparations compared to unstimulated PBMC (Figure 6.22B).

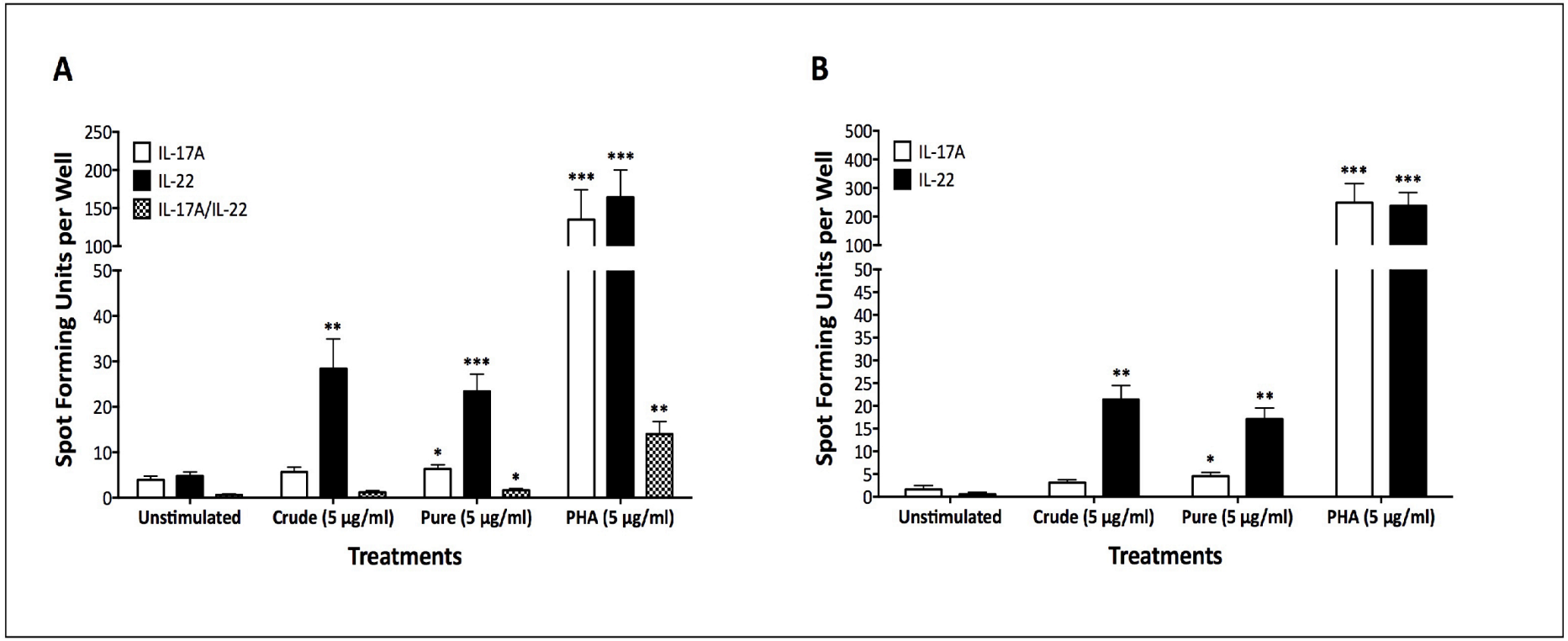

Figure 6.17 Secretion of IL-17A and IL-22 in PBMC exposed to *B. oleronius* proteins by FluoroSpot and ELISpot. Secretion of the cytokines, IL-17A (green fluorescence) and IL-22 (red fluorescence), by isolated PBMC from healthy volunteers (n = 6), following a 48 hour incubation period with stimulation by untreated (culture media), crude *B. oleronius* protein (5 µg/ml), pure *B. oleronius* protein (5 µg/ml), or anti-CD3 (1 ng/ml) (positive control), determined by (**A**) FluoroSpot and (**B**) ELISpot. PBMC co-expressing IL-17A and IL-22 (IL-17A/IL-22) (yellow fluorescence) were detected. (Significance: * = $p < 0.05$, ** = $p < 0.01$, *** = $p < 0.001$).

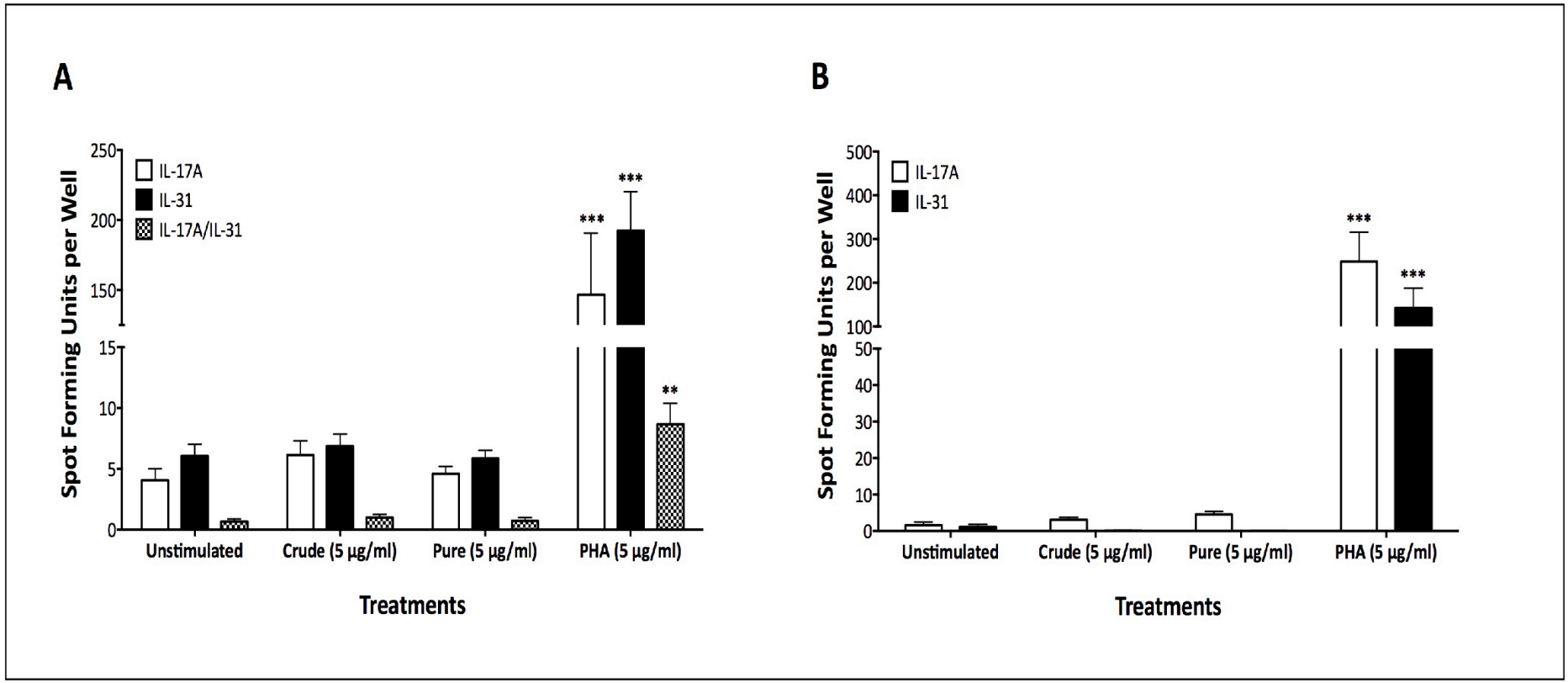

Figure 6.18 Secretion of IL-17A and IL-31 in PBMC exposed to *B. oleronius* proteins by FluoroSpot and ELISpot. Secretion of the cytokines, IL-17A (green fluorescence) and IL-31 (red fluorescence), by isolated PBMC from healthy volunteers (n = 6), following a 48 hour incubation period with stimulation by untreated (culture media), crude *B. oleronius* protein (5 µg/ml), pure *B. oleronius* protein (5 µg/ml), or anti-CD3 (1 ng/ml) (positive control), determined by (**A**) FluoroSpot and (**B**) ELISpot. PBMC co-expressing IL-17A and IL-31 (IL-17A/IL-31) (yellow fluorescence) were detected. (Significance: * = $p < 0.05$, ** = $p < 0.01$, *** = $p < 0.001$).

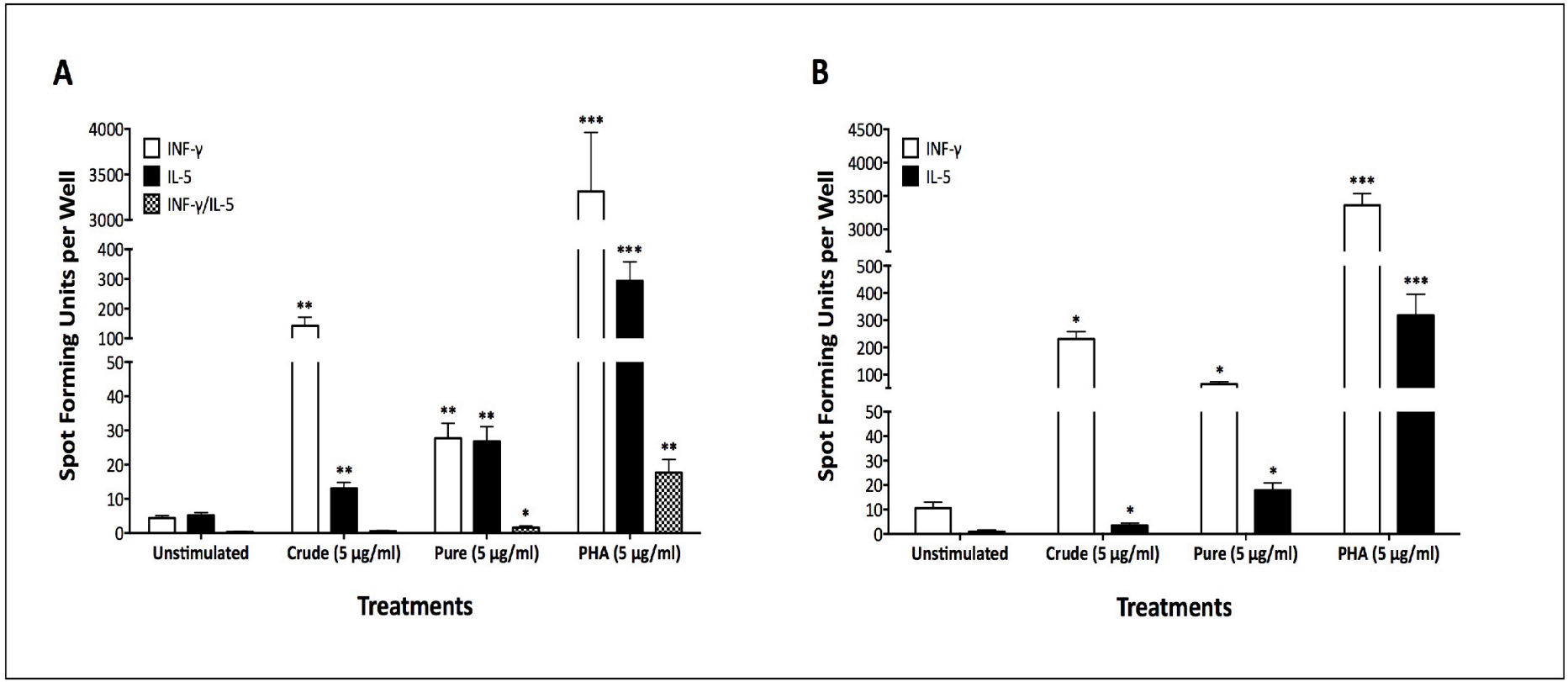

Figure 6.19 Secretion of IFN-γ and IL-5 in PBMC exposed to *B. oleronius* proteins by FluoroSpot and ELISpot. Secretion of the cytokines, IFN-γ (green fluorescence) and IL-5 (red fluorescence), by isolated PBMC from healthy volunteers (n = 6), following a 48 hour incubation period with stimulation by untreated (culture media), crude *B. oleronius* protein (5 µg/ml), pure *B. oleronius* protein (5 µg/ml), or anti-CD3 (1 ng/ml) (positive control), determined by (**A**) FluoroSpot and (**B**) ELISpot. PBMC co-expressing IFN-γ and IL-5 (IFN-γ/IL-5) (yellow fluorescence) were detected. (Significance: * = $p < 0.05$, ** = $p < 0.01$, *** = $p < 0.001$).

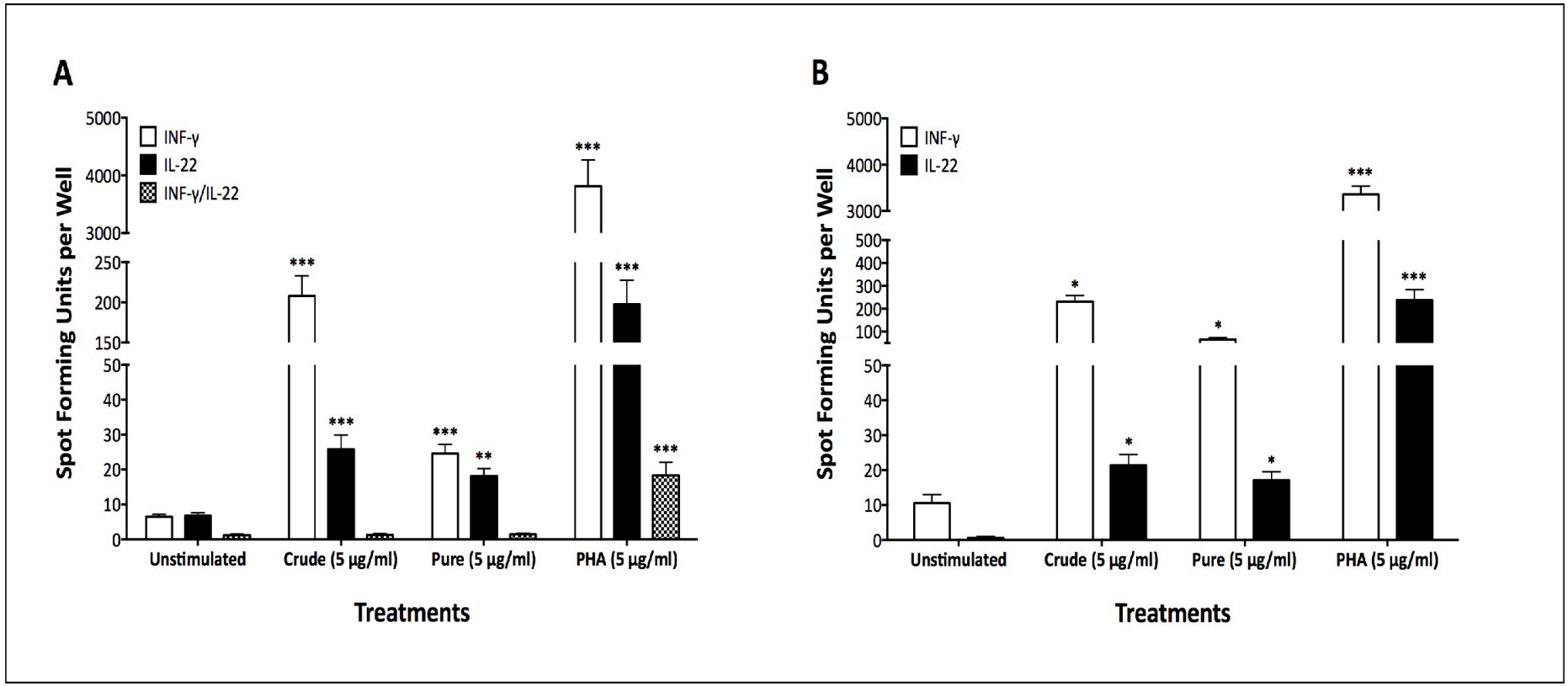

Figure 6.20 Secretion of IFN-γ and IL-22 in PBMC exposed to *B. oleronius* proteins by FluoroSpot and ELISpot. Secretion of the cytokines, IFN-γ (green fluorescence) and IL-22 (red fluorescence), by isolated PBMC from healthy volunteers (n = 6), following a 48 hour incubation period with stimulation by untreated (culture media), crude *B. oleronius* protein (5 µg/ml), pure *B. oleronius* protein (5 µg/ml), or anti-CD3 (1 ng/ml) (positive control), determined by (**A**) FluoroSpot and (**B**) ELISpot. PBMC co-expressing IFN-γ and IL-22 (IFN-γ/IL-22) (yellow fluorescence) were detected. (Significance: ** = $p < 0.01$, *** = $p < 0.001$).

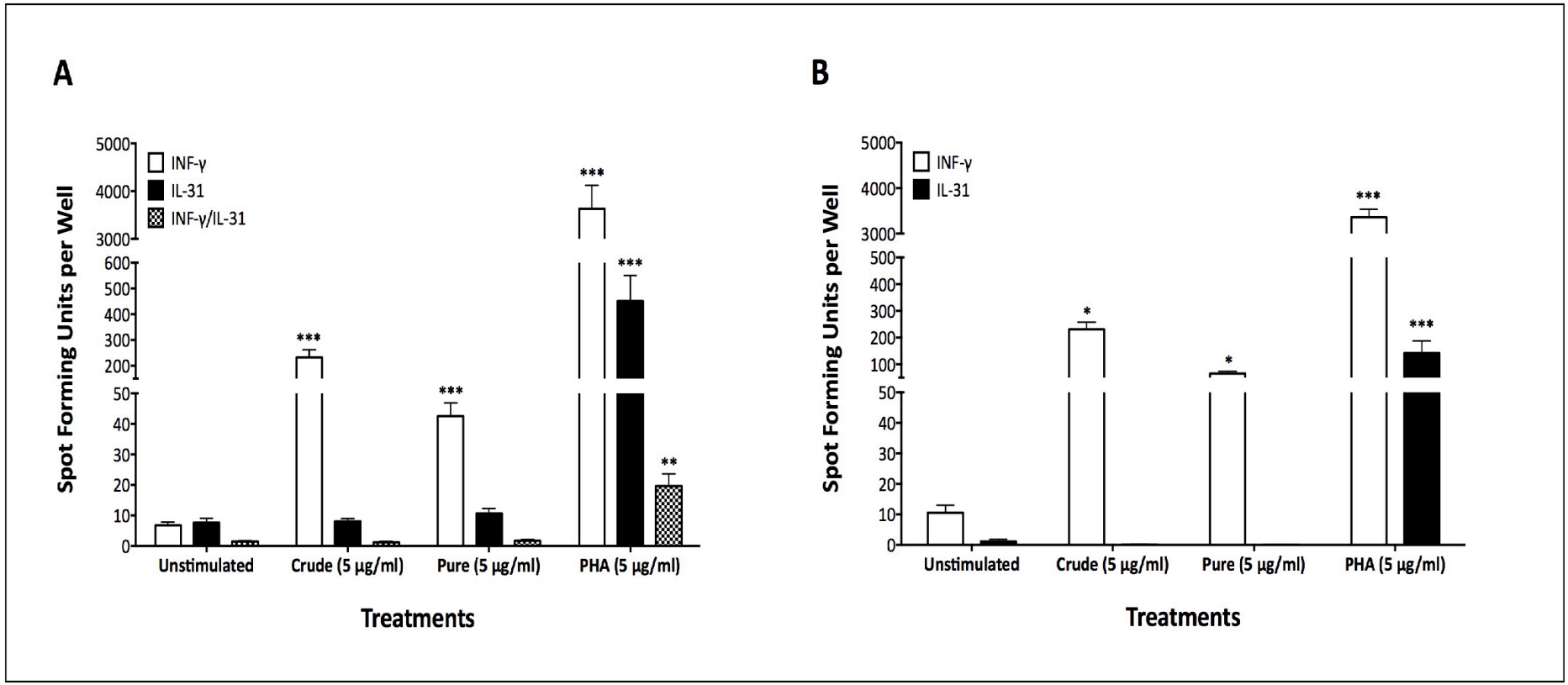

Figure 6.21 Secretion of IFN-γ and IL-31 in PBMC exposed to *B. oleronius* proteins by FluoroSpot and ELISpot. Secretion of the cytokines, IFN-γ (green fluorescence) and IL-31 (red fluorescence), by isolated PBMC from healthy volunteers (n = 6), following a 48 hour incubation period with stimulation by untreated (culture media), crude *B. oleronius* protein (5 µg/ml), pure *B. oleronius* protein (5 µg/ml), or anti-CD3 (1 ng/ml) (positive control), determined by (**A**) FluoroSpot and (**B**) ELISpot. PBMC co-expressing IFN-γ and IL-31 (IFN-γ/IL-31) (yellow fluorescence) were detected. (Significance: ** = $p < 0.01$, *** = $p < 0.001$).

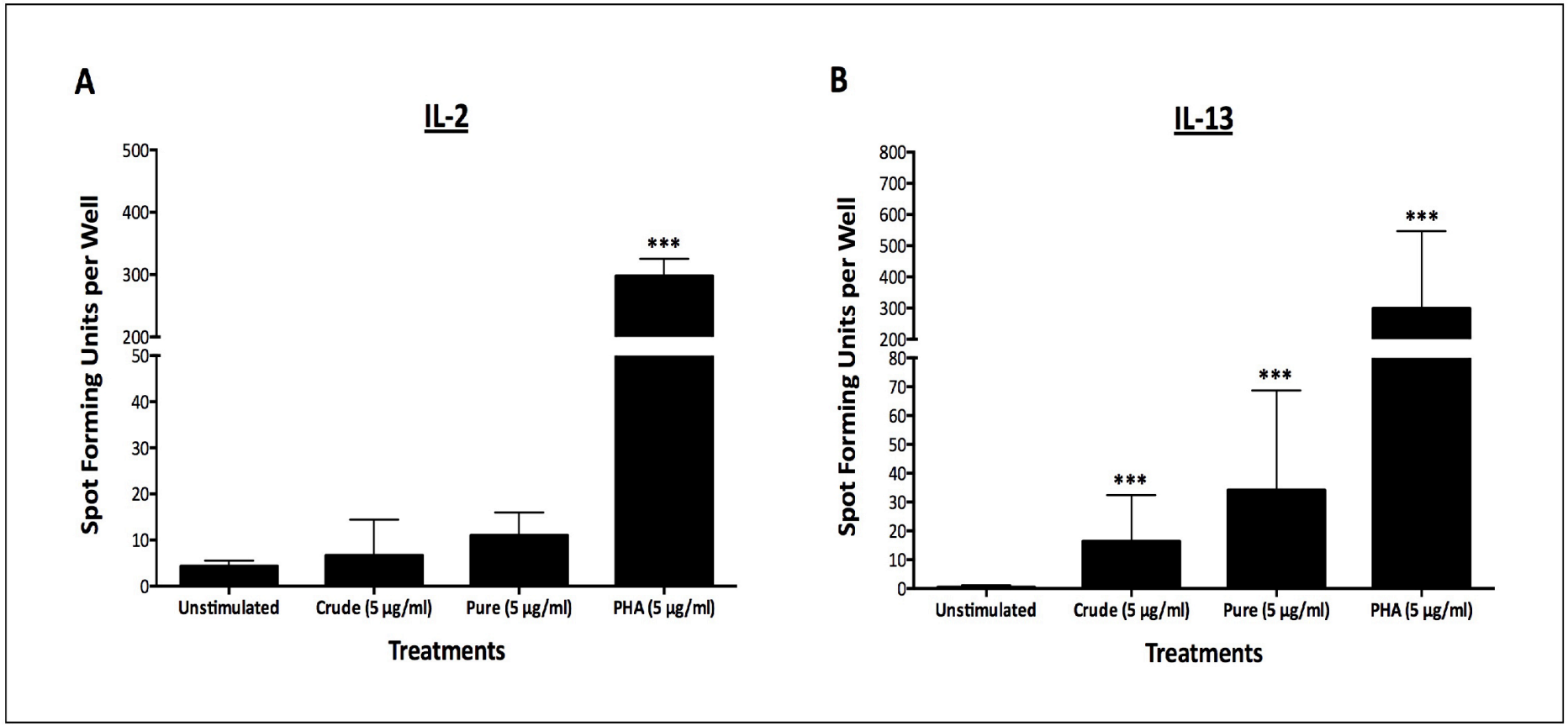

Figure 6.22 Secretion of IL-2 and IL-13 in PBMC exposed to *B. oleronius* proteins by ELISpot. Secretion of the cytokines, (**A**) IL-2 and (**B**) IL-13, by isolated PBMC from healthy volunteers (n = 6), following a 48 hour incubation period with stimulation by untreated (culture media), crude *B. oleronius* protein (5 µg/ml), pure *B. oleronius* protein (5 µg/ml), or anti-CD3 (1 ng/ml) (positive control), determined by ELISpot. (Significance: *** = $p < 0.001$).

6.10 Discussion

Rosacea is a chronic inflammatory dermatosis that affects the skin of the face, the eyelid margins and the eyes (Holmes, 2013; Jarmuda *et al*., 2012; Powell, 2005). The condition affects all skin types but is most obvious in those with fair skin. A number of forms of rosacea have been recognized and include papulopustular, ocular, phytamous and erythematotelangiectatic (Crawford, 2004; Wilkin *et al*., 2002). While the aetiology of rosacea is complex, and may involve a variety of factors, treatment of the condition has relied upon the use of antibiotics (e.g. azelic acid, metronidazole, tetracycline), and the response to therapy is characterised by periods of remission and relapse once antibiotic therapy has been discontinued (Jarmuda *et al*., 2012; Yamasaki and Gallo, 2009; Gupta and Chaudhry, 2005; Pelle *et al*., 2004). The efficacy of antibiotics in controlling the condition may be due to their anti-inflammatory properties, although anti-inflammatory agents such as steroids and tacrolimus are not effective in treating the condition and their use can lead to deterioration of the condition (Gupta and Chaudhry, 2005). Many agents used in the treatment of rosacea, such as tetracyclines, azelaic acid, retinoids and metronidazole inhibit reactive oxygen species (ROS) production by neutrophils and lead to clearance of the condition (Akamatsu *et al*., 1991; Yoshioka *et al.*, 1986; Miyachi *et al*., 1986).

Neutrophils may induce tissue damage by the release of proteolytic enzymes during degranulation which can degrade collagen and activate key signaling pathways which can result in inflammation (Kuwahara *et al*., 2006; Devaney *et al*., 2003; Berton *et al*., 2000; Starkey *et al*., 1977). Neutrophil influx and activation is considered a key factor in the induction of erythema in the skin of rosacea patients (Yamasaki and Gallo, 2009; Gupta and Chaudhry, 2005). It has previously been demonstrated that exposure of neutrophils to *B. oleronius* proteins leads to increased migration, and elevated release of MMP-9 and cathelicidin (O'Reilly *et al*., 2012c). This may contribute to the tissue damage and inflammation evident in areas of skin erythema characteristic of rosacea patients. The aims of this Chapter, were to characterise the signaling mechanisms of the IP_3 pathway of neutrophil activation, and to elucidate the role of *B. oleronius* in the induction of inflammation in rosacea.

The 'crude' protein preparation employed here consists of all the protein released by *B. oleronius*, and may represent all of those released from dead *Demodex* mites in the pilosebaceous unit. The 'pure' protein preparation consists of proteins to which the sera of rosacea patients are reactive, and have been shown to be capable of

inducing an immune response and an inflammatory response in neutrophils, PBMC, and in a corneal epithelial cell line (hTCEpi) (O'Reilly *et al*., 2012a, 2012b; Li *et al*., 2010; Lacey *et al*., 2007). Analysis of the crude *B. oleronius* protein and pure *B. oleronius* protein preparations in TNF-α ELISpot assays confirmed the absence of LPS contamination as the number of cytokine-secreting cells were not significantly reduced following the addition of polymyxin B, an inhibitor of LPS activity, thus indicating that the effects observed from the *in vitro* assays are not attributable to endotoxin presence (Figure 6.1 – 6.3).

The IP_3 pathway involves the transduction of a number of intracellular signals leading to neutrophil activation. The activation of neutrophils is characterised by the rapid movement of intracellular Ca^{2+} ions stored in the calciosomes induced by IP_3 receptor binding (Thelen and Wirthmueller, 1994; Billah, 1993; Lew, 1990; Rossi, 1986). The regulation of intracellular neutrophil signal transduction for chemotaxis and degranulation requires an increase in the cytosolic Ca^{2+} levels (Tintinger *et al.*, 2005). Chemoattractant signaling molecules such as fMLP or IL-8, bind to a G protein-coupled receptor (GPCR) leading to the activation of the β isoform of phospholipase C (PLC), and the generation of the second messenger, IP_3 (Reeves *et al*., 2013; Bokoch, 1995). This results in the rapid release of stored Ca^{2+} from Ca^{2+}-gated ion channels of calciosomes, and neutrophil activation (Bokoch, 1995). The signaling cascade for rapid release of internally stored Ca^{2+} following the generation of IP_3 has been proposed as a potential therapeutic target against the inflammatory response of neutrophils in a range of diseases (Wacker *et al.*, 2009; Tintinger *et al.*, 2005; Binah *et al.*, 2004).

Neutrophils exposed to the *B. oleronius* protein preparations demonstrated elevated levels of IP_1 indicating the activation of GPCR signaling leading to the generation of the second messenger IP_3 (Bokoch, 1995) (Figure 6.4). Neutrophils activated through the IP_3 pathway exhibit a rapid release of internally stored Ca^{2+} following the occupancy of IP_3 and it's receptors on the Ca^{2+}-gated ion channels of the calciosomes, with a return to the basal level of cystolic Ca^{2+} by the action of plasma membrane and sacro(endo)plasmic reticulum Ca^{2+}-ATPase (SERCA) pumps (Putney, 2007; Tintinger *et al.*, 2005; Taylor *et al*., 2004; Berridge, 1995; Bokoch, 1995). The results presented here indicate that exposure of neutrophils to *B. oleronius* protein preparations leads to a rapid release of stored Ca^{2+} which begins to decline 50 seconds after the application of the proteins (Figure 6.5). Following stimulation of

neutrophils by the *B. oleronius* proteins, activated neutrophils also demonstrated elevated levels of F-actin (Figure 6.6), increased chemotaxis, indicating movement towards the *B. oleronius* proteins (Figure 6.7), and increased production of the pro-inflammatory cytokines, IL-1β and IL-6 (Figure 6.8, and Figure 6.9, respectively).

One scenario that might explain the follicular orientated inflammation characteristic of papulopustular rosacea suggests the release of immunogenic *B. oleronius* proteins from dead *Demodex* mites within the pilosebaceous unit. These are released from the pilosebaceous unit, attracting neutrophils to the surrounding area of infection. Activated neutrophils degranulate, release MMP-9 and cathelicidin (LL-37) which can cause tissue degradation (O'Reilly *et al*., 2012a; Yamasaki and Gallo, 2011). Neutrophils also produce elevated levels of IL-8 and TNF-α attracting more neutrophils to infiltrate the vicinity, and induce an exaggerated inflammatory response (O'Reilly *et al*., 2012c). The current work demonstrates that exposure of neutrophils to the *B. oleronius* proteins induced chemotaxis and the activation of neutrophils along the IP_3 pathway of intracellular signal transduction. Activated neutrophils release elevated levels of IL-6 and IL-1β which play a central role in inducing an inflammatory reaction in dermal tissue (Brink *et al*., 2000; Grossman *et al*., 1989). The IP_3 pathway has been a pharmacological target as a treatment for diseases to regulate the immune response and reduce inflammation, thus alleviating the symptoms associated with the condition (Eishingdrelo and Kongsamut, 2013; Brown and Tracy, 2013; Kliem *et al*., 2012; Galeotti *et al*., 2004). This may be a potential anti-inflammatory target to prevent relapses of the persistent non-transient erythema and flushing episodes that are a hallmark of rosacea.

Investigating the activation of master transcription factors, nuclear factor (NF)-κB, and the NF-κB pathway would be the basis for further research to elucidate the effect of *B. oleronius* proteins, and the underlying signaling mechanisms that result in the progression of the disease. The secretion of IL-1β and TNF-α is associated with the expression of NF-κB (Lawrence, 2009). Azelaic acid, a therapy for the treatment of rosacea, has been shown to modulate the inflammatory responses by suppressing IL-1β, TNF-α, and IL-6 secretion in normal human keratinocytes by activation of peroxisome proliferators-activated receptor (PPAR)-γ along the NF-κB pathway (Mastrofrancesco *et al*., 2010). Here, the secretion of IL-1β was assessed by ELISA and demonstrated the expression levels of IL-1β to be increased in neutrophils stimulated with the *B. oleronius* protein preparations. It has previously been

demonstrated that stimulation of neutrophils with the *B. oleronius* proteins increases TNF-α secretion (O'Reilly *et al*., 2012a).

Cytokines play an important role in the regulation of the immune response and inflammation, functioning in a pro-inflammatory or an anti-inflammatory capacity (Dinarello, 2000). However, the dysregulation of cytokine activity can lead to the development of chronic diseases and persistent inflammation (Zhang and An, 2007; Watkins *et al*., 2003; Dinarello, 2000). The effect of crude and pure *B. oleronius* proteins on PBMC cytokine secretion was analysed using FlouroSpot and ELISpot assays (Section 6.8 and 6.9). The aim of this body of work was to characterise the secretion of a range of cyokines which are specific for monocytes or T cells, from a PBMC population isolated from healthy volunteers following exposure to the crude or pure *B. oleronius* protein preparation.

IL-6 is a pleiotropic cytokine that acts in a pro-inflammatory or an anti-inflammatory capacity (Chalaris *et al*., 2011; Scheller *et al*., 2011; Muraguchi *et al*., 1988). The secretion of IL-6 was investigated by FluoroSpot, and it was shown that exposure of PBMC to crude *B. oleronius* protein or pure *B. oleronius* protein significantly increases the production of IL-6 compared to unstimulated PBMC ($p < 0.001$, and $p < 0.001$, respectively) (Figure 6.10 – 6.16). The increased secretion of IL-6 by PBMC treated with the crude or pure *B. oleronius* protein demonstrates a possible role for *B. oleronius* in the induction of an inflammatory response in rosacea.

The IL-1 family of cytokines are secreted by many cell types, and function as a pro-inflammatory mediator. It has been widely reported that increased levels of IL-1β can be detected in psoriatic skin lesions, and together with the down-regulation of IL-1α, it is thought that the increase of IL-1β results in the appearance of hyperproliferative inflammatory lesions (Schön *et al*., 2001; Debets *et al*., 1997; Yoshinaga *et al*., 1995; Uyemura *et al*., 1993; Kim *et al*., 1992; Nickoloff *et al*., 1991; Prens *et al*., 1990). The secretion of IL-1β was found to be significantly increased in PBMC stimulated by the crude or pure *B. oleronius* protein preparation compared to unstimulated PBMC ($p < 0.001$, and $p < 0.001$, respectively) (Figure 6.10). Thus, demonstrating that *B. oleronius* proteins are capable of inducing an inflammatory response, and that the increased secretion of IL-1β may play a role in the appearance of redness on the skin of rosacea patients due to the persistent inflammation and erythema that is associated with the condition.

TNF-α is a pro-inflammatory cyokine that functions as a key regulator of

inflammation, exerting a biological effect through a number of cell types including macrophages, monocytes, neutrophils, cardiac muscle cells, endothelial cells, epithelial cells, fibroblasts, and osteoclasts (Bradley *et al*., 2008; Popa *et al*., 2007; Abrahams *et al*., 2000; van der Bruggen *et al*., 1999). The secretion of TNF-α was observed to be significantly increased in PBMC stimulated with the crude or pure *B. oleronius* protein preparation compared to unstimulated PBMC ($p < 0.001$, and $p < 0.001$, respectively) (Figure 6.11). The increased secretion levels of TNF-α suggest that this cytokine may be involved in the induction of an inflammatory response in rosacea, and may therefore present itself as a potential therapeutic target for alleviating the persistent erythema and red appearance of the skin that is associated with the disease.

GM-CSF is a cytokine that functions as a hematopoietic growth factor and immune modulator acting in a paracrine manner to recruit circulating neutrophils, monocytes and leukocytes to enhance the immune sytstem in response to an infection, and has also been shown to increase dendritic cell maturation and the phagocytosis activity of macrophages (Shi *et al*., 2006). The secretion of GM-CSF was observed to be significantly increased in PBMC treated with the crude *B. oleronius* protein or pure *B. oleronius* protein preparations relative to the unstimulated PBMC ($p < 0.001$, and $p < 0.001$, respectively) (Figure 6.12). The increase of GM-CSF in PBMC treated with *B. oleronius* proteins implies that GM-CSF may be involved in the recruitment of immune cells to the site of infection in rosacea.

IL-10 is a pleiotropic cytokine that has a critical role in regulating inflammatory and immune responses, inactivating macrophages and expression of pro-inflammatory cytokines such as IL-6 or TNF-α, to suppress cytokine activity and inflammation (Williams *et al*., 2002; Moore *et al*., 1993). IL-10 modulates the immune response by inhibiting the expression of the major histocompatibility complex class II (MHC class II), B7-1, and B7-2, thus blocking the antigen presenting cell activation of T cell mechanism (Cao *et al*., 2002; Williams *et al*., 2002; Chang *et al*., 1995; Buelens *et al*., 1995; Ding *et al*., 1993). The anti-inflammatory activity of IL-10 has been shown to be regulated by the release of TNF receptors (R) agonists and IL-1R agonists, with the activity of IL-10 being implicated in a range of skin conditions such as psoriatic arthritis, *Leishmania major* infection, and dermatitis herpetiforms (Antiga *et al*., 2015; Weiss *et al*., 2004; McInnes *et al*., 2001; Belkaid *et al*., 2001; Joyce *et al*., 1994). The secretion of IL-10 was demonstrated to be significantly elevated in PBMC

treated with the crude or pure *B. oleronius* protein relative to unstimulated PBMC ($p < 0.001$, and $p < 0.001$, respectively) (Figure 6.13). Thus, exposure of PBMC to *B. oleronius* proteins results in the activation of an immune response that may be regulated by the increased secretion of IL-10.

IL-12p70 is an immunoregulatory cytokine that functions in Th1 cell differentiation and cell-mediated immuntiy in response to the recognition of invading microbial pathogens by antigen presenting cells (Hölscher, 2004; Trinchieri, 1993, 1995; Hsieh *et al*., 1993; Manetti *et al*., 1993). IL-12p40 secretion was analysed in PBMC stimulated with the crude *B. oleronius* protein or pure *B. oleronius* protein preparation, and observed to be significantly increased relative to unstimulated PBMC ($p < 0.001$, and $p < 0.001$, respectively) (Figure 6.14). The increased secretion of IL-12p40 by PBMC treated with *B. oleronius* protein demonstrates that exposure to *B. oleronius* leads to the activation of an immune response that may be modulated by IL-12p70.

The heterodimeric cytokine IL-23 is a member of the IL-12 family of cytokines, consisting of the IL-12p40 subunit coupled to a novel IL-23p19 subunit that binds with high affinity to the IL-23R and IL-12Rβ1 on the cell membrane, respectively (Kleinschek *et al*., 2006; Oppmann *et al*., 2000). IL-23 functions in the regulation of monocyte recruitment in response to a systemic bacterial infection such as *Listeria monocytogenes*, and has been suggested to enhance inflammation in a range of skin and autoimmune disorders including chronic spontaneous urticaria, *Cryptococcus neoformans*, and psoriasis (Atwa *et al*., 2014; Indramohan *et al*., 2012; Fitch *et al*., 2007; Kleinschek *et al*., 2006; Lee *et al*., 2004). Recently, Tang *et al*. (2012) proposed IL-23 as a potential therapeutic target for autoimmune diseases. PBMC exposed to the crude or pure *B. oleronius* protein preparation significantly increased the secretion of IL-23 compared to unstimulated PBMC ($p < 0.001$, and $p < 0.001$, respectively) (Figure 6.15). Thus, IL-23 secretion may be involved in the induction of an inflammatory response in rosacea, and could possibly be a potential therapeutic target for the treatment of this skin disease.

ApoE is a major protein component of very-low-density lipoproteins and high-density lipoproteins that exert anti-artherogenic effects to prevent build up of plaques on arteries (Greenow *et al*., 2005). PBMC exposed to the *B. oleronius* protein preparations did not show difference in the secretion of ApoE compared to unstimulated PBMC, suggesting that ApoE is not involved in the pathogenesis of

rosacea (Figure 6.16).

IL-17A has been implicated with a role in the defence against invading skin pathogens, and elevated levels of IL-17A has been associated with chronic inflammatory diseases such as rheumatoid arthritis and psoriasis (Harper *et al*., 2009; Johansen *et al*., 2009; Pitta *et al*., 2009; Eyerich *et al*., 2008; Murphy *et al*., 2003; Chabaud *et al*., 1999; Teunissen *et al*., 1998). PBMC treated with the crude *B. oleronius* protein ($p < 0.05$) or pure *B. oleronius* protein ($p < 0.01$) preparation were shown to significantly increase the secretion of IL-17A relative to unstimulated PBMC (Figure 6.17 and Figure 6.18). Thus, the secretion of IL-17A may induce an epithelial immune response in rosacea against the *B. oleronius* proteins, implying a role for *B. oleronius* in the disease.

In inflammatory skin disorders, a specific T cell subset, Th22, has been shown to be implicated in epidermal immunity and tissue remodeling by the secretion of IL-22 and TNF-α (Eyerich *et al*., 2009). IL-22 secretion was shown to be significantly increased in PBMC stimulated with the crude *B. oleronius* protein ($p < 0.001$) or pure *B. oleronius* protein ($p < 0.001$) compared to unstimulated PBMC (Figure 6.17 and Figure 6.20). Increased IL-22 secretion induced by *B. oleronius* proteins suggests that IL-22 could possibly be involved in the mediation of infiltrating immune cells to a site of infection that may lead to chronic inflammation and alterations to the extracellular matrix and tissue damage in rosacea.

IFN-γ is a type II interferon, a cytokine produced by natural killer (NK) T cells, $CD4^+$ Th1 cells, and $CD8^+$ cytotoxic T lymphocytes, that functions as a immunomodulator of the innate and adaptive immune responses against viral and parasitic infections (Schoenborn and Wilson, 2007; Gomez-Marin *et al*., 1998; Urban *et al*., 1996; Pernis *et al*., 1995; Schofield *et al*., 1987; Wheelock, 1965). Elevated levels of IFN-γ were observed in PBMC following exposure to the crude *B. oleronius* protein ($p < 0.001$) or pure *B. oleronius* protein ($p < 0.001$) compared to unstimulated PBMC (Figure 6.19 – 6.21). The increased secretion of IFN-γ by PBMC exposed to *B. oleronius* protein suggests a role for the cytokine in rosacea, as a modulator of the innate and adaptive immune responses against a persistent infection.

The cytokine, IL-2, is a T cell growth factor, promoting the development of T regulatory cells, and the expansion of T cells in the mediation of an immune response (Malek, 2003; Smith, 1988). Elevated secretion of IL-2 was demonstrated in treated PBMC following exposure to the crude *B. oleronius* or pure *B. oleronius*

protein preparations. However, a significant increase of IL-2 induced by the *B. oleronius* proteins was not observed (Figure 6.22A). Thus, the increased secretion of IL-2 implies that this cytokine may be involved in the induction of a T cell-mediated response due to *B. oleronius* proteins at the site of infection on the skin of rosacea patients.

IL-13 is mainly secreted by Th2 cells that have been shown to induce inflammation in allergenic diseases, and to activate matrix MMPs in airway epithelia, resulting in degradation and tissue remodeling of the extracellular matrix (Matsumura, 2012; Finkelman *et al*., 2010; Lee *et* al., 2001; Zhu *et* al., 1999). IL-13 secretion was shown to be significantly increased in PBMC treated with the crude ($p < 0.001$) or pure ($p < 0.001$) *B. oleronius* proteins compared to unstimulated PBMC (Figure 6.22B). Following exposure to *B. oleronius* proteins, IL-13 secretion may play a role in the induction of an inflammatory response, and the activation of MMPs in rosacea. It was previously demonstrated that *B. oleronius* proteins induce the expression of MMP-9 in neutrophils and corneal epithelial (hTCEpi) cells, and the increase of MMP-9 activity may result in damage to the corneal surface in ocular rosacea (O'Reilly *et al*., 2012a).

In conclusion, the results presented in this Chapter demonstrate that *B. oleronius* proteins are capable of inducing an immune and inflammatory response that may elucidate the mechanisms underlying development of the persistent erythema and inflammation associated with the disease. Exposure of neutrophils to the *B. oleronius* protein preparations lead to increased production of IP_1, a breakdown product of IP_3 generation, the release of stored Ca^{2+}, cytoskeletal reassembly and conversion to F-actin, and increased chemotaxis. The secretion levels of IL-1β and IL-6 were demonstrated to be significantly elevated in *B. oleronius* protein stimulated neutrophils.

The secretion of cytokines in isolated PBMC following exposure to crude or pure *B. oleronius* proteins was investigated by ELISpot or FluoroSpot assays using PBMC isolated from healthy volunteers. The secretion of ApoE, IL-2, and IL-31 were not increased relative to unstimulated PBMC, following stimulation with the crude or pure *B. oleronius* protein. FluoroSpot assays showed that the levels of secreted IL-1β, IL-10, IL-12p40, IL-23, TNF-α, and GM-CSF were significantly elevated following stimulation of PBMC with the crude or pure *B. oleronius* protein preparations compared to unstimulated PBMC ($p < 0.0001$, and $p < 0.0001$, respectively).

ELISpot and FluoroSpot anaylsis demonstrated that IL-5, IL-13, IL-17A, IL-22, and IFN-γ were significantly increased in PBMC exposed to crude or pure *B. oleronius* proteins compared to unstimulated PBMC ($p < 0.0001$, and $p < 0.0001$, respectively).

These results demonstrate that the *B. oleronius* proteins can mediate an inflammatory response that is characteristic of rosacea. The significance of this work lies in the fact that if elevated cytokine production occurs *in vivo* this could lead to the tissue damage (corneal scarring) and inflammation on the surface of the eye (keratitis) observed in ocular rosacea. The elucidation of the role of *B. oleronius* in the induction of ocular rosacea will facilitate the development of more effective and targeted therapies for the control of this disease.

Chapter 7

An Analysis of the Role of *Bacillus oleronius* Proteins in Erythematotelangiectatic Rosacea, Ocular Rosacea, and *Demodex*-Related Blepharitis

7.0 Introduction

The possible role of *D. folliculorum* mites in the pathogenesis of rosacea, especially by passive transfer of other microorganisms has been speculated upon for many years (Jarmuda *et al*., 2012). The incidence of *Demodex* on the facial skin of patients with rosacea is significantly higher than in controls (Erbağci and Ozgöztaşi, 1998; Bonner *et al*., 1993; Vance, 1986). A significantly greater density of the mites per cm^2 was detected in patients with papulopustular rosacea, and the composition of the lipids from their sebum revealed differences in comparison with controls which might facilitate the development of larger populations of mites (Ní Raghallaigh *et al*., 2012; Bonnar *et al*., 1993). The presence of *D. folliculorum* in the sebum secretions from the pilosebaceous unit was found in 90.2% of papulopustular patients and only in 11.9% of healthy controls. Additionally, histological tests of skin samples obtained from these patients revealed that the presence of *Demodex* was strongly correlated with substantial perifollicular lymphocytic infiltration (Georgala *et al*., 2001).

B. oleronius was successfully isolated from a *Demodex* mite obtained from a papulopustular rosacea patient, and it is believed that it may play a role in facilitating digestion, as it does in the termite, *Reticulitermes santonensis* (Lacey *et al*., 2007; Kuhnigk *et al*., 1995). This bacterium produced two highly immunogenic proteins that showed sera reactivity in erythematotelangiectatic rosacea patients, papulopustular rosacea patients, and facial rosacea patients with ocular *Demodex* mite infestation (O'Reilly *et al*., 2012c; Li *et al*., 2010; Lacey *et al*., 2007). The *B. oleronius* produces proteins that activate neutrophils, and induce an aberrant wound healing response and an inflammatory response in a corneal epithelial (hTCEpi) cell line (O'Reilly *et al*., 2012a, 2012b). Szkaradkiewicz *et al*. (2012), recently identified *B. oleronius* from epilated eyelashes of severe *Demodex*-associated blepharitis patients (18/36) and control subjects (5/30).

The aim of this Chapter was to investigate the role of *B. oleronius* proteins in rosacea, in studies involving (1) erythematotelangiectatic rosacea patients, (2) ocular rosacea patients (Subtype IV group) and ocular rosacea patients with erythematotelangiectatic rosacea (Subtype I & IV group), and (3) *Demodex*-related blepharitis patients.

7.1 Investigating the Role of *B. oleronius* in Erythematotelangiectatic Rosacea

It has previously been established by Western blotting, that erythematotelangiectatic rosacea patients show serum reactivity to *B. oleronius* proteins (O'Reilly *et al*., 2012c). Seventy-five erythematotelangiectatic rosacea patients were recruited to investigate the role of *B. oleronius* in this rosacea subtype. Controls, acne vulgaris, and seborrheic dermatitis patients were also enrolled in the study. Further details can be seen in Section 2.4.1. A list of the study population data is given in Table A7.1 of the appendix.

The aim of the work presented here was to establish whether a correlation existed between the sebaceous condition of the skin, the density of *Demodex* mites and reactivity of sera obtained from erythematotelangiectatic rosacea patients to *B. oleronius* proteins in order to determine the possible role of *B. oleronius* in the induction of this disfiguring condition.

7.1.1 Reactivity of Patient Sera to *B. oleronius* Protein

Protein was extracted from *B. oleronius* cells, resolved by 1-D SDS-PAGE, and transferred to membranes for Western blotting as described in Section 2.14, and Section 2.19, respectively. Serum from rosacea, acne vulgaris, seborrheic dermatitis patients, and controls was isolated, and used to probe nitrocellulose membranes containing the *B. oleronius* proteins. The number of sera samples showing reactivity to the 62 kDa and 83 kDa proteins of *B. oleronius* was calculated for each cohort (Figure 7.1). The results revealed that 26.92% (14/52) of controls showed reactivity to the *B. oleronius* proteins while 82.67% (62/75) ($p = 0.0246$) of patients diagnosed with rosacea showed reactivity to the *B. oleronius* proteins (Figure 7.2). Rosacea patients could be divided into two classes on the basis of their reactivity (62/75) or non-reactivity (13/75) to the *B. oleronius* proteins, and were termed antigen-reactive or antigen non-reactive, respectively. Acne vulgaris patients demonstrated non-reactivity to the *B. oleronius* proteins (92.86% (13/14)). Sera samples from patients diagnosed with seborrheic dermatitis demonstrated 44.44% (4/9) reactivity to the *B. oleronius* proteins while 55.56% (5/9) were non-reactive to the *B. oleronius* proteins. The study population data can be seen in Table 7.1. Western blot images recorded for the study participants can be seen the appendix (Figure A7.1 – A7.14). Analylsis of sera reactivity to *B. oleronius* proteins demonstrated that there was no

significant difference between male and female sera reactivity for each of the participant cohorts of this study population.

7.1.2 Analysis of Severity of Skin Lesions in Rosacea Patients

The severity of skin lesions in rosacea patients in the study population was evaluated by Dr Stanisław Jarmuda and colleagues, and graded 1 (mild facial erythema), 2 (moderate facial erythema), or 3 (severe facial erythema), depending upon severity of skin lesions, and the appearance of facial erythema. In the rosacea study population, only grade 1 and grade 2 skin lesions were observed, and not grade 3 (Figure 7.3). A difference between the severity of skin lesions amongst rosacea patients and serum-reactivity to the *B. oleronius* proteins was not observed in this study. Rosacea patients with grade 1 skin lesions, were 81.13% (43/53) serum reactive to the *B. oleronius* proteins, and 18.87% (10/53) serum non-reactive. Amongst rosacea patients classified with grade 2 skin lesions, 86.36% (19/22) of patients were serum reactive to the *B. oleronius* proteins while 13.64% (3/22) were assessed as serum non-reactive (Figure 7.3).

7.1.3 Analysis of *Demodex* Mite Population in Study Participants

The density of *Demodex* mites on the faces of study participants was measured using a standard surface biopsy (SSSB) by Dr Stanisław Jarmuda and colleagues (Section 2.38). Analysis of the *Demodex* mite population in the skin of rosacea patients, acne vulgaris patients, seborrheic dermatitis patients, and controls revealed a statistically greater number of *Demodex* mites in the skin of rosacea patients that showed reactivity to the 62 kDa and 83 kDa *B. oleronius* proteins ($p < 0.0001$) (Figure 7.4). There is a slightly lower although statistically non-significant *Demodex* mite population in the skin of non-reactive *B. oleronius* protein rosacea patients. The density of *Demodex* mites in the skin of acne vulgaris and seborrheic dermatitis patients was similar to the *Demodex* mite observed in controls.

7.1.4 *B. oleronius* Protein Reactive Rosacea Patients Display Reduced Levels of Sebum in Their Skin

The sebum level in the skin of study participants was measured by a sebumetric test by Dr Stanisław Jarmuda and colleagues (Section 2.39). Results demonstrated

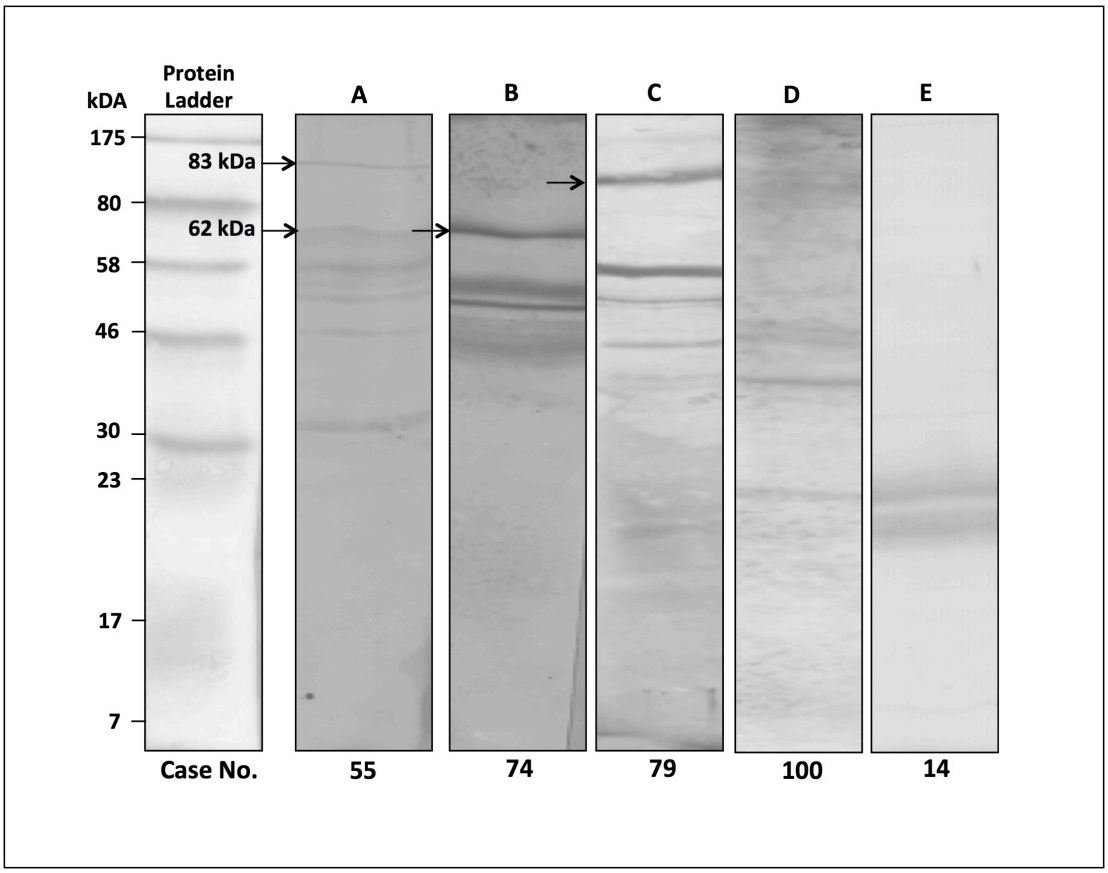

Figure 7.1 Representative Western blots of sera reactivity of participants in erythematotelangiectatic rosacea study to *B. oleronius* proteins. Positive serum immunoreactivity to (**A**) both 83 and 62 kDa protein bands (marked by arrows, case no. 55), (**B**) the 62 kDa protein band (case no. 74), (**C**) the 83 kDa protein band (case no. 10), (**D**) negative serum immunoreactivity reactivity to both protein bands (case no. 100), and (**E**) serum from a control patient negative for reactivity to both bands (case no. 14).

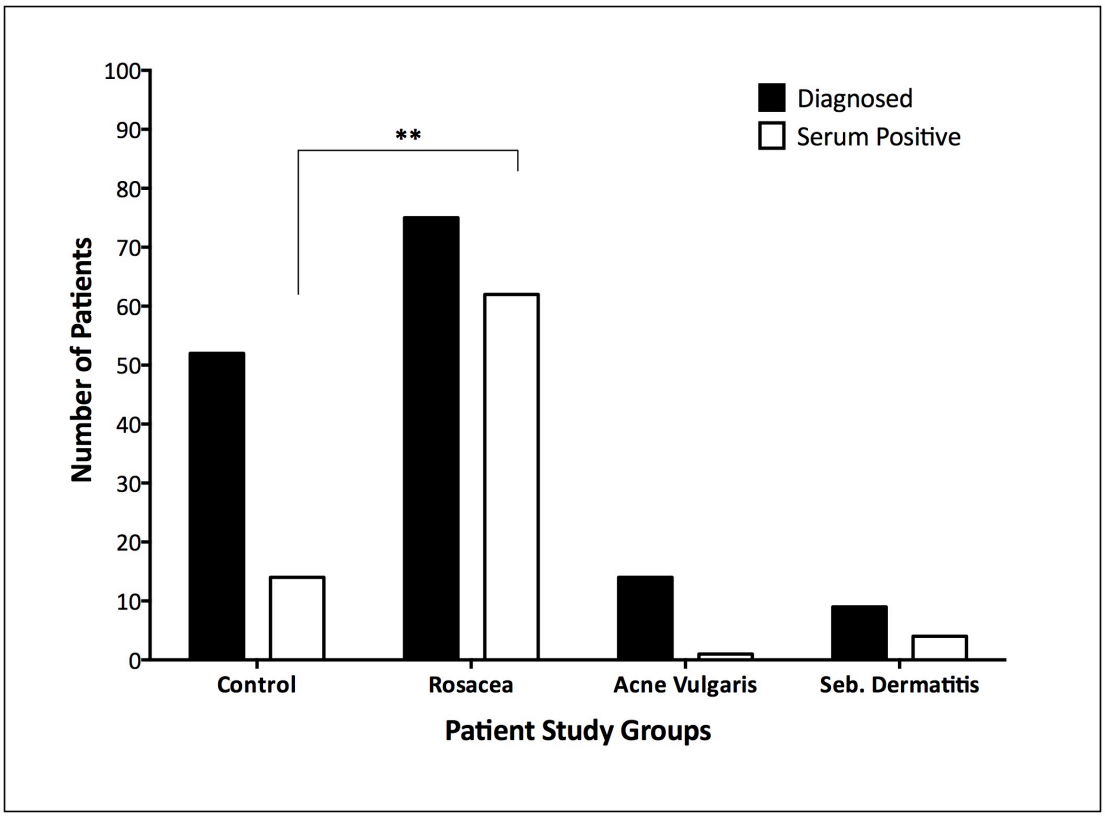

Figure 7.2 Distribution of sera reactivity of participants in erythematotelangiectatic rosacea study to *B. oleronius* protein. Subtype I rosacea patient, acne vulgaris patient, seborrheic dermatitis patient (Seb. Dermatitis), and control sera reactivity to 62 and 83 kDa proteins of *B. oleronius*. Reactivity of patient sera to 62 and 83 kDa proteins of *B. oleronius* were recorded by Western blot. (Significance: ** = $p < 0.01$).

Table 7.1 Erythematotelangiectatic rosacea study population sera reactivity of participants to *B. oleronius* protein. Erythematotelangiectatic **s**tudy population data describing gender, age, rosacea type and subtype, and the percentage serum reactivity/non-reactivity to *B. oleronius* 62 kDa protein for the control patient group, the subtype I rosacea, control, acne vulgaris, and seborrheic dermatitis.

Study Population	Average Age (yrs)	Age Range	Male	Female	Population Number	Positive Serum-Reactivity	Negative Serum-Reactivity
Control	46.26	18-89	24	29	53	26.92% (14/52)	3.08% (28/52)
Erythematotelangiectatic Rosacea	47.07	20-81	33	42	75	82.67% (62/75)	17.33% (13/75)
Acne Vulgaris	22.93	15-29	6	8	14	7.14% (1/14)	92.86% (13/14)
Seborrheic Dermatitis	30.11	22-45	4	5	9	44.44% (4/9)	55.56% (5/9)

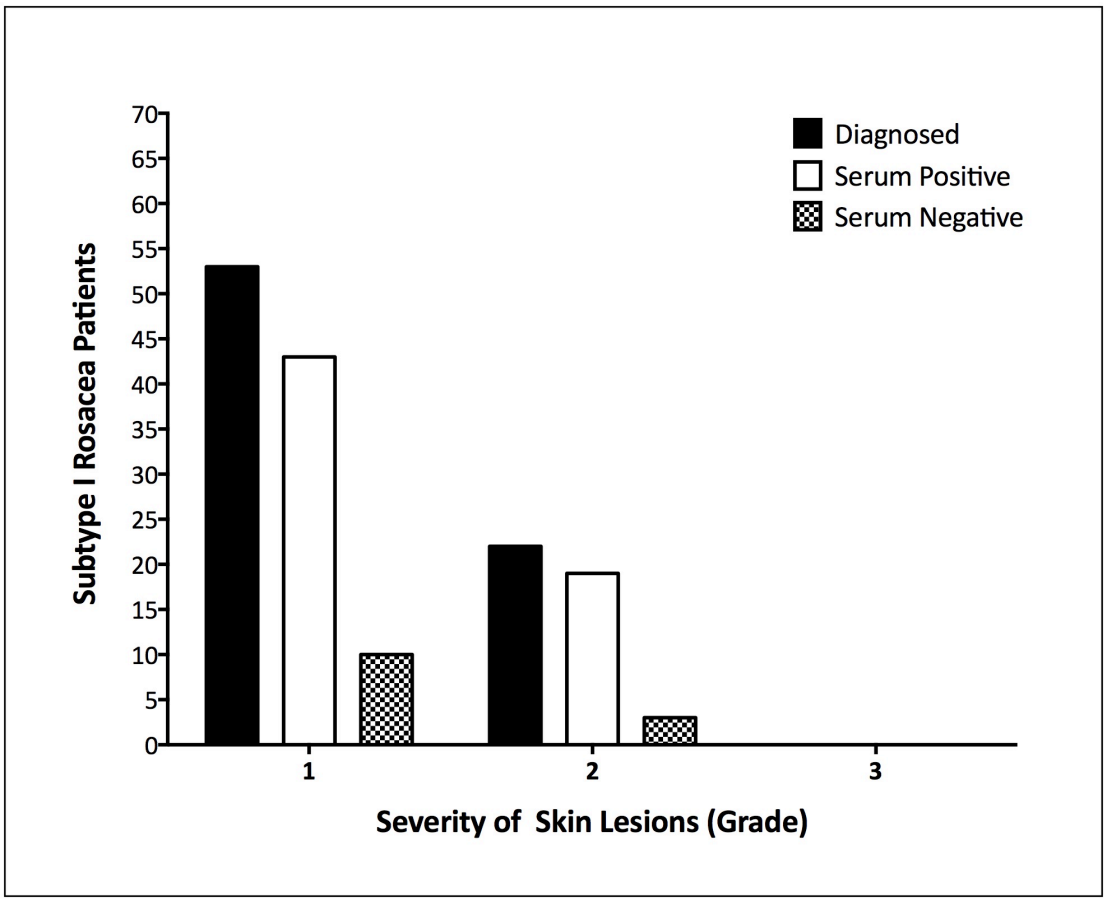

Figure 7.3 Severity of skin lesions amongst erythematotelangiectatic rosacea patients. The severity grade of skin lesions distributed amongst subtype I rosacea patients serum negative, and serum positive for reactivity to *B. oleronius* protein within the population study group. Participants of the study were graded, grade 1 (mild facial erythema), 2 (moderate facial erythema), or 3 (severe facial erythema), depending upon severity of skin lesions, and the appearance of facial erythema.

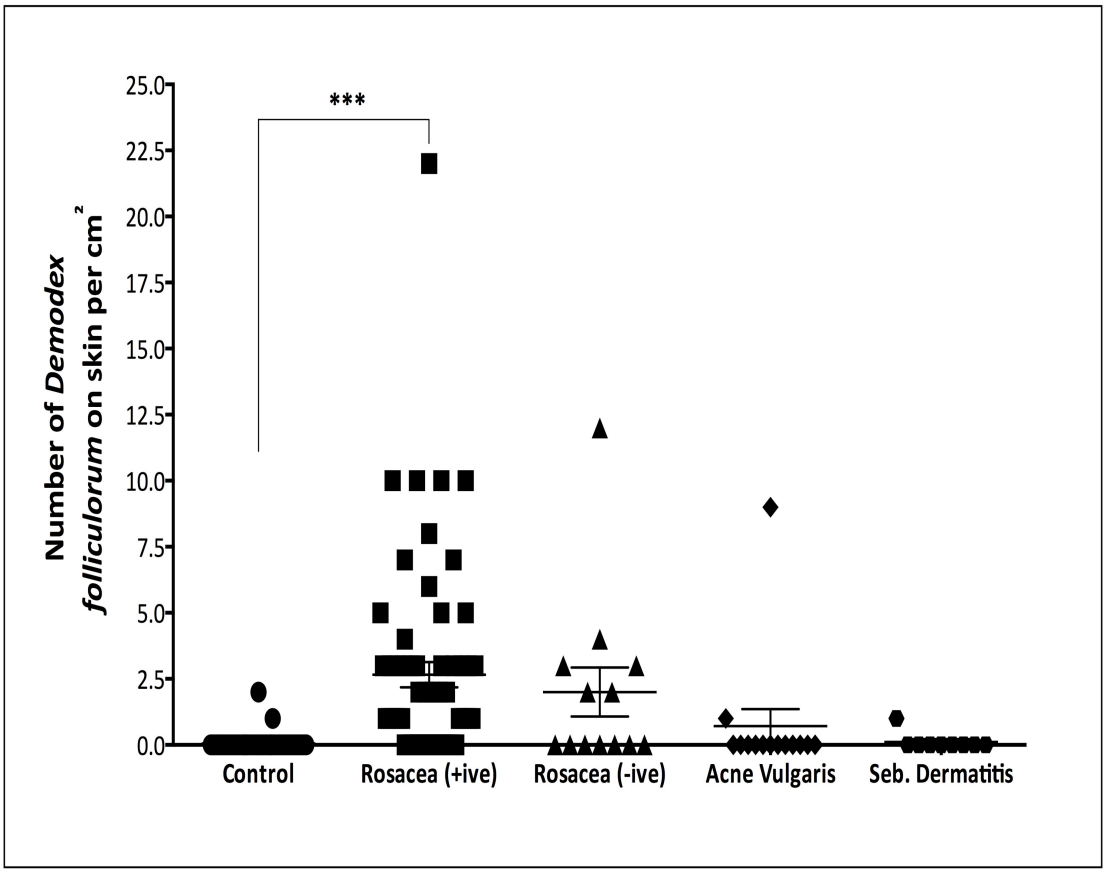

Figure 7.4 Density of *Demodex* mites in participants of erythematotelangiectatic rosacea study. Variations in *Demodex* population on faces of rosacea patients, acne vulgaris patients, seborrheic dermatitis patients (Seb. Dermatitis), and controls. *Demodex* mites were extracted from the skin of study participants, and enumerated as described. Rosacea (+ive) indicates rosacea patients who were reactive to the *B. oleronius* proteins; Rosacea (-ive) indicates rosacea patients who did not react to the *B. oleronius* proteins. (Significance: *** = $p < 0.001$).

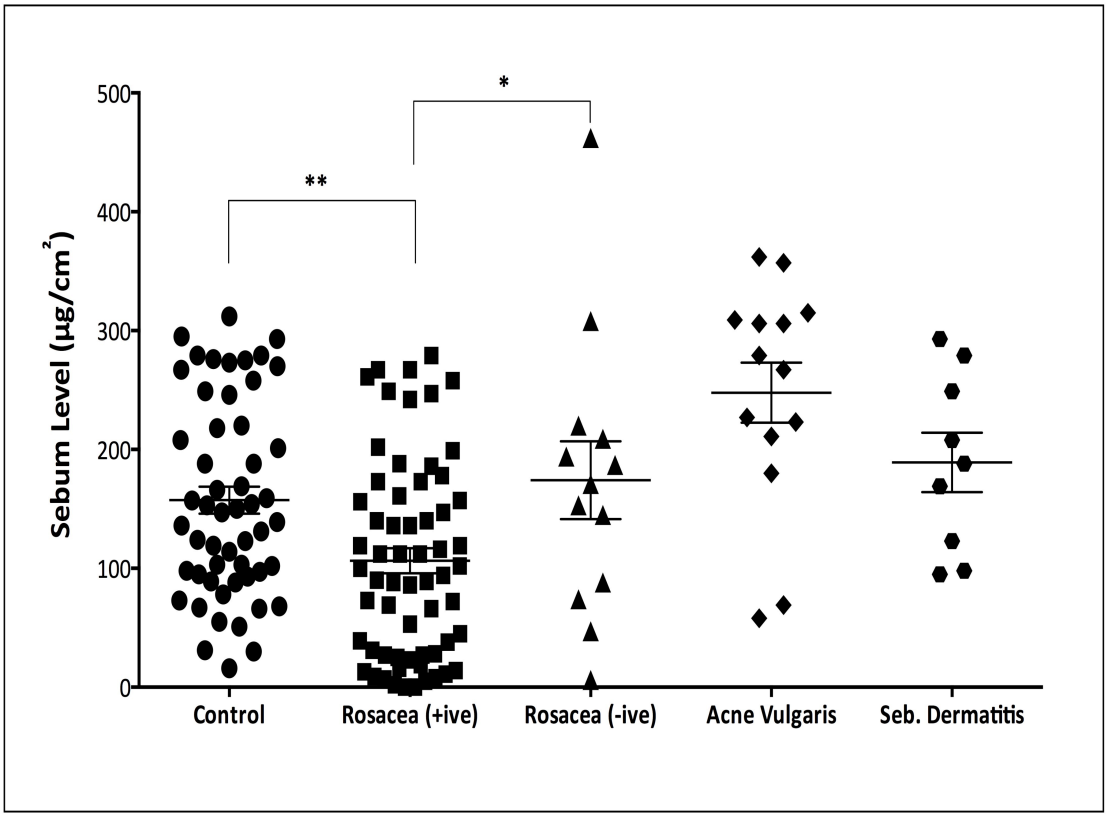

Figure 7.5 Quantity of sebum on the skin of participants in erythematotelangiectatic rosacea study. Variation in sebum level on skin of rosacea patients, acne vulgaris patients, seborrheic dermatitis patients (Seb. Dermatitis), and controls. The sebum level on the skin of study participants was measured, and expressed as $\mu g/cm^{-2}$. Rosacea (+ive) indicates rosacea patients who were reactive to the *B. oleronius* proteins; Rosacea (-ive) indicates rosacea patients who did not react to the *B. oleronius* proteins. (Significance: * = $p < 0.05$, ** = $p < 0.01$).

that *B. oleronius* protein reactive rosacea patients showed a lower level of sebum compared to the control population ($p = 0.0013$) (Figure 7.5). Interestingly, the *B. oleronius* protein reactive rosacea patients showed a significantly lower level of sebum than the *B. oleronius* protein non-reactive rosacea patients ($p = 0.0159$). Acne vulgaris and seborrheic dermatitis patients showed greater abundance of sebum compared to the *B. oleronius* protein reactive rosacea patients, and similar sebum levels to the *B. oleronius* protein non-reactive rosacea patients.

7.1.5 Investigating Cytokine Secretion Levels in Study Participants

The secretion of the cytokines IL-17, TNF-α, and IL-8 by lymphocytes in sera samples was investigated in study participants, and measured by ELISA (Section 2.39). The levels of secreted IL-17 were slightly reduced in rosacea patients who showed sera reactivity to the *B. oleronius* proteins compared to controls but the difference was not significant. Similar low levels of IL-17 secretion were detected for each cohort of the study (Figure 7.6). Analysis of the secretion of the pro-inflammatory cytokine TNF-α demonstrated no significant difference in the production of TNF-α in rosacea patients, acne vulgaris patients, seborrheic dermatitis patients, and controls (Figure 7.7). Similarly, the inflammatory mediator IL-8 did not demonstrate a significant change in secretion levels in each of the patient groups, and controls in the study (Figure 7.8).

7.1.6 Summary

Western blotting demonstrated that erythematotelangiectatic rosacea patients were 82.67% (62/75) sera positive to the *B. oleronius* proteins compared to 26.92% (14/52) sera reactivity in controls. Erythematotelangiectatic rosacea patients sera reactive to the *B. oleronius* proteins were shown to be grade 1 (mild facial erythema) or grade 2 (moderate facial erythema) skin facial lesions, and have an increased density of *Demodex* mites, and reduced levels of sebum, present on the surface of their skin compared to controls, and acne vulgaris and seborrheic dermatitis patients. The secretion levels of the cytokines IL-17, TNF-α, and IL-8 were similar for all cohort of the study, and a difference was not observed.

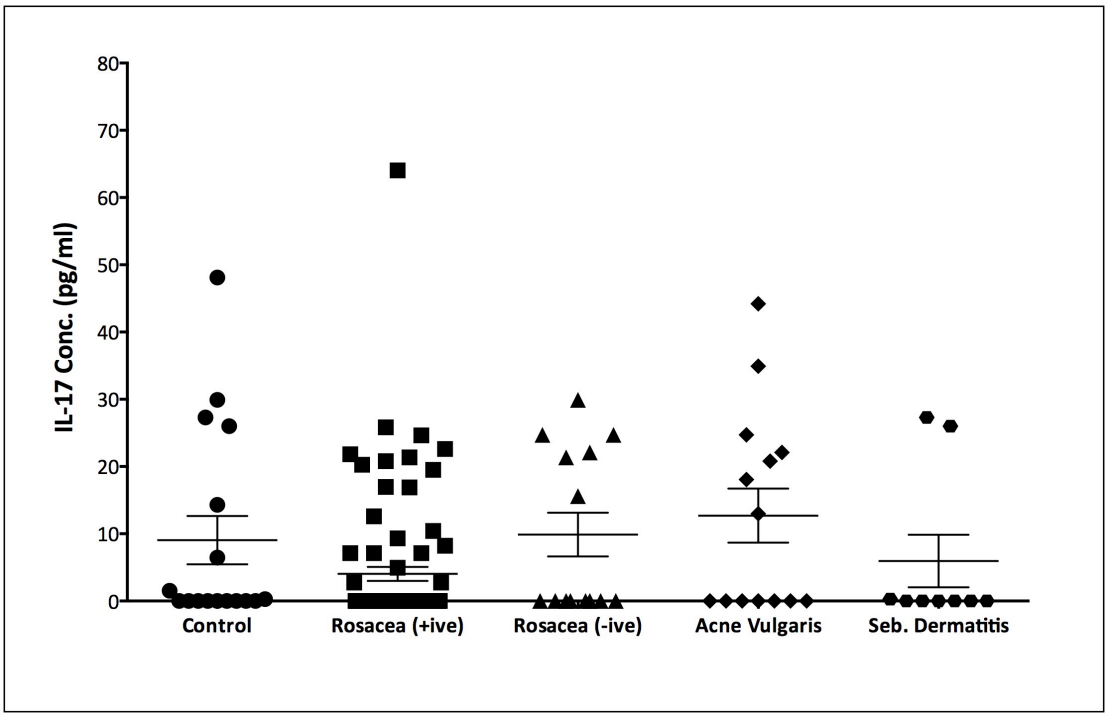

Figure 7.6 Secretion of IL-17 in participants of erythematotelangiectatic rosacea study. Secretion of IL-17 in rosacea patients, acne vulgaris patients, seborrheic dermatitis patients (Seb. Dermatitis), and controls, detected by ELISA. Rosacea (+ive) indicates rosacea patients who were reactive to the *B. oleronius* proteins; Rosacea (-ive) indicates rosacea patients who did not react to the *B. oleronius* proteins.

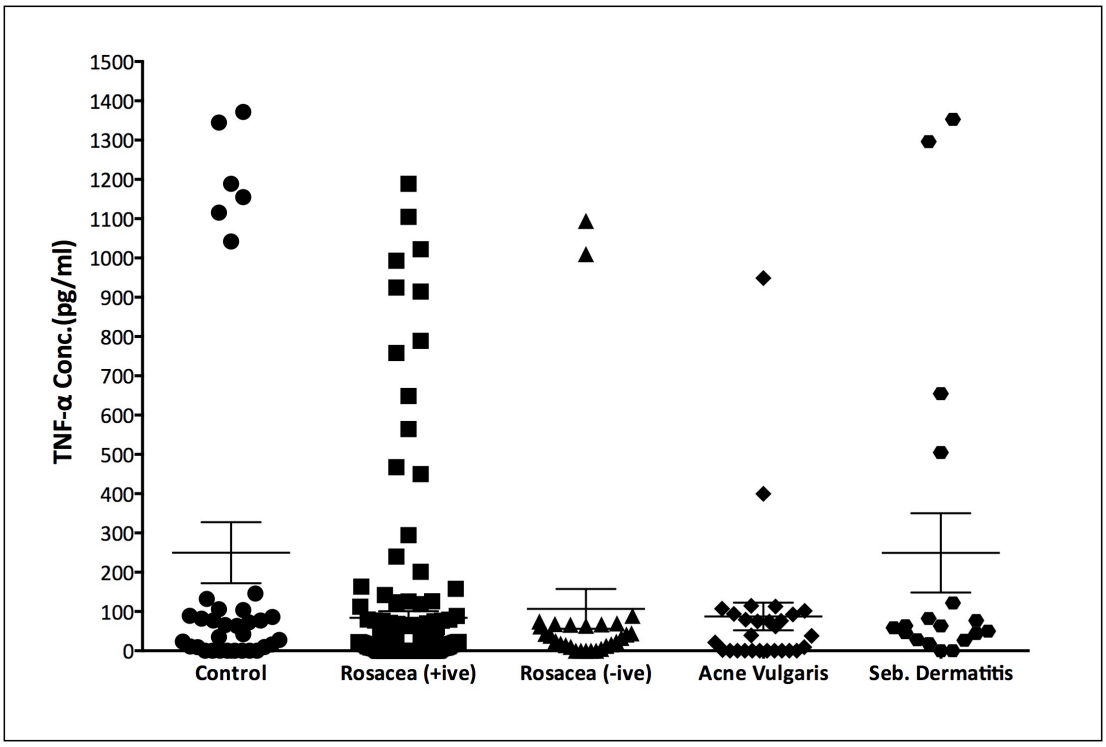

Figure 7.7 Secretion of TNF-α in participants of erythematotelangiectatic rosacea study. Secretion of TNF-α in rosacea patients, acne vulgaris patients, seborrheic dermatitis patients (Seb. Dermatitis), and controls, detected by ELISA. Rosacea (+ive) indicates rosacea patients who were reactive to the *B. oleronius* proteins; Rosacea (-ive) indicates rosacea patients who did not react to the *B. oleronius* proteins.

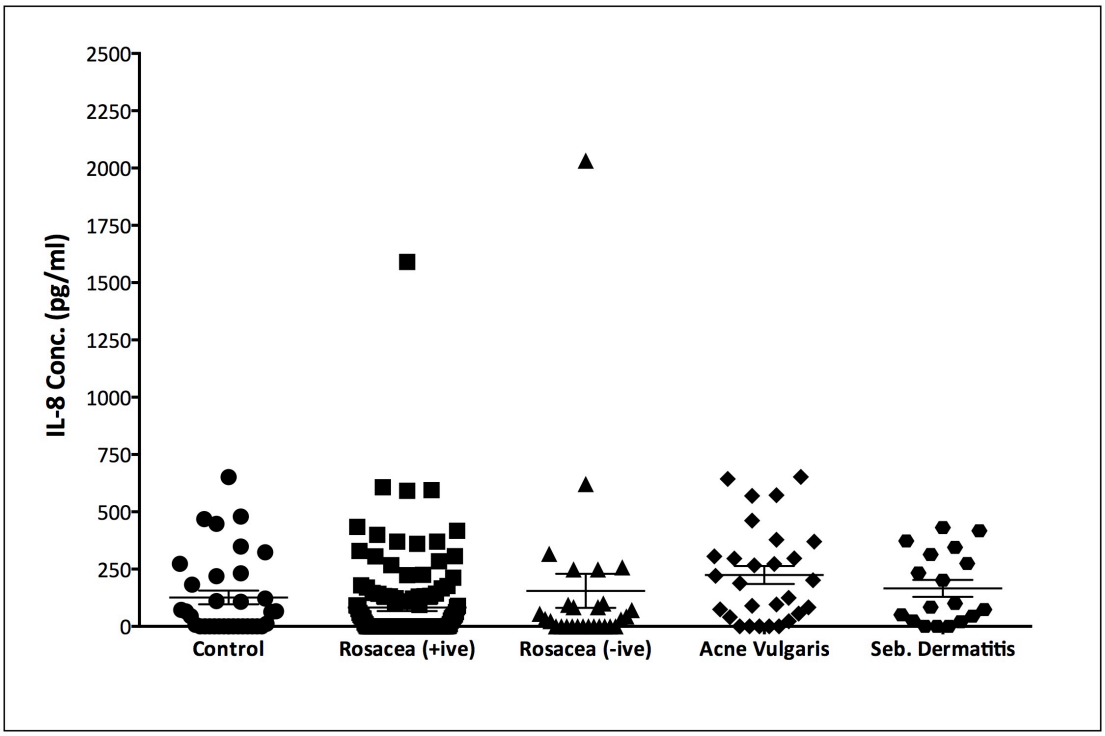

Figure 7.8 Secretion of IL-8 in participants of erythematotelangiectatic rosacea study. Secretion of IL-8 in rosacea patients, acne vulgaris patients, seborrheic dermatitis patients (Seb. Dermatitis), and controls, detected by ELISA. Rosacea (+ive) indicates rosacea patients who were reactive to the *B. oleronius* proteins; Rosacea (-ive) indicates rosacea patients who did not react to the *B. oleronius* proteins.

7.2 Analysis of *B. oleronius* Proteins in the Induction of Ocular Rosacea

Ocular rosacea has a range of symptoms such as burning or stinging sensation of the eyes, light sensitivity, blurred vision, itching, watery or bloodshot appearance, and telangiectases of the conjunctiva and eyelid margin, and blepharitis (Wilkin *et al*., 2002). This condition can appear without other symptoms typical of rosacea, and if left untreated, patients with ocular rosacea may result in visual impairment (Powell, 2005). Li *et al*. (2010) showed a positive correlation between serum immunoreactivity to *B. oleronius* proteins and facial rosacea ($p = 0.009$), eyelid margin inflammation ($p = 0.04$), and ocular *Demodex* infestation ($p = 0.48$), and demonstrated a correlation between facial rosacea and eyelid margin inflammation ($p = 0.016$). It has also been shown that *B. oleronius* proteins induce an aberrant wound healing response in a corneal epithelial cell line (hTCEpi), demonstrating a possible role for *B. oleronius* in ocular rosacea (O'Reilly *et al*., 2012b).

Eighteen participants were recruited to analyse the role of *B. oleronius* proteins in the induction of ocular rosacea (Section 2.4.2). As ocular rosacea patients can also display symptoms associated with erythematotelangiectatic rosacea, patients diagnosed with ocular rosacea and erythematotelangiectatic rosacea were also recruited into the study. A list of the study population data is given in Table 7.2.

The aim of this study was to determine serum reactivity to *B. oleronius* proteins in each of the investigated groups and to characterise a T cell specific-cytokine response in controls (control group), ocular rosacea patients (Subtype IV group) and ocular rosacea patients with erythematotelangiectatic rosacea (Subtype I & IV group) by ELISpot (Section 2.23). The crude and pure *B. oleronius* protein preparations have previously been shown to be sera reactive in patients with rosacea, and induce an inflammatory response in a corneal epithelial cell line (hTCEpi) (O'Reilly *et al*., 2012b, 2012c; Li *et al*., 2010).

7.2.1 Assessement of Reactivity to *B. oleronius* Immuno-Reactive 62 kDa and 83 kDa Protein

The study population was divided into three groups, and the reactivity of patient sera to the 62 kDa and 83 kDa proteins was evaluted by Western blotting (Figure 7.9A). The control group showed 83.3% (5/6) negative serum-reactivity to the *B. oleronius* 62 kDa and 83 kDa protein bands (Code R) (Figure 7.9B). The ocular rosacea group (Subtype IV group), and the ocular rosacea with

erythematotelangiectatic rosacea group (Subtype I & IV group) both demonstrated 100% (6/6) positive serum-reactivity to *B. oleronius* 62 kDa and 83 kDa proteins (Figure 7.9C and 7.9D, respectively) (Table 7.3).

7.2.2 Investigation of the T Cell Cytokine Response Following Exposure to *B. oleronius* Protein

Elevated IL-13 production was observed by PBMC extracted from control subjects, following exposure to crude or pure *B. oleronius* protein preparations but the increase was not significant ($p = 0.0625$). In contrast, PBMC isolated from rosacea patients of the Subtype I, and the Subtype I & IV group, and exposed to the crude or pure *B. oleronius* proteins showed reduced levels of IL-13 secreting cells relative to *B. oleronius* protein stimulated PBMC from controls. Intrestingly, the untreated PBMC from the rosacea patients of Subtype I group, and the Subtype I & IV group displayed greater levels of IL-13 secreting cells compared to untreated control group PBMC (Figure 7.10). For Figures 7.11 to 7.15, the positive control, PBMC exposed to anti-CD3 (1 ng/ml) is excluded for ease of interpreting the results. A representative positive control response induced by anti-CD3 (1 ng/ml) is given in Figure 7.10.

An increase of IL-2 secretion was observed in untreated PBMC from rosacea Subtype IV, and Subtype I & IV patients compared to control. However, the observed increase was not significant (Figure 7.11). Exposure of PBMC extracted from controls, to the *B. oleronius* proteins resulted in slightly elevated levels of IL-2 secretion, and relative to control PBMC treated with the *B. oleronius* proteins, rosacea patient PBMC exposed to the *B. oleronius* proteins increased IL-2 secretion. Rosacea patient PBMC stimulated by the crude or pure *B. oleronius* proteins showed a decline in IL-2 secreting cells compared to untreated PBMC isolated from rosacea patients, and a significant reduction of IL-2 secretion was recorded following treatment of Subtype IV rosacea patient PBMC to pure *B. oleronius* proteins relative to untreated PBMC isolated from Subtype IV rosacea patients (Figure 7.11).

Untreated PBMC from rosacea patients within the Subtype IV, and Subtype I & IV groups displayed elevated IL-22 secretion compared to untreated PBMC from the control group. Exposure of PBMC isolated from controls and Subtype I & IV rosacea patients to the crude or pure *B. oleronius* proteins (5 μg/ml), resulted in a significant increase in IL-22 secreting cells relative to untreated PBMC in the control group ($p < 0.05$). Rosacea patients PBMC stimulated by *B. oleronius* protein

demonstrated a slight decrease in IL-22 secretion compared to *B. oleronius* protein treated PBMC of controls (Figure 7.12).

Untreated PBMC from the Subtype IV group, and Subtype I & IV group displayed elevated levels of IL-17A secretion compared to untreated PBMC from the control group. Exposure of PBMC to the pure *B. oleronius* protein (5 μg/ml) preparation increased the production of IL-17A secreting cells in control PBMC relative to untreated PBMC in the control group but not in the Subtype IV, and Subtype I & IV groups where a significant inhibition of IL-17A secreting cells was observed ($p < 0.05$) (Figure 7.13). A significant reduction of IL-17A production was recorded between the control group treated with the pure *B. oleronius* protein (5 μg/ml), and the pure *B. oleronius* protein (5 μg/ml) treated PBMC from the Subtype I & IV group ($p < 0.05$). Isolated PBMC treated with the crude *B. oleronius* protein (5 μg/ml) from the Subtype IV group of rosacea patients, displayed a similar inhibitory effect of IL-17A secretion, and the decrease was significant relative to untreated PBMC from the ocular rosacea patients of the Subtype IV group ($p < 0.05$). A similar reduction of IL-17A levels was recorded for PBMC extracted from the Subtype I & IV group of rosacea patients, untreated and treated with pure *B. oleronius* protein ($p < 0.05$) (Figure 7.13).

The levels of secreted IL-31 were shown to be similar in untreated PBMC in rosacea patients and controls. There was no difference in IL-31 production between rosacea patients and controls following PBMC treatment with the pure *B. oleronius* protein preparation. However, treatment of rosacea patient PBMC with the crude *B. oleronius* protein preparation resulted in a marginal increase of IL-31 secreting cells, but the observed increase was not deemed significant (Figure 7.14).

Exposure of control PBMC to crude *B. oleronius* protein, had the greatest effect in inducing IFN-γ secretion compared to the other T cell specific-cytokines investigated. Crude or pure *B. oleronius* protein treated PBMC extracted from controls demonstrated a significant increase in IFN-γ secretion compared to untreated PBMC ($p < 0.05$) (Figure 7.15). Interestingly, the PBMC of rosacea patients exposed to crude *B. oleronius* protein preparation, exhibited a significant reduction of IFN-γ secreting cells relative to crude *B. oleronius* protein treated PBMC of controls ($p < 0.05$). Similar levels of IFN-γ secretion were observed in PBMC exposed to pure *B. oleronius* proteins. However, there were greater numbers of IFN-γ secreting cells recorded from PBMC isolated from Subtype I & IV rosacea patients following

exposure to the crude or pure *B. oleronius* protein (5 μg/ml) compared to PBMC isolated from rosacea Subtype IV patients, and treated with the *B. oleronius* protein preparations ($p < 0.05$) (Figure 7.15).

7.2.3 Summary

Untreated PBMC from rosacea patients displayed an altered immune response compared to controls, with increased levels of secreted IL-13, IL-2, IL-22, and IFN-γ, demonstrating an active immune response. Rosacea patient PBMC exposed to crude or pure *B. oleronius* proteins (5 μg/ml) demonstrated decreased secretion of T cell specific-cytokines, IL-13, IL-22, IL-17A, and IFN-γ. The cytokines IL-2 and IL-31, were shown to be increased in secretion following stimulation by the *B. oleronius* proteins.

Table 7.2 List of study participants in ocular rosacea study and serum reactivity to *B. oleronius* protein. Study population data describing gender, age, rosacea type and subtype, and reactivity to *B. oleronius* 62 kDa protein for each participant. (-: negative serum-reactivity, +: positive serum-reactivity).

Patient Code Identifier	Gender	Age (yrs)	Rosacea Type	Subtype	Anti-62 kDa Sera-reactivity (+/-)
B	Male	49	Ocular Rosacea	IV	+
C*	Male	39	Ocular Rosacea with Erythematotelangiectatic Rosacea	I & IV	+
D	Male	69	Ocular Rosacea	IV	+
E	Male	27	Ocular Rosacea with Erythematotelangiectatic Rosacea	I & IV	+
F	Male	32	Ocular Rosacea with Erythematotelangiectatic Rosacea	I & IV	+
I	Male	37	Ocular Rosacea	IV	+
J	Male	51	Ocular Rosacea	IV	+
K*	Female	66	Ocular Rosacea	IV	+
L	Female	52	Ocular Rosacea with Erythematotelangiectatic Rosacea	I & IV	+
M	Male	21	Ocular Rosacea	IV	+
N	Male	50	Ocular Rosacea with Erythematotelangiectatic Rosacea	I & IV	+
O	Male	49	Ocular Rosacea with Erythematotelangiectatic Rosacea	I & IV	+
R	Male	32	Control	-	+
S	Male	63	Control	-	-
T	Female	58	Control	-	-
U	Male	31	Control	-	-
V	Male	72	Control	-	-
W	Female	42	Control	-	-

* indicates patient was on a course of doxycyclone oral antibiotics

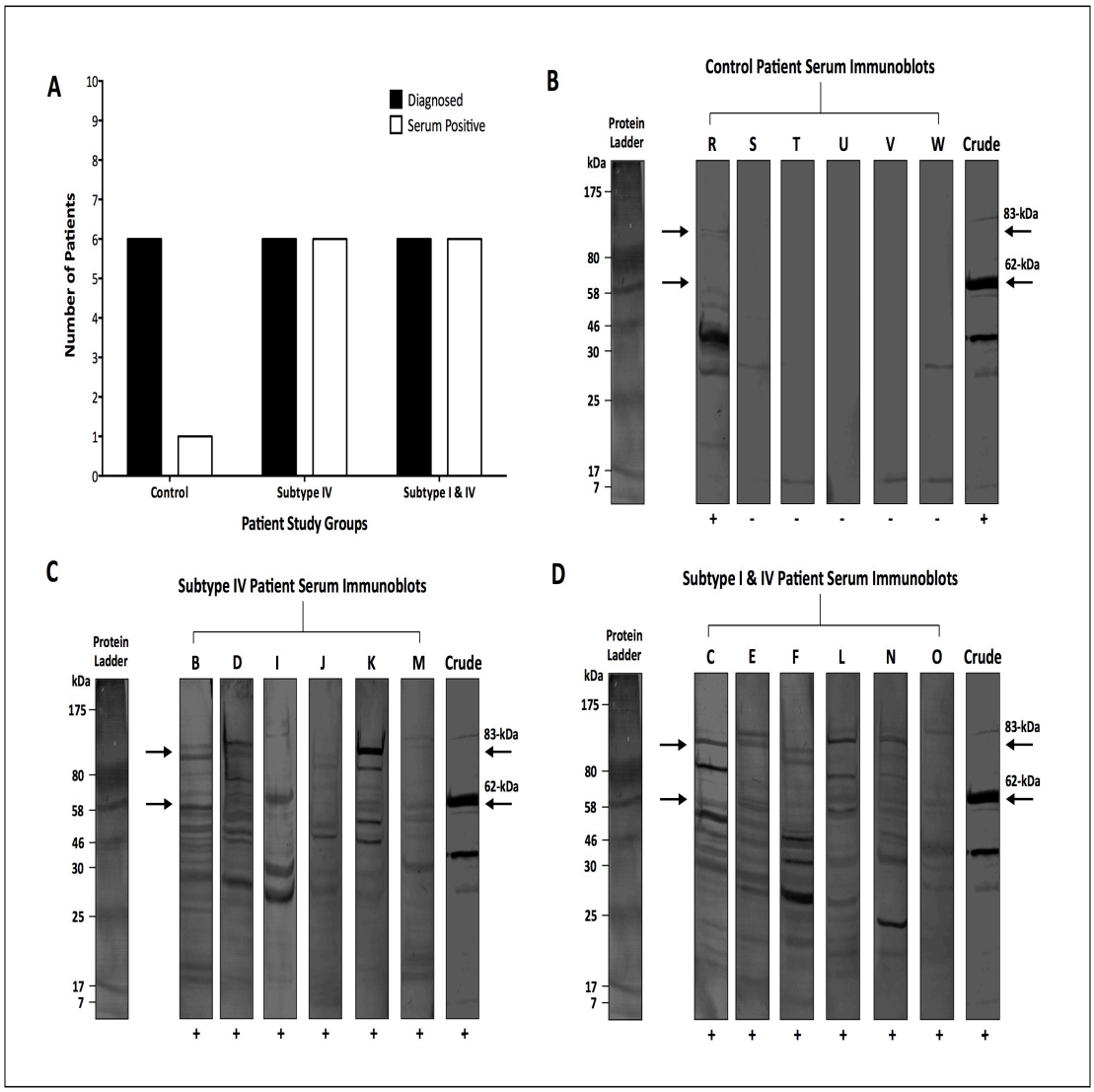

Figure 7.9 Western blots of sera reactivity of study participants to *B. oleronius* protein in ocular rosacea study. (**A**) Subtype IV rosacea patient (ocular rosacea), Subtype I & IV rosacea patient (ocular rosacea with erythematotelangiectatic rosacea), and control sera reactivity to 62 and 83 kDa proteins of *B. oleronius*. Reactivity of patient sera to 62 and 83 kDa proteins of *B. oleronius* were recorded by Western blot. Open symbols indicate patients or controls, and closed symbols indicate those showing reactivity to *B. oleronius* proteins. Immunoblots of (**B**) control patient sera samples, (**C**) Subtype IV, ocular rosacea patient sera samples, and (**D**) Subtype I & IV, erythematotelangiectatic and ocular rosacea patient sera samples, to determine reactivity to *B. oleronius* protein, and in particular, sera-reactivity to the anti-62 kDa protein. Crude (crude *B. oleronius* protein (1 µg/µl)) represents a positive control for reactivity to the 62 kDa protein. (n = 6 patients for each population). (-: negative serum-reactivity, +: positive serum-reactivity).

Table 7.3 Ocular rosacea study population sera reactivity of participants to *B. oleronius* protein. Study population data describing gender, age, rosacea type and subtype, and reactivity to *B. oleronius* 62 kDa protein for the control patient group, the subtype IV, ocular rosacea group, and subtype I & IV, erythematotelangiectatic and ocular rosacea patient group.

Study Population	Average Age (yrs)	Age Range	Male	Female	Population Number	Positive Anti-62 kDa Protein Reactivity	Negative Anti-62 kDa Protein Reactivity
Control Group	49.7	29 - 70	4	2	6	0% (0/6)	100% (6/6)
Ocular Group (Subtype IV)	48.8	21 - 69	5	1	6	100% (6/6)	0% (0/6)
Ocular Rosacea and Erythematotelangiectatic Rosacea Group (Subtype I & IV)	42.2	27 - 52	4	2	6	100% (6/6)	0% (0/6)

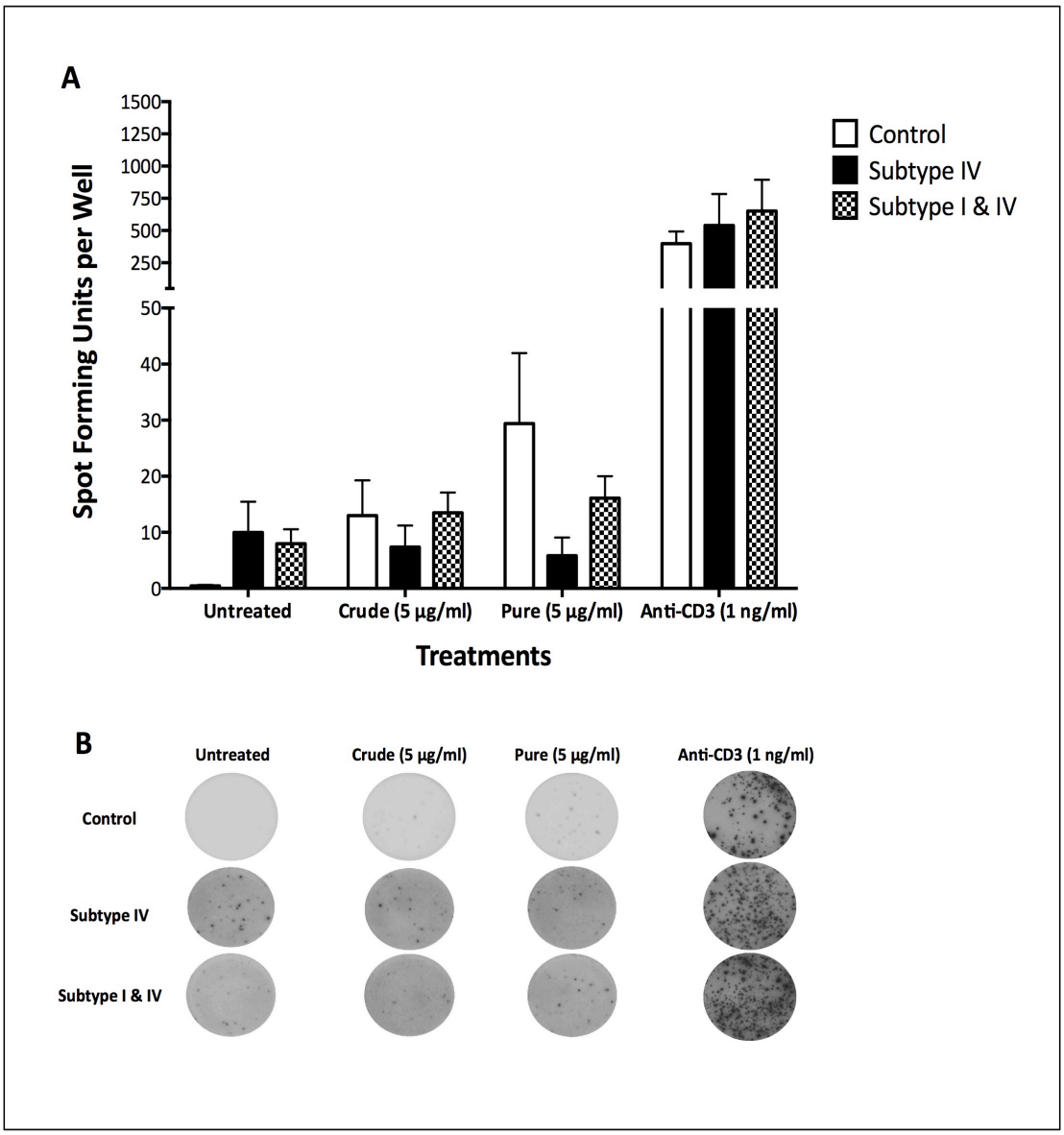

Figure 7.10 IL-13 secretion by PBMC from controls and patients exposed to *B. oleronius* proteins or anti-CD3 (positive control) in ocular rosacea study. (**A**) Secretion of IL-13 by isolated PBMC following 48 hour incubation with stimulation by untreated (culture media), crude *B. oleronius* protein (5 µg/ml), pure *B. oleronius* protein (5 µg/ml), or anti-CD3 (1 ng/ml) (positive control), determined by ELISpot. (**B**) Representative well images of spot formation for each treatment of the control, Subtype IV, and Subtype I & IV subjects. (n = 6 patients for each population).

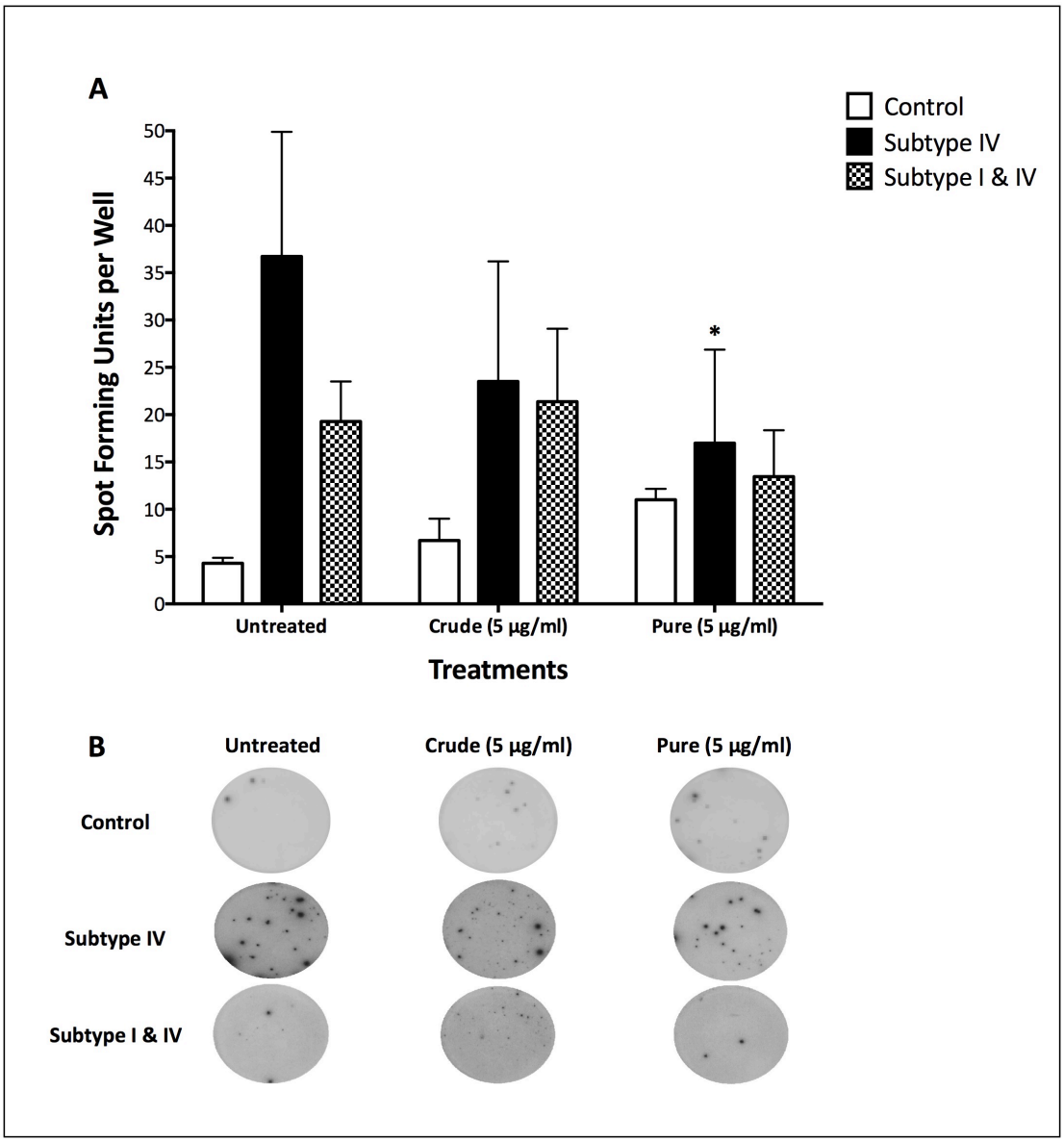

Figure 7.11 IL-2 secretion by PBMC from controls and patients exposed to *B. oleronius* proteins in ocular rosacea study. (**A**) Secretion of IL-2 by isolated PBMC following 48 hour incubation with stimulation by untreated (culture media), crude *B. oleronius* protein (5 µg/ml), or pure *B. oleronius* protein (5 µg/ml), determined by ELISpot. (**B**) Representative well images of spot formation for each treatment of the control, Subtype IV, and Subtype I & IV subjects. (n = 6 patients for each population). (Significance: * = $p < 0.05$).

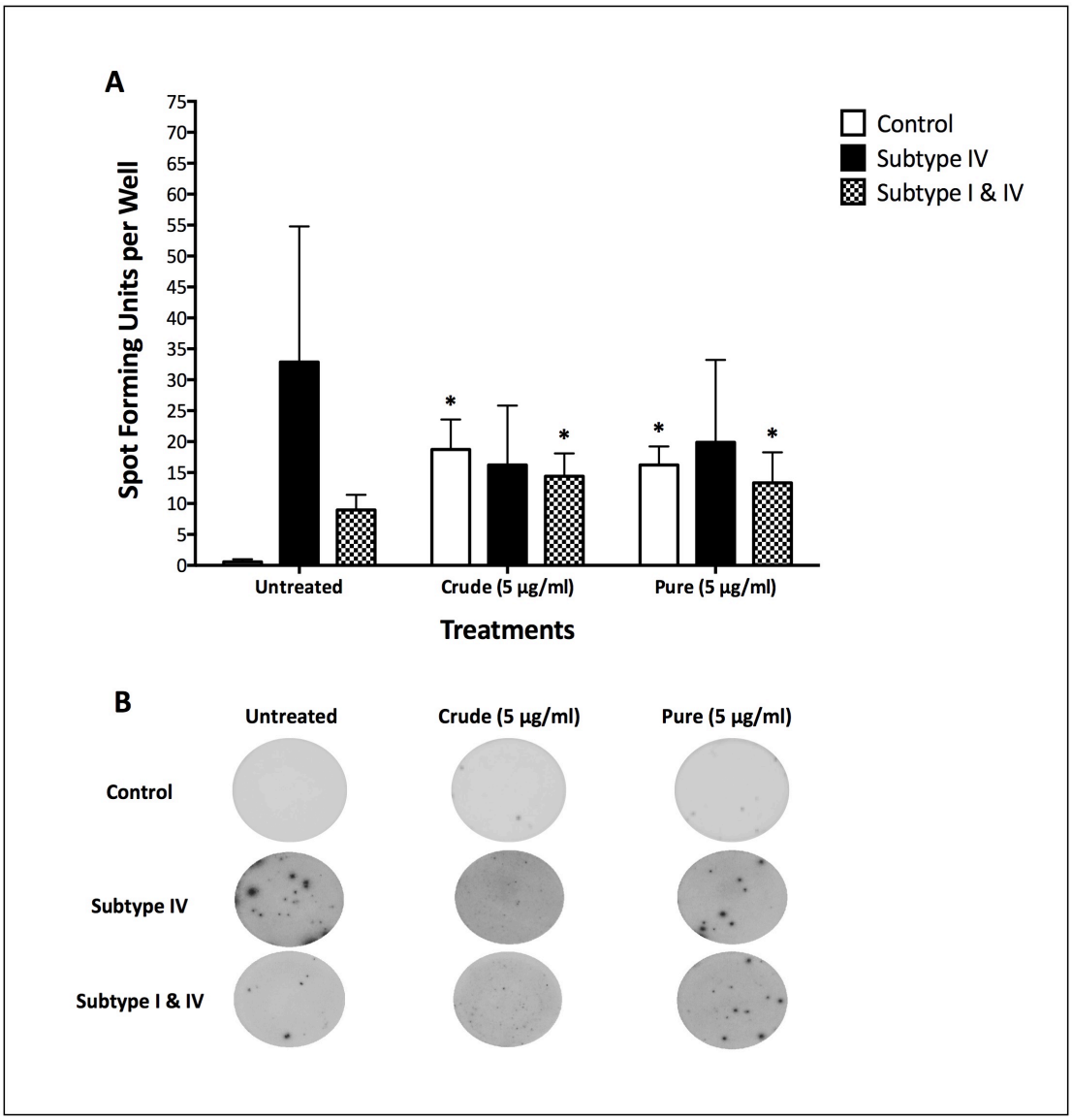

Figure 7.12 IL-22 secretion by PBMC from controls and patients exposed to *B. oleronius* proteins in ocular rosacea study. (**A**) Secretion of IL-22 by isolated PBMC following 48 hour incubation with stimulation by untreated (culture media), crude *B. oleronius* protein (5 µg/ml), or pure *B. oleronius* protein (5 µg/ml), determined by ELISpot. (**B**) Representative well images of spot formation for each treatment of the control, Subtype IV, and Subtype I & IV subjects. (n = 6 patients for each population). (Significance: * = $p < 0.05$).

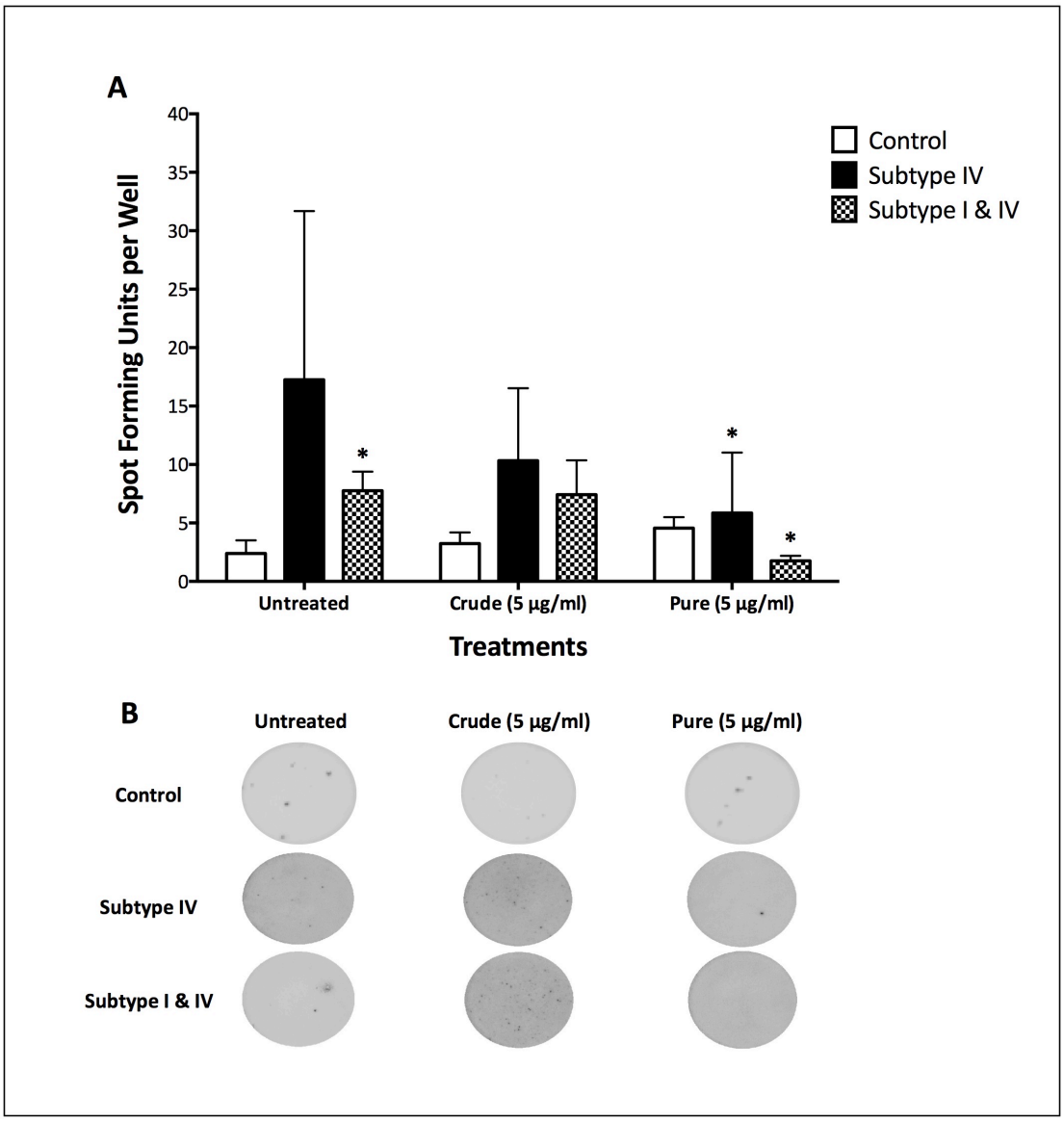

Figure 7.13 IL-17A secretion by PBMC from controls and patients exposed to *B. oleronius* proteins in ocular rosacea study. (**A**) Secretion of IL-17A by isolated PBMC following 48 hour incubation with stimulation by untreated (culture media), crude *B. oleronius* protein (5 µg/ml), or pure *B. oleronius* protein (5 µg/ml), determined by ELISpot. (**B**) Representative well images of spot formation for each treatment of the control, Subtype IV, and Subtype I & IV subjects. (n = 6 patients for each population). (Significance: * = $p < 0.05$).

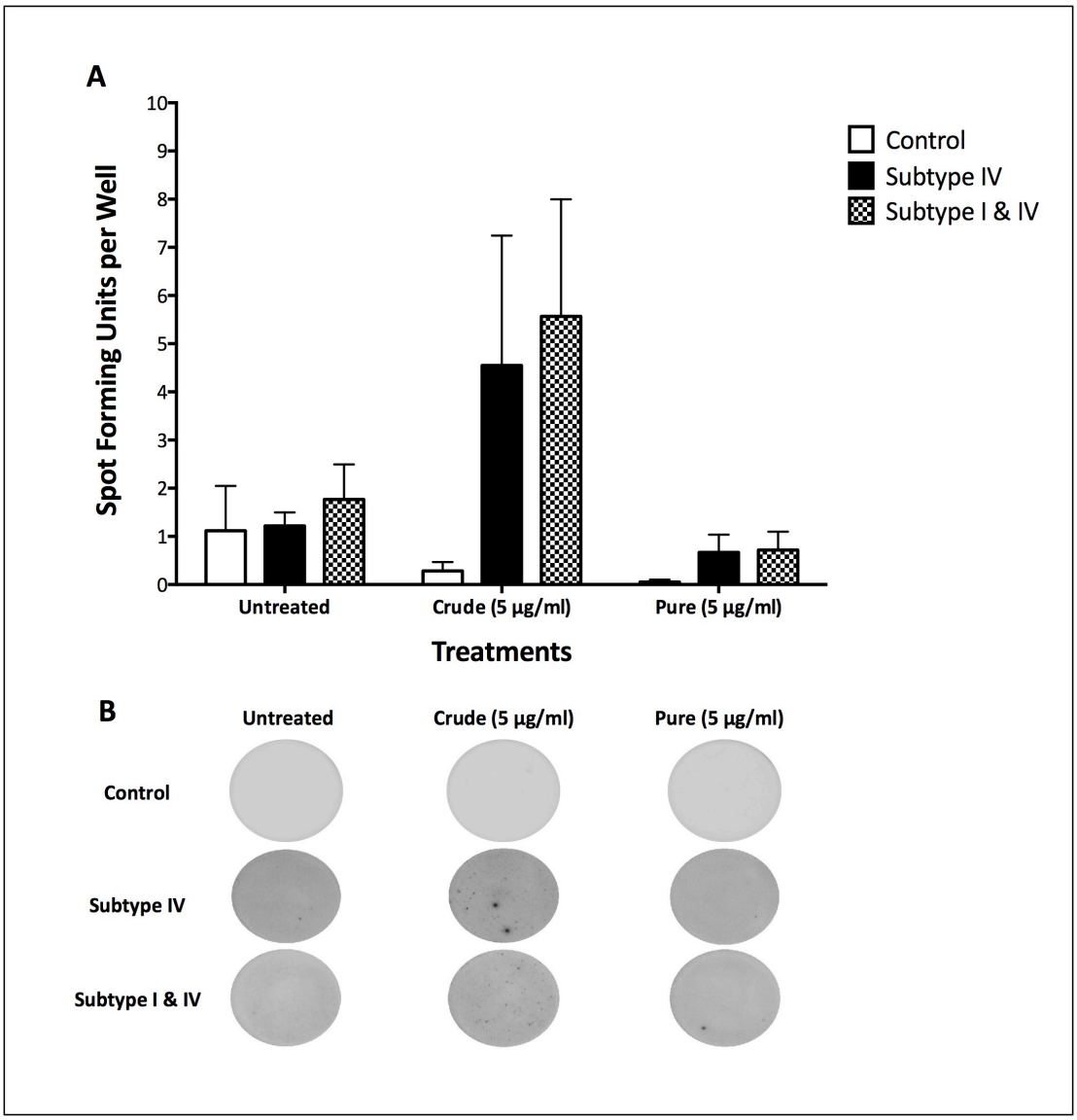

Figure 7.14 IL-31 secretion by PBMC from controls and patients exposed to *B. oleronius* proteins in ocular rosacea study. (**A**) Secretion of IL-31 by isolated PBMC following 48 hour incubation with stimulation by untreated (culture media), crude *B. oleronius* protein (5 µg/ml), or pure *B. oleronius* protein (5 µg/ml), determined by ELISpot. (**B**) Representative well images of spot formation for each treatment of the control, Subtype IV, and Subtype I & IV subjects. (n = 6 patients for each population).

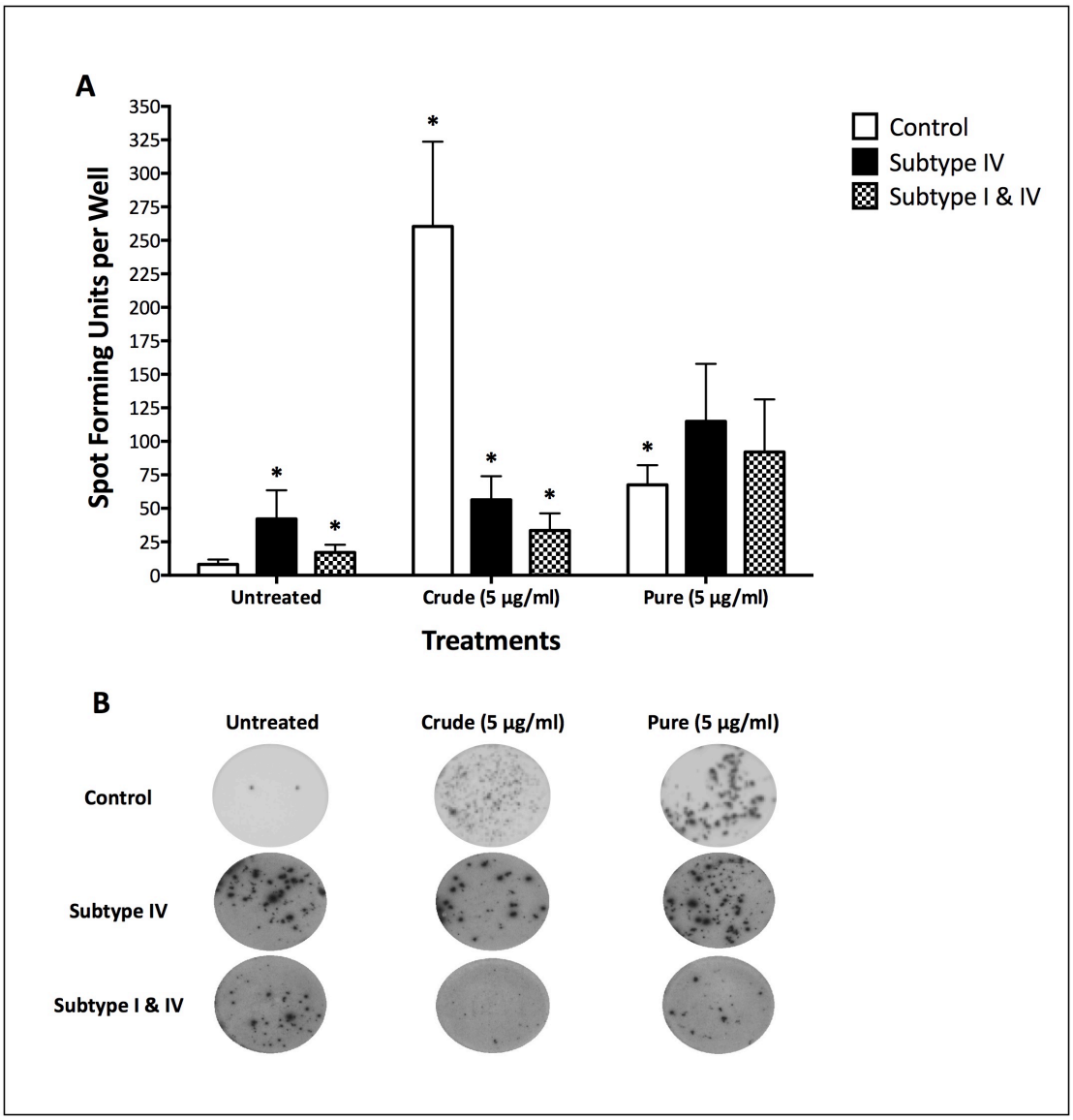

Figure 7.15 IFN-γ secretion by PBMC from controls and patients exposed to *B. oleronius* proteins in ocular rosacea study. (**A**) Secretion of IFN-γ by isolated PBMC following 48 hour incubation with stimulation by untreated (culture media), crude *B. oleronius* protein (5 µg/ml), or pure *B. oleronius* protein (5 µg/ml), determined by ELISpot. (**B**) Representative well images of spot formation for each treatment of the control, Subtype IV, and Subtype I & IV subjects. (n = 6 patients for each population). (Significance: * = $p < 0.05$).

7.3 An Assessment of the Role of *B. oleronius* Proteins in *Demodex*-Related Blepharitis

Blepharitis is an inflammatory condition affecting the eyelids, resulting in dry eye, meibomian gland dysfunction, and if left untreated, the disease can persist to impair vision (Jackson, 2008). In recent years, *Demodex* mites have been implicated in the disease, in a form of the condition classified as *Demodex*-related blepharitis. Patients with high ocular *Demodex* infestation were shown to be sera reactive to *B. oleronius* proteins ($p = 0.048$) (Li *et al*., 2010; Liu *et al*., 2010). Seventy consenting volunteers were recruited to assess the role of *B. oleronius* proteins in *Demodex*-related blepharitis (Section 2.4.3). A list of the study population data is given in Table A7.2 of the appendix.

7.3.1 Reactivity of Patient Sera to *B. oleronius* Protein

Protein from cultures of *B. oleronius* was extracted as described in Section 2.12.1, resolved by electrophoresis in denaturing conditions before protein transfer onto a nitrocellulose membrane, and probed with patient serum before blot development to determine serum-reactivity to *B. oleronius* proteins in a double-blind experimental set up. Each patient serum blot was assessed in duplicate (Trial 1 and Trial 2), and it was revealed that patients of Group 1 with blepharitis and high infestation of *Demodex* mites, were 78.4% (29/37) sera reactive to the *B. oleronius* protein, as 21.8% (8/37) were assessed as serum non-reactive to the *B. oleronius* protein ($p = 0.0613$) (Figure 7.16). Group 2, consisting of individuals with *Demodex* infestation and blepharitis-negative, were 64.7% (11/17) sera reactive, and 35.3% (6/17) serum non-reactive to the *B. oleronius* protein. The control subjects, without *Demodex* mite infestation and blepharitis, were recorded as 50.0% (8/16) sera reactive and sera non-reactive to the *B. oleronius* protein (Table 7.4). Representative immunoblots observed to be sera reactive and sera non-reactive to the *B. oleronius* anti-62 kDa protein in blepharitis and control patients can be seen in Figure 7.17. Immunoblot images recorded for the blepharitis study participants can be seen in the appendix (Figure A7.15 – A7.30).

Following the assessment of sera immunoreactivity to the *B. oleronius* protein, the study participant information was further analysed to establish a correlation between blepharitis, *Demodex* mite infestation, keratitis, and/or acne with sera reactivity to the *B. oleronius* anti-62 kDa protein. The statistical significance of the

results was calculated using the Chi-square test. The participants of the study diagnosed as blepharitis-positive were 78.4% (29/37) sera reactive, and 21.6% (8/37) sera non-reactive to *B. oleronius* protein while blepharitis-negative individuals were 57.6% (19/33) sera reactive, and 42.4% (14/33) sera non-reactive to *B. oleronius* protein ($p = 0.0613$) (Table 7.5). The outcome of Chi-square test did not demonstrate a significant correlation between the incidence of blepharitis and sera immunoreactivity to the *B. oleronius* anti-62 kDa protein but it did show a p - value near to $p < 0.05$.

Epilated eyelashes were analysed under a light microscope by Dr Lingyi Liang and colleagues, and enhanced with a fluorescein-containing solution as a method for the identification and counting of *D. brevis* and *D. folliculorum* mites in study participants (Liang *et al*., 2014; Kheirkhah *et al*., 2007a; Gao *et al*., 2005). The results showed that 74.1% (40/54) of participants with *Demodex* mites were sera reactive to the *B. oleronius* protein while 25.9% (14/54) were sera non-reactive (Table 7.6). However, the controls were observed to be 50.0% (8/16) sera reactive to the *B. oleronius* protein. The number of participants for each group of the study suggested that more control sera samples are required for the study, as this may be more representative when inferring the correlation between sera reactivity to *B. oleronius* protein and blepharitis, and *Demodex* mite infestation.

The correlation between patients diagnosed with keratitis and sera reactive to the *B. oleronius* protein was shown not to be significant ($p = 0.2064$). The results revealed that 77.7% (23/30) of keratitis patients were sera reactive to the *B. oleronius* protein compared with 62.5% (25/40) of controls sera (Table 7.7). Similarly, the number of patients sera reactive to the *B. oleronius* protein between acne patients (71.4%; 19/27), and controls (67.4%; 29/43) was calculated not to be significant ($p = 0.7972$) (Table 7.8). However, it is worth noting that despite a non-significant difference between the incidence of keratitis and acne in this study population, there was a high level of participants' sera reactive to the immunogenic *B. oleronius* proteins.

7.3.2 Summary

Western blotting demonstrated that the blepharitis patients with high *Demodex* mite infestation of Group 1 were 78.4% (29/37) sera reactive, patients with *Demodex* mite infestation of Group 2 were 64.7% (11/37) sera reactive, and controls of Group 3 were 50.0% (8/16) sera reactive to *B. oleronius* proteins. Participants observed to be sera reactive among the keratitis patients ($p = 0.2064$), and the acne patients ($p = 0.7972$) did not show a significant correlation to the *B. oleronius* proteins. The results of the Chi-square test showed that there was not a significant correlation between sera immunoreactivity to the *B. oleronius* protein and blepharitis ($p = 0.0613$), and *Demodex* mite infestation ($p = 0.0685$) but that there was a trend towards a significant correlation.

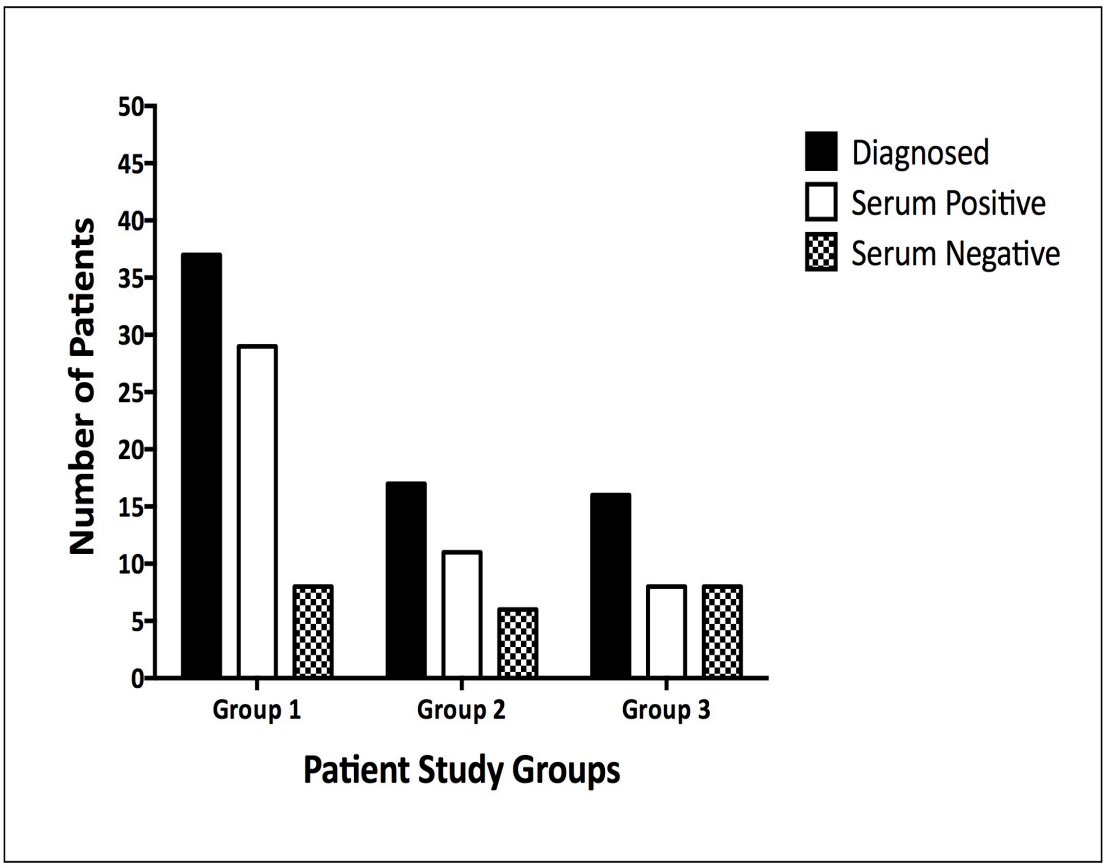

Figure 7.16 Sera reactivity of participants in *Demodex*-related blepharitis study to *B. oleronius* protein. Assessment of serum reactivity of 70 subjects (blepharitis and control patients) to the *B. oleronius* 62-kDa protein in a double-blind immunoblot study. Group 1 was clinically diagnosed with blepharitis and *Demodex* mite infestation. Group 2 was clinically diagnosed with *Demodex* mite infestation and blepharitis-negative. Group 3 was clinically diagnosed with *Demodex* mite infestation-negative and blepharitis-negative.

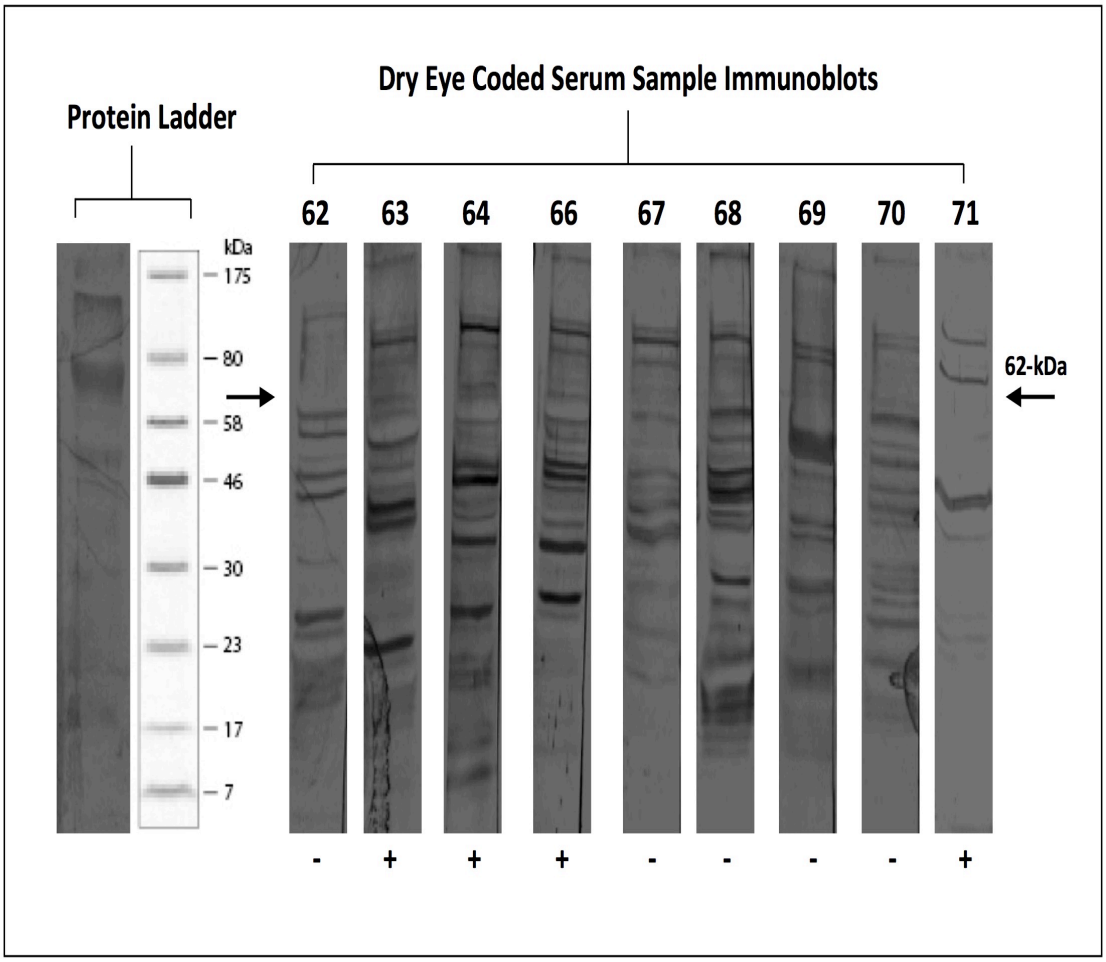

Figure 7.17 Representative Western blots of serum reactivity of participants in *Demodex*-related blepharitis study to *B. oleronius* protein. Representative immunoblots to determine sera reactivity to *B. oleronius* anti-62 kDa protein in blepharitis and control patients. (-: negative serum-reactivity, +: positive serum-reactivity).

Table 7.4 *Demodex*-related blepharitis study population sera reactivity of participants to *B. oleronius* protein. All participants in the study were divided into Group 1, 2, or 3, on the basis on the level of *Demodex* infestation present on the eyelash, and the values for positive- and negative-serum reactivity for each Group is given. Group 1 was clinically diagnosed with blepharitis and *Demodex* mite infestation. Group 2 was clinically diagnosed with *Demodex* mite infestation and blepharitis-negative. Group 3 was clinically diagnosed with *Demodex* mite infestation-negative and blepharitis-negative.

Study Population	Average Age (yrs)	Age Range	Male	Female	Population Number	Serum Reactive	Serum Non-Reactive
Group 1	19.9	6-37	11	26	37	78.4% (29/37)	21.6% (8/37)
Group 2	25.4	12-35	3	14	17	64.7% (11/17)	35.3% (6/17)
Group 3	21.2	6-31	9	7	16	50.0% (8/16)	50.0% (8/16)

Table 7.5 Sera reactivity of blepharitis patients to *B. oleronius* protein in *Demodex*-related blepharitis study. The participants of the study were categorised into blepharitis-positive diagnosis (+), and blepharitis-negative diagnosis (-), and the values for positive- and negative-serum reactivity are given (p = 0.0613).

Study Population	Total Population Number	Serum Reactive	Serum Non-Reactive
Blepharitis (+)	37	78.4% (29/37)	21.6% (8/37)
Blepharitis (-)	33	57.6% (19/33)	42.4% (14/33)
Total	70	48	22

Table 7.6 Sera reactivity of blepharitis patients with ocular Demodicosis infestation to *B. oleronius* protein in *Demodex*-related blepharitis study. The participants of the study were categorised into *Demodex*-positive diagnosis (+), and *Demodex*-negative diagnosis (-), and the values for positive- and negative-serum reactivity are given (p = 0.0685).

Study Population	Total Population Number	Serum Reactive	Serum Non-Reactive
Demodex (+)	54	74.1% (40/54)	25.9% (14/54)
Demodex (-)	16	50.0% (8/16)	50.0% (8/16)
Total	70	48	22

Table 7.7 Sera reactivity of keratitis patients to *B. oleronius* protein in *Demodex*-related blepharitis study. The participants of the study were categorised into keratitis-positive diagnosis (+), and keratitis-negative diagnosis (-), and the values for positive- and negative-serum reactivity are given (p = 0.2064).

Study Population	Total Population Number	Serum Reactive	Serum Non-Reactive
Keratitis (+)	30	77.7% (23/30)	23.3% (7/30)
Keratitis (-)	40	62.5% (25/40)	37.5% (15/40)
Total	70	48	22

Table 7.8 Sera reactivity of acne patients to *B. oleronius* protein in *Demodex*-related blepharitis study. The participants of the study were categorised into acne-positive diagnosis (+), and acne-negative diagnosis (-), and the values for positive- and negative-serum reactivity are given (p = 0.7972).

Study Population	Total Population Number	Serum Reactive	Serum Non-Reactive
Acne (+)	27	70.4% (19/27)	29.6% (8/27)
Acne (-)	43	67.4% (29/43)	32.6% (14/43)
Total	70	48	22

7.4 Discussion

A possible role for microorganisms in the aetiology of rosacea has been the subject of significant debate (Jarmuda *et al*., 2012; Li *et al*., 2010). Investigators have attempted to uncover the significance of the increased density of *Demodex* mites on the facial skin of rosacea patients, and their role in the pathogenesis of the disease (Yamasaki and Gallo, 2009; Erbağı and Ozgöstaşi, 1998). One of the suggested pathogenic mechanisms is connected with the fact that *Demodex* mites may transport various bacteria around the face. This theory is supported by the effectiveness of the antibiotic treatment (e.g. doxycycline, minocycline tetracycline), although these antibiotics may also function as anti-inflammatory agents (Gupta and Chaudhry, 2005).

The bacterium *B. oleronius* was originally isolated from a *D. folliculorum* mite of a papulopustular rosacea patient. Proteins from *B. oleronius* were shown to initiate PBMC proliferation in 16 of 22 (73%) rosacea patients ($p = 0.0105$) but only in 5 of 17 (29%) control subjects, and it has been suggested that *B. oleronius* may play a role in the development of dermatological changes associated with rosacea (Lacey *et al*., 2007). Two proteins derived from *B. oleronius* (62 kDa and 83 kDa) were isolated and demonstrated to be highly immunogenic. Exposure of neutrophils to *B. oleronius* proteins leads to their activation, and triggers the release of MMP-9 and cathelicidin. The stimulation of IL-8 and TNF-α production may result in the development of an inflammatory process *in vivo* (O'Reilly *et al*., 2012a). The exposure of neutrophils to *B. oleronius* proteins may occur in and around the pilosebaceous unit, when the proteins of *B. oleronius* are released from the dead *D. folliculorum* and *D. brevis* mites (O'Reilly *et al*., 2012a). As a result of the induced inflammatory process, the structures of the tissue surrounding the pilosebaceous unit may be damaged, and promote the persistent inflammation associated with the disease (Kafienah *et al*., 1998).

It is possible that exposure to low levels of *B. oleronius* protein in normal skin does not sufficiently challenge the immune response but that the large amounts of material released within the pilosebaceous unit in rosacea patients may induce neutrophil migration and activation (O'Reilly *et al*., 2012a). Antibiotics that are commonly used in the treatment of rosacea do not reduce the population of *Demodex* but inhibit the growth of *B. oleronius*, and thus may prevent the release of *B. oleronius*-associated proteins into and around the pilosebaceous unit (Lacey *et al*.,

2007). After antibiotic therapy is discontinued, rosacea symptoms may return, possibly due to the gradual revival of the *B. oleronius* population in the digestive system of the *Demodex* mites, and other host-microorganisms that reside in the *Demodex* mites (Murillo *et al*., 2014; Jarmuda *et al*., 2012).

The revival of the *B. oleronius* population is possible due to the fact that this bacterium, like other members of the *Bacillus* family, exists in two possible stages: vegetative and endosporic (Szkaradkiewicz *et al*., 2012). *Demodex* mites migrate on the surface of the host skin, and most probably feed on the sebum components and epithelial cells. *B. oleronius* endospores enter their digestive systems in the process and germinate into their vegetative forms. Papulopustular rosacea patients have higher pH and reduced levels of hydration of their facial skin (Ní Raghallaigh and Powell, 2009). They also display a different composition of fatty acids in the sebum, with elevated levels of myristic acids and reduced levels of specific saturated fatty acids (Ní Raghallaigh *et al*., 2012). Perhaps such conditions, not necessarily connected with the levels of sebum but rather with its composition, create a favourable environment for the development of the mite population, and thus, the increased bacteria population.

Alterations in the nature of the sebum produced in the face may facilitate the increase in the density of *Demodex* mites in the skin of rosacea patients. These may transport bacteria upon their death in and around the pilosebaceous unit, and the immunogenic proteins of *B. oleronius* have been shown to induce an inflammatory reaction (O'Reilly *et al*., 2012a). This scenario would implicate bacteria as having a key role in the induction of rosacea, but this role might only come into play once other factors (e.g. vascular damage, altered sebum, increased *Demodex* density) have occurred. A clear understanding of the factors that contribute to the aetiology of rosacea will assist in the development of more effective therapies for the control of this chronic, disfiguring condition.

The results presented here from the erythematotelangiectatic rosacea study (Section 7.1) demonstrated that sera from 82.67% of erythematotelangiectatic rosacea patients reacted with the 62 kDa and/or 83 kDa protein(s) of *B. oleronius* (Figure 7.2), and patients were assessed as having grade 1 (mild facial erythema) or grade 2 (moderate facial erythema) skin lesions (Figure 7.3). Similar levels of rosacea patient serum reactivity to the *B. oleronius* proteins has been observed in previous studies examining erythematotelangiectatic rosacea, papulopustular rosacea, and ocular

rosacea (O'Reilly *et al*., 2012c; Li *et al*., 2010; Lacey *et al*., 2007). In addition, these patients displayed a higher population of *Demodex* mites in their skin (Figure 7.4), and a lower level of sebum than controls (Figure 7.5). An increase of *Demodex* mite infestation in rosacea patients has been established from previous findings, and it has been suggested that the greater number of *Demodex* mites may be due to altering levels of sebum, and it's composition on the skin of individuals with rosacea that may provide a suitable environment for mite infestation (Ní Raghallaigh *et al*., 2012; Erbağci and Ozgöztaşi, 1998; Bonner *et al*., 1993; Vance, 1986). In the rosacea patients examined in this population, there was no discernible difference detected from the serum samples examined for the secretion of the immunostimulatory and pro-inflammatory cytokines IL-17, TNF-α, and IL-8 compared to controls, acne vulgaris patients, and seborrheic dermatitis patients (Figure 7.6 – 7.8).

The secretion of cytokines by immune cells is a key component of the regulatory mechanisms of the innate and adaptive immune systems, and cell signaling in response to a foreign agent. Akilov and Mumcuoglu (2003) suggest that rosacea patients may be genetically susceptible to the disease and possess a weakened immune response, as they showed that individuals with the human leukocyte antigen (HLA) Cw2 and Cw4 haplotypes were more suseptible to suffer with Demodicosis, an increased density of *Demodex* mites, and have a decreased natural killer T cell population, respectively. The activation of a dermal innate immune response in erythematotelangiectatic rosacea and papulopustular rosacea patients has been investigated, and demonstrated that genes coding for IL-8, IL-1β, TNF-α, and Cox-1 were increased following examination of facial skin swabs and epidermal scrapings of rosacea patients' skin lesions, and observed an overexpression of genes coding for the inflammasome (Casas *et al*., 2012).

The results presented from the ocular rosacea study (Section 7.2) showed an altered immune response in rosacea Subtype IV, and rosacea Subtype I & IV patients compared to controls. Following Western blot analysis, a positive correlation between patient serum and reactivity to *B. oleronius* proteins was demonstrated (Figure 7.9). PBMC isolated from controls demonstrated low secretion levels for each of the cytokines analysed. In comparison, the untreated PBMC cytokine secretion profile was altered in rosacea patients with increased expression of IL-13, IL-2, IL-22, and IFN-γ, suggesting an active immune response that is primed to react to an invading foreign stimulus (Figure 7.10 – 7.15).

The main role of the cytokine, IL-2, is as a T cell growth factor, to promote the development of T regulatory cells, and the expansion of T cells in the mediation of an immune response (Malek, 2003; Smith, 1988). Increased secretion of IL-2 was shown in untreated PBMC isolated from rosacea patients (Figure 7.11). Exposure of PBMC from rosacea patients with the *B. oleronius* proteins did not alter IL-2 secretion. Thus, the increased level of secreted IL-2 by untreated rosacea patient PBMC suggests that in rosacea, IL-2 is actively secreted to recruit and proliferate T cells against an infection, and increased secretion of IL-2 may lead to the development of a chronic disease against an infection.

IL-22 is secreted by activated dendritic cells and T lympocytes in response to a bacterial infection of epithelial cells, and has been shown to be produced by Th17 cells functioning in the mediation of an adaptive innate immune response of epithelial tissues, and expression of antimicrobial peptides such as S100A7 (Martin *et al*., 2014; Sonnenberg *et al*., 2011; Wolk *et* al., 2004; Radaeva *et al*., 2004; Ong *et al*., 2002). In inflammatory skin disorders, a specific T cell subset, Th22, has been shown to be implicated in epidermal immunity and tissue remodeling by the secretion of IL-22 and TNF-α (Eyerich *et al*., 2009). IL-22 secretion was shown to be increased in untreated PBMC from rosacea patients compared to untreated PBMC from control subjects. IL-22 secretion was observed to be significantly increased in control subjects following stimulation with the *B. oleronius* protein preparations ($p < 0.05$) (Figure 7.12). Thus, exposure of control PBMC to the *B. oleronius* proteins demonstrates a capacity for *B. oleronius* proteins to increase the secretion of IL-22 and induce an adaptive immune response.

IL-17A is a cytokine that functions in the regulation of the transcription factor NF-κB and mitogen-activated protein kinases, and is produced by the Th17 subset of T helper cells for the induction of an epithelial immune response (Bulek *et al*., 2011; Kryczek *et al*., 2011; Sun *et al*., 2011; Liu *et al*., 2009; Afzali *et al*., 2007; Harrington *et al*., 2005; Park *et al*., 2005). Elevated levels of IL-17A have been associated with chronic inflammatory diseases including rheumatoid arthritis and psoriasis, and in defence against invading skin pathogens (Harper *et al*., 2009; Johansen *et al*., 2009; Pitta *et al*., 2009; Eyerich *et al*., 2008; Murphy *et al*., 2003; Chabaud *et al*., 1999; Teunissen *et al*., 1998). Levels of IL-17A were elevated in untreated PBMC from rosacea patients (Subtype IV and Subtype I & IV groups) compared to untreated PBMC from control subjects (Figure 7.13). In rosacea patients of the Subtype I & IV

group, the levels of secreted IL-17A significantly decreased following exposure to the pure *B. oleronius* protein preparation suggesting that the secretion of IL-17A may be reduced by the presence of the *B. oleronius* proteins. Thus, *B. oleronius* may lead to an altered epithelial immune response in rosacea.

IFN-γ is a type II interferon, a cytokine produced by natural killer (NK) T cells, $CD4^+$ Th1 cells, and $CD8^+$ cytotoxic T lymophocytes, that functions as a immunomodulator of the innate and adaptive immune responses against viral and parasitic infections (Schoenborn and Wilson, 2007; Gomez-Marin *et al*., 1998; Urban *et al*., 1996; Pernis *et al*., 1995; Schofield *et al*., 1987; Wheelock, 1965). Increased IFN-γ levels were observed in the untreated PBMC of ocular rosacea patients (Subtype IV group) but not from the Subtype I & IV group. Following exposure to the *B. oleronius* proteins, the levels of IFN-γ increased in the controls, and exposure to the crude *B. oleronius* proteins exhibited an inhibitory effect, with reduced IFN-γ levels detected in rosacea PBMC relative to controls (Figure 7.15). Thus, the PBMC from controls increase the secretion of IFN-γ in response to the *B. oleronius* proteins, inducing an adaptive immune response while PBMC from rosacea patients demonstrate reduced IFN-γ secretion, and an altered immune response due to the *B. oleronius* proteins.

Exposure of isolated PBMC from controls to the crude or pure *B. oleronius* proteins showed an increase in cytokine secretion compared to untreated PBMC from controls. However, a change in the cytokine secretion profile of rosacea patients PBMC exposed to the *B. oleronius* protein preparations was not observed relative to untreated PBMC from rosacea patients. Thus, suggesting an active immune response to the *B. oleronius* proteins in controls, and a reduced immune response with an altered cytokine expression profile in rosacea patients. The alternatively regulated immune system observed in rosacea patients, may lead to a weakened immune response, that is unable to clear a bacterial infection leading to the characteristic persistent inflammation and erythema seen in rosacea.

Blepharitis is an inflammatory condition of the eyelid margins causing ocular discomfort and irritation with persistence leading to a decline in visual acuity and function (Jackson, 2008). The high frequency of the *Demodex* mites has been well established in rosacea, and in recent years the prevalence of *Demodex* mites has been recorded in diseases affecting the eye and surrounding areas in *Demodex*-related blepharitis and chalazia (Liang *et al*., 2014; Skaradkiewicz *et al*., 2012; Li *et al*.,

2010; Erbağci and Ozgöztaşi, 1998; Bonner *et al*., 1993; Vance, 1986). Ocular demodicosis has been associated as a causative factor for a number of ocular disorders including eyelash loss or abnormal alignment, lipid tear deficiency of the meibomian gland due to chronic inflammation, and chronic conjunctivitis that may result in the formation of keratitis on the corneal surface and visual impairment (Liang *et al*., 2014; Lee *et al*., 2010; Li *et al*., 2010; Liu *et al*., 2010; Gao *et al*., 2007; Kheirkhah *et al*., 2007b).

The positive results of the blepharitis study (Section 7.3) has demonstrated a trend towards a correlation between blepharitis ($p = 0.0613$), and *Demodex* mite infestation ($p = 0.0685$), and serum immunoreactivity to the *B. oleronius* proteins (Table 7.5, and Table 7.6, respectively), and that the number of *Demodex* mite residing in the eyelashes and meibomian glands may have a role in the pathogenesis of blepharitis. It is currently believed that the severity of the eye disorder observed in patients with ocular demodicosis may be a consequence of the abundance of *Demodex* mite species present in the eyelashes or hair follicle of the skin, and that the pathogenicity of blepharitis and other eye conditions may also be related to the depth that the mites penetrate as they reside in the sebaceous units of the skin, and meibomian glands of the eyes (Liang *et al*., 2014; Liu *et* al., 2010; Lacey *et al*., 2009). Interestingly, *B. oleronius* has been isolated from epilated eyelashes of severe *Demodex*-related chronic blepharitis patients (18/36) and control subjects (5/30) (Szkaradkiewicz *et al*., 2012).

In this Chapter, it has been demonstrated that sera from erythematotelangiectatic rosacea patients (82.67%; 62/75), and ocular rosacea patients (100%; 6/6) positively react to *B. oleronius* proteins. A high level of reactivity to the *B. oleronius* protein was also observed in patients with blepharitis (78.4%; 29/37). Improved counting techniques using a fluorescein-containing solution, and a molecular approach involving amplification of the 16S rRNA gene has lead to increased identification and counting of *D. brevis* and *D. folliculorum* mites in populations (Liang *et al*., 2014; Thoemmes *et al*., 2014; Kheirkhah *et al*., 2007a; Gao *et al*., 2005). The *Demodex* mites naturally occur on the skin of humans, and even though they are not believed to be pathogenic, it is believed that the microbes released upon mite death may be capable of initiating an immune response and an inflammatory response given suitable environmental conditions of the human host. As the *Demodex* mite life cycle lasts for 14 – 21 days, the microbe population is

replenished at the site of infection, either in the pilosebaceous unit in the skin or at the meibomian glands of the eyes. The microbes may operate as a co-pathogen, resulting in an immune response leading to chronic inflammation associated with skin and eye conditions such as rosacea, and blepharitis, and as demonstrated in the ocular rosacea study, patients display a reduced immune response to *B. oleronius* proteins.

Chapter 8

General Discussion

8.0 General Discussion

The aetiology of rosacea remains unknown, and currently the exact mechanisms that lead to the development of the condition are widely debated. Some research groups focus on the trigger factors involved in the disease such as alcohol consumption, spicy food intake, or UV exposure, which result in a transient flushing episode that is characteristic of the disease, whereas other groups have focused on alterations to the vascular network, changes in the levels of ROS in the skin, and the innate immune response (Steinhoff *et al*., 2011, 2013; Yamasaki *et al*., 2011; Yamasaki and Gallo, 2009; Gupta and Chaudhry, 2005; Kligman, 2004). More recently, studies have begun to focus on the role of the adaptive immune response in the induction of rosacea (Buhl *et al*., 2015). As patients with rosacea display increased densities of *Demodex* mites on their skin relative to controls, many research studies have investigated the role of *Demodex* mites and the role of these mites in the skin condition (Casa *et al*., 2012; Zhao *et al*., 2009; Erbağci and Ozgöztaşi, 1998; Bonnar *et al*., 1993; Vance, 1986). However, despite great effort, the pathogeneis of rosacea remains unknown, and as a result, the condition remains difficult to treat.

In the last decade, the potential role of bacteria in the pathogenesis of rosacea has been discussed (Holmes, 2013; Jarmuda *et al*., 2012; Whitfeld *et al*., 2011; Lacey *et al*., 2007; Dahl *et al*., 2004). The potential candidate pathogenic bacteria include *B. oleronius*, *S. epidermidis*, *H. pylori*, and *C. pneumoniae*. It has been suggested that the *Demodex* mites may act as vehicles for the transport of bacteria that may reside within the mites, and that increased densities of mites may allow for an increase in the population of the pathogenic potential of *Demodex*-associated microorganisms (Holmes, 2013; Jarmuda *et al*., 2012; Lacey *et al*., 2009; Gupta and Chaudhry, 2005).

Of the potential candidate pathogenic bacteria, *B. oleronius* has been demonstrated to have a possible role in the induction and persistence of rosacea. The bacterium was first isolated from a micro-disected *D. folliculorum* mite of a papulopustular rosacea patient (Delaney, 2004). Delaney (2004) highlighted two immuno-stimulatory proteins, a 62 kDa protein and an 83 kDa protein, that may be implicated in the induction of rosacea. These proteins were observed to be highly sera reactive in rosacea patients and were the focus of further studies. Recently, Murillo *et al*. (2014) characterised the microbiota of patients with erythematotelangiectatic rosacea, papulopustular rosacea, and controls, and identified a diverse community of *Demodex*-associated microorganisms that were subtype-specific for each study

population. Interestingly, the authors identified *Bacillus* species in *Demodex* mites, further implicating a possible role for a *Bacillus* species in the induction of this disease. The aim of this project was to establish whether there is a possible role for *B. oleronius* proteins in the pathogenesis of ocular rosacea.

The aim of Chapter 3 was to investigate the effect of different culture conditions on the *B. oleronius* proteome, and in particular, on the expression of the 62 kDa immuno-reactive protein. Lacey *et al*. (2007) identified the immunogenic proteins to be homologous to a bacterial heat shock protein, molecular chaperone GroEL in the case of the 62 kDa protein, and the 83 kDa protein was found to be involved in the phosphoenolpyruvate phosphotransferase sensory system. The 62 kDa molecular chaperone GroEL protein has previously been observed to be highly sera reactive in rosacea patients (O'Reilly *et al*., 2012c; Li *et al*., 2010; Lacey *et al*., 2007). The expression of the 62 kDa GroEL protein was analysed under different culture conditions by Western blotting. It was demonstrated that the *B. oleronius* increased expression of the 62 kDa GroEL protein in response to stress following alterations in temperature, pH, ROS presence, and oxygen availability of the local environment. The expression of the 62 kDa GroEL protein is reduced in an environment that most closely resembles the aerobic, pH 8 environment in the hindgut of the *Demodex* mite (Erban and Hubert, 2010; König et al., 2002).

There are many features of the skin microenvironment including aerobicity, temperature, pH, and lipid composition, that can influence the natural skin microflora and the *Demodex* mite population, and therefore can directly affect *Demodex*-associated microorganisms (Holmes, 2013; Ní Raghallaigh *et al*., 2012; Grice and Segre, 2011; Leyden *et al*., 1975; Somerville, 1969). Variations in temperature have previously been suggested to alter the phenotypic characteristics of the *Demodex* microbiota, and may lead to non-pathogenic microbes switching to pathogenic microbes, as is believed to be the case for *B. oleronius* (Jarmuda *et al*., 2012; Lacey *et al*., 2009; Dahl *et al*., 2004). It was observed that an increase of temperature correlated with a significant rise in the production of the 62 kDa protein ($p = 0.0206$). Similarly, in culture conditions that most closely resemble that of the skin (pH 6 and 37°C), the expression of the 62 kDa GroEL protein was elevated compared to the pH 8 conditions that resemble the hindgut of the *Demodex* mite ($p < 0.0001$). This suggests that *B. oleronius* produced increased levels of the immuno-reactive 62 kDa GroEL protein in response to stress from the surrounding environment, and that a

change in the local environment following the death of the *Demodex* mite, from the the hindgut of the mite to the pilosebaceous unit or meibomian gland of the human host, may be a trigger for the induction of an oxidative stress response.

S. epidermidis is the most abundant microbe to naturally colonise the skin micro-environment. *S. epidermidis* isolated from rosacea patients' skin was shown to be consistently β-hemolytic compared to non-hemolytic in controls, and it was demonstrated that the β-hemolytic *S. epidermidis* isolates secreted more protein and different proteins at 37°C compared to cells grown at 30°C (Cheung *et al*., 2012; Dahl *et al*., 2004). Pure cultures of *S. epidermidis* were isolated from pustules on the cheeks (9/15), and eyelids (4/15), of papulopustular rosacea patients, implicating *S. epidermidis* in the pathogenesis of the disease (Whitfeld *et al*., 2011). The transient episodes of flushing are believed to result in an elevated skin temperature in rosacea patients relative to healthy individuals, and it was suggested that alterations in temperature and the microenvironment of the *B. oleronius* can result in the *B. oleronius* upregulating the secretion of proteins, such as the 62 kDa GroEL protein, that mediate an inflammatory response in rosacea.

The composition of sebum on the skin of rosacea patients has been of interest as it is postulated that sebum is a source of food for the *Demodex* and that a plentiful supply of sebum and epithelial cells may result in an increase in the *Demodex* population in the pilosebaceous units of the skin and the meibomian glands of the eyes (Liang *et al*., 2014; Forton, 2012; Liu *et* al., 2010; Lacey *et al*., 2009; Pye *et al*., 1976). Ní Raghallaigh *et al*. (2012) demonstrated that the composition of fatty acids in sebum is altered in rosacea patients compared to controls, suggesting that fatty acid composition present on the skin may be related to the skin barrier integrity, and that it is the quality of sebum available and not the quantity that is a factor in rosacea.

The analysis of lipase activity present in *B. oleronius* cultures grown under different environmental conditions was assessed using tributyrin agar, and it was observed that lipase activity was elevated in conditions resembling that of the *Demodex* mite hindgut, and that a change in temperature, from 30°C to 37°C, significantly increased the activity of lipase in the bacterium ($p = 0.002$). Thus, demonstrating that a change in temperature alters the secretion of proteins, and may lead to a non-pathogenic bacteria switching to a pathogenic bacteria.

In Chapter 4, the isolation and purification of *B. oleronius* proteins by ÄKTA FPLC™ for use in further assays involving corneal epithelial (hTCEpi) cells,

neutrophils, or PBMC was demonstrated. The pure *B. oleronius* protein preparations have been shown using LC/MS to contain proteins implicated in response to oxidative stress, i.e. Kat E1, vegetative catalase 1, superoxide dismutase, and alkyl hydroperoxide reductase (small subunit), in the formation of bacterial cell wall, hypothetical protein Noc_2222, bacterial cell mobility, flagellin, and bacterial heat shock protein (Hsp) and chaperone protein, GroEL (O'Reilly *et al*., 2012a). The 'pure' *B. oleronius* protein preparation demonstrated a capacity to induce an immune response, and the implication for *B. oleronius* proteins in the induction of rosacea has been demonstrated in previous studies (O'Reilly *et al*., 2012a, 2012b, 2012c; Li *et al*., 2010; Lacey *et al*., 2007).

The aim of Chapter 4 was to characterise the effect of *B. oleronius* proteins on corneal epithelial (hTCEpi) cells. It has been established that an increased densitiy of *Demodex* mites on the eyelashes is a feature of ocular rosacea but their role in the aetiology of the condition has not been fully elucidated (Oltz and Check, 2011; Yamasaki and Gallo, 2009; Kheirkhah *et al*., 2007b; Diaz-Perez, 1994; Vance, 1986). The role of *B. oleronius* was previously analysed in ocular rosacea patients, and it was demonstrated that the incidences of ocular rosacea and eyelid inflammation correlated with ocular *Demodex* infestation and sera-reactivity to *B. oleronius* proteins (Li *et al*., 2010). The effect of *B. oleronius* proteins on a corneal epithelial (hTCEpi) cell line was investigated, and it was demonstrated that exposure of corneal epithelial cells to the *B. oleronius* proteins resulted in an aberrant wound healing response with a dose-dependent increase in gene expression of *MMP-3* (61-fold) and *MMP-9* (300-fold), and increased MMP-9 activity (O'Reilly *et al*., 2012b). The authors also demonstrated reduced levels of β-integrin (1.25-fold; $p = 0.01$), and increased levels of vinculin (2.7-fold; $p = 0.0009$), suggesting that the corneal epithelial (hTCEpi) cells become more motile in response to the *B. oleronius* proteins, and this may contribute to ocular scarring *in vivo* (O'Reilly *et al*., 2012b).

In this study, it was observed that exposure of corneal epithelial (hTCEpi) cells to *B. oleronius* proteins resulted in a reduced hTCEpi cell proliferation. This was most evident at day 3 where exposure of hTCEpi cells to 2 µg/ml and 6 µg/ml pure *B. oleronius* protein preparations lead to an increased mean generation time (MGT) of 91 hour and 123 hour, respectively, compared to control hTCEpi cells with a MGT of 76 hour. The reduction in hTCEpi cell proliferation was significant in the case of the 6 µg/ml pure *B. oleronius* protein preparation ($p = 0.0185$). It was observed that

caspase-3 and caspase-7 were not induced in hTCEpi cells following exposure to pure *B. oleronius* proteins, thus suggesting that the effect induced by the *B. oleronius* proteins was anti-proliferative, and it was observed that exposure to pure *B. oleronius* proteins inhibited hTCEpi cell progression at the G_1/S transition. Exposure of hTCEpi cells to *B. oleronius* proteins also resulted in increased antimicrobial peptide CCL20 and S100A7 secretion, increased MMP-9 expression and activity, and increased secretion of IL-6 and IL-8. These findings demonstrate the potential of *B. oleronius* proteins to induce an inflammatory response that would contribute to the degradation of corneal tissue that would lead to corneal scarring and ulcer formation *in vivo*. By understanding the interaction of *B. oleronius* proteins with the corneal surface it would allow for the development of therapeutics that could target this bacterial response and reduce the severity of symptoms arising from this interaction.

In Chapter 5, the proteome of corneal epithelial (hTCEpi) cells was analysed following exposure to *B. oleronius* proteins. Alterations in the proteome of hTCEpi cells induced by exposure to *B. oleronius* proteins was investigated using 1-D and 2-D SDS-PAGE followed by liquid chromatography mass spectrometry (LC/MS), and also by performing in-gel solution digestion and label-free mass spectrometry (LF/MS). The identification of changes in the abundance of hTCEpi cell proteins may potentially help to elucidate the pathogenic effect of *B. oleronius* proteins on the corneal epithelial surface and in the induction of the symptoms associated with ocular rosacea.

Hsps are necessary for maintaining the differentiated structures of the eye such as the retinal pigment epithelium, and Hsps are up-regulated to facilitate the folding of damaged proteins and to reorganise the tissues of the eye in response to stress (Urbak and Vorum, 2010; Arrigo and Simon, 2010; Li *et al*., 2003; Strunnikova *et al*., 2001; Omar and Papolla, 1993; Georgopolous and Welch, 1993; Dasgupta *et al*., 1992; Linquist and Craig, 1988). Hsps have been shown to be involved in regulating cell growth and cell cycle events, with Hsp70 previously demonstrated to mediate cell cycle progression by regulating G_1 cyclin abundance (Truman *et al*., 2012). It was observed in the 1-D and 2-D SDS-PAGE proteomic studies that exposure of hTCEpi cells to *B. oleronius* proteins leads to an increase in the abundance of Hsps that may be involved in mediating hTCEpi cell cycle progression. Similarly, it was observed that exposure of hTCEpi cells to pure *B. oleronius* protein inhibited the hTCEpi cell cycle at the G_1/S transition, with an increase of hTCEpi cells observed at the G_1-phase

of the cell cycle. It can be hypothesised that the increased abundance of Hsps observed in hTCEpi cells and the inhibition of the hTCEpi cell cycle at the G_1/S transition may be due to the presence of the *B. oleronius* 62 kDa GroEL protein. A number of ocular pathologies have been associated with an increase of Hsps such as uveal melanoma, glaucoma, and cataracts, and it can be suggested that an increase of Hsps in ocular rosacea may be contributing to disorganization of corneal tissues and scarring (Urbak and Vorum, 2010; Missotten *et al*., 2003; Tezel *et al*., 2000).

Interestingly, leukocyte elastase inhibitor was the only common protein identified to be exclusive to hTCEpi cells treated with either crude or pure *B. oleronius* protein. Leukocyte elastase inhibitor is a serine protease inhibitor that has been demonstrated to exhibit both pro-survival and pro-apoptotic characteristics, and increased expression has been reported during wound healing in corneal endothelial cells (Justet *et al*., 2015; Huntington, 2011; Pardon-Barthe *et al*., 2007, 2008; Torriglia *et al*., 2008). The skin of rosacea patients has previously been demonstrated to have a higher abundance of ROS (Tisma *et al*., 2009; Yamasaki and Gallo, 2009). It has been suggested that an increase in ROS production may result in an increase in the expression of leukocyte elastase inhibitor (Justet *et al*., 2015). Thus, it has been demonstrated that exposure of hTCEpi cells to *B. oleronius* proteins results in increased abundance of leukocyte elastase inhibitor, and this may contribute to the aberrant wound healing response in hTCEpi cells.

LF/MS analysis demonstrated that hTCEpi cells exposed to crude or pure *B. oleronius* proteins results in minor changes to the hTCEpi proteome but many of the proteins that are altered in abundance were observed by String network analysis to share a similar function that is specific for poly (A) RNA binding. Poly (A) RNA binding proteins have been demonstrated to play an important role in a range of physiological processes including signal transduction, target degradation of proteins and protein synthesis, cell survival, cell cycle and migration, cell proliferation, apoptosis, regulation of transcription, and response to DNA damage (Zhao *et al*., 2015; Zhou *et al*., 2014; Vlachostergios *et al*., 2012; Yamaguchi *et al*., 2012; Wei and Lin, 2012; Kim *et al*., 2008; Ciechanover, 2005; Sakamoto *et al*., 2003). Thus, changes to the hTCEpi proteome following exposure to *B. oleronius* proteins results in alterations in hTCEpi cells at a RNA processing level that may lead a disruption of the corneal epithelial surface.

The first part of Chapter 6 focused on examing the effect of *B. oleronius*

proteins on neutrophils by the IP_3 pathway of activation. Neutrophils exposed to *B. oleronius* proteins demonstrated increased migration and elevated release of MMP-9, an enzyme known to degrade collagen, and cathelicidin, an antimicrobial peptide (O'Reilly *et al*., 2012a). Exposure of neutrophils to the bacterial proteins resulted in elevated production of IL-8 and TNF-α (O'Reilly *et al*., 2012a). Increased production of IL-8 which is a trigger for neutrophil recruitment to the site of infection, and TNF-α is indicative of an inflammatory response. Here, it was observed that neutrophils exposed to *B. oleronius* proteins increase production of IP_1, an indicator for the generation of the secondary messenger IP_3, by GPCR receptor signaling activation (Reeves *et al*., 2013; Bokoch, 1995). The activation of *B. oleronius* protein stimulated neutrophils was followed by Ca^{2+} release, and cytoskeletal rearrangement of G-actin to F-actin, and increased neutrophil chemotaxis (Putney, 2007; Tintinger *et al.*, 2005; Taylor *et al*., 2004; Berridge, 1995; Bokoch, 1995). The IP_3 pathway has been established as a pharmacological target for the treatment of diseases that affect the immune response and leads to chronic inflammation (Eishingdrelo and Kongsamut, 2013; Brown and Tracy, 2013; Kliem *et al*., 2012; Galeotti *et al*., 2004). The identification of the IP_3 pathway of neutrophil activation induced by exposure to *B. oleronius* proteins may facilitate the development of new therapies to reduce the inflammation that is charcateristic of the condition.

The second part of Chapter 6 involved investigating the cytokine secretion profile of PBMC exposed to *B. oleronius* proteins by ELISpot and/or FlouroSpot assay techniques. PBMC from healthy volunteers were shown to significantly increase secretion of a range of cytokines including IL-1β, IL-10, IL-12p40, IL-23, TNF-α, GM-CSF, IL-5, IL-13, IL-17A, IL-22, and IFN-γ following exposure to crude or pure *B. oleronius* protein preparation compared to unstimulated PBMC ($p < 0.0001$). Cytokines function in cell communication, mediating inflammation and regulating the immune response. Exposure of PBMC to *B. oleronius* proteins signals increased secretions of these cytokines that may have implications for the regulation of inflammatory and adaptive innate immune responses in rosacea.

Chapter 7 focused on characterising the role of *B. oleronius* proteins in three collaborative studies involving patients with erythematotelangiectatic rosacea, ocular rosacea, and *Demodex*-related blepharitis. It has been observed that rosacea patients are highly sera reactive to *B. oleronius* proteins relative to control subjects. Proteins extracted from the *B. oleronius* were observed to induce an inflammatory immune

response in 72% (16/22) of papulopustular rosacea patients but only 29% (5/17) of controls ($p = 0.01$) (Lacey *et al*., 2007). A strong correlation was demonstrated between ocular *Demodex* inflammation and serum reactivity to these bacterial proteins in patients with ocular rosacea (Li *et al*., 2010). In addition, the presence of eyelid margin inflammation (74.6%; 44/59) ($p = 0.04$) and ocular rosacea (80%; 47/59) ($p = 0.009$) correlated with reactivity to these proteins (Li *et al*., 2010). Similarly, patients with erythematelangiectatic rosacea have been shown to be highly sera reactive to *B. oleronius* proteins (80%; 21/26) (O'Reilly *et al*., 2012c).

Here, in our collaborative studies, similar levels of serum immunoreactivity were observed in erythematotelangiectatic rosacea patients with 82.6% (62/75) sera reactive to the *B. oleronius* proteins compared to 26.9% (14/52) sera reactivity in controls. This population of rosacea patients demonstrated an increased density of *D. folliculorum* mites in the skin but sera reactive rosacea patients also had reduced levels of sebum which supports previous reports suggesting that the composition of fatty acids and quality of sebum on the skin of rosacea patients plays a role in the proliferation of *Demodex* mites, and disrupting the intergrity and barrier of skin (Ní Raghallaigh *et al*., 2012).

The study of ocular rosacea patients demonstrated that patients with ocular rosacea (Subtype IV group) or ocular and erythematotelangiectatic rosacea (Subtype I & IV group) have an altered cytokine secretion profile relative to controls, with increased levels of secreted IL-13, IL-2, IL-22, and IFN-γ, demonstrating an active immune response. Recently, Buhl *et al*. (2015) observed activation of a Th1/Th17 pathways in rosacea patients, suggesting an altered immune response, and that this results in a weakened immune response. It can be suggested that a weakened immune response may lead to the body being unable to clear a bacterial infection leading to the characteristic persistent inflammation and erythema seen in rosacea. However, treatment of rosacea patient PBMC with *B. oleronius* protein did not significantly alter the cytokine secretion profile for the cytokines but control PBMC exposed to *B. oleronius* protein demonstrated a significant increase in the secretion of IL-2 ($p < 0.05$) and IFN-γ ($p < 0.05$), and this may have implications in the regulation of the adaptive immune response in rosacea.

The role of *B. oleronius* proteins in the induction of *Demodex*-related blepharitis was investigated. A number of studies have implicated *Demodex* mites with ocular pathologies such as *Demodex*-related blepharitis, ocular Demodicosis, chalzia, and

ocular rosacea (Liang *et al*., 2014; Skaradkiewicz *et al*., 2012; Li *et al*., 2010; Erbağci and Ozgöztaşi, 1998; Bonner *et al*., 1993; Vance, 1986). *B. oleronius* has been isolated from epilated eyelashes of severe *Demodex*-related chronic blepharitis patients (18/36) and control subjects (5/30), suggesting a possible role for the bacterium in the induction of the disease and damage to the corneal surface (Szkaradkiewicz *et al*., 2012). Similar levels of sera reactivity to *B. oleronius* proteins were observed in this study population, and a trend towards a correlation between blepharitis ($p = 0.0613$), and *Demodex* mite infestation ($p = 0.0685$) and sera reactivity to *B. oleronius* proteins was observed.

From the research presented here, there are many potential avenues to consider for future studies. These include the generation of a recombinant form of the pure *B. oleronius* protein preparation, and in particular, the 62 kDa GroEL protein to design assays that specifically investigate this protein to determine its role in rosacea and to elucidate possible reasons why individuals are highly sera reactive to this protein. As more research studies have focused on the adaptive immune system and its regulation in rosacea, it would be beneficial to investigate the effect of *B. oleronius* proteins on Toll-like receptor signaling and B cell proliferation, and the effect on NF-κB. This could be approached by FACS analysis, immunoblotting, or B cell-specific ELISpot/FluoroSpot assays. Of the TLR pathways, TLR-2 and TLR-5, would be of interest as these have previously been associated with rosacea (O'Reilly *et al*., 2012a; Yamasaki and Gallo, 2011; Yamasaki *et al*., 2007, 2011).

It has previously been demonstrated that exposure of neutrophils to *B. oleronius* proteins induced neutrophil activation, and the activation of neutrophils has been characterised via the IP_3 pathway (O'Reilly *et al*., 2012a). Future research could focus on the receptor that is activated along this pathway by the *B. oleronius* proteins as this would greatly facilitate the develpoment of target therapeutics that would help to alleviate the persistent erythema that is associated with rosacea. A future project could also use the LF/MS to perform a proteomic study investigating the effect of *B. oleronius* proteins on human neutrophils. The high resolution of the Q Exactive™ mass spectrometer, employed for LF/MS studies, would allow for the identification of small antimicrobial peptides that may have a role in the induction of rosacea, and it be would of great interest to elucidate if the effect on poly (A) RNA binding observed in hTCEpi cells exposed to *B. oleronius* proteins corresponds to *B. oleronius* protein treated neutrophils.

It was observed that exposure of *B. oleronius* proteins leads to reduced hTCEpi cell proliferation with a halt in the hTCEpi cell cycle at the G_1/S transition, and the induction of an inflammatory response. This study used a corneal epithelial (hTCEpi) cell line as an *in vitro* model of the human cornea. However, it would be beneficial for future studies to use an air-lift *in vitro* cell culture model of the cornea, to assess the effect of *B. oleronius* proteins on corneal epithelia in multiple cell layer model and to investigate if exposure to *B. oleronius* proteins results in the formation of ocular sterile ulcers and scarring, and if this can be blocked in a similar manner that is routinely used in a clinic for the treatment of similar ocular pathologies.

Alterations in the abundance of proteins specific for poly (A) RNA binding was observed in the hTCEpi LF/MS proteomic study. This can be studied further with the possibility of identifying microRNAs (miRNAs) that may be involved in this process. The identification of these miRNAs may allow for the development of a molecular diagnostic tool for rosacea and more therapeutic targets.

It can be hypothesized that a series of events are required to trigger the onset of rosacea and it's associated symptoms such as the persistent eythema and flushing episodes to arise in a patient. Rosacea is normally shown to appear in patients who are in their mid-thirties and it is observed that the population of *Demodex* mites is higher compared to people without rosacea. Over a period of time, this may allow for a gradual deterioration in the integrity of the skin barrier, and as the density of *Demodex* mites increases, so too may the populations of bacteria that reside within these potential vectors. The condition of the host's skin, along with the composition of sebum may allow for the increased growth of *Demodex* mites, and may provide a suitable environment for a potential bacterial role in the disease. It has been descibed that alterations in an environment such as an increase in temperature, can result in a non-pathogenic bacterium becoming a pathogenic bacterium. *Demodex*-associated microorganisms may exploit the life cycle and vehicular role of *Demodex* mites, as the *Demodex* travel around the facial skin and, following death, they release their contents into the pilosebaceous units or meibomian glands on the face. This may be a possible route of transmission involved in rosacea, with *B. oleronius* possibly utilizing this process. In conclusion, the aetiology of rosacea remains unknown but the results presented here demonstrate that *B. oleronius* proteins may be implicated in the pathogenesis of rosacea, and that the action of these proteins can lead to the induction of an inflammatory response that is a hallmark of the disease.

Chapter 9

Bibliography

ABD-EL-AL, A. M., BAYOUMY, A. M. & ABOU SALEM, E. A. 1997. A study on Demodex folliculorum in rosacea. J Egypt Soc Parasitol, 27, 183-95.

ABRAHAMS, V. M., CAMBRIDGE, G., LYDYARD, P. M. & EDWARDS, J. C. 2000. Induction of tumor necrosis factor alpha production by adhered human monocytes: a key role for Fcgamma receptor type IIIa in rheumatoid arthritis. Arthritis Rheum, 43, 608-16.

ABRAM, K., SILM, H. & OONA, M. 2010. Prevalence of rosacea in an Estonian working population using a standard classification. Acta Derm Venereol, 90, 269-73.

AEBERSOLD, R. & MANN, M. 2003. Mass spectrometry-based proteomics. Nature, 422, 198-207.

AFONSO, A. A., SOBRIN, L., MONROY, D. C., SELZER, M., LOKESHWAR, B. & PFLUGFELDER, S. C. 1999. Tear fluid gelatinase B activity correlates with IL-1alpha concentration and fluorescein clearance in ocular rosacea. Invest Ophthalmol Vis Sci, 40, 2506-12.

AFZALI, B., LOMBARDI, G., LECHLER, R. I. & LORD, G. M. 2007a. The role of T helper 17 (Th17) and regulatory T cells (Treg) in human organtransplantation and autoimmune disease. Clin Exp Immunol, 148, 32-46.

AGOSTINI, L., MARTINON, F., BURNS, K., MCDERMOTT, M. F., HAWKINS, P. N. & TSCHOPP, J. 2004. NALP3 forms an IL-1beta-processing inflammasome with increased activity in Muckle-Wells autoinflammatory disorder. Immunity, 20, 319-25.

AHMAD, S., KOLLI, S., LAKO, M., FIGUEIREDO, F. & DANIELS, J. T. 2010. Stem cell therapies for ocular surface disease. Drug Discov Today, 15, 306-13.

AHN, E. Y., DEKELVER, R. C., LO, M. C., NGUYEN, T. A., MATSUURA, S., BOYAPATI, A., PANDIT, S., FU, X. D. & ZHANG, D. E. 2011. SON controls cell-cycle progression by coordinated regulation of RNA splicing. Mol Cell, 42, 185-98.

AKAMATSU, H., KOMURA, J., ASADA, Y., MIYACHI, Y. & NIWA, Y. 1991. Inhibitory effect of azelaic acid on neutrophil functions: a possible cause for its efficacy in treating pathogenetically unrelated diseases. Arch Dermatol Res, 283, 162-6.

AKAMATSU, H., OGUCHI, M., NISHIJIMA, S., ASADA, Y., TAKAHASHI, M., USHIJIMA, T. & NIWA, Y. 1990. The inhibition of free radical generation by

human neutrophils through the synergistic effects of metronidazole with palmitoleic acid: a possible mechanism of action of metronidazole in rosacea and acne. Arch Dermatol Res, 282, 449-54.

AKILOV, O. E. & MUMCUOGLU, K. Y. 2003. Association between human demodicosis and HLA class I. Clin Exp Dermatol, 28, 70-3.

ALLEN, K. J., DAVIS, C. L., BILLINGS, S. D. & MOUSDICAS, N. 2007. Recalcitrant papulopustular rosacea in an immunocompetent patient responding to combination therapy with oral ivermectin and topical permethrin. Cutis, 80, 149-51.

ALOI, F., TOMASINI, C., SORO, E. & PIPPIONE, M. 2000. The clinicopathologic spectrum of rhinophyma. J Am Acad Dermatol, 42, 468-72.

ALOMAR, A., BERTH-JONES, J., BOS, J. D., GIANNETTI, A., REITAMO, S., RUZICKA, T., STALDER, J. F., THESTRUP-PEDERSEN, K. & DERMATITIS, E. W. G. O. A. 2004. The role of topical calcineurin inhibitors in atopic dermatitis. Br J Dermatol, 151 Suppl 70 Dec 2004, 3-27.

ANDREWS, P., HE, Y. J. & XIONG, Y. 2006. Cytoplasmic localized ubiquitin ligase cullin 7 binds to p53 and promotes cell growth by antagonizing p53 function. Oncogene, 25, 4534-48.

ANTIGA, E., QUAGLINO, P., PIERINI, I., VOLPI, W., LAMI, G., BIANCHI, B., DEL BIANCO, E., RENZI, D., BARONI, G., NOVELLI, M., PONTI, R., PAPINI, M., DI LOLLO, S., CALABRÒ, A. S., FABBRI, P. & CAPRONI, M. 2015. Regulatory T cells as well as IL-10 are reduced in the skin of patients with dermatitis herpetiformis. J Dermatol Sci, 77, 54-62.

ANTILLE, C., SAURAT, J. H. & LÜBBE, J. 2004. Induction of rosaceiform dermatitis during treatment of facial inflammatory dermatoses with tacrolimus ointment. Arch Dermatol, 140, 457-60.

ANTONICKA, H., SASARMAN, F., NISHIMURA, T., PAUPE, V. & SHOUBRIDGE, E. A. 2013. The mitochondrial RNA-binding protein GRSF1 localizes to RNA granules and is required for posttranscriptional mitochondrial gene expression. Cell Metab, 17, 386-98.

ARAI, H., KOIZUMI, H., AOKI, J. & INOUE, K. 2002. Platelet-activating factor acetylhydrolase (PAF-AH). J Biochem, 131, 635-40.

ARAKI-SASAKI, K., OHASHI, Y., SASABE, T., HAYASHI, K., WATANABE, H., TANO, Y. & HANDA, H. 1995. An SV40-immortalized human corneal

epithelial cell line and its characterization. Invest Ophthalmol Vis Sci, 36, 614-21.

ARPITHA, P., GAO, C. Y., TRIPATHI, B. K., SARAVANAMUTHU, S. & ZELENKA, P. 2013. Cyclin-dependent kinase 5 promotes the stability of corneal epithelial cell junctions. Molecular Vision, 19, 319-332.

ARRIGO, A. P. & SIMON, S. 2010. Expression and Functions of Heat Shock Proteins in the Normal and Pathological Mammalian Eye. Current Molecular Medicine, 10, 776-793.

ATWA, M. A., EMARA, A. S., YOUSSEF, N. & BAYOUMY, N. M. 2014. Serum concentration of IL-17, IL-23 and TNF-α among patients with chronic spontaneous urticaria: association with disease activity and autologous serum skin test. J Eur Acad Dermatol Venereol, 28, 469-74.

AYLESWORTH, R. & VANCE, J. C. 1982. Demodex-Folliculorum And Demodex Brevis In Cutaneous Biopsies. Journal of the American Academy of Dermatology, 7, 583-589.

AYRES, S. & ANDERSON, N. P. 1932. Demodex folliculorum: its role on the etiology of acne rosacea. Arch Dermatol Syphilol, 25, 89–98.

AYRES, S. & ANDERSON, N. P. 1933. Acne rosacea. Response to local treatment for Demodex folliculorum. JAMA, 100, 645–647.

AYRES, S. 1930. Pityriasis folliculorum (Demodex). Arch Dermatol Syphilol, 1930, 21, 19–24.

AYRES, S. 1961. Demodectic eruptions (demodicidosis) in the human. 30 years' experience with 2 commonly unrecognized entities: pityriasis folliculorum (Demodex) and acne rosacea (Demodex type). Arch Dermatol, 83, 816-27.

BABIOR, B. M., KIPNES, R. S. & CURNUTTE, J. T. 1973. Biological defense mechanisms. The production by leukocytes of superoxide, a potential bactericidal agent. J Clin Invest, 52, 741-4.

BABIOR, B. M., LAMBETH, J. D. & NAUSEEF, W. 2002. The neutrophil NADPH oxidase. Arch Biochem Biophys, 397, 342-4.

BADWEY, J. A., CURNUTTE, J. T., ROBINSON, J. M., LAZDINS, J. K., BRIGGS, R. T., KARNOVSKY, M. J. & KARNOVSKY, M. L. 1980. Comparative aspects of oxidative metabolism of neutrophils from human blood and guinea pig peritonea: magnitude of the respiratory burst, dependence upon stimulating agents, and localization of the oxidases. J Cell Physiol, 105, 541-5.

BAIMA, B. & STICHERLING, M. 2002. Demodicidosis revisited. Acta Derm Venereol, 82, 3-6.

BAKAR, O., DEMIRCAY, Z., TOKER, E. & CAKIR, S. 2009. Ocular signs, symptoms and tear function tests of papulopustular rosacea patients receiving azithromycin. J Eur Acad Dermatol Venereol, 23, 544-9.

BALDRIDGE, C. W. & GERARD, R. W. 1933. The extra respiration of phagocytosis. Amer Jour Physiol, 103, 235-236.

BAMFORD, J. T., GESSERT, C. E., RENIER, C. M., JACKSON, M. M., LAABS, S. B., DAHL, M. V. & ROGERS, R. S., 3RD 2006. Childhood stye and adult rosacea. J Am Acad Dermatol, 55, 951-5.

BANDYOPADHYAY, J., LEE, J., LEE, J. I., YU, J. R., JEE, C., CHO, J. H., JUNG, S., LEE, M. H., ZANNONI, S., SINGSON, A., KIM, D. H., KOO, H. S. & AHNN, J. 2002. Calcineurin, a calcium/calmodulin-dependent protein phosphatase, is involved in movement, fertility, egg laying, and growth in Caenorhabditis elegans. Mol Biol Cell, 13, 3281-93.

BASTA-JUZBASIC, A., SUBIC, J. S. & LJUBOJEVIC, S. 2002. Demodex folliculorum in development of dermatitis rosaceiformis steroidica androsacea related diseases. Clin Dermatol, 20, 135-40.

BASTOS, M. C., CEOTTO, H., COELHO, M. L. & NASCIMENTO, J. S. 2009. Staphylococcal antimicrobial peptides: relevant properties and potential biotechnological applications. Curr Pharm Biotechnol, 10, 38-61.

BEALE, K. 2012. Feline demodicosis: a consideration in the itchy or overgrooming cat. J Feline Med Surg, 14, 209-13.

BELKAID, Y., HOFFMANN, K. F., MENDEZ, S., KAMHAWI, S., UDEY, M. C., WYNN, T. A. & SACKS, D. L. 2001. The role of interleukin (IL)-10 in the persistence of Leishmania major in the skin after healing and the therapeutic potential of anti-IL-10 receptor antibody for sterile cure. J Exp Med, 194, 1497-506.

BELLOCCHIO, S., MORETTI, S., PERRUCCIO, K., FALLARINO, F., BOZZA, S., MONTAGNOLI, C., MOSCI, P., LIPFORD, G. B., PITZURRA, L. & ROMANI, L. 2004. TLRs govern neutrophil activity in aspergillosis. J Immunol, 173, 7406-15.

BERG, M. & LIDEN, S. 1989. An epidemiological study of rosacea. Acta Derm Venereol, 69, 419-23.

BERGIN, D. A., REEVES, E. P., MELEADY, P., HENRY, M., MCELVANEY, O. J., CARROLL, T. P., CONDRON, C., CHOTIRMALL, S. H., CLYNES, M., O'NEILL, S. J. & MCELVANEY, N. G. 2010. alpha-1 Antitrypsin regulates human neutrophil chemotaxis induced by soluble immune complexes and IL-8. J Clin Invest, 120, 4236-50.

BERNARDES, T. F. & BONFIOLI, A. A. 2010. Blepharitis. Semin Ophthalmol, 25, 79-83.

BERRIDGE, M. J. 1995. Capacitative calcium entry. Biochem J, 312 (Pt 1), 1-11.

BERTON, A., GODEAU, G., EMONARD, H., BABA, K., BELLON, P., HORNEBECK, W. & BELLON, G. 2000. Analysis of the ex vivo specificity of human gelatinases A and B towards skin collagen and elastic fibers by computerized morphometry. Matrix Biol, 19, 139-48.

BHATIA, N. D. & DEL ROSSO, J. Q. 2012. Optimal management of papulopustular rosacea: rationale for combination therapy. J Drugs Dermatol, 11, 838-44.

BILLAH, M. M. 1993. Phospholipase D and cell signaling. Curr Opin Immunol, 5, 114-23.

BINAH, O., SHILKRUT, M., YANIV, G. & LARISCH, S. 2004. The Fas receptor 1,4,5-IP3 cascade: a potential target for treating heart failure and arrhythmias. Ann N Y Acad Sci, 1015, 338-50.

BLASI, F., TARSIA, P. & ALIBERTI, S. 2009. Chlamydophila pneumoniae. Clin Microbiol Infect, 15, 29-35.

BLAZQUEZ-DOMINGO, M., GRECH, G. & VON LINDERN, M. 2005. Translation initiation factor 4E inhibits differentiation of erythroid progenitors. Mol Cell Biol, 25, 8496-506.

BLENCOWE, B. J., BAUREN, G., ELDRIDGE, A. G., ISSNER, R., NICKERSON, J. A., ROSONINA, E. & SHARP, P. A. 2000. The SRm160/300 splicing coactivator subunits. Rna, 6, 111-20.

BLENCOWE, B. J., ISSNER, R., NICKERSON, J. A. & SHARP, P. A. 1998. A coactivator of pre-mRNA splicing. Genes Dev, 12, 996-1009.

BLOUNT, B. W. & PELLETIER, A. L. 2002. Rosacea: a common, yet commonly overlooked, condition. Am Fam Physician, 66, 435-40.

BOCHKAREVA, E. S., LISSIN, N. M. & GIRSHOVICH, A. S. 1988. Transient association of newly synthesized unfolded proteins with the heat-shock GroEL protein. Nature, 336, 254-7.

BOCHUD, P. Y., BOCHUD, M., TELENTI, A. & CALANDRA, T. 2007. Innate immunogenetics: a tool for exploring new frontiers of host defence. Lancet Infect Dis, 7, 531-42.

BODNAR, A. G., OUELLETTE, M., FROLKIS, M., HOLT, S. E., CHIU, C. P., MORIN, G. B., HARLEY, C. B., SHAY, J. W., LICHTSTEINER, S. & WRIGHT, W. E. 1998. Extension of life-span by introduction of telomerase into normal human cells. Science, 279, 349-52.

BOHM, D., SCHWANITZ, P., STOCK GISSENDANNER, S., SCHMID-OTT, G. & SCHULZ, W. 2014. Symptom severity and psychological sequelae in rosacea: results of a survey. Psychol Health Med, 19, 586-91.

BOIXEDA DE MIQUEL, D., VAZQUEZ ROMERO, M., VAZQUEZ SEQUEIROS, E., FORUNY OLCINA, J. R., BOIXEDA DE MIQUEL, P., LOPEZ SAN ROMAN, A., ALEMAN VILLANUEVA, S. & MARTIN DE ARGILA DE PRADOS, C. 2006. Effect of Helicobacter pylori eradication therapy in rosacea patients. Rev Esp Enferm Dig, 98, 501-9.

BOKOCH, G. M. 1995. Chemoattractant signaling and leukocyte activation. Blood, 86, 1649-60.

BONNAR, E., EUSTACE, P. & POWELL, F. C. 1993. The Demodex mite population in rosacea. J Am Acad Dermatol, 28, 443-8.

BORREGAARD, N., SORENSEN, O. E. & THEILGAARD-MONCH, K. 2007. Neutrophil granules: a library of innate immunity proteins. Trends Immunol,28, 340-5.

BRADLEY, J. R. 2008. TNF-mediated inflammatory disease. J Pathol, 214, 149-60.

BRECHARD, S. & TSCHIRHART, E. J. 2008. Regulation of superoxide production in neutrophils: role of calcium influx. J Leukoc Biol, 84, 1223-37.

BRINK, N., SZAMEL, M., YOUNG, A. R., WITTERN, K. P. & BERGEMANN, J. 2000. Comparative quantification of IL-1beta, IL-10, IL-10r, TNFalpha and IL-7 mRNA levels in UV-irradiated human skin in vivo. Inflamm Res, 49, 290-6.

BROERING, T. J., WANG, Y. L., PANDEY, R. N., HEGDE, R. S., WANG, S. C. & NAMEKAWA, S. H. 2015. BAZ1B is dispensable for H2AX phosphorylation on Tyrosine 142 during spermatogenesis. Biol Open, 4, 873-84.

BROWN, K. M. & TRACY, D. K. 2013. Lithium: the pharmacodynamic actions of the amazing ion. Ther Adv Psychopharmacol, 3, 163-76.

BROWN, T. T., CHOI, E. Y., THOMAS, D. G., HRISTOV, A. C. & CHAN, M. P. 2014. Comparative analysis of rosacea and cutaneous lupus erythematosus: histopathologic features, T-cell subsets, and plasmacytoid dendritic cells. J Am Acad Dermatol, 71, 100-7.

BROWNE, N., HEELAN, M. & KAVANAGH, K. 2013. An analysis of the structural and functional similarities of insect hemocytes and mammalian phagocytes. Virulence, 4, 597-603.

BRUININK, A., SIDLER, C. & BIRCHLER, F. 1996. Neurotrophic effects of transferrin on embryonic chick brain and neural retinal cell cultures. Int J Dev Neurosci, 14, 785-95.

BUELENS, C., WILLEMS, F., DELVAUX, A., PIERARD, G., DELVILLE, J. P., VELU, T. & GOLDMAN, M. 1995. Interleukin-10 differentially regulates B7-1 (CD80) and B7-2 (CD86) expression on human peripheral blood dendritic cells. Eur J Immunol, 25, 2668-72.

BUHL, T., SULK, M., NOWAK, P., BUDDENKOTTE, J., MCDONALD, I., AUBERT, J., CARLAVAN, I., DERET, S., REINICHE, P., RIVIER, M., VOEGEL, J. J. & STEINHOFF, M. 2015. Molecular and Morphological Characterization of Inflammatory Infiltrate in Rosacea Reveals Activation of Th1/Th17 Pathways. J Invest Dermatol, 135, 2198-208.

BULEK, K., LIU, C., SWAIDANI, S., WANG, L., PAGE, R. C., GULEN, M. F., HERJAN, T., ABBADI, A., QIAN, W., SUN, D., LAUER, M., HASCALL, V., MISRA, S., CHANCE, M. R., ARONICA, M., HAMILTON, T. & LI, X. 2011. The inducible kinase IKKi is required for IL-17-dependent signaling associated with neutrophilia and pulmonary inflammation. Nat Immunol, 12, 844-52.

CAMPBELL, E. J., CAMPBELL, M. A. & OWEN, C. A. 2000. Bioactive proteinase 3 on the cell surface of human neutrophils: quantification, catalytic activity, and susceptibility to inhibition. J Immunol, 165, 3366-74.

CAO, S., LIU, J., CHESI, M., BERGSAGEL, P. L., HO, I. C., DONNELLY, R. P. & MA, X. 2002. Differential regulation of IL-12 and IL-10 gene expression in macrophages by the basic leucine zipper transcription factor c-Maf fibrosarcoma. J Immunol, 169, 5715-25.

CARLEVARO, M. F., ALBINI, A., RIBATTI, D., GENTILI, C., BENELLI, R., CERMELLI, S., CANCEDDA, R. & CANCEDDA, F. D. 1997. Transferrin

promotes endothelial cell migration and invasion: implication in cartilage neovascularization. J Cell Biol, 136, 1375-84.

CARLSSON, R., ENGVALL, E., FREEMAN, A. & RUOSLAHTI, E. 1981. Laminin and fibronectin in cell adhesion: enhanced adhesion of cells from regenerating liver to laminin. Proc Natl Acad Sci U S A, 78, 2403-6.

CASAS, C., PAUL, C., LAHFA, M., LIVIDEANU, B., LEJEUNE, O., ALVAREZ GEORGES, S., SAINT-MARTORY, C., DEGOUY, A., MENGEAUD, V., GINISTY, H., DURBISE, E., SCHMITT, A. M. & REDOULES, D. 2012. Quantification of Demodex folliculorum by PCR in rosacea and its relationship to skin innate immune activation. Exp Dermatol, 21, 906-10.

CASTELLANO, E. & DOWNWARD, J. 2011. RAS Interaction with PI3K: More Than Just Another Effector Pathway. Genes Cancer, 2, 261-74.

CHABAUD, M., DURAND, J. M., BUCHS, N., FOSSIEZ, F., PAGE, G., FRAPPART, L. & MIOSSEC, P. 1999. Human interleukin-17: A T cell derived proinflammatory cytokine produced by the rheumatoid synovium. Arthritis Rheum, 42, 963-70.

CHALARIS, A., GARBERS, C., RABE, B., ROSE-JOHN, S. & SCHELLER, J. 2011. The soluble Interleukin 6 receptor: generation and role in inflammation and cancer. Eur J Cell Biol, 90, 484-94.

CHANG, C. H., FURUE, M. & TAMAKI, K. 1995. B7-1 expression of Langerhans cells is up-regulated by proinflammatory cytokines, and is down-regulated by interferon-gamma or by interleukin-10. Eur J Immunol, 25, 394-8.

CHAPLIN, D. D. 2010. Overview of the immune response. J Allergy Clin Immunol, 125, S3-23.

CHAUDHARY, P., THAMAKE, S. I., SHETTY, P. & VISHWANATHA, J. K. 2014. Inhibition of triple-negative and Herceptin-resistant breast cancer cell proliferation and migration by Annexin A2 antibodies. Br J Cancer, 111, 2328-41.

CHEN, C. H. 2004. Platelet-activating factor acetylhydrolase: is it good or bad for you? Curr Opin Lipidol, 15, 337-41.

CHESNEY, C. J. 1988. An unusual species of demodex mite in a cat. Vet Rec, 123, 671-3.

CHEUNG, G. Y., DUONG, A. C. & OTTO, M. 2012. Direct and synergistic hemolysis caused by Staphylococcus phenol-soluble modulins: implications for diagnosis and pathogenesis. Microbes Infect, 14, 380-6.

CHIANG, M. C., JUO, C. G., CHANG, H. H., CHEN, H. M., YI, E. C. & CHERN, Y. 2007. Systematic uncovering of multiple pathways underlying the pathology of Huntington disease by an acid-cleavable isotope-coded affinity tag approach. Mol Cell Proteomics, 6, 781-97.

CHUNG, U., IGARASHI, T., NISHISHITA, T., IWANARI, H., IWAMATSU, A., SUWA, A., MIMORI, T., HATA, K., EBISU, S., OGATA, E., FUJITA, T. & OKAZAKI, T. 1996. The interaction between Ku antigen and REF1 protein mediates negative gene regulation by extracellular calcium. J Biol Chem, 271, 8593-8.

CIECHANOVER, A. 2005. Intracellular protein degradation: from a vague idea, through the lysosome and the ubiquitin-proteasome system, and onto human diseases and drug targeting (Nobel lecture). Angew Chem Int Ed Engl, 44, 5944-67.

CODA, A. B., HATA, T., MILLER, J., AUDISH, D., KOTOL, P., TWO, A., SHAFIQ, F., YAMASAKI, K., HARPER, J. C., DEL ROSSO, J. Q. &GALLO, R. L. 2013. Cathelicidin, kallikrein 5, and serine protease activity is inhibited during treatment of rosacea with azelaic acid 15% gel. J Am Acad Dermatol, 69, 570-7.

COGEN, A. L., YAMASAKI, K., MUTO, J., SANCHEZ, K. M., CROTTY ALEXANDER, L., TANIOS, J., LAI, Y., KIM, J. E., NIZET, V. & GALLO, R. L. 2010. Staphylococcus epidermidis antimicrobial delta-toxin (phenol soluble modulin-gamma) cooperates with host antimicrobial peptides to kill group A Streptococcus. PLoS One, 5, e8557.

COLLET, J. F. & MESSENS, J. 2010. Structure, function, and mechanism of thioredoxin proteins. Antioxid Redox Signal, 13, 1205-16.

CONESA, A. & GOTZ, S. 2008. Blast2GO: A comprehensive suite for functional analysis in plant genomics. Int J Plant Genomics, 2008, 619832.

CONG, Y. S., WRIGHT, W. E. & SHAY, J. W. 2002. Human telomerase and its regulation. Microbiol Mol Biol Rev, 66, 407-25, table of contents.

COPPO, A., MANZI, A., PULITZER, J. F. & TAKAHASHI, H. 1973. Abortive bacteriophage T4 head assembly in mutants of Escherichia coli. J Mol Biol, 76, 61-87.

COSTER, D. J., AGGARWAL, R. K. & WILLIAMS, K. A. 1995. Surgical management of ocular surface disorders using conjunctival and stem cell allografts. Br J Ophthalmol, 79, 977-82.

COX, J. & MANN, M. 2008. MaxQuant enables high peptide identification rates, individualized p.p.b.-range mass accuracies and proteome-wide protein quantification. Nat Biotechnol, 26, 1367-72.

COX, J., NEUHAUSER, N., MICHALSKI, A., SCHELTEMA, R. A., OLSEN, J. V. & MANN, M. 2011. Andromeda: a peptide search engine integrated into the MaxQuant environment. J Proteome Res, 10, 1794-805.

CRAWFORD, G. H., PELLE, M. T. & JAMES, W. D. 2004. Rosacea: I. Etiology, pathogenesis, and subtype classification. J Am Acad Dermatol, 51, 327-41; quiz 342-4.

CURNUTTE, J. T., KUVER, R. & BABIOR, B. M. 1987. Activation of the respiratory burst oxidase in a fully soluble system from human neutrophils. J Biol Chem, 262, 6450-2.

CZEPITA, D., KUZNA-GRYGIEL, W., CZEPITA, M. & GROBELNY, A. 2007. Demodex folliculorum and Demodex brevis as a cause of chronic marginal blepharitis. Ann Acad Med Stetin, 53, 63-7; discussion 67.

D'AGOSTINO, P., ARCOLEO, F., BARBERA, C., DI BELLA, G., LA ROSA, M., MISIANO, G., MILANO, S., BRAI, M., CAMMARATA, G., FEO, S. & CILLARI, E. 1998. Tetracycline inhibits the nitric oxide synthase activity induced by endotoxin in cultured murine macrophages. Eur J Pharmacol, 346, 283-90.

DAHL, M. V., ROSS, A. J. & SCHLIEVERT, P. M. 2004. Temperature regulates bacterial protein production: possible role in rosacea. J Am Acad Dermatol, 50, 266-72.

DANIELS, J. T., GEERLING, G., ALEXANDER, R. A., MURPHY, G., KHAW, P. T. & SAARIALHO-KERE, U. 2003. Temporal and spatial expression of matrix metalloproteinases during wound healing of human corneal tissue. Exp Eye Res, 77, 653-64.

DASGUPTA, B., CORKILL, M., KIRKHAM, B., GIBSON, T. & PANAYI, G. 1992. Serial estimation of interleukin 6 as a measure of systemic disease in rheumatoid arthritis. J Rheumatol, 19, 22-5.

DAVANGER, M. & EVENSEN, A. 1971. Role of the pericorneal papillary structure in renewal of corneal epithelium. Nature, 229, 560-1.

DEBETS, R., HEGMANS, J. P., CROUGHS, P., TROOST, R. J., PRINS, J. B., BENNER, R. & PRENS, E. P. 1997. The IL-1 system in psoriatic skin: IL-1 antagonist sphere of influence in lesional psoriatic epidermis. J Immunol, 158, 2955-63.

DECKERS-HEBESTREIT, G. & ALTENDORF, K. 1996. The F0F1-type ATP synthases of bacteria: structure and function of the F0 complex. Annu Rev Microbiol, 50, 791-824.

DEL ROSSO, J. Q. 2006. Update on rosacea pathogenesis and correlation with medical therapeutic agents. Cutis, 78, 97-100.

DEL ROSSO, J. Q. 2012. Advances in understanding and managing rosacea: part 2: the central role, evaluation, and medical management of diffuse and persistent facial erythema of rosacea. J Clin Aesthet Dermatol, 5, 26-36.

DEL ROSSO, J. Q., GALLO, R. L., TANGHETTI, E., WEBSTER, G. & THIBOUTOT, D. 2013a. An evaluation of potential correlations between pathophysiologic mechanisms, clinical manifestations, and management of rosacea. Cutis, 91, 1-8.

DEL ROSSO, J. Q., THIBOUTOT, D., GALLO, R., WEBSTER, G., TANGHETTI, E., EICHENFIELD, L., STEIN-GOLD, L., BERSON, D. & ZAENGLEIN, A. 2013b. Consensus recommendations from the American Acne & Rosacea Society on the management of rosacea, part 1: a status report on the disease state, general measures, and adjunctive skin care. Cutis, 92, 234-40.

DEL ROSSO, J. Q., THIBOUTOT, D., GALLO, R., WEBSTER, G., TANGHETTI, E., EICHENFIELD, L., STEIN-GOLD, L., BERSON, D. & ZAENGLEIN, A. 2013c. Consensus recommendations from the American Acne & Rosacea Society on the management of rosacea, part 2: a status report on topical agents. Cutis, 92, 277-84.

DELANEY, S. 2004. The role of bacterial Antigen(s) in the Induction and Persistence of Papulopustular Rosacea. *PhD Thesis.*

DESCH, C. & NUTTING, W. B. 1972. Demodex folliculorum (Simon) and D. brevis akbulatova of man: redescription and reevaluation. J Parasitol, 58, 169-77.

DESCH, C. E. & NUTTING, W. B. 1974. Demodex adocoilei sp. nov. from the white-tailed deer, Odocoileus virginianus. Can J Zool, 52, 785-9.

DEVANEY, J. M., GREENE, C. M., TAGGART, C. C., CARROLL, T. P., O'NEILL, S. J. & MCELVANEY, N. G. 2003. Neutrophil elastase up regulates interleukin-8 via toll-like receptor 4. FEBS Lett, 544, 129-32.

DI CERA, E. 2009. Serine proteases. IUBMB Life, 61, 510-5.

DIAZ, C., O'CALLAGHAN, C. J., KHAN, A. & ILCHYSHYN, A. 2003. Rosacea: a cutaneous marker of Helicobacter pylori infection? Results of a pilot study. Acta Derm Venereol, 83, 282-6.

DIAZ-PEREZ, J. L. 1994. Demodex mites in rosacea. J Am Acad Dermatol, 30, 812-3.

DINARELLO, C. A. 1986. Interleukin-1: amino acid sequences, multiple biological activities and comparison with tumor necrosis factor (cachectin). Year Immunol, 2, 68-89.

DINARELLO, C. A. 1996. Biologic basis for interleukin-1 in disease. Blood, 87, 2095-147.

DINARELLO, C. A. 2000. Proinflammatory cytokines. Chest, 118, 503-8.

DINARELLO, C. A. 2011. Interleukin-1 in the pathogenesis and treatment of inflammatory diseases. Blood, 117, 3720-32.

DING, L., LINSLEY, P. S., HUANG, L. Y., GERMAIN, R. N. & SHEVACH, E. M. 1993. IL-10 inhibits macrophage costimulatory activity by selectively inhibiting the up-regulation of B7 expression. J Immunol, 151, 1224-34.

DOBRZANSKI, P., RYSECK, R. P. & BRAVO, R. 1994. Differential interactions of Rel-NF-kappa B complexes with I kappa B alpha determine pools of constitutive and inducible NF-kappa B activity. Embo j, 13, 4608-16.

DOMON, B. & AEBERSOLD, R. 2006. Mass spectrometry and protein analysis. Science, 312, 212-7.

DOUGHERTY, J. M. & MCCULLEY, J. P. 1986. Bacterial lipases and chronic blepharitis. Invest Ophthalmol Vis Sci, 27, 486-91.

DOWD, S. E., SUN, Y., SECOR, P. R., RHOADS, D. D., WOLCOTT, B. M., JAMES, G. A. & WOLCOTT, R. D. 2008. Survey of bacterial diversity in

chronic wounds using pyrosequencing, DGGE, and full ribosome shotgun sequencing. BMC Microbiol, 8, 43.

DROGE, M. J., BOERSMA, Y. L., VAN POUDEROYEN, G., VRENKEN, T. E., RUGGEBERG, C. J., REETZ, M. T., DIJKSTRA, B. W. & QUAX, W. J. 2006. Directed evolution of Bacillus subtilis lipase A by use of enantiomeric phosphonate inhibitors: crystal structures and phage display selection. Chembiochem, 7, 149-57.

DRUMMOND, P. D. & SU, D. 2012. Blushing in rosacea sufferers. J Psychosom Res, 72, 153-8.

DUA, H. S. & AZUARA-BLANCO, A. 2000. Limbal stem cells of the corneal epithelium. Surv Ophthalmol, 44, 415-25.

DUA, H. S., FARAJ, L. A., SAID, D. G., GRAY, T. & LOWE, J. 2013. Human corneal anatomy redefined: a novel pre-Descemet's layer (Dua's layer). Ophthalmology, 120, 1778-85.

DUA, H. S. & FORRESTER, J. V. 1990. The corneoscleral limbus in human corneal epithelial wound healing. Am J Ophthalmol, 110, 646-56.

DUA, H. S., MIRI, A. & SAID, D. G. 2010. Contemporary limbal stem cell transplantation - a review. Clin Experiment Ophthalmol, 38, 104-17.

DURSUN, D., KIM, M. C., SOLOMON, A. & PFLUGFELDER, S. C. 2001. Treatment of recalcitrant recurrent corneal erosions with inhibitors of matrix metalloproteinase-9, doxycycline and corticosteroids. Am J Ophthalmol, 132, 8-13.

DUSTIN, M. L., ROTHLEIN, R., BHAN, A. K., DINARELLO, C. A. & SPRINGER, T. A. 1986. Induction by IL 1 and interferon-gamma: tissue distribution, biochemistry, and function of a natural adherence molecule (ICAM-1). J Immunol, 137, 245-54.

DZIARSKI, R. 2004. Peptidoglycan recognition proteins (PGRPs). Mol Immunol, 40, 877-86.

ECKERT, R. L., BROOME, A. M., RUSE, M., ROBINSON, N., RYAN, D. & LEE, K. 2004. S100 proteins in the epidermis. J Invest Dermatol, 123, 23-33.

EDER, C. 2009. Mechanisms of interleukin-1beta release. Immunobiology, 214, 543-53.

EGGERT, T., BROCKMEIER, U., DROGE, M. J., QUAX, W. J. & JAEGER, K. E. 2003. Extracellular lipases from Bacillus subtilis: regulation of gene

expression and enzyme activity by amino acid supply and external pH. FEMS Microbiol Lett, 225, 319-24.

EGGERT, T., PENCREAC'H, G., DOUCHET, I., VERGER, R. & JAEGER, K. E. 2000. A novel extracellular esterase from Bacillus subtilis and its conversion to a monoacylglycerol hydrolase. Eur J Biochem, 267, 6459-69.

EICHNER, R. D., AL SALAMI, M., WOOD, P. R. & MULLBACHER, A. 1986. The effect of gliotoxin upon macrophage function. Int J Immunopharmacol, 8, 789-97.

EISHINGDRELO, H. & KONGSAMUT, S. 2013. Minireview: Targeting GPCR Activated ERK Pathways for Drug Discovery. Curr Chem Genom Transl Med, 7, 9-15.

EL-SHAZLY, A. M., GHANEUM, B. M., MORSY, T. A. & AATY, H. E. 2001. The pathogenesis of Demodex folliculorum (hair follicular mites) in females with and without rosacea. J Egypt Soc Parasitol, 31, 867-75.

ELDRIDGE, A. G., LI, Y., SHARP, P. A. & BLENCOWE, B. J. 1999. The SRm160/300 splicing coactivator is required for exon-enhancer function. Proc Natl Acad Sci U S A, 96, 6125-30.

ELEWSKI, B. E., DRAELOS, Z., DRENO, B., JANSEN, T., LAYTON, A. & PICARDO, M. 2011. Rosacea - global diversity and optimized outcome: proposed international consensus from the Rosacea International Expert Group. J Eur Acad Dermatol Venereol, 25, 188-200.

ELEWSKI, B. E., FLEISCHER, A. B., JR. & PARISER, D. M. 2003. A comparison of 15% azelaic acid gel and 0.75% metronidazole gel in the topical treatment of papulopustular rosacea: results of a randomized trial. Arch Dermatol, 139, 1444-50.

ELKINGTON, P. T., O'KANE, C. M. & FRIEDLAND, J. S. 2005. The paradox of matrix metalloproteinases in infectious disease. Clin Exp Immunol, 142, 12-20.

ELSTON, C. A. & ELSTON, D. M. 2014. Demodex mites. Clin Dermatol, 32, 739-43.

ELSTON, D. M. 2010. Demodex mites: Facts and controversies. Clinics in Dermatology, 28, 502-504.

ELSTON, D. M., LAWLER, K. B. & IDDINS, B. O. 2001. What's eating you? Demodex folliculorum. Cutis, 68, 93-4.

ENGEL, A., JOHNSON, M. L. & HAYNES, S. G. 1988. Health effects of sunlight exposure in the United States. Results from the first National Health and Nutrition Examination Survey, 1971-1974. Arch Dermatol, 124, 72-9.

ERBAGCI, Z. & OZGOZTASI, O. 1998. The significance of Demodex folliculorum density in rosacea. Int J Dermatol, 37, 421-5.

ERBAN, T. & HUBERT, J. 2010. Determination of pH in regions of the midguts of acaridid mites. J Insect Sci, 10, 42.

EYERICH, K., FOERSTER, S., ROMBOLD, S., SEIDL, H. P., BEHRENDT, H., HOFMANN, H., RING, J. & TRAIDL-HOFFMANN, C. 2008. Patients with chronic mucocutaneous candidiasis exhibit reduced production of Th17 associated cytokines IL-17 and IL-22. J Invest Dermatol, 128, 2640-5.

EYERICH, K., PENNINO, D., SCARPONI, C., FOERSTER, S., NASORRI, F., BEHRENDT, H., RING, J., TRAIDL-HOFFMANN, C., ALBANESI, C. & CAVANI, A. 2009. IL-17 in atopic eczema: linking allergen-specific adaptive and microbial-triggered innate immune response. J Allergy Clin Immunol, 123, 59-66.e4.

FENN, J. B., MANN, M., MENG, C. K., WONG, S. F. & WHITEHOUSE, C. M. 1989. Electrospray ionization for mass spectrometry of large biomolecules. Science, 246, 64-71.

FERNANDEZ, I. S., BAI, X. C., HUSSAIN, T., KELLEY, A. C., LORSCH, J. R., RAMAKRISHNAN, V. & SCHERES, S. H. 2013. Molecular architecture of a eukaryotic translational initiation complex. Science, 342, 1240585.

FERNANDEZ-OBREGON, A. & PATTON, D. L. 2007. The role of Chlamydia pneumoniae in the etiology of acne rosacea: response to the use of oral azithromycin. Cutis, 79, 163-7.

FERRY, G., LONCHAMPT, M., PENNEL, L., DE NANTEUIL, G., CANET, E. & TUCKER, G. C. 1997. Activation of MMP-9 by neutrophil elastase in an in vivo model of acute lung injury. FEBS Lett, 402, 111-5.

FIELD, J., BROEK, D., KATAOKA, T. & WIGLER, M. 1987. Guanine nucleotide activation of, and competition between, RAS proteins from Saccharomyces cerevisiae. Mol Cell Biol, 7, 2128-33.

FINGAR, D. C., RICHARDSON, C. J., TEE, A. R., CHEATHAM, L., TSOU, C. & BLENIS, J. 2004. mTOR controls cell cycle progression through its cell

growth effectors S6K1 and 4E-BP1/eukaryotic translation initiation factor 4E. Mol Cell Biol, 24, 200-16.

FINI, M. E., COOK, J. R. & MOHAN, R. 1998. Proteolytic mechanisms in corneal ulceration and repair. Arch Dermatol Res, 290 Suppl, S12-23.

FINI, M. E., PARKS, W. C., RINEHART, W. B., GIRARD, M. T., MATSUBARA, M., COOK, J. R., WEST-MAYS, J. A., SADOW, P. M., BURGESON, R. E., JEFFREY, J. J., RAIZMAN, M. B., KRUEGER, R. R. & ZIESKE, J. D. 1996. Role of matrix metalloproteinases in failure to re-epithelialize after corneal injury. Am J Pathol, 149, 1287-302.

FINKELMAN, F. D., HOGAN, S. P., HERSHEY, G. K., ROTHENBERG, M. E. & WILLS-KARP, M. 2010. Importance of cytokines in murine allergic airway disease and human asthma. J Immunol, 184, 1663-74.

FITCH, E., HARPER, E., SKORCHEVA, I., KURTZ, S. E. & BLAUVELT, A. 2007. Pathophysiology of psoriasis: recent advances on IL-23 and Th17 cytokines. Curr Rheumatol Rep, 9, 461-7.

FORTON, F., GERMAUX, M. A., BRASSEUR, T., DE LIEVER, A., LAPORTE, M., MATHYS, C., SASS, U., STENE, J. J., THIBAUT, S., TYTGAT, M. & SEYS, B. 2005. Demodicosis and rosacea: epidemiology and significance in daily dermatologic practice. J Am Acad Dermatol, 52, 74-87.

FORTON, F. & SEYS, B. 1993. Density of Demodex folliculorum in rosacea: a case control study using standardized skin-surface biopsy. Br J Dermatol, 128, 650-9.

FORTON, F. & SONG, M. 1998. Limitations of standardized skin surface biopsy in measurement of the density of Demodex folliculorum. A case report. Br J Dermatol, 139, 697-700.

FORTON, F. M. 2012. Papulopustular rosacea, skin immunity and Demodex: pityriasis folliculorum as a missing link. J Eur Acad Dermatol Venereol, 26, 19-28.

FOSSATI, G., MOOTS, R. J., BUCKNALL, R. C. & EDWARDS, S. W. 2002. Differential role of neutrophil Fcgamma receptor IIIB (CD16) in phagocytosis, bacterial killing, and responses to immune complexes. Arthritis Rheum, 46, 1351-61.

FRANK, L. A., KANIA, S. A., CHUNG, K. & BRAHMBHATT, R. 2013. A molecular technique for the detection and differentiation of Demodex mites on cats. Vet Dermatol, 24, 367-9, e82-3.

FU, J., LV, X., LIN, H., WU, L., WANG, R., ZHOU, Z., ZHANG, B., WANG, Y. L., TSANG, B. K., ZHU, C. & WANG, H. 2010. Ubiquitin ligase cullin 7 induces epithelial-mesenchymal transition in human choriocarcinoma cells. J Biol Chem, 285, 10870-9.

FUCHS, E., TUMBAR, T. & GUASCH, G. 2004. Socializing with the neighbors: stem cells and their niche. Cell, 116, 769-78.

FUJII, J. & IKEDA, Y. 2002. Advances in our understanding of peroxiredoxin, a multifunctional, mammalian redox protein. Redox Rep, 7, 123-30.

GALEOTTI, N., BARTOLINI, A., CALVANI, M., NICOLAI, R. & GHELARDINI, C. 2004. Acetyl-L-carnitine requires phospholipase C-IP3 pathway activation to induce antinociception. Neuropharmacology, 47, 286-94.

GALLO, R. L. & NAKATSUJI, T. 2011. Microbial symbiosis with the innate immune defense system of the skin. J Invest Dermatol, 131, 1974-80.

GAO, Y. Y., DI PASCUALE, M. A., ELIZONDO, A. & TSENG, S. C. 2007. Clinical treatment of ocular demodecosis by lid scrub with tea tree oil. Cornea, 26, 136-43.

GAO, Y. Y., DI PASCUALE, M. A., LI, W., LIU, D. T., BARADARAN-RAFII, A., ELIZONDO, A., KAWAKITA, T., RAJU, V. K. & TSENG, S. C. 2005. High prevalence of Demodex in eyelashes with cylindrical dandruff. Invest Ophthalmol Vis Sci, 46, 3089-94.

GARCIA-VARGAS, A., MAYORGA-RODRIGUEZ, J. A. & SANDOVAL-TRESS, C. 2007. Scalp demodicidosis mimicking favus in a 6-year-old boy. J Am Acad Dermatol, 57, S19-21.

GARREIS, F., GOTTSCHALT, M., SCHLORF, T., GLASER, R., HARDER, J., WORLITZSCH, D. & PAULSEN, F. P. 2011. Expression and regulation of antimicrobial peptide psoriasin (S100A7) at the ocular surface and in the lacrimal apparatus. Invest Ophthalmol Vis Sci, 52, 4914-22.

GEIGER, T., COX, J. & MANN, M. 2010. Proteomics on an Orbitrap benchtop mass spectrometer using all-ion fragmentation. Mol Cell Proteomics, 9, 2252-61.

GEORGALA, S., KATOULIS, A. C., KYLAFIS, G. D., KOUMANTAKI MATHIOUDAKI, E., GEORGALA, C. & ARONI, K. 2001. Increased

density of Demodex folliculorum and evidence of delayed hypersensitivity reaction in subjects with papulopustular rosacea. J Eur Acad Dermatol Venereol, 15, 441-4.

GEORGOPOULOS, C. & WELCH, W. J. 1993. Role of the major heat shock proteins as molecular chaperones. Annu Rev Cell Biol, 9, 601-34.

GEORGOPOULOS, C. P., HENDRIX, R. W., CASJENS, S. R. & KAISER, A. D. 1973. Host participation in bacteriophage lambda head assembly. J Mol Biol, 76, 45-60.

GILMORE, W. S., OLWILL, S., MCGLYNN, H. & ALEXANDER, H. D. 2004. Annexin A2 expression during cellular differentiation in myeloid cell lines. Biochem Soc Trans, 32, 1122-3.

GIPSON, I. K., SPURR-MICHAUD, S. J., TISDALE, A. S., KUBLIN, C., CINTRON, C. & KEUTMANN, H. 1995. Stratified squamous epithelia produce mucin-like glycoproteins. Tissue Cell, 27, 397-404.

GOLDBERG, M. F. & BRON, A. J. 1982. Limbal palisades of Vogt. Trans Am Ophthalmol Soc, 80, 155-71.

GOLLNICK, H. & LAYTON, A. 2008. Azelaic acid 15% gel in the treatment of rosacea. Expert Opin Pharmacother, 9, 2699-706.

GOLOUBINOFF, P., GATENBY, A. A. & LORIMER, G. H. 1989. GroE heat-shock proteins promote assembly of foreign prokaryotic ribulose bisphosphate carboxylase oligomers in Escherichia coli. Nature, 337, 44-7.

GOMES, J. A., ROMANO, A., SANTOS, M. S. & DUA, H. S. 2005. Amniotic membrane use in ophthalmology. Curr Opin Ophthalmol, 16, 233-40.

GOMEZ-MARIN, J. E., VALERE, A., BONHOMME, A., EL'BTAOURI, H., ANTONICELLI, F., BURLET, H., AUBERT, D., VILLENA, I., GUENOUNOU, M., HAYE, B. & PINON, J. M. 1998. Interferon-gamma signal transduction during parasite infection: modulation of MAP kinases in the infection of human monocyte cells (THP1) by Toxoplasma gondii. Parasite Immunol, 20, 631-5.

GOMME, P. T., MCCANN, K. B. & BERTOLINI, J. 2005. Transferrin: structure, function and potential therapeutic actions. Drug Discov Today, 10, 267-73.

GORDON, G. M., LEDEE, D. R., FEUER, W. J. & FINI, M. E. 2009. Cytokines and signaling pathways regulating matrix metalloproteinase-9 (MMP-9) expression in corneal epithelial cells. J Cell Physiol, 221, 402-11.

GREENOW, K., PEARCE, N. J. & RAMJI, D. P. 2005. The key role of apolipoprotein E in atherosclerosis. J Mol Med (Berl), 83, 329-42.

GRELLNER, W., GEORG, T. & WILSKE, J. 2000. Quantitative analysis of proinflammatory cytokines (IL-1beta, IL-6, TNF-alpha) in human skinwounds. Forensic Sci Int, 113, 251-64.

GRICE, E. A. & SEGRE, J. A. 2011. The skin microbiome. Nat Rev Microbiol, 9, 244-53.

GRIFFIN, N. M., YU, J., LONG, F., OH, P., SHORE, S., LI, Y., KOZIOL, J. A. & SCHNITZER, J. E. 2010. Label-free, normalized quantification of complex mass spectrometry data for proteomic analysis. Nat Biotechnol, 28, 83-9.

GRIFFITH, M., OSBORNE, R., MUNGER, R., XIONG, X., DOILLON, C. J., LAYCOCK, N. L., HAKIM, M., SONG, Y. & WATSKY, M. A. 1999. Functional human corneal equivalents constructed from cell lines. Science, 286, 2169-72.

GROENEN, P. J., MERCK, K. B., DE JONG, W. W. & BLOEMENDAL, H. 1994. Structure and modifications of the junior chaperone alpha-crystallin. From lens transparency to molecular pathology. Eur J Biochem, 225, 1-19.

GROSSMAN, R. M., KRUEGER, J., YOURISH, D., GRANELLIPIPERNO, A., MURPHY, D. P., MAY, L. T., KUPPER, T. S., SEHGAL, P. B. & GOTTLIEB, A. B. 1989. Interleukin-6 Is Expressed In High Levels In Psoriatic Skin And Stimulates Proliferation Of Cultured Human Keratinocytes. Proceedings of the National Academy of Sciences of the United States of America, 86, 6367-6371.

GUNDESLI, H., TALIM, B., KORKUSUZ, P., BALCI-HAYTA, B., CIRAK, S., AKARSU, N. A., TOPALOGLU, H. & DINCER, P. 2010. Mutation in exon 1f of PLEC, leading to disruption of plectin isoform 1f, causes autosomal recessive limb-girdle muscular dystrophy. Am J Hum Genet, 87, 834-41.

GUPTA, A. K. & CHAUDHRY, M. M. 2005. Rosacea and its management: an overview. Journal of the European Academy of Dermatology and Venereology, 19, 273-285.

HAN, X., ASLANIAN, A. & YATES, J. R., 3RD 2008. Mass spectrometry for proteomics. Curr Opin Chem Biol, 12, 483-90.

HARDMAN, M. & MAKAROV, A. A. 2003. Interfacing the orbitrap mass analyzer to an electrospray ion source. Anal Chem, 75, 1699-705.

HARPER, E. G., GUO, C., RIZZO, H., LILLIS, J. V., KURTZ, S. E., SKORCHEVA, I., PURDY, D., FITCH, E., IORDANOV, M. & BLAUVELT, A. 2009. Th17 cytokines stimulate CCL20 expression in keratinocytes in vitro and in vivo: implications for psoriasis pathogenesis. J Invest Dermatol, 129, 2175-83.

HARRINGTON, L. E., HATTON, R. D., MANGAN, P. R., TURNER, H., MURPHY, T. L., MURPHY, K. M. & WEAVER, C. T. 2005. Interleukin 17 producing CD4+ effector T cells develop via a lineage distinct from the T helper type 1 and 2 lineages. Nat Immunol, 6, 1123-32.

HARTL, F. U. & HAYER-HARTL, M. 2002. Molecular chaperones in the cytosol: from nascent chain to folded protein. Science, 295, 1852-8.

HAU, S. & BARTON, K. 2009. Corneal complications of glaucoma surgery. Curr Opin Ophthalmol, 20, 131-6.

HE, Q. Y., MASON, A. B., NGUYEN, V., MACGILLIVRAY, R. T. & WOODWORTH, R. C. 2000. The chloride effect is related to anion binding in determining the rate of iron release from the human transferrin N-lobe. Biochem J, 350 Pt 3, 909-15.

HEIMER, S. R., YAMADA, A., RUSSELL, H. & GILMORE, M. 2010. Response of corneal epithelial cells to Staphylococcus aureus. Virulence, 1, 223-35.

HEMMINGSEN, S. M., WOOLFORD, C., VAN DER VIES, S. M., TILLY, K., DENNIS, D. T., GEORGOPOULOS, C. P., HENDRIX, R. W. & ELLIS, R. J. 1988. Homologous plant and bacterial proteins chaperone oligomeric protein assembly. Nature, 333, 330-4.

HENDRIX, R. W. 1979. Purification and properties of groE, a host protein involved in bacteriophage assembly. J Mol Biol, 129, 375-92.

HERBERT, J. & NEVYAS, A. S. 1980. Demodex folliculorum and Blepharitis. Cutaneous infestations of man and animal. Mol Microbiol, 63, 1275-1278.

HERMEKING, H., LENGAUER, C., POLYAK, K., HE, T. C., ZHANG, L., THIAGALINGAM, S., KINZLER, K. W. & VOGELSTEIN, B. 1997. 14-3-3 sigma is a p53-regulated inhibitor of G2/M progression. Mol Cell, 1, 3-11.

HERR, H. & YOU, C. H. 2000. Relationship between Helicobacter pylori and rosacea: It may be a myth. Journal of Korean Medical Science, 15, 551-554.

HIRAISHI, H., SHIN, B. S., UDAGAWA, T., NEMOTO, N., CHOWDHURY, W., GRAHAM, J., COX, C., REID, M., BROWN, S. J. & ASANO, K. 2013. Interaction between 25S rRNA A loop and eukaryotic translation initiation

factor 5B promotes subunit joining and ensures stringent AUG selection. Mol Cell Biol, 33, 3540-8.

HOFMANN, B., HECHT, H. J. & FLOHE, L. 2002. Peroxiredoxins. Biol Chem, 383, 347-64.

HOLMES, A. D. 2013. Potential role of microorganisms in the pathogenesis of rosacea. J Am Acad Dermatol, 69, 1025-32.

HOLSCHER, C. 2004. The power of combinatorial immunology: IL-12 and IL-12 related dimeric cytokines in infectious diseases. Med Microbiol Immunol, 193, 1-17.

HORANI, A., NATH, A., WASSERMAN, M. G., HUANG, T. & BRODY, S. L. 2013. Rho-associated protein kinase inhibition enhances airway epithelial Basal-cell proliferation and lentivirus transduction. Am J Respir Cell Mol Biol, 49, 341-7.

HOZONO, Y., UETA, M., HAMURO, J., KOJIMA, K., KAWASAKI, S., YAMAZAKI, K. & KINOSHITA, S. 2006. Human corneal epithelial cells respond to ocular-pathogenic, but not to nonpathogenic-flagellin. Biochem Biophys Res Commun, 347, 238-47.

HSIEH, C. S., MACATONIA, S. E., TRIPP, C. S., WOLF, S. F., O'GARRA, A. & MURPHY, K. M. 1993. Development of TH1 CD4+ T cells through IL-12 produced by Listeria-induced macrophages. Science, 260, 547-9.

HU, Q., NOLL, R. J., LI, H., MAKAROV, A., HARDMAN, M. & GRAHAM COOKS, R. 2005. The Orbitrap: a new mass spectrometer. J Mass Spectrom, 40, 430-43.

HUANG, L. C., JEAN, D., PROSKE, R. J., REINS, R. Y. & MCDERMOTT, A. M. 2007. Ocular surface expression and in vitro activity of antimicrobial peptides. Curr Eye Res, 32, 595-609.

HUEN, M. S., SY, S. M., LEUNG, K. M., CHING, Y. P., TIPOE, G. L., MAN, C., DONG, S. & CHEN, J. 2010. SON is a spliceosome-associated factor required for mitotic progression. Cell Cycle, 9, 2679-85.

HUNTINGTON, J. A. 2011. Serpin structure, function and dysfunction. J Thromb Haemost, 9 Suppl 1, 26-34.

INDIK, Z. K., PARK, J. G., HUNTER, S. & SCHREIBER, A. D. 1995. The molecular dissection of Fc gamma receptor mediated phagocytosis. Blood, 86, 4389-99.

INDRAMOHAN, M., SIEVE, A. N., BREAK, T. J. & BERG, R. E. 2012. Inflammatory monocyte recruitment is regulated by interleukin-23 during systemic bacterial infection. Infect Immun, 80, 4099-105.

IOCONO, J. A., COLLERAN, K. R., REMICK, D. G., GILLESPIE, B. W., EHRLICH, H. P. & GARNER, W. L. 2000. Interleukin-8 levels and activity in delayed-healing human thermal wounds. Wound Repair Regen, 8, 216-25.

ISHIHARA, K. & HIRANO, T. 2002. IL-6 in autoimmune disease and chronic inflammatory proliferative disease. Cytokine Growth Factor Rev, 13, 357-68.

IWASAKI, A. & MEDZHITOV, R. 2015. Control of adaptive immunity by the innate immune system. Nat Immunol, 16, 343-53.

JACKSON, W. B. 2008. Blepharitis: current strategies for diagnosis and management. Can J Ophthalmol, 43, 170-9.

JANEWAY, C. A., JR. 1989. Approaching the asymptote? Evolution and revolution in immunology. Cold Spring Harb Symp Quant Biol, 54 Pt 1, 1-13.

JANG, Y. H., SIM, J. H., KANG, H. Y., KIM ,Y. C. & LEE, E. S. 2011. Immunohistochemical expression of matrix metalloproteinases in the granulomatous rosacea compared with the non-granulomatous rosacea. J Eur Acad Dermatol Venereol, 25 (5), 544-48.

JARMUDA, S., O'REILLY, N., ZABA, R., JAKUBOWICZ, O., SZKARADKIEWICZ, A. & KAVANAGH, K. 2012. Potential role of Demodex mites and bacteria in the induction of rosacea. Journal of Medical Microbiology, 61, 1504-1510.

JARVIS, R. M., HUGHES, S. M. & LEDGERWOOD, E. C. 2012. Peroxiredoxin 1 functions as a signal peroxidase to receive, transduce, and transmit peroxide signals in mammalian cells. Free Radic Biol Med, 53, 1522-30.

JAYACHANDRAN, R., SUNDARAMURTHY, V., COMBALUZIER, B., MUELLER, P., KORF, H., HUYGEN, K., MIYAZAKI, T., ALBRECHT, I., MASSNER, J. & PIETERS, J. 2007. Survival of mycobacteria in macrophages is mediated by coronin 1-dependent activation of calcineurin. Cell, 130, 37-50.

JENKINS, C., TUFT, S., LIU, C. & BUCKLEY, R. 1993. Limbal transplantation in the management of chronic contact-lens-associated epitheliopathy. Eye (Lond), 7 (Pt 5), 629-33.

JENKINS, M. S., BROWN, S. I., LEMPERT, S. L. & WEINBERG, R. J. 1979. Ocular rosacea. Am J Ophthalmol, 88, 618-22.

JETHWANEY, D., ISLAM, M. R., LEIDAL, K. G., DE BERNABE, D. B., CAMPBELL, K. P., NAUSEEF, W. M. & GIBSON, B. W. 2007. Proteomic analysis of plasma membrane and secretory vesicles from human neutrophils. Proteome Sci, 5, 12.

JIN, L., FENG, X., RONG, H., PAN, Z., INABA, Y., QIU, L., ZHENG, W., LIN, S., WANG, R., WANG, Z., WANG, S., LIU, H., LI, S., XIE, W. & LI, Y. 2013. The antiparasitic drug ivermectin is a novel FXR ligand that regulates metabolism. Nat Commun, 4, 1937.

JING, X., SHULING, G. & YING, L. 2005. Environmental scanning electron microscopy observation of the ultrastructure of Demodex. Microsc Res Tech, 68, 284-9.

JOHANSEN, C., USHER, P. A., KJELLERUP, R. B., LUNDSGAARD, D., IVERSEN, L. & KRAGBALLE, K. 2009. Characterization of the interleukin 17 isoforms and receptors in lesional psoriatic skin. Br J Dermatol, 160, 319 24.

JOURDAIN, A. A., KOPPEN, M., WYDRO, M., RODLEY, C. D., LIGHTOWLERS, R. N., CHRZANOWSKA-LIGHTOWLERS, Z. M. & MARTINOU, J. C. 2013. GRSF1 regulates RNA processing in mitochondrial RNA granules. Cell Metab, 17, 399-410.

JOYCE, D. A., GIBBONS, D. P., GREEN, P., STEER, J. H., FELDMANN, M. & BRENNAN, F. M. 1994. Two inhibitors of pro-inflammatory cytokinerelease, interleukin-10 and interleukin-4, have contrasting effects on release of soluble p75 tumor necrosis factor receptor by cultured monocytes. Eur J Immunol, 24, 2699-705.

JULIO, G., MERINDANO, M. D., CANALS, M. & RALLO, M. 2008. Image processing techniques to quantify microprojections on outer corneal epithelial cells. Journal of Anatomy, 212, 879-886.

JUSTET, C., EVANS, F., TORRIGLIA, A. & CHIFFLET, S. 2015. Increase in the expression of leukocyte elastase inhibitor during wound healing in corneal endothelial cells. Cell Tissue Res.

KAFIENAH, W., BUTTLE, D. J., BURNETT, D. & HOLLANDER, A. P. 1998. Cleavage of native type I collagen by human neutrophil elastase. Biochem J,330 (Pt 2), 897-902.

KAHN, C. R., YOUNG, E., LEE, I. H. & RHIM, J. S. 1993. Human corneal epithelial primary cultures and cell lines with extended life span: in vitro model for ocular studies. Invest Ophthalmol Vis Sci, 34, 3429-41.

KAMOUN, B., FOURATI, M., FEKI, J., MLIK, M., KARRAY, F., TRIGUI, A., ELLOUZE, S., HAMMAMI, B., CHAABOUNI, M. & AYADI, A. 1999. [Blepharitis due to Demodex: myth or reality?]. J Fr Ophtalmol, 22, 525-7.

KANADA, K. N., NAKATSUJI, T. & GALLO, R. L. 2012. Doxycycline indirectly inhibits proteolytic activation of tryptic kallikrein-related peptidases and activation of cathelicidin. J Invest Dermatol, 132, 1435-42.

KARAS, M. & HILLENKAMP, F. 1988. Laser desorption ionization of proteins with molecular masses exceeding 10,000 daltons. Anal Chem, 60, 2299-301.

KARNOVSKY, M. L. & BADWEY, J. A. 1986. Respiratory burst during phagocytosis: an overview. Methods Enzymol, 132, 353-4.

KARTHIKEYAN, R. S., LEAL, S. M., JR., PRAJNA, N. V., DHARMALINGAM, K., GEISER, D. M., PEARLMAN, E. & LALITHA, P. 2011. Expression of innate and adaptive immune mediators in human corneal tissue infected with Aspergillus or fusarium. J Infect Dis, 204, 942-50.

KAWAI, T. & AKIRA, S. 2010. The role of pattern-recognition receptors in innate immunity: update on Toll-like receptors. Nat Immunol, 11, 373-84.

KAWASAKI, A., ITO, S., FURUKAWA, H., HAYASHI, T., GOTO, D., MATSUMOTO, I., KUSAOI, M., OHASHI, J., GRAHAM, R. R., MATSUTA, K., BEHRENS, T. W., TOHMA, S., TAKASAKI, Y., HASHIMOTO, H., SUMIDA, T. & TSUCHIYA, N. 2010. Association of TNFAIP3 interacting protein 1, TNIP1 with systemic lupus erythematosus in a Japanese population: a case-control association study. Arthritis Res Ther, 12, R174.

KELHALA, H. L., PALATSI, R., FYHRQUIST, N., LEHTIMAKI, S., VAYRYNEN, J. P., KALLIOINEN, M., KUBIN, M. E., GRECO, D., TASANEN, K., ALENIUS, H., BERTINO, B., CARLAVAN, I., MEHUL, B., DERET, S., REINICHE, P., MARTEL, P., MARTY, C., BLUME-PEYTAVI, U., VOEGEL, J. J. & LAUERMA, A. 2014. IL-17/Th17 pathway is activated in acne lesions. PLoS One, 9, e105238.

KEMAL, M., SUMER, Z., TOKER, M. I., ERDOGAN, H., TOPALKARA, A. & AKBULUT, M. 2005. The Prevalence of Demodex folliculorum in blepharitis patients and the normal population. Ophthalmic Epidemiol, 12, 287-90.

KENYON, K. R. & TSENG, S. C. 1989. Limbal autograft transplantation for ocular surface disorders. Ophthalmology, 96, 709-22; discussion 722-3.

KERESZTES, M. & LAJTOS, Z. 1997. Major laminin-binding and F-actin-linked glycoproteins of neutrophils. Cell Biol Int, 21, 543-50.

KERN, R., MALKI, A., HOLMGREN, A. & RICHARME, G. 2003. Chaperone properties of Escherichia coli thioredoxin and thioredoxin reductase. Biochem J, 371, 965-72.

KHEIRKHAH, A., BLANCO, G., CASAS, V. & TSENG, S. C. 2007a. Fluorescein dye improves microscopic evaluation and counting of demodex in blepharitis with cylindrical dandruff. Cornea, 26, 697-700.

KHEIRKHAH, A., CASAS, V., LI, W., RAJU, V. K. & TSENG, S. C. 2007b. Corneal manifestations of ocular demodex infestation. Am J Ophthalmol, 143, 743-749.

KIM, M. B., KIM, G. W., PARK, H. J., KIM, H. S., CHIN, H. W., KIM, S. H., KIM, B. S. & KO, H. C. 2011. Pimecrolimus 1% cream for the treatment of rosacea. J Dermatol, 38, 1135-9.

KIM, N. I., COOPER, K. D., FISHER, G. J., BAADSGAARD, O., VOORHEES, J. J. & HAMMERBERG, C. 1992. Psoriatic skin reveals the in vivo presence of an epidermal IL-1 inhibitor. Arch Dermatol Res, 284, 71-6.

KIM, Y. J., CHO, Y. E., KIM, Y. W., KIM, J. Y., LEE, S. & PARK, J. H. 2008. Suppression of putative tumour suppressor gene GLTSCR2 expression in human glioblastomas. J Pathol, 216, 218-24.

KIRK, H. 1949. Demodectic Mange. Can J Comp Med Vet Sci, 13, 255-7.

KLEBANOFF, S. J. 2005. Myeloperoxidase: friend and foe. J Leukoc Biol, 77, 598 625.

KLEBE, S., CALLAHAN, T. & POWER, J. H. 2014. Peroxiredoxin I and II in human eyes: cellular distribution and association with pterygium and DNA damage. J Histochem Cytochem, 62, 85-96.

KLEINSCHEK, M. A., MULLER, U., BRODIE, S. J., STENZEL, W., KOHLER, G., BLUMENSCHEIN, W. M., STRAUBINGER, R. K., MCCLANAHAN, T., KASTELEIN, R. A. & ALBER, G. 2006. IL-23 enhances the inflammatory cell

response in Cryptococcus neoformans infection and induces a cytokine pattern distinct from IL-12. J Immunol, 176, 1098-106.

KLIEM, C., MERLING, A., GIAISI, M., KOHLER, R., KRAMMER, P. H. & LI WEBER, M. 2012. Curcumin suppresses T cell activation by blocking Ca2+ mobilization and nuclear factor of activated T cells (NFAT) activation. J Biol Chem, 287, 10200-9.

KLIGMAN, A. M. 2004. A personal critique on the state of knowledge of Rosacea. Dermatology, 208, 191-7.

KOCA, R., ALTINYAZAR, H. C., ANKARALI, H., MUHTAR, S., TEKIN, N. S. & CINAR, S. 2010. A comparison of metronidazole 1% cream and pimecrolimus 1% cream in the treatment of patients with papulopustular rosacea: a randomized open-label clinical trial. Clin Exp Dermatol, 35, 251-6.

KOCZULLA, R., VON DEGENFELD, G., KUPATT, C., KROTZ, F., ZAHLER, S., GLOE, T., ISSBRUCKER, K., UNTERBERGER, P., ZAIOU, M., LEBHERZ, C., KARL, A., RAAKE, P., PFOSSER, A., BOEKSTEGERS, P., WELSCH, U., HIEMSTRA, P. S., VOGELMEIER, C., GALLO, R. L., CLAUSS, M. & BALS, R. 2003. An angiogenic role for the human peptide antibiotic LL-37/hCAP-18. J Clin Invest, 111, 1665-72.

KONDO, S., YAMAMOTO, N., MURAKAMI, T., OKUMURA, M., MAYEDA, A. & IMAIZUMI, K. 2004. Tra2 beta, SF2/ASF and SRp30c modulate the function of an exonic splicing enhancer in exon 10 of tau pre-mRNA. Genes Cells, 9, 121-30.

KÖNIG, H., FRÖHLICH, J., BERCHTOLD, M. & WENZEL, M. 2002. Diversity and microhabitats of the hindgut flora of termites. Recent Res Devel Microbiology, 6, 125–156.

KONIG, H. 2006. Bacillus species in the intestine of termites and other soil invertebrates. J Appl Microbiol, 101, 620-7.

KOSTER, J., GEERTS, D., FAVRE, B., BORRADORI, L. & SONNENBERG, A. 2003. Analysis of the interactions between BP180, BP230, plectin and the integrin alpha6beta4 important for hemidesmosome assembly. J Cell Sci, 116, 387-99.

KRYCZEK, I., WU, K., ZHAO, E., WEI, S., VATAN, L., SZELIGA, W., HUANG, E., GREENSON, J., CHANG, A., ROLINSKI, J., RADWAN, P., FANG, J., WANG, G. & ZOU, W. 2011. IL-17+ regulatory T cells in the

microenvironments of chronic inflammation and cancer. J Immunol, 186, 4388-95.

KUHNIGK, T., BORST, E. M., BREUNIG, A., KONIG, H., COLLINS, M. D., HUTSON, R. A. & KAMPFER, P. 1995. Bacillus oleronius sp.nov., a member of the hindgut flora of the termite Reticulitermes santonensis (Feytaud). Can J Microbiol, 41, 699-706.

KURPAKUS, M. A., DANESHVAR, C., DAVENPORT, J. & KIM, A. 1999. Human corneal epithelial cell adhesion to laminins. Curr Eye Res, 19, 106-14.

KUSUKAWA, N., YURA, T., UEGUCHI, C., AKIYAMA, Y. & ITO, K. 1989. Effects of mutations in heat-shock genes groES and groEL on protein exportin Escherichia coli. Embo j, 8, 3517-21.

KUWAHARA, I., LILLEHOJ, E. P., LU, W., SINGH, I. S., ISOHAMA, Y., MIYATA, T. & KIM, K. C. 2006. Neutrophil elastase induces IL-8 gene transcription and protein release through p38/NF-{kappa}B activation via EGFR transactivation in a lung epithelial cell line. Am J Physiol Lung Cell Mol Physiol, 291, L407-16.

KYRIAKIS, K. P., PALAMARAS, I., TERZOUDI, S., EMMANUELIDES, S., MICHAILIDES, C. & PAGANA, G. 2005. Epidemiologic aspects of rosacea. J Am Acad Dermatol. United States.

LACEY, N., DELANEY, S., KAVANAGH, K. & POWELL, F. C. 2007. Mite-related bacterial antigens stimulate inflammatory cells in rosacea. Br J Dermatol, 157, 474-81.

LACEY, N., KAVANAGH, K. & TSENG, S. C. 2009. Under the lash: Demodex mites in human diseases. Biochem (Lond), 31, 2-6.

LACEY, N. 2009. An Investigation of the Factors Involved in the Induction and Persistence of papulopustular rosacea. *Phd Thesis*.

LAI, X., WANG, L. & WITZMANN, F. A. 2013. Issues and applications in label-free quantitative mass spectrometry. Int J Proteomics, 2013, 756039.

LAMBETH, J. D. 2000. Regulation of the phagocyte respiratory burst oxidase by protein interactions. Journal of Biochemistry and Molecular Biology, 33, 427 439.

LANDINO, L. M., SKRESLET, T. E. & ALSTON, J. A. 2004. Cysteine oxidation of tau and microtubule-associated protein-2 by peroxynitrite: modulation of microtubule assembly kinetics by the thioredoxin reductase system. J Biol

Chem, 279, 35101-5.

LANDIS, G. N. & TOWER, J. 2005. Superoxide dismutase evolution and life span regulation. Mech Ageing Dev, 126, 365-79.

LAPINET, J. A., SCAPINI, P., CALZETTI, F., PEREZ, O. & CASSATELLA, M. A. 2000. Gene expression and production of tumor necrosis factor alpha, interleukin-1beta (IL-1beta), IL-8, macrophage inflammatory protein 1alpha (MIP-1alpha), MIP-1beta, and gamma interferon-inducible protein 10 by human neutrophils stimulated with group B meningococcal outer membrane vesicles. Infect Immun, 68, 6917-23.

LARSEN, B. & WHITE, S. 1995. Antifungal effect of hydrogen peroxide on catalase producing strains of Candida spp. Infect Dis Obstet Gynecol, 3, 73-8.

LAWRENCE, T. 2009. The nuclear factor NF-kappaB pathway in inflammation. Cold Spring Harb Perspect Biol, 1, a001651.

LAZAROW, P. B. & FUJIKI, Y. 1985. Biogenesis of peroxisomes. Annu Rev Cell Biol, 1, 489-530.

LEE, C. G., HOMER, R. J., ZHU, Z., LANONE, S., WANG, X., KOTELIANSKY, V., SHIPLEY, J. M., GOTWALS, P., NOBLE, P., CHEN, Q., SENIOR, R. M. & ELIAS, J. A. 2001. Interleukin-13 induces tissue fibrosis by selectively stimulating and activating transforming growth factor beta(1). J Exp Med, 194, 809-21.

LEE, E., TREPICCHIO, W. L., OESTREICHER, J. L., PITTMAN, D., WANG, F., CHAMIAN, F., DHODAPKAR, M. & KRUEGER, J. G. 2004. Increased expression of interleukin 23 p19 and p40 in lesional skin of patients with psoriasis vulgaris. J Exp Med, 199, 125-30.

LEE, J. Y. & HSU, C. K. 2007. Granulomatous rosacea-like demodicidosis. Dermatol Online J, 13, 9.

LEE, M. H. & LOZANO, G. 2006. Regulation of the p53-MDM2 pathway by 14-3-3 sigma and other proteins. Semin Cancer Biol, 16, 225-34.

LEE, S. H., CHUN, Y. S., KIM, J. H., KIM, E. S. & KIM, J. C. 2010. The relationship between demodex and ocular discomfort. Invest Ophthalmol Vis Sci, 51, 2906-11.

LEVIS, H. & DANIELS, J. T. 2009. New technologies in limbal epithelial stem cell transplantation. Curr Opin Biotechnol, 20, 593-7.

LEVIS, H. J., BROWN, R. A. & DANIELS, J. T. 2010. Plastic compressed collagen

as a biomimetic substrate for human limbal epithelial cell culture. Biomaterials, 31, 7726-37.

LEW, P. D. 1990. Receptors and intracellular signaling in human neutrophils. Am Rev Respir Dis, 141, S127-31.

LEY, K., LAUDANNA, C., CYBULSKY, M. I. & NOURSHARGH, S. 2007. Getting to the site of inflammation: the leukocyte adhesion cascade updated. Nat Rev Immunol, 7, 678-89.

LEYDEN, J. J., MCGINLEY, K. J., MILLS, O. H. & KLIGMAN, A. M. 1975. Propionibacterium levels in patients with and without acne vulgaris. J Invest Dermatol, 65, 382-4.

LI, F., LIU, X., ZHOU, W., YANG, X. & SHEN, Y. 2015. Auto-inhibitory Mechanism of the Human Mitochondrial RNase P Protein Complex. Sci Rep, 5, 9878.

LI, J., O'REILLY, N., SHEHA, H., KATZ, R., RAJU, V. K., KAVANAGH, K. & TSENG, S. C. 2010. Correlation between ocular Demodex infestation and serum immunoreactivity to Bacillus proteins in patients with Facial rosacea. Ophthalmology, 117, 870-877.e1.

LI, X., KLINTMAN, D., WEITZ-SCHMIDT, G., SCHRAMM, R. & THORLACIUS, H. 2004. Lymphocyte function antigen-1 mediates leukocyte adhesion and subsequent liver damage in endotoxemic mice. Br J Pharmacol, 141, 709-16.

LI, Y., ROTH, S., LASER, M., MA, J. X. & CROSSON, C. E. 2003. Retinal preconditioning and the induction of heat-shock protein 27. Invest Ophthalmol Vis Sci, 44, 1299-304.

LI, Z., BURNS, A. R., MILLER, S. B. & SMITH, C. W. 2011. CCL20, gammadelta T cells, and IL-22 in corneal epithelial healing. Faseb j, 25, 2659-68. LIANG, L., DING, X. & TSENG, S. C. 2014. High prevalence of demodex brevis infestation in chalazia. Am J Ophthalmol, 157, 342-348.e1.

LINDQUIST, S. & CRAIG, E. A. 1988. The heat-shock proteins. Annu Rev Genet, 22, 631-77.

LIU, C., QIAN, W., QIAN, Y., GILTIAY, N. V., LU, Y., SWAIDANI, S., MISRA, S., DENG, L., CHEN, Z. J. & LI, X. 2009. Act1, a novel U-box E3 ubiquitin ligase for IL-17R-mediated signalling. Cytokine, 48, 27-27.

LIU, J., SHEHA, H. & TSENG, S. C. 2010. Pathogenic role of Demodex mites in blepharitis. Current opinion in allergy and clinical immunology, 10, 505.

LOEWEN, P. C. & SWITALA, J. 1987. Multiple Catalases In Bacillus Subtilis. Journal of Bacteriology, 169, 3601-3607.

LOMHOLT, G. 1964. Prevalence Of Skin Diseases In A Population; A Census Study From The Faroe Islands. Dan Med Bull, 11, 1-7.

LOMINADZE, G., POWELL, D. W., LUERMAN, G. C., LINK, A. J., WARD, R. A. & MCLEISH, K. R. 2005. Proteomic analysis of human neutrophil granules. Mol Cell Proteomics, 4, 1503-21.

LU, H., YANG, Y., ALLISTER, E. M., WIJESEKARA, N. & WHEELER, M. B. 2008. The identification of potential factors associated with the development of type 2 diabetes: a quantitative proteomics approach. Mol Cell Proteomics, 7, 1434-51.

LU, Y. & WAHL, L. M. 2005. Production of matrix metalloproteinase-9 by activated human monocytes involves a phosphatidylinositol-3 kinase/Akt/IKKalpha/NF kappaB pathway. J Leukoc Biol, 78, 259-65.

MACEK, B., WAANDERS, L. F., OLSEN, J. V. & MANN, M. 2006. Top-down protein sequencing and MS3 on a hybrid linear quadrupole ion trap-orbitrap mass spectrometer. Mol Cell Proteomics, 5, 949-58.

MACLENNAN, I. C., GULBRANSON-JUDGE, A., TOELLNER, K. M., CASAMAYOR-PALLEJA, M., CHAN, E., SZE, D. M., LUTHER, S. A. & ORBEA, H. A. 1997. The changing preference of T and B cells for partners as T-dependent antibody responses develop. Immunol Rev, 156, 53-66.

MACLEOD, M. K., KAPPLER, J. W. & MARRACK, P. 2010. Memory CD4 T cells: generation, reactivation and re-assignment. Immunology, 130, 10-5.

MACNAB, R. M. 2003. How bacteria assemble flagella. Annu Rev Microbiol, 57,77-100.

MAKAROV, A. 2000. Electrostatic axially harmonic orbital trapping: a high performance technique of mass analysis. Anal Chem, 72, 1156-62.

MAKAROV, A., DENISOV, E., KHOLOMEEV, A., BALSCHUN, W., LANGE, O., STRUPAT, K. & HORNING, S. 2006. Performance evaluation of a hybrid linear ion trap/orbitrap mass spectrometer. Anal Chem, 78, 2113-20.

MALEK, T. R. 2003. The main function of IL-2 is to promote the development of T regulatory cells. J Leukoc Biol, 74, 961-5.

MALTSEVA, I. A., FLEISZIG, S. M., EVANS, D. J., KERR, S., SIDHU, S. S., MCNAMARA, N. A. & BASBAUM, C. 2007. Exposure of human corneal epithelial cells to contact lenses in vitro suppresses the upregulation of human beta-defensin-2 in response to antigens of Pseudomonas aeruginosa. Exp Eye Res, 85, 142-53.

MANARA, F. S., CHIN, J. & SCHNEIDER, D. L. 1991. Role of degranulation in activation of the respiratory burst in human neutrophils. J Leukoc Biol, 49, 489-98.

MANSSON, P., ZHANG, X. W., JEPPSSON, B., JOHNELL, O. & THORLACIUS, H. 2000. Critical role of P-selectin-dependent rolling in tumor necrosis factor alpha-induced leukocyte adhesion and extravascular recruitment in vivo. Naunyn Schmiedebergs Arch Pharmacol, 362, 190-6.

MARKSON, G., KIEL, C., HYDE, R., BROWN, S., CHARALABOUS, P., BREMM, A., SEMPLE, J., WOODSMITH, J., DULEY, S., SALEHI ASHTIANI, K., VIDAL, M., KOMANDER, D., SERRANO, L., LEHNER, P. & SANDERSON, C. M. 2009. Analysis of the human E2 ubiquitin conjugating enzyme protein interaction network. Genome Res, 19, 1905-11.

MARTIN, J. C., BAETEN, D. L. & JOSIEN, R. 2014. Emerging role of IL-17 and Th17 cells in systemic lupus erythematosus. Clin Immunol, 154, 1-12.

MASTROFRANCESCO, A., OTTAVIANI, M., ASPITE, N., CARDINALI, G., IZZO, E., GRAUPE, K., ZOUBOULIS, C. C., CAMERA, E. & PICARDO, M. 2010. Azelaic acid modulates the inflammatory response in normal human keratinocytes through PPARgamma activation. Exp Dermatol, 19, 813-20.

MATSUMURA, Y. 2012. Role of Allergen Source-Derived Proteases in Sensitization via Airway Epithelial Cells. J Allergy (Cairo), 2012, 903659.

MC ALEER, M. A., LACEY, N. & POWELL, F. C. 2009. The pathophysiology of rosacea. Giornale Italiano Di Dermatologia E Venereologia, 144, 663-671.

MCALEER, M. A., FITZPATRICK, P. & POWELL, F. C. 2010. Papulopustular rosacea: prevalence and relationship to photodamage. J Am Acad Dermatol, 63, 33-9.

MCCARTHY, J. B., BASARA, M. L., PALM, S. L., SAS, D. F. & FURCHT, L. T. 1985. The role of cell adhesion proteins--laminin and fibronectin--in the movement of malignant and metastatic cells. Cancer Metastasis Rev, 4, 125-52.

MCCRACKEN, S., LAMBERMON, M. & BLENCOWE, B. J. 2002. SRm160 splicing coactivator promotes transcript 3'-end cleavage. Mol Cell Biol, 22, 148-60.

MCCULLEY, J. P. & SHINE, W. E. 2003. Meibomian gland function and the tear lipid layer. Ocul Surf, 1, 97-106.

MCINNES, I. B., ILLEI, G. G., DANNING, C. L., YARBORO, C. H., CRANE, M., KUROIWA, T., SCHLIMGEN, R., LEE, E., FOSTER, B., FLEMMING, D., PRUSSIN, C., FLEISHER, T. A. & BOUMPAS, D. T. 2001. IL-10 improves skin disease and modulates endothelial activation and leukocyte effector function in patients with psoriatic arthritis. J Immunol, 167, 4075-82.

MCKEE, H. D., IRION, L. C., CARLEY, F. M., BRAHMA, A. K., JAFARINASAB, M. R., RAHMATI-KAMEL, M., KANAVI, M. R. & FEIZI, S. 2014. Re: Dua et al.: Human corneal anatomy redefined: a novel pre-Descemet layer (Dua's layer) (Ophthalmology 2013;120:1778-85). Ophthalmology, 121, e24-5.

MEANS, A. R. 1994. Calcium, calmodulin and cell cycle regulation. FEBS Lett, 347, 1-4.

MELLER, D., PAUKLIN, M., THOMASEN, H., WESTEKEMPER, H. & STEUHL, K. P. 2011. Amniotic membrane transplantation in the human eye. Dtsch Arztebl Int, 108, 243-8.

MEYER-HOFFERT, U. & SCHRODER, J. M. 2011. Epidermal proteases in the pathogenesis of rosacea. J Investig Dermatol Symp Proc, 15, 16-23.

MICHALSKI, A., DAMOC, E., HAUSCHILD, J. P., LANGE, O., WIEGHAUS, A., MAKAROV, A., NAGARAJ, N., COX, J., MANN, M. & HORNING, S. 2011. Mass spectrometry-based proteomics using Q Exactive, a high performance benchtop quadrupole Orbitrap mass spectrometer. Mol Cell Proteomics, 10, M111.011015.

MISSOTTEN, G. S., JOURNEE-DE KORVER, J. G., DE WOLFF-ROUENDAAL, D., KEUNEN, J. E., SCHLINGEMANN, R. O. & JAGER, M. J. 2003. Heat shock protein expression in the eye and in uveal melanoma. Invest Ophthalmol Vis Sci, 44, 3059-65.

MIYACHI, Y. 2001. Potential antioxidant mechanism of action for metronidazole: implications for rosacea management. Adv Ther, 18, 237-43.

MIYACHI, Y., YOSHIOKA, A., IMAMURA, S. & NIWA, Y. 1986. Effect of antibiotics on the generation of reactive oxygen species. J Invest Dermatol, 86, 449-53.

MIZEL, S. B., WEST, A. P. & HANTGAN, R. R. 2003. Identification of a sequence in human toll-like receptor 5 required for the binding of Gram-negative flagellin. J Biol Chem, 278, 23624-9.

MOHAN, K., DING, Z., HANLY, J. & ISSEKUTZ, T. B. 2002. IFN-gamma inducible T cell alpha chemoattractant is a potent stimulator of normal human blood T lymphocyte transendothelial migration: differential regulation by IFN-gamma and TNF-alpha. J Immunol, 168, 6420-8.

MOHAN, R. R., POSSIN, D. E., SINHA, S. & WILSON, S. E. 2003. Development of genetically engineered tet HPV16-E6/E7 transduced human corneal epithelial clones having tight regulation of proliferation and normal differentiation. Exp Eye Res, 77, 395-407.

MOORE, J. E., MCMULLEN, C. B., MAHON, G. & ADAMIS, A. P. 2002. The corneal epithelial stem cell. DNA Cell Biol, 21, 443-51.

MOORE, K. W., O'GARRA, A., DE WAAL MALEFYT, R., VIEIRA, P. & MOSMANN, T. R. 1993. Interleukin-10. Annu Rev Immunol, 11, 165-90. MORIOKA, Y., YAMASAKI, K., LEUNG, D. & GALLO, R. L. 2008. Cathelicidin antimicrobial peptides inhibit hyaluronan-induced cytokine release and modulate chronic allergic dermatitis. Journal of Immunology, 181, 3915-3922.

MURAGUCHI, A., HIRANO, T., TANG, B., MATSUDA, T., HORII, Y., NAKAJIMA, K. & KISHIMOTO, T. 1988. The essential role of B cell stimulatory factor 2 (BSF-2/IL-6) for the terminal differentiation of B cells. J Exp Med, 167, 332-44.

MURAKAMI, M. S. & MORRISON, D. K. 2001. Raf-1 without MEK? Sci STKE, 2001, pe30.

MURILLO, N., AUBERT, J. & RAOULT, D. 2014. Microbiota of Demodex mites from rosacea patients and controls. Microb Pathog, 71-72, 37-40.

MURPHY, C. A., LANGRISH, C. L., CHEN, Y., BLUMENSCHEIN, W., MCCLANAHAN, T., KASTELEIN, R. A., SEDGWICK, J. D. & CUA, D. J.

2003. Divergent pro- and antiinflammatory roles for IL-23 and IL-12 in joint autoimmune inflammation. J Exp Med, 198, 1951-7.

NAIR, R. P., DUFFIN, K. C., HELMS, C., DING, J., STUART, P. E., GOLDGAR, D., GUDJONSSON, J. E., LI, Y., TEJASVI, T., FENG, B. J., RUETHER, A., SCHREIBER, S., WEICHENTHAL, M., GLADMAN, D., RAHMAN, P., SCHRODI, S. J., PRAHALAD, S., GUTHERY, S. L., FISCHER, J., LIAO, W., KWOK, P. Y., MENTER, A., LATHROP, G. M., WISE, C. A., BEGOVICH, A. B., VOORHEES, J. J., ELDER, J. T., KRUEGER, G. G., BOWCOCK, A. M. & ABECASIS, G. R. 2009. Genome-wide scan reveals association of psoriasis with IL-23 and NF-kappaB pathways. Nat Genet, 41, 199-204.

NAKAMURA, T., NAKAMURA, H., HOSHINO, T., UEDA, S., WADA, H. & YODOI, J. 2005. Redox regulation of lung inflammation by thioredoxin. Antioxid Redox Signal, 7, 60-71.

NARAYANAN, S., HUNERBEIN, A., GETIE, M., JACKEL, A. & NEUBERT, R. H. 2007. Scavenging properties of metronidazole on free oxygen radicals in a skin lipid model system. J Pharm Pharmacol, 59, 1125-30.

NEMETH, N. M., RUDER, M. G., GERHOLD, R. W., BROWN, J. D., MUNK, B. A., OESTERLE, P. T., KUBISKI, S. V. & KEEL, M. K. 2014. Demodectic mange, dermatophilosis, and other parasitic and bacterial dermatologic diseases in free-ranging white-tailed deer (Odocoileus virginianus) in the United States from 1975 to 2012. Vet Pathol, 51, 633-40.

NEUMANN, C. A., CAO, J. & MANEVICH, Y. 2009. Peroxiredoxin 1 and its role in cell signaling. Cell Cycle, 8, 4072-8.

NI RAGHALLAIGH, S. & POWELL, F. C. 2009. The cutaneous microenvironment in papulopustular rosacea. Br J Dermatol, 161 (Suppl. 1), 25.

NI RAGHALLAIGH, S., BENDER, K., LACEY, N., BRENNAN, L. & POWELL, F. C. 2012. The fatty acid profile of the skin surface lipid layer in papulopustular rosacea. Br J Dermatol, 166, 279-87.

NICKOLOFF, B. J. 1991. The cytokine network in psoriasis. Arch Dermatol, 127, 871-84.

NORRIS, J. D., FAN, D., SHERK, A. & MCDONNELL, D. P. 2002. A negative coregulator for the human ER. Mol Endocrinol, 16, 459-68.

NOTARA, M. & DANIELS, J. T. 2010. Characterisation and functional features of a spontaneously immortalised human corneal epithelial cell line with progenitor- like characteristics. Brain Res Bull, 81, 279-86.

NUTTING, W. B. & GREEN, A. C. 1976. PATHOGENESIS ASSOCIATED WITH HAIR FOLLICLE MITES (DEMODEX SPP) IN AUSTRALIAN ABORIGINES. British Journal of Dermatology, 94, 307-312.

O'REILLY, N., BERGIN, D., REEVES, E. P., MCELVANEY, N. G. & KAVANAGH, K. 2012a. Demodex-associated bacterial proteins induce neutrophil activation. British Journal of Dermatology, 166, 753-760.

O'REILLY, N., GALLAGHER, C., KATIKIREDDY, K. R., CLYNES, M., O'SULLIVAN, F. & KAVANAGH, K. 2012b. Demodex-Associated Bacillus Proteins Induce an Aberrant Wound Healing Response in a Corneal Epithelial Cell Line: Possible Implications for Corneal Ulcer Formation in Ocular Rosacea. Investigative Ophthalmology & Visual Science, 53, 3250-3259.

O'REILLY, N., MENEZES, N. & KAVANAGH, K. 2012c. Positive correlation between serum immunoreactivity to Demodex-associated Bacillus proteins and erythematotelangiectatic rosacea. British Journal of Dermatology, 167, 1032-1036.

OEHLKE, O., MARTIN, H. W., OSTERBERG, N. & ROUSSA, E. 2011. Rab11b and its effector Rip11 regulate the acidosis-induced traffic of V-ATPase in salivary ducts. J Cell Physiol, 226, 638-51.

OFFORD, E. A., SHARIF, N. A., MACE, K., TROMVOUKIS, Y., SPILLARE, E. A., AVANTI, O., HOWE, W. E. & PFEIFER, A. M. 1999. Immortalized human corneal epithelial cells for ocular toxicity and inflammation studies. Invest Ophthalmol Vis Sci, 40, 1091-101.

OGUNLEYE, T. & JAMES, W. D. 2008. Ethanol-induced flushing with topical pimecrolimus use. Dermatitis, 19, E1-2.

OH, P., BORGSTROM, P., WITKIEWICZ, H., LI, Y., BORGSTROM, B. J., CHRASTINA, A., IWATA, K., ZINN, K. R., BALDWIN, R., TESTA, J. E. & SCHNITZER, J. E. 2007. Live dynamic imaging of caveolae pumping targeted antibody rapidly and specifically across endothelium in the lung. Nat Biotechnol, 25, 327-37.

OH, P., LI, Y., YU, J., DURR, E., KRASINSKA, K. M., CARVER, L. A., TESTA, J. E. & SCHNITZER, J. E. 2004. Subtractive proteomic mapping of the endothelial surface in lung and solid tumours for tissue-specific therapy. Nature, 429, 629-35.

OHTSUKA, N., URASE, K., MOMOI, T. & NOGAWA, H. 2001. Induction of bud formation of embryonic mouse tracheal epithelium by fibroblast growth factor plus transferrin in mesenchyme-free culture. Dev Dyn, 222, 263-72.

OKA, M., NOROSE, K., MATSUSHIMA, K., NISHIGORI, C. & HERLYN, M. 2006. Overexpression of IL-8 in the cornea induces ulcer formation in the SCID mouse. Br J Ophthalmol, 90, 612-5.

OKUMOTO, K., SHIMOZAWA, N., KAWAI, A., TAMURA, S., TSUKAMOTO, T., OSUMI, T., MOSER, H., WANDERS, R. J., SUZUKI, Y., KONDO, N. & FUJIKI, Y. 1998. PEX12, the pathogenic gene of group III Zellweger syndrome: cDNA cloning by functional complementation on a CHO cell mutant, patient analysis, and characterization of PEX12p. Mol Cell Biol, 18, 4324-36.

OLSON, M. O., DUNDR, M. & SZEBENI, A. 2000. The nucleolus: an old factory with unexpected capabilities. Trends Cell Biol, 10, 189-96.

OLTZ, M. & CHECK, J. 2011. Rosacea and its ocular manifestations. Optometry, 82, 92-103.

OMAR, R. & PAPPOLLA, M. 1993. Oxygen free radicals as inducers of heat shock protein synthesis in cultured human neuroblastoma cells: relevance to neurodegenerative disease. Eur Arch Psychiatry Clin Neurosci, 242, 262-7.

ONG, P. Y., OHTAKE, T., BRANDT, C., STRICKLAND, I., BOGUNIEWICZ, M., GANZ, T., GALLO, R. L. & LEUNG, D. Y. 2002. Endogenous antimicrobial peptides and skin infections in atopic dermatitis. N Engl J Med, 347, 1151-60.

OPPMANN, B., LESLEY, R., BLOM, B., TIMANS, J. C., XU, Y., HUNTE, B., VEGA, F., YU, N., WANG, J., SINGH, K., ZONIN, F., VAISBERG, E. CHURAKOVA, T., LIU, M., GORMAN, D., WAGNER, J., ZURAWSKI, S., LIU, Y., ABRAMS, J. S., MOORE, K. W., RENNICK, D., DE WAAL MALEFYT, R., HANNUM, C., BAZAN, J. F. & KASTELEIN, R. A. 2000. Novel p19 protein engages IL-12p40 to form a cytokine, IL-23, with biological activities similar as well as distinct from IL-12. Immunity, 13, 715-25.

OSHIMA, S., TURER, E. E., CALLAHAN, J. A., CHAI, S., ADVINCULA, R., BARRERA, J., SHIFRIN, N., LEE, B., BENEDICT YEN, T. S., WOO, T., MALYNN, B. A. & MA, A. 2009. ABIN-1 is a ubiquitin sensor that restricts cell death and sustains embryonic development. Nature, 457, 906-9.

OSTERMANN, J., HORWICH, A. L., NEUPERT, W. & HARTL, F. U. 1989. Protein folding in mitochondria requires complex formation with hsp60 and ATP hydrolysis. Nature, 341, 125-30.

PADRON-BARTHE, L., COURTA, J., LEPRETRE, C., NAGBOU, A. & TORRIGLIA, A. 2008. Leukocyte Elastase Inhibitor, the precursor of L DNase II, inhibits apoptosis by interfering with caspase-8 activation. Biochim Biophys Acta, 1783, 1755-66.

PADRON-BARTHE, L., LEPRETRE, C., MARTIN, E., COUNIS, M. F. & TORRIGLIA, A. 2007. Conformational modification of serpins transforms leukocyte elastase inhibitor into an endonuclease involved in apoptosis. Mol Cell Biol, 27, 4028-36.

PAEZ, P. M., MARTA, C. B., MORENO, M. B., SOTO, E. F. & PASQUINI, J. M. 2002. Apotransferrin decreases migration and enhances differentiation of oligodendroglial progenitor cells in an in vitro system. Dev Neurosci, 24, 47-58.

PAGE, M. J. & DI CERA, E. 2008. Serine peptidases: classification, structure and function. Cell Mol Life Sci, 65, 1220-36.

PAK, J. H., KIM, T. I., JOON KIM, M., YONG KIM, J., CHOI, H. J., KIM, S. A. & TCHAH, H. 2006. Reduced expression of 1-cys peroxiredoxin in oxidative stress-induced cataracts. Exp Eye Res, 82, 899-906.

PALAU, N., JULIA, A., FERRANDIZ, C., PUIG, L., FONSECA, E., FERNANDEZ, E., LOPEZ-LASANTA, M., TORTOSA, R. & MARSAL, S. 2013. Genome wide transcriptional analysis of T cell activation reveals differential gene expression associated with psoriasis. BMC Genomics, 14, 825.

PARADA, C. A. & ROEDER, R. G. 1999. A novel RNA polymerase II-containing complex potentiates Tat-enhanced HIV-1 transcription. Embo j, 18, 3688-701.

PARK, H., LI, Z., YANG, X. O., CHANG, S. H., NURIEVA, R., WANG, Y. H., WANG, Y., HOOD, L., ZHU, Z., TIAN, Q. & DONG, C. 2005. A distinct lineage of CD4 T cells regulates tissue inflammation by producing interleukin 17. Nat Immunol, 6, 1133-41.

PARKKINEN, J., VON BONSDORFF, L., EBELING, F. & SAHLSTEDT, L. 2002. Function and therapeutic development of apotransferrin. Vox Sang, 83 Suppl 1, 321-6.

PARTIDA-SANCHEZ, S., COCKAYNE, D. A., MONARD, S., JACOBSON, E. L., OPPENHEIMER, N., GARVY, B., KUSSER, K., GOODRICH, S., HOWARD, M., HARMSEN, A., RANDALL, T. D. & LUND, F. E. 2001. Cyclic ADP-ribose production by CD38 regulates intracellular calcium release, extracellular calcium influx and chemotaxis in neutrophils and is required for bacterial clearance in vivo. Nat Med, 7, 1209-16.

PARTIDA-SANCHEZ, S., IRIBARREN, P., MORENO-GARCIA, M. E., GAO, J. L., MURPHY, P. M., OPPENHEIMER, N., WANG, J. M. & LUND, F. E. 2004. Chemotaxis and calcium responses of phagocytes to formyl peptide receptor ligands is differentially regulated by cyclic ADP ribose. J Immunol, 172, 1896-906.

PATEL, S., MCLAREN, J., HODGE, D. & BOURNE, W. 2001. Normal human keratocyte density and corneal thickness measurement by using confocal microscopy in vivo. Invest Ophthalmol Vis Sci, 42, 333-9.

PATEL, V. J., THALASSINOS, K., SLADE, S. E., CONNOLLY, J. B., CROMBIE, A., MURRELL, J. C. & SCRIVENS, J. H. 2009. A comparison of labeling and label-free mass spectrometry-based proteomics approaches. J Proteome Res, 8, 3752-9.

PAULL, A. C. & WHIKEHART, D. R. 2005. Expression of the p53 family of proteins in central and peripheral human corneal endothelial cells. Mol Vis, 11, 328-34.

PEDERSON, T. 1998. The plurifunctional nucleolus. Nucleic Acids Res, 26, 3871-6. PELLE, M. T., CRAWFORD, G. H. & JAMES, W. D. 2004. Rosacea: II. Therapy. J Am Acad Dermatol, 51, 499-512; quiz 513-4.

PERNIS, A., GUPTA, S., GOLLOB, K. J., GARFEIN, E., COFFMAN, R. L., SCHINDLER, C. & ROTHMAN, P. 1995. Lack of interferon gamma receptor beta chain and the prevention of interferon gamma signaling in TH1 cells. Science, 269, 245-7.

PFLUGFELDER, S. C., FARLEY, W., LUO, L., CHEN, L. Z., DE PAIVA, C. S., OLMOS, L. C., LI, D. Q. & FINI, M. E. 2005. Matrix metalloproteinase-9

knockout confers resistance to corneal epithelial barrier disruption in experimental dry eye. Am J Pathol, 166, 61-71.

PIGORS, M., SCHWIEGER-BRIEL, A., COSGAREA, R., DIACONEASA, A., BRUCKNER-TUDERMAN, L., FLECK, T. & HAS, C. 2015. Desmoplakin mutations with palmoplantar keratoderma, woolly hair and cardiomyopathy. Acta Derm Venereol, 95, 337-40.

PITTA, M. G., ROMANO, A., CABANTOUS, S., HENRI, S., HAMMAD, A., KOURIBA, B., ARGIRO, L., EL KHEIR, M., BUCHETON, B., MARY, C., EL-SAFI, S. H. & DESSEIN, A. 2009. IL-17 and IL-22 are associated with protection against human kala azar caused by Leishmania donovani. J Clin Invest, 119, 2379-87.

POLLARD, T. D. & COOPER, J. A. 2009. Actin, a central player in cell shape and movement. Science, 326, 1208-12.

POPA, C., NETEA, M. G., VAN RIEL, P. L., VAN DER MEER, J. W. & STALENHOEF, A. F. 2007. The role of TNF-alpha in chronic inflammatory conditions, intermediary metabolism, and cardiovascular risk. J Lipid Res, 48, 751-62.

POTTS, J. R. & CAMPBELL, I. D. 1996. Structure and function of fibronectin modules. Matrix Biol, 15, 313-20; discussion 321.

POWELL, F. C. 2004. Rosacea and the pilosebaceous follicle. Cutis, 74, 9-12, 32-4.

POWELL, F. C. 2005. Clinical practice. Rosacea. N Engl J Med, 352, 793-803.

PRADA, J., NOELLE, B., BAATZ, H., HARTMANN, C. & PLEYER, U. 2003. Tumour necrosis factor alpha and interleukin 6 gene expression in keratocytes from patients with rheumatoid corneal ulcerations. Br J Ophthalmol, 87, 548-50.

PREKERIS, R., KLUMPERMAN, J. & SCHELLER, R. H. 2000. A Rab11/Rip11 protein complex regulates apical membrane trafficking via recycling endosomes. Mol Cell, 6, 1437-48.

PRENS, E. P., BENNE, K., VAN DAMME, J., BAKKUS, M., BRAKEL, K., BENNER, R. & VAN JOOST, T. 1990. Interleukin-1 and interleukin-6 in psoriasis. J Invest Dermatol, 95, 121s-124s.

PUTNEY, J. W., JR. 2007. Recent breakthroughs in the molecular mechanism of capacitative calcium entry (with thoughts on how we got here). Cell Calcium, 42, 103-10.

PYE, R. J., MEYRICK, G. & BURTON, J. L. 1976. Skin surface lipid composition in rosacea. Br J Dermatol, 94, 161-4.

RADAEVA, S., SUN, R., PAN, H. N., HONG, F. & GAO, B. 2004. Interleukin 22 (IL-22) plays a protective role in T cell-mediated murine hepatitis: IL-22 is a survival factor for hepatocytes via STAT3 activation. Hepatology, 39, 1332-42.

RAMOS, H. C., RUMBO, M. & SIRARD, J. C. 2004. Bacterial flagellins: mediators of pathogenicity and host immune responses in mucosa. Trends Microbiol, 12, 509-17.

RAPPOLD, I., IWABUCHI, K., DATE, T. & CHEN, J. 2001. Tumor suppressor p53 binding protein 1 (53BP1) is involved in DNA damage-signaling pathways. J Cell Biol, 153, 613-20.

RASHMI, R. N., ECKES, B., GLOCKNER, G., GROTH, M., NEUMANN, S., GLOY, J., SELLIN, L., WALZ, G., SCHNEIDER, M., KARAKESISOGLOU, I., EICHINGER, L. & NOEGEL, A. A. 2012. The nuclear envelope protein Nesprin-2 has roles in cell proliferation and differentiation during wound healing. Nucleus, 3, 172-86.

RATH, O., PARK, S., TANG, H. H., BANFIELD, M. J., BRADY, R. L., LEE, Y. C., DIGNAM, J. D., SEDIVY, J. M., KOLCH, W. & YEUNG, K. C. 2008. The RKIP (Raf-1 Kinase Inhibitor Protein) conserved pocket binds to the phosphorylated N-region of Raf-1 and inhibits the Raf-1-mediated activated phosphorylation of MEK. Cell Signal, 20, 935-41.

RATHINAM, V. A., VANAJA, S. K. & FITZGERALD, K. A. 2012. Regulation of inflammasome signaling. Nat Immunol, 13, 333-42.

REBORA, A., DRAGO, F. & PICCIOTTO, A. 1994. Helicobacter pylori in patients with rosacea. Am J Gastroenterol, 89, 1603-4.

REEVES, E. P., BANVILLE, N., RYAN, D. M., O'REILLY, N., BERGIN, D. A., POHL, K., MOLLOY, K., MCELVANEY, O. J., ALSALEH, K., ALJORFI, A., KANDALAFT, O., O'FLYNN, E., GERAGHTY, P., O'NEILL, S. J. & MCELVANEY, N. G. 2013. Intracellular Secretory Leukoprotease Inhibitor Modulates Inositol 1,4,5-Triphosphate Generation and Exerts an Anti Inflammatory Effect on Neutrophils of Individuals with Cystic Fibrosis and Chronic Obstructive Pulmonary Disease. Biomed Research International.

REEVES, E. P., LU, H., JACOBS, H. L., MESSINA, C. G., BOLSOVER, S., GABELLA, G., POTMA, E. O., WARLEY, A., ROES, J. & SEGAL, A. W.

2002. Killing activity of neutrophils is mediated through activation of proteases by K+ flux. Nature, 416, 291-7.

REINHARD, L., SRIDHARA, S. & HALLBERG, B. M. 2015. Structure of the nuclease subunit of human mitochondrial RNase P. Nucleic Acids Res, 43, 5664-72.

REINSTEIN, D. Z., ARCHER, T. J., GOBBE, M., SILVERMAN, R. H. & COLEMAN, D. J. 2009. Stromal thickness in the normal cornea: three dimensional display with artemis very high-frequency digital ultrasound. J Refract Surg, 25, 776-86.

RHEE, S. G., KANG, S. W., CHANG, T. S., JEONG, W. & KIM, K. 2001. Peroxiredoxin, a novel family of peroxidases. IUBMB Life, 52, 35-41.

RIAU, A. K., WONG, T. T., BEUERMAN, R. W. & TONG, L. 2009. Calcium binding S100 protein expression in pterygium. Mol Vis, 15, 335-42.

RIAZ, A. A., WAN, M. X., SCHAEFER, T., SCHRAMM, R., EKBERG, H., MENGER, M. D., JEPPSSON, B. & THORLACIUS, H. 2002. Fundamental and distinct roles of P-selectin and LFA-1 in ischemia/reperfusion-induced leukocyte-endothelium interactions in the mouse colon. Ann Surg, 236, 777 84; discussion 784.

RIDDELL, J. R., WANG, X. Y., MINDERMAN, H. & GOLLNICK, S. O. 2010. Peroxiredoxin 1 stimulates secretion of proinflammatory cytokines by binding to TLR4. J Immunol, 184, 1022-30.

RIOS-YUIL, J. M. & MERCADILLO-PEREZ, P. 2013. Evaluation of Demodex folliculorum as a Risk Factor for the Diagnosis of Rosacea In Skin Biopsies. Mexico's General Hospital (1975-2010). Indian J Dermatol, 58, 157.

ROBERTS, S. A., STRANDE, N., BURKHALTER, M. D., STROM, C., HAVENER, J. M., HASTY, P. & RAMSDEN, D. A. 2010. Ku is a 5'-dRP/AP lyase that excises nucleotide damage near broken ends. Nature, 464, 1214-7.

ROBERTSON, D. M., LI, L., FISHER, S., PEARCE, V. P., SHAY, J. W., WRIGHT, W. E., CAVANAGH, H. D. & JESTER, J. V. 2005. Characterization of growth and differentiation in a telomerase-immortalized human corneal epithelial cell line. Invest Ophthalmol Vis Sci, 46, 470-8.

ROSS, P. L., HUANG, Y. N., MARCHESE, J. N., WILLIAMSON, B., PARKER, K., HATTAN, S., KHAINOVSKI, N., PILLAI, S., DEY, S., DANIELS, S., PURKAYASTHA, S., JUHASZ, P., MARTIN, S., BARTLET-JONES, M.,

HE, F., JACOBSON, A. & PAPPIN, D. J. 2004. Multiplexed protein quantitation in Saccharomyces cerevisiae using amine-reactive isobaric tagging reagents. Mol Cell Proteomics, 3, 1154-69.

ROSS, S. J., FINDLAY, V. J., MALAKASI, P. & MORGAN, B. A. 2000. Thioredoxin peroxidase is required for the transcriptional response to oxidative stress in budding yeast. Mol Biol Cell, 11, 2631-42.

ROSSI, F. 1986. The O2- -forming NADPH oxidase of the phagocytes: nature, mechanisms of activation and function. Biochim Biophys Acta, 853, 65-89.

ROTHMAN, J. E. 1989. Polypeptide chain binding proteins: catalysts of protein folding and related processes in cells. Cell, 59, 591-601.

ROXRUD, I., RAIBORG, C., PEDERSEN, N. M., STANG, E. & STENMARK, H. 2008. An endosomally localized isoform of Eps15 interacts with Hrs to mediate degradation of epidermal growth factor receptor. J Cell Biol, 180, 1205-18.

RUFLI, T. & BUCHNER, S. A. 1984. T-cell subsets in acne rosacea lesions and the possible role of Demodex folliculorum. Dermatologica, 169, 1-5.

RUFLI, T. & MUMCUOGLU, Y. 1981. The hair follicle mites Demodex folliculorum and Demodex brevis: biology and medical importance. A review. Dermatologica, 162, 1-11.

SAKAMOTO, K. M., KIM, K. B., VERMA, R., RANSICK, A., STEIN, B., CREWS, C. M. & DESHAIES, R. J. 2003. Development of Protacs to target cancer promoting proteins for ubiquitination and degradation. Mol Cell Proteomics,2, 1350-8.

SAKIMOTO, T., YAMADA, A., KANNO, H. & SAWA, M. 2008. Upregulation of tumor necrosis factor receptor 1 and TNF-alpha converting enzyme during corneal wound healing. Jpn J Ophthalmol, 52, 393-8.

SARIKAS, A., XU, X., FIELD, L. J. & PAN, Z. Q. 2008. The cullin7 E3 ubiquitin ligase: a novel player in growth control. Cell Cycle, 7, 3154-61.

SASTRE, N., RAVERA, I., VILLANUEVA, S., ALTET, L., BARDAGI, M., SANCHEZ, A., FRANCINO, O. & FERRER, L. 2012. Phylogenetic relationships in three species of canine Demodex mite based on partial sequences of mitochondrial 16S rDNA. Vet Dermatol, 23, 509-e101.

SATOH, T., NAKAMURA, S. & KAZIRO, Y. 1987. Induction of neurite formation in PC12 cells by microinjection of proto-oncogenic Ha-ras protein

preincubated with guanosine-5'-O-(3-thiotriphosphate). Mol Cell Biol, 7, 4553-6.

SCHAEFER, I., RUSTENBACH, S. J., ZIMMER, L. & AUGUSTIN, M. 2008. Prevalence of skin diseases in a cohort of 48,665 employees in Germany. Dermatology, 217, 169-72.

SCHEINFELD, N. & BERK, T. 2010. A review of the diagnosis and treatment of rosacea. Postgrad Med, 122, 139-43.

SCHELLER, J., CHALARIS, A., SCHMIDT-ARRAS, D. & ROSE-JOHN, S. 2011. The pro- and anti-inflammatory properties of the cytokine interleukin-6. Biochim Biophys Acta, 1813, 878-88.

SCHERMER, A., GALVIN, S. & SUN, T. T. 1986. Differentiation-related expression of a major 64K corneal keratin in vivo and in culture suggests limbal location of corneal epithelial stem cells. J Cell Biol, 103, 49-62.

SCHILDERS, G., VAN DIJK, E. & PRUIJN, G. J. 2007. C1D and hMtr4p associate with the human exosome subunit PM/Scl-100 and are involved in pre-rRNA processing. Nucleic Acids Res, 35, 2564-72.

SCHOENBORN, J. R. & WILSON, C. B. 2007. Regulation of interferon-gamma during innate and adaptive immune responses. Adv Immunol, 96, 41-101.

SCHOFIELD, L., FERREIRA, A., ALTSZULER, R., NUSSENZWEIG, V. & NUSSENZWEIG, R. S. 1987. Interferon-gamma inhibits the intrahepatocytic development of malaria parasites in vitro. J Immunol, 139, 2020-5.

SCHON, M., BEHMENBURG, C., DENZER, D. & SCHON, M. P. 2001. Pathogenic function of IL-1 beta in psoriasiform skin lesions of flaky skin (fsn/fsn) mice. Clin Exp Immunol, 123, 505-10.

SCHWABE, R. F. & BRENNER, D. A. 2006. Mechanisms of Liver Injury. I. TNF alpha-induced liver injury: role of IKK, JNK, and ROS pathways. Am J Physiol Gastrointest Liver Physiol, 290, G583-9.

SEGAL, A. W. 2005. How neutrophils kill microbes. Annu Rev Immunol, 23, 197-223.

SHARMA, V. K., LYNN, A., KAMINSKI, M., VASUDEVA, R. & HOWDEN, C. W. 1998. A study of the prevalence of Helicobacter pylori infection and other markers of upper gastrointestinal tract disease in patients with rosacea. Am J Gastroenterol, 93, 220-2.

SHEPPARD, F. R., KELHER, M. R., MOORE, E. E., MCLAUGHLIN, N. J., BANERJEE, A. & SILLIMAN, C. C. 2005. Structural organization of the neutrophil NADPH oxidase: phosphorylation and translocation during priming and activation. J Leukoc Biol, 78, 1025-42.

SHEVCHENKO, A., TOMAS, H., HAVLIS, J., OLSEN, J. V. & MANN, M. 2006. In-gel digestion for mass spectrometric characterization of proteins and proteomes. Nat Protoc, 1, 2856-60.

SHI, Y., LIU, C. H., ROBERTS, A. I., DAS, J., XU, G., REN, G., ZHANG, Y., ZHANG, L., YUAN, Z. R., TAN, H. S., DAS, G. & DEVADAS, S. 2006. Granulocyte-macrophage colony-stimulating factor (GM-CSF) and T-cell responses: what we do and don't know. Cell Res, 16, 126-33.

SHIIO, Y., DONOHOE, S., YI, E. C., GOODLETT, D. R., AEBERSOLD, R. & EISENMAN, R. N. 2002. Quantitative proteomic analysis of Myc oncoprotein function. Embo j, 21, 5088-96.

SHIIO, Y., SUH, K. S., LEE, H., YUSPA, S. H., EISENMAN, R. N. & AEBERSOLD, R. 2006. Quantitative proteomic analysis of myc-induced apoptosis: a direct role for Myc induction of the mitochondrial chloride ion channel, mtCLIC/CLIC4. J Biol Chem, 281, 2750-6.

SHIMO-OKA, T., HAGIWARA, Y. & OZAWA, E. 1986. Class specificity of transferrin as a muscle trophic factor. J Cell Physiol, 126, 341-51.

SHIRANE, J., NAKAYAMA, T., NAGAKUBO, D., IZAWA, D., HIESHIMA, K., SHIMOMURA, Y. & YOSHIE, O. 2004. Corneal epithelial cells and stromal keratocytes efficently produce CC chemokine-ligand 20 (CCL20) and attract cells expressing its receptor CCR6 in mouse herpetic stromal keratitis. Curr Eye Res, 28, 297-306.

SHORTT, A. J., SECKER, G. A., MUNRO, P. M., KHAW, P. T., TUFT, S. J. & DANIELS, J. T. 2007. Characterization of the limbal epithelial stem cell niche: novel imaging techniques permit in vivo observation and targeted biopsy of limbal epithelial stem cells. Stem Cells, 25, 1402-9.

SIEZEN, R. J. & LEUNISSEN, J. A. 1997. Subtilases: the superfamily of subtilisin like serine proteases. Protein Sci, 6, 501-23.

SINGH, C. R., CURTIS, C., YAMAMOTO, Y., HALL, N. S., KRUSE, D. S., HE, H., HANNIG, E. M. & ASANO, K. 2005. Eukaryotic translation initiation

factor 5 is critical for integrity of the scanning preinitiation complex and accurate control of GCN4 translation. Mol Cell Biol, 25, 5480-91.

SIRBASKU, D. A., PAKALA, R., SATO, H. & EBY, J. E. 1991. Thyroid hormone dependent pituitary tumor cell growth in serum-free chemically defined culture. A new regulatory role for apotransferrin. Biochemistry, 30, 7466-77.

SMEDMAN, C., ERNEMAR, T., GUDMUNDSDOTTER, L., GILLE-JOHNSON, P., SOMELL, A., NIHLMARK, K., GARDLUND, B., ANDERSSON, J. & PAULIE, S. 2012. FluoroSpot Analysis of TLR-Activated Monocytes Reveals Several Distinct Cytokine-Secreting Subpopulations. Scand J Immunol, 75, 249-58.

SMEDMAN, C., GARDLUND, B., NIHLMARK, K., GILLE-JOHNSON, P., ANDERSSON, J. & PAULIE, S. 2009. ELISpot analysis of LPS-stimulated leukocytes: human granulocytes selectively secrete IL-8, MIP-1beta and TNF alpha. J Immunol Methods, 346, 1-8.

SMITH, A., ROWAN, R., MCCANN, M. & KAVANAGH, K. 2012. Exposure of Staphylococcus aureus to silver(I) induces a short term protective response. Biometals, 25, 611-6.

SMITH, J. R., LANIER, V. B., BRAZIEL, R. M., FALKENHAGEN, K. M., WHITE, C. & ROSENBAUM, J. T. 2007. Expression of vascular endothelial growth factor and its receptors in rosacea. Br J Ophthalmol, 91, 226-9.

SMITH, K. A. 1988. Interleukin-2: inception, impact, and implications. Science, 240, 1169-76.

SMITH, K. D., ANDERSEN-NISSEN, E., HAYASHI, F., STROBE, K., BERGMAN, M. A., BARRETT, S. L., COOKSON, B. T. & ADEREM, A. 2003. Toll-like receptor 5 recognizes a conserved site on flagellin required for protofilament formation and bacterial motility. Nat Immunol, 4, 1247-53.

SOHN, E. J., PAAPE, M. J., CONNOR, E. E., BANNERMAN, D. D., FETTERER, R. H. & PETERS, R. R. 2007. Bacterial lipopolysaccharide stimulates bovine neutrophil production of TNF-alpha, IL-1beta, IL-12 and IFN-gamma. Vet Res, 38, 809-18.

SOMERVILLE, D. A. 1969. The normal flora of the skin in different age groups. Br J Dermatol, 81, 248-58.

SON, S. W., KIM, I. H., OH, C. H. & KIM, J. G. 1999. The response of rosacea to eradication of Helicobacter pylori. Br J Dermatol. England.

SONNENBERG, G. F., FOUSER, L. A. & ARTIS, D. 2011. Border patrol: regulation of immunity, inflammation and tissue homeostasis at barrier surfaces by IL- 22. Nat Immunol, 12, 383-90.

SPICKETT, S. G. 1961. Studies on Demodex folliculorum Simon. Parasitology, 51, 181-192.

SPRINGER, T. A. 1990. Adhesion receptors of the immune system. Nature, 346, 425-34.

SPRINGER, T. A. 1994. Traffic signals for lymphocyte recirculation and leukocyte emigration: the multistep paradigm. Cell, 76, 301-14.

STARKEY, P. M., BARRETT, A. J. & BURLEIGH, M. C. 1977. The degradation of articular collagen by neutrophil proteinases. Biochim Biophys Acta, 483, 386-97.

STEIN, L., KIRCIK, L., FOWLER, J., TAN, J., DRAELOS, Z., FLEISCHER, A., APPELL, M., STEINHOFF, M., LYNDE, C., LIU, H. & JACOVELLA, J. 2014. Efficacy and safety of ivermectin 1% cream in treatment of papulopustular rosacea: results of two randomized, double-blind, vehicle controlled pivotal studies. J Drugs Dermatol, 13, 316-23.

STEINHOFF, M., BUDDENKOTTE, J., AUBERT, J., SULK, M., NOVAK, P., SCHWAB, V. D., MESS, C., CEVIKBAS, F., RIVIER, M., CARLAVAN, I., DERET, S., ROSIGNOLI, C., METZE, D., LUGER, T. A. & VOEGEL, J. J. 2011. Clinical, cellular, and molecular aspects in the pathophysiology of rosacea. J Investig Dermatol Symp Proc, 15, 2-11.

STEINHOFF, M., SCHAUBER, J. & LEYDEN, J. J. 2013. New insights into rosacea pathophysiology: a review of recent findings. J Am Acad Dermatol, 69, S15-26.

STERNBERG, N. 1973. Properties of a mutant of Escherichia coli defective in bacteriophage lambda head formation (groE). I. Initial characterization. J Mol Biol, 76, 1-23.

STRUNNIKOVA, N., BAFFI, J., GONZALEZ, A., SILK, W., COUSINS, S. W. & CSAKY, K. G. 2001. Regulated heat shock protein 27 expression in human retinal pigment epithelium. Invest Ophthalmol Vis Sci, 42, 2130-8.

SUAREZ-FARINAS, M., DHINGRA, N., GITTLER, J., SHEMER, A., CARDINALE, I., DE GUZMAN STRONG, C., KRUEGER, J. G. & GUTTMAN-YASSKY, E. 2013. Intrinsic atopic dermatitis shows similar TH2

and higher TH17 immune activation compared with extrinsic atopic dermatitis. J Allergy Clin Immunol, 132, 361-70.

SUN, D., NOVOTNY, M., BULEK, K., LIU, C., LI, X. & HAMILTON, T. 2011. Treatment with IL-17 prolongs the half-life of chemokine CXCL1 mRNA via the adaptor TRAF5 and the splicing-regulatory factor SF2 (ASF). Nat Immunol, 12, 853-60.

SZKARADKIEWICZ, A., CHUDZICKA-STRUGALA, I., KARPINSKI, T. M., GOSLINSKA-PAWLOWSKA, O., TULECKA, T., CHUDZICKI, W., SZKARADKIEWICZ, A. K. & ZABA, R. 2012. Bacillus oleronius and Demodex mite infestation in patients with chronic blepharitis. Clin Microbiol Infect, 18, 1020-5.

SZYMCZYNA, B. R., BOWMAN, J., MCCRACKEN, S., PINEDA-LUCENA, A., LU, Y., COX, B., LAMBERMON, M., GRAVELEY, B. R., ARROWSMITH, C. H. & BLENCOWE, B. J. 2003. Structure and function of the PWI motif: a novel nucleic acid-binding domain that facilitates pre-mRNA processing. Genes Dev, 17, 461-75.

TAN, S. R. & TOPE, W. D. 2004. Pulsed dye laser treatment of rosacea improves erythema, symptomatology, and quality of life. J Am Acad Dermatol, 51, 592-9.

TANAKA, K., HATADA, T., KOBAYASHI, M., MOHRI, Y., TONOUCHI, H., MIKI, C., NOBORI, T. & KUSUNOKI, M. 2004. The clinical implication of 14-3-3 sigma expression in primary gastrointestinal malignancy. Int J Oncol, 25, 1591-7.

TANG, C., CHEN, S., QIAN, H. & HUANG, W. 2012. Interleukin-23: as a drug target for autoimmune inflammatory diseases. Immunology, 135, 112-24.

TANGHETTI, E., DEL ROSSO, J. Q., THIBOUTOT, D., GALLO, R., WEBSTER, G., EICHENFIELD, L. F., STEIN-GOLD, L., BERSON, D. & ZAENGLEIN, A. 2014. Consensus Recommendations From the American Acne & Rosacea Society on the Management of Rosacea, Part 4: A Status Report on Physical Modalities and Devices. Cutis, 93, 71-76.

TAYLOR, C. W., DA FONSECA, P. C. & MORRIS, E. P. 2004. IP(3) receptors: the search for structure. Trends Biochem Sci, 29, 210-9.

TECKCHANDANI, A., MULKEARNS, E. E., RANDOLPH, T. W., TOIDA, N. & COOPER, J. A. 2012. The clathrin adaptor Dab2 recruits EH domain scaffold

proteins to regulate integrin beta1 endocytosis. Mol Biol Cell, 23, 2905-16.
TEEHAN, G. S., BAHDOUCH, D., RUTHAZER, R., BALAKRISHNAN, V. S., SNYDMAN, D. R. & JABER, B. L. 2004. Iron storage indices: novel predictors of bacteremia in hemodialysis patients initiating intravenous iron therapy. Clin Infect Dis, 38, 1090-4.
TERAKI, Y., HITOMI, K., SATO, Y. & IZAKI, S. 2012. Tacrolimus-induced rosacea-like dermatitis: a clinical analysis of 16 cases associated with tacrolimus ointment application. Dermatology, 224, 309-14.
TEUNISSEN, M. B., KOOMEN, C. W., DE WAAL MALEFYT, R., WIERENGA, E. A. & BOS, J. D. 1998. Interleukin-17 and interferon-gamma synergize in the enhancement of proinflammatory cytokine production by human keratinocytes. J Invest Dermatol, 111, 645-9.
TEZEL, G., HERNANDEZ, R. & WAX, M. B. 2000. Immunostaining of heat shock proteins in the retina and optic nerve head of normal and glaucomatous eyes. Arch Ophthalmol, 118, 511-8.
THELEN, M. & WIRTHMUELLER, U. 1994. Phospholipases and protein kinases during phagocyte activation. Curr Opin Immunol, 6, 106-12.
THOEMMES, M. S., FERGUS, D. J., URBAN, J., TRAUTWEIN, M. & DUNN, R. R. 2014. Ubiquity and diversity of human-associated Demodex mites. PloS One, 9, e106265.
THORLACIUS, H., VOLLMAR, B., GUO, Y., MAK, T. W., PFREUNDSCHUH, M. M., MENGER, M. D. & SCHMITS, R. 2000. Lymphocyte function antigen 1 (LFA-1) mediates early tumour necrosis factor alpha-induced leucocyte adhesion in venules. Br J Haematol, 110, 424-9.
TING, J. P., LOVERING, R. C., ALNEMRI, E. S., BERTIN, J., BOSS, J. M., DAVIS, B. K., FLAVELL, R. A., GIRARDIN, S. E., GODZIK, A., HARTON, J. A., HOFFMAN, H. M., HUGOT, J. P., INOHARA, N., MACKENZIE, A., MALTAIS, L. J., NUNEZ, G., OGURA, Y., OTTEN, L. A., PHILPOTT, D., REED, J. C., REITH, W., SCHREIBER, S., STEIMLE, V. & WARD, P. A. 2008. The NLR gene family: a standard nomenclature. Immunity, 28, 285-7.

TINTINGER, G., STEEL, H. C. & ANDERSON, R. 2005. Taming the neutrophil: calcium clearance and influx mechanisms as novel targets for pharmacological control. Clin Exp Immunol, 141, 191-200.

TISMA, V. S., BASTA-JUZBASIC, A., JAGANJAC, M., BRCIC, L., DOBRIC, I., LIPOZENCIC, J., TATZBER, F., ZARKOVIC, N. & POLJAK-BLAZI, M. 2009. Oxidative stress and ferritin expression in the skin of patients with rosacea. J Am Acad Dermatol, 60, 270-6.

TO, W. S. & MIDWOOD, K. S. 2011. Plasma and cellular fibronectin: distinct and independent functions during tissue repair. Fibrogenesis Tissue Repair, 4, 21.

TODD, R. F., 3RD 1996. The continuing saga of complement receptor type 3 (CR3). J Clin Invest, 98, 1-2.

TOPCU-YILMAZ, P., ATAKAN, N., BOZKURT, B., IRKEC, M., ABAN, D., MESCI, L. & TEZCAN, I. 2013. Determination of tear and serum inflammatory cytokines in patients with rosacea using multiplex bead technology. Ocul Immunol Inflamm, 21, 351-9.

TORRIGLIA, A., LEPRETRE, C., PADRON-BARTHE, L., CHAHORY, S. & MARTIN, E. 2008. Molecular mechanism of L-DNase II activation and function as a molecular switch in apoptosis. Biochem Pharmacol, 76, 1490-502.

TOZAWA, Y., YOSHIKAWA, H., KAWAMURA, F., ITAYA, M. & TAKAHASHI, H. 1992. Isolation and characterization of the groES and groEL genes of Bacillus subtilis Marburg. Biosci Biotechnol Biochem, 56, 1995-2002.

TRINCHIERI, G. 1993. Interleukin-12 and its role in the generation of TH1 cells. Immunol Today, 14, 335-8.

TSAI, R. J., LI, L. M. & CHEN, J. K. 2000. Reconstruction of damaged corneas by transplantation of autologous limbal epithelial cells. N Engl J Med, 343, 86- 93.

TSENG, S. C. 1989. Concept and application of limbal stem cells. Eye (Lond), 3 (Pt 2), 141-57.

TSENG, S. C. 1996. Regulation and clinical implications of corneal epithelial stem cells. Mol Biol Rep, 23, 47-58.

TSENG, S. C., PRABHASAWAT, P., BARTON, K., GRAY, T. & MELLER, D. 1998. Amniotic membrane transplantation with or without limbal allografts for corneal surface reconstruction in patients with limbal stem cell deficiency. Arch Ophthalmol, 116, 431-41.

TSENG, S. H., CHENG, C. Y., HUANG, M. Z., CHUNG, M. Y. & SU, T. S. 2013. Modulation of formation of the 3'-end of the human argininosuccinate synthetase mRNA by GT-repeat polymorphism. Int J Biochem Mol Biol, 4, 179-90.

TU, C. L., CHANG, W. & BIKLE, D. D. 2001. The extracellular calcium-sensing receptor is required for calcium-induced differentiation in human keratinocytes. J Biol Chem, 276, 41079-85.

TUTEJA, N., TUTEJA, R., OCHEM, A., TANEJA, P., HUANG, N. W., SIMONCSITS, A., SUSIC, S., RAHMAN, K., MARUSIC, L., CHEN, J., ZHANG, J., WANG, S., PONGOR, S. & FALASCHI, A. 1994. Human DNA helicase II: a novel DNA unwinding enzyme identified as the Ku autoantigen. Embo j, 13, 4991-5001.

TWO, A. M. & DEL ROSSO, J. Q. 2014. Kallikrein 5-mediated inflammation in rosacea: clinically relevant correlations with acute and chronic manifestations in rosacea and how individual treatments may provide therapeutic benefit. J Clin Aesthet Dermatol, 7, 20-5.

UCKAY, I., PITTET, D., VAUDAUX, P., SAX, H., LEW, D. & WALDVOGEL, F. 2009. Foreign body infections due to Staphylococcus epidermidis. Ann Med, 41, 109-19.

URBAK, L. & VORUM, H. 2010. Heat shock proteins in the human eye. Int J Proteomics, 2010, 479571.

URBAN, J. F., JR., FAYER, R., SULLIVAN, C., GOLDHILL, J., SHEA DONOHUE, T., MADDEN, K., MORRIS, S. C., KATONA, I., GAUSE, W., RUFF, M., MANSFIELD, L. S. & FINKELMAN, F. D. 1996. Local TH1 and TH2 responses to parasitic infection in the intestine: regulation by IFN-gamma and IL-4. Vet Immunol Immunopathol, 54, 337-44.

URIARTE, S. M., POWELL, D. W., LUERMAN, G. C., MERCHANT, M. L., CUMMINS, T. D., JOG, N. R., WARD, R. A. & MCLEISH, K. R. 2008. Comparison of proteins expressed on secretory vesicle membranes and plasma membranes of human neutrophils. J Immunol, 180, 5575-81.

UYEMURA, K., YAMAMURA, M., FIVENSON, D. F., MODLIN, R. L. & NICKOLOFF, B. J. 1993. The cytokine network in lesional and lesion-free psoriatic skin is characterized by a T-helper type 1 cell-mediated response. J Invest Dermatol, 101, 701-5.

VAN DER BRUGGEN, T., NIJENHUIS, S., VAN RAAIJ, E., VERHOEF, J. & VAN ASBECK, B. S. 1999. Lipopolysaccharide-induced tumor necrosis factor alpha production by human monocytes involves the raf-1/MEK1 MEK2/ERK1-ERK2 pathway. Infect Immun, 67, 3824-9.

VAN DER LOOP, F. T., SCHAART, G., TIMMER, E. D., RAMAEKERS, F. C. & VAN EYS, G. J. 1996. Smoothelin, a novel cytoskeletal protein specific for smooth muscle cells. J Cell Biol, 134, 401-11.

VAN DERVORT, A. L., YAN, L., MADARA, P. J., COBB, J. P., WESLEY, R. A., CORRIVEAU, C. C., TROPEA, M. M. & DANNER, R. L. 1994. Nitric oxide regulates endotoxin-induced TNF-alpha production by human neutrophils. J Immunol, 152, 4102-9.

VAN DYK, T. K., GATENBY, A. A. & LAROSSA, R. A. 1989. Demonstration by genetic suppression of interaction of GroE products with many proteins. Nature, 342, 451-3.

VAN ZUUREN, E. J., KRAMER, S. F., CARTER, B. R., GRABER, M. A. & FEDOROWICZ, Z. 2011. Effective and evidence-based management strategies for rosacea: summary of a Cochrane systematic review. Br J Dermatol, 165, 760-81.

VANCE, R. E., ISBERG, R. R. & PORTNOY, D. A. 2009. Patterns of pathogenesis: discrimination of pathogenic and nonpathogenic microbes by the innate immune system. Cell Host Microbe, 6, 10-21.

VANCE. J. 1986. Demodicidosis—do Demodex mites cause disease? Curr Conc Skin Disorder, 10–18.

VASIOUKHIN, V., BOWERS, E., BAUER, C., DEGENSTEIN, L. & FUCHS, E. 2001. Desmoplakin is essential in epidermal sheet formation. Nat Cell Biol, 3, 1076-85.

VAZIRI, H. & BENCHIMOL, S. 1998. Reconstitution of telomerase activity in normal human cells leads to elongation of telomeres and extended replicative life span. Curr Biol, 8, 279-82.

VEMUGANTI, G. K., FATIMA, A., MADHIRA, S. L., BASTI, S. & SANGWAN, V. S. 2009. Limbal stem cells: application in ocular biomedicine. Int Rev Cell Mol Biol, 275, 133-81.

VENABLE, J. D., WOHLSCHLEGEL, J., MCCLATCHY, D. B., PARK, S. K. & YATES, J. R., 3RD 2007. Relative quantification of stable isotope labeled

peptides using a linear ion trap-Orbitrap hybrid mass spectrometer. Anal Chem, 79, 3056-64.

VERSTREPEN, L., CARPENTIER, I., VERHELST, K. & BEYAERT, R. 2009. ABINs: A20 binding inhibitors of NF-kappa B and apoptosis signaling. Biochem Pharmacol, 78, 105-14.

VLACHOSTERGIOS, P. J., VOUTSADAKIS, I. A. & PAPANDREOU, C. N. 2012. The ubiquitin-proteasome system in glioma cell cycle control. Cell Div, 7, 18.

VOLLMER, R. T. 1996. Demodex-associated folliculitis. Am J Dermatopathol, 18, 589-91.

WACKER, M. J., KOSLOSKI, L. M., GILBERT, W. J., TOUCHBERRY, C. D., MOORE, D. S., KELLY, J. K., BROTTO, M. & ORR, J. A. 2009. Inhibition of thromboxane A2-induced arrhythmias and intracellular calcium changes in cardiac myocytes by blockade of the inositol trisphosphate pathway. J Pharmacol Exp Ther, 331, 917-24.

WALKER, W., VINIK, A., HELDSINGER, A. & KAVEH, R. 1983. Role of calcium and calmodulin in activation of the oxyntic cell by histamine and carbamylcholine in the guinea pig. J Clin Invest, 72, 955-64.

WANG, C., GUO, Y., WANG, J. & MIN, Z. 2015. Annexin A2 knockdown inhibits hepatoma cell growth and sensitizes hepatoma cells to 5-fluorouracil by regulating beta-catenin and cyclin D1 expression. Mol Med Rep, 11, 2147-52.

WANG, C. Y., CHEN, C. L., TSENG, Y. L., FANG, Y. T., LIN, Y. S., SU, W. C., CHEN, C. C., CHANG, K. C., WANG, Y. C. & LIN, C. F. 2012. Annexin A2 silencing induces G2 arrest of non-small cell lung cancer cells through p53 dependent and -independent mechanisms. J Biol Chem, 287, 32512-24.

WANG, J., GAO, Q. S., WANG, Y., LAFYATIS, R., STAMM, S. & ANDREADIS, A. 2004. Tau exon 10, whose missplicing causes frontotemporal dementia, is regulated by an intricate interplay of cis elements and trans factors. J Neurochem, 88, 1078-90.

WANG, Y., WANG, J., GAO, L., LAFYATIS, R., STAMM, S. & ANDREADIS, A. 2005. Tau exons 2 and 10, which are misregulated in neurodegenerative diseases, are partly regulated by silencers which bind a SRp30c.SRp55 complex that either recruits or antagonizes htra2beta1. J Biol Chem, 280, 14230-9.

WARD, I. M., MINN, K., VAN DEURSEN, J. & CHEN, J. 2003. p53 Binding protein 53BP1 is required for DNA damage responses and tumor suppression in mice. Mol Cell Biol, 23, 2556-63.

WATKINS, L. R., HANSEN, M. K., NGUYEN, K. T., LEE, J. E. & MAIER, S. F. 1999. Dynamic regulation of the proinflammatory cytokine, interleukin-1beta: molecular biology for non-molecular biologists. Life Sci, 65, 449-81.

WATKINS, L. R., MILLIGAN, E. D. & MAIER, S. F. 2003. Glial proinflammatory cytokines mediate exaggerated pain states: implications for clinical pain. Adv Exp Med Biol, 521, 1-21.

WEI, W. & LIN, H. K. 2012. The key role of ubiquitination and sumoylation in signaling and cancer: a research topic. Front Oncol, 2, 187.

WEISS, E., MAMELAK, A. J., LA MORGIA, S., WANG, B., FELICIANI, C., TULLI, A. & SAUDER, D. N. 2004. The role of interleukin 10 in the pathogenesis and potential treatment of skin diseases. J Am Acad Dermatol, 50, 657-75; quiz 676-8.

WELLBROCK, C., KARASARIDES, M. & MARAIS, R. 2004. The RAF proteins take centre stage. Nat Rev Mol Cell Biol, 5, 875-85.

WENG, N. P., HATHCOCK, K. S. & HODES, R. J. 1998. Regulation of telomere length and telomerase in T and B cells: a mechanism for maintaining replicative potential. Immunity, 9, 151-7.

WHEELOCK, E. F. 1965. Interferon-Like Virus-Inhibitor Induced in Human Leukocytes by Phytohemagglutinin. Science, 149, 310-311.

WHITELOCK, R. B., FUKUCHI, T., ZHOU, L., TWINING, S. S., SUGAR, J., FEDER, R. S. & YUE, B. Y. 1997. Cathepsin G, acid phosphatase, and alpha 1-proteinase inhibitor messenger RNA levels in keratoconus corneas. Invest Ophthalmol Vis Sci, 38, 529-34.

WHITFELD, M., GUNASINGAM, N., LEOW, L. J., SHIRATO, K. & PREDA, V. 2011. Staphylococcus epidermidis: a possible role in the pustules of rosacea. J Am Acad Dermatol, 64, 49-52.

WILKIN, J., DAHL, M., DETMAR, M., DRAKE, L., FEINSTEIN, A., ODOM, R. & POWELL, F. 2002. Standard classification of rosacea: Report of the National Rosacea Society Expert Committee on the Classification and Staging of Rosacea. J Am Acad Dermatol, 46, 584-7.

WILKIN, J., DAHL, M., DETMAR, M., DRAKE, L., LIANG, M. H., ODOM, R. & POWELL, F. 2004. Standard grading system for rosacea: report of the National Rosacea Society Expert Committee on the classification and staging of rosacea. J Am Acad Dermatol, 50, 907-12.

WILLIAMS, D. L., RISSE, B., KIM, S., SAUNDERS, D., ORLIN, S., BAKER, M. S., JENSEN, P. J. & LAVKER, R. M. 1999. Plasminogen activator inhibitor type 2 in human corneal epithelium. Invest Ophthalmol Vis Sci, 40, 1669-75.

WILLIAMS, L., JARAI, G., SMITH, A. & FINAN, P. 2002. IL-10 expression profiling in human monocytes. J Leukoc Biol, 72, 800-9.

WILLIS, D. M., LOEWY, A. P., CHARLTON-KACHIGIAN, N., SHAO, J. S., ORNITZ, D. M. & TOWLER, D. A. 2002. Regulation of osteocalcin gene expression by a novel Ku antigen transcription factor complex. J Biol Chem, 277, 37280-91.

WILSON, S. E. & ESPOSITO, A. 2009. Focus on molecules: interleukin-1: a master regulator of the corneal response to injury. Exp Eye Res, 89, 124-5.

WITKO-SARSAT, V., ALLEN, R. C., PAULAIS, M., NGUYEN, A. T., BESSOU, G., LENOIR, G. & DESCAMPS-LATSCHA, B. 1996. Disturbed myeloperoxidase-dependent activity of neutrophils in cystic fibrosis homozygotes and heterozygotes, and its correction by amiloride. J Immunol, 157, 2728-35.

WITTINGHOFER, A. & PAI, E. F. 1991. The structure of Ras protein: a model for a universal molecular switch. Trends Biochem Sci, 16, 382-7.

WOJCIAK-STOTHARD, B., POTEMPA, S., EICHHOLTZ, T. & RIDLEY, A. J. 2001. Rho and Rac but not Cdc42 regulate endothelial cell permeability. J Cell Sci, 114, 1343-55.

WOLF, R., OPHIR, J., AVIGAD, J., LENGY, J. & KRAKOWSKI, A. 1988. The hair follicle mites (Demodex spp.). Could they be vectors of pathogenic microorganisms? Acta Derm Venereol, 68, 535-7.

WOLF, S. F., TEMPLE, P. A., KOBAYASHI, M., YOUNG, D., DICIG, M., LOWE, L., DZIALO, R., FITZ, L., FERENZ, C., HEWICK, R. M. & ET AL. 1991. Cloning of cDNA for natural killer cell stimulatory factor, a heterodimeric cytokine with multiple biologic effects on T and natural killer cells. J Immunol, 146, 3074-81.

WOLK, K., KUNZ, S., WITTE, E., FRIEDRICH, M., ASADULLAH, K. & SABAT, R. 2004. IL-22 increases the innate immunity of tissues. Immunity, 21, 241 54.

WOLLINA, U. 2007. The role of topical calcineurin inhibitors for skin diseases other than atopic dermatitis. Am J Clin Dermatol, 8, 157-73.

WOLLINA, U. 2014. Recent advances in the understanding and management of rosacea. F1000Prime Rep, 6, 50.

WU, J. & CHEN, Z. J. 2014. Innate immune sensing and signaling of cytosolic nucleic acids. Annu Rev Immunol, 32, 461-88.

YAGO, T., NANKE, Y., KAWAMOTO, M., FURUYA, T., KOBASHIGAWA, T., KAMATANI, N. & KOTAKE, S. 2007. IL-23 induces human osteoclastogenesis via IL-17 in vitro, and anti-IL-23 antibody attenuates collagen-induced arthritis in rats. Arthritis Res Ther, 9, R96.

YAMAGUCHI, H., HSU, J. L. & HUNG, M. C. 2012. Regulation of ubiquitination mediated protein degradation by survival kinases in cancer. Front Oncol, 2, 15.

YAMAGUCHI, Y. L., TANAKA, S. S., OSHIMA, N., KIYONARI, H., ASASHIMA, M. & NISHINAKAMURA, R. 2011. Translocon-associated protein subunit Trap-gamma/Ssr3 is required for vascular network formation in the mouse placenta. Dev Dyn, 240, 394-403.

YAMASAKI, K., DI NARDO, A., BARDAN, A., MURAKAMI, M., OHTAKE, T., CODA, A., DORSCHNER, R. A., BONNART, C., DESCARGUES, P., HOVNANIAN, A., MORHENN, V. B. & GALLO, R. L. 2007. Increased serine protease activity and cathelicidin promotes skin inflammation in rosacea. Nat Med, 13, 975-80.

YAMASAKI, K. & GALLO, R. L. 2008. Antimicrobial peptides in human skin disease. Eur J Dermatol, 18, 11-21.

YAMASAKI, K. & GALLO, R. L. 2009. The molecular pathology of rosacea. Journal of Dermatological Science, 55, 77-81.

YAMASAKI, K. & GALLO, R. L. 2011. Rosacea as a disease of cathelicidins and skin innate immunity. J Investig Dermatol Symp Proc, 15, 12-5.

YAMASAKI, K., KANADA, K., MACLEOD, D. T., BORKOWSKI, A. W., MORIZANE, S., NAKATSUJI, T., COGEN, A. L. & GALLO, R. L. 2011. TLR2 expression is increased in rosacea and stimulates enhanced serine protease production by keratinocytes. J Invest Dermatol, 131, 688-97.

YAMASAKI, K., SCHAUBER, J., CODA, A., LIN, H., DORSCHNER, R. A., SCHECHTER, N. M., BONNART, C., DESCARGUES, P., HOVNANIAN,A. & GALLO, R. L. 2006. Kallikrein-mediated proteolysis regulates the antimicrobial effects of cathelicidins in skin. Faseb j, 20, 2068-80.

YANG, H. Y., WEN, Y. Y., CHEN, C. H., LOZANO, G. & LEE, M. H. 2003. 14-3-3 sigma positively regulates p53 and suppresses tumor growth. Mol Cell Biol, 23, 7096-107.

YARDLEY, M. M., NEELY, M., HUYNH, N., ASATRYAN, L., LOUIE, S. G., ALKANA, R. L. & DAVIES, D. L. 2014. Multiday administration of ivermectin is effective in reducing alcohol intake in mice at doses shown to be safe in humans. Neuroreport, 25, 1018-23.

YATES, J. R., 3RD 2004. Mass spectral analysis in proteomics. Annu Rev Biophys Biomol Struct, 33, 297-316.

YATES, J. R., COCIORVA, D., LIAO, L. & ZABROUSKOV, V. 2006. Performance of a linear ion trap-Orbitrap hybrid for peptide analysis. Anal Chem, 78, 493-500.

YOSHINAGA, Y., HIGAKI, M., TERAJIMA, S., OHKUBO, E., NOGITA, T., MIYASAKA, N. & KAWASHIMA, M. 1995. Detection of inflammatory cytokines in psoriatic skin. Arch Dermatol Res, 287, 158-64.

YOSHIOKA, A., MIYACHI, Y., IMAMURA, S. & NIWA, Y. 1986. Anti-oxidant effects of retinoids on inflammatory skin diseases. Arch Dermatol Res, 278, 177-83.

YU, X., VOUGHT, V. E., CONRADT, B. & MAINE, E. M. 2006. Eukaryotic translation initiation factor 5B activity regulates larval growth rate and germline development in Caenorhabditis elegans. Genesis, 44, 412-8.

YUCEL, A. & YILMAZ, M. 2013. [Investigation of the prevalance of Demodex folliculorum and Demodex brevis in rosacea patients]. Turkiye Parazitol Derg, 37, 195-8.

ZHANG, H. J., YAO, D. F., YAO, M., HUANG, H., WANG, L., YAN, M. J., YAN, X. D., GU, X., WU, W. & LU, S. L. 2013. Annexin A2 silencing inhibits invasion, migration, and tumorigenic potential of hepatoma cells. World J Gastroenterol, 19, 3792-801.

ZHANG, J. M. & AN, J. 2007. Cytokines, inflammation, and pain. Int Anesthesiol Clin, 45, 27-37.

ZHAO, B., ZONG, G., XIE, Y., LI, J., WANG, H. & BIAN, E. 2015. Downregulation of ubiquitin-associated protein 2-like with a short hairpin RNA inhibits human glioma cell growth in vitro. Int J Mol Med, 36, 1012-8.

ZHAO, Y. E., GUO, N. & WU, L. P. 2009. The effect of temperature on the viability of Demodex folliculorum and Demodex brevis. Parasitol Res, 105, 1623-8.

ZHOU, B., TANG, Z., DENG, Y., HOU, S., LIU, N., LIN, W., LIU, X. & YAO, L. 2014. Tumor suppressor candidate gene, NDRG2 is frequently inactivated in human glioblastoma multiforme. Mol Med Rep, 10, 891-6.

ZHOU, L., BEUERMAN, R. W., CHAN, C. M., ZHAO, S. Z., LI, X. R., YANG, H., TONG, L., LIU, S., STERN, M. E. & TAN, D. 2009. Identification of tear fluid biomarkers in dry eye syndrome using iTRAQ quantitative proteomics. J Proteome Res, 8, 4889-905.

ZHU, J. & PAUL, W. E. 2008. CD4 T cells: fates, functions, and faults. Blood, 112, 1557-69.

ZHU, Z., HOMER, R. J., WANG, Z., CHEN, Q., GEBA, G. P., WANG, J., ZHANG, Y. & ELIAS, J. A. 1999. Pulmonary expression of interleukin-13 causes inflammation, mucus hypersecretion, subepithelial fibrosis, physiologic abnormalities, and eotaxin production. J Clin Invest, 103, 779-88.

Appendix

Appendix: List of Figures

Figure A4.1 Visualization of crude *B. oleronius* protein ÄKTA FPLC™ fractions 1 to 18 by Coomassie Staining and Western blotting 396

Figure A4.2 Visualization of crude *B. oleronius* protein ÄKTA FPLC™ fractions 19 to 36 by Coomassie Staining and Western blotting 397

Figure A4.3 Visualization of crude *B. oleronius* protein ÄKTA FPLC™ fractions 37 to 54 by Coomassie Staining and Western blotting 398

Figure A4.4 Visualization of crude *B. oleronius* protein ÄKTA FPLC™ fractions 55 to 72 by Coomassie Staining and Western blotting 399

Figure A4.5 Visualization of crude *B. oleronius* protein ÄKTA FPLC™ fractions 73 to 81 by Coomassie Staining and Western blotting 400

Figure A4.6 Visualization of ÄKTA FPLC™ generated pure *B. oleronius* protein preparation fractions 1 to 8 by Coomassie Staining and Western blotting 401

Figure A4.7 A representative 1-D gelatinase zymogram (10% w/v) gel image to assess MMP-9 activity present in hTCEpi cell supernatants following exposure to pure *B. oleronius* proteins..... 402

Figure A6.1 Assessment of endotoxin activity and IL-6 secretion in PBMC exposed to LPS by FluoroSpot..... 403

Figure A6.2 Representative ELISpot images of assessment of endotoxin activity and TNF-α secretion in PBMC exposed to LPS (A) without, or (B) with the addition of polymyxin B (10 μg/ml) 404

Figure A6.3 Representative FluoroSpot images of assessment of endotoxin activity and IL-6 secretion in PBMC exposed to LPS (A) without, or (B) with the addition of polymyxin B (10 μg/ml) 405

Figure A6.4 Representative ELISpot images of assessment of endotoxin activity and TNF-α secretion in PBMC exposed to pure *B. oleronius* protein (A) without, or (B) with the addition of polymyxin B (10 μg/ml) 406

Figure A6.5 Representative ELISpot images of assessment of endotoxin activity and TNF-α secretion in PBMC exposed to crude *B. oleronius* protein (A) without, or (B) with the addition of polymyxin B (10 μg/ml) 407

Figure A7.1 Western blots of sera reactivity of participants coded (A) 4 to 34 and (B) 35 to 42, to *B. oleronius* proteins in erythematotelangiectatic rosacea study 414

Figure A7.2 Western blots of sera reactivity of participants coded (A) 9 to 40 and (B) 43 to 101, to *B. oleronius* proteins in erythematotelangiectatic rosacea study 414

Figure A7.3 Western blots of sera reactivity of participants coded (A) 102 to 118 and (B) 28 to 46, to *B. oleronius* proteins in erythematotelangiectatic rosacea study 415

Figure A7.4 Western blots of sera reactivity of participants coded (A) 35 to 136 and (B) 103 to 130, to *B. oleronius* proteins in erythematotelangiectatic rosacea study 415

Figure A7.5 Western blots of sera reactivity of participants coded (A) 127 to 136 and (B) 60 to 67, to *B. oleronius* proteins in erythematotelangiectatic rosacea study 416

Figure A7.6 Western blots of sera reactivity of participants coded (A) 102 to 124 and (B) 7 to 101, to *B. oleronius* proteins in erythematotelangiectatic rosacea study 416

Figure A7.7 Western blots of sera reactivity of participants coded (A) 65 to 127 and (B) 128 to 136, to *B. oleronius* proteins in erythematotelangiectatic rosacea study 417

Figure A7.8 Western blots of sera reactivity of participants coded (A) GZ2 to 134 and (B) 135 to 136, to *B. oleronius* proteins in erythematotelangiectatic rosacea study 417

Figure A7.9 Western blots of sera reactivity of participants coded (A) 69 to 81 and (B) 79 to 87, to *B. oleronius* proteins in erythematotelangiectatic rosacea study 418

Figure A7.10 Western blots of sera reactivity of participants coded (A) 91 to GT2 and (B) 47 to 55, to *B. oleronius* proteins in erythematotelangiectatic rosacea study 418

Figure A7.11 Western blots of sera reactivity of participants coded (A) 65 to 73 and (B) 56 to 64, to *B. oleronius* proteins in erythematotelangiectatic rosacea study 419

Figure A7.12 Western blots of sera reactivity of participants coded (A) N1 to N8 and (B) N9 to N16, to *B. oleronius* proteins in erythematotelangiectatic rosacea study 419

Figure A7.13 Western blots of sera reactivity of participants coded (A) N17 to N23 and (B) N24 to N27, to *B. oleronius* proteins in erythematotelangiectatic rosacea study 420

Figure A7.14 Western blots of sera reactivity of participants coded (A) 74 to 77, (B) 7 to 65, and (C) 47 to 68, to *B. oleronius* proteins in erythematotelangiectatic rosacea study 420

Figure A7.15 Serum reactivity of participant 1 to 14 to *B. oleronius* protein in *Demodex*-related blepharitis study (Trial 1)..... 424

Figure A7.16 Serum reactivity of participant 1 to 14 to *B. oleronius* protein in *Demodex*-related blepharitis study (Trial 2)..... 424

Figure A7.17 Serum reactivity of participant 15 to 33 to *B. oleronius* protein in *Demodex*-related blepharitis study (Trial 1)..... 425

Figure A7.18 Serum reactivity of participant 15 to 33 to *B. oleronius* protein in *Demodex*-related blepharitis study (Trial 2)..... 425

Figure A7.19 Serum reactivity of participant 34 to 46 to *B. oleronius* protein in *Demodex*-related blepharitis study (Trial 1)..... 426

Figure A7.20 Serum reactivity of participant 34 to 46 to *B. oleronius* protein in *Demodex*-related blepharitis study (Trial 2)..... 426

Figure A7.21 Serum reactivity of participant 49 to 61 to *B. oleronius* protein in *Demodex*-related blepharitis study (Trial 1)..... 427

Figure A7.22 Serum reactivity of participant 49 to 61 to *B. oleronius* protein in *Demodex*-related blepharitis study (Trial 2)..... 427

Figure A7.23 Serum reactivity of participant 62 to 71 to *B. oleronius* protein in *Demodex*-related blepharitis study (Trial 1)..... 428

Figure A7.24 Serum reactivity of participant 62 to 71 to *B. oleronius* protein in *Demodex*-related blepharitis study (Trial 2)..... 428

Figure A7.25 Serum reactivity of participant 72 to 82 to *B. oleronius* protein in *Demodex*-related blepharitis study (Trial 1)..... 429

Figure A7.26 Serum reactivity of participant 72 to 82 to *B. oleronius* protein in *Demodex*-related blepharitis study (Trial 2)..... 429

Figure A7.27 Serum reactivity of participant 83 to 94 to *B. oleronius* protein in *Demodex*-related blepharitis study (Trial 1)..... 430

Figure A7.28 Serum reactivity of participant 83 to 94 to *B. oleronius* protein in *Demodex*-related blepharitis study (Trial 2)..... 430

Figure A7.29 Serum reactivity of participant 96 to 102 to *B. oleronius* protein in *Demodex*-related blepharitis study (Trial 1)..... 431

Figure A7.30 Serum reactivity of participant 96 to 102 to *B. oleronius* protein in *Demodex*-related blepharitis study (Trial 2)..... 431

Appendix: List of Tables

Table A3.1 Fold change of LC/MS protein band identities from 1-D SDS-PAGE *B. oleronius* cultures under different environmental conditions 393

Table A7.1 List of study participants in erythematotelangiectatic rosacea study and serum reactivity to *B. oleronius* protein 408

Table A7.2 List of study participants in *Demodex*-related blepharitis study and serum reactivity to *B. oleronius* protein 421

Table A3.1 Fold change of LC/MS protein band identities from 1-D SDS-PAGE *B. oleronius* cultures under different environmental conditions. Fold change values are relative to the optimal environmental condition of the *B. oleronius* residing in the hindgut of the *Demodex* mite (Sample number 1 at pH 8) (nutrient broth medium (pH 8), aerobic, - 10 mM H_2O_2, 30°C).

Band Number	Protein Identity	pH of Medium	Environmental Culture Condition															
			1	2	3	4	5	6	7	8	9	10	11	12	13	14	15	16
1	Molecular Chaperone GroEL	pH 6	0.7	1.3	0.5	0.7	1.5	0.6	0.4	0.7	0.4	0.9	0.6	0.5	0.8	0.8	0.5	0.6
		pH 7	1.1	1.5	1.3	0.5	0.8	1.7	1.2	0.8	0.8	0.6	0.5	0.6	0.9	1.0	0.8	0.8
		pH 8	1.0	0.5	0.5	0.4	0.9	1.0	0.8	1.2	0.7	1.4	1.2	0.5	1.0	1.0	0.7	0.9
2	30S Ribosomal Protein S1	pH 6	1.1	1.4	0.7	0.9	1.6	0.8	0.5	0.7	0.9	1.7	1.1	1.0	1.0	1.0	0.8	0.9
		pH 7	1.4	1.5	1.9	0.7	1.3	1.9	1.6	1.0	1.4	1.2	1.3	1.4	1.4	1.4	1.2	1.4
		pH 8	1.0	0.9	0.9	0.7	1.2	1.1	1.2	1.3	0.7	1.2	1.8	1.1	1.3	1.1	1.3	1.1
3	Cyclase	pH 6	0.9	0.8	0.4	0.5	1.2	0.7	0.4	0.6	0.8	1.5	1.1	0.9	0.6	0.6	0.8	1.0
		pH 7	0.5	0.6	1.3	0.6	0.8	1.0	1.2	0.9	1.1	0.9	1.0	1.1	1.0	1.2	1.1	1.2
		pH 8	1.0	0.8	0.7	0.8	1.1	0.6	1.2	1.2	0.4	0.7	1.3	0.7	1.2	1.2	0.7	1.0
4	Thioredoxin	pH 6	1.2	0.8	0.6	0.7	1.0	0.8	0.4	0.7	0.9	1.3	1.2	1.1	0.7	0.6	0.7	0.9
		pH 7	0.9	0.8	1.4	1.1	1.1	1.0	1.1	0.9	1.1	0.8	1.5	1.6	1.2	1.4	1.3	1.2
		pH 8	1.0	0.7	0.9	0.9	0.8	0.6	0.9	0.9	0.5	0.6	1.5	1.0	1.2	1.1	0.6	1.1
5	1-Pyrroline-5-Carboxylate Dehydrogenase	pH 6	0.5	0.8	0.2	0.4	1.3	0.4	0.2	0.4	0.5	1.1	0.6	0.5	0.9	0.8	0.5	0.6
		pH 7	0.9	1.3	1.2	0.2	0.4	1.4	1.0	0.7	1.1	0.7	0.5	0.4	0.9	1.0	0.8	1.1
		pH 8	1.0	0.5	0.5	0.4	0.9	0.8	0.9	1.5	0.8	1.2	1.5	0.6	1.2	1.0	1.1	1.2
6	Enolase	pH 6	0.6	0.8	0.4	0.6	1.8	0.5	0.4	0.8	0.8	1.8	1.0	1.0	1.1	1.2	1.1	1.3
		pH 7	1.1	0.6	1.8	0.4	0.6	1.8	1.8	1.0	1.5	0.9	0.7	0.9	1.0	1.3	1.3	1.6
		pH 8	1.0	0.5	0.7	0.4	0.9	0.7	1.6	2.3	0.7	1.2	2.2	0.9	1.4	1.0	1.9	1.8
7	Enolase	pH 6	0.6	0.9	0.3	0.5	1.5	0.5	0.5	0.7	0.7	1.5	0.9	0.9	1.2	1.1	1.0	1.1
		pH 7	0.9	0.5	1.5	0.4	0.6	1.7	1.4	0.7	1.3	0.9	0.6	0.8	0.9	1.2	1.4	1.6
		pH 8	1.0	0.7	0.7	0.5	1.2	1.0	1.4	1.8	0.5	1.0	2.0	0.8	1.2	0.7	1.8	1.2
8	Peptidase M29	pH 6	1.1	1.0	0.3	0.6	1.6	0.8	0.6	0.8	1.0	2.2	1.4	1.0	1.2	1.1	1.1	1.3
		pH 7	0.8	0.6	1.8	0.9	0.8	1.5	1.3	0.9	1.2	0.6	0.7	0.8	0.6	0.9	1.1	1.5
		pH 8	1.0	0.8	0.7	0.6	0.7	0.7	1.2	2.4	0.5	1.2	2.1	0.7	1.1	1.1	1.0	1.4

Table A3.1 (Continued) Fold change of LC/MS protein band identities from 1-D SDS-PAGE *B. oleronius* cultures under different environmental conditions. Fold change values are relative to the optimal environmental condition of the *B. oleronius* residing in the hindgut of the *Demodex* mite (Sample number 1 at pH 8) (nutrient broth medium (pH 8), aerobic, - 10 mM H_2O_2, 30°C).

Band Number	Protein Identity	pH of Medium	Environmental Culture Condition															
			1	2	3	4	5	6	7	8	9	10	11	12	13	14	15	16
9	Inorganic Pyrophosphatase	pH 6	1.1	1.5	0.6	0.9	3.0	0.7	0.5	1.0	1.4	2.9	2.0	1.5	2.6	2.3	1.8	2.5
		pH 7	1.6	1.5	3.6	1.3	1.2	3.2	3.5	2.2	1.9	1.3	1.3	1.5	1.6	1.5	2.7	3.1
		pH 8	1.0	1.0	1.2	1.1	0.4	1.2	2.5	4.6	0.9	3.1	3.1	1.0	2.3	2.6	2.8	2.0
10	Putative Secreted Protein	pH 6	0.8	0.7	0.4	0.4	1.3	0.4	0.4	0.6	1.0	1.7	1.1	0.7	1.4	1.4	1.1	1.6
		pH 7	1.0	1.1	2.0	0.6	0.5	1.1	1.3	0.8	1.1	1.0	1.2	0.8	1.0	1.2	1.4	1.0
		pH 8	1.0	0.5	0.8	0.5	-0.1	0.3	1.3	2.5	0.4	1.7	1.5	0.5	0.8	1.2	1.5	1.4
11	Peptidase S8	pH 6	1.1	1.5	0.6	0.9	3.0	0.7	0.5	1.0	1.4	2.9	2.0	1.5	2.6	2.3	1.8	2.5
		pH 7	1.6	1.5	3.6	1.3	1.2	3.2	3.5	2.2	1.9	1.3	1.3	1.5	1.6	1.5	2.7	3.1
		pH 8	1.0	1.0	1.2	1.1	0.4	1.2	2.5	4.6	0.9	3.1	3.1	1.0	2.3	2.6	2.8	2.0
12	Peptidase S8	pH 6	0.9	0.9	0.4	0.6	0.9	0.6	0.4	0.5	0.8	1.4	0.9	0.9	0.7	0.5	0.8	1.2
		pH 7	0.5	0.4	1.2	0.6	0.4	0.7	1.0	0.5	0.4	0.1	0.4	0.4	0.0	0.1	0.3	0.4
		pH 8	1.0	0.6	1.0	1.2	0.7	0.6	1.0	1.5	0.2	0.4	1.1	0.5	0.9	0.9	0.6	0.8
13	Clp Protease ClpX	pH 6	1.0	1.1	0.4	0.8	2.0	0.5	0.4	0.8	1.3	2.6	1.6	1.3	1.8	1.8	1.6	2.3
		pH 7	0.8	0.9	2.8	0.7	0.5	1.8	2.9	2.7	2.0	1.4	1.8	2.0	2.3	1.9	2.0	2.7
		pH 8	1.0	0.4	1.1	0.8	0.1	0.7	2.0	3.8	0.4	1.7	3.4	1.2	1.9	1.5	1.9	2.1
14	ATP F0F1 Synthase Subunit Beta	pH 6	1.1	1.4	0.6	0.8	1.5	0.7	0.4	0.6	0.8	1.6	1.0	0.9	0.9	0.8	0.7	0.8
		pH 7	1.4	1.8	1.3	0.9	1.3	1.6	1.4	0.7	1.6	1.6	1.3	1.4	1.5	1.6	1.2	1.2
		pH 8	1.0	0.8	0.7	0.5	1.2	0.8	1.1	1.2	0.8	1.3	1.8	1.0	1.3	0.8	1.0	1.2
15	Peroxidase	pH 6	2.2	2.1	0.7	1.3	1.6	0.7	0.6	0.9	0.8	2.0	1.1	0.9	1.0	0.8	0.8	1.0
		pH 7	0.9	1.6	1.5	0.9	1.5	2.2	1.3	0.8	1.2	0.9	0.9	1.0	0.8	1.0	1.1	1.3
		pH 8	1.0	0.7	0.9	0.9	1.0	0.8	1.3	1.6	0.5	1.0	1.9	1.0	1.2	1.1	0.8	1.3
16	Thioredoxin	pH 6	1.2	0.7	0.4	0.5	1.3	0.8	0.4	0.7	1.1	1.5	1.0	0.8	0.7	0.5	0.7	1.2
		pH 7	0.6	0.3	0.6	0.5	0.4	0.3	0.5	0.2	1.1	0.4	0.5	0.7	0.3	0.3	0.5	0.7
		pH 8	1.0	0.6	0.7	0.8	0.5	0.6	0.8	2.0	0.2	0.6	1.5	0.6	1.0	1.2	0.8	1.1

Table A3.1 (Continued) Fold change of LC/MS protein band identities from 1-D SDS-PAGE *B. oleronius* cultures under different environmental conditions. Fold change values are relative to the optimal environmental condition of the *B. oleronius* residing in the hindgut of the *Demodex* mite (Sample number 1 at pH 8) (nutrient broth medium (pH 8), aerobic, - 10 mM H_2O_2, 30°C).

Band Number	Protein Identity	pH of Medium	Environmental Culture Condition															
			1	2	3	4	5	6	7	8	9	10	11	12	13	14	15	16
17	Fructose-Bisphosphate Aldolase	pH 6	1.0	0.8	0.4	0.5	1.1	0.7	0.4	0.7	0.8	1.4	0.9	0.8	0.5	0.4	0.6	1.1
		pH 7	0.6	0.3	0.8	0.5	0.3	0.5	0.7	0.4	1.2	0.6	0.7	0.7	0.4	0.7	1.1	1.5
		pH 8	1.0	0.5	0.8	0.9	0.6	0.6	1.5	1.7	0.4	0.7	1.6	0.8	0.9	1.2	0.8	1.1
18	Elongation Factor Tu	pH 6	0.5	0.8	0.2	0.4	1.3	0.4	0.2	0.4	0.5	1.1	0.6	0.5	0.9	0.8	0.5	0.6
		pH 7	0.9	1.3	1.2	0.2	0.4	1.4	1.0	0.7	1.1	0.7	0.5	0.4	0.9	1.0	0.8	1.1
		pH 8	1.0	0.5	0.5	0.4	0.9	0.8	0.9	1.5	0.8	1.2	1.5	0.6	1.2	1.0	1.1	1.2
19	Aconitate Hydratase	pH 6	1.0	1.1	0.4	0.8	2.0	0.5	0.4	0.8	1.3	2.6	1.6	1.3	1.8	1.8	1.6	2.3
		pH 7	0.8	0.9	2.8	0.7	0.5	1.8	2.9	2.7	2.0	1.4	1.8	2.0	2.3	1.9	2.0	2.7
		pH 8	1.0	0.4	1.1	0.8	0.1	0.7	2.0	3.8	0.4	1.7	3.4	1.2	1.9	1.5	1.9	2.1
20	Sugar ABC Transporter Substrate-Binding Protein	pH 6	0.7	1.3	0.5	0.7	1.5	0.6	0.4	0.7	0.4	0.9	0.6	0.5	0.8	0.8	0.5	0.6
		pH 7	1.1	1.5	1.3	0.5	0.8	1.7	1.2	0.8	0.8	0.6	0.5	0.6	0.9	1.0	0.8	0.8
		pH 8	1.0	0.5	0.5	0.4	0.9	1.0	0.8	1.2	0.7	1.4	1.2	0.5	1.0	1.0	0.7	0.9
21	Superoxide Dismutase	pH 6	0.8	0.6	0.2	0.4	1.2	0.6	0.4	0.6	0.7	1.5	1.0	0.8	1.0	0.8	0.8	1.1
		pH 7	0.9	0.7	1.8	0.8	0.7	1.3	1.2	0.8	1.0	0.5	1.0	0.9	0.6	0.9	0.7	1.0
		pH 8	1.0	0.6	0.7	0.4	0.7	0.6	1.3	2.0	0.4	1.0	2.0	0.8	1.0	0.9	1.0	1.3
22	Protein prkA	pH 6	0.8	1.3	0.4	0.7	1.6	0.5	0.5	0.7	0.7	1.5	0.9	0.9	1.2	1.1	1.0	1.1
		pH 7	0.9	0.5	1.5	0.4	0.6	1.7	1.4	0.7	1.3	0.9	0.6	0.8	0.9	1.2	1.4	1.6
		pH 8	1.0	0.7	0.7	0.5	1.2	1.0	1.4	1.8	0.5	1.0	2.0	0.8	1.2	0.7	1.8	1.2
23	ATP F0F1 Synthase Subunit Beta	pH 6	1.1	1.4	0.6	0.8	1.5	0.7	0.4	0.6	0.8	1.6	1.0	0.9	0.9	0.8	0.7	0.8
		pH 7	1.4	1.8	1.3	0.9	1.3	1.6	1.4	0.7	1.6	1.6	1.3	1.4	1.5	1.6	1.2	1.2
		pH 8	1.0	0.8	0.7	0.5	1.2	0.8	1.1	1.2	0.8	1.3	1.8	1.0	1.3	0.8	1.0	1.2
24	Flagellin	pH 6	1.1	1.4	0.7	0.9	1.6	0.8	0.5	0.7	0.9	1.7	1.1	1.0	1.0	1.0	0.8	0.9
		pH 7	1.4	1.5	1.9	0.7	1.3	1.9	1.6	1.0	1.4	1.2	1.3	1.4	1.4	1.4	1.2	1.4
		pH 8	1.0	0.9	0.9	0.7	1.2	1.1	1.2	1.3	0.7	1.2	1.8	1.1	1.3	1.1	1.3	1.1
25	C4-Dicarboxylate ABC Transporter Substrate-Binding Protein	pH 6	1.1	0.7	0.3	0.6	1.5	0.6	0.4	0.6	0.7	1.5	1.0	0.8	1.0	0.8	0.8	1.1
		pH 7	0.9	0.7	1.8	0.8	0.7	1.3	1.2	0.8	1.0	0.5	1.0	0.9	0.6	0.9	0.7	1.0
		pH 8	1.0	0.6	0.7	0.4	0.7	0.6	1.3	2.0	0.4	1.0	2.0	0.8	1.0	0.9	1.0	1.3

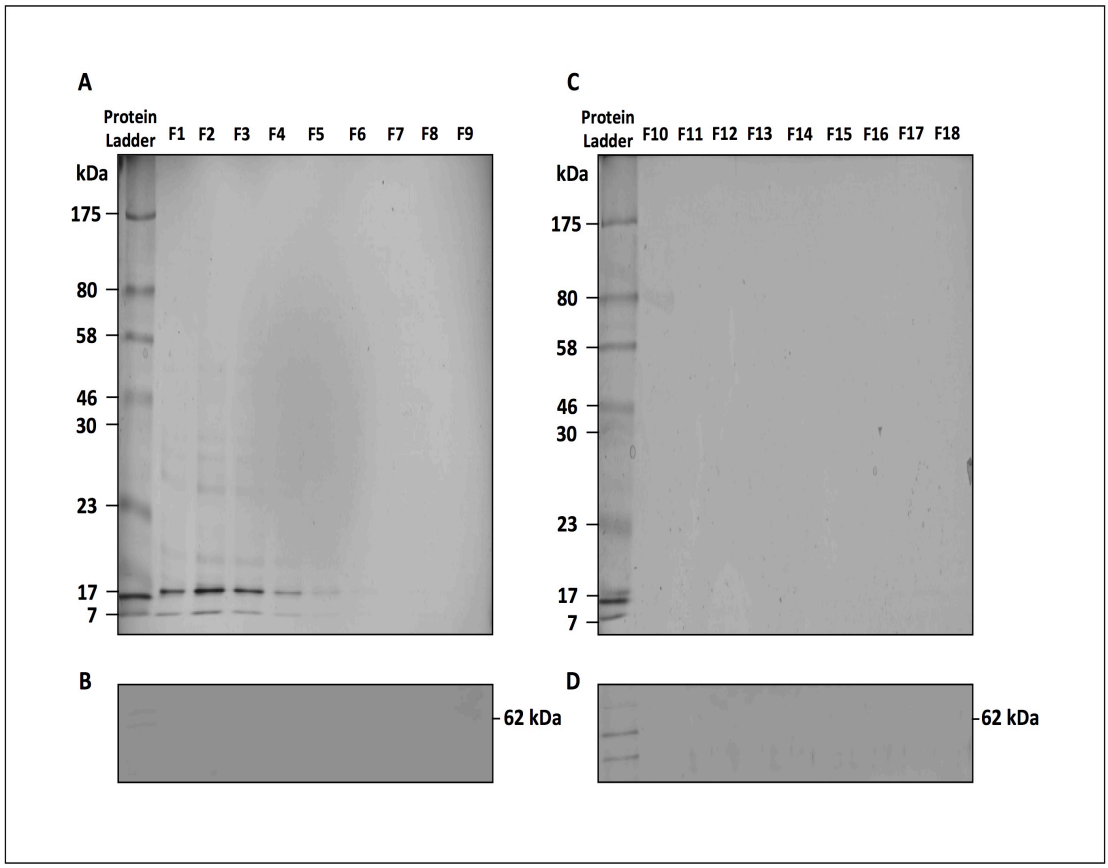

Figure A4.1 Visualization of crude *B. oleronius* protein ÄKTA FPLC™ fractions 1 to 18 by Coomassie Staining and Western blotting. Preparation of pure *B. oleronius* protein by assessing fractions for the abundance of the protein of interest, the 62 kDa *B. oleronius* protein. (**A**) Fractions 1 to 9 (F1 – F9) of crude *B. oleronius* protein eluted from the Q-sepharose™ high performance beads of the ÄKTA FPLC™ column were resolved by 1-D SDS-PAGE with visualization by Coomassie staining, and (**B**) assessment of reactivity to anti-62 kDa *B. oleronius* protein by western blotting. (**C**) Fractions 10 to 18 (F10 – F18) of crude *B. oleronius* protein eluted from the Q-sepharose™ high performance beads of the ÄKTA FPLC™ column were resolved by 1-D SDS-PAGE with visualization by Coomassie staining, and (**D**) assessment of reactivity to anti-62 kDa protein by western blotting.

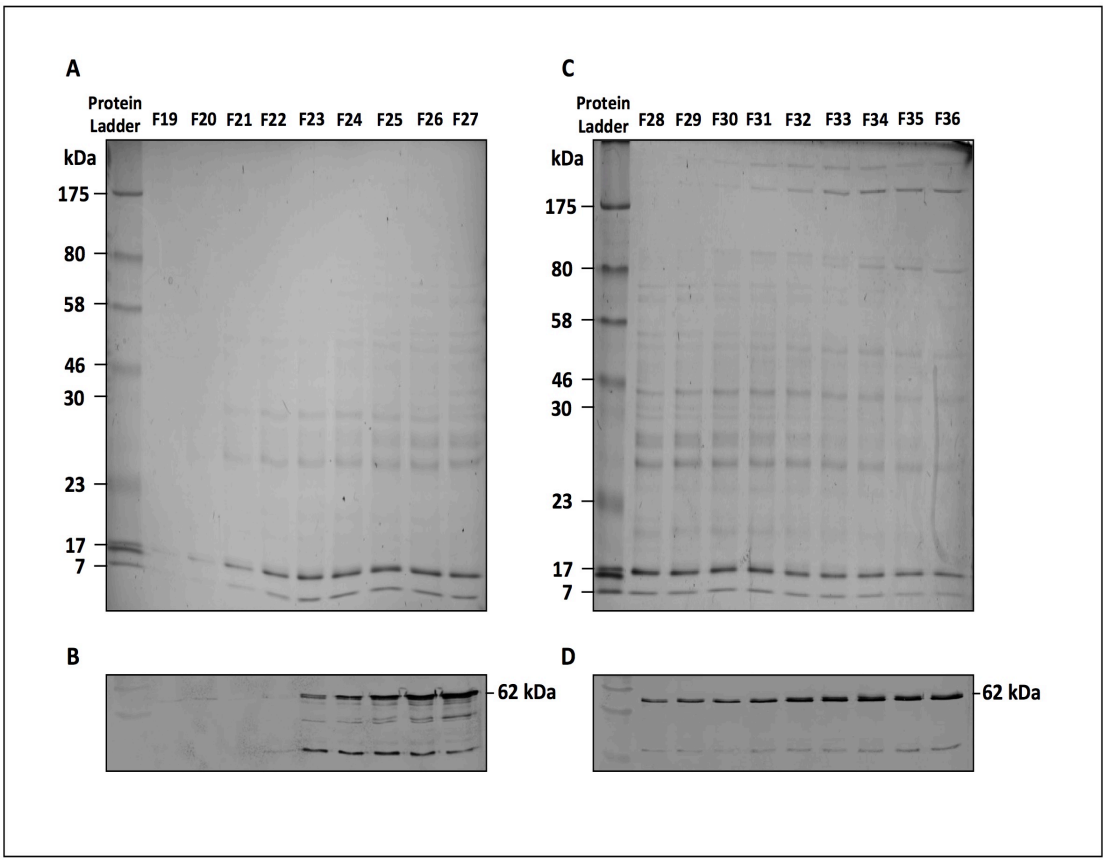

Figure A4.2 Visualization of crude *B. oleronius* protein ÄKTA FPLC™ fractions 19 to 36 by Coomassie Staining and Western blotting. Preparation of pure *B. oleronius* protein by assessing fractions for the abundance of the protein of interest, the 62 kDa *B. oleronius* protein. (**A**) Fractions 19 to 27 (F19 – F27) of crude *B. oleronius* protein eluted from the Q-sepharose™ high performance beads of the ÄKTA FPLC™ column were resolved by 1-D SDS-PAGE with visualization by Coomassie staining, and (**B**) assessment of reactivity to anti-62 kDa *B. oleronius* protein by western blotting. (**C**) Fractions 28 to 36 (F28 – F36) of crude *B. oleronius* protein eluted from the Q-sepharose™ high performance beads of the ÄKTA FPLC™ column were resolved by 1-D SDS-PAGE with visualization by Coomassie staining, and (**D**) assessment of reactivity to anti-62 kDa protein by western blotting.

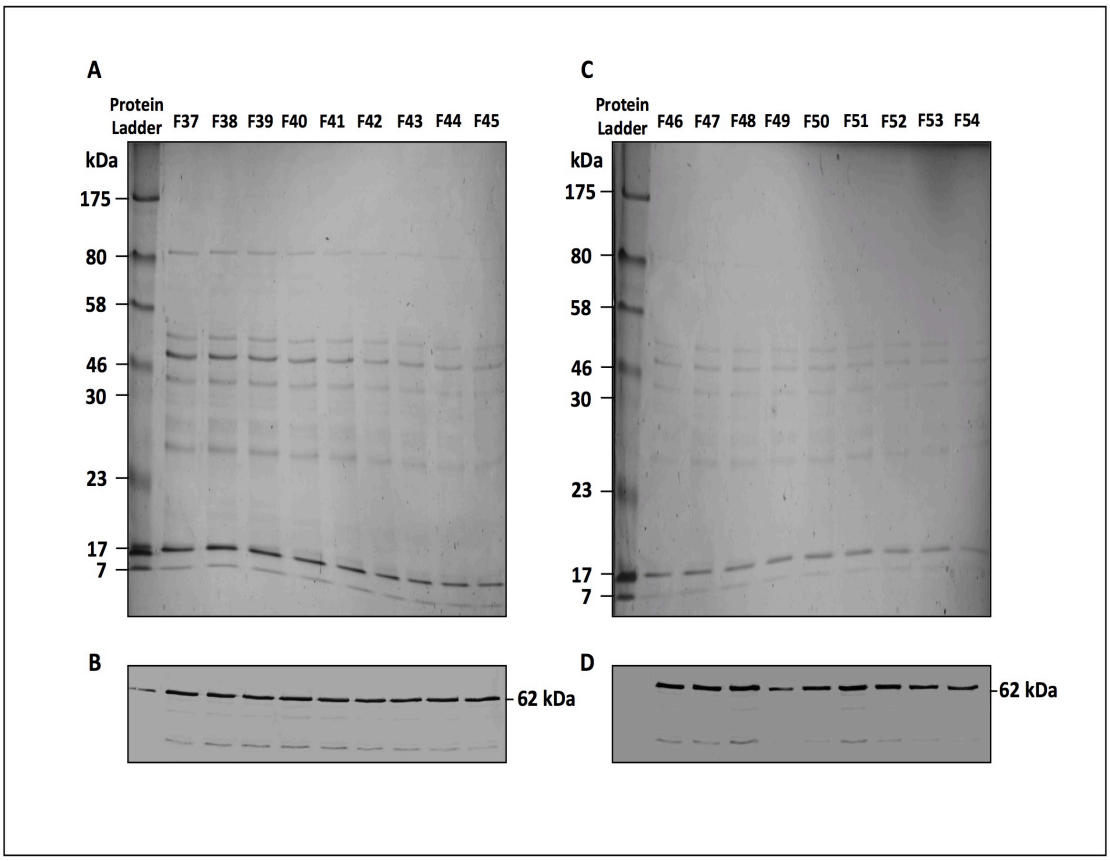

Figure A4.3 Visualization of crude *B. oleronius* protein ÄKTA FPLC™ fractions 37 to 54 by Coomassie Staining and Western blotting. Preparation of pure *B. oleronius* protein by assessing fractions for the abundance of the protein of interest, the 62 kDa *B. oleronius* protein. (**A**) Fractions 37 to 45 (F37 – F45) of crude *B. oleronius* protein eluted from the Q-sepharose™ high performance beads of the ÄKTA FPLC™ column were resolved by 1-D SDS-PAGE with visualization by Coomassie staining, and (**B**) assessment of reactivity to anti-62 kDa *B. oleronius* protein by western blotting. (**C**) Fractions 46 to 54 (F46 – F54) of crude *B. oleronius* protein eluted from the Q-sepharose™ high performance beads of the ÄKTA FPLC™ column were resolved by 1-D SDS-PAGE with visualization by Coomassie staining, and (**D**) assessment of reactivity to anti-62 kDa protein by western blotting.

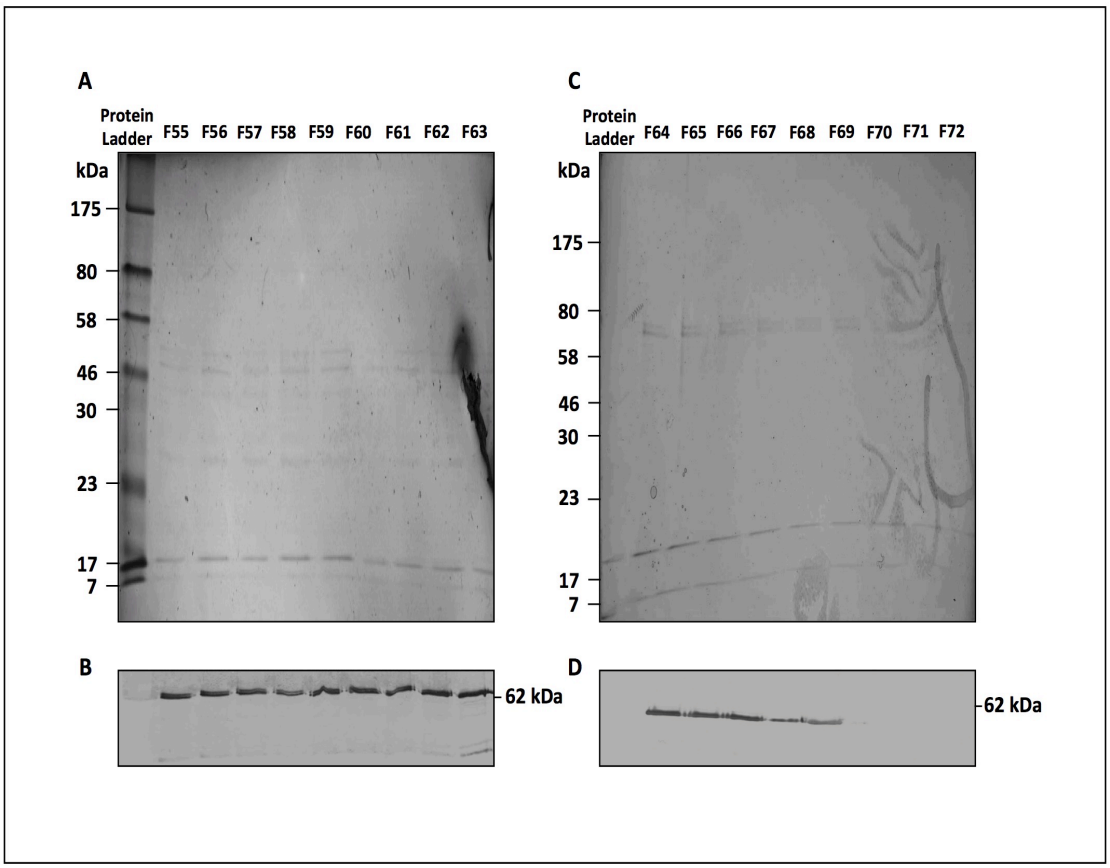

Figure A4.4 Visualization of crude *B. oleronius* protein ÄKTA FPLC™ fractions 55 to 72 by Coomassie Staining and Western blotting. Preparation of pure *B. oleronius* protein by assessing fractions for the abundance of the protein of interest, the 62 kDa *B. oleronius* protein. (**A**) Fractions 55 to 63 (F55 – F63) of crude *B. oleronius* protein eluted from the Q-sepharose™ high performance beads of the ÄKTA FPLC™ column were resolved by 1-D SDS-PAGE with visualization by Coomassie staining, and (**B**) assessment of reactivity to anti-62 kDa *B. oleronius* protein by western blotting. (**C**) Fractions 64 to 72 (F64 – F72) of crude *B. oleronius* protein eluted from the Q-sepharose™ high performance beads of the ÄKTA FPLC™ column were resolved by 1-D SDS-PAGE with visualization by Coomassie staining, and (**D**) assessment of reactivity to anti-62 kDa protein by western blotting.

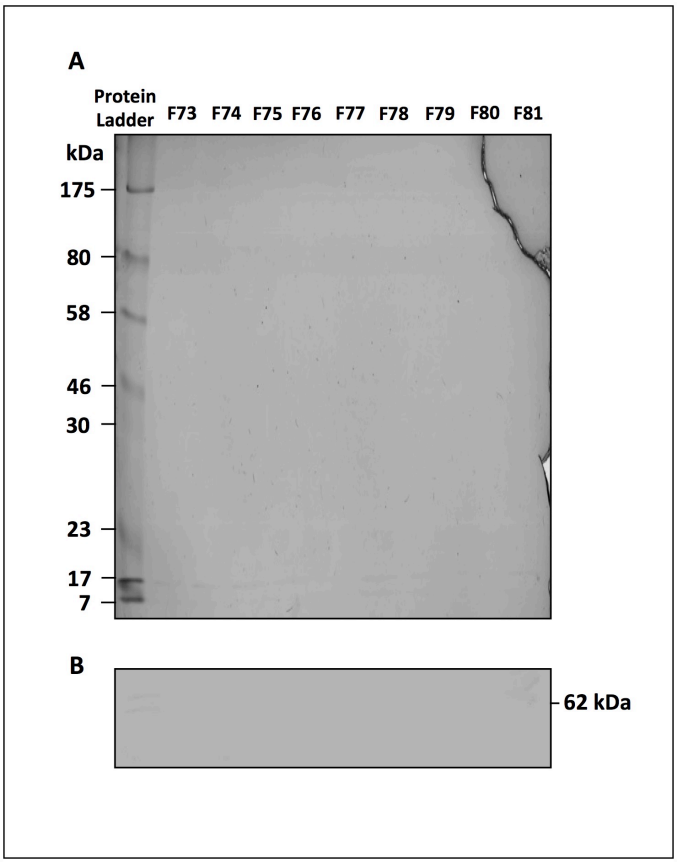

Figure A4.5 Visualization of crude *B. oleronius* protein ÄKTA FPLC™ fractions 73 to 81 by Coomassie Staining and Western blotting. Preparation of pure *B. oleronius* protein by assessing fractions for the abundance of the protein of interest, the 62 kDa *B. oleronius* protein. (**A**) Fractions 73 to 81 (F73 – F81) of crude *B. oleronius* protein eluted from the Q-sepharose™ high performance beads of the ÄKTA FPLC™ column were resolved by 1-D SDS-PAGE with visualization by Coomassie staining, and (**B**) assessment of reactivity to anti-62 kDa *B. oleronius* protein by western blotting.

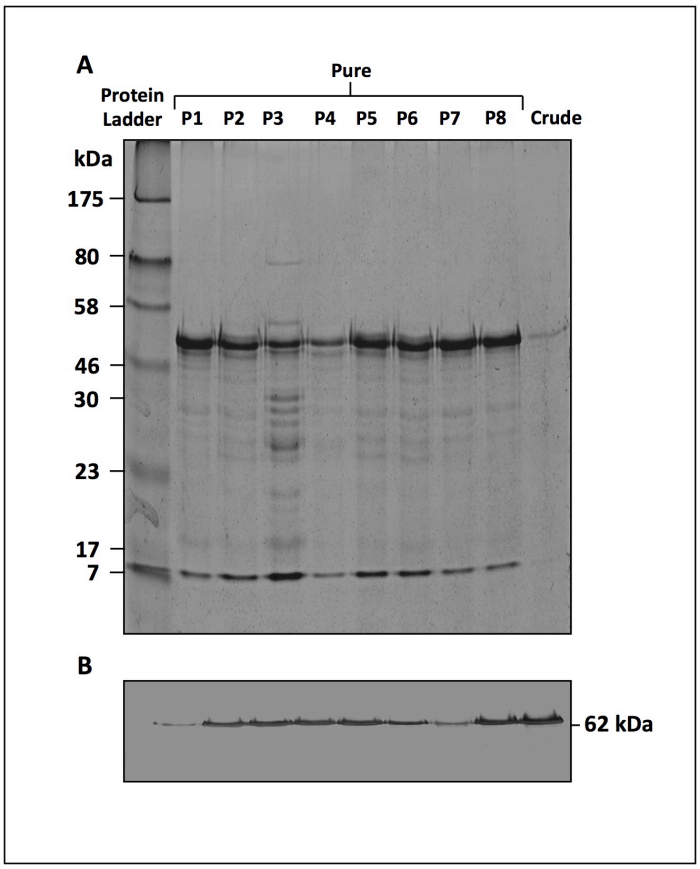

Figure A4.6 Visualization of ÄKTA FPLC™ generated pure *B. oleronius* protein preparation fractions 1 to 8 by Coomassie Staining and Western blotting. (**A**) Fractions of pure *B. oleronius* protein preparations labeled P1 to P8 (P1 – P8) obtained from separation of crude *B. oleronius* protein from the Q-sepharose™ high performance beads of the ÄKTA FPLC™ column were resolved by 1-D SDS-PAGE with visualization by Coomassie staining, and (**B**) assessment of reactivity to anti-62 kDa *B. oleronius* protein by Western blotting. Crude *B. oleronius* protein (20 µg) was resolved, and immunoblotted alongside the pure *B. oleronius* protein preparations to assess the abundance and purification of the anti-62 kDa protein.

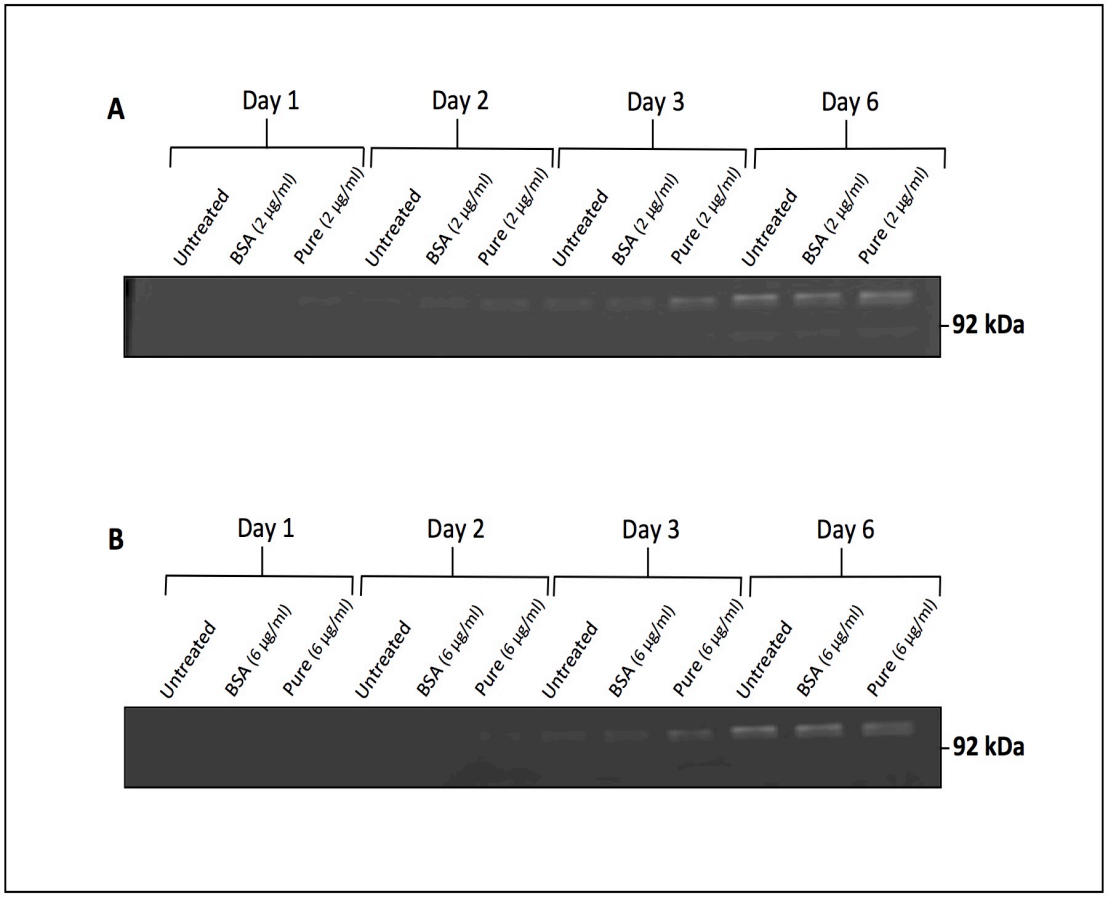

Figure A4.7 A representative 1-D gelatinase zymogram (10% w/v) gel image to assess MMP-9 activity present in hTCEpi cell supernatants following exposure to pure *B. oleronius* proteins. A representative 1-D gelatinase zymogram (10% w/v) gel image of filter-concentrated hTCEpi supernatant samples exposed to (**A**) 2 µg/ml or (**B**) 6 µg/ml pure *B. oleronius* protein. Corneal epithelial (hTCEpi) cell samples were resolved using gelatinase zymogram (10%, w/v) gels to detect MMP-9 activity (92 kDa). The gel was stained and de-stained using Coomassie brilliant blue staining protocol (Section 2.16.1). BSA (2 and 6 µg/ml) was used as a protein control for the assay.

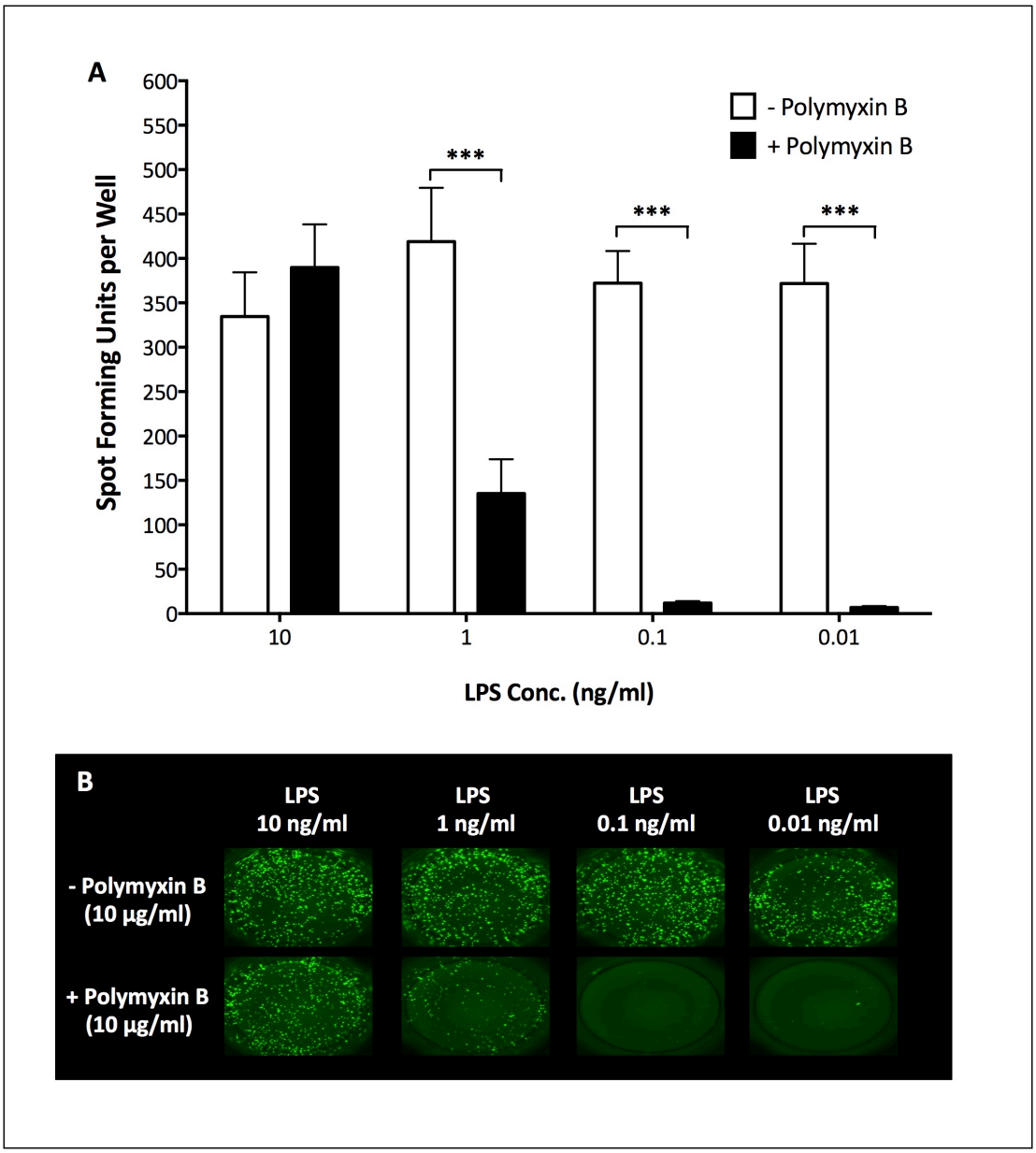

Figure A6.1 Assessment of endotoxin activity and IL-6 secretion in PBMC exposed to LPS by FluoroSpot. (**A**) Investigating the endotoxin properties of pure and crude *B. oleronius* protein preparations through FluoroSpot, by performing titrations of LPS (10 – 0.01 ng/ml) to examine spot formation induced by endotoxin activity, and inhibition of endotoxin activity by polymyxin B (10 µg/ml) at 0.1 ng/ml LPS. The inhibition of spot formation at 0.1 ng/ml and 0.001 ng/ml LPS following the addition of polymyxin B was significant. (**B**) Representative FluoroSpot images of spot formation and inhibition were recorded. (n = 3, experiment performed in triplicate). (Significance: *** = $p < 0.001$).

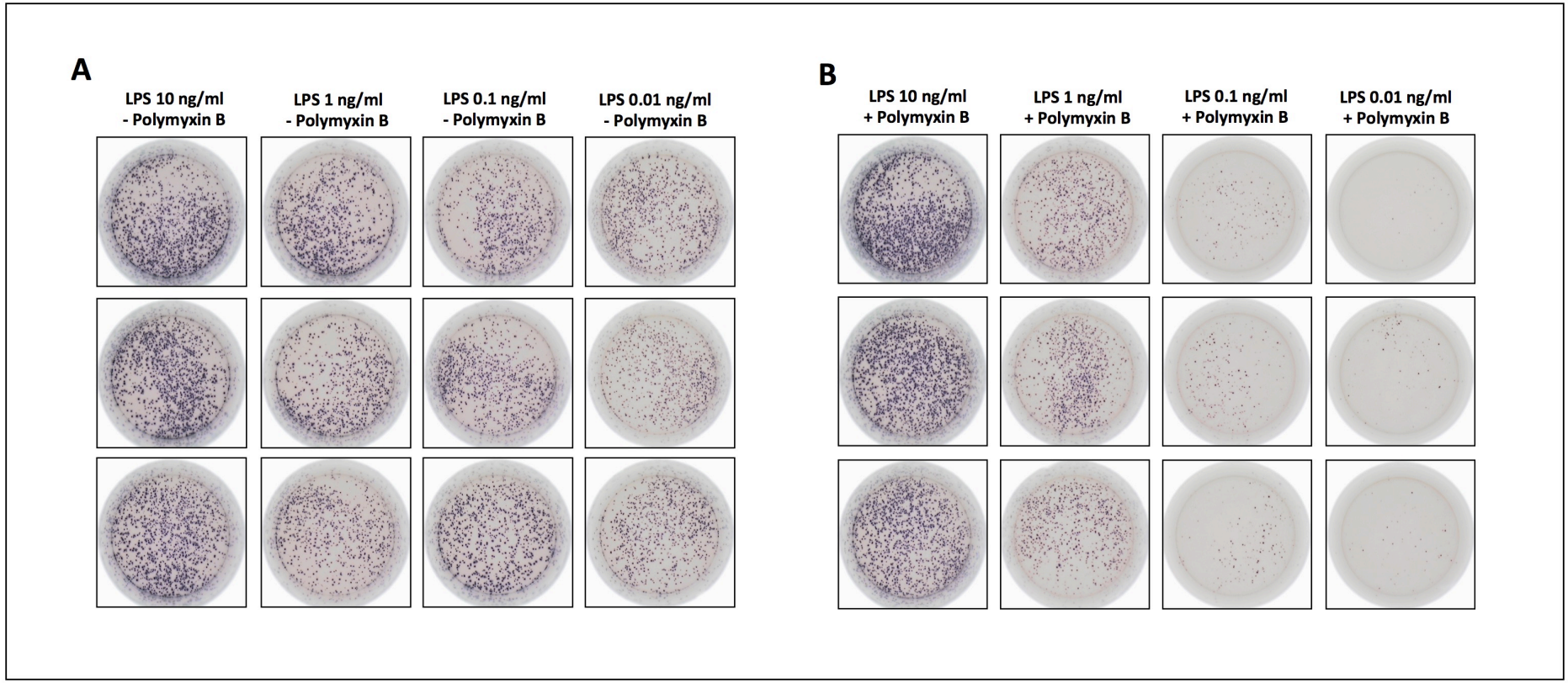

Figure A6.2 Representative ELISpot images of assessment of endotoxin activity and TNF-α secretion in PBMC exposed to LPS (A) without, or (B) with the addition of polymyxin B (10 µg/ml). Investigating the endotoxin properties of pure and crude *B. oleronius* protein preparations through TNF-α ELISpot, by performing titrations of LPS (10 – 0.01 ng/ml) to examine spot formation induced by endotoxin activity, and inhibition of endotoxin activity by polymyxin B (10 µg/ml) at 0.1 ng/ml LPS. The inhibition of spot formation at 0.1 ng/ml and 0.001 ng/ml LPS following the addition of polymyxin B was significant. (n = 3, experiment performed in triplicate).

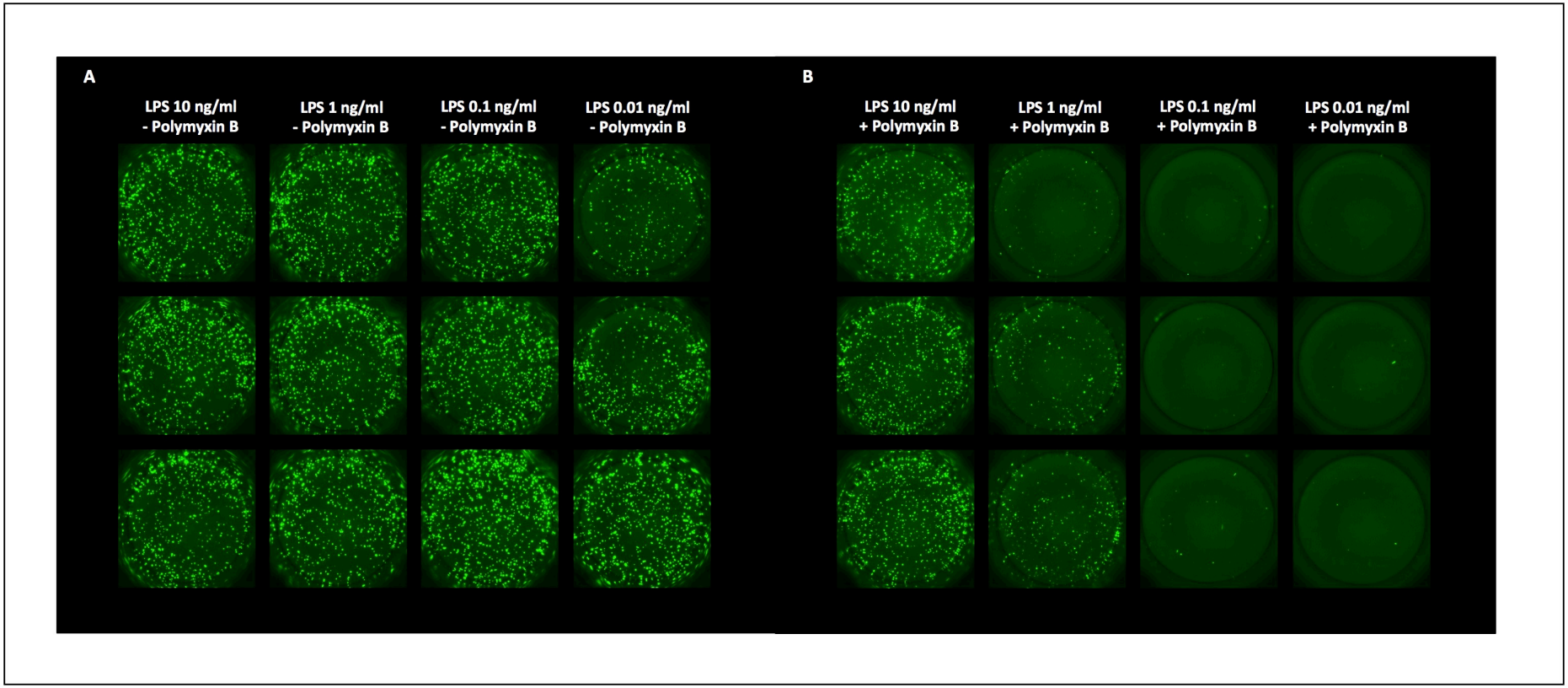

Figure A6.3 Representative FluoroSpot images of assessment of endotoxin activity and IL-6 secretion in PBMC exposed to LPS (A) without, or (B) with the addition of polymyxin B (10 µg/ml). Investigating the endotoxin properties of pure and crude *B. oleronius* protein preparations through IL-6 FluoroSpot, by performing titrations of LPS (10 – 0.01 ng/ml) to examine spot formation induced by endotoxin activity, and inhibition of endotoxin activity by polymyxin B (10 µg/ml) at 0.1 ng/ml LPS. The inhibition of spot formation at 0.1 ng/ml and 0.001 ng/ml LPS following the addition of polymyxin B was significant. (n = 3, experiment performed in triplicate).

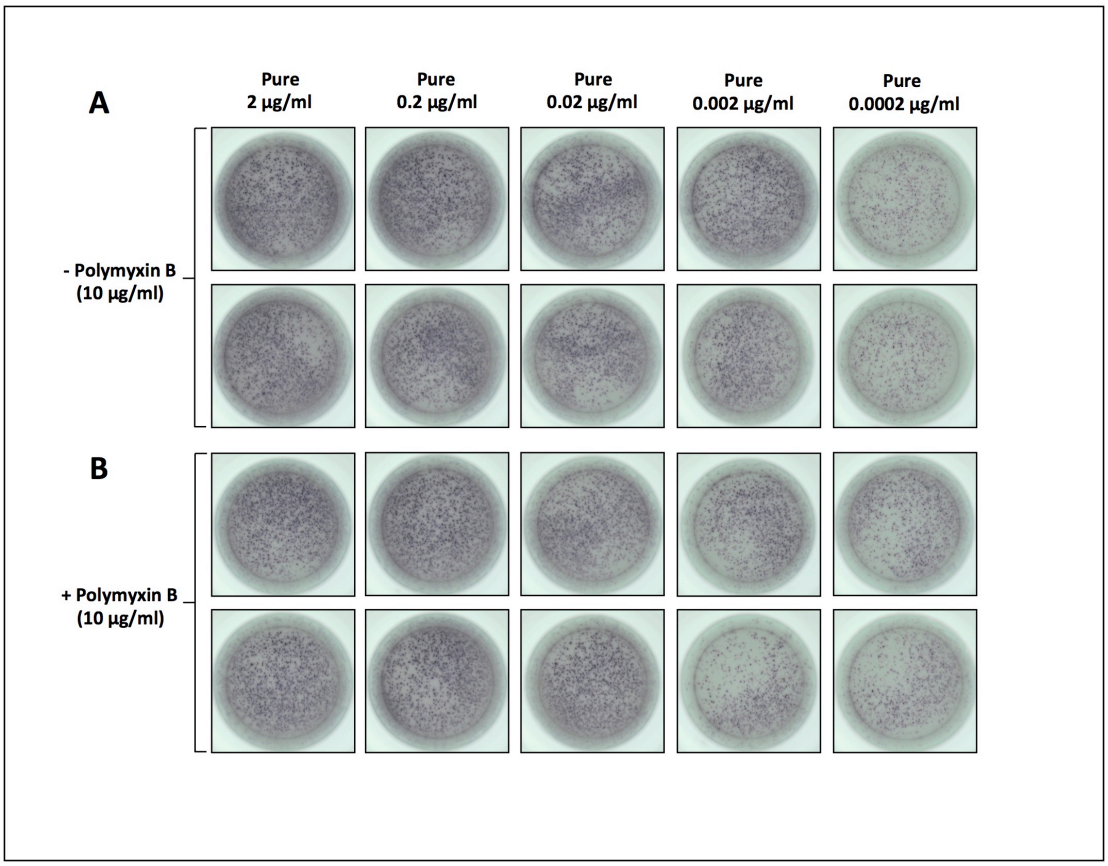

Figure A6.4 Representative ELISpot images of assessment of endotoxin activity and TNF-α secretion in PBMC exposed to pure *B. oleronius* protein (A) without, or (B) with the addition of polymyxin B (10 µg/ml). Investigating the endotoxin properties of pure *B. oleronius* protein preparations (2, 0.2, 0.002, and 0.0002 µg/ml) through TNF-α ELISpot. (n = 3, experiment performed in triplicate).

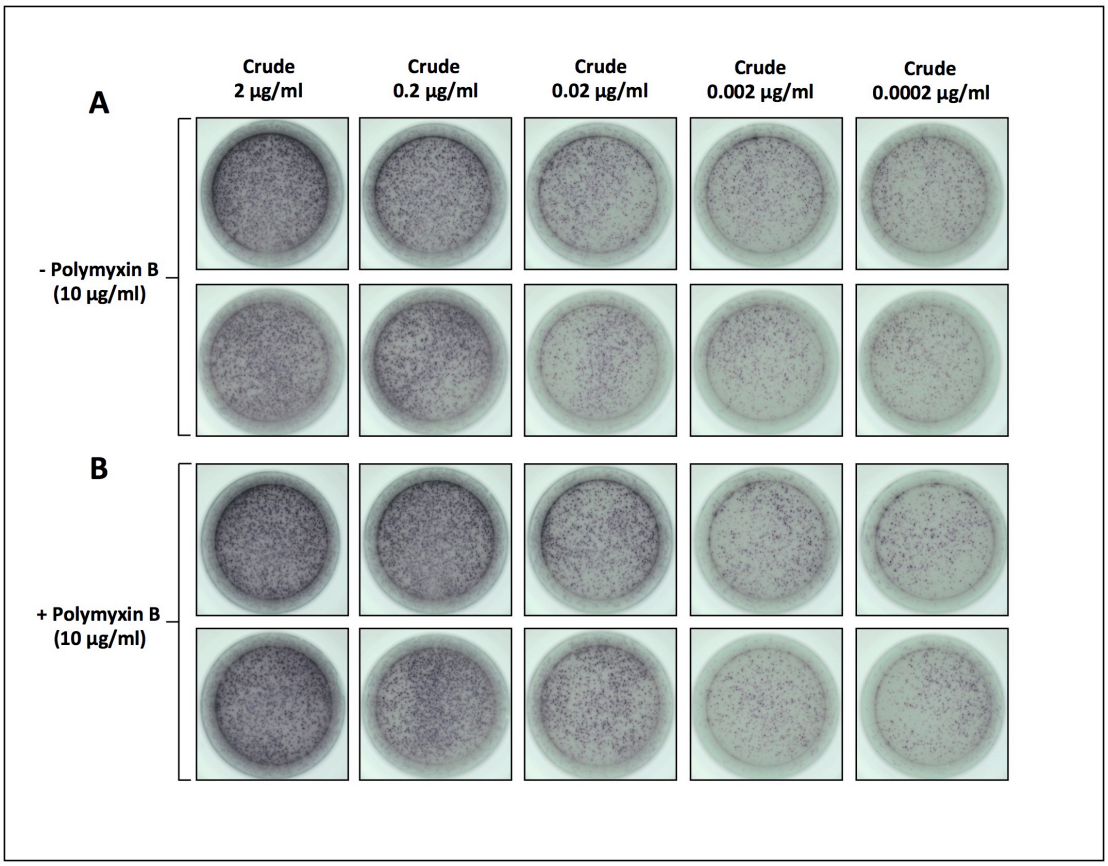

Figure A6.5 Representative ELISpot images of assessment of endotoxin activity and TNF-α secretion in PBMC exposed to crude *B. oleronius* protein (A) without, or (B) with the addition of polymyxin B (10 µg/ml). Investigating the endotoxin properties of crude *B. oleronius* protein (2, 0.2, 0.002, and 0.0002 µg/ml) preparations through TNF-α ELISpot. (n = 3, experiment performed in triplicate).

Table A7.1 List of study participants in erythematotelangiectatic rosacea study and serum reactivity to *B. oleronius* protein. Study population data describing gender, age, skin condition, and reactivity to *B. oleronius* 62 kDa protein for each participant. (-: negative serum-reactivity, +: positive serum-reactivity). (R: rosacea; C: control; AV: acne vulgairs; SD: seborrheic dermatitis).

Serum Code	Gender (M/F)	Age (yrs)	Skin Condition	Serverity of Skin Lesions	Number of *D. folliculorum* on skin / cm2	62-kDa P; 83-kDa P	62-kDa P; 83-kDa A	62-kDa A; 83-kDa P	62-kDa A; 83-kDa A
P2	F	35	R	1	1	+	-	-	-
P3	F	20	R	1	0	-	+	-	-
P4	F	38	R	1	1	-	+	-	-
P5	F	28	R	2	0	-	+	-	-
P6	F	63	R	2	2	-	+	-	-
P7	M	44	R	1	1	-	-	+	-
P8	F	58	R	1	3	-	+	-	-
P9	M	21	R	2	0	+	-	-	-
P11	F	58	R	2	10	-	+	-	-
P12	M	60	R	1	0	-	+	-	-
P13	F	65	R	1	2	-	+	-	-
P14	M	74	R	1	1	-	+	-	-
P15	M	51	R	1	1	+	-	-	-
P16	F	29	R	1	0	-	+	-	-
P17	F	47	R	2	3	-	+	-	-
P18	F	81	R	2	7	-	+	-	-
P19	F	56	R	1	0	-	+	-	-
P20	M	58	R	2	2	-	+	-	-
P22	M	55	R	1	3	-	+	-	-
P24	M	61	R	1	3	-	+	-	-
P25	M	47	R	1	1	+	-	-	-

Table A7.1 (Continued) List of study participants in erythematotelangiectatic rosacea study and serum reactivity to *B. oleronius* protein. Study population data describing gender, age, skin condition, and reactivity to *B. oleronius* 62 kDa protein for each participant. (-: negative serum-reactivity, +: positive serum-reactivity). (R: rosacea; C: control; AV: acne vulgairs; SD: seborrheic dermatitis).

Serum Code	Gender (M/F)	Age (yrs)	Skin Condition	Serverity of Skin Lesions	Number of *D. folliculorum* on skin / cm2	62-kDa P; 83-kDa P	62-kDa P; 83-kDa A	62-kDa A; 83-kDa P	62-kDa A; 83-kDa A
P26	M	58	R	1	1	+	-	-	-
P27	F	60	R	1	5	-	-	+	-
P28	M	52	R	2	3	+	-	-	-
P29	F	48	R	2	0	-	+	-	-
P30	M	42	R	1	8	-	+	-	-
P31	F	33	R	1	0	-	+	-	-
P32	F	52	R	1	0	-	-	+	-
P33	M	47	R	1	5	-	+	-	-
P34	M	35	R	1	1	-	-	+	-
P35	F	52	R	2	10	+	-	-	-
P36	M	36	R	1	1	+	-	-	-
P37	F	34	R	1	3	+	-	-	-
P38	F	38	R	2	0	+	-	-	-
P39	M	37	R	2	1	+	-	-	-
P40	F	37	R	1	0	+	-	-	-
P41	M	69	R	1	2	+	-	-	-
P43	F	59	R	1	3	-	+	-	-
P44	F	37	R	2	0	-	+	-	-
P45	F	20	R	1	5	-	+	-	-
P46	M	62	R	1	7	+	-	-	-
P50	M	72	R	1	10	-	-	+	-

Table A7.1 (Continued) List of study participants in erythematotelangiectatic rosacea study and serum reactivity to *B. oleronius* protein. Study population data describing gender, age, skin condition, and reactivity to *B. oleronius* 62 kDa protein for each participant. (-: negative serum-reactivity, +: positive serum-reactivity). (R: rosacea; C: control; AV: acne vulgairs; SD: seborrheic dermatitis).

Serum Code	Gender (M/F)	Age (yrs)	Skin Condition	Serverity of Skin Lesions	Number of *D. folliculorum* on skin / cm2	62-kDa P; 83-kDa P	62-kDa P; 83-kDa A	62-kDa A; 83-kDa P	62-kDa A; 83-kDa A
P52	M	64	R	1	10	-	-	+	-
P53	F	27	R	1	2	-	-	+	-
P55	M	30	R	2	0	-	-	+	-
P56	F	46	R	1	0	-	-	+	-
P60	F	31	R	1	0	+	-	-	-
P62	F	53	R	1	4	+	-	-	-
P64	F	41	R	1	0	+	-	-	-
P65	F	58	R	1	4	-	-	-	+
P67	F	50	R	1	0	-	-	-	+
P68	F	39	R	1	3	+	-	-	-
P70	M	72	R	2	6	+	-	-	-
P71	F	52	R	1	1	+	-	-	-
P72	M	69	R	2	12	-	-	-	+
P73	M	52	R	1	3	-	+	-	-
P74	F	37	R	1	0	-	+	-	-
P75	M	53	R	2	22	+	-	-	-
P76	F	26	R	1	0	-	-	-	+
P79	F	57	R	2	2	-	-	-	+
P80	M	31	R	1	3	-	-	-	+
P82	M	35	R	1	0	-	-	-	+
P84	F	31	R	1	0	-	-	-	+
P85	F	35	R	1	0	-	-	+	-
P86	M	55	R	1	0	-	-	-	+
P87	M	56	R	2	1	-	+	-	-
P89	F	29	R	1	0	-	+	-	-
P91	F	64	R	1	0	-	-	-	+
P92	M	26	R	1	2	-	-	-	+
P94	M	50	R	2	0	-	-	-	+

Table A7.1 (Continued) List of study participants in erythematotelangiectatic rosacea study and serum reactivity to *B. oleronius* protein. Study population data describing gender, age, skin condition, and reactivity to *B. oleronius* 62 kDa protein for each participant. (-: negative serum-reactivity, +: positive serum-reactivity). (R: rosacea; C: control; AV: acne vulgairs; SD: seborrheic dermatitis).

Serum Code	Gender (M/F)	Age (yrs)	Skin Condition	Serverity of Skin Lesions	Number of *D. folliculorum* on skin / cm2	62-kDa P; 83-kDa P	62-kDa P; 83-kDa A	62-kDa A; 83-kDa P	62-kDa A; 83-kDa A
P108	F	65	R	2	3	+	-	-	-
P109	F	55	R	1	1	-	+	-	-
P125	M	26	R	1	3	-	-	-	+
P131	F	44	R	1	0	-	+	-	-
P132	M	42	R	2	3	-	-	+	-
p128	M	33	C	-	1	+	-	-	-
p117	M	26	C	-	0	-	-	-	+
p133	F	29	C	-	0	-	-	+	-
p111	F	45	C	-	0	-	-	-	+
p104	F	19	C	-	0	+	-	-	-
p78	F	32	C	-	0	-	-	-	+
p105	M	41	C	-	0	-	-	+	-
p113	F	22	C	-	0	-	-	-	+
p114	M	24	C	-	0	+	-	-	-
p130	F	26	C	-	0	-	+	-	-
p124	F	18	C	-	0	-	-	-	+
GZ 2	M	38	C	-	0	-	+	-	-
p134	F	61	C	-	0	-	-	+	-
p135	M	19	C	-	2	-	-	+	-
p136	M	23	C	-	0	-	-	+	-
p115	F	29	C	-	0	-	+	-	-
p116	F	72	C	-	0	-	-	-	+
p110	F	19	C	-	0	-	-	-	+
p69	M	47	C	-	0	-	+	-	-
p102	F	55	C	-	0	-	-	-	+
p103	F	31	C	-	0	-	-	+	-
p100	F	27	C	-	0	-	-	-	+
p96	F	46	C	-	0	-	-	-	+
p97	F	58	C	-	0	-	-	-	+
p98	M	29	C	-	0	-	-	-	+

Table A7.1 (Continued) List of study participants in erythematotelangiectatic rosacea study and serum reactivity to *B. oleronius* protein. Study population data describing gender, age, skin condition, and reactivity to *B. oleronius* 62 kDa protein for each participant. (-: negative serum-reactivity, +: positive serum-reactivity). (R: rosacea; C: control; AV: acne vulgairs; SD: seborrheic dermatitis).

Serum Code	Gender (M/F)	Age (yrs)	Skin Condition	Serverity of Skin Lesions	Number of *D. folliculorum* on skin / cm2	62-kDa P; 83-kDa P	62-kDa P; 83-kDa A	62-kDa A; 83-kDa P	62-kDa A; 83-kDa A
p81	M	24	C	-	0	-	+	-	-
N1	F	89	C	-	0	-	-	-	+
N2	M	59	C	-	0	-	+	-	-
N3	F	67	C	-	0	-	-	-	+
N4	M	49	C	-	0	+	-	-	-
N5	F	64	C	-	0	-	-	-	+
N6	F	48	C	-	0	-	-	-	+
N7	F	61	C	-	0	-	-	-	+
N8	M	58	C	-	0	-	+	-	-
N9	M	69	C	-	0	-	-	-	+
N10	M	76	C	-	0	-		-	+
N11	F	49	C	-	0	-	-	-	+
N12	F	59	C	-	0	-	-	+	-
N13	F	78	C	-	0	-	-	+	-
N14	M	68	C	-	0	-	-	-	+
N15	M	57	C	-	0	-	-	-	+
N16	M	47	C	-	0	-	-	-	+
N17	M	44	C	-	0	-	-	-	+
N18	M	45	C	-	0	-	+	-	-
N19	M	47	C	-	0	-	-	-	+
N20	F	53	C	-	0	-	-	-	+
N21	F	64	C	-	0	-	+	-	-
N22	F	38	C	-	0	-	-	-	+
N23	M	45	C	-	0	-	-	-	+
N24	F	55	C	-	0	-	-	-	+
N25	M	39	C	-	0	-	-	-	+
N26	M	69	C	-	0	-	-		+
N27	F	62	C	-	0	-	-	-	+

Table A7.1 (Continued) List of study participants in erythematotelangiectatic rosacea study and serum reactivity to *B. oleronius* protein. Study population data describing gender, age, skin condition, and reactivity to *B. oleronius* 62 kDa protein for each participant. (-: negative serum-reactivity, +: positive serum-reactivity). (R: rosacea; C: control; AV: acne vulgairs; SD: seborrheic dermatitis).

Serum Code	Gender (M/F)	Age (yrs)	Skin Condition	Serverity of Skin Lesions	Number of *D. folliculorum* on skin / cm2	62-kDa P; 83-kDa P	62-kDa P; 83-kDa A	62-kDa A; 83-kDa P	62-kDa A; 83-kDa A
GZ 1	M	21	AV	-	0	-	-	-	+
GT 1	F	29	AV	-	0	-	-	-	+
GT 2	F	22	AV	-	0	-	-	-	+
p51	F	22	AV	-	0	-	-	-	+
p118	F	28	AV	-	0	-	-	-	+
p112	F	26	AV	-	0	-	-	-	+
p119	M	22	AV	-	0	-	-	-	+
p120	M	23	AV	-	0	-	-	-	+
p121	M	19	AV	-	1	-	-	-	+
p93	M	25	AV	-	0	-	-	-	+
p99	F	19	AV	-	0	-	-	-	+
p129	F	15	AV	-	0	-	-	-	+
p101	M	21	AV	-	9	-	-	-	+
p122	F	29	AV	-	0	-	+	-	-
p128	M	33	SD	-	1	+	-	-	-
p117	M	26	SD	-	0	-	-	-	+
p133	F	29	SD	-	0	-	-	+	-
p111	F	45	SD	-	0	-	-	-	+
p104	F	19	SD	-	0	+	-	-	-
p78	F	32	SD	-	0	-	-	-	+
p105	M	41	SD	-	0	-	-	+	-
p113	F	22	SD	-	0	-	-	-	+
p114	M	24	SD	-	0	+	-	-	-

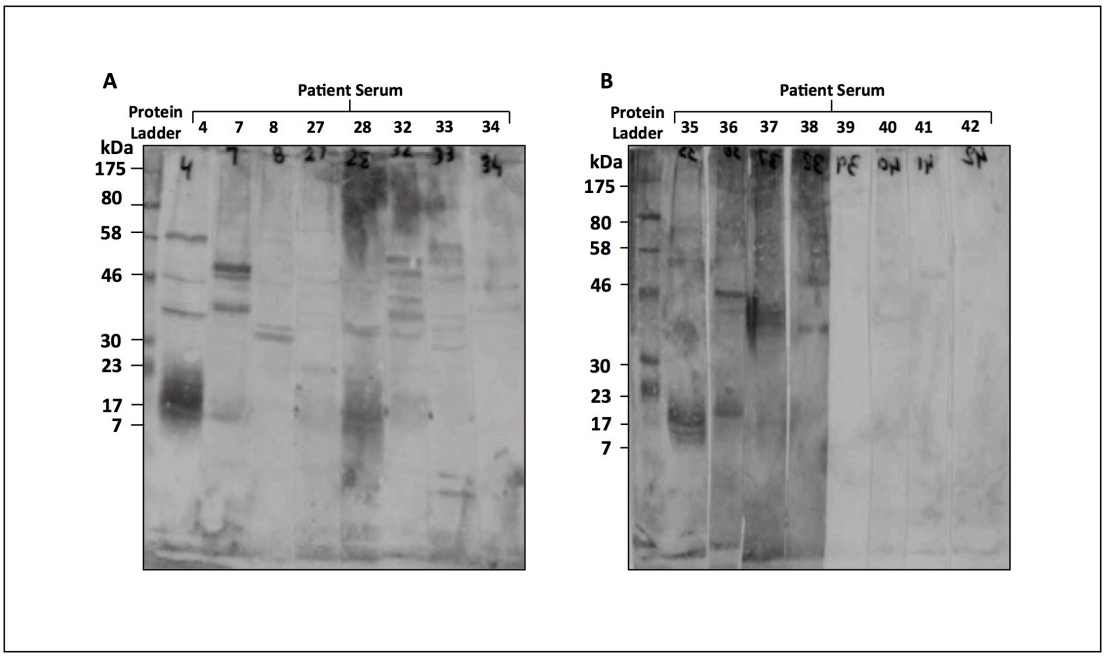

Figure A7.1 Western blots of sera reactivity of participants coded (A) 4 to 34 and (B) 35 to 42, to *B. oleronius* proteins in erythematotelangiectatic rosacea study.

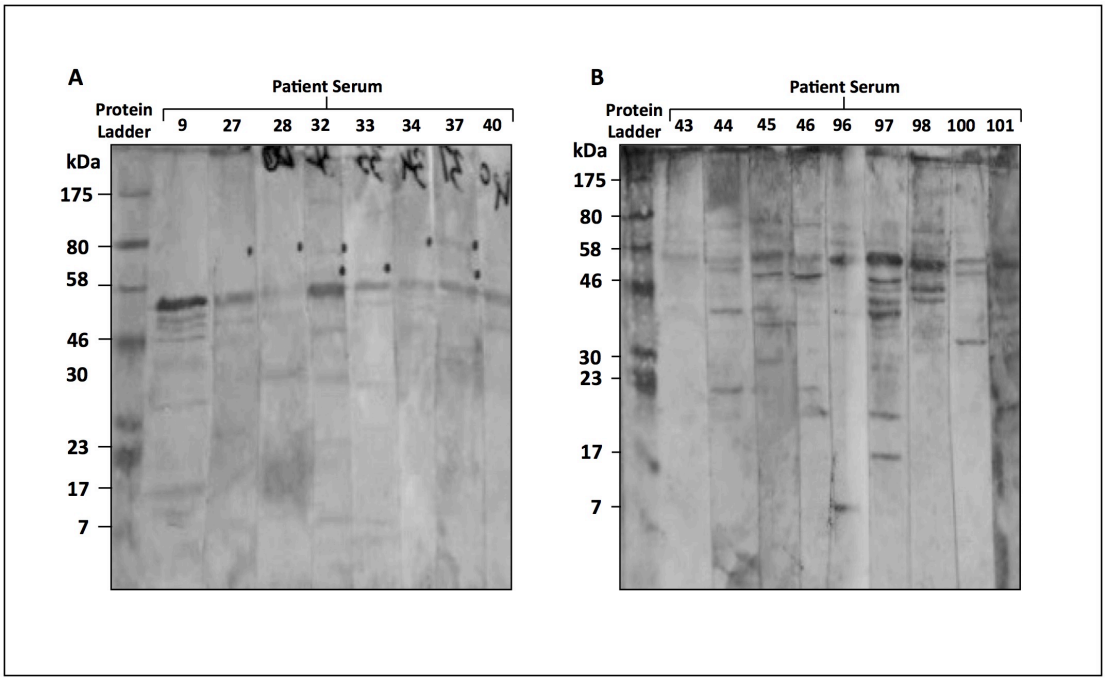

Figure A7.2 Western blots of sera reactivity of participants coded (A) 9 to 40 and (B) 43 to 101, to *B. oleronius* proteins in erythematotelangiectatic rosacea study.

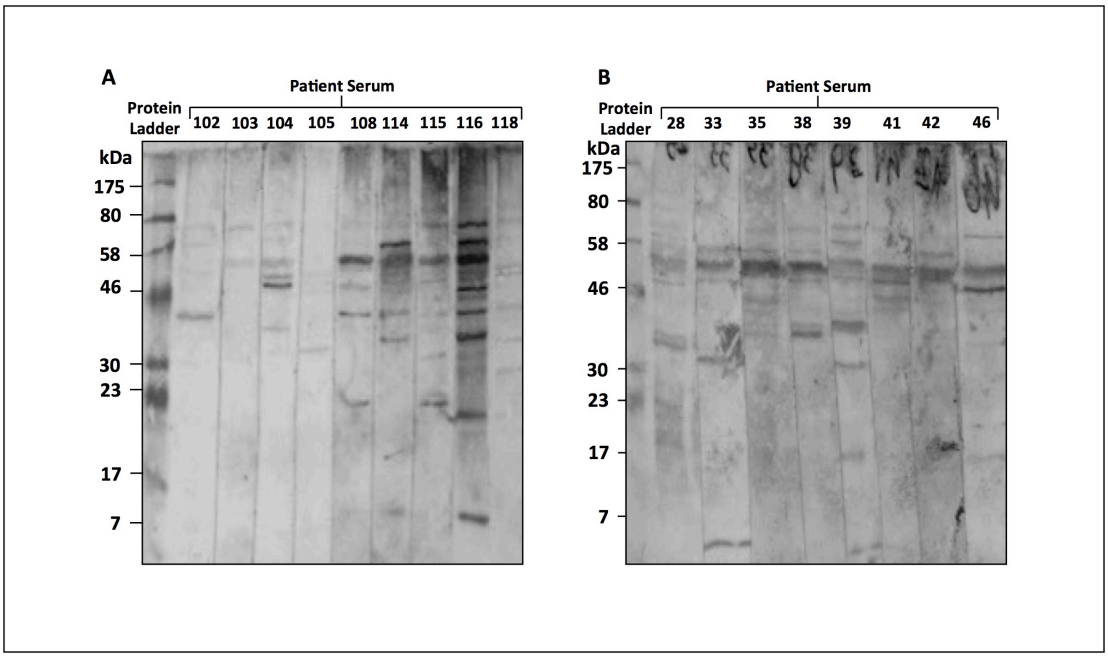

Figure A7.3 Western blots of sera reactivity of participants coded (A) 102 to 118 and (B) 28 to 46, to *B. oleronius* proteins in erythematotelangiectatic rosacea study.

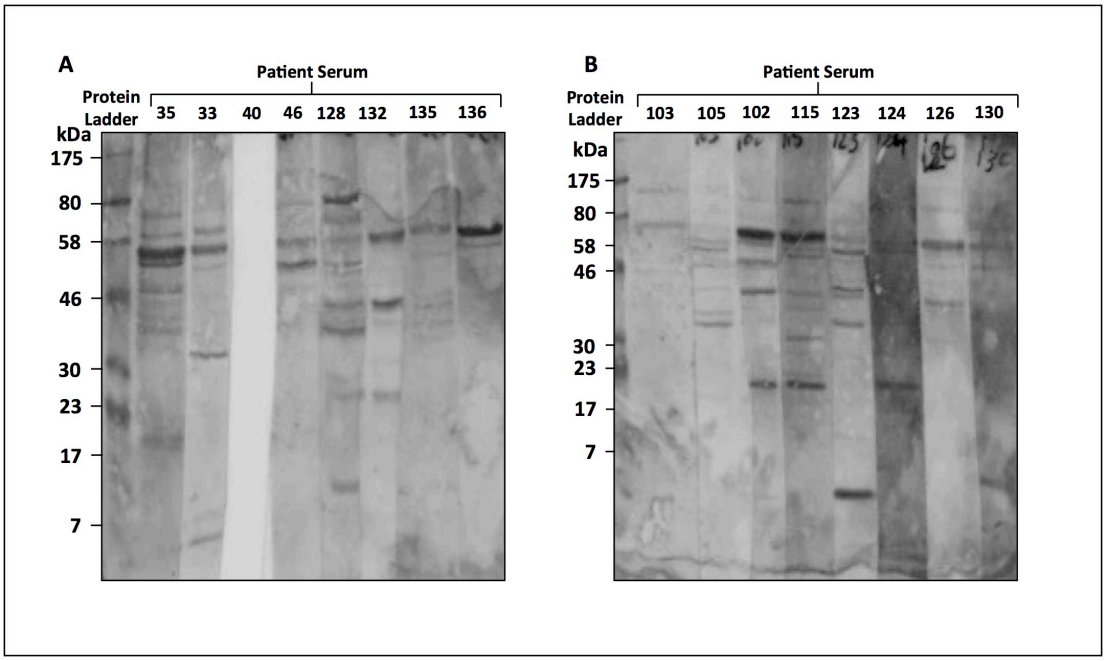

Figure A7.4 Western blots of sera reactivity of participants coded (A) 35 to 136 and (B) 103 to 130, to *B. oleronius* proteins in erythematotelangiectatic rosacea study.

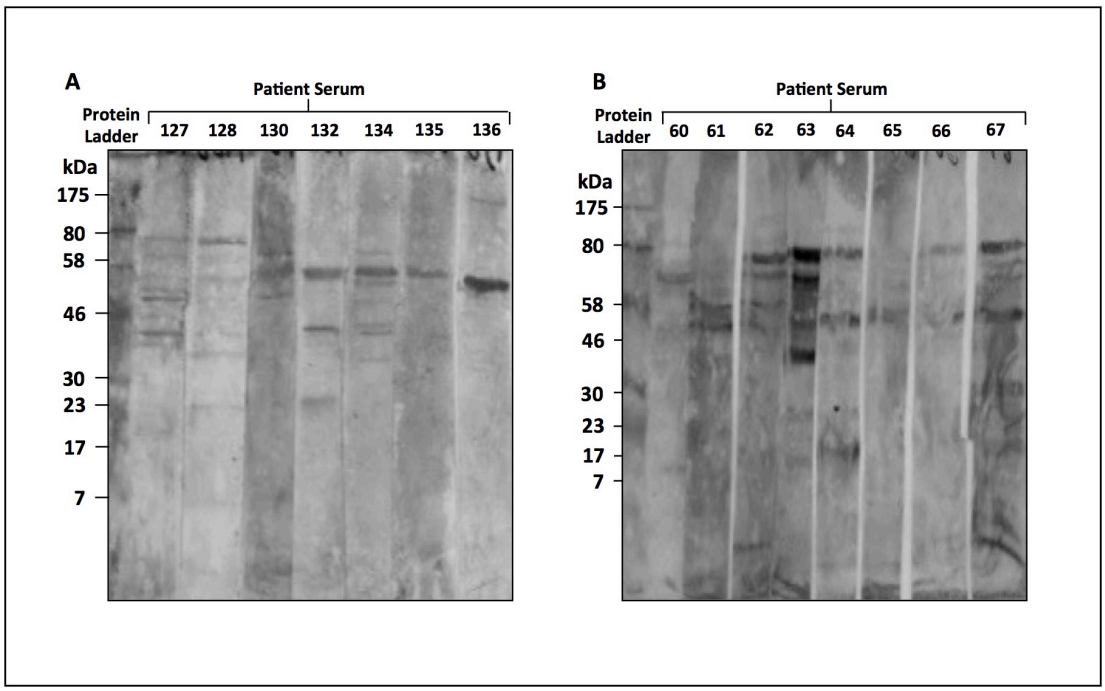

Figure A7.5 Western blots of sera reactivity of participants coded (A) 127 to 136 and (B) 60 to 67, to *B. oleronius* proteins in erythematotelangiectatic rosacea study.

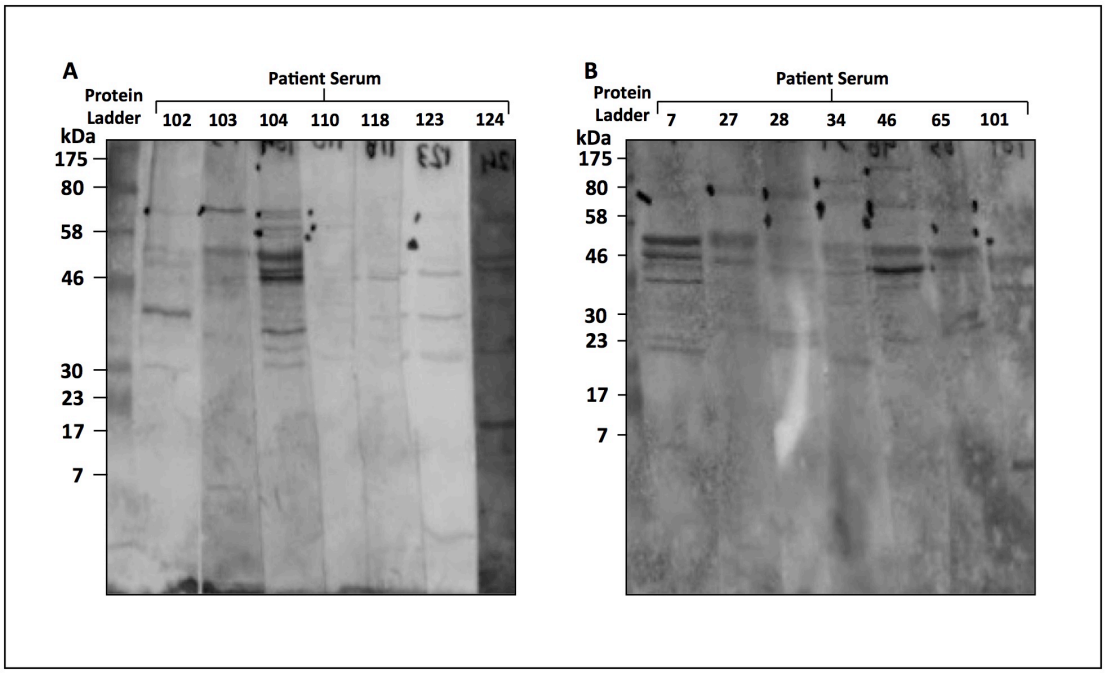

Figure A7.6 Western blots of sera reactivity of participants coded (A) 102 to 124 and (B) 7 to 101, to *B. oleronius* proteins in erythematotelangiectatic rosacea study.

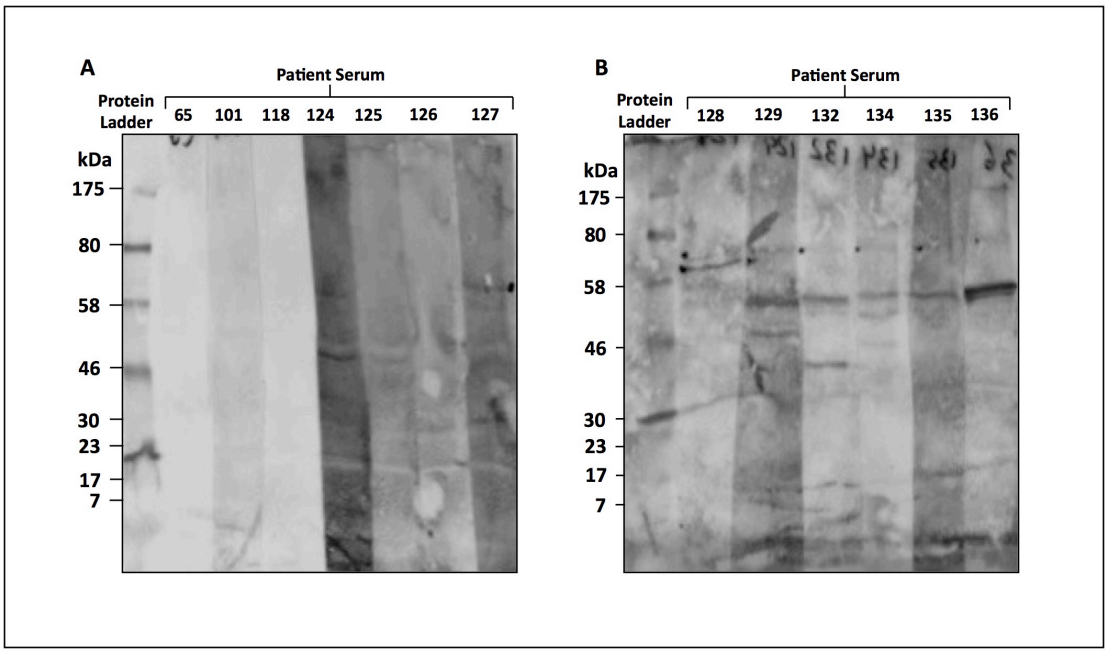

Figure A7.7 Western blots of sera reactivity of participants coded (A) 65 to 127 and (B) 128 to 136, to *B. oleronius* proteins in erythematotelangiectatic rosacea study.

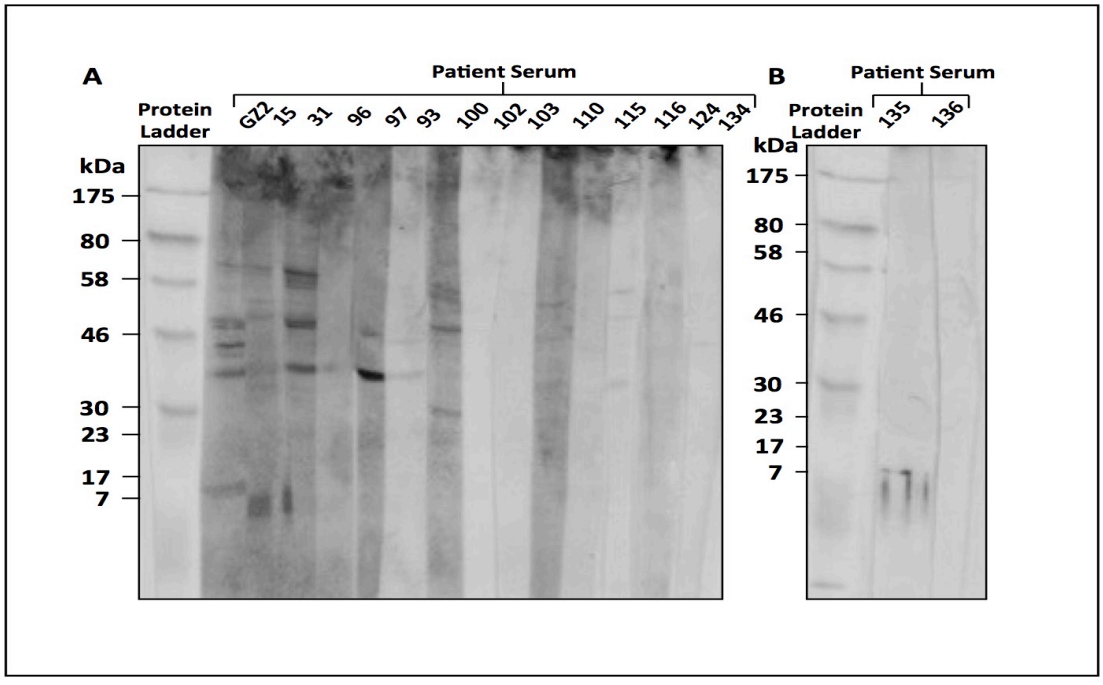

Figure A7.8 Western blots of sera reactivity of participants coded (A) GZ2 to 134 and (B) 135 to 136, to *B. oleronius* proteins in erythematotelangiectatic rosacea study.

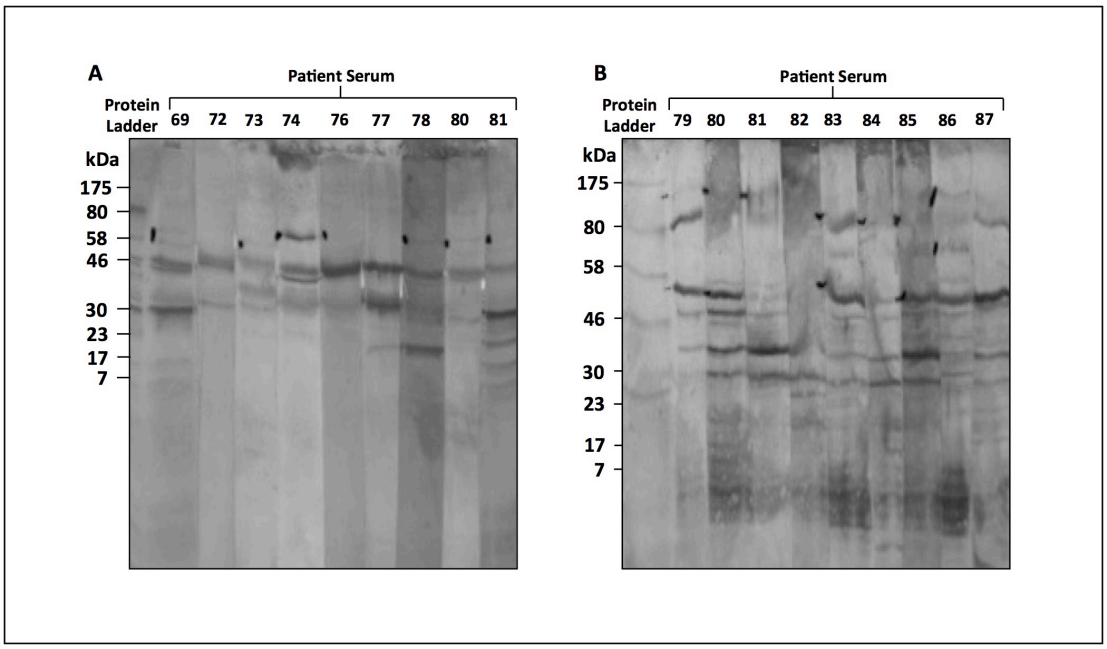

Figure A7.9 Western blots of sera reactivity of participants coded (A) 69 to 81 and (B) 79 to 87, to *B. oleronius* proteins in erythematotelangiectatic rosacea study.

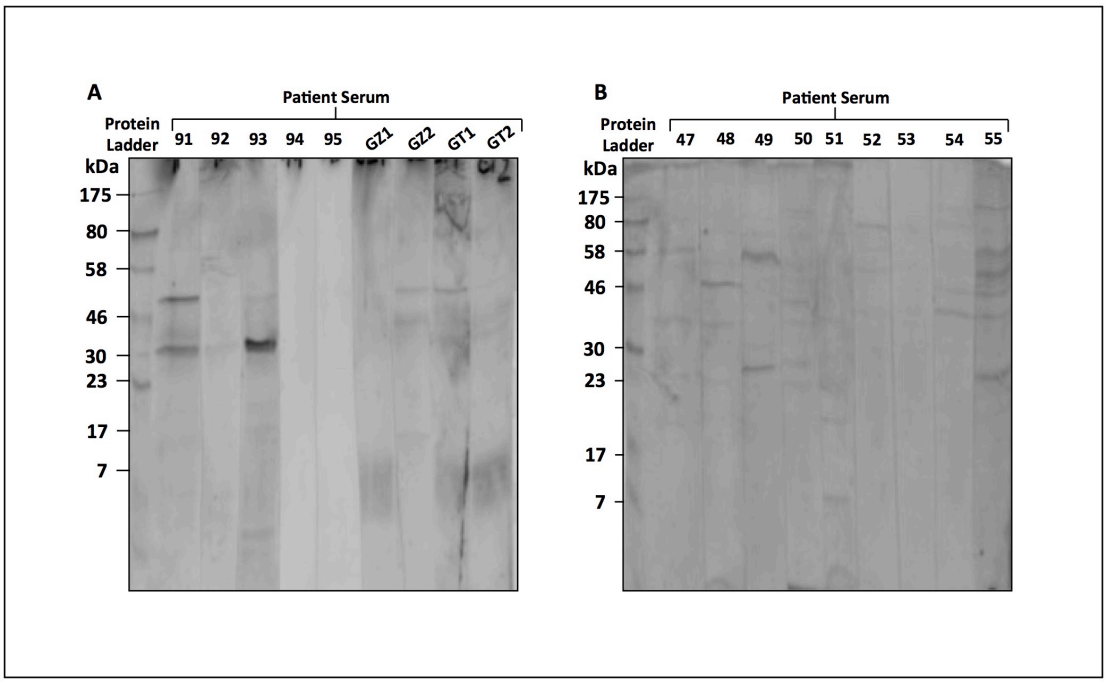

Figure A7.10 Western blots of sera reactivity of participants coded (A) 91 to GT2 and (B) 47 to 55, to *B. oleronius* proteins in erythematotelangiectatic rosacea study.

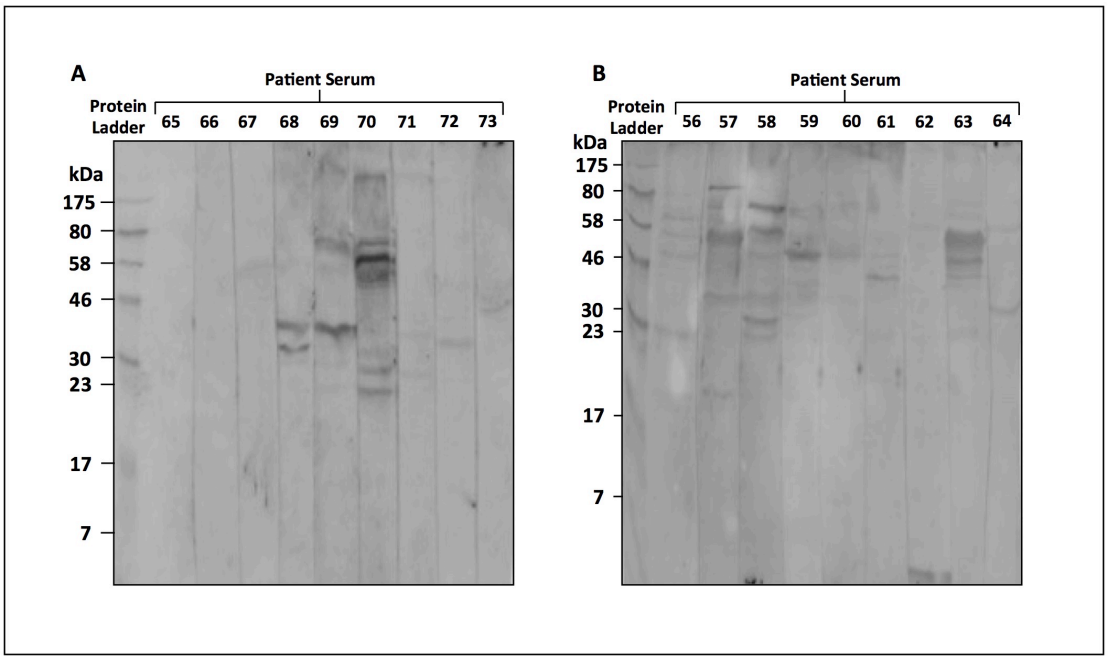

Figure A7.11 Western blots of sera reactivity of participants coded (A) 65 to 73 and (B) 56 to 64, to *B. oleronius* proteins in erythematotelangiectatic rosacea study.

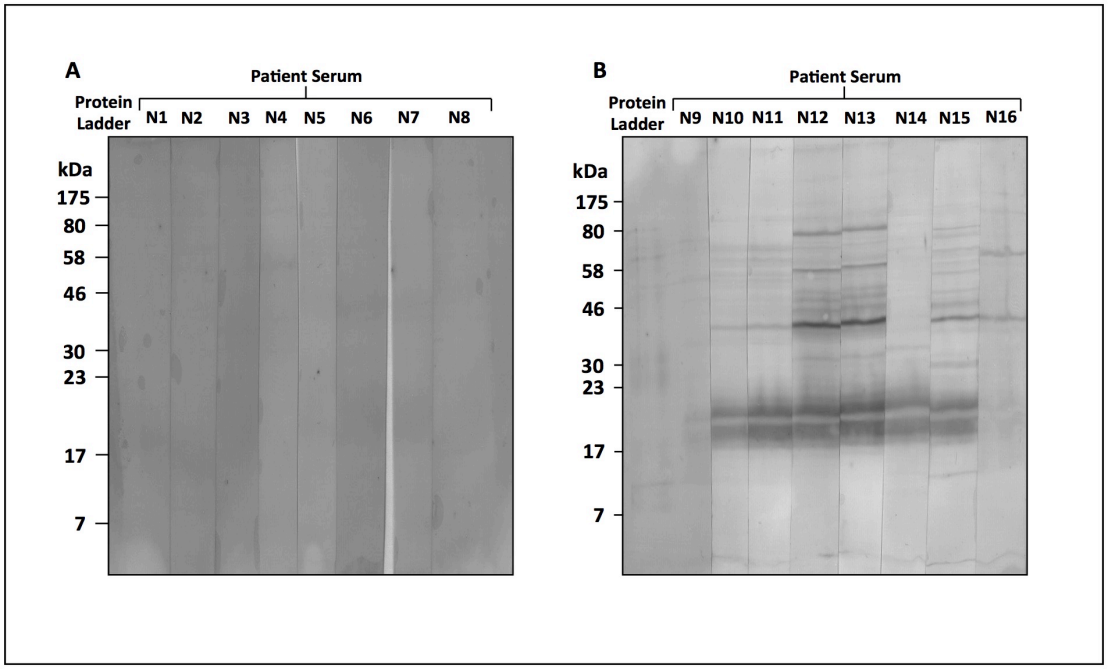

Figure A7.12 Western blots of sera reactivity of participants coded (A) N1 to N8 and (B) N9 to N16, to *B. oleronius* proteins in erythematotelangiectatic rosacea study.

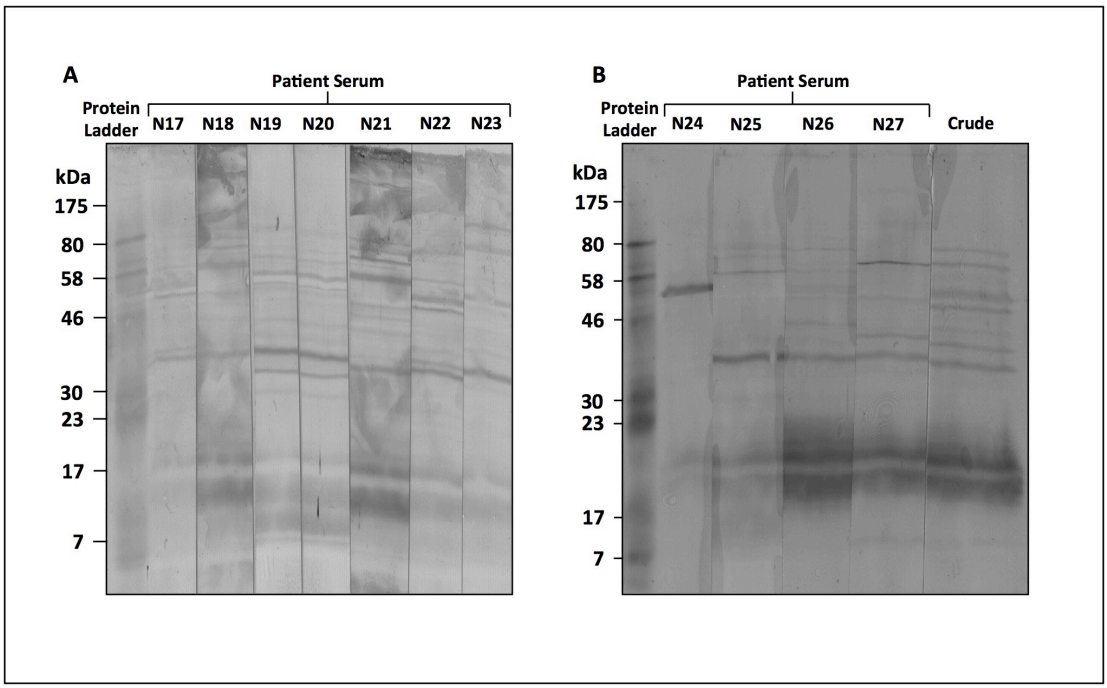

Figure A7.13 Western blots of sera reactivity of participants coded (A) N17 to N23 and (B) N24 to N27, to *B. oleronius* proteins in erythematotelangiectatic rosacea study.

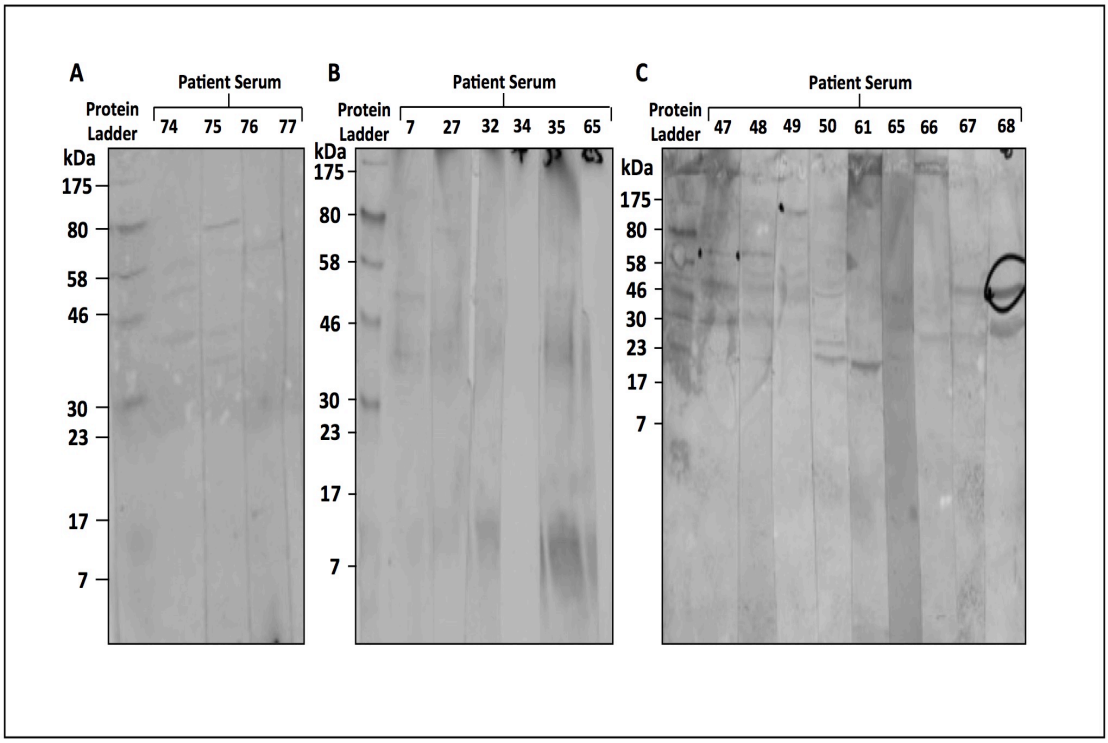

Figure A7.14 Western blots of sera reactivity of participants coded (A) 74 to 77, (B) 7 to 65, and (C) 47 to 68, to *B. oleronius* proteins in erythematotelangiectatic rosacea study.

Table A7.2 List of study participants in *Demodex*-related blepharitis study and serum reactivity to *B. oleronius* protein. Study population data describing gender, age, skin condition, and reactivity to *B. oleronius* 62 kDa protein for each participant. (-: negative serum-reactivity, +: positive serum-reactivity).

Serum Code Identifier	Reactivity to 62-kDa Protien (+/-)		Group	Serum Reactivity	*Demodex* on Lashes		Keratitis	Meiboscore	Blepharitis	Sex	Age	Acne
	Trial 1	Trial 2			*D. Brevis*	*D. Folliculorum*						
1	+	+	1	+	8	7	+	6	+	F	18	-
2	+	+	1	+	2	5	+	2	+	F	23	-
3	-	-	1	-	5	6	+	6	+	F	21	+
4	+	+	1	+	3	3	+	6	+	F	16	+
5	+	+	1	+	5	2	+	3	+	F	20	+
6	+	+	1	+	7	6	+	5	+	F	22	+
11	-	-	1	-	3	1	+	6	+	F	16	+
14	-	-	1	-	2	1	+	6	+	F	23	+
15	+	+	1	+	2	3	-	1	+	F	33	-
19	+	+	1	+	2	1	+	2	+	F	25	+
25	+	+	1	+	4	2	+	6	+	F	20	+
26	+	+	1	+	3	3	+	5	+	M	17	+
31	+	+	1	+	2	1	-	2	+	M	12	-
33	+	+	1	+	6	2	+	4	+	F	19	+
34	-	-	1	-	2	1	-	1	+	M	8	-
35	+	+	1	+	11	11	+	4	+	F	17	-
42	+	+	1	+	2	1	+	1	+	F	14	-
46	-	-	1	-	5	3	+	5	+	F	23	+
50	+	+	1	+	12	2	+	6	+	M	26	+
51	-	-	1	-	1	1	+	5	+	M	12	-
52	+	+	1	+	3	1	+	2	+	M	13	+
54	+	+	1	+	12	10	+	3	+	M	22	+
55	+	+	1	+	4	3	+	4	+	F	20	+
56	+	+	1	+	4	4	+	4	+	F	16	+
61	+	+	1	+	2	3	-	0	+	M	20	+
62	-	-	1	-	2	0	+	4	+	F	6	-
63	+	+	1	+	1	2	-	3	+	F	22	-

Table A7.2 (Continued) List of study participants in *Demodex*-related blepharitis study and serum reactivity to *B. oleronius* protein. Study population data describing gender, age, skin condition, and reactivity to *B. oleronius* 62 kDa protein for each participant. (-: negative serum-reactivity, +: positive serum-reactivity).

Serum Code Identifier	Reactivity to 62-kDa Protien (+/-)		Group	Serum Reactivity	*Demodex* on Lashes		Keratitis	Meiboscore	Blepharitis	Sex	Age	Acne
	Trial 1	Trial 2			*D. Brevis*	*D. Folliculorum*						
71	+	+	1	+	2	7	+	3	+	F	29	-
76	+	+	1	+	2	6	-	2	+	M	37	-
77	+	+	1	+	8	16	+	5	+	F	20	+
78	+	+	1	+	2	4	+	3	+	F	17	-
79	+	+	1	+	3	3	+	5	+	F	14	+
82	+	+	1	-	3	1	+	6	+	M	21	-
87	+	+	1	+	2	4	+	5	+	F	25	-
89	+	+	1	+	7	2	+	5	+	M	20	-
90	+	+	1	+	2	3	+	6	+	F	20	+
102	+	+	1	+	2	2	-	2	+	F	28	-
12	-	-	2	-	1	3	-	2	-	F	18	+
27	+	+	2	+	1	4	-	1	-	M	30	-
29	-	-	2	-	0	3	-	2	-	F	12	-
36	+	+	2	+	2	2	-	1	-	F	35	-
38	+	+	2	+	0	6	-	1	-	M	28	-
44	+	+	2	+	0	2	-	1	-	F	32	+
49	-	-	2	-	1	5	-	1	-	F	33	-
68	-	-	2	-	2	2	-	0	-	F	32	-
83	-	-	2	-	0	3	-	0	-	M	12	-
84	+	+	2	+	2	4	-	1	-	F	27	-
92	+	+	2	+	0	1	-	1	-	F	25	-
93	+	+	2	+	1	1	-	1	-	F	25	+
94	+	+	2	+	0	2	-	1	-	F	25	+
96	+	+	2	-	0	2	-	1	-	F	24	-
98	-	-	2	+	0	3	-	1	-	F	25	-
100	+	+	2	+	1	0	-	1	-	F	25	-
101	-	-	2	+	2	0	-	0	-	F	23	-
28	-	-	3	-	0	0	-	2	-	M	21	+

Table A7.2 (Continued) List of study participants in *Demodex*-related blepharitis study and serum reactivity to *B. oleronius* protein. Study population data describing gender, age, skin condition, and reactivity to *B. oleronius* 62 kDa protein for each participant. (-: negative serum-reactivity, +: positive serum-reactivity).

Serum Code Identifier	Reactivity to 62-kDa Protien (+/-)		Group	Serum Reactivity	*Demodex* on Lashes		Keratitis	Meiboscore	Blepharitis	Sex	Age	Acne
	Trial 1	Trial 2			*D. Brevis*	*D. Folliculorum*						
39	-	-	3	-	0	0	-	0	-	M	6	+
40	-	-	3	-	0	0	-	0	-	F	29	-
53	+	+	3	+	0	0	-	0	-	M	31	-
64	+	+	3	+	0	0	-	1	-	F	26	-
66	+	+	3	+	0	0	-	1	-	F	7	-
67	-	-	3	-	0	0	-	1	-	M	17	-
69	-	-	3	-	0	0	-	0	-	M	28	-
70	-	-	3	-	0	0	-	1	-	M	19	-
72	+	+	3	-	0	0	-	0	-	F	25	+
73	+	+	3	+	0	0	-	0	-	M	27	-
74	+	+	3	+	0	0	-	0	-	F	21	-
75	+	+	3	+	0	0	-	0	-	M	23	-
86	-	-	3	+	0	0	-	1	-	M	10	-
97	+	+	3	+	0	0	-	0	-	F	24	-
99	-	-	3	-	0	0	-	0	-	F	25	-

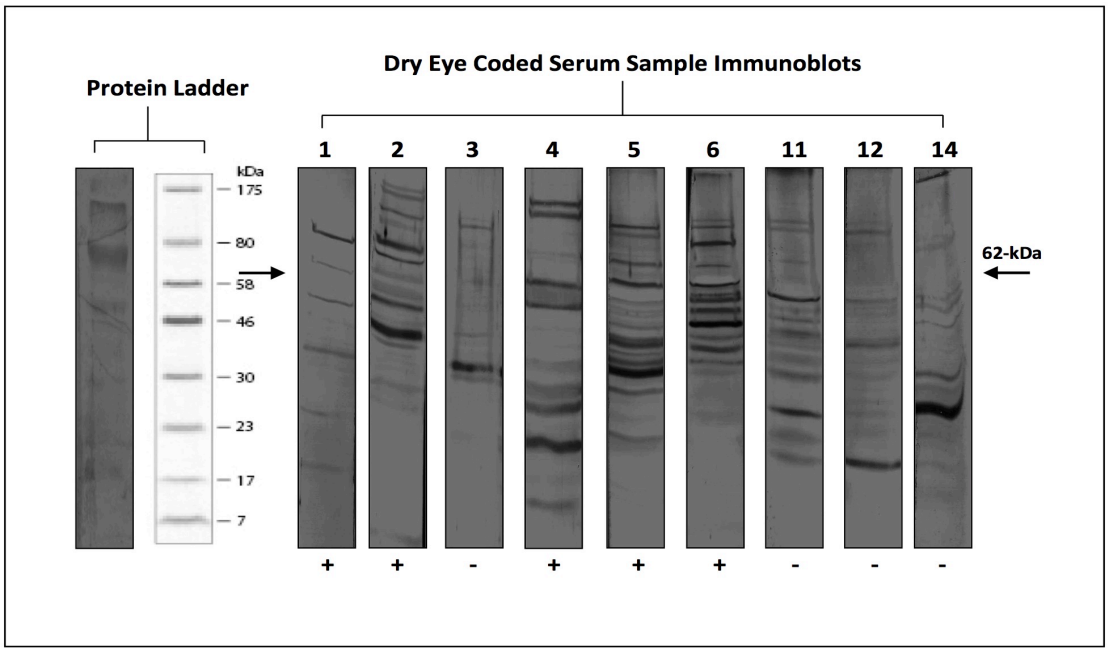

Figure A7.15 Serum reactivity of participant 1 to 14 to *B. oleronius* protein in *Demodex*-related blepharitis study (Trial 1). (-: negative serum reactivity, +: positive serum reactivity).

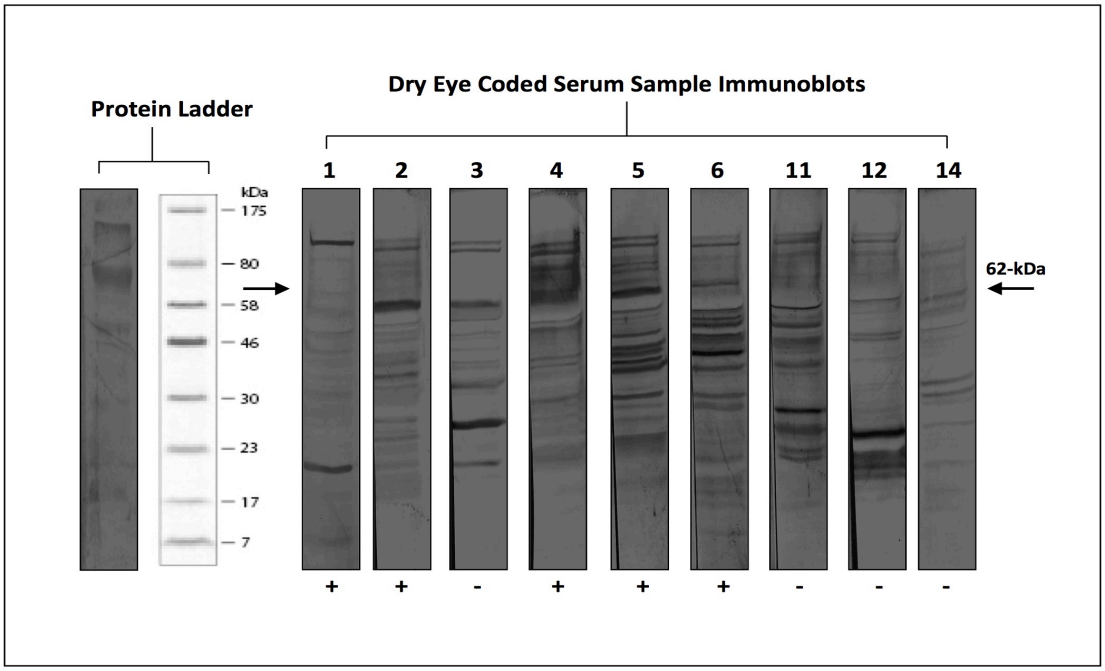

Figure A7.16 Serum reactivity of participant 1 to 14 to *B. oleronius* protein in *Demodex*-related blepharitis study (Trial 2). (-: negative serum reactivity, +: positive serum reactivity).

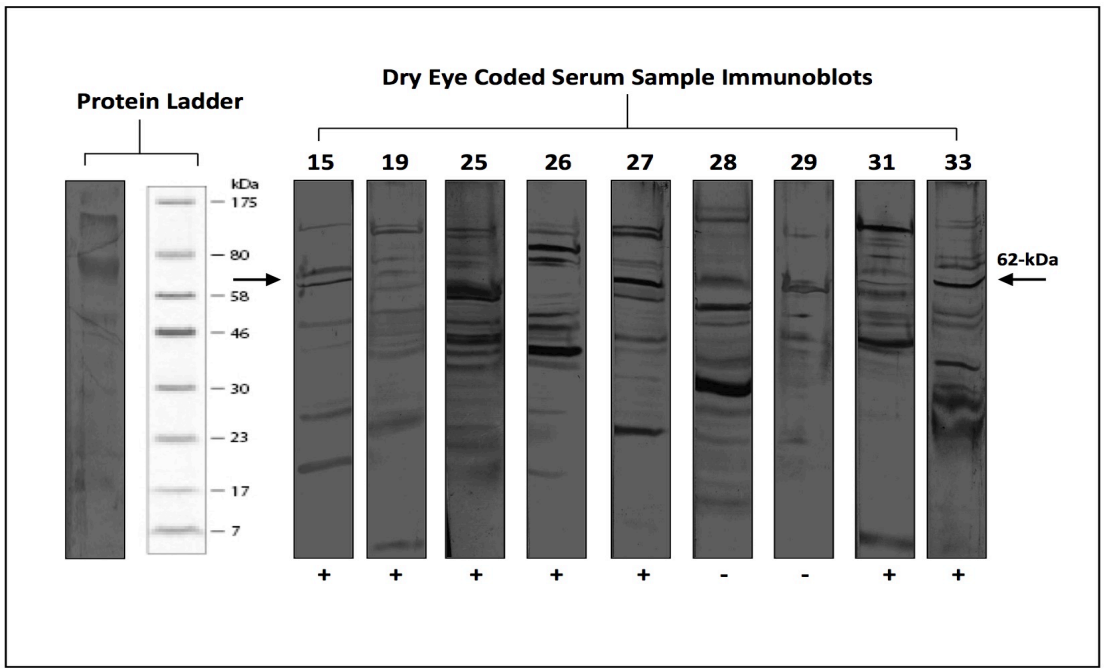

Figure A7.17 Serum reactivity of participant 15 to 33 to *B. oleronius* protein in *Demodex*-related blepharitis study (Trial 1). (-: negative serum reactivity, +: positive serum reactivity).

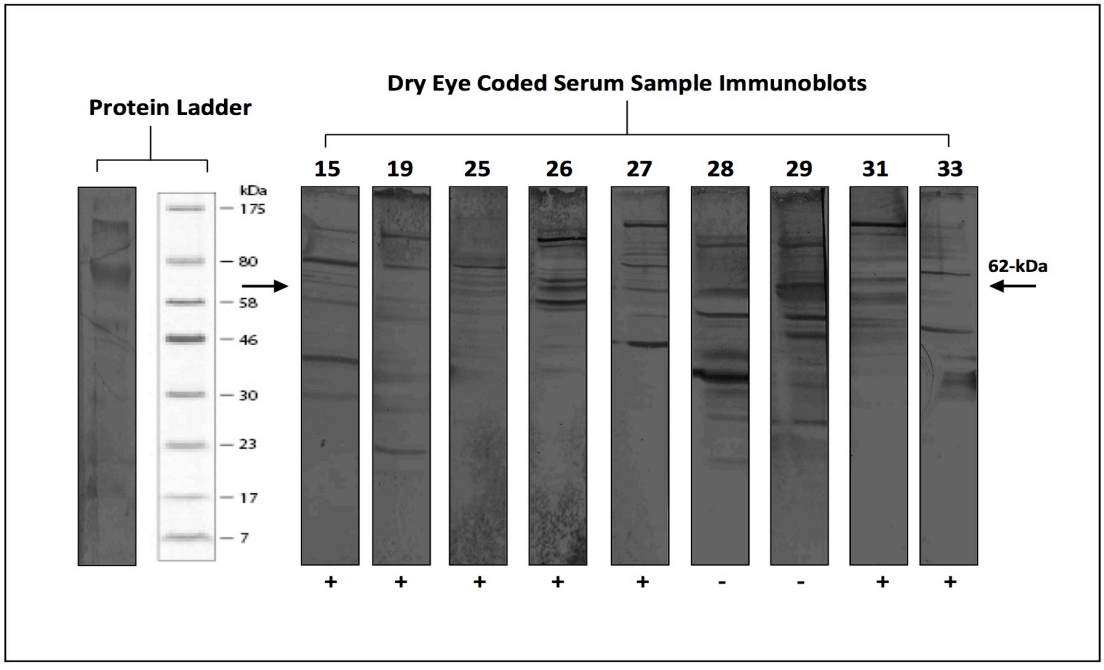

Figure A7.18 Serum reactivity of participant 15 to 33 to *B. oleronius* protein in *Demodex*-related blepharitis study (Trial 2). (-: negative serum reactivity, +: positive serum reactivity).

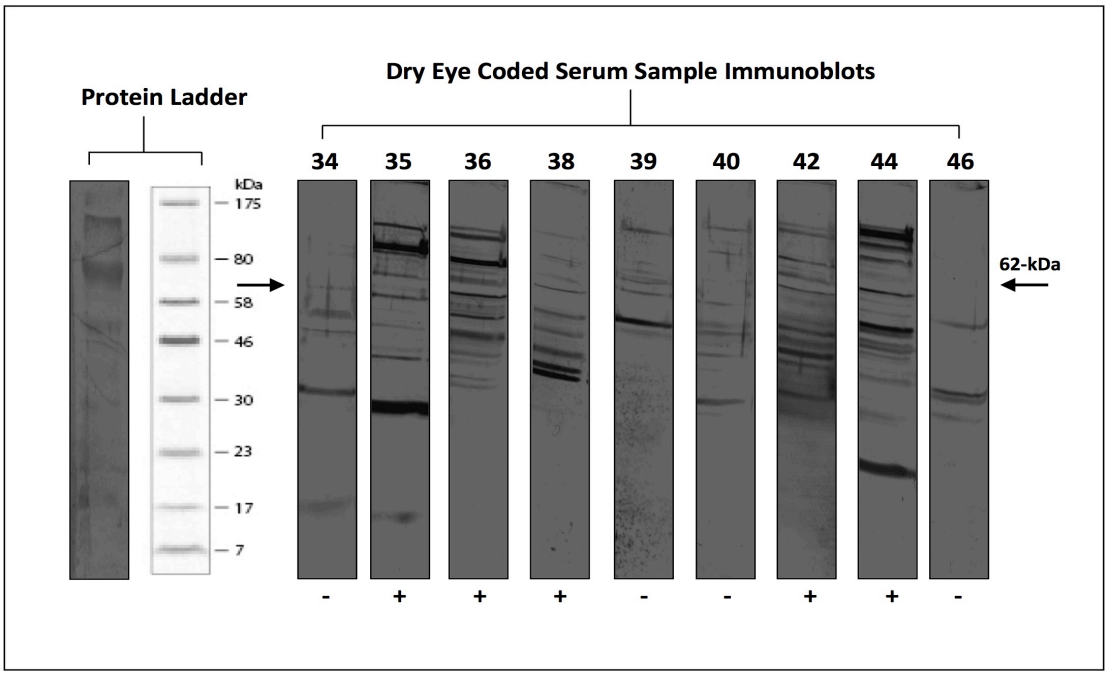

Figure A7.19 Serum reactivity of participant 34 to 46 to *B. oleronius* protein in *Demodex*-related blepharitis study (Trial 1). (-: negative serum reactivity, +: positive serum reactivity).

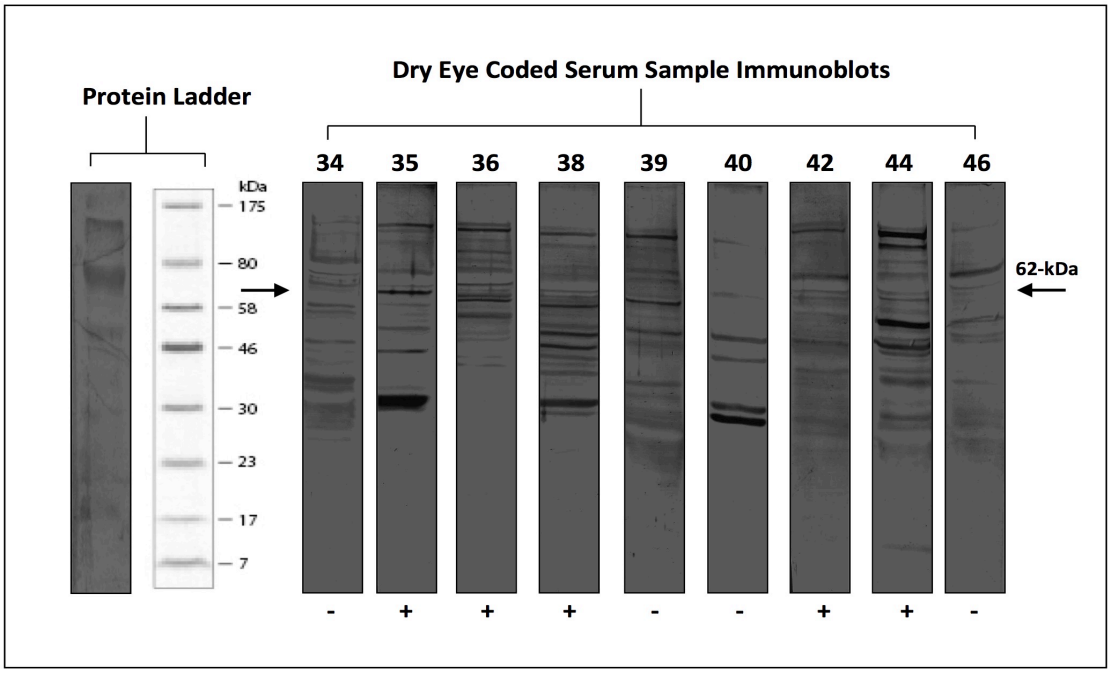

Figure A7.20 Serum reactivity of participant 34 to 46 to *B. oleronius* protein in *Demodex*-related blepharitis study (Trial 2). (-: negative serum reactivity, +: positive serum reactivity).

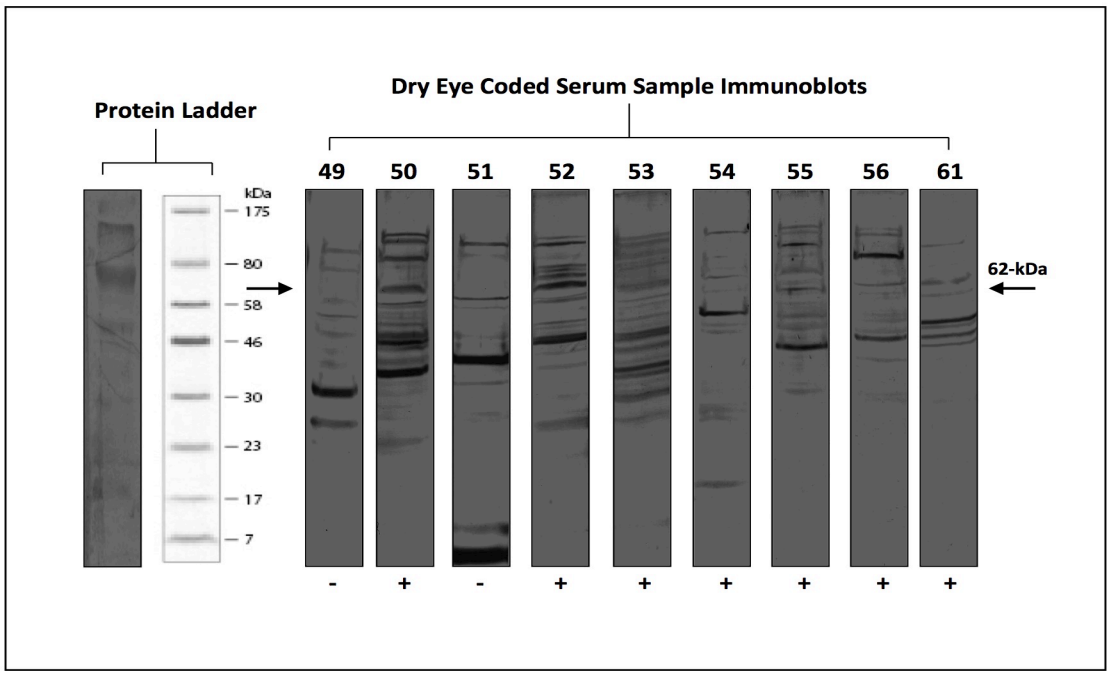

Figure A7.21 Serum reactivity of participant 49 to 61 to *B. oleronius* protein in *Demodex*-related blepharitis study (Trial 1). (-: negative serum reactivity, +: positive serum reactivity).

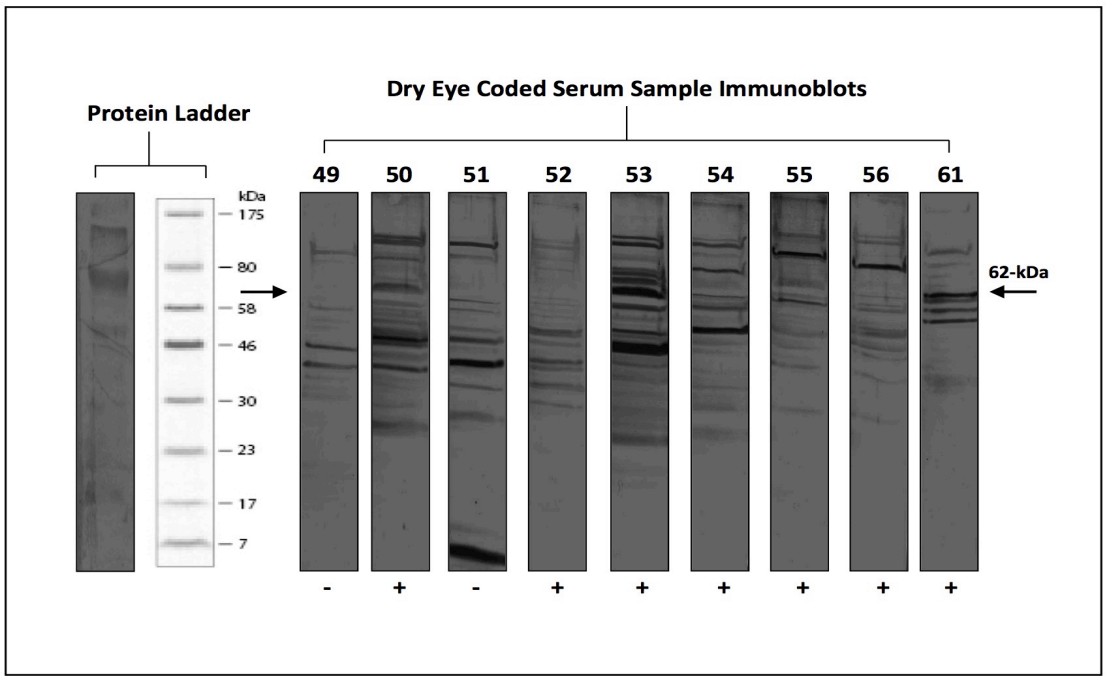

Figure A7.22 Serum reactivity of participant 49 to 61 to *B. oleronius* protein in *Demodex*-related blepharitis study (Trial 2). (-: negative serum reactivity, +: positive serum reactivity).

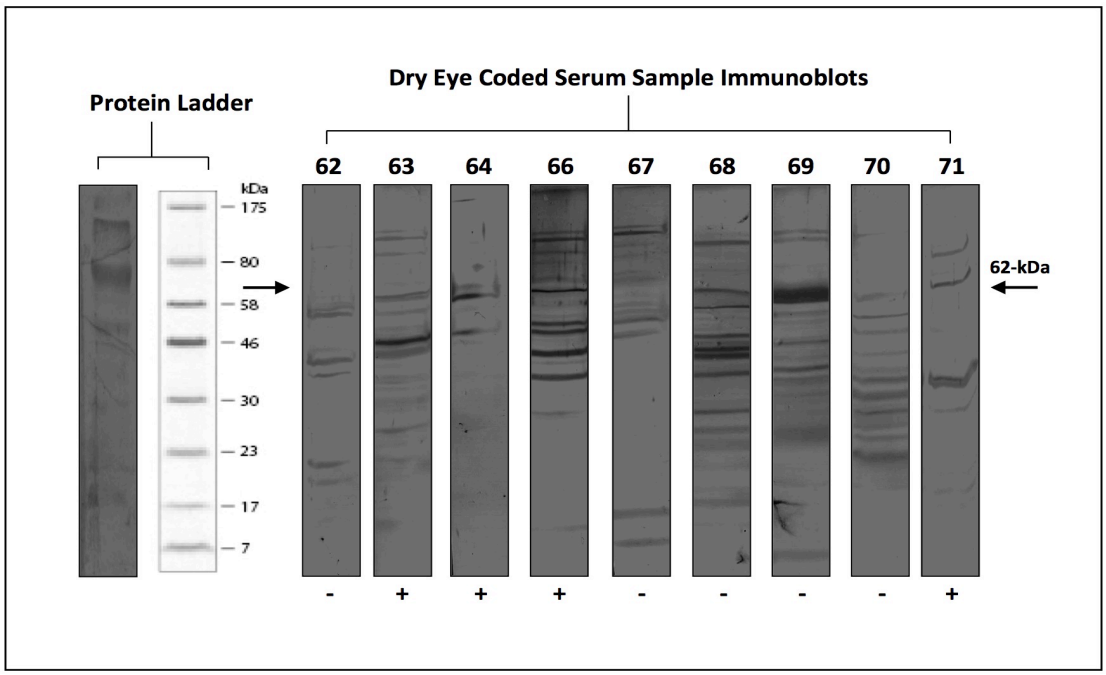

Figure A7.23 Serum reactivity of participant 62 to 71 to *B. oleronius* protein in *Demodex*-related blepharitis study (Trial 1). (-: negative serum reactivity, +: positive serum reactivity).

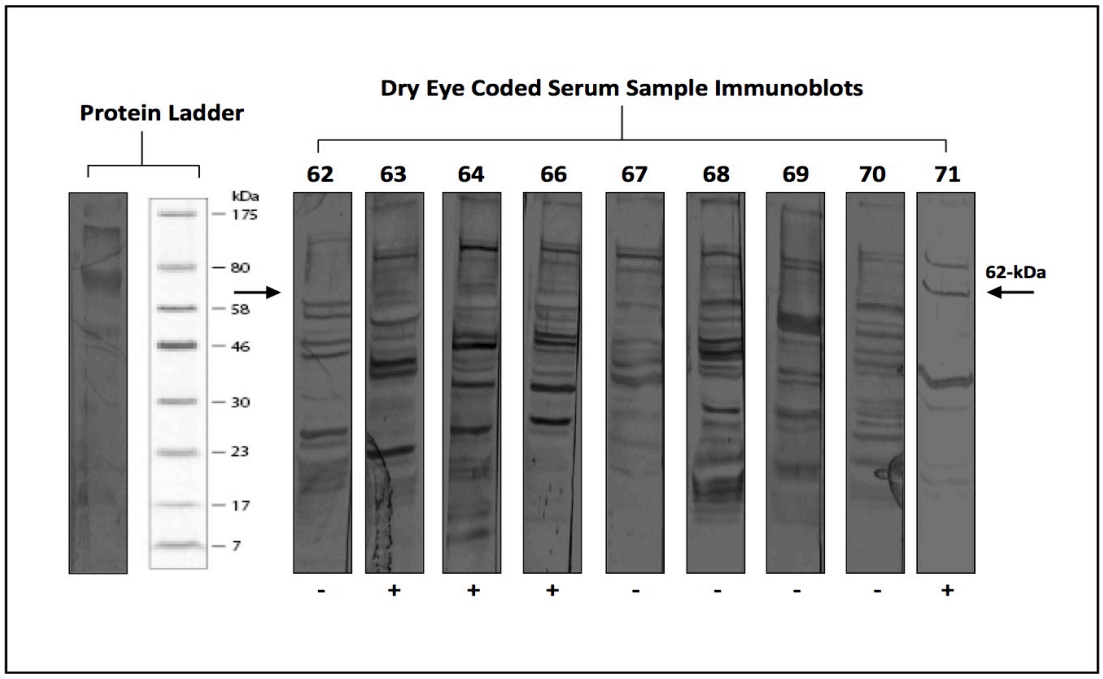

Figure A7.24 Serum reactivity of participant 62 to 71 to *B. oleronius* protein in *Demodex*-related blepharitis study (Trial 2). (-: negative serum reactivity, +: positive serum reactivity).

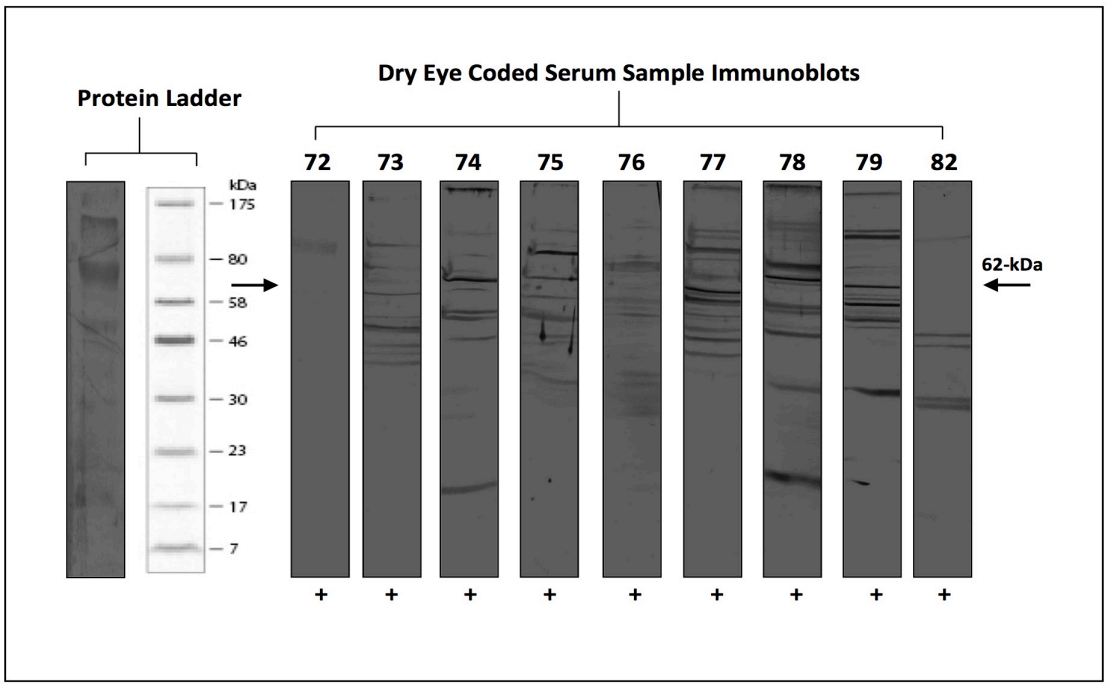

Figure A7.25 Serum reactivity of participant 72 to 82 to *B. oleronius* protein in *Demodex*-related blepharitis study (Trial 1). (-: negative serum reactivity, +: positive serum reactivity).

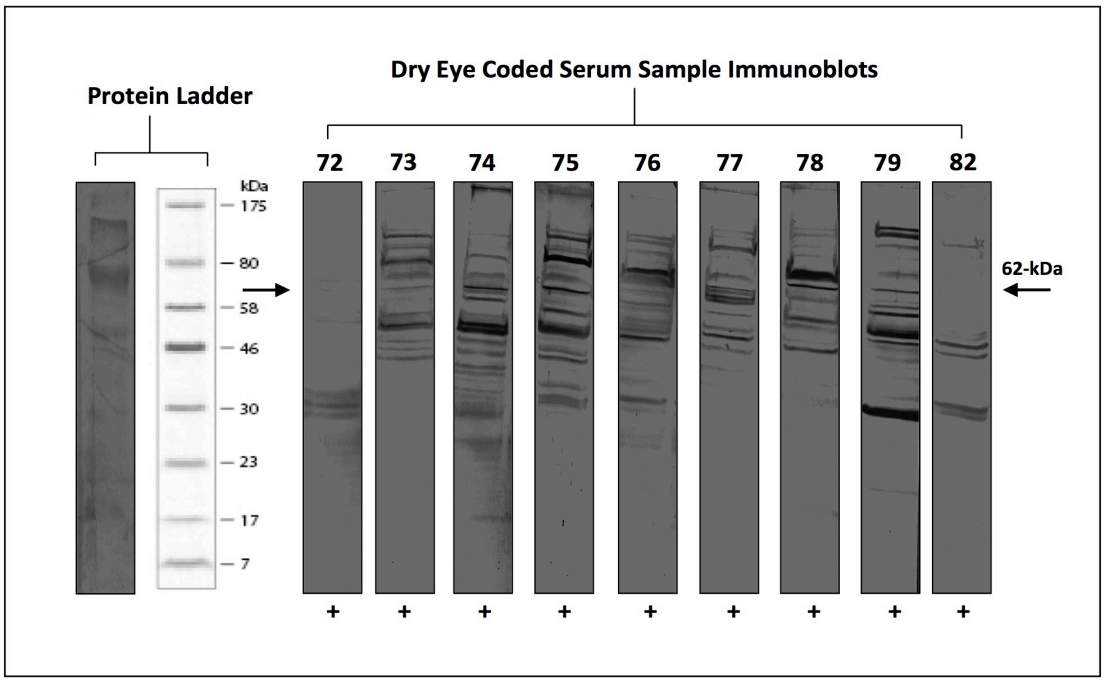

Figure A7.26 Serum reactivity of participant 72 to 82 to *B. oleronius* protein in *Demodex*-related blepharitis study (Trial 2). (-: negative serum reactivity, +: positive serum reactivity).

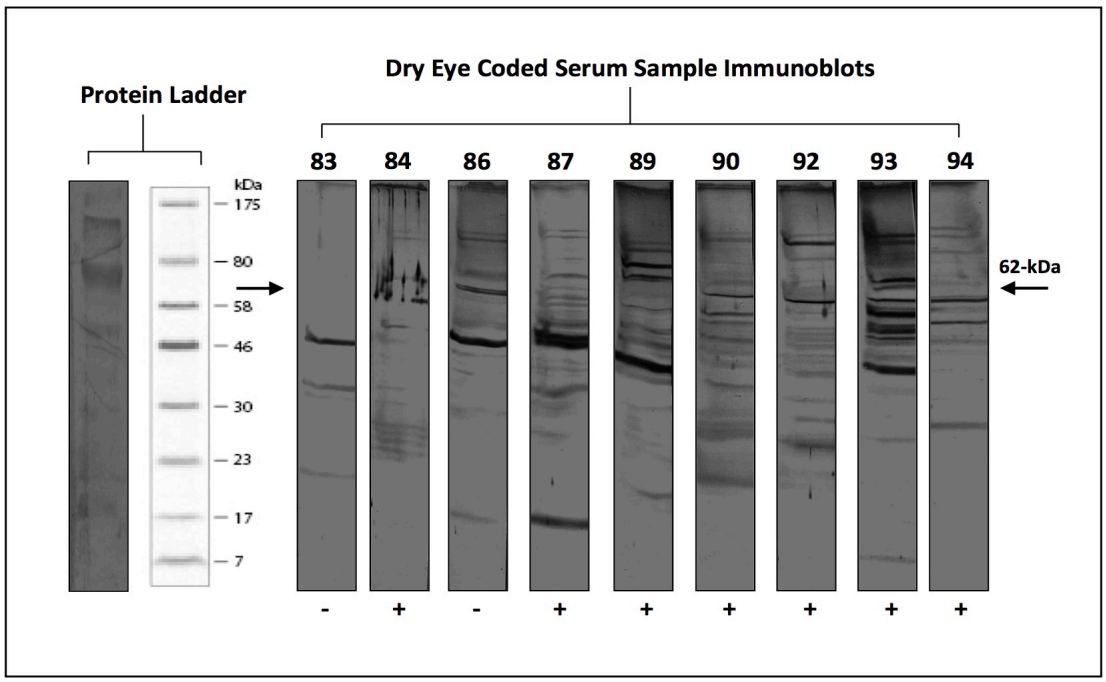

Figure A7.27 Serum reactivity of participant 83 to 94 to *B. oleronius* protein in *Demodex*-related blepharitis study (Trial 1). (-: negative serum reactivity, +: positive serum reactivity).

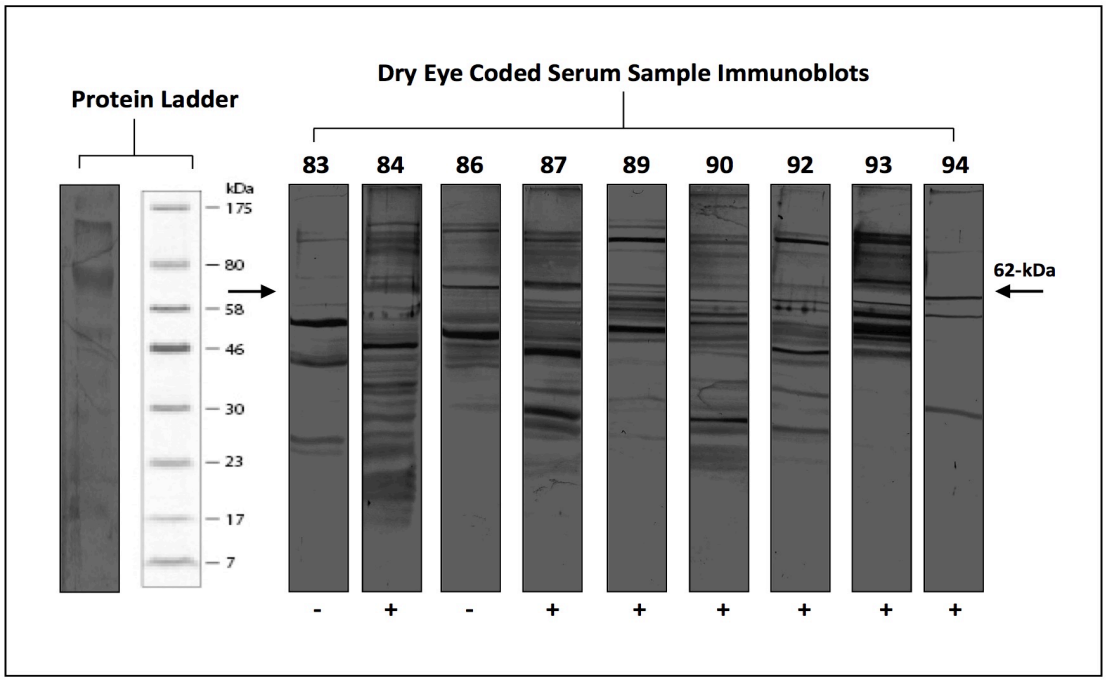

Figure A7.28 Serum reactivity of participant 83 to 94 to *B. oleronius* protein in *Demodex*-related blepharitis study (Trial 2). (-: negative serum reactivity, +: positive serum reactivity).

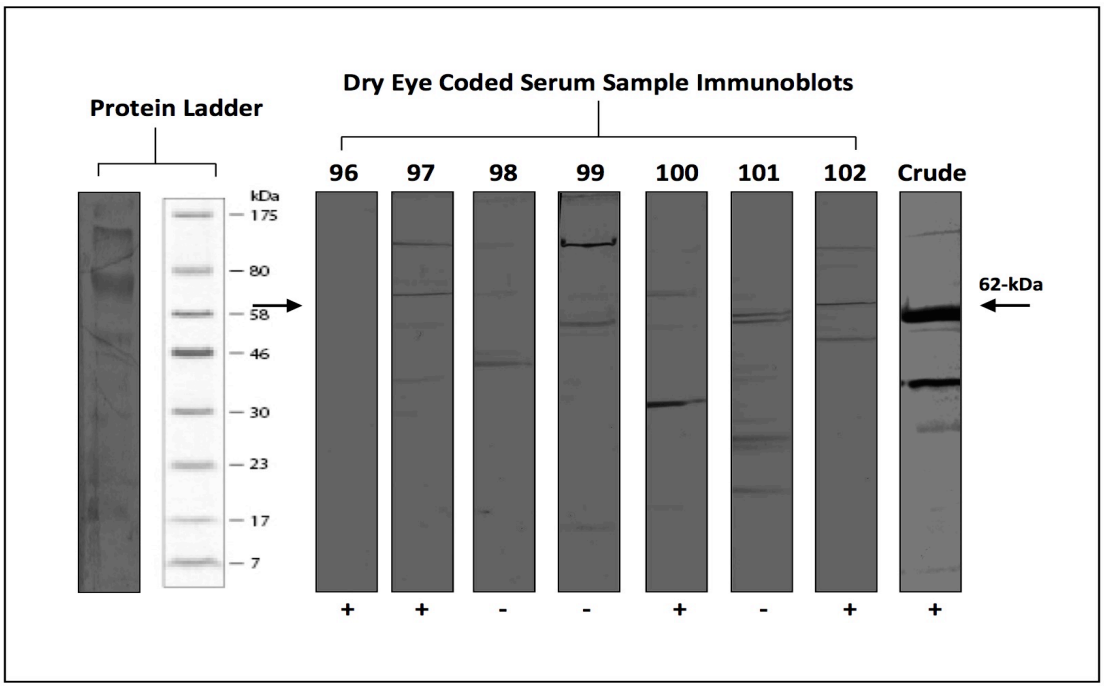

Figure A7.29 Serum reactivity of participant 96 to 102 to *B. oleronius* protein in *Demodex*-related blepharitis study (Trial 1). (-: negative serum reactivity, +: positive serum reactivity).

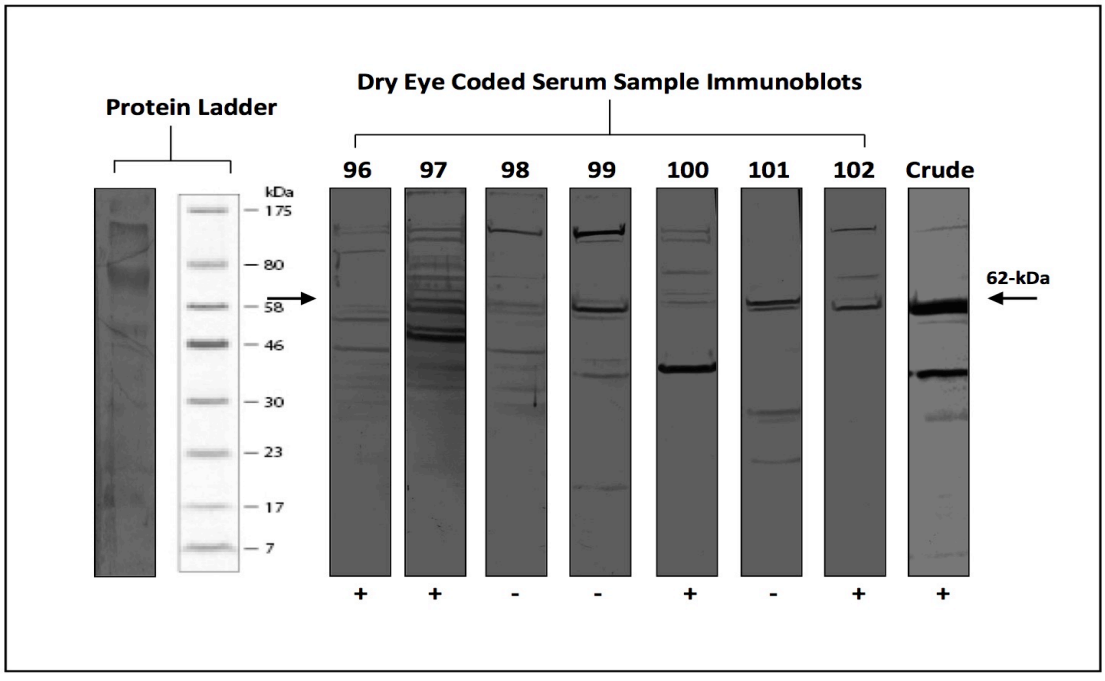

Figure A7.30 Serum reactivity of participant 96 to 102 to *B. oleronius* protein in *Demodex*-related blepharitis study (Trial 2). (-: negative serum reactivity, +: positive serum reactivity).